

YEREVAN STATE UNIVERSITY

# ASTROPHYSICS, GRAVITATION AND QUANTUM PHYSICS

A VOLUME IN HONOUR OF ACADEMICIAN  
EDVARD CHUBARYAN

YEREVAN – 2012

YEREVAN STATE UNIVERSITY

# **ASTROPHYSICS, GRAVITATION AND QUANTUM PHYSICS**

**A VOLUME IN HONOUR OF PROFESSOR  
EDVARD CUBARYAN  
ON HIS 75<sup>TH</sup> BIRTHDAY**

---

**YEREVAN**  
**YSU PUBLISHING HOUSE**  
**2012**

ՀՏ  
ԳՄԴ  
Ս

Խմբագիր Փիզ. մաթ. գիտ. դոկ.,  
պրոֆ. **Ա. Ա. Սահարյան**

Աստղաֆիզիկա, գրավիտացիա և քվանտային ֆիզիկա: Երևան:  
ԵՊՀ հրատ., 2012 թ., 300 էջ:

Գիրքը ներառում է «Աստղաֆիզիկա, գրավիտացիա և քվանտային ֆիզիկա» կոնֆերանսին ներկայացված զեկուցումները: Կոնֆերանսը կազմակերպվել է Երևանի պետական համալսարանի ֆիզիկայի ֆակուլտետի կողմից և նվիրված է եղել պրոֆեսոր Էդվարդ Չուբարյանի ծննդյան 75-ամյակին: Գիրքը օգտակար կլինի աստղաֆիզիկայի, գրավիտացիայի ու քվանտային ֆիզիկայի բնագավառներում աշխատող ֆիզիկոսների, ինչպես նաև այդ ուղղություններով մասնագիտացող ուսանողների համար:

Editor Dr. Phys. Math. Sciences,  
**Prof. A. A. Saharian**

Astrophysics, gravitation and quantum physics. Yerevan. YSU Publishing House, 2012, 300 pages.

The book includes the contributions to the conference “Astrophysics, Gravitation and Quantum Physics” in honour of Professor Edvard Chubaryan on his 75<sup>th</sup> birthday organized by the Department of Physics of the Yerevan State University (20 – 21 May, 2011). It will be useful for physicists working in astrophysics, gravity and quantum physics and also for students specializing in these directions.

ISBN

ՀՏ  
ԳՄԴ

© ԵՊՀ հրատարակչություն, 2012 թ.  
© YSU Publishing House, 2012



**Professor Edvard Chubaryan**

# Contents

<b>Preface.....</b>	6
<b>R. M. Avagyan, Edvard Chubaryan .....</b>	7
<b>V. N. Melnikov, Gravity and Cosmology in Arbitrary Dimensions and Fundamental Constants.....</b>	9
<b>E. Chubaryan, R. Avagyan, G. Harutunyan, A. Piloyan, Tensor-Scalar Theories of Gravity in the Context of Modern Cosmology....</b>	35
<b>R. M. Avagyan, G. Harutunyan, Modified Cosmological Models in JBD Theory.....</b>	48
<b>E. R. Bezerra de Mello, Induced Self-Interactions in the Spacetime of a Global Monopole with Finite Core.....</b>	55
<b>A. A. Saharian, Quantum Vacuum in de Sitter Spacetime.....</b>	76
<b>D. M. Sedrakian, Generation of a Toroidal Magnetic Field in Rotating Neutron Stars.....</b>	102
<b>E. E. Khachikyan, Physical Peculiarities of UV Galaxies.....</b>	107
<b>M. G. Abrahamyan, Tornado Mechanism of Astrophysical Jets Generation.....</b>	122
<b>A. P. Mahtessian, Dependence of Galaxy Luminosity Function on the Morphological Type and on Surrounding Medium.....</b>	139
<b>G. A. Ohanian, Formation and Evolution of Galaxies: Two Different Approaches.....</b>	178
<b>H. M. Khudaverdian, Th. Th. Voronov, Second Order Operators on the Algebra of Densities and a Groupoid of Connections.....</b>	188
<b>L. A. Hovhannисyan, G. Muradyan, A. Zh. Muradyan, Quantum Superpositional Beam-Splitter for a Two-Bunch Atom Interferometer.....</b>	223
<b>E. M. Khazaryan, H. A. Sarkisyan, Adiabatic Description of Ring-Like Nanostructures.....</b>	231

<b>T. V. Gevorgyan and G. Yu. Kryuchkyan</b> , Pulsed "Three-Photon" Light.....	244
<b>A. E. Allahverdyan and K. V. Hovhannisyan</b> , Work Extraction from Microcanonical Bath.....	258
<b>M. Samsonyan</b> , M theory on $AdS_7 \times S^4$ and $AdS_4 \times S^7 = Z_k$ .....	271
<b>A. S. Kotanjyan, A. A. Saharian, V. M. Bardeghyan</b> , Casimir-Polder Forces in the Geometry of Cosmic String.....	283
<b>V. M. Mekhitarian</b> , In Response to Edward Chubaryan's Beloved History on the Abandoned Paper by S. Goudsmit and G. Uhlenbeck about the Spin.....	292

## Preface

On May 5, 2011 Professor Edvard Chubaryan, a world-known Armenian scientist in the area of theoretical physics and astrophysics, celebrated his 75<sup>th</sup> birthday. This volume consists of the contributions to the conference “Astrophysics, Gravitation and Quantum Physics” in honour of Professor Edvard Chubaryan on his 75<sup>th</sup> birthday hosted by the Department of Physics of the Yerevan State University (20 – 21 May, 2011). The research activity by Edvard Chubaryan is very wide and covers various topics of gravity, astrophysics and quantum physics. The volume includes the papers in all these directions and will be interesting for physicists working in these topics. The contributors present this book to Professor Edvard Chubaryan as a gift on his 75<sup>th</sup> anniversary. All of them, together with researchers of the Department of Physics of the Yerevan State University wish him excellent health for many years and even more brilliant scientific achievements.

Editor Professor A. A. Saharian (Yerevan State University)



# Edvard Chubaryan

R. M. Avagyan

*Department of Physics, Yerevan State University  
1 Alex Manoogian Street, 0025 Yerevan, Armenia*

Edvard Chubaryan, theoretical physicist, one of the founders of the Armenian school of physics of superdense celestial bodies, Honored Scientist, Academician of NAS of Armenia, Doctor of Physical and Mathematical Sciences, Professor, Head of the Theoretical Physics Department of Yerevan State University, celebrated his 75<sup>th</sup> anniversary.

Professor Edvard Chubaryan was born on May 5, 1936. In 1953 he left school № 20 named after Dzerzhinsky with honors and gold medal. In the same year he entered the Department of Physics of Faculty of Physics and Mathematics of Yerevan State University. Still a student he was actively engaged in research work. His first scientific paper, which became his thesis was devoted to the question of parity violation in the processes of  $\beta$ -decay - a very topical issue in the 1950s. After graduating from the University, in 1958-1961 E. Chubaryan continued his postgraduate studies at the Department of Theoretical Physics. After defending his PhD dissertation in 1964 he began working at the same department, first as a senior lecturer, from 1967 - as an Associate professor and since the defense of his doctoral dissertation in 1972 he is a professor of the Department of Theoretical Physics.

Edvard Chubaryan's scientific research is devoted to thermodynamics of degenerate superdense matter and the theory of superdense celestial bodies, whose bases in the early 1960s were laid by academicians Victor Hambartsumyan and Gurgen Sahakian. For his research work in this field in 1970 Edvard Chubaryan together with Davit Sedrakyan and Vladimir Papoyan was awarded the Prize of Lenin Komsomol.

In subsequent years Edvard Chubaryan together with the staff members of the Department of Theoretical Physics carried out a series of works devoted to the theory of pulsars, rotating magnetized neutron stars.

There is every reason to believe that in the case of extremely strong gravitational fields, Einstein's general theory of relativity needs substantial clarification. On this basis there have been a number of attempts at the Department of Theoretical Physics to study alternative theories of gravitation. In this respect Edvard Chubaryan's input into the development of bimetric gravitational theory, Kaluza-Klein's projective theory and others is very important.

A number of significant problems were solved within the framework of bimetric theory of gravitation. In particular, it has been shown how to self-consistently determine the background and a curved metrics. With prof. Chubaryan's direct participation models of static spherical as well as those of stationary rotating stellar configurations were built, their integral parameters -

weight, size, quadrupole moments, etc. – were calculated in the framework of bimetric gravitational theory. The analytic vacuum solution of the field equations of the bimetric gravitational theory has been found, which is unique in scientific literature.

Edvard Chubaryan is the author of over 140 scientific papers published in national and international journals. They were presented at many conferences, symposia, and received recognition of the scientific community.

E. Chubaryan is one of the authors (with G. Sahakian) of the textbook "Quantum Mechanics" in Russian and Armenian languages, co-author of Collected Problems in Theoretical Physics, as well as of the Collected Problems in Physics for University entrants.

E.Chubaryan plays a major role in the education of qualified physicists. He teaches a course in "Quantum Mechanics", as well as special courses in theoretical physics at the Faculty of Physics. Six PhD theses were defended under his supervision. From 1991 to 2006, Professor E. Chubaryan, being the vice-rector of Yerevan State University for Natural Sciences, devoted much attention to the organization of educational process and actively participated in the reform of university education.

One cannot but mention his significant role in the formation and development of the Ijevan branch of Yerevan State University. The school education has not been left unattended either. E. Chubaryan was chairman of the educational-methodical council in physics of the USSR Ministry of Education, the chairman of the jury of Republican school Olympiads in physics, and in 1984 the chairman of All-Union School Olympiad jury. On his initiative in secondary schools, particularly in schools with physical and mathematical bias, extensive work was carried out to identify the gifted students.

Professor Chubaryan's role in building up and strengthening the scientific links between the Joint Institute for Nuclear Research (Dubna, Russia) and the Physics Department of Yerevan State University is also noteworthy. Up to now graduates of the Faculty of Physics, Yerevan State University, specialists in Nuclear and Theoretical Physics, work at this Institute.

In addition to the fruitful scientific and pedagogical activity E. Chubaryan takes an active part in public activities. He is a board member of the Problem-solving Council in Physics of NAS of Armenia, a member of specialized councils for defense of doctoral dissertations, a member of the Academic Councils of Yerevan State University and of the Faculty of Physics.

Edvard Chubaryan, an honest, direct and humble scientific worker, enjoys the confidence and affection of his students and colleagues. The hero of the day is full of strength, vigour and willingness to work actively. This is evidenced by the fact that during the last two years he substantially revised and republished the textbook "Quantum Mechanics" and "Problems in quantum mechanics."

Our congratulations to Professor Chubaryan. We wish him health, longevity and success in all his future endeavors.

# Gravity and cosmology in arbitrary dimensions and fundamental constants

V. N. Melnikov

*Center for Gravitation and Fundamental Metrology, VNIIMS  
and*

*Institute of Gravitation and Cosmology  
Peoples' Friendship University of Russia  
46 Ozernaya Str., Moscow, 119361, Russia*

## Abstract

Integrable multidimensional models of gravitation and cosmology make up one of the proper approaches to study basic issues and strong field objects, the Early and present Universe and black hole physics in particular [1, 2, 3]. Our main results within this approach are described both for cosmology and for BH physics. Problems of the absolute  $G$  measurements and its possible time and range variations are reflections of the unification problem.

The choice, nature, classification and precision of determination of fundamental physical constants and also their role in expected transfer to new definitions of main units of SI , supposed to be based on fundamental physical constants and stable quantum phenomena are described. The problem of temporal variations of constants is also discussed, temporal and range variations of  $G$  in particular. A need for further absolute measurements of  $G$ , its possible range and time variations is pointed out. The multipurpose space project SEE is shortly described, aimed for measuring  $G$  and its stability in space and time 3-4 orders better than at present. It may answer many important questions posed by gravitation, cosmology and unified theories. Laboratory experiment project to test possible deviations from the Newton Law is presented also.

## 1. Introduction

Gravitation as a fundamental interaction that governs all phenomena at large and very small scales, but still not well understood at a quantum level, is a missing cardinal link to unification of all physical interactions. Discovery of present acceleration of the Universe, dark matter and dark energy problems are also a great challenge to modern physics, which may bring to a new revolution in it. Studies in the previous century in the field of gravitation were devoted mainly to theoretical investigations and experimental verification of general relativity and alternative theories of gravitation with a strong stress on relations between macro and microworld phenomena or, in other words, between classical gravitation and quantum physics.

As a motivation there were: singularities in cosmology and black hole physics, role of gravity at large and very small (planckian) scales, attempts to create a quantum theory of gravity as for other physical fields, problem of possible variations of fundamental physical constants etc. A lot of work was done in our group [4] along such topics as :

- exact solutions with different fields as sources in GR,
- particle-like solutions with a gravitational field,
- quantum theory of fields in a classical gravitational background,
- quantum cosmology with fields like a scalar one, with the cosmological constant etc.,
- self-consistent treatment of quantum effects in cosmology,
- development of alternative theories of gravitation: scalar-tensor, with extra dimensions etc.,
- possible variations of fundamental physical constants [5, 6, 7, 8, 9].

As our main results of this period one may mention [4] the first quantum cosmological model with a cosmological constant (creation from nothing) (1972); first classical models for conformal scalar field (1968) and quantum cosmological models with minimal and conformal scalar fields (1971), first nonsingular cosmological model with spontaneous symmetry breaking (1978-79) of the nonlinear conformal scalar field, exact solutions for nonlinear electrodynamics, including Born-Infeld one, first exact solution for dilaton-type interaction with electro-magnetic field in GR. First non-singular field particle-like solution with gravitational field (1979). Also, the conclusion that only G may vary with respect to atomic system of measurements in Brans-Dicke frame (1978).

As all attempts to quantize general relativity in a usual manner failed and it was proved that it is not renormalizable, it became clear that the promising trend is along the lines of unification of all physical interactions which started in the 70's. About this time the experimental investigation of gravity in strong fields and gravitational waves started giving a powerful speed up in theoretical studies of such objects as pulsars, black holes, QSO's, AGN's, early Universe etc., which continues now.

In experimental activities some crucial next generation gravitational experiments verifying predictions of unified schemes will be important. Among them are: STEP - testing the corner stone Equivalence Principle, SEE - testing the inverse square law (or new non-Newtonian interactions), EP, possible variations of the newtonian constant G with time, measurements of the absolute value of G with unprecedented accuracy [10, 11]. Of course, gravitational waves problem, verification of torsional, rotational, 2nd order and strong field effects remain important also.

Other very important feature, which may be envisaged, is an increasing role of fundamental physics studies, gravitation, cosmology and astrophysics in particular, in space experiments [12]. Unique microgravity environments and modern technology outbreak give nearly ideal place for gravitational experiments which suffer a lot on Earth from its relatively strong gravitational field and gravitational fields of nearby objects due to the fact that there is no ways of screening gravity.

In the development of relativistic gravitation and dynamical cosmology we may

notice three distinct stages: first, investigation of models with matter sources in the form of a perfect fluid, as was originally done by Einstein and Friedmann. Second, studies of models with sources as different physical fields, starting from electromagnetic and scalar ones, both in classical and quantum cases (see [4]). And third, which is really topical now, application of ideas and results of unified models for treating fundamental problems of cosmology, black hole and wormholes physics, especially in high energy regimes and for explanation of the present acceleration of the Universe, dark matter and dark energy problems. Multidimensional gravitational models play an essential role in the latter approach.

The necessity of studying multidimensional models of gravitation and cosmology [1, 2] is motivated by several reasons. First, the main trend of modern physics is the unification of all known fundamental physical interactions: electromagnetic, weak, strong and gravitational ones. During the recent decades there has been a significant progress in unifying weak and electromagnetic interactions, some more modest achievements in GUT, supersymmetric, string and superstring theories.

Now, theories with membranes,  $p$ -branes and M-theory are being created and studied. Having no definite successful theory of unification now, it is desirable to study the common features of these theories and their applications to solving basic problems of modern gravity and cosmology. Second, multidimensional gravitational models, as well as scalar-tensor theories of gravity, are theoretical frameworks for describing possible temporal and range variations of fundamental physical constants [4, 5, 6, 7]. The possible discovery of the fine structure constant variations and its anisotropy is now at a critical further investigation.

Lastly, applying multidimensional gravitational models to basic problems of modern cosmology and black hole physics, we hope to find answers to such long-standing problems as singular or nonsingular initial states, creation of the Universe, creation of matter and its entropy, cosmological constant, coincidence problem, origin of inflation and specific scalar fields which may be necessary for its realization, isotropization and graceful exit problems, stability and nature of fundamental constants [5, 12, 13], possible number of extra dimensions, their stable compactification, new data on present acceleration of the Universe, dark matter and dark energy etc.

Multidimensional gravitational models are certain generalizations of GR which is tested reliably for weak fields up to 0.0001 and partially in strong fields (binary pulsars), so it is quite natural to inquire about their possible observational or experimental windows. From what we already know, among these windows are:

- possible deviations from the Newton and Coulomb laws, or new interactions,

- possible variations of the effective gravitational constant with a time rate smaller than the Hubble one,

- possible existence of monopole modes in gravitational waves,

- different behaviour of strong field objects, such as multidimensional black holes, wormholes and AGN,

- standard cosmological tests,

- possible non-conservation of energy in strong field objects and accelerators, if braneworld or similar ideas about gravity in the bulk turn out to be true, etc.

Since modern cosmology has already become a unique laboratory for testing standard unified models of physical interactions at energies that are far beyond the level of existing and future man-made accelerators, there exists a possibility of using cosmological and astrophysical data for discriminating between future unified schemes. Data on possible time variations or possible deviations from the Newton law should also contribute to the unified theory choice.

As no accepted unified model exists, in our approach [1, 2, 14, 15] we adopted models, based on multidimensional Einstein equations with or without sources of different nature as: cosmological constant, perfect and viscous fluids, scalar and electromagnetic fields and their possible interactions, dilaton and moduli fields, fields of antisymmetric forms (related to  $p$ -branes) etc.

Our program's main objective was and is to obtain exact self-consistent solutions (integrable models) for these models and then to analyze them in cosmological, spherically and axially symmetric cases. It is done mainly within Riemannian geometry. In many cases we tried to single out models, which do not contradict available experimental or observational data on variations of  $G$ .

As our model [1, 2] we use  $n$  Einstein spaces of constant curvature with sources as  $(m+1)$ -component perfect fluid, (or fields or form-fields,), cosmological or spherically symmetric metric, manifold as a direct product of factor-spaces of arbitrary dimensions. Then in harmonic time gauge we show that Einstein multidimensional equations are equivalent to Lagrange equations with non-diagonal in general minisuperspace metric and some exponential potential. After diagonalization of this metric we perform reduction to sigma-model and Toda-like systems, further to Liouville, Abel, generalized Emden-Fowler Eqs. etc. and try to find exact solutions. We suppose that behavior of extra spaces is the following: they are constant, or dynamically compactified, or like torus, or large, but with barriers, walls etc.

So, we realized the program in arbitrary dimensions (from 1988) [1, 2, 3, 14, 15] in **cosmology** obtaining exact general solutions of multidimensional Einstein equations with sources:

- $\Lambda$ ,  $\Lambda +$  scalar field (singled out nonsingular, dynamically compactified, inflationary, 1994);
- perfect fluid, PF + scalar field (e.g. nonsingular, inflationary solutions);
- viscous fluid (e.g. nonsingular, generation of mass and entropy, quintessence and coincidence in 2-component model);
- stochastic behavior near the singularity, billiards in Lobachevsky space,  $D=11$  is critical,  $\varphi$  destroys billiards (1994);
- for all above cases Ricci-flat solutions above were obtained for any  $n$ , also with curvature in one factor-space; with curvatures in 2 factor-spaces only for total  $N=10, 11$ ;
- fields: scalar, dilatons, forms of arbitrary rank (1998) - inflationary,  $\Lambda$  generation by forms ( $p$ -branes) [16];
- first billiards for dilaton-forms ( $p$ -branes) interaction (1999);
- quantum variants (solutions of WDW-equation [17]) for all above cases where classical solutions were obtained;

- dilatonic fields with potentials [18, 19], billiard behavior for them also.

For many of these integrable models we calculated also the variation with time of the effective gravitational constant and comparison with present experimental bounds allowed to choose particular models or single out some classes of solutions.

### Solutions depending on $r$ in any dimensions:

- generalized Schwarzschild, generalized Tangerlini (BH's are singled out), also with minimal scalar field (no BH's);
- generalized Reissner-Nordstrom (BH's also are singled out), the same plus  $\varphi$  (no BH's);
- multi-temporal;
- for dilaton-like interaction of  $\varphi$  and e.-m. fields (BH's exist only for a special case);
- stability studies (stable solutions only for BH case above);
- the same for dilaton-forms (p-branes) interaction, stability found only in some cases, e.g. for one form in particular.

PPN parameters for most of the models were calculated.

## 2. Multidimensional Models

The history of the multidimensional approach begins with the well-known papers of T.K. Kaluza and O. Klein on 5-dimensional theories which opened an interest to investigations in multidimensional gravity. A revival of ideas of many dimensions started in the 70's and continues now. Now, it is heated by expectations connected with the overall M-theory. In all these theories, 4-dimensional gravitational models with extra fields were obtained from some multidimensional model by dimensional reduction based on the decomposition of the manifold

$$M = M^4 \times M_{\text{int}}, \quad (1)$$

where  $M^4$  is our 4-dimensional manifold and  $M_{\text{int}}$  is some internal manifold (mostly considered to be compact).

The earlier papers on multidimensional gravity and cosmology dealt with multidimensional Einstein equations and with a block-diagonal cosmological or spherically symmetric metric defined on the manifold  $M = R \times M_0 \times \dots \times M_n$  of the form

$$g = -dt \otimes dt + \sum_{r=0}^n a_r^2(t) g^r \quad (2)$$

where  $(M_r, g^r)$  are Einstein spaces,  $r = 0, \dots, n$ . In some of them a cosmological constant and simple scalar fields were also used [17].

Such models are usually reduced to pseudo-Euclidean Toda-like systems with the Lagrangian

$$L = \frac{1}{2} G_{ij} \dot{x}^i \dot{x}^j - \sum_{k=1}^m A_k e^{u_i^k x^i} \quad (3)$$

and the zero-energy constraint  $E = 0$ .

It should be noted that pseudo-Euclidean Toda-like systems are not well-studied yet. There exists a special class of equations of state that gives rise to Euclidean Toda models [20].

Cosmological solutions are closely related to solutions with spherical symmetry [21]. Moreover, the scheme of obtaining the latter is very similar to the cosmological approach [1, 22]. In [23] the Schwarzschild solution was generalized to the case of  $n$  internal Ricci-flat spaces and it was shown that a black hole configuration takes place when the scale factors of internal spaces are constants. It was shown there also that a minimally coupled scalar field is incompatible with the existence of black holes. In [24] an analogous generalization of the Tangherlini solution was obtained, and an investigation of singularities was performed in [25]. These solutions were also generalized to the electrovacuum case with and without a scalar field [26, 27, 28]. Here, it was also proved that BH's exist only when a scalar field is switched off. Deviations from the Newton and Coulomb laws were obtained depending on mass, charge and number of dimensions. In [28] spherically symmetric solutions were obtained for a system of scalar and electromagnetic fields with a dilaton-type interaction and also deviations from the Coulomb law were calculated depending on charge, mass, number of dimensions and dilaton coupling. Multidimensional dilatonic black holes were singled out. A theorem was proved in [28] that "cuts" all non-black-hole configurations as being unstable under even monopole perturbations. In [29] the extremely charged dilatonic black hole solution was generalized to a multi-center (Majumdar-Papapetrou) case when the cosmological constant is non-zero.

We note that for  $D = 4$  the pioneering Majumdar-Papapetrou solutions with a conformal scalar field and an electromagnetic field were considered in [30].

At present there exists a special interest to the so-called M- and F-theories etc. These theories are "super-membrane" analogues of the superstring models in  $D = 11, 12$  etc. The low-energy limit of these theories leads to multidimensional models with p-branes.

### **Exact solutions with "branes"**

In our papers several classes of the exact solutions for the multidimensional gravitational model governed by the Lagrangian

$$\mathcal{L} = R[g] - 2\Lambda - h_{\alpha\beta}g^{MN}\partial_M\varphi^\alpha\partial_N\varphi^\beta - \sum_a \frac{1}{n_a!} \exp(2\lambda_{a\alpha}\varphi^\alpha)(F^a)^2, \quad (4)$$

were considered. Here  $g$  is metric,  $F^a = dA^a$  are forms of ranks  $n_a$  and  $\varphi^\alpha$  are scalar fields and  $\Lambda$  is a cosmological constant (the matrix  $h_{\alpha\beta}$  is invertible).

It was proposed earlier that *IIB* string may have its origin in a 12-dimensional theory, known as *F*-theory (Vafa). A low energy effective (bosonic) Lagrangian for *F*-theory was also suggested. The field content of this 12-dimensional field model is the following one: metric, one scalar field (with negative kinetic term), 4-form and 5-form. In our work [31] a chain of so-called  $B_D$ -models in dimensions  $D = 11, 12, \dots$  was suggested.  $B_D$ -model contains  $l = D - 11$  scalar fields with negative kinetic terms (i.e. scalar fields are so-called "phantom" fields) coupled to  $(l + 1)$  different

forms of ranks  $4, \dots, 4+l$ . These models were constructed using  $p$ -brane intersection rules that will be discussed below. For  $D = 11$  ( $l = 0$ )  $B_D$ -model coincides with the truncated bosonic sector of  $D = 11$  supergravity. For  $D = 12$  ( $l = 1$ ) it coincides with truncated  $D = 12$  model. It was conjectured by us in [31] that these  $B_D$ -models for  $D > 12$  may correspond to low energy limits of some unknown  $F_D$ -theories (analogues of  $M$ - and  $F$ -theories).

### Description of the models.

In [15] certain classes of  $p$ -brane solutions to field equations corresponding to the Lagrangian (4), obtained by us earlier, were presented.

These solutions have a block-diagonal metrics defined on  $D$ -dimensional product manifold, i.e.

$$g = e^{2\gamma} g^0 + \sum_{i=1}^n e^{2\phi^i} g^i, \quad M_0 \times M_1 \times \dots \times M_n, \quad (5)$$

where  $g^0$  is a metric on  $M_0$  (our space) and  $g^i$  are fixed Ricci-flat (or Einstein) metrics on  $M_i$  (internal space,  $i > 0$ ). The moduli  $\gamma, \phi^i$  and scalar fields  $\varphi^\alpha$  are functions on  $M_0$  and fields of forms are also governed by several scalar functions on  $M_0$ . Any  $F^a$  is supposed to be a sum of monoms, corresponding to electric or magnetic  $p$ -branes ( $p$ -dimensional analogues of membranes), i.e. the so-called composite  $p$ -brane ansatz is considered [32, 33].

(In non-composite case we have no more than one monom for each  $F^a$ .)  $p = 0$  corresponds to a particle,  $p = 1$  to a string,  $p = 2$  to a membrane etc. The  $p$ -brane world-volume (world-line for  $p = 0$ , world-surface for  $p = 1$  etc.) is isomorphic to some product of internal manifolds:  $M_I = M_{i_1} \times \dots \times M_{i_k}$  where  $1 \leq i_1 < \dots < i_k \leq n$  and has dimension  $p+1 = d_{i_1} + \dots + d_{i_k} = d(I)$ , where  $I = \{i_1, \dots, i_k\}$  is a multi-index describing the location of  $p$ -brane and  $d_i = \dim M_i$ . Any  $p$ -brane is described by the triplet ( $p$ -brane index)  $s = (a, v, I)$ , where  $a$  is the color index labelling the form  $F^a$ ,  $v = e(\text{lectric}), m(\text{agnetic})$ . For the electric and magnetic branes corresponding to form  $F^a$  the world-volume dimensions are  $d(I) = n_a - 1$  and  $d(I) = D - n_a - 1$ , respectively. The sum of this dimensions is  $D - 2$ . For  $D = 11$  supergravity we get  $d(I) = 3$  and  $d(I) = 6$ , corresponding to electric  $M2$ -brane and magnetic  $M5$ -brane.

### Sigma model representation.

In [34] the model under consideration was reduced to gravitating self-interacting sigma-model with certain constraints imposed. The sigma-model representation for non-composite electric case was obtained earlier in [32, 33], for electric composite case see also [35]).

The  $\sigma$ -model Lagrangian, obtained from (2.4), has the form [34]

$$\mathcal{L}_\sigma = R[g^0] - \hat{G}_{AB} g^{0\mu\nu} \partial_\mu \sigma^A \partial_\nu \sigma^B - \sum_s \varepsilon_s \exp(-2U^s) g^{0\mu\nu} \partial_\mu \Phi^s \partial_\nu \Phi^s - 2V, \quad (6)$$

where  $(\sigma^A) = (\phi^i, \varphi^\alpha)$ ,  $V$  is a potential,  $(\hat{G}_{AB})$  are components of (truncated) target

space metric,  $\varepsilon_s = \pm 1$ ,

$$U^s = U_A^s \sigma^A = \sum_{i \in I_s} d_i \phi^i - \chi_s \lambda_{a_s \alpha} \varphi^\alpha$$

are linear functions,  $\Phi^s$  are scalar functions on  $M_0$  (corresponding to forms), and  $s = (a_s, v_s, I_s)$ . Here parameter  $\chi_s = +1$  for the electric brane ( $v_s = e$ ) and  $\chi_s = -1$  for the magnetic one ( $v_s = m$ ).

A pure gravitational sector of the sigma-model was considered earlier in our paper [21]. For  $p$ -brane applications  $g^0$  is Euclidean,  $(\hat{G}_{AB})$  is positive definite (for  $d_0 > 2$ ) and  $\varepsilon_s = -1$ , if pseudo-Euclidean (electric and magnetic)  $p$ -branes in a pseudo-Euclidean space-time are considered. The sigma-model (6) may be also considered for the pseudo-Euclidean metric  $g^0$  of signature  $(-, +, \dots, +)$  (e.g. in investigations of gravitational waves). In this case for a positive definite matrix  $(\hat{G}_{AB})$  and  $\varepsilon_s = 1$  we get a non-negative kinetic energy terms.

The co-vectors  $U^s$  play a key role in studying the integrability of the field equations [34, 37] and possible existence of stochastic behavior near the singularity, see our paper [36]. An important mathematical characteristic here is the matrix of scalar products  $(U^s, U^{s'}) = \hat{G}^{AB} U_A^s U_B^{s'}$ , where  $(\hat{G}^{AB}) = (\hat{G}_{AB})^{-1}$ . The scalar products for co-vectors  $U^s$  were calculated in [34] (for electric case see [32, 33, 35] )

$$(U^s, U^{s'}) = d(I_s \cap I_{s'}) + \frac{d(I_s)d(I_{s'})}{2 - D} + \chi_s \chi_{s'} \lambda_{a_s \alpha} \lambda_{a_{s'} \beta} h^{\alpha \beta},$$

where  $(h^{\alpha \beta}) = (h_{\alpha \beta})^{-1}$ ;  $s = (a_s, v_s, I_s)$ ,  $s' = (a_{s'}, v_{s'}, I_{s'})$ . They depend upon brane intersections (first term), dimensions of brane world-volumes and total dimension  $D$  (second term), scalar products of dilatonic coupling vectors and electromagnetic types of branes (third term). As will be shown below the so-called “intersections rules”(i.e. relations for  $d(I_s \cap I_{s'})$ ) are defined by scalar products of  $U^s$ -vectors.

### Cosmological and spherically symmetric solutions.

A family of general cosmological type  $p$ -brane solutions with  $n$  Ricci-flat internal spaces was considered, where also a generalization to the case of  $n - 1$  Ricci-flat spaces and one Einstein space of non-zero curvature (say  $M_1$ ) was obtained. These solutions are defined up to solutions to Toda-type equations and may be obtained using the Lagrange dynamics following from our sigma-model approach [31]. The solutions contain a subclass of spherically symmetric solutions (for  $M_1 = S^{d_1}$ ). Special solutions with orthogonal and block-orthogonal sets of  $U$ -vectors were considered earlier in our works [31] and [14], respectively. (For non-composite case, see [39, 40]) and references therein.)

### Toda solutions.

In [31] the reduction of  $p$ -brane cosmological type solutions to Toda-like systems was first performed. General classes of  $p$ -brane solutions (cosmological and spherically symmetric ones) related to Euclidean Toda lattices associated with Lie algebras (mainly  $\mathbf{A}_m$ ,  $\mathbf{C}_m$  ones) were obtained in [41, 43, 44, 46, 47].

A class of space-like brane ( $S$ -brane) solutions (related to Toda-type systems) with product of Ricci-flat internal spaces and  $S$ -brane solutions with special orthogonal intersection rules were considered in [55, 56] and solutions with accelerated expansion (e.g. with power-law and exponential behavior of scale factors) were singled out.

### Black brane solutions.

In [46, 47] a family of spherically-symmetric solutions was investigated and a subclass of black-hole configurations related to Toda-type equations with certain asymptotical conditions imposed was singled out. These black hole solutions are governed by functions  $H_s(z) > 0$ , defined on the interval  $(0, (2\mu)^{-1})$ , where  $\mu > 0$  is the extremality parameter, and obey a set of differential equations (equivalent to Toda-type ones)

$$\frac{d}{dz} \left( \frac{(1 - 2\mu z)}{H_s} \frac{d}{dz} H_s \right) = \bar{B}_s \prod_{s'} H_{s'}^{-A_{ss'}},$$

with the following boundary conditions imposed: **(i)**  $H_s((2\mu)^{-1} - 0) = H_{s0} \in (0, +\infty)$ ; **(ii)**  $H_s(+0) = 1$ ,  $s \in S$ . Here  $\bar{B}_s \neq 0$  and  $(A_{ss'})$  is a quasi-Cartan matrix.

In refs. [45, 46, 47] the following hypothesis was suggested: the functions  $H_s$  are polynomials when intersection rules

$$1.12d(I_s \cap I_{s'}) = \frac{d(I_s)d(I_{s'})}{D - 2} - \chi_s \chi_{s'} \lambda_{a_s \alpha} \lambda_{a'_{s'} \beta} h^{\alpha \beta} + \frac{1}{2}(U^{s'}, U^{s'}) A_{ss'}, \quad s \neq s'. \quad (7)$$

correspond to semi-simple Lie algebras, i.e. when  $(A_{ss'})$  is a Cartan matrix.

Here

$$(A_{ss'}) \equiv \left( \frac{2(U^s, U^{s'})}{(U^{s'}, U^{s'})} \right),$$

$s, s' \in S$ , is a quasi-Cartan matrix.

This hypothesis was verified for Lie algebras:  $\mathbf{A_m}$ ,  $\mathbf{C_{m+1}}$ ,  $m = 1, 2, \dots$ , in [46, 47]. It was also confirmed by special black-hole "block orthogonal" solutions considered earlier in [14, 42].

In [45, 46, 47] explicit formulas for the solution corresponding to the algebra  $\mathbf{A_2}$  are presented. These formulas are illustrated by two examples of  $\mathbf{A_2}$ -dyon solutions: a dyon in  $D = 11$  supergravity (with  $M2$  and  $M5$  branes intersecting at a point) and Kaluza-Klein dyon. Extremal configurations (e.g. with multi-black-hole extension) were also obtained.

We note, that special black hole solutions with orthogonal  $U$ -vectors were considered in [38] (for non-composite case) and [31]. These solutions have analogous in models with multicomponent perfect fluid [49, 51, 52].

The black brane solution, corresponding to Lie algebras  $\mathbf{C_2}$  and  $\mathbf{A_3}$  where obtained in [50].

In [38] some propositions related to i) interconnection between the Hawking temperature and the singularity behavior, and ii) multitemporal configurations were proved.

It should be noted that polynomial structure was found also for the so-called flux brane solutions, that occur as generalizations of the well-known Melvin solution.

### **Cosmological models in diverse dimensions**

Scalar fields play an essential role in modern cosmology. They are attributed to inflation models of the hypothetical early universe and the models describing the present stage of the accelerated expansion as well. There is no unique candidate for the potential of the minimally coupled scalar field. Typically a potential is a sum of exponents. Such potentials appear quite generically in a large class of theories: multidimensional, Kaluza-Klein models, supergravity and string/M - theories.

Single exponential potential was extensively studied within Friedmann-Robertson-Walker (FRW) 4D-model containing both a minimally coupled scalar field and a perfect fluid with the linear barotropic equation of state . The attention was mainly focussed on the qualitative behavior of solutions, stability of the exceptional solutions to curvature and shear perturbations and their possible applications within the known cosmological scenario such as inflation and scaling ("tracking") . In particular, it was found by a phase plane analysis that for "flat" positive potentials there exists an unique late-time attractor in the form of the scalar dominated solution. It is stable within homogeneous and isotropic models with non-zero spatial curvature with respect to spatial curvature perturbations and provides the power-law inflation. For "intermediate" positive potentials an unique late-time attractor is the scaling solution, where the scalar field "mimics" the perfect fluid, adopting its equation of state. The energy-density of the scalar field scales with that of the perfect fluid. Using our methods for multidimensional cosmology the problem of integrability by quadratures of the model in 4-dimensions was also studied. Four classes of general solutions, when the parameter characterizing the steepness of the potential and the barotropic parameter obey some relations, were found [60]. For the case of multiple exponential potential of the scalar field and dust integrable model in 4D was obtained in [61].

As to scalar fields with the multiple exponential potential in any dimensions, a wide class of exact solutions was obtained in [18, 19]. In [54] a behavior of this system near the singularity was studied using a billiard approach suggested earlier in [53, 36]. A number of S-brane solutions may be found in [55, 56].

Details for 2-component D-dimensional integrable models see in [63, 58, 59]. Quite different model with dilaton, branes and cosmological constant and static internal spaces was investigated in [16], where possible generation of the effective cosmological constant by branes was demonstrated. Model with variable equations of state see in [62] with acceleration of our space and compactification of internal spaces.

### **Cosmological models with time variations of $G$ .**

As we mentioned before cosmological models in scalar-tensor and multidimensional theories are the framework for describing possible variations of fundamental

physical constants with time due to scalar fields present explicitly in STT or generated by extra dimensions in multidimensional approach. In [66] we obtained solutions for the system of conformal scalar and gravitational fields in 4D and calculated the present possible relative variation of  $G$  at the level of less than  $5 \times 10^{-13} \text{year}^{-1}$ . Later, in the frames of a multidimensional model with a perfect fluid and 2 factor spaces (our 3D space of Friedmann open, closed and flat models) and internal 6D Ricci-flat one, we obtained the same limit for such variation of  $G$  [9].

We estimated also the possible variations of the gravitational constant  $G$  in the framework of a generalized (Bergmann-Wagoner-Nordtvedt) scalar-tensor theory of gravity on the basis of the field equations, without using their special solutions. Specific estimates were essentially related to the values of other cosmological parameters (the Hubble and acceleration parameters, the dark matter density etc.), but the values of  $G\text{-dot}/G$  compatible with modern observations do not exceed  $5 \times 10^{-13}$  per year [74].

In [73] we continued the studies of models in arbitrary dimensions and obtained the relations for  $G\text{-dot}$  in multidimensional model with Ricci-flat internal space and multicomponent perfect fluid. A two-component example: dust + 5-brane, was considered. It was shown that  $G\text{-dot}/G$  is less than  $5 \times 10^{-13} \text{year}^{-1}$ . Expressions for  $G\text{-dot}$  were considered also in a multidimensional model with an Einstein internal space and a multicomponent perfect fluid [76]. In the case of two factor-spaces with non-zero curvatures without matter, a mechanism for prediction of small  $G\text{-dot}$  was suggested. The result was compared with exact (1+3+6)-dimensional solutions, obtained by us earlier [75, 76].

Multidimensional cosmological model describing the dynamics of  $n+1$  Ricci-flat factor-spaces  $M_i$  in the presence of a one-component anisotropic fluid was considered in [82]. The pressures in all spaces were supposed to be proportional to the density:  $p_i = w_i \rho$ ,  $i = 0, \dots, n$ . Solutions with accelerated power-law expansion of our 3-space  $M_0$  and small enough variation of the gravitational constant  $G$  were found. These solutions exist for two branches of the parameter  $w_0$ . The first branch describes the super-stiff matter with  $w_0 > 1$ , the second one may contain a phantom matter with  $w_0 < -1$ , e.g., when  $G$  grows with time, so this branch may describe not present, but earlier stages only.

Similar exact solutions, but nonsingular and with an exponential behaviour of the scale factors were considered in [83] for the same multidimensional cosmological model describing the dynamics of  $n+1$  Ricci-flat factor spaces  $M_i$  in the presence of a one-component perfect fluid. Solutions with accelerated exponential expansion of our 3-space  $M_0$  and small variation of the gravitational constant  $G$  were found also.

Exact S-brane solutions with 2 electric branes and 2 phantom scalar fields in the manifold

$$M = (0, +\infty) \times \mathbb{R} \times M_2 \times M_3 \times M_4 \times M_5. \quad (8)$$

were obtained and studied in [84]. We got the asymptotic accelerated expansion

of our 3-dimensional factor space and variations obeying the present experimental constraints of  $G$ -dot/ $G$  equal or less than  $5 \cdot 10^{-13} \text{year}^{-1}$ .

### Spherically-symmetric solutions, black holes and PPN parameters.

In [34] it was shown that, after dimensional reduction on the manifold  $M_0 \times M_1 \times \dots \times M_n$  and when the composite  $p$ -brane ansatz is considered, the problem is reduced to the gravitating self-interacting  $\sigma$ -model with certain constraints. For electric  $p$ -branes see also [33, 35] (in [35] the composite electric case was considered). This representation may be considered as a powerful tool for obtaining different solutions with intersecting  $p$ -branes. In [34, 37] Majumdar-Papapetrou type solutions were obtained (for the non-composite electric case see [33] and for the composite electric case see [35]). These solutions correspond to Ricci-flat  $(M_i, g^i)$ ,  $i = 1, \dots, n$  and were generalized to the case of Einstein internal spaces [34]. The obtained solutions take place when certain *orthogonality relations* (on couplings parameters, dimensions of “branes”, total dimension) are imposed. In this situation a class of cosmological and spherically symmetric solutions was obtained [31]. Solutions with a horizon (black branes) were considered in detail in [38, 31].

It should be noted that multidimensional and multitemporal generalizations of the Schwarzschild and Tangherlini solutions were considered in [27, 64], where the generalized Newton formulas in a multitemporal case were obtained.

We also calculated the Post-Newtonian Parameters  $\beta$  and  $\gamma$  (Eddington parameters) for general spherically symmetric solutions and black holes in particular [14]. These parameters depending on  $p$ -brane charges, their worldvolume dimensions, dilaton couplings and number of dimensions may be useful for possible physical applications.

Some specific models in classical and quantum multidimensional cases with  $p$ -branes were analysed. Exact solutions for the system of scalar fields and fields of forms with a dilatonic type interactions for *generalized intersection rules* were studied in [46], where the PPN parameters were also calculated. Other problems connected with observations and general properties of BH's were studied in a braneworld in [57].

Also, a *stability* analysis for solutions with  $p$ -branes was carried out [48, 71]. It was shown there that for some simple  $p$ -brane systems multidimensional black branes are stable under monopole perturbations while other (non-BH) spherically symmetric solutions turned out to be unstable.

Below we dwell mainly upon some problems of fundamental physical constants, the gravitational constant in particular, upon the SEE and laboratory projects to measure  $G$  and its possible variations shortly and on some theoretical models with variations of the effective gravitational constant.

## 3. Fundamental physical constants

In any physical theory we meet with constants which characterize the stability properties of different types of matter: of objects, processes, classes of processes and

so on. These constants are important because they arise independently in different situations and have the same value, at any rate within accuracies we have gained nowadays. That is why they are called fundamental physical constants (FPC) [4, 12]. It is impossible to define strictly this notion. It is because the constants, mainly dimensional, are present in definite physical theories. In the process of scientific progress some theories are replaced by more general ones with their own constants, some relations between old and new constants arise. So, we may talk not about an absolute choice of FPC, but only about a choice corresponding to the present state of physical sciences.

Really, before the creation of the electroweak interaction theory and some Grand Unification Models, this *choice* was considered as follows:

$$c, \hbar, \alpha, G_F, g_s, m_p \text{ (or } m_e\text{)}, G, H, \rho, \Lambda, k, I, \quad (9)$$

where  $\alpha$ ,  $G_F$ ,  $g_s$  and  $G$  are constants of electromagnetic, weak, strong and gravitational interactions,  $H$ ,  $\rho$  and  $\Lambda$  are cosmological parameters (the Hubble constant, mean density of the Universe and cosmological constant),  $k$  and  $I$  are the Boltzmann constant and the mechanical equivalent of heat which play the role of conversion factors between temperature on the one hand, energy and mechanical units on the other. After adoption in 1983 of a new definition of the meter ( $\lambda = ct$  or  $\ell = ct$ ) this role is partially played also by the speed of light  $c$ . It is now also a conversion factor between units of time (frequency) and length, it is defined with the absolute (null) accuracy. With the new suggested definitions of basic units of the International System of Units (SI) such a role may play also  $\hbar$  and  $N_A$ , where  $N_A$  is the Avogadro number.

Now, when the theory of electroweak interactions has a firm experimental basis and we have some good models of strong interactions, a more preferable choice is as follows:

$$\hbar, (c), e, m_e, \theta_w, G_F, \theta_c, \Lambda_{QCD}, G, H, \rho, \Lambda, k, I \quad (10)$$

and, possibly, three angles of Kobayashi-Maskawa —  $\theta_2$ ,  $\theta_3$  and  $\delta$ . Here  $\theta_w$  is the Weinberg angle,  $\theta_c$  is the Cabibbo angle and  $\Lambda_{QCD}$  is a cut-off parameter of quantum chromodynamics. Of course, if a theory of four known now interactions will be created (M-, F-or other), then we will probably have another choice. As we see, the macro constants remain the same, though in some unified models, i.e. in multidimensional ones, they may be related in some manner (see below). From the point of view of these unified models the above mentioned ones are low energy constants.

All these constants are known with different accuracies. The most precisely defined constant was and remain the speed of light  $c$ : its accuracy was  $10^{-10}$  and now it is defined with the null accuracy. Atomic constants,  $e$ ,  $\hbar$ ,  $m$  and others are determined with errors  $10^{-6} \div 10^{-8}$ ,  $G$  up to  $10^{-4}$  or even worse,  $\theta_w$  — up to  $10^{-3}$ ; the accuracy of  $H$  is about several percents. Other cosmological parameters (FPC): mean density estimations vary also within 2 percent; for  $\Lambda$  we have now data that its corresponding energy density exceeds the matter density (0.7 and 0.3 of the total universe mass correspondingly).

As to the nature of the FPC, we may mention several approaches. One of the first hypotheses belongs to J.A. Wheeler: in each cycle of the Universe evolution the FPC arise anew along with physical laws which govern this evolution. Thus, the nature of the FPC and physical laws are connected with the origin and evolution of our Universe.

A less global approach to the nature of dimensional constants suggests that they are needed to make physical relations dimensionless or they are measures of asymptotic states. Really, the speed of light appears in relativistic theories in factors like  $v/c$ , at the same time velocities of usual bodies are smaller than  $c$ , so it plays also the role of an asymptotic limit. The same sense have some other FPC:  $\hbar$  is the minimal quantum of action,  $e$  is the minimal observable charge (if we do not take into account quarks which are not observable in a free state) etc.

Finally, FPC or their combinations may be considered as natural scales determining the basic units. While the earlier basic units were chosen more or less arbitrarily, i.e., the second, meter and kilogram, now the first two are based on stable (quantum) phenomena. Their stability is believed to be ensured by the physical laws which include FPC. There appeared similar suggestions for a new reproducible realization of a  $kg$ , fixing values of  $N_A$  or other constants, e.g.  $\hbar$  [91].

An exact knowledge of FPC and precision measurements are necessary for testing main physical theories, extension of our knowledge of nature and, in the long run, for practical applications of fundamental theories. Within this, such theoretical problems arise:

- 1) development of models for confrontation of theory with experiment in critical situations (i.e. for verification of GR, QED, QCD, GUT or other unified models);
- 2) setting limits for spacial and temporal variations of FPC. It is becoming especially important now with the idea to introduce new basic units of International System of Units (SI), based completely on FPC.

As to a classification of FPC, we may set them now into four groups according to their generality:

- 1) Universal constants such as  $\hbar$ , which divides all phenomena into quantum and non-quantum ones (micro- and macro-worlds) and to a certain extent  $c$ , which divides all motions into relativistic and non-relativistic ones;
- 2) constants of interactions like  $\alpha$ ,  $\theta_w$ ,  $\Lambda_{QCD}$  and  $G$ ;
- 3) constants of elementary constituencies of matter like  $m_e$ ,  $m_w$ ,  $m_x$ , etc., and
- 4) transformation multipliers such as  $k$ ,  $I$  and partially  $c$  (conversion from the second to the meter). Soon there may be more after modernization of SI - values of  $\hbar$ ,  $e$ ,  $k$  and  $N_A$  may be fixed with zero uncertainty.

Of course, this division into classes is not absolute. Many constants move from one class to another. Some of the constants ceased to be fundamental (i.e. densities, magnetic moments, etc.) as they are calculated via other FPC.

As to the number of FPC, there are two opposite tendencies: the number of “old” FPC is usually diminishing when a new, more general theory is created, but at the same time new fields of science arise, new processes are discovered in which new constants appear. So, in the long run we may come to some minimal choice

which is characterized by one or several FPC, maybe connected with the so-called Planck parameters — combinations of  $c$ ,  $\hbar$  and  $G$  (natural, or Planck system of units [12, 13]):

$$\begin{aligned} L &= \left( \frac{\hbar G}{c^3} \right)^{1/2} \sim 10^{-33} \text{ cm}, \\ m_L &= (c\hbar/2G)^{1/2} \sim 10^{-5} \text{ g}, \\ \tau_L &= L/c \sim 10^{-43} \text{ s}. \end{aligned} \quad (11)$$

The role of these parameters is important since  $m_L$  characterizes the energy of unification of four known fundamental interactions: strong, weak, electromagnetic and gravitational ones, and  $L$  is a scale where the classical notions of space-time loose their meaning. There are other ideas about the final number of FPC (2, 1, or none). Of course, all will depend on a future unified theory.

The problem of the gravitational constant  $G$  measurement and its stability is a part of a rapidly developing field, called gravitational-relativistic metrology (GRM). It has appeared due to the growth of measurement technology precision, spread of measurements over large scales and a tendency to the unification of fundamental physical interaction [7], where main problems arise and are concentrated on the gravitational interaction.

The main subjects of GRM are:

- general relativistic models for different astronomical scales: Earth, Solar System, galaxies, cluster of galaxies, cosmology;
- time transfer, VLBI, space dynamics, relativistic astrometry etc.(pioneering works were done in Russia by Arifov and Kadyev, Brumberg in 60's);
- development of generalized gravitational theories and unified models for testing their effects in experiments;
- fundamental physical constants,  $G$  in particular, and their stability in space and time; projects  $\mu$ SCOPE, STEP, SEE...
- fundamental cosmological parameters as FPC: cosmological models studies (quintessence, k-essence, phantom, multidimensional ones), measurements and observations; WMAP, PLANCK, ...
- gravitational waves (3d generations of detectors, study of sources...); LIGO, VIRGO, TAMA, LISA, RADIOASTRON,...
- basic standards (clocks) and other modern precision devices (atomic and neutron interferometry, atomic force spectroscopy etc.) in fundamental gravitational experiments, especially in space for testing GR and other theories : rotational, torsional and second order effects (need uncertainty  $10^{-6}$ ), e.g. LAGEOS, Gravity Probe B, ASTROD, LATOR etc.

We are now on the level  $2.3 \cdot 10^{-5}$  in measuring PPN-parameter  $\gamma$  and  $5 \cdot 10^{-4}$  - for  $\beta$ , Brans-Dicke parameter  $\omega > 40000$ . Proposed several future missions aimed to increase the accuracy of  $\gamma$ .

There are three problems related to  $G$ , which origin lies mainly in unified models predictions: 1) absolute  $G$  measurements, 2) possible time variations of  $G$ , 3) possible range variations of  $G$  – non-Newtonian, or new interactions.

*Absolute measurements of  $G$ .* There are many laboratory determinations of  $G$  with errors of the order  $10^{-3}$  and some are on the level of  $10^{-4}$ .

The most recent and precise  $G$  measurements do not agree with each other and some differ from the CODATA value of 2010:

$$G = 6.67384(80) \cdot 10^{-11} \cdot m^3 \cdot kg^{-1} \cdot s^{-2} \quad (12)$$

with relative standard uncertainty  $1.2 \cdot 10^{-4}$ .

So, we see that we are not too far (about two orders) from Cavendish, who obtained value of  $G$  2 centuries ago at the level  $10^{-2}$ . The situation with the measurement of the absolute value of  $G$  is really different from atomic constants values and their uncertainties ( $10^{-8}$ ). This means that either the limit of terrestrial accuracies of defining  $G$  has been reached or we have some new physics entering the measurement procedure [7]. The first means that, maybe we should turn to space experiments to measure  $G$  [12, 11], and the second means that a more thorough study of theories, generalizing GR, or unified theories is necessary.

There exist also some satellite determinations of  $G$  (namely  $G \cdot M_{\text{Earth}}$ ) on the level of  $10^{-9}$  (so, should we know  $G$  much better, our knowledge of masses of the Earth and other planets will be much better and consequently their models).

The precise knowledge of  $G$  is necessary, first of all, as it is a FPC; next, for the evaluation of mass of the Earth, planets, their mean density and, finally, for construction of Earth models; for transition from mechanical to electromagnetic units and back; for evaluation of other constants through relations between them given by unified theories; for finding new possible types of interactions and geophysical effects; for some practical applications like increasing of gradiometers precision, as they demand a calibration by a gravitational field of a standard body depending on  $G$ : high accuracy of their calibration ( $10^{-5} - 10^{-6}$ ) requires the same accuracy of  $G$ .

The knowledge of constants values has not only a fundamental meaning but also a metrological one. The modern system of standards is based mainly on stable physical phenomena. So, the stability of constants plays a crucial role. As all physical laws were established and tested during the last 2-3 centuries in experiments on the Earth and in the near space, i.e. at a rather short space and time intervals in comparison with the radius and age of the Universe, the possibility of slow *variations* of constants (i.e. with the rate of the evolution of the Universe or slower) cannot be excluded a priori.

So, the assumption of absolute stability of constants is an extrapolation and each time we must test it.

*Time Variations of  $G$ .* The problem of FPC variations arose with the attempts to explain the relations between micro- and macro-world phenomena. Dirac was the first to introduce (1937) the so-called “Large Numbers Hypothesis” which relates some known very big (or very small) numbers with the dimensionless age of the

Universe  $T \sim 10^{40}$  (age of the Universe is  $10^{17}$  s, divided by the characteristic elementary particle time  $10^{-23}$  s). He suggested that the ratio of the gravitational to strong interaction strengths,  $Gm_p^2/\hbar c \sim 10^{-40}$ , is inversely proportional to the age of the Universe:  $Gm_p^2/\hbar c \sim T^{-1}$ . Then, as the age varies, some constants or their combinations must vary as well. Atomic constants seemed to Dirac to be more stable, so he chose the variation of  $G$  as  $T^{-1}$ .

After the original Dirac hypothesis some new ones appeared (Gamov, Teller, Landau, Terazawa, Staniukovich etc., see [4, 12]) and also some generalized theories of gravitation admitting the variations of an effective gravitational coupling. We may single out three stages in the development of this field:

1. Study of theories and hypotheses with variations of FPC, their predictions and confrontation with experiments (1937-1977).
2. Creation of theories admitting variations of an effective gravitational constant in a particular system of units, analyses of experimental and observational data within these theories [65, 4] (1977-present).
3. Analyses of FPC variations within unified models [7, 5, 1] (present).

Within the development of the first stage from the analysis of the whole set of existed astronomical, astrophysical, geophysical and laboratory data, a conclusion was made [65, 66] that variations of atomic constants are excluded, but variation of the effective gravitational constant in the atomic system of units does not contradict the available experimental data on the level  $10^{-12} \div 10^{-13} \text{ year}^{-1}$ . Moreover, in [65, 66] the conception was worked out that variations of constants are not absolute but depend on the system of measurements (choice of standards, units and devices using this or that fundamental interaction). Each fundamental interaction through dynamics, described by the corresponding theory, defines the system of units and the corresponding system of basic standards, e.g. atomic and gravitational (ephemeris) seconds.

There are different astronomical, geophysical and laboratory *data* on possible variations of FPC [12].

But the most strict present data on variations of strong, electromagnetic, gravitational and week interaction constants are the following:

$$\begin{aligned} |\dot{G}_s/G_s| &< 5 \cdot 10^{-19} \text{ year}^{-1}, \\ |\dot{\alpha}/\alpha| &< 10^{-17} \text{ year}^{-1}, \\ |\dot{G}/G| &< 5 \cdot 10^{-13} \text{ year}^{-1}, \\ |\dot{G}_F/G_F| &< 2 \cdot 10^{-12} \text{ year}^{-1}. \end{aligned} \quad (13)$$

Some studies of strong interaction constant and its dependance on transferred momenta may be found in [81]. The recent review on variations of  $\alpha$  see in [90].

There appeared some data on a possible variation of  $\alpha$  on the level of  $10^{-16}$  at some  $z$  [79]. Other groups do not support these results. Also appeared data on possible violation of  $m_e/m_p$  (Varshalovich et al.) The problem may be that even if they are correct, all these results are mean values of variations at some epoch of the evolution of the Universe (certain  $z$  interval). In essence variations

may be different at different epochs (if they exist at all) and at the next stage observational data should be analyzed with the account of evolution of corresponding ("true") cosmological models.

Now we still have no unified theory of all four interactions. So it is possible to construct systems of measurements based on any of these four interactions. But practically it is done now on the basis of the mostly worked out theory — on electrodynamics (more precisely on QED). Of course, it may be done also on the basis of the gravitational interaction (as it was partially earlier). Then, different units of basic physical quantities arise based on dynamics of the given interaction, i.e. the atomic (electromagnetic) second, defined via frequency of atomic transitions or the gravitational second defined by the mean Earth motion around the Sun (ephemeris time).

It does not follow from anything that these two seconds are always synchronized in time and space. So, in principle they may evolve relative to each other, for example at the rate of the evolution of the Universe or at some slower rate.

That is why, in general, variations of the gravitational constant are possible in the atomic system of units ( $c, \hbar, m$  are constant, Jordan frame) and masses of all particles — in the gravitational system of units ( $G, \hbar, c$  are constant by definition, Einstein frame). Practically we can test only the first variant since the modern basic standards are defined in the atomic system of measurements. Possible variations of FPC must be tested experimentally but for this it is necessary to have the corresponding theories admitting such variations and their certain effects.

Mathematically these systems of measurement may be realized as conformally related metric forms. Arbitrary conformal transformations give us a transition to an arbitrary system of measurements.

We know that scalar-tensor and multidimensional theories are corresponding frameworks for these variations. So, one of the ways to describe variable gravitational coupling is the introduction of a *scalar field* as an additional variable of the gravitational interaction. It may be done by different means (e.g. Jordan, Brans-Dicke, Canuto and others). We have suggested a variant of gravitational theory with a conformal scalar field (Higgs-type field [67, 4]) where Einstein's general relativity may be considered as a result of spontaneous symmetry breaking of conformal symmetry (Domokos, 1976) [4]. In our variant spontaneous symmetry breaking of the global gauge invariance leads to a nonsingular cosmology [68]. Besides, we may get variations of the effective gravitational constant in the atomic system of units when  $m, c, \hbar$  are constant and variations of all masses in the gravitational system of units ( $G, c, \hbar$  are constant). It is done on the basis of approximate [69] and exact cosmological solutions with local inhomogeneity [70].

As to other experimental or observational data, the results are of different quality. The most reliable ones are based on lunar laser ranging (Nordtvedt, 2003; Turyshev, 2008) and Pitjeva's result (2006, 2010) on radar ranging and optical observations. They are less than  $5 \cdot 10^{-1}$  per year. Here, once more we see that there is a need for corresponding theoretical and experimental studies. Probably, future space missions like Earth SEE-satellite [10, 11, 12, 13] or missions to other planets and lunar laser

ranging will be a decisive step in solving the problem of temporal variations of  $G$  and determining the fates of different theories which predict them, since the greater is the time interval between successive measurements and, of course, the more precise they are, the more stringent results will be obtained.

As was shown in [5, 72, 1] temporal variations of FPC are connected with each other in *multidimensional models* of unification of interactions. So, experimental tests on  $\dot{\alpha}/\alpha$  may at the same time be used for estimation of  $\dot{G}/G$  and vice versa. Moreover, variations of  $G$  are related also to the cosmological parameters  $\rho$ ,  $\Omega$  and  $q$  which gives opportunities of raising the precision of their determination.

As variations of FPC are closely connected with the behavior of internal scale factors [8], it is a direct probe of properties of extra dimensions and the corresponding unified theories [8, 9, 1]. From this point of view it is an additional test of not only gravity and cosmology, but unified theories of physical interactions as well.

*Non-Newtonian interactions, or range variations of  $G$ .* Nearly all modified theories of gravity and unified theories predict also some deviations from the Newton law (inverse square law, ISL) or composition-dependent violations of the Equivalence Principle (EP) due to appearance of new possible massive particles (partners) [5]. Experimental data exclude the existence of these particles on a very good level at nearly all ranges except less than *micrometer* and also at *meters and hundreds of meters* ranges. Our recent analysis of experimental bounds and new limits on possible ISL violation using the new method and modern precession data from satellites, planets, binary pulsar and LLR data were obtained in [77].

In the Einstein theory  $G$  is a true constant. But, if we think that  $G$  may vary with time, then, from a relativistic point of view, it may vary with distance as well. In GR massless gravitons are mediators of the gravitational interaction, they obey second-order differential equations and interact with matter with a constant strength  $G$ . If any of these requirements is violated, we come in general to deviations from the Newton law with range (or to generalization of GR).

In [6] we analyzed several classes of such theories:

1. Theories with massive gravitons like bimetric ones or theories with a  $\Lambda$ -term.
2. Theories with an effective gravitational constant like the general scalar-tensor ones.
3. Theories with torsion.
4. Theories with higher derivatives (4th-order equations etc.), where massive modes appear leading to short-range additional forces.
5. More elaborated theories with other mediators besides gravitons (partners), like supergravity, superstrings, M-theory etc.
6. Theories with nonlinearities induced by any known physical interactions (Born-Infeld etc.)
7. Phenomenological models where the detailed mechanism of deviation is not known (fifth or other force).
8. Modifications of the Newton law at large ranges (MOND etc.), small acceleration at  $a > a_0$  (Pioneer anomaly, etc.)

In all these theories some effective or real masses appear leading to Yukawa-type (or power-law) deviations from the Newton law, characterized by strength  $\alpha$  and range  $\lambda$ .

There exist some model-dependant estimations of these forces.

Some  $p$ -brane models (ADD, branewolds) also predict non-Newtonian additional interactions of both Yukawa or power-law, in particular in the less than 10nm range, what is intensively discussed nowadays [13, 78]. About PPN parameters for multi-dimensional models with  $p$ -branes see above, section 2.

More serious evidence on a possible violation of Newton's Law has come to us from space, namely, from data processing on the motion of the spacecrafts Pioneer 10 and 11, referring to length ranges of the order of or exceeding the size of the Solar system. The discovered anomalous (additional) acceleration is  $(8.60 \pm 1.34) \cdot 10^{-8} \text{ cm/s}^2$ . It acts on the spacecrafts and is directed towards the Sun. This acceleration is not explained yet completely by known effects, bodies or influences related to the design of the spacecrafts themselves (leakage etc.), as was confirmed by independent calculations.

Many different approaches have been analyzed both in the framework of standard theories and invoking new physics, but none of them now seems to be sufficiently convincing and generally accepted.

This Pioneer anomaly has caused new proposals of space missions with more precise experiments and a wide spectrum of research at the Solar system length range and beyond:

- Cosmic Vision 2015-2025, suggested by the European Space Agency, and
- Pioneer Anomaly Explorer, suggested by NASA. So, we hope they contribute a lot to our knowledge of gravity and unified models.

*SEE - Project.* We saw that there are three problems connected with  $G$ . There is a promising new multi-purpose space experiment SEE - Satellite Energy Exchange [10, 11], which addresses all these problems and may be more effective in solving them than other laboratory or space experiments.

This experiment is based on a limited 3-body problem of celestial mechanics: small and large masses in a drag-free satellite and the Earth. Unique horse-shoe orbits, which are effectively one-dimensional, are used in it.

The aims of the SEE-project are to measure: Inverse Square law (ISL) and Equivalence Principle (EP) at ranges of meters and the Earth radius,  $G$ -dot and the absolute value of  $G$  with unprecedented accuracies.

We studied many aspects of the SEE-project [11, 12] and the general conclusion is that realization of the SEE-project may improve our knowledge of  $G$ ,  $G$ -dot and  $G(r)$  by 3-4 orders.

Another laboratory variant was suggested in our paper [80] to test possible range variations of  $G$ . It is the experiment on possible detection of new forces, or test of the inverse square law, parameterized by Yukawa-type potential with strength  $\alpha$  and range  $\lambda$ . The installation comprises a ball with a spherical cavity whose

center is shifted with respect to the ball center. The ball is placed on a turn-table being rotated uniformly. Torsion balance as a sensitive element is inside the cavity. Uniform gravitational field created inside the ball do not influence the balance, but any non-gravitational forces create a torque, which acts periodically during the rotation of the ball. The spectrum of harmonics was calculated. It is shown that preferable to use the first harmonic in the measurements. Sensitivity of the method was evaluated, which is limited by uncertainties due to manufacturing of elements and temperature fluctuations of the sensitive element. It was shown that the sensitivity of the method suggested may be on the level of  $\alpha - 10^{-10}$  in the range of  $\lambda - (0.1 - 10^7)m$  in the space of Yukawa parameters  $(\alpha, \lambda)$ .

Our recent results on theoretical models with variations of G, FPC, billiards, solutions with branes and black branes as well as transition to new SI units see also in [85, 87], [86], [88], [89, 92] and [91, 93] correspondingly.

### Acknowledgments

The work was supported in part by the RFBR grants 09-02-00677a, 11-02-91155-GFENa and by the FTsP “Nauchnie i nauchno-pedagogicheskie kadry innovatsionnoy Rossii” for 2009-2013.

## References

- [1] V.N. Melnikov, “Multidimensional Classical and Quantum Cosmology and Gravitation. Exact Solutions and Variations of Constants.” CBPF-NF-051/93, Rio de Janeiro, 1993;  
V.N. Melnikov, in: “Cosmology and Gravitation”, ed. M. Novello, Editions Frontieres, Singapore, 1994, p. 147.
- [2] V.N. Melnikov, “Multidimensional Cosmology and Gravitation”, CBPF-MO-002/95, Rio de Janeiro, 1995, 210 pp.;  
V.N. Melnikov. In: *Cosmology and Gravitation. II*, ed. M. Novello, Editions Frontieres, Singapore, 1996, p. 465.
- [3] V.N.Melnikov. ”Exact Solutions in Multidimensional Gravity and Cosmology III.” CBPF-MO-03/02, Rio de Janeiro, 2002, 297 pp.
- [4] K.P. Staniukovich and V.N. Melnikov, “Hydrodynamics, Fields and Constants in the Theory of Gravitation”, Energoatomizdat, Moscow, 1983, 256 pp. (in Russian). See English translation of first 5 sections in:  
V.N. Melnikov, Fields and Constraints in the Theory of Gravitation, CBPF MO-02/02, Rio de Janeiro, 2002, 145 pp.
- [5] V.N. Melnikov, Int. J. Theor. Phys. **33**, 1569 (1994).
- [6] V. de Sabbata, V.N. Melnikov and P.I. Pronin, Prog. Theor. Phys. **88**, 623 (1992).

- [7] V.N. Melnikov. In: "Gravitational Measurements, Fundamental Metrology and Constants", eds. V. de Sabbata and V.N. Melnikov, Kluwer Academic Publ., Dordrecht, 1988, p. 283.
- [8] V.D. Ivashchuk and V.N. Melnikov, Nuovo Cimento **B** **102**, 131 (1988).
- [9] K.A. Bronnikov, V.D. Ivashchuk and V.N. Melnikov, Nuovo Cimento **B** **102**, 209 (1988).
- [10] A. Sanders and W. Deeds. Phys. Rev. D **46**, 480 (1992).
- [11] A.D. Alexeev, K.A. Bronnikov, N.I. Kolosnitsyn, M.Yu. Konstantinov, V.N. Melnikov and A.G. Radynov. *Izmeritel'naya tekhnika*, 1993, N 8, p.6; N 9, p.3; N 10, p.6; 1994, N1, p.3; Int. J. Mod. Phys. D **3**, 773 (1994).  
 P.N. Antonyuk, K.A. Bronnikov and V.N. Melnikov. Astron. Lett. **20**, 59 (1994); Grav. Cosm. **3**, N 4(12) (1997).  
 K.A. Bronnikov, M.Yu. Konstantinov and V.N. Melnikov, Grav. Cosm. **2**, 361 (1996); *Izmerit. Tekhnika*, N 5, p.3 (1996).  
 A.D. Alexeev, V.N. Melnikov et al. Ibid., N 10, p.3 (1997); Grav. Cosm. **5**, 67 (1999).  
 A.J. Sanders, V.N. Melnikov et al. Ibid, **3**, 287 (1997); Meas. Sci. Technol. **10**, 514 (1999); Class. Quant. Grav. **17**, N 1 (2000).  
 V.N. Melnikov. Science in Russia, N 6, p.3 (2000).
- [12] V.N. Melnikov. Gravity as a Key Problem of the Millennium. Proc.2000 NASA/JPL Conference on Fundamental Physics in Microgravity, NASA Document D-21522, 2001, p.4.1-4.17, Solvang, CA, USA.
- [13] S.A. Kononogov and V.N. Melnikov, The Fundamental Physical Constants, the Gravitational Constant, and the SEE Space Experiment Project. Izm. Tekhnika **6**, 1 (2005) - in Russian; English translation: Measurement Techniques **48**, 6, 521 (2005).
- [14] V.D. Ivashchuk and V.N. Melnikov. Multidimensional cosmological and spherically symmetric solutions with intersecting p-branes. In Lecture Notes in Physics, Vol. 537, "Mathematical and Quantum Aspects of Relativity and Cosmology Proceedings of the Second Samos Meeting on Cosmology, Geometry and Relativity held at Pythagoreon, Samos, Greece, 1998, eds: S. Cotsakis, G.W. Gibbons., Berlin, Springer, 2000.
- [15] V.D. Ivashchuk and V.N. Melnikov, Class. Quantum Grav. **18**, R82-R157 (2001); hep-th/0110274.
- [16] M.A. Grebeniuk, V.D. Ivashchuk and V.N. Melnikov, Grav. Cosmol. **4**, 145 (1998).

- [17] U. Bleyer, V.D. Ivashchuk, V.N. Melnikov and A.I. Zhuk, Nucl. Phys. **B** **429**, 117 (1994).
- [18] V.D. Ivashchuk, V.N. Melnikov and A.B. Selivanov, JHEP 0309 (2003) 059.
- [19] J.-M. Alimi, V.D. Ivashchuk and V.N. Melnikov, Grav. Cosmol. **11**, 111 (2005).
- [20] V.R. Gavrilov, V.D. Ivashchuk and V.N. Melnikov, J. Math. Phys. **36**, 5829 (1995).
- [21] V.D. Ivashchuk and V.N. Melnikov, Grav. Cosmol. **2**, 177 (1996).
- [22] V.D. Ivashchuk and V.N. Melnikov, Int. J. Mod. Phys. D **3**, 795 (1994).
- [23] K.A. Bronnikov and V.D. Ivashchuk. In: Abstr. 8th Sov. Grav. Conf., Erevan, EGU, 1988, p.156.
- [24] S.B. Fadeev, V.D. Ivashchuk and V.N. Melnikov, Phys. Lett. A **161**, 98 (1991).
- [25] V.D. Ivashchuk and V.N. Melnikov, Grav. Cosmol. **1**, 204 (1996).
- [26] S.B. Fadeev, V.D. Ivashchuk and V.N. Melnikov, Chinese Phys. Lett. **8**, 439 (1991).
- [27] V.D. Ivashchuk and V.N. Melnikov, Class. Quantum Grav. **11**, 1793 (1994).
- [28] K.A. Bronnikov and V.N. Melnikov, Annals of Physics **239**, 40 (1995).
- [29] V.D. Ivashchuk and V.N. Melnikov, Phys. Lett. B **384**, 58 (1996).
- [30] N.M. Bocharova, K.A. Bronnikov and V.N. Melnikov, *Vestnik MGU (Moscow Univ.)*, **6**, 706 (1970)(in Russian, English transl.: Moscow Univ. Phys. Bull., **25**, 6, 80 (1970)) — the first MP-type solution with a conformal scalar field; K.A. Bronnikov and V.N. Melnikov, in *Problems of Theory of Gravitation and Elementary Particles*, **5**, 80 (1974) (in Russian) — the first MP-type solution with conformal scalar and electromagnetic fields.
- [31] V.D. Ivashchuk and V.N. Melnikov, J. Math. Phys. **39**, 2866 (1998).
- [32] V.D. Ivashchuk and V.N. Melnikov, Grav. Cosmol. **2**, 297 (1996).
- [33] V.D. Ivashchuk and V.N. Melnikov, Phys. Lett. B **403**, 23 (1997).
- [34] V.D. Ivashchuk and V.N. Melnikov, Class. Quantum Grav. **14**, 3001 (1997); Corrigenda *ibid.* **15**, 3941 (1998).
- [35] V.D. Ivashchuk, V.N. Melnikov and M. Rainer, Gravit. Cosmol. **4**, 73 (1998).
- [36] V.D. Ivashchuk and V.N. Melnikov, J. Math. Phys. **41**, 6341 (2000).

- [37] V.D. Ivashchuk and V.N. Melnikov, Class. Quantum Grav. **16**, 849 (1999).  
 bibitem{IMJ1} V.D. Ivashchuk and V.N. Melnikov., J. Math. Phys. **40**, 6558 (1999).
- [38] K.A. Bronnikov, V.D. Ivashchuk and V.N. Melnikov, Grav. Cosmol. **3**, 203 (1997).
- [39] M.A. Grebeniuk, V.D. Ivashchuk and V.N. Melnikov, Grav. Cosmol. **3**, 243 (1997).
- [40] K.A. Bronnikov, M.A. Grebeniuk, V.D. Ivashchuk and V.N. Melnikov, Grav. and Cosmol. **3**, 105 (1997).
- [41] V.R. Gavrilov and V.N. Melnikov, Toda Chains with Type  $A_m$  Lie Algebra for Multidimensional Classical Cosmology with Intersecting  $p$ -branes, In : Proceedings of the International seminar "Current topics in mathematical cosmology", (Potsdam, Germany , 30 March - 4 April 1998), Eds. M. Rainer and H.-J. Schmidt, World Scientific, 1998, p. 310.
- [42] S. Cotsakis, V.D. Ivashchuk and V.N. Melnikov, Grav. and Cosmol. **5**, 52 (1999).
- [43] V.R. Gavrilov and V.N. Melnikov, Theor. Math. Phys. **123**, 374 (2000).
- [44] S. Cotsakis, V.R. Gavrilov and V.N. Melnikov, Grav. and Cosmol. **6**, 66 (2000).
- [45] V.D. Ivashchuk and V.N. Melnikov, Grav. and Cosmol. **5**, 313 (1999).
- [46] V.D. Ivashchuk and V.N. Melnikov, Grav. and Cosmol. **6**, 27 (2000).
- [47] V.D. Ivashchuk and V.N. Melnikov, Class. Quantum Gravity **17**, 2073 (2000).
- [48] K.A. Bronnikov and V.N. Melnikov, Nucl. Phys. **B 584**, 436 (2000).
- [49] V.D. Ivashchuk, V.N. Melnikov and A.B. Selivanov, Grav. Cosmol. **7**, 308 (2001).
- [50] M.A. Grebeniuk, V.D. Ivashchuk and V.N. Melnikov Phys. Lett. B **543**, 98 (2002).
- [51] V.D. Ivashchuk, V.N. Melnikov and A.B. Selivanov, Grav. Cosmol. **9**, 50 (2003).
- [52] H. Dehnen, V.D. Ivashchuk and V.N. Melnikov, Grav. Cosmol. **9**, 153 (2003).
- [53] V.D. Ivashchuk and V.N. Melnikov, Clas. Quantum Grav. **12**, 809 (1995).
- [54] H. Dehnen, V.D. Ivashchuk and V.N. Melnikov, Gen. Rel. Gravit. **36**, 1563 (2004).

- [55] V.D. Ivashchuk, V.N. Melnikov and A.B. Selivanov, Gen. Rel. Gravit. **36**, 1593 (2004).
- [56] V.D. Ivashchuk, V.N. Melnikov and S.-W. Kim, Grav. Cosm. **10**, 141 (2004).
- [57] K.A. Bronnikov, H. Dehnen and V.N. Melnikov, Phys. Rev. D **68** 024025 (2003).
- [58] V.R. Gavrilov and V.N. Melnikov, Grav. Cosmol. **7**, 301 (2001).
- [59] V.R. Gavrilov and V.N. Melnikov, Modern trends in multidimensional gravity and cosmology, In: Advances in the Interplay Between Quantum and Gravity Physics, P.G. Bergmann and V. de Sabbata (eds.), Kluwer Academic Publishers, 2002, p. 285-315.
- [60] H. Dehnen, V.R. Gavrilov and V.N. Melnikov, Grav. Cosmol. **8**, 189 (2003).
- [61] V.R. Gavrilov, V.N. Melnikov and S.T. Abdryakhmanov, Gen. Rel. Gravit. **36** 1579 (2004).
- [62] J.-M. Alimi, V. R. Gavrilov and V. N. Melnikov, Multicomponent perfect fluid with variable parameters in n Ricci-flat spaces, Proceedings of ICGA6, 6-9 October 2003, Seoul, Korea *J. Korean Phys. Soc.* 2004, v.44, p. S148.
- [63] V.N. Melnikov and V.R. Gavrilov, 2-component cosmological models with perfect fluid: exact solutions. In: The Gravitational Constant: Generalized Gravitational Theories and Experiments, V. de Sabbata, G. Gillies and V.N. Melnikov eds., 2004, Kluwer Academic Publishers, p. 247-268.
- [64] V.D. Ivashchuk and V.N. Melnikov, Int. J. Mod. Phys. D **4**, 167 (1995).
- [65] V.N. Melnikov and K.P. Staniukovich. In: “Problems of Gravitation and Elementary Particle Theory (PGEPT)”, Atomizdat, Moscow, 1978, v.9, p.3 (in Russian).
- [66] N.A. Zaitsev and V.N. Melnikov. In: PGEPT, 1979, v.10, p.131.
- [67] K.A. Bronnikov, V.N. Melnikov and K.P. Staniukovich. ITP-68-69, Kiev, 1968.
- [68] V.N. Melnikov. Dokl. Acad. Nauk **246**, N 6, 1351 (1979);  
V.N. Melnikov and S.V. Orlov, Phys.Lett. A **70**, 263 (1979).
- [69] V.N. Melnikov and A.G. Radynov. In: PGEPT, 1984, v.14, p.73.
- [70] V.N. Melnikov and A.G. Radynov. In: “On Relativity Theory”, Singapore, WS, 1985, v.2, p.196.
- [71] K.A. Bronnikov and V.N. Melnikov. Grav. Cosmol. **5**, 306 (1999).
- [72] V.N. Melnikov. In: “Results of Science and Technology. Gravitation and Cosmology”. Ed.: V.N. Melnikov, 1991, v.1, p.49 (in Russian).

- [73] V.D. Ivashchuk and V.N. Melnikov. Problems of G and Multidimensional Models. In Proc. JGRG11, Eds. J. Koga et al., Waseda Univ., Tokyo, 2002, pp. 405-409.
- [74] K.A. Bronnikov, V.N. Melnikov and M. Novello, Gravit. Cosmol. **8**, 18 (2002).
- [75] V.N. Melnikov. Time Variations of G in Different Models. Proc. 5 Int. Friedmann Seminar, Joao Pessoa, Brazil. *Int. J.Mod. Phys. A* **17**, 4325 (2002).
- [76] H. Dehnen, V.D. Ivashchuk, S.A. Kononogov and V.N. Melnikov, Grav. Cosmol. **11**, N4.
- [77] N.I. Kolosnitsyn and V.N. Melnikov, Gen. Rel. Gravit. **36**, 1619 (2004).
- [78] K.A. Bronnikov, S.A. Kononogov, V.N. Melnikov, Gen. Rel. Gravit. **38**, 1215 (2006).
- [79] J. Webb et al., Phys. Rev. Lett. **87**, 091301 (2001).
- [80] N.I. Kolosnitsyn, S.A. Kononogov, V.N. Melnikov, Izmeritel'naya Technika, 2007, N4.
- [81] V.V. Khruschev, S.A. Kononogov, V.N. Melnikov. Izmeritel'naya Technika, 2007, N3.
- [82] J.-M. Alimi, V.D. Ivashchuk, S.A. Kononogov, V.N. Melnikov. Grav. Cosmol. **12**, 173 (2006).
- [83] V.D. Ivashchuk, S.A. Kononogov, V.N. Melnikov, M. Novello, Grav. Cosmol. **12**, 273 (2006).
- [84] J.-M. Alimi, V.D. Ivashchuk, V.N. Melnikov, Grav. Cosmol. **13** (2007).
- [85] V.N. Melnikov, Progr. Theor. Phys., Suppl., Japan, N 172, (2008) 182-191.
- [86] V.N. Melnikov, Int. J. Mod. Phys. A **24**, 1473 (2009).
- [87] V.N. Melnikov, Frontiers of Physics **4**, 75 (2009).
- [88] V.D. Ivashchuk, V.N. Melnikov, Grav. Cosmol. **15**, 49 (2009).
- [89] V.D. Ivashchuk and V.N. Melnikov, SIGMA **5**, 070 (2009).
- [90] K.A. Bronnikov and V.N. Melnikov, Izmerit. Tekhn. **N11** 3 (2010).
- [91] V.N. Melnikov, Int. J. Mod. Phys. A **26**, 3788 (2011).
- [92] V. D. Ivashchuk and V. N. Melnikov, Grav. Cosmol. **17**, 7 (2011).
- [93] V.N. Melnikov, Fundamental Physics and Fundamental Metrology. *Mir Izmereniy* **N1** (2011) 7-19.

# Tensor-scalar theories of gravitation in the context of modern cosmology

E. Chubaryan, R. Avagyan, G. Harutunyan, A. Piloyan

*Department of Physics, Yerevan State University*

*1 Alex Manoogian Street, 0025 Yerevan, Armenia*

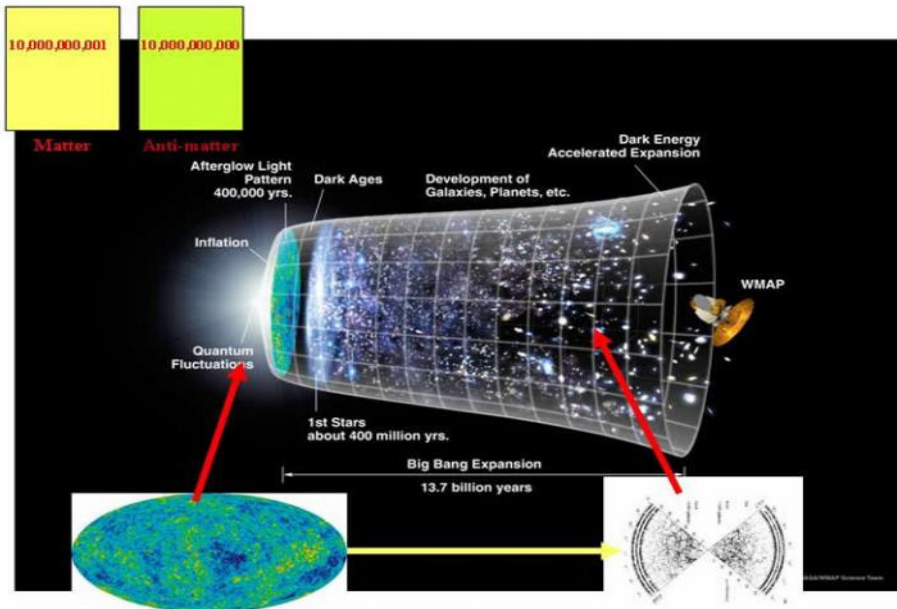
Recently discovered accelerated expansion of the Universe is of current interest in theoretical research on the evolution of the Universe. The cause of this behavior is presumably the presence of dark energy, which has been estimated to form up to 70% of the universe and generates a “repulsive gravitational force”. In this paper we present the approach based on tensor-scalar theories. After the discussion of the action for Tensor-scalar (TS) theories, we will describe conformal correspondence between JBD and Einstein theories. Cosmological models are considered in the framework of the Jordan-Brans-Dicke (JBD) theory in the Einstein frame. The cases of scalar field, the cosmological constant and the matter, being described by the equation of state  $P=\alpha\epsilon$  ( $P$  is the pressure,  $\epsilon$  is the energy density), are separately discussed. The analysis of obtained results is carried out in the light of modern observational data. It is shown that, in the case of  $q=-1/2$  ( $q$  is the “deceleration” parameter), the contributions of the scalar field and the cosmological constant  $\Lambda$  ( $\Lambda>0$ ) compensate each other, thus leading to Einstein’s theory.

## 1. Introduction

In the present paper, first we will briefly speak about the problems of the modern cosmology raised after new observational data, and then we will mention approaches and theories created to solve these problems, and finally we will pick up from these theories tensor-scalar one and discuss it in detail.

What are the most exiting points in cosmology? Of course, we can point out at least 4 problems related with the words Dark Matter, Dark Energy, Large scale structure, and Inflation[1-7]. In the Fig. 1 the universe evolution is shown as a result of recent cosmological observational data and theory. One can see in the first stage of the universe evolution the inflation, exponential expansion of the universe, the existence of which is demanded by observations and theory, then another accelerating expanding stage of the universe evolution in the late epoch takes place. These both stages need to be explained by new theories, introducing a new type of field or by changing the action of General Relativity (GR).

From Fig. 2, we can see how the observed rotational curves for stars far from the Galaxy center differ from those predicted by Newtonian gravity. The dark



matter or alternative theories of gravity are coming to help somehow explain this behavior [8-13].

Figure 1: Schematic view of the Universe evolution.

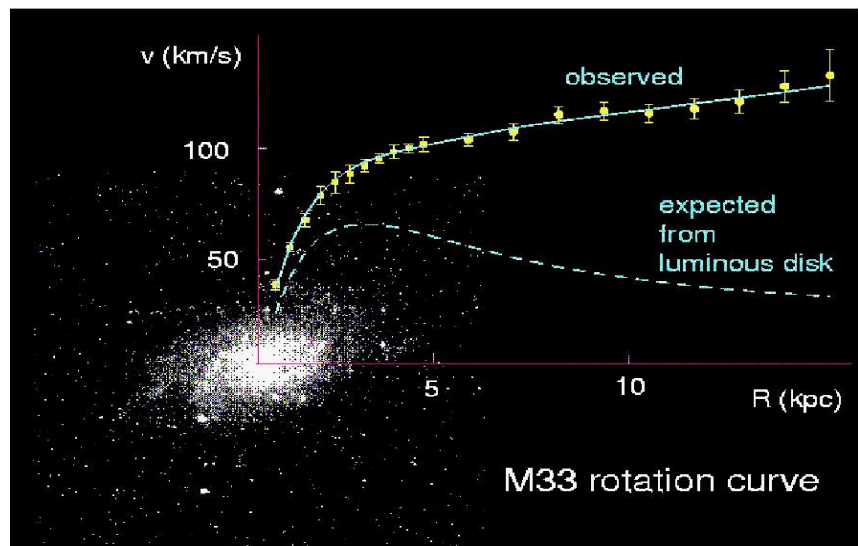


Figure 2: Rotational Curve of M33 Galaxy.

Modern cosmological observations of the large scale structure (LSS), Ia type supernova and cosmic microwave background (CMB) voted about current acceleration of the Universe expansion. As an illustration, in the Fig. 3 we present the data coming from Ia type supernova observations. One of the most popular theoretical explanations of the accelerated expansion is related with the consideration of a non-gravitational source (dark energy) for which  $\epsilon+3P<0$  ( $\epsilon$  is the energy density and  $P$  is the pressure). The positive cosmological constant is the simplest source of this type.

An alternative approach for the explanation of the accelerated expansion is based on the use of theories of gravity different from GR. Among the most popular alternatives are tensor-scalar (TS) theories. There are several motivations for this. In particular, superstring theories lead to TS theories in the low-energy limit. TS theories also provide a solution for the graceful exit problem from the inflationary stage to the radiation dominated phase.

In the first part of the present paper we will give a general introduction to TS theories. The conformal relation between GR and Jordan-Brans-Dicke (JBD) theory is discussed. The remained part of the paper is devoted to the investigation of cosmological models considered in the Einstein frame of JBD theory, in the phase dominated by a scalar field, and also in the presence of the cosmological constant and the matter described by the barotropic equation of state  $P=\alpha\epsilon$ . The analysis of the obtained results is done by comparing with the modern observational data. It is shown that for  $q=1/2$  ( $q$  is the deceleration parameter) the contributions of the scalar field and the  $\Lambda$ -term ( $\Lambda>0$ ) compensate each other and the situation becomes similar to that for the GR.

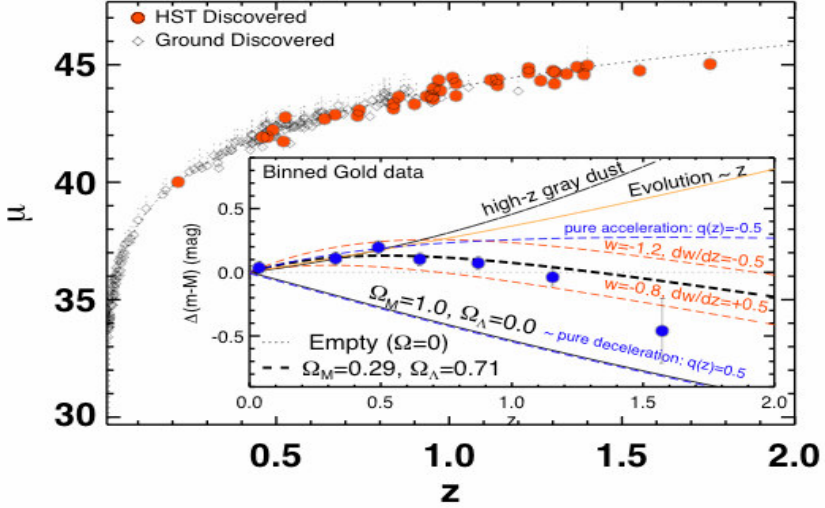


Figure 3: Ia Type Supernova observational data showing the late time acceleration of the Universe expansion.

## 2. Conformal correspondence of the JBD and GR theories

Let suppose that in the same manyfold two conformally related Riemann structures are given:

$$d\bar{s}^2 = ds^2 \sigma^2(x) = \sigma^2(x) \cdot g_{\mu\nu} \cdot dx^\mu dx^\nu, \bar{g}_{\mu\nu} = \sigma^2(x) \cdot g_{\mu\nu}, g_{\mu\nu} = \sigma^{-2}(x) \cdot \bar{g}_{\mu\nu} \quad (2.1)$$

Besides the mathematical content we try to give a physical interpretation to conformal transformation (2.1) by relating it with the scale transformation of units of measurements.

The idea of relationship between different systems of units for physical quantities and the local conformal transformations goes back to Weil [14], Eddington [15], Dicke [16]. It is natural to assume that the universal constants such as the speed of light and the Planck constant are invariant under conformal transformations:

$$\bar{c}^- = c, \bar{\hbar} = \hbar. \quad (2.2)$$

We also assume that those 1-forms in the definition of which does not appear the metric tensor are unchanged under the transformations (2.1), for example  $A_\mu = \bar{A}_\mu$  for the potential of the electromagnetic field. On the other hand, the components of the 4-velocity are transformed according to

$$u^\mu = \frac{dx^\mu}{ds} = \frac{dx^\mu}{\sigma^{-1} d\bar{s}} = \sigma \bar{u}^\mu, \quad u_\mu = g_{\mu\nu} \cdot u^\nu = \sigma^{-1} \bar{u}_\mu$$

(relation  $u_\mu \cdot u^\mu = 1$  in the space conserves its form:  $\bar{u}^\mu \cdot \bar{u}_\mu = 1$ , as it should be).

It is easy to establish the relationship between physical quantities of different units on the base of (2.2). For example, for distance  $\bar{l} = \sigma \cdot l$ , for time  $\bar{t} = \sigma \cdot t$ , for mass  $\bar{m} = \sigma^{-1} \cdot m$ , for energy density  $\bar{\varepsilon} = \sigma^{-4} \cdot \varepsilon$  and so on. It is pertinent to note that if we postulate the conformal invariance of electrodynamics, then such a requirement would be the conservation of the speed of light, the size of the elementary charge  $e = \bar{e}$  and the vector potential  $A_\mu$  for the electromagnetic field with respect to the conformal transformation.

Let us suppose that the metric tensor obeys the equations of TS theory of gravity, which are obtained as a result of the variations of the action

$$W = \int \sqrt{-g} \left[ -F(\phi)R + \frac{1}{2}\Phi(\phi)g^{\mu\nu}\phi_\mu\phi_\nu + L_m \right] dx^4 \quad (2.3)$$

with respect to  $g_{\mu\nu}$  and  $\phi$ . In (2.3),  $L_m$  is the Lagrangian for the matter and non-gravitational fields,  $\phi$  is the gravitational scalar, and  $f_{,\alpha} = \partial f / \partial x^\alpha$ . We consider the conformal transformation

$$\bar{g}_{\mu\nu} = \frac{F(\phi)}{F_0} \cdot g_{\mu\nu}, \quad F_0 = \text{const.}$$

The action takes the form

$$\overline{W} = \int \sqrt{-\bar{g}} \left[ -F_0 \bar{R} + \frac{1}{2} \bar{g}^{\mu\nu} \psi_\mu \psi_\nu + \bar{L}_m \right] dx^4 \quad (2.4)$$

where

$$\psi_\alpha = \phi_\alpha \sqrt{3F_0 \frac{F'^2}{F^2} + F_0 \frac{\Phi}{F}}, \quad F' = \frac{\partial F}{\partial \phi}.$$

The corresponding equations have the form:

$$\bar{G}_{\alpha\beta} = \frac{1}{2F_0} (\bar{T}_{\alpha\beta}^m + \bar{T}_{\alpha\beta}^s), \quad \bar{g}^{\alpha\beta} \nabla_\alpha \psi_\beta = 0, \quad \bar{T}_{\alpha\beta}^s = \psi_\alpha \psi_\beta - \frac{1}{2} \bar{g}_{\alpha\beta} \bar{g}^{\mu\nu} \psi_\mu \psi_\nu.$$

If we take  $F_0 = 1/2k_0 = c^3/16\pi G$ , then the conformally transformed action corresponds to the GR action with minimally coupled scalar field  $\psi$ . The latter satisfies the homogenous wave equation.

### 3. Cosmological Scalar in the Jordan-Brans-Dicke theory

In this section the cosmological problem in the proper representation of the JBD theory is considered in presence of a non-minimally coupled scalar field. As it will be shown the introduction of the cosmological scalar provides a possibility for the transition from the decelerated expansion of the Universe to the accelerated one. It was noted in [17-23] that the modern conceptions of the Universe give rise to the introduction of the cosmological constant in the GR, therefore it is worth to introduce a similar quantity in the JBD theory. Having assumed that the field corresponding to this quantity should be scalar but cannot be dynamical (its changes should be controlled by the gravitational scalar  $y = y(x^\mu)$ ), we introduce the cosmological scalar  $\varphi = \varphi(y)$  in the JBD theory action similar to the introduction of the cosmological constant in the GR action:

$$W = \frac{1}{c} \int \left\{ -\frac{y}{2\chi} \left[ R + 2\varphi(y) - \zeta \frac{g^{\mu\nu} y_\mu y_\nu}{y^2} \right] + L_m \right\} \sqrt{-g} d^4x, \quad \chi = \frac{8\pi}{c^4}, \quad (3.1)$$

Here,  $\zeta$  is a dimensionless coupling constant of the JBD theory. The presence of the cosmological scalar means that in addition to the kinetic term the potential one is also considered for the scalar field.

We consider the conformal transformation

$$\tilde{g}_{\mu\nu} = \frac{y}{y_0} \cdot g_{\mu\nu}, \quad y_0 = \frac{2(2+\zeta)}{G(3+2\zeta)}, \quad (3.2)$$

$$\phi_\alpha = \frac{y_\alpha}{y} \sqrt{\frac{(3+2\zeta)y_0}{2\chi}}.$$

The field equations in the conformally transformed frame take the form

$$\tilde{g}^{\alpha\beta}\tilde{\nabla}_\alpha\psi_{,\beta}=0, \quad \tilde{G}_{\alpha\beta}-\Lambda\tilde{g}_{\alpha\beta}=\frac{\chi}{y_0}(\tilde{T}_{\alpha\beta}+\tilde{\tau}_{\alpha\beta}), \quad (3.3)$$

where

$$\tilde{\tau}_{\alpha\beta}=\psi_{,\alpha}\psi_{,\beta}-\frac{1}{2}\tilde{g}_{\alpha\beta}\tilde{g}^{\mu\nu}\psi_{,\mu}\psi_{,\nu}, \quad (3.4)$$

For the action one finds

$$\tilde{W}=\int\sqrt{-\tilde{g}}\left[-\frac{y_0}{2\chi}(\tilde{R}+2\Lambda)+\frac{1}{2}\bar{g}^{\alpha\beta}\psi_{,\alpha}\psi_{,\beta}+\tilde{L}_m\right]dx^4, \quad (3.5)$$

So we can see how due to the conformal transformation we got the action with a constant coefficient for the Ricci scalar.

It is well-known that the large scale properties of the Universe are described by the Friedmann-Robertson-Walker (FRW) metric. Eqs. (3.3) for the scale factor  $a(t)$  and the scalar field take the form (units with  $c = 1$  are used)

$$\frac{d}{dt}\left(\dot{\Phi}a^3\right)=0, \quad \dot{\Phi}=c_1\left(\frac{a_0}{a}\right)^3, \quad (3.6)$$

$$3\left(\frac{\dot{a}^2}{a^2}+\frac{k}{a^2}\right)=8\pi G\left(\varepsilon+\frac{1}{2}\dot{\Phi}^2\right)+\Lambda, \quad (3.7)$$

$$2\cdot\frac{\ddot{a}}{a}+\frac{\dot{a}^2}{a^2}+\frac{k}{a^2}=-8\pi G\left(\alpha\varepsilon+\frac{1}{2}\dot{\Phi}^2\right)+\Lambda, \quad (3.8)$$

$$\varepsilon(t)=\varepsilon_0\left(\frac{a_0}{a}\right)^n, \quad n=3(1+\alpha), \quad (3.9)$$

$$P(t)=\alpha\varepsilon(t), \quad \alpha=-1, 0, \frac{1}{3}, 1, \quad (3.10)$$

where the dot denotes the derivative with respect to the time,  $a_0$  is the scale factor  $a(t)$  in a fixed moment of time  $t_0$ , and

$$c_1^2=\frac{2H_0^2}{8\pi G}(1-q_o)-\varepsilon_o=\frac{3H_0^2}{8\pi G}\left[\frac{2}{3}(1-q_o)-\overset{\circ}{\Omega}_m\right].$$

In GR one has  $q_0=-1/2$  and  $\overset{\circ}{\Omega}_m=1$  and  $c_1=0$ .

Eqs. (3.6)-(3.10) are written in a more compact form, by using the Hubble constant  $H\equiv\dot{a}/a$  and the ratio  $\Omega(t)\equiv\frac{\varepsilon}{\varepsilon_c}$ , where  $\varepsilon_c\equiv\frac{3H^2}{8\pi G}$ , is introduced by analogy with the critical energy density  $\varepsilon_c=\frac{3H_0^2}{8\pi G}$  in GR. Eq. (3.8) is presented as:

$$1 + \frac{k}{a^2 H^2} = \frac{8\pi G}{3H^2} \epsilon + \frac{8\pi G}{3H^2} \frac{\dot{\Phi}^2}{2} + \frac{\Lambda}{3H^2}, 1 = \frac{\epsilon}{\epsilon_c} + \frac{\epsilon_{ck}}{\epsilon_c} + \frac{\epsilon_\Lambda}{\epsilon_c} - \frac{\epsilon_k}{\epsilon_c}, \quad (3.11)$$

where  $\epsilon_{ck} = \frac{1}{2} c_1 \left( \frac{a_0}{a} \right)^6$ ,  $\epsilon_\Lambda = \frac{\Lambda}{8\pi G}$ ,  $\epsilon_k = \frac{3k}{8\pi G a^2}$  are respectively the energy densities for the scalar field, for the  $\Lambda$ -term and generated by the spatial curvature. Introducing also the so-called “deceleration” parameter  $q = \ddot{a}a/\dot{a}^2$ , we get

$$2q + 1 = -3\alpha \frac{\epsilon}{\epsilon_c} - \frac{3\epsilon_{ck}}{\epsilon_c} + \frac{3\epsilon_\Lambda}{\epsilon_c} - \frac{\epsilon_k}{\epsilon_c}. \quad (3.12)$$

Finally, we obtain the following set of equations:

$$\Omega_m + \Omega_{ck} + \Omega_\Lambda = 1 + \Omega_k, 2q + 1 = -3\alpha \Omega_m - 3\Omega_{ck} + 3\Omega_\Lambda - \Omega_k, \quad (3.13)$$

with the notations  $\Omega_m \equiv \epsilon/\epsilon_c$ ,  $\Omega_{ck} \equiv \epsilon_{ck}/\epsilon_c$ ,  $\Omega_\Lambda \equiv \epsilon_\Lambda/\epsilon_c$ ,  $\Omega_k \equiv \epsilon_k/\epsilon_c$ . Eq. (3.13) can also be written in the form:

$$\frac{3}{2} \frac{\dot{H}}{H^2} + 1 = -\alpha \Omega_m - \Omega_{ck} + \Omega_\Lambda - \frac{1}{3} \Omega_k, \quad (3.14)$$

from which it follows that when the contributions of the scalar field,  $\Omega_{ck}$ , and the cosmological constant,  $\Omega_\Lambda$ , compensate each other, the dynamics of the changing of  $H$  with time becomes similar to that in GR. As a result we obtain

$$q = \Omega_\Lambda - 2\Omega_{ck} - (1 + 3\alpha) \frac{\Omega_m}{2}, \quad (3.15)$$

from which it follows that  $\Omega_m = 1 - 2\Omega_{ck}$ , for  $q = -1/2$ . Thus, within the framework of the considered model during the certain period of time, when  $\Omega_{ck} = \Omega_\Lambda$  occurs, the Universe expands with deceleration, similar to that in GR. Then the situation changes in a way that  $q$  becomes positive [24]. It is natural to assume that at some intermediate moment of time,  $q$  becomes zero. According to our estimations it occurs when  $\Omega_\Lambda \approx 0.52$  and  $\Omega_{ck} \approx 0.18$ , when  $\Omega_m \approx 0.3$  as estimated in the set of works [25].

Let us try to find the dynamical picture for the time variation of the scale factor  $a(t)$ . In Ref. [26] exact analytical expressions for  $a(t)$  are obtained for some cases of the equation of state. We rewrite these relations using the above-mentioned notations. For the function  $q(t)$  it is convenient to use the formula

$$q = \frac{3}{2} (\Omega_\Lambda - \Omega_{ck}) - \frac{1}{2}. \quad (3.16)$$

The scale factor  $a(t)$  for the Universe with the dust takes the following forms:

a)  $\Lambda > 0$ . If the condition  $4\overset{o}{\Omega}_{ck}\overset{o}{\Omega}_\Lambda > \left(\frac{\overset{o}{\Omega}_m}{\overset{o}{\Omega}_\Lambda}\right)^2$  is satisfied, then

$$\left(\frac{a}{a_0}\right)^3 = b^+ sh[3H_0\sqrt{\overset{o}{\Omega}_\Lambda}(t-t_0) + \delta^+] - \frac{1}{2} \frac{\overset{o}{\Omega}_m}{\overset{o}{\Omega}_\Lambda}. \quad (3.17)$$

In the case of  $4\overset{o}{\Omega}_{ck}\overset{o}{\Omega}_\Lambda < \left(\frac{\overset{o}{\Omega}_m}{\overset{o}{\Omega}_\Lambda}\right)^2$ ,

$$\left(\frac{a}{a_0}\right)^3 = b^- ch[3H_0\sqrt{\overset{o}{\Omega}_\Lambda}(t-t_0) + \delta^-] - \frac{1}{2} \frac{\overset{o}{\Omega}_m}{\overset{o}{\Omega}_\Lambda}. \quad (3.18)$$

For both cases, the symbol "o" denotes the values corresponding to the fixed moment of time  $t_0$ . The constants have the following forms

$$(b^+)^2 = \frac{\overset{o}{\Omega}_m}{\overset{o}{\Omega}_\Lambda} - \frac{1}{4} \left( \frac{\overset{o}{\Omega}_m}{\overset{o}{\Omega}_\Lambda} \right)^2, \quad (3.19)$$

$$(b^-)^2 = \frac{1}{4} \left( \frac{\overset{o}{\Omega}_m}{\overset{o}{\Omega}_\Lambda} \right)^2 - \frac{\overset{o}{\Omega}_m}{\overset{o}{\Omega}_\Lambda}, \quad (3.20)$$

$$e^{\delta^\pm} = \frac{1 + \frac{1}{2} \frac{\overset{o}{\Omega}_m}{\overset{o}{\Omega}_\Lambda} + \sqrt{\left(1 + \frac{1}{2} \frac{\overset{o}{\Omega}_m}{\overset{o}{\Omega}_\Lambda}\right)^2 + b^{\pm 2}}}{b^\pm}. \quad (3.21)$$

b)  $\Lambda < 0$ . General solutions for  $a(t)$  follow in this case from the equation

$$\frac{d}{dt} \left( \frac{a}{a_0} \right)^3 = 3H_0 \sqrt{\overset{o}{\Omega}_\Lambda} \sqrt{\left| \frac{\overset{o}{\Omega}_{ck}}{\overset{o}{\Omega}_\Lambda} \right| + \frac{1}{4} \left( \frac{\overset{o}{\Omega}_m}{\overset{o}{\Omega}_\Lambda} \right)^2 - \left[ \left( \frac{a}{a_0} \right)^3 - \frac{1}{2} \frac{\overset{o}{\Omega}_m}{\overset{o}{\Omega}_\Lambda} \right]^2}, \quad (3.22)$$

where the expression under the square root must be positive, i.e. only one of the possibilities for the Universe expansion can be realized.

$$\left( \frac{a}{a_0} \right)^3 > \frac{1}{2} \left| \frac{\overset{o}{\Omega}_m}{\overset{o}{\Omega}_\Lambda} \right| + \sqrt{\left| \frac{\overset{o}{\Omega}_{ck}}{\overset{o}{\Omega}_\Lambda} \right| + \frac{1}{4} \left( \frac{\overset{o}{\Omega}_m}{\overset{o}{\Omega}_\Lambda} \right)^2}. \quad (3.23)$$

The solution of (3.22) has the form

$$\left(\frac{a}{a_0}\right)^3 = \sqrt{\left|\frac{\overset{o}{\Omega}_{ck}}{\overset{o}{\Omega}_\Lambda}\right| + \frac{1}{4} \left(\frac{\overset{o}{\Omega}_m}{\overset{o}{\Omega}_\Lambda}\right)^2} \sin(3H_0 \sqrt{\frac{o}{\overset{o}{\Omega}_\Lambda}} t) \frac{1}{2} \frac{\overset{o}{\Omega}_m}{\left|\overset{o}{\Omega}_\Lambda\right|}. \quad (3.24)$$

Now we can estimate the age of the Universe. For the light coming from a stellar object, the redshift is typical, which is due to the expansion of the Universe. The wavelength increases linearly proportional to the scale factor  $a(t)$ . This effect can be described by introducing the redshift  $z$ :

$$1+z = \frac{\lambda_0}{\lambda} = \frac{a_0}{a}. \quad (3.25)$$

where the index "o" corresponds to the moment of observation. From Eq. (3.25) it follows that

$$\dot{z} = -H(1+z), \quad (3.26)$$

which makes it possible to evaluate the age of the Universe

$$\Delta t_u = \int_0^{t_0} dt = \int_0^{\infty} \frac{dz}{H(1+z)}. \quad (3.27)$$

From Eqs. (3.15) and (3.27) we get

$$\Delta t_u = \frac{1}{H_0} \int_0^{\infty} \frac{dz}{(1+z) \sqrt{\overset{o}{\Omega}_{ck}(1+z)^6 + \overset{o}{\Omega}_m(1+z)^3 - \overset{o}{\Omega}_k(1+z)^2 + \overset{o}{\Omega}_\Lambda}}. \quad (3.28)$$

Introducing a new integration variable  $y = (1+z)^{-3}$ , this result is presented in the form

$$\Delta t_u = \frac{1}{3H_0} \int_0^1 \frac{dz}{\sqrt{\overset{o}{\Omega}_{ck} + \overset{o}{\Omega}_m y + \overset{o}{\Omega}_\Lambda y^2}}. \quad (3.29)$$

For  $\overset{o}{\Omega}_\Lambda = 0$ ,  $\overset{o}{\Omega}_{ck} = 0$ ,  $\overset{o}{\Omega}_m = 1$ , Eq. (3.29) gives the Einsteinian estimate for the age of the Universe

$$\Delta t_B^r = \frac{2}{3} H_0^{-1} \approx 8 \div 10 \text{ Gyr}, \quad (3.30)$$

where we used the value of the Hubble constant according to the Hubble Space Telescope Key Project  $H_o^{-1} = 9.77 \cdot h^{-1} \text{ Gyr}$ ,  $0.64 < h < 0.8$ . The obtained estimate for the age disagrees with the estimates of stellar lifetimes, giving the lifetimes larger than  $11 \div 12$  Gyr. Thus in GR there exist the problem of age.

In our case, the integral (3.27) is equal to

$$\Delta t_u = \frac{1}{3H_0\sqrt{\Omega_\Lambda}} \ln \left( \frac{2\sqrt{\Omega_\Lambda + 2\Omega_\Lambda + \Omega_m}}{2\sqrt{\Omega_\Lambda \Omega_{ck} + \Omega_m}} \right) \quad (3.31)$$

$$= \frac{\Delta t_B^3}{\sqrt{\Omega_\Lambda}} \ln \left( \frac{2\sqrt{\Omega_\Lambda + 2\Omega_\Lambda + \Omega_m}}{2\sqrt{\Omega_\Lambda \Omega_{ck} + \Omega_m}} \right).$$

In the case  $\Omega_\Lambda = \Omega_{ck}$ , the age of the Universe is close to that in GR:

$$\Delta t_u = \Delta t_u^e \frac{\ln(1 + 2\sqrt{\Omega_\Lambda})}{2\sqrt{\Omega_\Lambda}}. \quad (3.32)$$

The standard cosmological model is investigated within the framework of the Einstein frame of JBD theory, from the viewpoint of the contribution of different components' energy densities. It is shown that for the value  $q = -1/2$  (estimated by the WMAP experiment [27]) contributions of the energies due to the scalar field and  $\Lambda$ -term, compensate each other and the expansion occurs by the scheme similar to that in GR. In the future, when this condition is violated, the parameter  $q$  becomes zero for the values  $\Omega_m \approx 0.3, \Omega_\Lambda = 0.52, \Omega_{ck} = 0.18$ , after which it becomes positive.

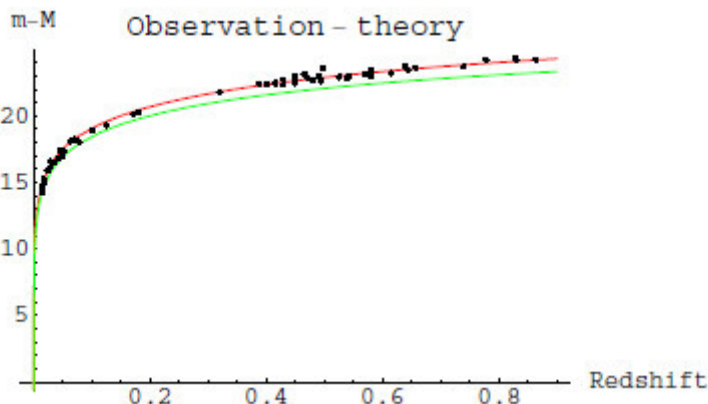


Figure 4: The black points are the observational data from Ia type Supernovae. The green line is the theoretical curve for the case  $\Omega_\Lambda = 0.65$ . The red is the theoretical curve for the case  $\Omega_\Lambda = 0.5$ . The vertical axis corresponds to the effective stellar magnitude  $m - M = 5 \log_{10}(d_L / Mpc) + 25$ .

As a result of this work, it is worthwhile to present the time dependences of  $a(t)$  and  $H(t)$  in order to qualitatively describe the dynamics of the Universe evolution

in the limited case of minimally-coupled scalar and tensor fields. As can be seen in Fig. 4, where the dependence of effective stellar magnitude on the redshift is depicted, the theoretical curve is closer to the observational data in the case of bigger values of  $\Omega_\Lambda$ . Here we used the observational data for Ia type supernovae [28,29]. For a more complete picture of the Universe evolution, in Fig. 3, we also present the dependence on time for the different contributions. The red curve represents the  $\Omega_{ck}(t)$ , the green curve represents the  $\Omega_m(t)$ , and the blue curve represents the  $\Omega_\Lambda(t)$ . From this figure, the growth of  $\Omega_\Lambda(t)$  is obvious. According to our cosmological model, the transition of the Universe expansion from a decelerating to an accelerating one can be realized as shown in Fig. 6. One can also see the behavior of the Hubble rate.

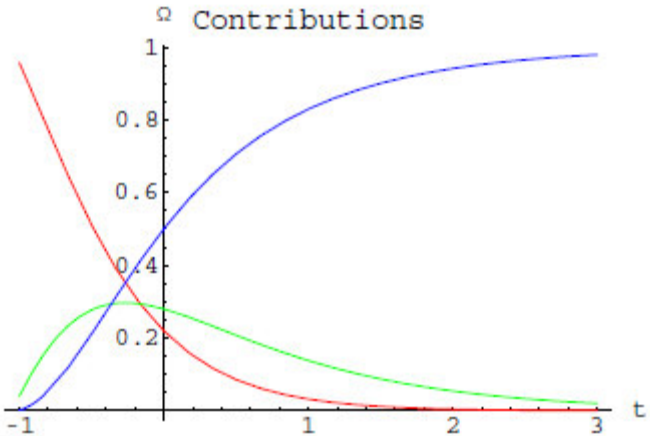


Fig. 5. Red/green/blue curves correspond to  $\Omega_{ck}(t)/\Omega_m(t)/\Omega_\Lambda(t)$ . The time on the horizontal axis is measured in units of  $3H_0\sqrt{\frac{o}{\Omega_\Lambda}} \approx (4 \div 5)\sqrt{\frac{o}{\Omega_\Lambda}}$  Gyr, and the zero point corresponds to the moment of the observation.

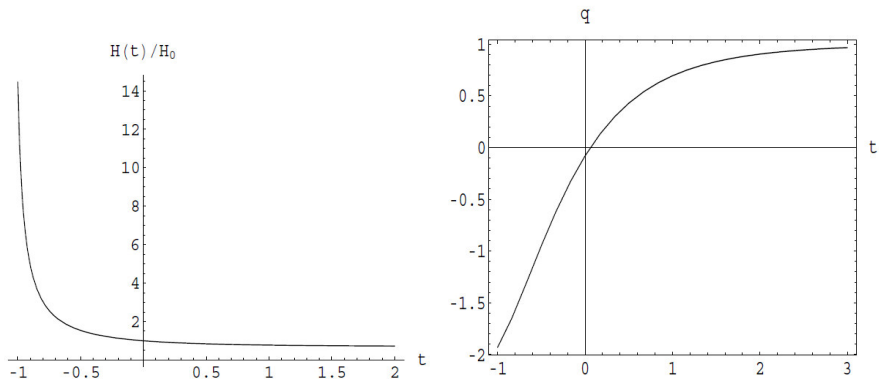


Figure 6. Left plot is the theoretical curve for the Hubble rate and the right one is the theoretical curve for the "deceleration" parameter. For both cases, the time is

measured in units of  $3H_0\sqrt{\frac{e}{\Omega_\Lambda}} \approx (4 \div 5)\sqrt{\frac{e}{\Omega_\Lambda}}$  Gyr, and the zero point corresponds to the moment of observation.

## 4. Conclusion

In the first part of this work the cosmological model with non-minimally coupled scalar field is considered in the presence of a cosmological scalar  $\phi = y\Lambda/y_0$  in the proper frame of the JBD theory. The cosmological scalar is chosen similar to that in the Einstein frame, where it becomes a cosmological constant. It is shown that in this case, a phase with an accelerated expansion appears in the scale of cosmological times.

The corresponding action has the form (2.3) and we have considered a special case of the function  $\phi(y) = y\Lambda/y_0$ . With this choice the gravitational part of the JBD action in the Einstein frame coincides with that in GR and the cosmological expansion in the Jordan frame is always decelerated. When the cosmological scalar is present in the case of non-minimally coupled scalar field, the Universe with transition from the phase of the decelerated expansion to the accelerated expansion phase is realized. At late stages we have an exponential expansion and the scalar field tends to a constant value. In the case of minimally coupled scalar field the situation is basically the same. In the second part, a cosmological model of the Universe is considered in the Einstein frame of JBD theory in the presence of the cosmological constant. The obtained analytical results are in agreement with modern observational data about the expansion of the Universe. From the presented results we can see the change of the sign for the “deceleration” parameter which describes the transition from the decelerated expansion to the accelerated one near the present time.

## References

- [1] P.J.E. Peebles and B. Ratra, Rev. Mod. Phys. **75**, 559 (2003).
- [2] A.R. Liddle and D.H. Lyth, *Cosmological Inflation and Large Scale structure* (Cambridge University Press, Cambridge, 2000).
- [3] V. Mukhanov, *Physical Foundations of Cosmology* (Cambridge University Press, Cambridge, 2005).
- [4] E. Kolb and E. Turner, *The Early Universe* (Westview Press, 1988).
- [5] K. Sato, Mon. Not. R. Astron. Soc. **195**, 467 (1981).
- [6] N.G. Tyson and D. Goldsmith, *Origins: Fourteen Billion Years of Cosmic Evolution* (W. W. Norton & Co., pp. 84-5, 2004).
- [7] A. Guth, Phase transitions in the very early universe, in *The Very Early Universe*, Editors G.W. Gibbons and S.W. Hawking (Cambridge University Press, Cambridge, 1983).
- [8] W. J. G. de Blok and S. McGaugh, Mon. Not. R. Astron. Soc. **290**, 533 (1997).
- [9] M.A. Zwaan, J. M. van der Hulst, W. J. G. de Blok, and S. McGaugh, Mon. Not. R. Astron. Soc. **273**, L35 (1995).
- [10] W. J. G. de Blok and A. Bosma, *Astronomy & Astrophysics* **385** (3), (2002).

- [11] M. Milgrom, *Astrophys. J.* **270**, 365 (1983).
- [12] M. Milgrom, M. "MD or DM? Modified dynamics at low accelerations for dark matter". *Proceedings of Scienc.*(2010).
- [13] J.D. Bekenstein, *Contemp. Phys.* **47**, 387 (2006).
- [14] H. Weyl, *Raum, Zeit, Materie* (Berlin, 1923).
- [15] A. Eddington, *Fundamental Theory* (Cambridge Univ. Press, 1948).
- [16] R. Dicke, *Phys. Rev.* **125**, 2163 (1963).
- [17] R. M. Avagyan, G. G. Harutyunyan, and V. V. Papoyan, *Astrophysica* **51**, 653 (2005).
- [18] J. Garriga and V.F. Mukhanov, *Phys. Lett. B* **458**, 219 (1999).
- [19] N.Panagia, *Nuovo Cim. B* **120**, 667 (2005).
- [20] Y.Fujii and K. Maeda, *The Scalar Tensor Theory of Gravitation* (Cambridge University Press, Cambridge , 2003).
- [21] S. Weinberg, *Gravitation and Cosmology* (John Wiley and Sons, New Jork, 1972).
- [22] R. J. Scherrer, *Phys. Rev. Lett.* **93**, 011301 (2004).
- [23] R. M. Avagyan, and G. Harutunyan, *Astrophysica* **48**, 633 (2005).
- [24] N. Brown, *Nuovo Gim. B* **120**, 667 (2005).
- [25] E.T. Copeland, M. Sami, and S. Tsujikawa, *Int.J.Mod.Phys. D* **15**, 1753 (2006).
- [26] R.M. Avagyan, and G. Harutunyan, *Astrophysica* **48**, 455 (2005).
- [27] G. Bennet et al., arxiv:astro-ph/0302207 (2003).
- [28] Moncy V. Jonn, *Astrophys. J.* **614**, 1 (2004).
- [29] V. Sahni, and A. A. Starobinsky, *Int. J. Mod. Phys. D* **9**, 373 (2000).

# Modified cosmological models in Jordan-Brans-Dicke theory

R.M. Avagyan, G.H. Harutunyan

*Department of Physics, Yerevan State University  
1 Alex Manoogian Street, 0025 Yerevan, Armenia*

This paper is based on the modified Jordan-Brans-Dicke (JBD) tensor-scalar theory. By taking into account the importance of vacuum effects in recent cosmology, we consider cosmological models with a scalar field and the vacuum energy in various conformal frames of the JBD theory.

## 1. Introduction

Recent observational data on the expansion of the universe raised a number of problems for cosmological investigations. The observations of supernovae and cosmic microwave background [1-4] indicate that the universe is accelerating. Within the framework of General Relativity this requires a special type of the energy source for this expansion with the equation of state close to the one for cosmological constant. Other classes of models are based on slowly varying scalar fields dominating at large scales. In the present paper we consider cosmological models within the framework of so called Einstein frame for Jordan tensor-scalar theory [5], when the scalar field is minimally coupled to the tensor field, and in the proper frame of this theory with self-consistent scalar field [6]. In the first case the cosmological constant  $\Lambda$  is responsible for the effects related to the vacuum energy. In the second case, in analogy with  $\Lambda$ , we introduce a cosmological scalar  $\varphi(y)$ , which as a result of special conformal transformation goes to  $\Lambda$  in the Einstein frame. It is well-known that quantum vacuum effects may be responsible for the cosmological constant  $\Lambda$ . In the early de Sitter stage of the cosmological expansion  $\Lambda \sim H^4$  with  $H$  being the Hubble constant, whereas the vacuum energy, induced by the QCD condensate at late stages of the evolution, is of the order  $\sim H$  [7-9].

In accordance with the abovementioned, at the first step it makes sense to ignore a possible contribution from other forms of energy and to consider the role of  $\Lambda$  in the Einstein frame and the role of a cosmological scalar in the modified version of JBD theory.

## 2. Dominating scalar field in presence of the vacuum energy

We consider the Friedmann-Robertson-Walker line element with flat spatial sections

$$dS^2 = dt^2 - a^2(t) \left[ dr^2 + r^2 (d\theta^2 + \sin \theta d\varphi^2) \right] \quad (1)$$

The field equations of the Jordan theory have the form

$$\frac{d}{dt} (\dot{\Phi} a^3) = 0, \quad (2)$$

$$\frac{3\dot{a}^2}{a^2} = 8\pi G \frac{\dot{\Phi}^2}{2} + \Lambda, \quad (3)$$

$$\frac{2\ddot{a}}{a} + \frac{\dot{a}^2}{a^2} = -8\pi G \frac{1}{2} \dot{\Phi}^2 + \Lambda \quad (4)$$

with the energy density  $\varepsilon = \Lambda + \frac{\dot{\Phi}^2}{2} 8\pi G$  and the pressure  $P = -\Lambda + \frac{\dot{\Phi}^2}{2} 8\pi G$ .

Equations (2)-(4) are obtained by the variation of the action [10].

In analogy with the Einsteinian critical energy density,

$$\varepsilon_{co} = \frac{3H_0^2}{8\pi G}$$

( $H_0$  is the Hubble constant), we may introduce  $\varepsilon_c = \frac{3H^2}{8\pi G}$  [11]. In terms of the latter, the field equations (2)-(4) are written in a physically transparent form. Equation (3) is written as

$$1 = \frac{\varepsilon_{ck}}{\varepsilon_c} + \frac{\varepsilon_\Lambda}{\varepsilon_c} = \Omega_{ck} + \Omega_\Lambda \quad (6)$$

where  $\varepsilon_{ck} = \frac{\dot{\Phi}^2}{2}$ ,  $\varepsilon_\Lambda = \frac{\Lambda}{8\pi G}$ ,  $\Omega_{ck} = \frac{\varepsilon_{ck}}{\varepsilon_c}$ ,  $\Omega_\Lambda = \frac{\varepsilon_\Lambda}{\varepsilon_c}$ . Hence, the sum of the contributions from the energy of the scalar field,  $\Omega_{ck}$ , and from the energy generated by  $\Lambda$  is equal to unity.

In a similar way, (4) takes the form

$$2q + 1 = -3\Omega_{ck} + 3\Omega_\Lambda, \quad (7)$$

where  $q = \frac{\ddot{a}a}{\dot{a}^2}$  is the dimensionless deceleration parameter, or in a more convenient form

$$\frac{2}{3} \frac{\dot{H}}{H^2} + 1 = -\Omega_{ck} + \Omega_\Lambda. \quad (8)$$

From relations (7) (or (8)) it follows that under the compensation of the contributions from scalar and vacuum fields and also in the absence of them one has  $q = -\frac{1}{2}$ , similar to the case of General Relativity.

Eliminating  $\Omega_\Lambda$  from (6) и (8), one has

$$\frac{\dot{H}}{3H^2} = -\Omega_{ck} = -\frac{\dot{\Phi}^2}{2} \frac{8\pi G}{3H^2}, \quad (9)$$

from which, making a natural assumption  $H = H(\Phi)$ , we find

$$\dot{\Phi} = -\frac{2H'}{8\pi G} \quad (10)$$

and the equation (3) takes the form

$$3H^2 = \frac{2H'^2}{8\pi G} + \Lambda. \quad (11)$$

From (11) we have

$$\frac{dH}{d\Phi} = \sqrt{\frac{8\pi G}{2}(3H^2 - \Lambda)} \quad (12)$$

and after the integration

$$H = \sqrt{\frac{\Lambda}{3}} ch\left(\sqrt{\frac{3}{2}} 8\pi G (\Phi - \Phi_0)\right), \quad \text{for } \Lambda > 0 \quad (13)$$

$$H = \sqrt{\frac{|\Lambda|}{3}} sh\left(\sqrt{\frac{3}{2}} 8\pi G (\Phi - \Phi_0)\right), \quad \text{for } \Lambda < 0 \quad (14)$$

Then, from (10) we get

$$\Lambda > 0 \Rightarrow H = \sqrt{\frac{\Lambda}{3}} cth\left(\sqrt{3\Lambda}(t - t_0)\right), \quad (15)$$

$$\Lambda < 0 \Rightarrow H = \sqrt{\frac{|\Lambda|}{3}} tg\left(\sqrt{3|\Lambda|} + (t - t_0)\right). \quad (16)$$

The deceleration parameter  $q$  is determined from (7), by taking into account (6),

$$q = -3\Omega_{ck} + 1 = 1 - 3\left(1 - \frac{\Lambda}{3H^2}\right). \quad (17)$$

By taking into account (13) and (14), we have

$$\Lambda > 0 \Rightarrow q = -2 + \frac{3}{cth^2\left(\sqrt{3\Lambda}(t - t_0)\right)}, \quad (18)$$

$$\Lambda < 0 \quad \Rightarrow \quad q = -2 - \frac{3}{tg\left(\sqrt{3|\Lambda|}(t-t_0)\right)}, \quad (19)$$

from which it follows that  $q \rightarrow 1$  for  $t \rightarrow \infty$ , and hence the accelerated expansion is possible only in the case  $\Lambda > 0$ .

Therefore, for sufficiently large  $t$  ( $t \rightarrow \infty$ ) for the behavior of  $H = \frac{\dot{a}}{a}$  to

the leading order one has  $H = \sqrt{\frac{\Lambda}{3}}$ . From here we see that,  $\Lambda$ , which in the present problem plays the role of the vacuum energy density, at late stages of the universe expansion is proportional to  $H^2$  ( $\Lambda = 3H^2$ ).

In order to clarify the role of the cosmological scalar in the proper frame of the Jordan theory, as in the previous problem, we ignore the contribution from all types of the matter, keeping only the scalar field and the vacuum effects induced by this field, determined by  $\varphi(y)$ .

The equations for the traditional cosmological problem, corresponding to the modified action of the JBD theory [6]

$$W = \frac{1}{c} \int \left\{ -\frac{y}{2k} \left[ R + 2\varphi(y) - \varsigma g^{\mu\nu} \frac{y_\mu y_\nu}{y^2} \right] \right\} \sqrt{-g} d^4x, \quad (20)$$

have the form

$$\frac{\ddot{y}}{y} + \frac{3\dot{y}}{y} \frac{\dot{R}}{R} = \frac{2\varphi(y)}{2+2\varsigma} \left( 1 - \frac{y}{\dot{y}} \frac{\dot{\varphi}}{\varphi} \right), \quad (21)$$

$$\frac{2\ddot{R}}{R} + \frac{\dot{R}^2}{R^2} = -\frac{\ddot{y}}{y} - \frac{2\dot{R}}{R} \frac{\dot{y}}{y} - \frac{\varsigma}{2} \frac{\dot{y}^2}{y^2} + \varphi(y), \quad (22)$$

$$\frac{3\dot{R}^2}{R^2} = \frac{1}{2} \varsigma \frac{\dot{y}^2}{y^2} - \frac{3\dot{R}}{R} \frac{\dot{y}}{y} + \varphi(y). \quad (23)$$

As it was noted before, the investigations on the quantum level evidence about the proportionality of the vacuum energy density to  $H^n$  with  $H$  being the Hubble parameter and  $n$  takes different values at different stages of the cosmological expansion.

On the base of the results obtained in the case of a minimally coupled scalar field at late stages of the universe evolution ( $\Lambda = 3H^2$ ), we may assume that in an analog problem where the cosmological scalar  $\varphi(y)$  plays the role of the vacuum energy density one has

$$\varphi(y) = \alpha H^2, \quad (24)$$

where  $\alpha$  is a dimensionless constant.

Introducing the notations  $\psi = \frac{\dot{y}}{y}$ ,  $H = \frac{\dot{R}}{R}$ , the set of field equations

takes the form

$$\dot{\psi} + \psi^2 + 3\psi H = \frac{2\alpha H^2}{3+2\zeta} \left( 1 - \frac{2\dot{H}}{H\psi} \right), \quad (25)$$

$$2\dot{H} + 3H^2 = -\dot{\psi} - \psi^2 \left( 1 + \frac{\zeta}{2} \right) - 2\psi H + \alpha H^2, \quad (26)$$

$$3H^2 = \frac{1}{2}\zeta\psi^2 - 3\psi H + \alpha H^2. \quad (27)$$

From (27) it follows that

$$\frac{\psi}{H} = \frac{3 \pm \sqrt{9 + 2\zeta(3-\alpha)}}{\zeta} \equiv \gamma, \quad (28)$$

From which we get  $\alpha \leq 3 + \frac{9}{2\zeta}$ .

By taking into account (28) and (26), we obtain

$$\frac{\dot{H}}{H^2} = \frac{\gamma(1 - \gamma(1 + \zeta))}{2 + \gamma} \equiv -A. \quad (29)$$

From here one finds

$$H = \frac{H_0}{1 + AH_0(t - t_0)}, \quad (30)$$

$$\frac{a}{a_0} = (1 + AH_0(t - t_0))^{\frac{1}{A}}, \quad (31)$$

$$\frac{y}{y_0} = \left( \frac{a}{a_0} \right)^{\gamma} = (1 + AH_0(t - t_0))^{\frac{\gamma}{A}}, \quad (32)$$

$$Q = 1 - A. \quad (33)$$

Estimating  $\gamma$  and  $A$  for large positive values of  $\zeta$  (which follow from the observational data within the framework of solar system [6]), we have

$$\gamma \approx \pm \sqrt{\frac{2(3-\alpha)}{\zeta}}, \quad A \approx (3-\alpha)$$

Negative values for  $\gamma$  are excluded from the consideration as  $H > 0 \left( \frac{\dot{a}}{a} > 0 \right)$  for

the expanding universe. Positive  $q$  is obtained for  $A < 1$ , which corresponds to  $\alpha > 2$ , and from (28) one has the estimate  $\alpha < 3$ . From here it follows that within the framework of the given model the expanding universe is obtained for the

vacuum energy density  $\varphi = \alpha H^2$  or for  $2 < \alpha < 3$ .

### 3. Conclusion

In the present paper we have tried to construct classical cosmological models by taking into account the vacuum energy. It is based on considerations related to that at the quantum field-theoretical level the vacuum energy is responsible for the cosmological constant  $\Lambda$  in the classical theory of gravity [14] and  $\Lambda$  can be taken proportional to the power of the Hubble parameter,  $H^n$  (the exponent  $n$  depends on the stage of evolution under consideration).

We have considered various variants of cosmological models within the framework of Jordan's modified tensor-scalar theory. It is assumed that the cosmological scalar  $\varphi(y)$  in the Lagrangian is related to vacuum effects. The cases of dominating scalar field are considered by taking into account the vacuum energy for FRW models with flat space. First, the problem is presented within the framework of the Einstein frame for the Jordan theory, in which  $\varphi(y)$  transforms to the usual cosmological constant  $\Lambda$ . In this frame, the minimally coupled scalar field allows to write the field equations through the quantities which play the role of contributions of densities for various types of energy [15]. As a result, the interpretation of the obtained results becomes simpler and is reduced to that, first, the accelerated expansion is possible only for and, second, at late stages of the evolution the Hubble constant  $H$  is related to  $\Lambda$  in the form  $H = \sqrt{\frac{\Lambda}{3}}$ . Further, the analog problem is considered in the proper frame of the modified variant for Jordan's theory. Here, on the base of the relation obtained before for  $H$  and  $\Lambda$ , we have taken the cosmological scalar in the form  $\varphi(y) = \alpha H^2$ . As a result, the accelerated expansion is realized if  $2 < \alpha < 3$ .

### References

1. N.Brown, High redshift Supernovae: Cosmological implications, *Nuovo Cim. B* **120**, 667 (2005).
2. E.T.Copeland, M.Sami, S.Tsujikawa, “Dynamics of Dark Energy” *Int. J. Mod. Phys. D* **15**, 1753 (2006).
3. V.Sahni, A.A.Starobinsky. *Int. J. Mod. Phys. D* **9**, 273 (2000).
4. E.G .Aman, M.A Markov, *Theor. Math. Phys.* **58**, 163 (1994).
5. R.M.Avagyan, G.G.Harutunyan, *Astrophisica* **48**, 633 (2005).
6. R.M.Avagyan, G.G.Harutunyan, V.V.Papoyan, *Astrophisica* **48**, 455 (2005).
7. S. Carneiro, *Int. J. Mod. Phys. D* **15**, 2241 (2006).
8. R. Schutzhold, *Phys. Rev. Lett.* **89**, 081302 (2002).

9. A.A.Starobinsky, Phys. Rev. Lett. D **91**, 99 (1980).
10. G.G.Harutunyan , V.V. Papoyan, Astrophisica **44**, 483 (2001).
11. R.M.Avagyan, G.G.Harutunyan, A.V.Hovsepyan, Astrophisica **53**, 317 (2010).
12. S.Weinderg, *Gravitation and Cosmology* (John Wiley and Sons, Nev York, 1972).
13. R.M.Avagyan, G.G. Harutunyan, Astrophisica **51**, 151 (2008).
14. A.A.Starobinsky, Phys.Lett., B **117**, 175 (1982).
15. E.V.Chubaryan, R.V.Avagyan, G.G.Harutunyan, A.S.Piloyan, “Universe evolution in the Einstein frame of Jordan-Brans -Dicke theory” Proccedings of YSU, 49-58, 2010.

# Induced self-interactions in the spacetime of a global monopole with finite core

E. R. Bezerra de Mello\*

*Departamento de Física-CCEN, Universidade Federal da Paraíba  
58.059-970, C. Postal 5.008, J. Pessoa, PB, Brazil*

## Abstract

In this paper we analyze induced self-interactions for point-like particles with electric and scalar charges placed at rest in the spacetime of a global monopole admitting a general spherically symmetric inner structure to it. In order to develop this analysis we calculate the three-dimensional Green function associated with the physical system under consideration. As we shall see for the charged particle outside the monopole core, the corresponding Green functions are composed by two distinct contributions, the firsts ones are induced by the non-trivial topology of the global monopole considered as a point-like defect and the seconds are corrections induced by the non-vanishing inner structure attributed to it. For both cases, the self-energies present a similar structure, having also two distinct contributions as well. For a specific model considered for region inside the monopole, named flower-pot, we shall see that the particle with electric charge will be always subject to a repulsive self-force with respect to the monopole core's boundary, on the other scalar charged particle exhibits peculiar behavior. Depending on the curvature coupling the self-force can be repulsive or attractive with respect to the core's boundary. Moreover, the contribution due to the point-like global monopole vanishes for massless particle conformally coupled with three dimensional space section of the manifold, and the only contribution comes from the core-induced part.

## 1. Introduction

It is well known that different types of topological objects may have been formed by the vacuum phase transition in the early Universe after Planck time [1, 2]. These include domain walls, cosmic strings and monopoles. Global monopoles are heavy spherically symmetric topological objects which may have been formed by the vacuum phase transition in the early Universe after Planck time. Although the global monopole was first introduced by Sokolov and Starobinsky in [3], its gravitational effects has been analyzed by Barriola and Vilenkin [4]. In the latter it is shown that

---

\*E-mail: emello@fisica.ufpb.br

for points far away from the monopole's center, the geometry of the spacetime can be given by the line element below:

$$ds^2 = -dt^2 + dr^2 + \alpha^2 r^2(d\theta^2 + \sin^2 \theta d\varphi^2) . \quad (1)$$

In (1) the parameter  $\alpha^2$ , which is smaller than unity, depends on the energy scale  $\eta$  where the phase transition spontaneously occur. This spacetime has a non-vanishing scalar curvature,  $R = \frac{2(1-\alpha^2)}{\alpha^2 r^2}$  and presents a solid angle deficit  $\delta\Omega = 4\pi^2(1 - \alpha^2)$ .

Although the geometric properties of the spacetime outside the monopole are very well understood, there are no explicit expressions for the components of the metric tensor in the region inside. Consequently many interesting investigations of physical effects associated with global monopole consider this object as a point-like defect. Adopting this simplified model, many calculations of vacuum polarization effects associated with bosonic [5] and fermionic quantum fields [6], in four-dimensional global monopole spacetime, present divergence on the monopole's core.

A very well known phenomenon that occur with an electric charged test particle placed at rest in a curved spacetime, is that it may become subjected to an electrostatic self-interactions. The origin of this induced self-interaction resides on the non-local structure of the field caused by the spacetime curvature and/or non-trivial topology. This phenomenon has been analyzed in an idealized cosmic string spacetime by Linet [7] and Smith [8], independently, and also in the spacetime of a global monopole considered as a point-like defect in [9]. In these analysis, the corresponding self-forces are always repulsive; moreover they present divergences on the respective defects' core. A possible way to avoid the divergence problem is to consider these defects as having a non-vanishing radius, and attributing for the region inside a structure. For the cosmic string, two different models have been adopted to describe the geometry inside it: the ballpoint-pen model proposed independently by Gott and Hiscock [10], replaces the conical singularity at the string axis by a constant curvature spacetime in the interior region, and flower-pot model [11], presents the curvature concentrated on a ring with the spacetime inside the string been flat. Khusnutdinov and Bezerra in [12], revisited the induced electrostatic self-energy problem considering the Hiscock and Gott model for the region inside the string. As to the global monopole the electrostatic self-energies problem have been analyzed considering for the region inside, the flower-pot model in [13] and ballpoint pen in [14]. In both analysis it was observed that the corresponding self-forces are finite at the monopole's core center.

In the context of self-interactions the induced self-energy on scalar charged point-like particles on a curved spacetime reveals peculiarities [15, 16] due to the non-minimal curvature coupling with the geometry. In the case of Schwarzschild spacetime, the self-force on a scalar charged particle at rest vanishes for minimal coupling [17]. The self-energy on scalar particle on the global monopole spacetime considering a non-trivial inner structure been developed recently in [18].

In this present paper, mainly supported by two previous publications, [13, 18], we shall analyze the self-interaction problems associate with electric and scalar charged

particles placed at rest in the global monopole spacetime, considering a non-trivial structure for the region inside to it. This paper is organized as follows: In section 2 we present the model to consider the geometry of the global in the whole space and the relevant field equations associated with the electric and scalar charged particles placed at rest in this background. We calculate the effective three-dimensional Green functions for points outside and inside the monopole's core. As a consequence, we provide a general expression for the electrostatic and scalar self-energies and their related self-forces. In section 3 we calculate explicit expressions for the self-energies considering, as application of previous formalism, the flower-pot model for the region inside the monopole. Finally in section 4, we present our conclusions and more relevant remarks.

## 2. The system

Many investigations concerning physical effects around a global monopole are developed considering it as idealized point-like defect. In this way the geometry of the spacetime is described by line element (1) for all values of the radial coordinate. However, a realistic model for a global monopole should present a non-vanishing characteristic core radius. For example, considering the model proposed by Barriola and Vilenkin [4], the line element given by (1) is attained for the radial coordinate much larger than its characteristic core radius, which depends on the inverse of the energy scale where the global  $O(3)$  symmetry is spontaneously broken to  $U(1)$ . Explicit expressions for the components of the metric tensor in whole space have not yet been found. Here, in this paper we shall not go into the details about this calculation. Instead, we shall consider a spherically symmetric model for describing the metric tensor for the region inside the shell of radius  $a$ . In the exterior region corresponding to  $r > a$ , the line element is given by (1), while in the interior region,  $r < a$ , the geometry is described by the static spherically symmetric line element

$$ds^2 = -dt^2 + v^2(r)dr^2 + w^2(r)(d\theta^2 + \sin^2\theta d\varphi^2) . \quad (2)$$

Because the metric tensor must be continuous at the boundary of the core, the functions  $v(r)$  and  $w(r)$  must satisfy the conditions

$$v(a) = 1 \text{ and } w(a) = \alpha a . \quad (3)$$

### 2.1. Self-interactions

In this subsection we shall develop a general formalism to analysis self-interactions associated with electric and scalar charged particles in global monopole spacetime.

#### 2.1.1. Electrostatic self-interaction

Here we investigate the electrostatic self-energy and the self-force for a point-like charged particle at rest, induced by the spacetime geometry associated with a global

monopole with the core of finite radius. We shall assume that in the region inside the monopole core the geometry is described by line element (2), and in the exterior region we have the standard line element (1). From the Maxwell equations, the covariant components of the electromagnetic four-vector potential,  $A_\mu$ , obey the equation below,

$$\partial_\lambda \left[ \sqrt{-g} g^{\mu\nu} g^{\lambda\sigma} (\partial_\nu A_\sigma - \partial_\sigma A_\nu) \right] = -4\pi \sqrt{-g} j^\mu, \quad (4)$$

where  $j^\mu$  is the four-vector electric current density. For a point-like particle at rest with coordinates  $\vec{r}_0 = (r_0, \theta_0, \varphi_0)$ , in the coordinate system corresponding to the line element (2), the static four-vector current and potential are expressed by:  $j^\mu = (j^0, 0, 0, 0)$  and  $A_\sigma = (A_0, 0, 0, 0)$ . The only nontrivial equation of (4) is  $\mu = 0$  with

$$j^0(x) = q \frac{\delta^{(3)}(\vec{r} - \vec{r}_0)}{\sqrt{-g}}, \quad (5)$$

where  $q$  is the electric charge of the particle. In the spherically symmetric spacetime defined by (2), the differential equation obeyed by  $A_0$  is:

$$\left[ \partial_r \left( \frac{w^2}{uv} \partial_r \right) - \frac{v}{u} \vec{L}^2 \right] A_0 = -\frac{4\pi q}{\sin \theta} \delta(\vec{r} - \vec{r}_0), \quad (6)$$

with  $\vec{L}$  being the operator orbital angular momentum. The solution of this equation can be written in terms of the Green function associated with the differential operator defined by the left-hand side, as follows:

$$A_0(\vec{r}) = 4\pi q G(\vec{r}, \vec{r}_0), \quad (7)$$

with the equation for the Green function

$$\left[ \partial_r \left( \frac{w^2}{uv} \partial_r \right) - \frac{v}{u} \vec{L}^2 \right] G(\vec{r}, \vec{r}_0) = -\frac{\delta(r - r_0)}{\sin \theta} \delta(\theta - \theta_0) \delta(\varphi - \varphi_0). \quad (8)$$

Having the electrostatic self-potential for the charge we can evaluate the corresponding self-force by using the standard formula

$$f_{el}^i(\vec{r}_0) = -q g^{ik} F_{km} u^m = -q \frac{g^{ik}}{u} \partial_k A_0|_{\vec{r}=\vec{r}_0} = -4\pi q^2 \frac{g^{ik}}{u} \lim_{\vec{r} \rightarrow \vec{r}_0} [\partial_k G(\vec{r}, \vec{r}_0)]. \quad (9)$$

An alternative way to obtain the self-force is to consider first the electrostatic self-energy given by [7, 8]

$$U_{el}(\vec{r}_0) = q A_0(\vec{r}_0)/2 = 2\pi q^2 \lim_{\vec{r} \rightarrow \vec{r}_0} G(\vec{r}, \vec{r}_0), \quad (10)$$

and then to derive the force on the base of the formula

$$f_{el}^i(\vec{r}_0) = -\frac{g^{ik}}{u} \partial_k U_{el}(\vec{r}_0). \quad (11)$$

In (9) and (10) the limit provides a divergent result. To obtain a finite and well defined result for the self-force, we should apply some renormalization procedure for the Green function. The procedure that we shall adopt is the standard one: we subtract from the Green function the terms in the corresponding DeWitt-Schwinger adiabatic expansion which are divergent in the coincidence limit. So, we define the renormalized Green function as

$$G_{ren}(\vec{r}, \vec{r}_0) = G(\vec{r}, \vec{r}_0) - G_{Sing}(\vec{r}, \vec{r}_0) . \quad (12)$$

In this way the renormalized self-energy,  $U_{el,ren}(\vec{r}_0)$ , and self-force,  $f_{el,ren}^i(\vec{r}_0)$ , are obtained by the formulas (9) and (10) substituting  $G(\vec{r}, \vec{r}_0)$  by  $G_{ren}(\vec{r}, \vec{r}_0)$ . Note that here the subtraction of the divergent part of the Green function corresponds to the renormalization of the particle mass.

Taking into account the spherical symmetry of the problem, we may express the Green function by the ansatz below,

$$G(\vec{r}, \vec{r}_0) = \sum_{l=0}^{\infty} \sum_{m=-l}^l g_l(r, r_0) Y_l^m(\theta, \varphi) Y_l^{m*}(\theta_0, \varphi_0) , \quad (13)$$

with  $Y_l^m(\theta, \varphi)$  being the ordinary spherical harmonics. Substituting (13) into (8) and using the well known addition theorem for the spherical harmonics, we arrive at the differential equation for the unknown radial function:

$$\left[ \frac{d}{dr} \left( \frac{w^2}{uv} \frac{d}{dr} \right) - \frac{v}{u} l(l+1) \right] g_l(r, r_0) = -\delta(r - r_0) . \quad (14)$$

As the functions  $u(r)$ ,  $v(r)$  and  $w(r)$  are continuous at  $r = a$ , from (14) it follows that the function  $g_l(r, r_0)$  and its first radial derivative are also continuous at this point. The function  $g_l(r, r_0)$  is also continuous at  $r = r_0$ . The discontinuity condition of the first radial derivative at  $r = r_0$  is obtained by the integration of (14) about this point. It reads,

$$\frac{dg_l(r, r_0)}{dr} \Big|_{r=r_0+} - \frac{dg_l(r, r_0)}{dr} \Big|_{r=r_0-} = -\frac{u(r_0)v(r_0)}{w^2(r_0)} . \quad (15)$$

Let us denote by  $R_{1l}(r)$  and  $R_{2l}(r)$  the two linearly independent solutions of the homogeneous equation corresponding to (14) in the region inside the monopole's core. We shall assume that the function  $R_{1l}(r)$  is regular at the core center  $r = r_c$  and that the solutions are normalized by the Wronskian relation

$$R_{1l}(r)R'_{2l}(r) - R'_{1l}(r)R_{2l}(r) = -\frac{u(r)v(r)}{w^2(r)} . \quad (16)$$

In the region outside the core the linearly independent solutions to the corresponding homogeneous equation are the functions  $r^{\lambda_1}$  and  $r^{\lambda_2}$ , where

$$\lambda_{1,2} = -\frac{1}{2} \pm \frac{1}{2\alpha} \sqrt{\alpha^2 + 4l(l+1)} . \quad (17)$$

Now, we can write  $g_l(r, r_0)$  as a function of the radial coordinate  $r$  in the separate regions  $[r_c, \min(r_0, a))$ ,  $(\min(r_0, a), \max(r_0, a))$ , and  $(\max(r_0, a), \infty)$  as a linear combination of the above mentioned solutions with arbitrary coefficients. The requirement of the regularity at the core center and at the infinity reduces the number of these coefficients to four. They are determined by the continuity condition at the monopole's core boundary and by the matching conditions at  $r = r_0$ . In this way we find the following expressions

$$g_l(r, r_0) = \frac{(ar_0)^{\lambda_1} R_{1l}(r)}{\alpha^2 [aR'_{1l}(a) - \lambda_2 R_{1l}(a)]}, \text{ for } r \leq a, \quad (18)$$

$$g_l(r, r_0) = \frac{r_-^{\lambda_1} r_+^{\lambda_2}}{\alpha^2 (\lambda_1 - \lambda_2)} \left[ 1 - \left( \frac{a}{r_-} \right)^{\lambda_1 - \lambda_2} D_{1l}(a) \right], \text{ for } r \geq a, \quad (19)$$

in the case  $r_0 > a$ , and

$$g_l(r, r_0) = R_{1l}(r_-) R_{2l}(r_+) - R_{1l}(r_0) R_{1l}(r) D_{2l}(a), \text{ for } r \leq a, \quad (20)$$

$$g_l(r, r_0) = \frac{a^{\lambda_1} r^{\lambda_2} R_{1l}(r_0)}{\alpha^2 [aR'_{1l}(a) - \lambda_2 R_{1l}(a)]}, \text{ for } r \geq a, \quad (21)$$

in the case  $r_0 < a$ . In these formulas,  $r_- = \min(r, r_0)$  and  $r_+ = \max(r, r_0)$ , and we have used the notation

$$D_{jl}(a) = \frac{aR'_{jl}(a) - \lambda_j R_{jl}(a)}{aR'_{1l}(a) - \lambda_2 R_{1l}(a)}, \quad j = 1, 2. \quad (22)$$

First let us consider the case when the charge is outside the monopole's core ( $r_0 > a$ ). Substituting the function (19) into (13), we observe that the Green function is presented in the form of the sum of two terms

$$G(\vec{r}, \vec{r}_0) = G_m(\vec{r}, \vec{r}_0) + G_c(\vec{r}, \vec{r}_0), \quad (23)$$

where

$$G_m(\vec{r}, \vec{r}_0) = \frac{1}{4\pi\alpha r_+} \sum_{l=0}^{\infty} \frac{2l+1}{\sqrt{\alpha^2 + 4l(l+1)}} \frac{r_-^{\lambda_1}}{r_+^{\lambda_1}} P_l(\cos \gamma), \quad (24)$$

is the Green function associated with the geometry of a point-like global monopole, and the term

$$G_c(\vec{r}, \vec{r}_0) = -\frac{1}{4\pi\alpha} \sum_{l=0}^{\infty} \frac{(2l+1)D_{1l}(a)}{\sqrt{\alpha^2 + 4l(l+1)}} (rr_0)^{\lambda_2} P_l(\cos \gamma), \quad (25)$$

is induced by non-trivial structure of the core. In formulas (24) and (25), the  $\gamma$  is the angle between the directions  $(\theta, \varphi)$  and  $(\theta_0, \varphi_0)$ , and  $P_l(x)$  represents the Legendre polynomials. As we can see, the contribution (25) depends on the structure of the core through the radial function  $R_{1l}(r)$ .

As we have already mentioned, the induced self-energy is obtained from the renormalized Green function taking the coincidence limit. We can observe that for points with  $r > a$ , the core-induced term (25) is finite in the coincidence limit and the divergence appears in the point-like monopole part only. So, in order to provide a finite and well defined value to (10), we have to renormalize Green function  $G_m(\vec{r}, \vec{r}_0)$  only:

$$G_{ren}(r_0, r_0) = G_{m,ren}(r_0, r_0) + G_c(r_0, r_0) . \quad (26)$$

As explained before, to obtain  $G_{m,ren}(r_0, r_0)$ , we subtract from (24) the terms in the corresponding DeWitt-Schwinger adiabatic expansion which are divergent in the coincidence limit:

$$G_{m,ren}(r_0, r_0) = \lim_{\vec{r} \rightarrow \vec{r}_0} [G_m(\vec{r}, \vec{r}_0) - G_{Sing}(\vec{r}, \vec{r}_0)] . \quad (27)$$

The part  $G_{Sing}(\vec{r}, \vec{r}_0)$  is found from the general formula given, for instance, in [19]. For simplicity, taking the separation of the points along the radial direction only ( $\gamma = 0$ ), we find

$$G_{Sing}(r, r_0) = \frac{1}{4\pi|r - r_0|} . \quad (28)$$

Now, by using formulas (24) and (28), one obtains

$$G_{m,ren}(r_0, r_0) = \frac{1}{4\pi r_0} \lim_{t \rightarrow 1} \left[ \frac{1}{\alpha} \sum_{l=0}^{\infty} \frac{2l+1}{\sqrt{\alpha^2 + 4l(l+1)}} t^{\lambda_1} - \frac{1}{1-t} \right] , \quad (29)$$

where  $t = r_</r_>$ . To evaluate the limit on the right, we note that

$$\lim_{t \rightarrow 1} \left( \frac{1}{\alpha} \sum_{l=0}^{\infty} t^{l/\alpha+1/2\alpha-1/2} - \frac{1}{1-t} \right) = 0 . \quad (30)$$

On the basis of this relation, replacing  $1/(1-t)$  in (29) by the first term in the brackets in (30), we find

$$G_{m,ren}(r_0, r_0) = \frac{S(\alpha)}{4\pi r_0} , \quad (31)$$

where we have introduced the notation

$$S(\alpha) = \frac{1}{\alpha} \sum_{l=0}^{\infty} \left[ \frac{2l+1}{\sqrt{\alpha^2 + 4l(l+1)}} - 1 \right] . \quad (32)$$

The function  $S(\alpha)$  is positive (negative) for  $\alpha < 1$  ( $\alpha > 1$ ) and, hence, the corresponding self-force is repulsive (attractive).

Combining formulas (10), (25) and (31), for the renormalized electrostatic self-energy we obtain

$$U_{el,ren}(r_0) = \frac{q^2 S(\alpha)}{2r_0} - \frac{q^2}{2\alpha r_0} \sum_{l=0}^{\infty} \frac{(2l+1)D_{1l}(a)}{\sqrt{\alpha^2 + 4l(l+1)}} \left( \frac{a}{r_0} \right)^{\sqrt{1+4l(l+1)/\alpha^2}} . \quad (33)$$

As we can see, the second term of the renormalized self-energy provides a convergent series for  $r_0 > a$ . Moreover, the dependence of the self-energy on the core structure is present in the function  $D_{1l}(a)$ . For large distances from the core,  $r_0 \gg a$ , the main contribution into the core-induced part comes from the term  $l = 0$  and one has

$$U_{el,ren}(r_0) \approx \frac{q^2}{2r_0} \left[ S(\alpha) - \frac{aD_{10}(a)}{\alpha^2 r_0} \right]. \quad (34)$$

The self-force is obtained from (33) by using formula (11):

$$\vec{f}_{el,ren}(\vec{r}_0) = U_{el,ren}(r_0) \frac{\vec{r}_0}{r_0^2} - \frac{q^2 \vec{r}_0}{2\alpha^2 r_0^3} \sum_{l=0}^{\infty} (2l+1) D_{1l}(a) \left( \frac{a}{r_0} \right)^{\sqrt{1+4l(l+1)/\alpha^2}}. \quad (35)$$

According to the symmetry of the problem, the self-force has only a radial component.

Now let us study the case when the charge is inside the core,  $r_0 < a$ . The corresponding Green function is obtained from (20) and is written in the form

$$G(\vec{r}, \vec{r}_0) = G_0(\vec{r}, \vec{r}_0) + G_\alpha(\vec{r}, \vec{r}_0), \quad (36)$$

where

$$G_0(\vec{r}, \vec{r}_0) = \frac{1}{4\pi} \sum_{l=0}^{\infty} (2l+1) R_{1l}(r_<) R_{2l}(r_>) P_l(\cos \gamma), \quad (37)$$

is the Green function for the background geometry described by the line element (2) for all values  $r_c \leq r < \infty$ , and the term

$$G_\alpha(\vec{r}, \vec{r}_0) = -\frac{1}{4\pi} \sum_{l=0}^{\infty} (2l+1) R_{1l}(r_0) R_{1l}(r) D_{2l}(a) P_l(\cos \gamma), \quad (38)$$

is due to the global monopole geometry in the region  $r > a$ . For the points away from the core boundary the latter is finite in the coincidence limit. The self-energy for the charge inside the core is written in the form

$$U_{el,ren}(r_0) = 2\pi q^2 G_{0,ren}(r_0, r_0) - \frac{q^2}{2} \sum_{l=0}^{\infty} (2l+1) D_{2l}(a) R_{1l}^2(r_0), \quad (39)$$

where

$$G_{0,ren}(r_0, r_0) = \lim_{\vec{r} \rightarrow \vec{r}_0} [G_0(\vec{r}, \vec{r}_0) - G_{Sing}(\vec{r}, \vec{r}_0)]. \quad (40)$$

The only contribution in the divergent part of the Green function comes from the first term of the DeWitt-Schwinger expansion. Note that near the center of the core one has  $R_{1l}(r_0) \propto (r_0 - r_c)^l$  and the main contribution into the second term on the right of (39) comes from the term with  $l = 0$ . Substituting the self-energy given by (39) into formula (11), we obtain the self-force for the charge inside the monopole core.

## 2.1.2. Scalar self-interaction

The action associated with a charged massive scalar field,  $\phi$ , coupled with a charge density,  $\rho$ , in a curved background spacetime reads

$$S = -\frac{1}{2} \int d^4x \sqrt{-g} (g^{\mu\nu} \nabla_\mu \phi \nabla_\nu \phi + \xi R \phi^2 + m^2 \phi^2) + \int d^4x \sqrt{-g} \rho \phi , \quad (41)$$

where the first part contains the Klein-Gordon action admitting an arbitrary curvature coupling,  $\xi$ , and the second part contains the interaction term. In the above equation  $R$  represents the scalar curvature. The field equation can be obtained by varying the action with respect to the field. This provides

$$(\square - \xi R - m^2) \phi = -\rho . \quad (42)$$

The physical system that we shall analyze corresponds to a particle at rest; so, there is no time dependence on the field. Moreover, because the metric tensor under consideration is also time-independent, the equation of motion above reduces effectively to a three-dimensional one:

$$(\nabla^2 - \xi R - m^2) \phi = -\rho . \quad (43)$$

The energy-momentum tensor associated with this system is obtained by taking the variation of (41) with respect to the metric tensor. It reads

$$\begin{aligned} T_{\mu\nu} &= \rho \phi g_{\mu\nu} + \nabla_\mu \phi \nabla_\nu \phi - \frac{1}{2} g_{\mu\nu} \left( g^{\lambda\chi} \nabla_\lambda \phi \nabla_\chi \phi + m^2 \phi^2 \right) \\ &+ \xi (G_{\mu\nu} \phi^2 + g_{\mu\nu} \square \phi^2 - \nabla_\mu \nabla_\nu \phi^2) , \end{aligned} \quad (44)$$

$G_{\mu\nu}$  being the Einstein tensor.

The energy for the scalar particle is obtained as shown below,

$$E = - \int d^3x \sqrt{-g} T_0^0 . \quad (45)$$

For static fields configurations and by using the motion equation (43), we have:

$$E = -\frac{1}{2} \int d^3x \sqrt{-g} \rho \phi . \quad (46)$$

By using the three-dimensional Green function defined by the differential operator in (43),

$$(\nabla^2 - \xi R - m^2) G(\vec{x}, \vec{x}') = -\frac{\delta^3(\vec{x} - \vec{x}')}{\sqrt{-g}} , \quad (47)$$

the energy given by (46) can be written as

$$E = -\frac{1}{2} \int \int d^3x \sqrt{-g(x)} d^3x' \sqrt{-g(x')} \rho(\vec{x}) G(\vec{x}, \vec{x}') \rho(\vec{x}') . \quad (48)$$

Considering now a point-like scalar charge at rest at the point  $\vec{r}_0$ , the charge density takes the form,

$$\rho(\vec{r}) = \frac{q}{\sqrt{-g}} \delta^3(\vec{r} - \vec{r}_0) . \quad (49)$$

Finally substituting (49) into (48), we obtain for the energy the following expression:

$$E = -\frac{q^2}{2} G(\vec{r}_0, \vec{r}_0) . \quad (50)$$

Here also, the evaluation of the Green function that we need for the calculation of the energy is divergent at the coincidence limit. In order to obtain a finite and well defined result for the energy we subtract from the Green function the corresponding DeWitt-Schwinger asymptotic expansion. Following the general procedure given in [19], the singular behavior of the three-dimensional Green function associated with a massive scalar field reads:

$$G_{Sing}(x, x') = \frac{1}{4\pi} \left[ \frac{1}{\sqrt{2\sigma}} - m \right] + O(\sigma) . \quad (51)$$

Adopting the above mentioned renormalization approach, the scalar self-energy is given by

$$\begin{aligned} E_{Ren} &= -\frac{q^2}{2} G_{Ren}(\vec{r}_0, \vec{r}_0) , \\ &= -\frac{q^2}{2} \lim_{\vec{r} \rightarrow \vec{r}_0} [G(\vec{r}, \vec{r}_0) - G_{Sing}(\vec{r}, \vec{r}_0)] . \end{aligned} \quad (52)$$

Once more, taking into account the spherical symmetry of the problem, the scalar Green function can be expressed by the ansatz below,

$$G(\vec{r}, \vec{r}_0) = \sum_{l=0}^{\infty} \sum_{m=-l}^l g_l(r, r_0) Y_l^m(\theta, \varphi) Y_l^{m*}(\theta_0, \varphi_0) . \quad (53)$$

Substituting (53) into (47), we arrive at the following differential equation for the unknown radial function  $g_l(r, r')$ :

$$\left[ \frac{d}{dr} \left( \frac{w^2}{v} \frac{d}{dr} \right) - l(l+1)v - \xi Rvw^2 - m^2 vw^2 \right] g_l = -\delta(r - r_0) , \quad (54)$$

with the Ricci scalar being given by

$$R = \frac{2}{w^2} + \frac{4v'w'}{wv^3} - \frac{4w''}{wv^2} - \frac{2(w')^2}{w^2 v^2} . \quad (55)$$

For  $\xi = 0$  and  $m = 0$  the differential equation above is similar to the previous one found in the analysis of electrostatic self-energy, Eq. (14). Moreover; as to the solution of (54) the junctions conditions are obtained as explain below:

- Because the function  $v(r)$  and  $w(r)$  are continuous at  $r = a$ , it follows that  $g_l(r, r')$  should be continuous at this point; however, due to the second radial derivative of the function  $w(r)$  in the Ricci scalar, a Dirac-delta function contribution on the Ricci scalar takes place if the first derivative of this function is not continuous at the boundary.<sup>1</sup> Naming by  $\check{R} = \bar{R}\delta(r - a)$  the Dirac-delta contribution of the Ricci scalar, the junction condition on the boundary is:

$$\frac{dg_l(r)}{dr}|_{r=a^+} - \frac{dg_l(r)}{dr}|_{r=a^-} = \xi \bar{R} g_l(a) . \quad (56)$$

- The function  $g_l(r)$  is continuous at  $r = r_0$ , however by integrating (54) about this point, the first radial derivative of this function obeys the junction condition below:

$$\frac{dg_l(r)}{dr}|_{r=r_0^+} - \frac{dg_l(r)}{dr}|_{r=r_0^-} = -\frac{v(r_0)}{w^2(r_0)} . \quad (57)$$

Now after this general discussion, let us analyze the solutions of the homogeneous differential equation associated with (54) for regions inside and outside the monopole's core. Let us denote by  $R_{1l}(r)$  and  $R_{2l}(r)$  the two linearly independent solutions of the equation in the region inside with  $R_{1l}(r)$  been the regular one at the core center  $r = r_c$ ; moreover, we shall assume that solutions are normalized by the Wronskian relation (16).

In the region outside, the two linearly independent solution are:

$$\frac{1}{\sqrt{r}} I_{\nu_l}(mr) \text{ and } \frac{1}{\sqrt{r}} K_{\nu_l}(mr) , \quad (58)$$

where  $I_\nu$  and  $K_\nu$  are the modified Bessel functions of order

$$\nu_l = \frac{1}{2\alpha} \sqrt{(2l+1)^2 + (1-\alpha^2)(8\xi-1)} . \quad (59)$$

Now we can write the function  $g_l(r)$  as a linear combination of the above solutions with arbitrary coefficients for the regions  $(r_c, \min(r_0, a))$ ,  $(\min(r_0, a), \max(r_0, a))$ , and  $(\max(r_0, a), \infty)$ . The requirement of the regularity at the core center and at the infinity reduces the number of these coefficients to four. These constants are determined by the continuity condition at the monopole's core boundary and at the point  $r = r_0$  by the junctions conditions given in (56) and (57), respectively. In this way we find the following expressions:

$$g_l(r, r_0) = \frac{K_{\nu_l}(mr_0)R_{1l}(r)}{\alpha^2 \sqrt{ar_0}} \frac{1}{a\mathcal{R}_l^{(1)}(a)K_{\nu_l}(ma) - R_{1l}(a)\tilde{K}_{\nu_l}(ma)}, \quad r \leq a , \quad (60)$$

$$g_l(r, r_0) = \frac{I_{\nu_l}(mr_-)K_{\nu_l}(mr_+)}{\alpha^2 \sqrt{rr_0}} - D_l^{(+)}(a) \frac{K_{\nu_l}(mr)K_{\nu_l}(mr_0)}{\alpha^2 \sqrt{rr_0}}, \quad r \geq a , \quad (61)$$

---

<sup>1</sup>For the flower-pot model this fact occur and has been considered in [13].

in the case of the charged particle is outside the monopole,  $r_0 > a$ , and

$$g_l(r, r_0) = R_{1l}(r_<) [R_{2l}(r_>) - D_l^{(-)}(a) R_{1l}(r_>)], \quad r \leq a, \quad (62)$$

$$g_l(r, r_0) = \frac{R_{1l}(r_0) K_{\nu_l}(mr)}{\alpha^2 \sqrt{ar}} \frac{1}{a \mathcal{R}_l^{(1)}(a) K_{\nu_l}(ma) - R_{1l}(a) \tilde{K}_{\nu_l}(ma)}, \quad r \geq a, \quad (63)$$

in the case of the charged particle is inside the monopole,  $r_0 < a$ . In these formulas,  $r_< = \min(r, r')$  and  $r_> = \max(r, r')$ , and we have used the notations:

$$D_l^{(+)}(a) = \frac{a \mathcal{R}_l^{(1)}(a) I_{\nu_l}(ma) - R_{1l}(a) \tilde{I}_{\nu_l}(ma)}{a \mathcal{R}_l^{(1)}(a) K_{\nu_l}(ma) - R_{1l}(a) \tilde{K}_{\nu_l}(ma)}, \quad (64)$$

$$D_l^{(-)}(a) = \frac{a \mathcal{R}_l^{(2)}(a) K_{\nu_l}(ma) - R_{2l}(a) \tilde{K}_{\nu_l}(ma)}{a \mathcal{R}_l^{(1)}(a) K_{\nu_l}(ma) - R_{1l}(a) \tilde{K}_{\nu_l}(ma)}. \quad (65)$$

For a given function  $F(z)$ , we use the notation

$$\tilde{F}(z) = z F'(z) - \frac{1}{2} F(z) \quad (66)$$

and for a solution  $R_{jl}(r)$ , with  $j = 1, 2$ ,

$$\mathcal{R}_l^{(j)}(a) = R'_{jl}(a) + \xi \bar{R} R_{jl}(a). \quad (67)$$

In the above definition  $R'_{jl}(a) = \frac{dR_{jl}(r)}{dr}|_{r=a}$ .

Before to go for a specific model, let us still continue the investigation of the self-energy for this general spherically symmetric spacetime. First we shall consider the case where the charge is outside the monopole's core. Substituting (61) into (53) we see that the Green function is expressed in terms of two contributions:

$$G(\vec{r}, \vec{r}_0) = G_{gm}(\vec{r}, \vec{r}_0) + G_c(\vec{r}, \vec{r}_0), \quad (68)$$

where

$$G_{gm}(\vec{r}, \vec{r}_0) = \frac{1}{4\pi\alpha^2 \sqrt{rr_0}} \sum_{l=0}^{\infty} (2l+1) I_{\nu_l}(mr_<) K_{\nu_l}(mr_>) P_l(\cos \gamma) \quad (69)$$

and

$$G_c(\vec{r}, \vec{r}_0) = -\frac{1}{4\pi\alpha^2 \sqrt{rr_0}} \sum_{l=0}^{\infty} (2l+1) D_l^{(+)}(a) K_{\nu_l}(mr_0) K_{\nu_l}(mr) P_l(\cos \gamma). \quad (70)$$

The first part corresponds to the Green function for the geometry of a point-like global monopole and the second is induced by the non-trivial structure of its core. In the formulas above,  $\gamma$  is the angle between both directions  $(\theta, \varphi)$  and  $(\theta_0, \varphi_0)$  and  $P_l(x)$  represents the Legendre polynomials of degree  $l$ .

The induced scalar self-energy is obtained by taking the coincidence limit in the renormalized Green function. We can observe that for points with  $r > a$ , the core-induced term (70) is finite and the divergence appears in the point-like monopole part only. So, in order to provide a finite and well defined result for (52), we have to renormalize the Green function  $G_{gm}(\vec{r}, \vec{r}_0)$  only. Let us first take  $\gamma = 0$  in the above expressions. The renormalized Green function is expressed by:

$$G_{Ren}(r_0, r_0) = G_{gm,ren}(r_0, r_0) + G_c(r_0, r_0) , \quad (71)$$

where

$$G_{gm,ren}(r_0, r_0) = \lim_{r \rightarrow r_0} [G_{gm}(r, r_0) - G_{Sing}(r, r_0)] . \quad (72)$$

For points outside the core, the radial one-half of geodesic distance becomes  $|r - r_0|/2$ , we have

$$G_{Sing}(r, r_0) = \frac{1}{4\pi} \left[ \frac{1}{|r - r_0|} - m \right] . \quad (73)$$

Now, by using  $G_m(r_0, r)$  given in (69), we have:

$$G_{gm,ren}(r_0, r) = \frac{1}{4\pi r_0} \lim_{r \rightarrow r_0} \left[ \frac{1}{\alpha^2} \sum_{l=0}^{\infty} (2l+1) I_{\nu_l}(mr_<) K_{\nu_l}(mr_>) - \frac{1}{1-t} \right] + \frac{m}{4\pi} , \quad (74)$$

where  $t = r_</r_>$ . In order to evaluate the limit on the right hand side of the above equation, we take the identity (30). So, as consequence of this relation and replacing in (74) the expression  $1/(1-t)$  by the first term in the brackets of that identity, we find

$$G_{gm,ren}(r', r') = \frac{S_{(\alpha)}(mr')}{4\pi\alpha r} + \frac{m}{4\pi} , \quad (75)$$

with

$$S_{(\alpha)}(mr') = \sum_{l=0}^{\infty} \left[ \frac{(2l+1)}{\alpha} I_{\nu_l}(mr') K_{\nu_l}(mr') - 1 \right] . \quad (76)$$

Two special situations deserve to be analyzed:

- For the case where  $\xi = 0$ , we have  $\nu_l = \frac{1}{2\alpha} \sqrt{4l(l+1) + \alpha^2}$ . Taking the limit  $m \rightarrow 0$  in (76), using [20, 21] we get a position independent expression named  $S_\alpha$ :

$$S_\alpha = \sum_{l=0}^{\infty} \left[ \frac{2l+1}{\sqrt{4l(l+1) + \alpha^2}} - 1 \right] . \quad (77)$$

Up to a factor  $1/\alpha$  this expression coincides with the similar one obtained in the previous analysis of the electrostatic self-energy, Eq (32).

- For  $\xi = 1/8$  we have  $\nu_l = \frac{1}{2\alpha}(2l+1)$ . Taking the limit  $m \rightarrow 0$  in (76) we see that the term inside the bracket vanishes, consequently  $G_{gm,ren}(r', r') = 0$  and the only contribution to the scalar self-energy comes from the core-induced part (70). In fact under these circumstance, the differential equation obeyed

by the Green function in the region outside the monopole is conformally related with the corresponding one in a flat space due to the conformal flatness of the space section of this metric tensor:

$$d\vec{t}^2 = dr^2 + \alpha^2 r^2 d\Omega_{(2)} = \rho^\lambda (d\rho^2 + \rho^2 d\Omega_{(2)}) , \quad (78)$$

with  $\rho = (\alpha r)^{1/\alpha}$  being  $\lambda = 2(\alpha - 1)$ . Moreover, by explicit calculation we can show that  $G_{gm}(\vec{r}, \vec{r}') = \rho^{-\lambda/4} G_M(\vec{\rho}, \vec{\rho}') \rho'^{-\lambda/4}$ .

Finally the complete expression for scalar self-energy reads

$$E_{Ren} = -\frac{q^2}{8\pi\alpha r_p} S_{(\alpha)}(mr_p) - \frac{q^2 m}{8\pi} + \frac{q^2}{8\pi\alpha^2 r_p} \sum_{l=0}^{\infty} (2l+1) D_l^{(+)}(a) (K_{\nu_l}(mr_p))^2 . \quad (79)$$

The self-force on a static test particle can be calculated by taking the negative gradient of the corresponding self-energy [15],

$$\vec{f} = \vec{\nabla} E_{Ren} . \quad (80)$$

Considering  $\vec{f} = f_r \hat{r}$ , the radial component of this force reads:

$$\begin{aligned} f_r &= \frac{q^2}{8\pi\alpha r_p^2} S_{(\alpha)}(mr_p) - \frac{q^2 m}{8\pi\alpha^2 r_p} \sum_{l=0}^{\infty} (2l+1) \left[ \left( I_{\nu_l+1}(mr_p) + \frac{\nu_l I_{\nu_l+1}(mr_p)}{mr_p} \right) \right. \\ &\quad \times K_{\nu_l}(mr_p) - I_{\nu_l}(mr_p) \left( K_{\nu_l+1}(mr_p) - \frac{\nu_l K_{\nu_l}(mr_p)}{mr_p} \right) \Big] \\ &\quad - \frac{q^2}{8\pi\alpha^2 r_p^2} \sum_{l=0}^{\infty} (2l+1) D_l^{(+)}(a) K_{\nu_l}^2(mr_p) - \frac{q^2 m}{4\pi\alpha^2 r_p} \sum_{l=0}^{\infty} (2l+1) D_l^{(+)}(a) \\ &\quad \times K_{\nu_l}(mr_p) \left( K_{\nu_l+1}(mr_p) - \frac{\nu_l K_{\nu_l}(mr_p)}{mr_p} \right) . \end{aligned} \quad (81)$$

The second analysis that can be formally developed here, is related with the case when the charge is inside the core. The corresponding Green function can be written in the form

$$G(\vec{r}, \vec{r}_0) = G_0(\vec{r}, \vec{r}_0) + G_\alpha(\vec{r}, \vec{r}_0) , \quad (82)$$

where

$$G_0(\vec{r}, \vec{r}_0) = \frac{1}{4\pi} \sum_{l=0}^{\infty} (2l+1) R_{1l}(r_<) R_{2l}(r_>) P_l(\cos \gamma) , \quad (83)$$

is the Green function for the background geometry described by the line element (2) and the term

$$G_\alpha(\vec{r}, \vec{r}_0) = -\frac{1}{4\pi} \sum_{l=0}^{\infty} (2l+1) D_l^{(-)}(a) R_{1l}(r) R_{1l}(r_0) P_l(\cos \gamma) , \quad (84)$$

is due to the global monopole geometry in the region  $r > a$ . For the points away from the core boundary the latter is finite in the coincidence limit. The renormalized scalar self-energy for the charge inside is written in the form

$$E_{Ren} = -\frac{q^2}{2} G_{0,Ren}(\vec{r}_0, \vec{r}_0) + \frac{q^2}{8\pi} \sum_{l=0}^{\infty} (2l+1) D_l^{(-)}(a) (R_{1l}(r_0))^2, \quad (85)$$

where the renormalized Green function is given by

$$G_{0,Ren}(\vec{r}_0, \vec{r}_0) = \lim_{\vec{r} \rightarrow \vec{r}_p} [G_0(\vec{r}, \vec{r}_0) - G_{Sing}(\vec{r}, \vec{r}_0)] . \quad (86)$$

Because the divergent part of the Green function should have the same structure as (51), the above expression provides a finite result; moreover, notice that near the center of the core one has  $R_{1l}(r) \approx \frac{I_{l+1/2}(m(r-r_c))}{\sqrt{r-r_c}}$  and the main contribution into the second term on the right of (85) comes from the term with  $l = 0$ . Finally we can say that the self-force is again obtained by taking the negative gradient of (85).

### 3. Flower-pot model

As we have mentioned before, there is no closed expression for the metric tensor in the region inside the global monopole. However, adopting the flower-pot model for this region, the calculations of vacuum polarization effects associated with massive scalar and fermionic fields have been developed in [22, 23], respectively. So, motived by these result we decided, as an illustration of the general procedure described before, to consider the flower-pot model in the present analysis of the induced electrostatic and scalar self-interactions. For this model the interior line element has the form [13]

$$ds^2 = -dt^2 + dr^2 + [r + (\alpha - 1)a]^2 (d^2\theta + \sin^2\theta d^2\varphi) . \quad (87)$$

In terms of the radial coordinate  $r$  the origin is located at  $r = r_c = (1 - \alpha)a$ . Defining  $\tilde{r} = r + (\alpha - 1)a$ , the line element takes the standard Minkowskian form. As we have mentioned before, from the Israel matching conditions for the metric tensors corresponding to (1) and (87), we find the singular contribution for the scalar curvature located on the bounding surface  $r = a$  [22]:

$$\bar{R} = 4 \frac{(1 - \alpha)}{\alpha a} . \quad (88)$$

In what follows, we shall consider, separately, the analysis of electrostatic and scalar self-interactions.

#### 3.1. Electrostatic self-interaction

Now we can express the renormalized Green function in the region outside the monopole core by taking into account that in the interior region we have two linearly

independent solutions of the homogeneous equation corresponding to (14):

$$R_{1l}(r) = \tilde{r}^l, \text{ and } R_{2l}(r) = \tilde{r}^{-l-1}/(2l+1). \quad (89)$$

So, from formula (33), the self-energy in the exterior region reads

$$\begin{aligned} U_{el,ren}(r_0) &= \frac{q^2 S(\alpha)}{2r_0} + \frac{2q^2(1-\alpha)}{\alpha r_0} \sum_{l=0}^{\infty} \frac{l(2l+1)}{\sqrt{\alpha^2 + 4l(l+1)}} \\ &\times \frac{(a/r_0)\sqrt{1+4l(l+1)/\alpha^2}}{\left[\sqrt{\alpha^2 + 4l(l+1)} + \alpha + 2l\right]^2}. \end{aligned} \quad (90)$$

The second term on the right of this formula is positive for  $\alpha < 1$  and negative for  $\alpha > 1$ . Combining this with the properties of the function  $S(\alpha)$  discussed in the previous section, we conclude that the electrostatic self-energy is positive for  $\alpha < 1$  and negative for  $\alpha > 1$ . The corresponding self-force is directly found from (35) and is repulsive in the first case and attractive in the second one. The core-induced part in (90) diverges at the core boundary,  $r_0 = a$ . Noting that for points near the boundary the main contribution into (90) comes from large values  $l$ , to the leading order we find

$$U_{el,ren}(r_0) \approx q^2 \frac{(\alpha-1)}{8\alpha a} \ln \left[ 1 - (a/r_0)^{1/\alpha} \right], \quad (91)$$

and the self-energy is dominated by the core-induced part.

Now we turn to the investigation of the self-energy for the particle inside the monopole core. Substituting the functions (89) into formulas (37) and (38), for the corresponding Green functions in the interior region one finds

$$G_0(\mathbf{r}, \mathbf{r}_0) = \frac{1}{4\pi|\mathbf{r} - \mathbf{r}_0|}, \quad (92)$$

$$G_\alpha(\mathbf{r}, \mathbf{r}_0) = \frac{1}{4\pi\alpha a} \sum_{l=0}^{\infty} \frac{2l+2-\alpha-\sqrt{\alpha^2+4l(l+1)}}{2l+\alpha+\sqrt{\alpha^2+4l(l+1)}} \frac{(\tilde{r}_0\tilde{r})^l}{(\alpha a)^{2l}} P_l(\cos\gamma), \quad (93)$$

Because in the flower-pot model the geometry in the region inside the monopole is a Minkowski one, we have  $G_{sing}(\vec{r}, \vec{r}_0) = G_0(\vec{r}, \vec{r}_0)$  and, hence,  $G_{0,ren}(r_0, r_0) = 0$ . Finally, the electrostatic self-energy in the region inside the monopole core reads:

$$U_{el,ren}(r_0) = 2\pi q^2 G_{ren}(r_0, r_0) = \frac{q^2}{2\alpha a} \sum_{l=0}^{\infty} \frac{2l+2-\alpha-\sqrt{\alpha^2+4l(l+1)}}{2l+\alpha+\sqrt{\alpha^2+4l(l+1)}} \left( \frac{\tilde{r}_0}{\alpha a} \right)^{2l}. \quad (94)$$

As in the case of the exterior region, this self-energy is positive for  $\alpha < 1$  and negative for  $\alpha > 1$ . The corresponding self-force is easily found from relation (11) and is repulsive with respect to the boundary of the monopole core in the first case and attractive in the second case. Near the core center the main contribution into the self-energy comes from the lowest modes and one has

$$U_{el,ren}(r_0) \approx \frac{q^2}{2\alpha a} \left[ \frac{1-\alpha}{\alpha} + \frac{4-\alpha-\sqrt{\alpha^2+8}}{2+\alpha+\sqrt{\alpha^2+8}} \left( \frac{\tilde{r}_0}{\alpha a} \right)^2 \right]. \quad (95)$$

### 3.2. Scalar self-interaction

In the region inside the global monopole the two linearly independent solutions for the homogeneous radial equation corresponding to (54) are:

$$R_{1l}(r) = \frac{I_{l+1/2}(m\tilde{r})}{\sqrt{\tilde{r}}} \text{ and } R_{2l}(r) = \frac{K_{l+1/2}(m\tilde{r})}{\sqrt{\tilde{r}}}. \quad (96)$$

Having obtained the above solutions, the expressions for the Green functions in both, inside and outside regions, can be explicitly constructed, consequently the corresponding self-energies. These expressions depend on the coefficients  $D_l^{(+)}(a)$  and  $D_l^{(-)}(a)$ , which can be explicitly provided as shown below:

$$D_l^{(+)}(a) = \frac{n_l^{(+)}(a)}{d_l(a)} \text{ and } D_l^{(-)}(a) = \frac{n_l^{(-)}(a)}{d_l(a)}, \quad (97)$$

with

$$\begin{aligned} n_l^{(+)}(a) &= I_{\nu_l}(ma)I_{l+1/2}(m\alpha a) \left[ \frac{(l + 4\xi(1 - \alpha))}{\alpha} - \nu_l + \frac{1}{2} \right] \\ &+ ma [I_{\nu_l}(ma)I_{l+3/2}(m\alpha a) - I_{l+1/2}(m\alpha a)I_{\nu_l+1}(ma)] , \end{aligned} \quad (98)$$

$$\begin{aligned} n_l^{(-)}(a) &= K_{\nu_l}(ma)K_{l+1/2}(m\alpha a) \left[ \frac{(l + 4\xi(1 - \alpha))}{\alpha} - \nu_l + \frac{1}{2} \right] \\ &- ma [K_{\nu_l}(ma)K_{l+3/2}(m\alpha a) - K_{l+1/2}(m\alpha a)K_{\nu_l+1}(ma)] \end{aligned} \quad (99)$$

and

$$\begin{aligned} d_l(a) &= K_{\nu_l}(ma)I_{l+1/2}(m\alpha a) \left[ \frac{(l + 4\xi(1 - \alpha))}{\alpha} - \nu_l + \frac{1}{2} \right] \\ &+ ma [K_{\nu_l}(ma)I_{l+3/2}(m\alpha a) + I_{l+1/2}(m\alpha a)K_{\nu_l+1}(ma)] . \end{aligned} \quad (100)$$

As in the first analyze, let us consider the core-induced part of the self-energy for the region outside, Eq. (79), adopting specific values for the parameter  $\xi$  and mass of the particle. Taking  $\xi = 0$ , and by using [21] to obtain the behavior of all functions contained in the coefficient defined in (97), (98) and (100), in the limit  $m \rightarrow 0$ , we have:

$$D_l^{(+)}(a) \approx \frac{2}{\nu_l} \left( \frac{ma}{2} \right)^{2\nu_l} \frac{(\alpha + 2l - 2\alpha\nu_l)}{(2\alpha\nu_l + \alpha + 2l)(\Gamma(\nu_l))^2} . \quad (101)$$

So the general term inside the summation of the core-induced part reads,

$$\frac{\alpha(2l + 1)}{\sqrt{4l^2 + 4l + \alpha^2}} \frac{4l(\alpha - 1)}{(\sqrt{4l^2 + 4l + \alpha^2} + 2l + \alpha)^2} \left( \frac{a}{r} \right)^{\sqrt{1+4l(l+1)/\alpha^2}} . \quad (102)$$

Which coincides with the result obtained for the electrostatic case.

We can see that the core-induced part in (79) is divergent near the boundary  $r = a$ . In order to verify this fact, we should analyze the general term in the summation for large value of  $l$ . Taking again the uniform asymptotic expansion for large orders of the modified Bessel functions in  $D^{(+)}(a)$  and the same for the Macdonald function,  $K_{\nu_l}(mr)$ , we get,

$$-\frac{[\alpha - 2\alpha\nu_l + 2l + 8\xi(1 - \alpha)]}{[\alpha + 2\alpha\nu_l + 2l + 8\xi(1 - \alpha)]} \left(\frac{a}{r}\right)^{2\nu_l}. \quad (103)$$

At this point we want to mention that the contribution proportional to the curvature coupling,  $\xi$ , in the above expression is consequence of the delta-Dirac contribution in the Ricci scalar, given by  $\xi R$ , present in (67).

For large value of  $l$  we have  $2\alpha\nu_l \approx (2l + 1) + \frac{(1 - \alpha^2)(8\xi - 1)}{2(2l + 1)} + O\left(\frac{1}{(2l + 1)^2}\right)$ . Substituting this expansion into (103), for the leading term in  $1/l$ , we obtain

$$-\alpha(1 - \alpha)\frac{(1 - 8\xi)}{4l} \left(\frac{a}{r}\right)^{2l/\alpha}. \quad (104)$$

Finally, after some intermediate steps we find:

$$E_{Ren} \approx q^2 \frac{(1 - \alpha)(1 - 8\xi)}{32\pi\alpha a} \ln \left[ 1 - (a/r_0)^{1/\alpha} \right]. \quad (105)$$

We can see that the above result does not depend on the mass of the particle. In fact this happens because the leading order term in the expansions of the coefficient  $D^{(+)}(a)$  there appear a power factor  $(ma)^{2\nu_l}$ , as to the square of the Macdonald function  $K_{\nu_l}(mr)$ , the leading power factor in the mass is  $(mr)^{-2\nu_l}$ . Moreover we can see from the above result that for  $\xi = 1/8$  there is no divergent contribution in the core-induced part, and that for  $\xi > 1/8$  this contribution becomes negative.

Now let us turn our investigation of the self-energy for the region inside the monopole. Substituting the functions (96) into the formulas (83) and (84) for the corresponding Green function in the interior region one finds [21],

$$G_0(\vec{r}, \vec{r}') = \frac{1}{4\pi} \frac{e^{-mR}}{R}, \quad (106)$$

with  $R = \sqrt{(\tilde{r}')^2 + (\tilde{r})^2 - 2\tilde{r}\tilde{r}' \cos\gamma}$ , being  $\gamma$  the angle between the two directions defined by the unit vectors  $\hat{\tilde{r}}'$  and  $\hat{\tilde{r}}$ . Taking  $\gamma = 0$  we get  $R = |r - r'|$ . Because in the flower-pot model the geometry in the region inside the monopole is a Minkowski one, we have  $G_0(\vec{r}, \vec{r}') = G_{Sing}(\vec{r}, \vec{r}')$ , consequently  $G_{0,Ren}(\vec{r}_0, \vec{r}_0) = 0$ . The scalar self-energy in this region is given only by the core-induced part:

$$E_{Ren} = \frac{q^2}{8\pi\tilde{r}_p} \sum_{l=0}^{\infty} (2l + 1) D_l^{(-)}(a) (I_{l+1/2}(m\tilde{r}_0))^2, \quad (107)$$

being  $\tilde{r}_0 = r_0 + (\alpha - 1)a$ . Near the core's center,  $\tilde{r}_0 \approx 0$ ,

$$I_{l+1/2}(m\tilde{r}_0) \approx \left(\frac{m\tilde{r}_0}{2}\right)^{l+1/2} \frac{1}{\Gamma(l + 3/2)}, \quad (108)$$

so the main contribution into the self-energy comes from the lowest mode,  $l = 0$ , resulting in

$$E_{Ren} \approx \frac{q^2 m D_0^{(-)}(a)}{4\pi^2}. \quad (109)$$

Taking the expression for the coefficient  $D_l^{(-)}(a)$ , for  $l = 0$ , and considering  $\xi = 0$ , after some steps we find

$$D_0^{(-)}(a) = \frac{1}{2} \frac{\pi e^{-m\alpha a}(\alpha - 1)}{\sinh(m\alpha a)(\alpha + \alpha a m - 1) + \alpha a m \cosh(m\alpha a)}. \quad (110)$$

Finally substituting the above expression into (109), and taking the limit  $m \rightarrow 0$  we obtain

$$E_{Ren}(r) \approx \frac{q^2(\alpha - 1)}{8\pi\alpha^2 a}. \quad (111)$$

Also we can calculate the core-induced contribution on the scalar self-energy near the boundary. Again, adopting a similar procedure as in the previous corresponding analysis, we can verify after some intermediate steps that the leading term inside the summation in (107) behaves as,

$$\frac{1}{4l} \frac{(1 - \alpha)(8\xi - 1)}{\alpha a} \left( \frac{\tilde{r}}{\alpha a} \right)^{2l}. \quad (112)$$

Finally, taking this expression back into (107) we obtain,

$$E_{Ren} \approx q^2 \frac{(1 - \alpha)(1 - 8\xi)}{32\pi\alpha a} \ln \left( 1 - \frac{\tilde{r}_0}{\alpha a} \right). \quad (113)$$

Once more we can see that this divergent contribution vanishes for  $\xi = 1/8$ .

Before to finish this application we want to cal attention that (105) and (113), for  $\xi = 0$ , coincide, up the numerical factor  $4\pi$ , with the corresponding core-induced electrostatic self-energies derived in [13].

#### 4. Concluding remarks

In this paper we have analyzed induced self-energies associated with particle with electric and scalar charges place at rest in the global monopole spacetime, considering a inner structure to it. These two distinct situations have been investigated separately along this paper.

As we could see, both investigations depend on the corresponding three-dimensional Green functions. For the general spherically symmetric static model of the core with finite thickness we have constructed the corresponding Green functions in both exterior and interior regions. In the region outside the core these functions are presented as a sum of two distinct contributions. The firsts ones corresponds to the Green functions for the geometry of a point-like global monopole and the seconds ones are

induced by the non-trivial structure of the monopole core. A similar structure is also presented by the Green functions for the region inside the monopole.

The self-energies are formally expressed in terms of the evaluation of the respective Green functions in the coincidence limit; however, because the results are divergent, we had to apply some renormalization procedure in order to obtain finite and well defined values. Here we used the point-splitting procedure. We analyze the divergent contributions associated with the Green functions at the coincidence limit, and extract all of them. In fact we did this in a manifest form by subtracting from the Green functions the DeWit-Schwinger adiabatic expansions which are divergent in the coincidence limit.

As an application of the general results, in section 3 we have considered a simple core model with a flat spacetime, the so called flower-pot model.

For the electrostatic case, the corresponding self-forces are repulsive with respect to the core boundary in the case  $\alpha < 1$  and attractive for  $\alpha > 1$ . In particular, for the first case, the charge placed at the core center is in a stable equilibrium position. Although in the flower-pot model, we have found a finite value of the self-energy at the monopole's center, it presents a logarithmic singular behavior at the core boundary.

As to the scalar charged particle the main conclusions found in this work, three deserves to be mentioned. They are: *i*) The renormalized self-energy depends strongly on the value adopted for the curvature coupling constant  $\xi$ . For specific values of this constant, the self-energy may provide repulsive, or attractive self-forces with respect to the boundary. *ii*) The self-energy presents a finite value at the monopole's core center, and *iii*) for conformally coupled massless field, the self-energy only depends on the core-induced part.

## Acknowledgment

The author thanks CNPq. for partial financial.

## References

- [1] T. W. Kibble, J. Phys. A. **9**, 1387 (1976).
- [2] A. Vilenkin and E. P. S. Shellard, *Cosmic Strings and Other Topological Defects* (Cambridge University Press, Cambridge, England, 1994).
- [3] D. D. Sokolov and A. A. Starobinsky, Dokl. Akad. Nauk USSR. **234**, 1043 (1977) [Sov. Phys. - Doklady **22**, 312 (1977)].
- [4] M. Barriola and A. Vilenkin, Phys. Rev. Lett. **63**, 341 (1989).
- [5] F. D. Mazzitelli and C. O. Lousto, Phys. Rev. D **43**, 468 (1991).

- [6] E. R. Bezerra de Mello, V. B. Bezerra and N. R. Khusnutdinov, Phys. Rev. D **60**, 063506 (1999).
- [7] B. Linet, Phys. Rev. D **33**, 1833 (1986).
- [8] A. G. Smith, in *The Formation and Evolution of Cosmic Strings*, Proceedings of the Cambridge Workshop, Cambridge, England, 1989, edited by G.W. Gibbons, S.W. Hawking, and T. Vachaspati (Cambridge University Press, Cambridge, England, 1990).
- [9] E. R. Bezerra de Mello and C. Furtado, Phys. Rev. D **56**, 1345 (1997).
- [10] J. R. Gott, Astrophys J. **288**, 422 (1985); W. A. Hiscock, Phys. Rev. D **31**, 3288 (1985).
- [11] B. Allen and A. C. Ottewill, Phys. Rev. D **42**, 2669 (1990).
- [12] N. R. Khusnutdinov and V.B. Bezerra, Phys. Rev. D **64**, 083506 (2001).
- [13] E. R. Bezerra de Mello and A. A. Saharian, Class. Quantum Grav. **24**, 2389 (2007).
- [14] D. Barbosa, J. Spinelly and E. R. Bezerra de Mello, Int. J. Mod. Phys. D **18**, 1085 (2009).
- [15] Lior M. Burko, Class. Quantum Grav. **17**, 227 (2000).
- [16] Alan G. Wiseman, Phys. Rev. D **61**, 084014 (2000).
- [17] A. I. Zelnikov and V. P. Frolov, Zh. Eksp. Teor. Fiz. **82**, 31 (1982) [Sov. Phys. JETP **51**, 191 (1982)].
- [18] D. Barbosa, U de Freitas and E. R. Bezerra de Mello, Class. Quantum Grav. **28**, 065009 (2011).
- [19] M. Christenssen, Phys. Rev. D **17**, 946 (1978).
- [20] I. S. Gradshteyn and I. M. Ryzhik, *Table of Integrals, Series and Products* (Academic Press, New York, 1980).
- [21] M. Abramowitz and I. A. Stegun, *Handbook of Mathematical Functions* (National Bureau of Standards, Washington DC, 1964).
- [22] E. R. Bezerra de Mello and A. A. Saharian, JHEP **610**, 049 (2006).
- [23] E. R. Bezerra de Mello and A. A. Saharian, Phys. Rev. D **75**, 065019 (2007).

# Quantum vacuum in de Sitter spacetime

A. A. Saharian

*Department of Physics, Yerevan State University  
1 Alex Manoogian Street, 0025 Yerevan, Armenia*

## Abstract

Local properties of the Bunch-Davies vacuum state are investigated for a massive scalar field with general curvature coupling parameter in background of  $D+1$ -dimensional de Sitter spacetime. The influence of the non-trivial topology of spatial dimensions and of the presence of boundaries on these properties are studied. Both the topological and boundary-induced parts in the vacuum energy-momentum tensor are time-dependent and they violate the local de Sitter symmetry.

## 1. Introduction

De Sitter (dS) spacetime is one of the simplest and most interesting spacetimes allowed by general relativity. Quantum field theory in this background has been extensively studied during the past two decades. Much of early interest to dS spacetime was motivated by the questions related to the quantization of fields propagating on curved backgrounds (for a review see [1]). This spacetime has a high degree of symmetry and numerous physical problems are exactly solvable on this background. The importance of this theoretical work increased by the appearance of the inflationary cosmology scenario [2]. In most inflationary models an approximately dS spacetime is employed to solve a number of problems in standard cosmology. During an inflationary epoch quantum fluctuations in the inflaton field introduce inhomogeneities and may affect the transition toward the true vacuum. These fluctuations play a central role in the generation of cosmic structures from inflation. More recently astronomical observations of high redshift supernovae, galaxy clusters and cosmic microwave background [3] indicate that at the present epoch the Universe is accelerating and can be well approximated by a world with a positive cosmological constant. If the Universe would accelerate indefinitely, the standard cosmology would lead to an asymptotic dS universe. Hence, the investigation of physical effects in dS spacetime is important for understanding both the early Universe and its future. In addition to the above, an interesting topic which has received increasing attention is related to string-theoretical models of dS spacetime and inflation. Recently a number of constructions of metastable dS vacua within the framework of string theory are discussed (see, for instance, [4, 5] and references therein).

In the present paper we discuss the quantization of a massive scalar field with general curvature coupling parameter on background of dS spacetime. A common problem in formulating quantum field theory on a curved background is ambiguity in the choice of vacuum. In de Sitter space there is a one-parameter family of vacua invariant under the de Sitter group, which have been dubbed the  $\alpha$  vacua [6]. It has long been suggested that the only physically sensible vacuum is the Bunch-Davies (Euclidean) vacuum. One reason for this choice is that the free propagators in the Bunch-Davies exhibit a Hadamard singularity, which matches with what is expected in the flat space limit. We will describe the local properties of the Bunch-Davies vacuum state. Among the most important quantities describing these properties are the vacuum expectation values (VEVs) of the field squared and the energy-momentum tensor. In addition, the VEV of the energy-momentum tensor acts as a source of gravity in the Einstein equations and, hence, plays an important role in modelling self-consistent dynamics involving the gravitational field. The VEV of the field squared for the inflaton field is the central quantity in discussing the generation of inhomogeneities during the inflationary expansion which are sources of large scale structure in the universe. For a scalar field on background of dS spacetime the renormalized vacuum expectation values of the field square and the energy-momentum tensor are investigated in Refs. [7]-[10] by using various regularization schemes. The corresponding effects upon phase transitions in an expanding universe are discussed in [11]. The non-trivial properties of the vacuum state in quantum field theory are manifested in its response to external influences. As simple models of the latter we consider boundary conditions imposed on the field operator due to the non-trivial topology of the background space or related to the presence of boundaries.

The paper is organized as follows. In the next section we consider the quantization of a massive scalar field with general curvature coupling parameter in classical dS background with trivial topology. dS-invariant vacuum states are discussed. By using the direct modes summation technique the Wightman function, the renormalized VEVs of the field squared and the energy-momentum tensor are evaluated for the Bunch-Davies vacuum state. The VEV of the energy-momentum tensor for dS spacetime with toroidally compactified spatial dimensions are considered in section 3. The VEV of the energy-momentum tensor and the Casimir forces for the geometry of two parallel plates in dS spacetime are discussed in section 4. The main results are summarized in section 5.

## 2. Scalar field in dS spacetime

As a background geometry we consider the  $(D + 1)$ -dimensional de Sitter spacetime ( $dS_{D+1}$ ) generated by a positive cosmological constant  $\Lambda$ .  $dS_{D+1}$  may be realized as the hyperboloid

$$\eta_{\mu\nu} Z^\mu Z^\nu = -\alpha^2, \quad \mu, \nu = 0, 1, \dots, D + 1, \quad (1)$$

in  $(D+2)$ -dimensional Minkowski spacetime with the line element  $ds_{D+2}^2 = \eta_{\mu\nu} dZ^\mu dZ^\nu$  with  $\eta_{\mu\nu}$  being the standard Minkowskian metric. In (1), the parameter  $\alpha = \sqrt{D(D-1)/(2\Lambda)}$  is called the dS radius. With this embedding the  $O(D+1, 1)$  symmetry, which is the isometry group of  $dS_{D+1}$ , is manifest. Different coordinate systems can be used on the hyperboloid. In this paper we employ the, so called, planar or inflationary coordinates,  $(t, z^1, \dots, z^D)$ , which are most appropriate for cosmological applications. These coordinates are related to the coordinates  $Z^\mu$  by the expressions

$$\begin{aligned} Z^0 &= \alpha \sinh(t/\alpha) + \frac{e^{t/\alpha}}{2\alpha} \sum_{l=1}^D (z^l)^2, \\ Z^l &= z^l e^{t/\alpha}, \quad l = 1, \dots, D, \\ Z^{D+1} &= \alpha \cosh(t/\alpha) - \frac{e^{t/\alpha}}{2\alpha} \sum_{l=1}^D (z^l)^2. \end{aligned} \quad (2)$$

They cover the half of hyperboloid (1) with  $Z^0 + Z^{D+1} > 0$ .

In planar coordinates the dS line element takes the form

$$ds^2 = dt^2 - e^{2t/\alpha} \sum_{l=1}^D (dz^l)^2. \quad (3)$$

In what follows, in addition to the synchronous time coordinate,  $t$ , we will also use the conformal time,  $\tau$ , defined as  $\tau = -\alpha e^{-t/\alpha}$ ,  $-\infty < \tau < 0$ . In terms of this coordinate the line element takes the conformally flat form:

$$ds^2 = \alpha^2 \tau^{-2} \left[ d\tau^2 - \sum_{l=1}^D (dz^l)^2 \right]. \quad (4)$$

Note that the line element (4) with  $0 < \tau < \infty$  covers the remained half of the hyperboloid (1). First we discuss the case of boundary-free geometry with trivial spatial topology. In this case we have  $-\infty < z^l < \infty$  for  $l = 1, 2, \dots, D$ .

We consider a scalar field  $\varphi(x)$  with curvature coupling parameter  $\xi$  in background of  $dS_{D+1}$ . The corresponding field equation has the form

$$\left( \nabla_l \nabla^l + m^2 + \xi R \right) \varphi = 0, \quad (5)$$

where  $\nabla_l$  is the covariant derivative operator and  $R = D(D+1)/\alpha^2$  is the Ricci scalar for the background spacetime. The most important special cases correspond to minimally and conformally coupled scalar fields with  $\xi = 0$  and  $\xi = \xi_D \equiv (D-1)/4D$ , respectively.

The quantization of the field  $\varphi(x)$  in dS spacetime is done by the standard methods of quantum field theory on curved backgrounds (for a review see [1]). Let

$\{\varphi_\sigma(x), \varphi_\sigma^*(x)\}$  be a complete set of solutions to the field equation (5) specified by a collective index  $\sigma$  and normalized by the condition

$$\int_{\Sigma} d\Sigma^\mu [\varphi_\sigma(x) \partial_\mu \varphi_{\sigma'}^*(x) - \varphi_{\sigma'}^*(x) \partial_\mu \varphi_\sigma(x)] = i\delta_{\sigma\sigma'}. \quad (6)$$

where  $\Sigma$  is a spacelike slice. Here and in what follows,  $\delta_{\sigma\sigma'}$  is understood as Dirac delta-function for continuous components of the collective index  $\sigma$  and as Kronecker delta for discrete ones. We expand the field operator in terms of the mode functions as

$$\varphi(x) = \sum_{\sigma} [a_{\sigma} \varphi_{\sigma}(x) + a_{\sigma}^+ \varphi_{\sigma}^*(x)], \quad (7)$$

where  $a_{\sigma}$  and  $a_{\sigma}^+$  are the annihilation and creation operators with the standard commutation relations  $[a_{\sigma}, a_{\sigma'}^+] = \delta_{\sigma\sigma'}$ ,  $[a_{\sigma}, a_{\sigma'}] = [a_{\sigma}^+, a_{\sigma'}^+] = 0$ . For continuous components of the collective index  $\sigma$  the summation in (7) is understood as an integration with an appropriate measure. Further, we define the vacuum state as follows:  $a_{\sigma} |0\rangle = 0$ . The multiparticle Fock states are constructed in the standard way acting by the creation operators on the vacuum state. In particular, a one-particle state is defined as  $|1_{\sigma}\rangle = a_{\sigma}^+ |0\rangle$ .

Note that, in general, the notion of the vacuum state depends on the choice of the mode functions. If  $\{\bar{\varphi}_\rho(x), \bar{\varphi}_\rho^*(x)\}$  is another set of mode functions with the corresponding vacuum state  $|\bar{0}\rangle$ , then this state contains  $\sum_{\rho} |\beta_{\rho\sigma}|^2$  particles in the  $\varphi_{\sigma}(x)$  mode, where  $\beta_{\rho\sigma} = -(\bar{\varphi}_{\rho}(x), \varphi_{\sigma}^*(x))$  is the Bogoliubov coefficients. The two vacuum states,  $|\bar{0}\rangle$  and  $|0\rangle$ , coincide only in the case  $\beta_{\rho\sigma} = 0$ .

In dS spacetime described by the inflationary coordinates, Eq. (3), the spatial coordinate dependence of the mode functions can be taken in the form  $e^{i\mathbf{k}\cdot\mathbf{z}}$  with  $\mathbf{z} = (z^1, \dots, z^D)$  and  $\mathbf{k} = (k_1, \dots, k_D)$ . For dS spacetime with trivial topology one has  $-\infty < k_l < +\infty$  and the collective index is specified as  $\sigma = (k_1, \dots, k_D)$ . From (5) we get the equation for the time-dependent part of the mode functions. The latter is solved in terms of the cylindrical functions and the mode functions are presented as

$$\varphi_{\sigma}(x) = \eta^{D/2} \sum_{j=1,2} c_j H_{\nu}^{(j)}(k\eta) e^{i\mathbf{k}\cdot\mathbf{z}}, \quad \eta = |\tau|, \quad (8)$$

where  $k = |\mathbf{k}|$ ,  $H_{\nu}^{(j)}(z)$ ,  $j = 1, 2$ , are the Hankel functions with the order

$$\nu = [D^2/4 - D(D+1)\xi - m^2\alpha^2]^{1/2}. \quad (9)$$

Note that the latter can be either real or imaginary in dependence of the curvature coupling parameter and the mass. From the normalization condition (6) we obtain the following relation between the coefficients  $c_j$ :

$$|c_1|^2 - e^{i(\nu - \nu^*)\pi} |c_2|^2 = \frac{e^{i(\nu - \nu^*)\pi/2}}{8(2\pi\alpha)^{D-1}}. \quad (10)$$

Different choices of one of the coefficients  $c_j$  correspond to different choices of the vacuum state in dS spacetime. The choice of the vacuum state is among the most

important steps in construction of a quantum field theory in a fixed classical gravitational background. dS spacetime is a maximally symmetric space and it is natural to choose a vacuum state having the same symmetry. In fact, there exists a one-parameter family of maximally symmetric quantum states [6] which are called  $\alpha$  vacua. In inflationary coordinates these states are realized by the mode functions (8) with the coefficients  $c_j$  being independent of  $\mathbf{k}$ . In the discussion below we will assume that the field is prepared in the dS-invariant Bunch-Davies vacuum state (otherwise known as the Euclidean vacuum) [10] for which  $c_2 = 0$ . As we have already mentioned before, among the set of dS-invariant quantum states the Bunch-Davies vacuum is the only one for which the short distance singularities of the two-point functions are of the Hadamard form. For a general  $\alpha$  vacuum, the subtractions in the renormalization procedure include nonlocal contributions to the effective action. In [12] it is shown that, except for the Bunch-Davies vacuum,  $\alpha$  vacua states are unphysical when gravitational interactions are included. This observation is applied to the quantum state of the inflaton, and it is found that strong fine tuning is required for states other than the Bunch-Davies vacuum to lead to observable features in the cosmic microwave background radiation anisotropy. In [13] it is proved that for an arbitrary homogeneous and isotropic physical initial state in de Sitter spacetime the expectation value of the energy-momentum tensor for a scalar field approaches the Bunch-Davies value at late times, independently of the initial state.

Hence, for the mode functions realizing the Bunch-Davies vacuum state one has

$$\varphi_\sigma(x) = c_1 \eta^{D/2} H_\nu^{(1)}(k\eta) e^{i\mathbf{k}\cdot\mathbf{z}}, \quad (11)$$

where the constant  $c_1$  is directly obtained from (10):

$$|c_1|^2 = \frac{e^{i(\nu-\nu^*)\pi/2}}{8(2\pi\alpha)^{D-1}}. \quad (12)$$

The free field theory may be defined in terms of its two-point functions. In particular, the information on the properties of the vacuum state is contained in these functions. Here we consider the Wightman function,  $W_{\text{dS}}(x, x') = \langle 0 | \varphi(x) \varphi(x') | 0 \rangle$ , where  $|0\rangle$  stands for the Bunch-Davies vacuum state. Our choice of the Wightman function is related to that, in addition to the VEVs of various physical observables, this function also determines the response of the Unruh-DeWitt particle detector at a given state of motion. Having the mode functions, the Wightman function may be evaluated by making use of the mode sum formula

$$W_{\text{dS}}(x, x') = \sum_\sigma \varphi_\sigma(x) \varphi_\sigma^*(x'). \quad (13)$$

Substituting the mode functions (11) and by taking into account (12), we find the following expression

$$W_{\text{dS}}(x, x') = \frac{e^{i(\nu-\nu^*)\pi/2} (\eta\eta')^D}{8(2\pi\alpha)^{D-1}} \int d^D \mathbf{k} H_\nu^{(1)}(k\eta) [H_\nu^{(1)}(k\eta')]^* e^{i\mathbf{k}\cdot\Delta\mathbf{z}}, \quad (14)$$

where  $\Delta\mathbf{z} = \mathbf{z} - \mathbf{z}'$ . For the further transformation of this expression, first we use the formula

$$\int d^D \mathbf{k} e^{i\mathbf{k}\cdot\Delta\mathbf{z}} F(k) = (2\pi)^{D/2} \int_0^\infty dk k^{D-1} F(k) \frac{J_{D/2-1}(k|\Delta\mathbf{z}|)}{(k|\Delta\mathbf{z}|)^{D/2-1}}, \quad (15)$$

for a given function  $F(k)$ , where  $J_\mu(x)$  is the Bessel function. This yield the formula

$$\begin{aligned} W_{\text{dS}}(x, x') &= \frac{e^{i(\nu-\nu^*)\pi/2}(\eta\eta')^D}{8(2\pi)^{D/2-1}\alpha^{D-1}|\Delta\mathbf{z}|^{D/2-1}} \int_0^\infty dk k^{D/2} \\ &\times H_\nu^{(1)}(k\eta)[H_\nu^{(1)}(k\eta')]^* J_{D/2-1}(k|\Delta\mathbf{z}|). \end{aligned} \quad (16)$$

As the next step, we write the product of the Hankel functions in terms of the Macdonald function:

$$e^{i(\nu-\nu^*)\pi/2} H_\nu^{(1)}(k\eta)[H_\nu^{(1)}(k\eta')]^* = \frac{4}{\pi^2} K_\nu(-ik\eta) K_\nu(ik\eta'), \quad (17)$$

and use the integral representation [14]

$$K_\nu(Z) K_\nu(z) = \frac{1}{4} \int_{-\infty}^{+\infty} dy \int_0^\infty \frac{dw}{w} e^{-\nu y - Z z w^{-1}} \cosh y \exp\left(-\frac{w}{2} - \frac{Z^2 + z^2}{2w}\right) \quad (18)$$

for the product of the Macdonald functions. Substituting this into (16) and changing the order of integration, the integral over  $k$  is evaluated with the help of the formula

$$\int_0^\infty dk k^{\nu+1} e^{-\alpha k^2} J_\nu(\beta x) = \frac{\beta^\nu e^{-\beta^2/4\alpha}}{(2\alpha)^{\nu+1}}. \quad (19)$$

The remained integral over  $w$  is expressed in terms of the gamma function and one gets the expression

$$W_{\text{dS}}(x, x') = \frac{\Gamma(D/2)}{4\pi^{D/2+1}\alpha^{D-1}} \int_0^\infty dz \frac{z^{D/2-\nu-1}}{[z^2 - 2u(x, x')z + 1]^{D/2}}, \quad (20)$$

where we have defined

$$u(x, x') = 1 + \frac{(\Delta\eta)^2 - |\Delta\mathbf{z}|^2}{2\eta\eta'}. \quad (21)$$

In deriving Eq. (20) we have assumed that  $|u| < 1$ . The integral in Eq. (20) is expressed in terms of the associated Legendre function  $P_{\nu-1/2}^{(1-D)/2}(u(x, x'))$  (see Ref. [15]). Expressing this function through the hypergeometric function, after some transformations, we get the final expression for the Wightman function in dS spacetime (for two-point functions in boundary-free dS spacetime see Ref. [7]):

$$\begin{aligned} W_{\text{dS}}(x, x') &= \frac{\alpha^{1-D}}{(4\pi)^{(D+1)/2}} \frac{\Gamma(D/2 + \nu)\Gamma(D/2 - \nu)}{\Gamma((D+1)/2)} \\ &\times {}_2F_1\left(\frac{D}{2} + \nu, \frac{D}{2} - \nu; \frac{D+1}{2}; \frac{1+u(x, x')}{2}\right). \end{aligned} \quad (22)$$

Note that, in terms of the coordinates  $Z^\mu$  in the higher-dimensional embedding space for dS spacetime, then one can write  $u(x, x') = 1 + [Z(x) - Z(x')]^2/(2\alpha^2)$ . The property that the Wightman function depends on spacetime points through  $[Z(x) - Z(x')]^2$  is related to the maximal symmetry of the Bunch-Davies vacuum state.

The Wightman function (22) is divergent in the coincidence limit and can not be directly used for the evaluation of the VEVs of the field squared and the energy-momentum tensor. In order to find the renormalized VEVs we can subtract from the Wightman function the corresponding DeWitt-Schwinger expansion truncated at the adiabatic order  $D + 1$ . After this subtraction the coincidence limit is finite. In this way, for the renormalized VEV of the field squared in the case  $D = 3$  one finds [7, 9, 10]

$$\langle \varphi^2 \rangle_{0,\text{ren}} = \frac{1}{8\pi^2\alpha^2} \left\{ \left( \frac{m^2\alpha^2}{2} + 6\xi - 1 \right) \left[ \psi\left(\frac{3}{2} + \nu\right) + \psi\left(\frac{3}{2} - \nu\right) - \ln(m^2\alpha^2) \right] - \frac{(6\xi - 1)^2}{m^2\alpha^2} + \frac{1}{30m^2\alpha^2} - 6\xi + \frac{2}{3} \right\}, \quad (23)$$

where  $\psi(x)$  is the logarithmic derivative of the gamma-function. Due to the maximal symmetry of the dS spacetime this VEV does not depend on the spacetime point. In a similar way, the renormalized VEV of the energy-momentum tensor takes the form [7, 9, 10] (see also [1])

$$\langle T_l^k \rangle_{0,\text{ren}} = \frac{\delta_l^k}{32\pi^2\alpha^4} \{ m^2\alpha^2 (m^2\alpha^2/2 + 6\xi - 1) [\psi(3/2 + \nu) + \psi(3/2 - \nu) - \ln(m^2\alpha^2)] - (6\xi - 1)^2 + 1/30 + (2/3 - 6\xi)m^2\alpha^2 \}. \quad (24)$$

By using the asymptotic expansion of the function  $\psi(x)$  for large values of the argument it can be seen that for large values of the parameter  $m\alpha$  from (24) one has

$$\langle T_l^k \rangle_{0,\text{ren}} \approx \frac{\delta_l^k}{32\pi^2m^2\alpha^6} \left( \frac{7}{12} - \frac{58\xi}{5} + 72\xi^2 - 144\xi^3 \right), \quad m\alpha \gg 1. \quad (25)$$

For a conformally coupled scalar field the coefficient in braces is equal  $-1/60$ . The energy-momentum tensor (24) is a gravitational source of the cosmological constant type. Due to the problem symmetry this will be the case for general values  $D$ . As a result, in combination with the initial cosmological constant  $\Lambda$ , the one-loop effects lead to the effective cosmological constant

$$\Lambda_{\text{eff}} = D(D - 1)/2\alpha^2 + 8\pi G \langle T_0^0 \rangle_{0,\text{ren}}, \quad (26)$$

where  $G$  is the Newton gravitational constant.

In figure 1 we have plotted the renormalized vacuum energy density in the uncompactified dS spacetime as a function of the parameter  $m\alpha$  for  $D = 3$  minimally and conformally coupled scalar fields. As it is seen from the plots, the one-loop correction to the cosmological constant for a minimally coupled scalar field is always positive, whereas for a conformally coupled scalar it can be also negative.

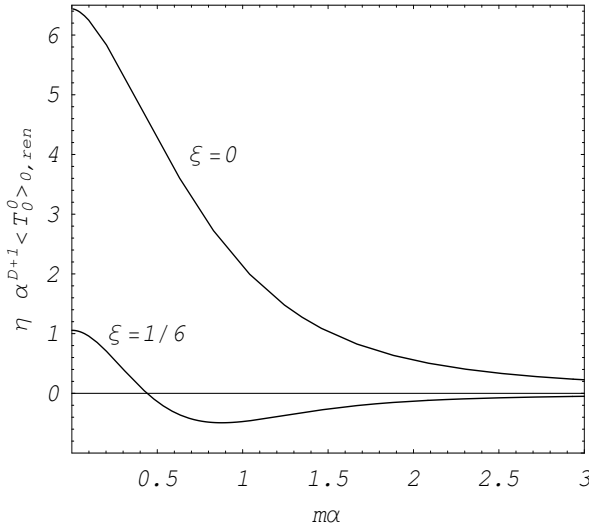


Figure 1: Renormalized vacuum energy density in uncompactified dS spacetime,  $\eta\alpha^{D+1} \langle T_0^0 \rangle_{\text{ren}}$  as a function of  $m\alpha$  for minimally and conformally coupled scalar fields in  $D = 3$ . The scaling coefficient  $\eta = 10^3(10^4)$  for minimally (conformally) coupled scalar fields.

### 3. dS spacetime with toroidally compact dimensions

#### 3.1. Mode functions

In recent years much attention has been paid to the possibility that a universe could have non-trivial topology [16, 17]. Many of high energy theories of fundamental physics are formulated in higher dimensional spacetimes and it is commonly assumed that the extra dimensions are compactified. In particular, the idea of compactified dimensions has been extensively used in supergravity and superstring theories. From an inflationary point of view universes with compact spatial dimensions, under certain conditions, should be considered a rule rather than an exception [18]. The models of a compact universe with non-trivial topology may play an important role by providing proper initial conditions for inflation (for physical motivations of considering compact universes see also [19]). There has been a large activity to search for signatures of non-trivial topology by identifying ghost images of galaxies, clusters or quasars. Recent progress in observations of the cosmic microwave background provides an alternative way to observe the topology of the universe [17]. If the scale of periodicity is close to the particle horizon scale then the changed appearance of the microwave background sky pattern offers a sensitive probe of the topology.

The compactification of spatial dimensions leads to a number of interesting quantum field theoretical effects which include instabilities in interacting field theories, topological mass generation, symmetry breaking. In the case of non-trivial topology

the boundary conditions imposed on fields give rise to the modification of the spectrum for vacuum fluctuations and, as a result, to the Casimir-type contributions in the vacuum expectation values of physical observables (for the topological Casimir effect and its role in cosmology see [20] and references therein). Compactification of extra dimensions have moduli parameters which parametrize the size and the shape of the extra dimensions and the Casimir effect has been used to stabilize these moduli. The topological Casimir energy can also serve as a model for dark energy needed for the explanation of the present accelerated expansion of the universe. The effects of the toroidal compactification of spatial dimensions in dS spacetime on the properties of quantum vacuum for a scalar field with general curvature coupling parameter are investigated in Refs. [21, 22]. The one-loop quantum effects for a fermionic field on background of dS spacetime are studied in [23, 24].

In this section we consider a general class of compactifications of dS spacetime having the spatial topology  $\mathbb{R}^p \times (\mathbb{S}^1)^q$ ,  $p + q = D$ . This geometry can be used to describe two types of models. For the first one  $p = 3$ ,  $q \geq 1$ , and which corresponds to the universe with Kaluza-Klein type extra dimensions. The presence of extra dimensions generates an additional gravitational source in the cosmological equations which is of barotropic type (gravitational source with a constant equation of state parameter) at late stages of the cosmological evolution. For the second model  $D = 3$  and the results given below describe how the properties of the universe with dS geometry are changed by one-loop quantum effects induced by the compactness of spatial dimensions.

We assume that the spatial coordinate  $z^l$ ,  $l = p + 1, \dots, D$ , is compactified to  $\mathbb{S}^1$  of the length  $L_l$ :  $0 \leq z^l \leq L_l$ , and for the other coordinates we have  $-\infty < z^l < +\infty$ ,  $l = 1, \dots, p$ . Let  $\mathbf{z}_p = (z^1, \dots, z^p)$  and  $\mathbf{z}_q = (z^{p+1}, \dots, z^D)$  be the position vectors along the uncompactified and compactified dimensions respectively. We impose the following boundary conditions along the compactified dimensions

$$\varphi(t, \mathbf{z}_p, \mathbf{z}_q + L_l \mathbf{e}_l) = \pm \varphi(t, \mathbf{z}_p, \mathbf{z}_q), \quad (27)$$

where  $l = p + 1, \dots, D$ , upper/lower sign corresponds to untwisted/twisted scalar field, and  $\mathbf{e}_l$  is the unit vector along the direction of the coordinate  $z^l$ .

As before, for the evaluation of the VEVs will use the direct mode-summation procedure assuming that the field is prepared in the Bunch-Davies vacuum state. The corresponding mode functions have the form

$$\varphi_\sigma(x) = \left[ \frac{e^{i(\nu - \nu^*)\pi/2} \eta^D}{2^{p+2} \pi^{p-1} V_q \alpha^{D-1}} \right]^{1/2} H_\nu^{(1)}(k\eta) e^{i\mathbf{k}_p \cdot \mathbf{z}_p + i\mathbf{k}_q \cdot \mathbf{z}_q}, \quad (28)$$

where  $V_q = L_{p+1} \cdots L_D$  is the volume of the compactified subspace, and

$$\begin{aligned} \mathbf{k}_p &= (k_1, \dots, k_p), \quad \mathbf{k}_q = (k_{p+1}, \dots, k_D), \quad k = \sqrt{\mathbf{k}_p^2 + \mathbf{k}_q^2}, \\ k_l &= 2\pi(n_l + g_l)/L_l, \quad n_l = 0, \pm 1, \pm 2, \dots, \quad l = p + 1, \dots, D. \end{aligned} \quad (29)$$

In (29),  $g_l = 0$  for untwisted scalar and  $g_l = 1/2$  for twisted scalar field.

### 3.2. Vacuum Energy-Momentum Tensor

Having the complete set of eigenfunctions we can evaluate the VEV of the energy-momentum tensor by using the mode-sum formula

$$\langle T_{ik} \rangle_{p,q} = \sum_{\sigma} T_{ik} \{ \varphi_{\sigma}(x), \varphi_{\sigma}^*(x) \}, \quad (30)$$

where the bilinear form  $T_{ik}\{f, g\}$  is determined by the form of the classical energy-momentum tensor for a scalar field. We implicitly assume the presence of a cutoff function in (30) which makes the sum finite. In the problem under consideration the set of quantum numbers  $\sigma$  is specified to  $(\mathbf{k}_p, \mathbf{n}_q)$  with  $\mathbf{n}_q = (n_{p+1}, \dots, n_D)$ . Substituting the eigenfunctions (28) into mode-sum (30) and applying to the series over  $n_{p+1}$  the Abel-Plana summation formula (see, for example, Refs. [25]), we find the following recurrence relation for the VEV of the energy-momentum tensor

$$\langle T_i^k \rangle_{p,q} = \langle T_i^k \rangle_{p+1,q-1} + \Delta_{p+1} \langle T_i^k \rangle_{p,q}. \quad (31)$$

Here  $\langle T_i^k \rangle_{p+1,q-1}$  is the part corresponding to dS spacetime with  $p+1$  uncompactified and  $q-1$  toroidally compactified dimensions and  $\Delta_{p+1} \langle T_i^k \rangle_{p,q}$  is induced by the compactness along the  $z^{p+1}$ -direction. For the corresponding energy density one has

$$\begin{aligned} \Delta_{p+1} \langle T_0^0 \rangle_{p,q} &= \frac{2\eta^D L_{p+1}}{(2\pi)^{(p+3)/2} V_q \alpha^{D+1}} \sum_{n=1}^{\infty} (\pm 1)^n \sum_{\mathbf{n}_{q-1}=-\infty}^{+\infty} \int_0^{\infty} dx \\ &\times \frac{x F_{\nu}^{(0)}(x\eta)}{(nL_{p+1})^{p-1}} f_{(p-1)/2}(nL_{p+1} \sqrt{x^2 + k_{\mathbf{n}_{q-1}}^2}), \end{aligned} \quad (32)$$

with the notations  $\mathbf{n}_{q-1} = (n_{p+2}, \dots, n_D)$ ,  $f_{\mu}(y) = y^{\mu} K_{\mu}(y)$ , and

$$\begin{aligned} F_{\nu}^{(0)}(y) &= y^2 [I'_{-\nu}(y) + I'_{\nu}(y)] K'_{\nu}(y) + D(1/2 - 2\xi)y [(I_{-\nu}(y) + I_{\nu}(y)) K_{\nu}(y)]' \\ &+ [I_{-\nu}(y) + I_{\nu}(y)] K_{\nu}(y) (\nu^2 + 2m^2\alpha^2 - y^2). \end{aligned} \quad (33)$$

In Eq. (32), the upper/lower sign corresponds to untwisted/twisted scalar field. The vacuum stresses are presented in the form (no summation over  $i$ )

$$\begin{aligned} \Delta_{p+1} \langle T_i^i \rangle_{p,q} &= A_{p,q} - \frac{4\eta^{D+2} L_{p+1}}{(2\pi)^{(p+3)/2} V_q \alpha^{D+1}} \sum_{n=1}^{\infty} (\pm 1)^n \sum_{\mathbf{n}_{q-1}=-\infty}^{+\infty} \int_0^{\infty} dx x K_{\nu}(x\eta) \\ &\times \frac{I_{-\nu}(x\eta) + I_{\nu}(x\eta)}{(nL_{p+1})^{p+1}} f_p^{(i)}(nL_{p+1} \sqrt{x^2 + k_{\mathbf{n}_{q-1}}^2}), \end{aligned} \quad (34)$$

where we have introduced the notations

$$\begin{aligned} f_p^{(i)}(y) &= f_{(p+1)/2}(y), \quad i = 1, \dots, p, \\ f_p^{(p+1)}(y) &= -y^2 f_{(p-1)/2}(y) - pf_{(p+1)/2}(y), \\ f_p^{(i)}(y) &= (nL_{p+1} k_i)^2 f_{(p-1)/2}(y), \quad i = p+2, \dots, D. \end{aligned} \quad (35)$$

The first term on the right of Eq. (34) is given by

$$A_{p,q} = \frac{2\eta^D L_{p+1}}{(2\pi)^{(p+3)/2} V_q \alpha^{D+1}} \sum_{n=1}^{\infty} (\pm 1)^n \sum_{\mathbf{n}_{q-1}=-\infty}^{+\infty} \int_0^{\infty} dx \frac{x F_{\nu}(x\eta)}{(nL_{p+1})^{p-1}} \\ \times f_{(p-1)/2}(nL_{p+1}\sqrt{x^2 + k_{\mathbf{n}_{q-1}}^2}), \quad (36)$$

with the notation

$$F_{\nu}(y) = [2(D+1)\xi - D/2] y ([I_{-\nu}(y) + I_{\nu}(y)] K_{\nu}(y))' + (4\xi - 1) y^2 K'_{\nu}(y) \\ \times [I'_{-\nu}(y) + I'_{\nu}(y)] + [I_{-\nu}(y) + I_{\nu}(y)] K_{\nu}(y) [(4\xi - 1)(y^2 + \nu^2)]. \quad (37)$$

As it is seen from the obtained formulae, the topological parts in the VEVs are time-dependent and, hence, the local dS symmetry is broken by them. By taking into account the relation between the conformal and synchronous time coordinates, we see that the VEV of the energy-momentum tensor is a function of the combinations  $L_l/\eta = L_l e^{t/\alpha}/\alpha$ , which is the comoving length of the compactified dimension measured in units of the dS curvature scale.

The recurring application of formula (31) allows us to write the VEV in the form

$$\langle T_i^k \rangle_{p,q} = \langle T_i^k \rangle_{\text{dS}} + \langle T_i^k \rangle_c, \quad \langle T_i^k \rangle_c = \sum_{l=1}^q \Delta_{D-l+1} \langle T_i^k \rangle_{D-l,l}, \quad (38)$$

where the part corresponding to uncompactified dS spacetime,  $\langle T_i^k \rangle_{\text{dS}}$ , is explicitly decomposed. The part  $\langle T_i^k \rangle_c$  is induced by the compactness of the  $q$ -dimensional subspace. This part is finite and the renormalization is needed for the uncompactified dS part only. We could expect this result, since the local geometry is not changed by the toroidal compactification.

For a conformally coupled massless scalar field  $\nu = 1/2$  and, by using the formulae for  $I_{\pm 1/2}(x)$  and  $K_{1/2}(x)$ , after the integration over  $x$  from formulae (32), (34) we find (no summation over  $i$ )

$$\Delta_{p+1} \langle T_i^i \rangle_{p,q} = -\frac{2(\eta/\alpha)^{D+1}}{(2\pi)^{p/2+1} V_{q-1}} \sum_{n=1}^{\infty} (\pm 1)^n \sum_{\mathbf{n}_{q-1}=-\infty}^{+\infty} \frac{g_p^{(i)}(nL_{p+1}k_{\mathbf{n}_{q-1}})}{(nL_{p+1})^{p+2}}, \quad (39)$$

with the notations

$$g_p^{(0)}(y) = g_p^{(i)}(y) = f_{p/2+1}(y), \quad i = 1, \dots, p, \\ g_p^{(p+1)}(y) = -(p+1)f_{p/2+1}(y) - y^2 f_{p/2}(y), \\ g_p^{(i)}(y) = (nL_{p+1}k_i)^2 f_{p/2}(y), \quad i = p+2, \dots, D. \quad (40)$$

In this case the topological part in the VEV of the energy-momentum tensor is traceless and the trace anomaly is contained in the uncompactified dS part only. Formula (39) could be obtained from the corresponding result in  $(D+1)$ -dimensional

Minkowski spacetime with spatial topology  $R^p \times (S^1)^q$ , taking into account that two problems are conformally related:  $\Delta_{p+1}\langle T_i^k \rangle_{p,q} = \Delta_{p+1}\langle T_i^k \rangle_{p,q}^{(M)}/a^{D+1}(\eta)$ , where  $a(\eta) = \alpha/\eta$  is the scale factor. This relation is valid for any conformally flat bulk. The similar formula takes place for the total topological part  $\langle T_i^k \rangle_c$ . Note that, in this case the expressions for  $\Delta_{p+1}\langle T_i^k \rangle_{p,q}$  are obtained from the formulae for  $\Delta_{p+1}\langle T_i^k \rangle_{p,q}^{(M)}$  replacing the lengths  $L_l$  of the compactified dimensions by the comoving lengths  $\alpha L_l/\eta$ ,  $l = p, \dots, D$ .

Now we turn to the investigation of the topological part in the VEV of the energy-momentum tensor in the asymptotic regions of the ratio  $L_{p+1}/\eta$ . For small values of this ratio,  $L_{p+1}/\eta \ll 1$ , to the leading order  $\Delta_{p+1}\langle T_i^k \rangle_{p,q}$  coincides with the corresponding result for a conformally coupled massless field, given by (39). For fixed value of the ratio  $L_{p+1}/\alpha$ , this limit corresponds to  $t \rightarrow -\infty$  and the topological part  $\langle T_i^k \rangle_c$  behaves like  $\exp[-(D+1)t/\alpha]$ . By taking into account that the part  $\langle T_i^k \rangle_{\text{ds}}$  is time independent, from here we conclude that in the early stages of the cosmological expansion the topological part dominates in the VEV of the energy-momentum tensor. In particular, in this limit the total energy density is negative.

For small values of the ratio  $\eta/L_{p+1}$ , we introduce a new integration variable  $y = L_{p+1}x$  and expand the integrand by using the formulae for the modified Bessel functions for small arguments. For real values of the parameter  $\nu$  we find

$$\begin{aligned} \Delta_{p+1}\langle T_0^0 \rangle_{p,q} &\approx \frac{2^\nu D [D/2 - \nu + 2\xi(2\nu - D - 1)]}{(2\pi)^{(p+3)/2} L_{p+1}^{-q} V_q \alpha^{D+1}} \Gamma(\nu) \left(\frac{\eta}{L_{p+1}}\right)^{D-2\nu} \\ &\times \sum_{n=1}^{\infty} (\pm 1)^n \sum_{\mathbf{n}_{q-1}=-\infty}^{+\infty} \frac{f_{(p+1)/2-\nu}(nL_{p+1}k_{\mathbf{n}_{q-1}})}{n^{(p+1)/2-\nu}}. \end{aligned} \quad (41)$$

In particular, this quantity is positive for a minimally coupled scalar field and for a conformally coupled massive scalar field. For a conformally coupled massless scalar the coefficient in (41) vanishes. For the vacuum stresses the second term on the right of formula (34) is suppressed with respect to the first term given by (36) by the factor  $(\eta/L_{p+1})^2$  for  $i = 1, \dots, p+1$ , and by the factor  $(\eta k_i)^2$  for  $i = p+2, \dots, D$ . As a result, to the leading order we have the relation (no summation over  $i$ )

$$\Delta_{p+1}\langle T_i^i \rangle_{p,q} \approx (2\nu/D)\Delta_{p+1}\langle T_0^0 \rangle_{p,q}, \quad \eta/L_{p+1} \ll 1, \quad (42)$$

between the energy density and stresses,  $i = 1, \dots, D$ . The coefficient in this relation does not depend on  $p$  and, hence, it takes place for the total topological part of the VEV as well. Hence, in the limit under consideration the topological parts in the vacuum stresses are isotropic. Note that this limit corresponds to late times in terms of synchronous time coordinate  $t$ ,  $(\alpha/L_{p+1})e^{-t/\alpha} \ll 1$ , and the topological part in the VEV is suppressed by the factor  $\exp[-(D-2\nu)t/\alpha]$ . For a conformally coupled massless scalar field the coefficient of the leading term vanishes and the topological parts are suppressed by the factor  $\exp[-(D+1)t/\alpha]$ . As the uncompactified dS part

is constant, it dominates the topological part at the late stages of the cosmological evolution.

For small values of the ratio  $\eta/L_{p+1}$  and for purely imaginary  $\nu$ , the energy density behaves like

$$\Delta_{p+1}\langle T_0^0 \rangle_{p,q} \approx \frac{4De^{-Dt/\alpha}B}{(2\pi)^{(p+3)/2}\alpha L_{p+1}^p V_q} \sin[2|\nu|t/\alpha + 2|\nu| \ln(L_{p+1}/\alpha) + \phi_0], \quad (43)$$

where the parameters  $B$  and  $\phi_0$  are defined by the relation

$$\begin{aligned} Be^{i\phi_0} = & 2^{i|\nu|} [|\nu|(1/2 - 2\xi) + i(D/4 - (D+1)\xi)]\Gamma(i|\nu|) \\ & \times \sum_{n=1}^{\infty} (\pm 1)^n \sum_{\mathbf{n}_{q-1}=-\infty}^{+\infty} n^{2i|\nu|-p-1} f_{(p+1)/2-i|\nu|}(nL_{p+1}k_{\mathbf{n}_{q-1}}). \end{aligned} \quad (44)$$

In the same limit, the main contribution into the vacuum stresses comes from the term  $A_{p,q}$  in (36) and one has (no summation over  $i$ )

$$\Delta_{p+1}\langle T_i^i \rangle_{p,q} \approx \frac{8|\nu|e^{-Dt/\alpha}B}{(2\pi)^{(p+3)/2}\alpha L_{p+1}^{p+1} V_{q-1}} \cos[2|\nu|t/\alpha + 2|\nu| \ln(L_{p+1}/\alpha) + \phi_0]. \quad (45)$$

Hence, in the case under consideration at late stages of the cosmological evolution the topological part is suppressed by the factor  $\exp(-Dt/\alpha)$  and the damping of the corresponding VEV has an oscillatory nature.

In the special case of topology  $R^{D-1} \times S^1$  with the length of the compactified dimension  $L_{p+1} = L$ , for the topological part in the energy density we have

$$\langle T_0^0 \rangle_c = \frac{2(\eta/L)^{D-2}}{(2\pi)^{D/2+1}\alpha^{D+1}} \sum_{n=1}^{\infty} \frac{(\pm 1)^n}{n^{D-2}} \int_0^\infty dx x F_\nu^{(0)}(x) f_{D/2-1}(nxL/\eta). \quad (46)$$

We recall that the quantity  $L/\eta$  is the comoving length of the compactified dimension measured in units of the dS curvature scale  $\alpha$ . Note that the corresponding quantity in the Minkowski spacetime with topology  $R^{D-1} \times S^1$  has the form

$$\langle T_0^0 \rangle_c^{(M)} = -\frac{2}{(2\pi)^{(D+1)/2} L^{D+1}} \sum_{n=1}^{\infty} \frac{(\pm 1)^n}{n^{D+1}} f_{(D+1)/2}(nLm), \quad (47)$$

and is always negative for an untwisted scalar field. In order to illustrate the oscillatory behavior, in figure 2 by the full curve we have plotted the topological part in the VEV of the energy density for an untwisted scalar field in  $dS_5$  with topology  $R^3 \times S^1$  as a function of the comoving length of the compactified dimension in units of  $\alpha$ :  $L_c = L/\eta$  for the value of the parameter  $\alpha m = 4$ . This topology corresponds to the original Kaluza-Klein model. The dashed curve presents the corresponding quantity in Minkowski spacetime with topology  $R^3 \times S^1$  (formula (47) with  $D = 4$ ) as a function of the length of the compactified dimension in the same units:  $L_c = L/\alpha$ .

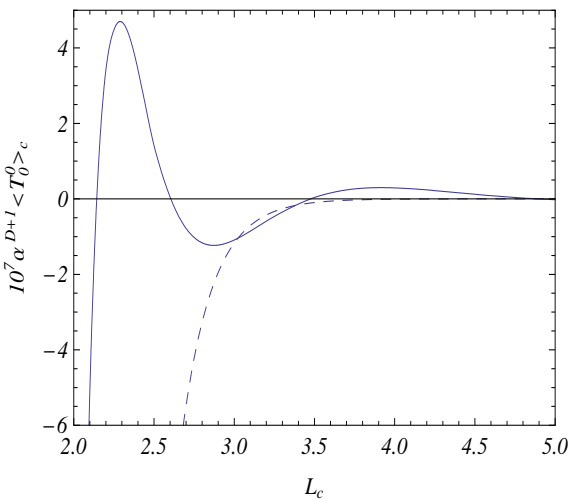


Figure 2: Topological part of the vacuum energy density,  $\alpha^{D+1}\langle T_0^0 \rangle_c$ , in dS<sub>5</sub> with topology  $R^3 \times S^1$  as a function of the comoving length of the compactified dimension in units of  $\alpha$ ,  $L_c = L/\eta$ , for the value of the parameter  $\alpha m = 4$ . The dashed curve presents the corresponding quantity in Minkowski spacetime with topology  $R^3 \times S^1$  as a function of the length of the compactified dimension in the same units:  $L_c = L/\alpha$ .

## 4. Casimir densities in dS spacetime

### 4.1. Boundary conditions and mode functions

The Casimir effect is now known to be common to systems of very different kind, involving fluctuating quantities on which external boundary conditions are imposed. It can have important implications on all scales, from subnuclear to cosmological. Imposing boundary conditions on a quantum field leads to a modification of the spectrum of zero-point fluctuations and results in the shifting in the vacuum expectation values for physical quantities, such as the energy density and stresses. In particular, the confinement of quantum fluctuations induces forces that act on the constraining boundaries. The particular features of the resulting vacuum forces depend on the nature of the quantum field, on the type of the spacetime manifold, the geometry of the boundaries, and on the specific boundary conditions imposed on the field.

An interesting topic in the investigation of the Casimir effect is its explicit dependence on the geometry of the background spacetime. As usual, the relevant information is encoded in the vacuum fluctuations spectrum and, not surprisingly, analytic solutions can be found for highly symmetric geometries only. The Casimir effect on the background of dS spacetime described in planar coordinates was investigated in Refs. [26] for a conformally coupled massless scalar field. In this last case the problem is conformally related to the corresponding problem in Minkowski space-

time and the vacuum characteristics are generated from those for the Minkowski counterpart, just by multiplying with the conformal factor. In particular, for the geometry of a single plate, the vacuum expectation value of the energy-momentum tensor vanishes. The Casimir densities induced by a single and two parallel plates for a massive scalar field with an arbitrary curvature coupling parameter has been considered in [27, 28]. The Casimir effect for a spherical boundary in dS spacetime was investigated in [29].

In this section, our main interest are the VEV of the energy-momentum tensor and the Casimir forces in the geometry of two infinite, parallel plates located at  $z^D = a_j$ ,  $j = 1, 2$ . On the plates the field obeys Robin boundary conditions (BCs)

$$(1 + \beta_j n^l \nabla_l) \varphi(x) = 0, \quad z^D = a_j, \quad (48)$$

with constant coefficients  $\beta_j$  and with  $n^l$  being the normal to the boundary. For the region between the plates one has  $n^l = (-1)^{j-1} \delta_D^l$ . Dirichlet and Neumann BCs correspond to special cases  $\beta_j = 0$  and  $\beta_j = \infty$ , respectively. The imposition of BCs leads to a modification of the VEVs for physical quantities, as compared with those in the situation without boundaries. Among the most important characteristics of the vacuum state is the VEV of the energy-momentum tensor. In addition to describing the physical structure of the quantum field at a given point, the energy-momentum tensor acts as the source in the Einstein equations and therefore plays an important role in modelling a self-consistent dynamics involving the gravitational field. The VEV is expressed as the mode-sum (30), where  $\{\varphi_\sigma(x), \varphi_\sigma^*(x)\}$  is a complete set of solutions to the classical field equation satisfying the boundary conditions (48).

In the region between the plates,  $a_1 < z^D < a_2$ , the eigenfunctions realizing the Bunch-Davies vacuum state and satisfying the BC on the plate at  $z^D = a_1$ , have the form

$$\varphi_\sigma(x) = C_\sigma \eta^{D/2} H_\nu^{(1)}(\eta K) \cos[k_D(z^D - a_1) + \alpha_1(k_D)] e^{i\mathbf{k}\cdot\mathbf{z}}, \quad (49)$$

with the notations  $K = \sqrt{k^2 + k_D^2}$  and  $e^{2i\alpha_1(x)} = (i\beta_1 x - 1)/(i\beta_1 x + 1)$ . In Eq. (49),  $\mathbf{z} = (z^1, \dots, z^{D-1})$  is the position vector along the dimensions parallel to the plates and  $\mathbf{k} = (k_1, \dots, k_{D-1})$ . For a conformally coupled massless field one has  $\nu = 1/2$ . From the boundary condition on the plate  $z^D = a_2$  it follows that the eigenvalues for  $k_D$  are solutions of the equation

$$(1 - b_1 b_2 y^2) \sin y - (b_1 + b_2) y \cos y = 0, \quad y = k_D a, \quad (50)$$

where  $b_j = \beta_j/a$  and  $a = a_2 - a_1$ . In the discussion below we will assume that all zeros are real. In particular, this is the case for the conditions  $b_j \leq 0$  (see Ref. [30]). The positive solutions of Eq. (50) will be denoted by  $y = \lambda_n$ ,  $n = 1, 2, \dots$ , and for the eigenvalues of  $k_D$  one has  $k_D = \lambda_n/a$ . Consequently, the eigenfunctions are specified by the set  $\sigma = (\mathbf{k}, n)$ . The coefficient  $C_\sigma$  in (49) is determined from the normalization condition and is given by the expression

$$C_\sigma^2 = \frac{(2\pi)^{2-D} \alpha^{1-D} e^{i(\nu-\nu^*)\pi/2}}{4a \{1 + \cos[\lambda_n + 2\alpha_1(\lambda_n/a)] \sin(\lambda_n)/\lambda_n\}}, \quad (51)$$

the star meaning complex conjugate.

It is well known that in dS spacetime without boundaries the Bunch–Davies vacuum state is not a physically realizable state for  $\text{Re } \nu \geq D/2$ . The corresponding two-point functions contain infrared divergences. In the presence of boundaries, the BCs on the quantized field may exclude long wavelength modes and the Bunch–Davies vacuum becomes a realizable state. An example of this type of situation is provided by the geometry of two parallel plates described above. In the region between the plates and for BCs with  $\beta_j \leq 0, \beta_j \neq \infty$ , there is a maximum wavelength,  $2\pi a/\lambda_1$ , and the two-point functions contain no infrared divergences. Mathematically, this situation corresponds to the one where in the argument of the Hankel function we have  $K \geq \lambda_1/a$ .

## 4.2. VEV of the energy-momentum tensor

Combining Eqs. (30),(28),(51), for the VEV of the energy-momentum tensor in the region between the plates we find the expression which contains series over  $\lambda_n$ . For the summation of this series we apply the Abel–Plana type summation formula from Refs. [30, 25]. This allows us to write the diagonal components in the decomposed form (no summation over  $l$ )

$$\begin{aligned} \langle T_l^l \rangle &= \langle T_l^l \rangle_j + \frac{A_D}{\alpha^{D+1}} \int_0^\infty dy y^{1-D} \int_y^\infty dx H(x, y) \\ &\quad \times [g(\beta_j x/\eta, |z^D - a_j| x/\eta) G_l(y) + 2G_l x^2 F_\nu(y)], \end{aligned} \quad (52)$$

where

$$\begin{aligned} A_D &= \frac{4(4\pi)^{-(D+1)/2}}{\Gamma((D-1)/2)}, \quad H(x, y) = \frac{(x^2 - y^2)^{(D-3)/2}}{c_1(x/\eta) c_2(x/\eta) e^{2ax/\eta} - 1}, \\ g(\beta_j u, yu) &= c_j(u) e^{2uy} + e^{-2uy}/c_j(u) + 2, \quad c_j(u) = \frac{\beta_j u - 1}{\beta_j u + 1}, \end{aligned} \quad (53)$$

and

$$F_\nu(y) = y^D [I_\nu(y) + I_{-\nu}(y)] K_\nu(y), \quad (54)$$

with  $I_\nu(y)$  and  $K_\nu(y)$  being the modified Bessel functions. In (52), we have introduced the notations

$$\begin{aligned} G_0(y) &= \left[ \frac{y^2}{4} \partial_y^2 - D(\xi + \xi_D) y \partial_y + D^2 \xi + m^2 \alpha^2 - y^2 + (1 - 4\xi) x^2 \right] F_\nu(y), \\ G_D(y) &= \left\{ \left( \xi - \frac{1}{4} \right) y^2 \partial_y^2 + \left[ \xi(2 - D) + \frac{D - 1}{4} \right] y \partial_y - \xi D \right\} F_\nu(y), \\ G_l(y) &= G_D(y) + \left[ \frac{y^2 - x^2}{D - 1} + (1 - 4\xi) x^2 \right] F_\nu(y), \quad l = 1, \dots, D - 1, \end{aligned} \quad (55)$$

and  $G_D = 1, G_l = 4\xi - 1$  for  $l = 0, 1, \dots, D - 1$ . In Eq. (52) (no summation over  $l$ ),

$$\langle T_l^l \rangle_j = \langle T_l^l \rangle_{\text{dS}} + \frac{A_D}{\alpha^{D+1}} \int_0^\infty dy y^{1-D} \int_y^\infty dx (x^2 - y^2)^{\frac{D-3}{2}} \frac{e^{-2x|z^D - a_j|/\eta}}{c_j(x/\eta)} G_l(y), \quad (56)$$

is the VEV for the geometry of a single plate at  $z^D = a_j$  when the second plate is absent [27] and  $\langle T_l^l \rangle_{\text{dS}}$  is the corresponding renormalized VEV in dS spacetime without boundaries discussed in section 2. For points away from the plates, renormalization is required for the latter part only. The last term on the right hand side of Eq. (52) is induced by the presence of the second plate. Note that in the formulas given above,  $|z^D - a_j|/\eta$  is the proper distance of the observation point from the plate at  $z^D = a_j$ , measured in units of the dS curvature radius  $\alpha$ . The VEVs depend on time through the combinations  $|z^D - a_j|/\eta$  and  $\beta_j/\eta$ . This property is a consequence of the maximal symmetry of dS spacetime and of Bunch–Davies vacuum.

For the non-zero off-diagonal component, we have

$$\begin{aligned} \langle T_0^D \rangle &= \langle T_0^D \rangle_j - \text{sgn}(z^D - a_j) \frac{A_D}{2\alpha^{D+1}} \int_0^\infty dy y^{1-D} G_{0D}(y) \\ &\quad \times \int_y^\infty dx x H(x, y) \left[ c_j(x/\eta) e^{2x|z^D - a_j|/\eta} - e^{-2x|z^D - a_j|/\eta} / c_j(x/\eta) \right], \end{aligned} \quad (57)$$

where the part corresponding to the geometry of a single plate is given by

$$\begin{aligned} \langle T_0^D \rangle_j &= \text{sgn}(z^D - a_j) \frac{2A_D}{\alpha^{D+1}} \int_0^\infty dy y^{1-D} G_{0D}(y) \\ &\quad \times \int_y^\infty dx x (x^2 - y^2)^{\frac{D-3}{2}} \frac{e^{-2x|z^D - a_j|/\eta}}{c_j(x/\eta)}. \end{aligned} \quad (58)$$

In these formulas we have defined the function

$$G_{0D}(y) = [(4\xi - 1)y\partial_y + 4\xi] F_\nu(y). \quad (59)$$

The off-diagonal component (57) corresponds to the energy flux along the direction perpendicular to the plates. Depending on the values of the coefficients in the boundary conditions and of the field mass this flux can be positive or negative. In the case when  $\beta_1 = \beta_2$ , the off-diagonal component  $\langle T_0^D \rangle$  vanishes at  $z^D = (a_1 + a_2)/2$ . This property is a direct consequence of the problem symmetry.

For a conformally coupled massless scalar field ( $\xi = \xi_D$ ,  $m = 0$ ) the single plate part in the VEV of the energy-momentum tensor vanishes and one finds (no summation over  $l$ )

$$\langle T_k^l \rangle = \langle T_k^l \rangle_{\text{dS}} - \frac{(\eta/\alpha)^{D+1} B_l \delta_l^k}{(4\pi)^{D/2} \Gamma(D/2 + 1)} \int_0^\infty dx \frac{x^D}{c_1(x)c_2(x)e^{2ax} - 1}, \quad (60)$$

where  $B_l = 1$  for  $l = 0, \dots, D-1$  and  $B_D = -D$ . The boundary induced part in this formula could have been obtained from the corresponding result for the Casimir effect in Minkowski spacetime, by using the fact that the two problems are conformally related. Note that the boundary induced part in Eq. (60) is traceless and the trace anomaly is contained in the boundary-free part only.

In the region  $z^D < a_1$  ( $z^D > a_2$ ) the VEV of the energy-momentum tensor coincides with the corresponding VEV for a single plate located at  $z^D = a_1$  ( $z^D = a_2$ )

and is given by the expressions (56) and (58), with  $j = 1$  ( $j = 2$ ). The results obtained in the present paper can be applied to a more general problem where the cosmological constant is different in separate regions  $z^D < a_1$ ,  $a_1 < z^D < a_2$ , and  $z^D > a_2$ . In this case the plate can be considered as a simple model of a thin domain wall separating the regions with different dS vacua.

### 4.3. Casimir Forces

Having the VEV of the energy-momentum tensor, we can evaluate the forces acting on the plates. The vacuum force acting per unit surface of the plate at  $z^D = a_j$  is determined by the  $D$ -component of the vacuum energy-momentum tensor evaluated at this point. For the region between the plates, the corresponding effective pressures can be written as  $p^{(j)} = p_1^{(j)} + p_{(\text{int})}^{(j)}$ ,  $j = 1, 2$ . The term  $p_1^{(j)}$  is the pressure for a single plate at  $z^D = a_j$ , when the second plate is absent. This term is divergent due to the surface divergences in the subtracted VEVs and needs additional renormalization. The term  $p_{(\text{int})}^{(j)}$  is the pressure induced by the second plate, and can be termed as an interaction force. This contribution is finite for all nonzero distances between the plates. In the regions  $z^D < a_1$  and  $z^D > a_2$  we have  $p^{(j)} = p_1^{(j)}$ . As a result, the contributions to the vacuum force coming from the term  $p_1^{(j)}$  are the same from the left and from the right sides of the plate, so that there is no net contribution to the effective force.

The interaction force on the plate at  $z^D = a_j$  is obtained from the last term on the right hand side of Eq. (52) for  $\langle T_D^D \rangle$  (with minus sign) taking  $z^D = a_j$ :

$$p_{(\text{int})}^{(j)} = -\frac{2A_D}{\alpha^{D+1}} \int_0^\infty dy y^{1-D} \int_y^\infty dx x^2 H(x, y) \left[ \frac{2(\beta_j/\eta)^2 G_D(y)}{(\beta_j x/\eta)^2 - 1} + F_\nu(y) \right], \quad (61)$$

where  $H(x, y)$  is defined by Eq. (53). The time dependence of the forces appears in the form  $a/\eta$  and  $\beta_j/\eta$ . Note that the ratio  $a/\eta$  is the proper distance between the plates measured in units of dS curvature radius  $\alpha$ . The effective pressures (61) can be either positive or negative, leading to repulsive or to attractive forces, respectively. For  $\beta_1 \neq \beta_2$  the Casimir forces acting on the left and on the right plates are different. For large values of  $\alpha$ , to leading order, the corresponding result for the geometry of two parallel plates in Minkowski spacetime is obtained:

$$p_{(\text{int})}^{(j)} \approx p_{(\text{M})}^{(j)} = -\frac{2(4\pi)^{-D/2}}{\Gamma(D/2)} \int_m^\infty dx \frac{x^2(x^2 - m^2)^{D/2-1}}{c_1(x)c_2(x)e^{2ax} - 1}. \quad (62)$$

Note that in the Minkowski spacetime the force is the same for both plates with independence of the values for the coefficients  $\beta_j$  and this force does not depend on the curvature coupling parameter.

In the special cases of Dirichlet and of Neumann boundary conditions one finds:

$$p_{(\text{int})}^{(\text{D})} = -\frac{4\alpha^{-D-1}}{(2\pi)^{\frac{D}{2}+1}} \sum_{n=1}^{\infty} \int_0^{\infty} dy y F_{\nu}(y) \left[ (D-1) f_{\frac{D}{2}}(yu_n) + f_{\frac{D}{2}-1}(yu_n) \right], \quad (63)$$

$$p_{(\text{int})}^{(\text{N})} = p_{(\text{int})}^{(\text{D})} - \frac{8\alpha^{-D-1}}{(2\pi)^{\frac{D}{2}+1}} \sum_{n=1}^{\infty} \int_0^{\infty} dy \frac{G_D(y)}{y} f_{\frac{D}{2}-1}(yu_n), \quad u_n = 2na/\eta, \quad (64)$$

where  $f_{\mu}(x) = K_{\mu}(x)/x^{\mu}$ . For  $0 \leq \nu < 1$  the integrand in the expression for  $p_{(\text{int})}^{(\text{D})}$  is positive which corresponds to an attractive force for all separations.

Now we turn to the investigation of the asymptotic behavior for the vacuum forces in the general case of Robin BC. In the limit of small proper distances between the plates,  $a/\eta \ll 1$ , to leading order we find

$$p_{(\text{int})}^{(j)} \approx -\frac{2(\eta/\alpha)^{D+1}}{(4\pi)^{D/2}\Gamma(D/2)} \int_0^{\infty} dx \frac{x^D}{c_1(x)c_2(x)e^{2ax} - 1}. \quad (65)$$

If, in addition,  $|\beta_j|/a \gg 1$ , one has

$$p_{(\text{int})}^{(j)} \approx -\frac{D\Gamma((D+1)/2)\zeta_R(D+1)}{(4\pi)^{(D+1)/2}(\alpha a/\eta)^{D+1}}, \quad (66)$$

and the corresponding force is attractive. In (66),  $\zeta_R(x)$  is the Riemann zeta function. The same result is obtained for Dirichlet BCs on both plates. In the case of Dirichlet BC on one plate and non-Dirichlet one on the other, the leading term is obtained from Eq. (66) with an additional factor  $(2^{-D} - 1)$ . In this case the vacuum force is repulsive at small distances.

In considering the large distance asymptotics, corresponding to  $a/\eta \gg 1$ , the cases of real and imaginary  $\nu$  must be studied separately. For positive values of  $\nu$ , one has

$$p_{(\text{int})}^{(j)} \approx -\frac{2\alpha^{-D-1}g_{\nu}^{(j)}\Gamma(\nu)}{\pi^{D/2+1}(2a/\eta)^{D-2\nu+2}}, \quad (67)$$

for non-Neumann BCs on the plate at  $z^D = a_j$  ( $|\beta_j| < \infty$ ) and

$$p_{(\text{int})}^{(j)} \approx -\frac{\alpha^{-D-1}g_{\nu}^{N(j)}\Gamma(\nu)}{\pi^{D/2+1}(2a/\eta)^{D-2\nu}}, \quad (68)$$

for Neumann BC ( $\beta_j = \infty$ ). Here the notations are as follows:

$$g_{\nu}^{(j)} = \left( \frac{D+1}{2} - \nu \right) \Gamma(D/2 - \nu + 1) \left[ 1 - 2 \left( \frac{\beta_j}{\eta} \right)^2 f_D \right] \sum_{n=1}^{\infty} \frac{(\delta_1 \delta_2)^n}{n^{D-2\nu+2}}, \quad (69)$$

$$g_{\nu}^{N(j)} = \Gamma(D/2 - \nu) f_D \sum_{n=1}^{\infty} \frac{(\delta_1 \delta_2)^n}{n^{D-2\nu}},$$

with  $f_D = -2\nu[\xi + (\xi - 1/4)(D - 2\nu)]$  and  $\delta_j = c_j(0)$ . Note that  $\delta_j = -1$  for non-Neumann BC, while  $\delta_j = 1$  if the BC is Neumann. In the case of non-Neumann BCs we have assumed that  $|\beta_j|/a \ll 1$ .

As it is seen from (68), for positive values of  $\nu$  and when  $f_D \neq 0$ , at large distances the ratio of the Casimir forces acting on the plate with Neumann and non-Neumann BCs is of the order  $(a/\eta)^2$ . Note that in neither of these cases does the force depend on the specific value of Robin coefficient in the BC on the second plate. For Dirichlet BC on the plate at  $z^D = a_j$  ( $\beta_j = 0$ ), at large separations the Casimir force acting on that plate is repulsive (attractive) for Neumann (non-Neumann) BCs on the other plate. The nature of the force acting on the plate with Neumann BC depends on the sign of  $f_D$  and can be either repulsive or attractive, in function of the curvature coupling parameter and of the field mass. For minimally and conformally coupled massive scalar fields one has  $f_D = \nu(D/2 - \nu)$  and  $f_D = \nu(1/2 - \nu)/D$ , respectively, and this parameter is positive. The corresponding force is attractive (repulsive) for Neumann (non-Neumann) BC on the second plate. Note that for the geometry of parallel plates in the Minkowski bulk the Casimir forces at large distances are repulsive for Neumann BC on one plate and for non-Neumann BC on the other plate. For all other cases of BCs the forces are attractive.

For imaginary  $\nu$ , the leading order terms at large separations between the plates are in the form

$$\begin{aligned} p_{(\text{int})}^{(j)} &\approx -\frac{4\alpha^{-D-1}|g_\nu^{(j)}|}{\pi^{D/2+1}(2a/\eta)^{D+2}} \cos[2|\nu|\ln(2a/\eta) + \phi_{(j)}], \quad |\beta_j| < \infty, \\ p_{(\text{int})}^{(j)} &\approx -\frac{2\alpha^{-D-1}|g_\nu^{\text{N}(j)}|}{\pi^{D/2+1}(2a/\eta)^D} \cos[2|\nu|\ln(2a/\eta) + \phi_{(j)}^{\text{N}}], \quad \beta_j = \infty, \end{aligned} \quad (70)$$

where the phases are defined in accordance with  $g_\nu^{(j)} = |g_\nu^{(j)}|e^{i\phi_{(j)}}$  and  $g_\nu^{\text{N}(j)} = |g_\nu^{\text{N}(j)}|e^{i\phi_{(j)}^{\text{N}}}$ . In this case the decay of the vacuum forces is oscillatory.

In Fig. 3, we have plotted the Casimir force for a  $D = 3$  scalar field with Dirichlet BC, minimally coupled to gravity, as a function of the proper distance between the plates, measured in units of the dS curvature scale  $\alpha$ . The figures near the curves correspond to the values of the parameter  $m\alpha$ . Values are taken in a way so to have both possibilities, with positive and purely imaginary values of the parameter  $\nu$ .

In Fig. 4 the dependence of the Casimir force on the parameter  $m\alpha$  is depicted for a given separation corresponding to  $a/\eta = 4$ . Conformally coupled scalar fields with Dirichlet and Neumann BCs are considered. For a massless field the force is the same for Dirichlet and Neumann BCs.

From the discussion given above it follows that for proper distances between the plates larger than the curvature radius of the dS spacetime,  $\alpha a/\eta \gtrsim \alpha$ , the gravitational field essentially changes the behavior of the Casimir forces compared with the case of the plates in Minkowski spacetime. The forces may become repulsive at large separations between the plates. In particular, for real values  $\nu$  and for Neumann BC on both plates, Casimir forces are repulsive at large separations, in the range of parameters for which  $f_D < 0$ . Recall that, for the geometry of parallel

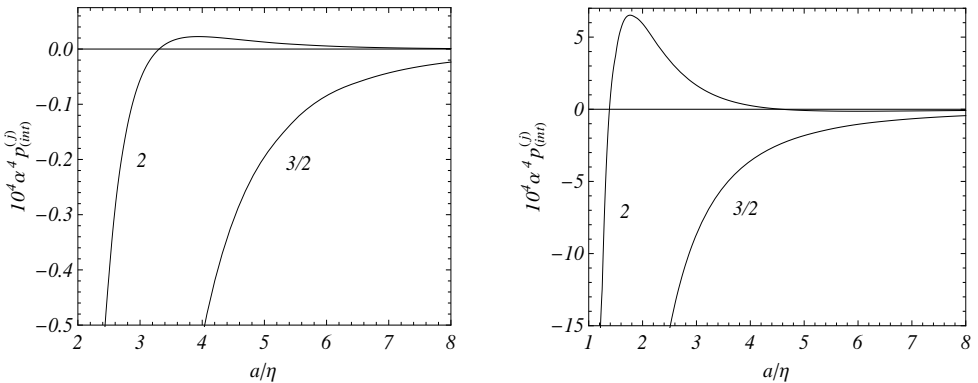


Figure 3: Interaction forces between the plates for a  $D = 3$  minimally coupled scalar field with Dirichlet (left plot) and Neumann (right plot) BCs. The figures near the curves are the values of the parameter  $\alpha m$ .

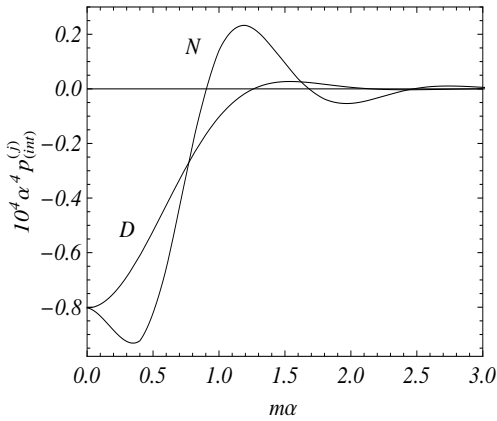


Figure 4: Interaction force between the plates for  $a/\eta = 4$  as a function of the field mass, for a  $D = 3$  conformally coupled scalar field with Dirichlet and Neumann BCs.

plates on the background of Minkowski spacetime, the only case with repulsive Casimir forces at large distances corresponds to Neumann BC on one plate and non-Neumann BC on the other. A remarkable feature of the influence of the gravitational field is the oscillatory behavior of the Casimir forces at large distances, which appears in the case of imaginary  $\nu$ . In this case, the values of the plate distance yielding zero Casimir force correspond to equilibrium positions. Among them, the positions with negative derivative of the force with respect to the distance are locally stable. As it follows from asymptotic formulas (67), (68), and (70), at large separations between the plates the decay of the Casimir forces as functions of the distance is power-law for both cases of massive and massless fields. Recall that, in Minkowski spacetime the corresponding Casimir forces decay as  $1/a^{D+1}$  for a massless field and they are exponentially suppressed by the factor  $\exp(-2ma)$  for a massive field.

It is also of interest to compare the features for the Casimir force in dS spacetime with the behavior of the Casimir forces for parallel plates in AdS spacetime. In Poincaré coordinates the corresponding line element is given by the expression

$$ds_{\text{AdS}}^2 = e^{-2\lambda y} \eta_{ik} dx^i dx^k - dy^2, \quad (71)$$

where  $\eta_{ik} = \text{diag}(1, -1, \dots, -1)$  is the metric tensor for  $D$ -dimensional Minkowski spacetime. For the corresponding Ricci scalar one has  $R = -D(D+1)\lambda^2$  and the AdS curvature radius is given by  $1/\lambda$ . For the general case of Robin BCs on two parallel plates, located at  $y = y_j$ ,  $j = 1, 2$ , the interaction forces between the plates are investigated in Ref. [31] (see also Refs. [32] for the case where an extra compact subspace is present). At large distances between the plates, as compared with the AdS curvature radius,  $\lambda(y_2 - y_1) \gg 1$ , the vacuum interaction forces per unit surface,  $p_{(\text{int})}^{(j)}$ , are exponentially suppressed by the factor  $\exp[2\nu_{\text{AdS}}\lambda(y_1 - y_2)]$  for the plate at  $y = y_1$  and by the factor  $\exp[(2\nu_{\text{AdS}} + D)\lambda(y_1 - y_2)]$  for the plate at  $y = y_2$ , where  $\nu_{\text{AdS}} = [D^2/4 - D(D+1)\xi + m^2/\lambda^2]^{1/2}$ . Note that in AdS spacetime the ground state becomes unstable for imaginary values of  $\nu_{\text{AdS}}$ . [33] Hence, in AdS spacetime the Casimir forces are exponentially suppressed for both massive and massless fields.

## 5. Conclusion

The natural appearance of dS spacetime in a variety of situations has stimulated considerable interest in the behavior of quantum fields propagating in this background. In the present paper we have discussed the properties of the quantum vacuum for a massive scalar field with general curvature coupling parameter. Among the most important local characteristics of the vacuum state are the VEVs of the field squared and the energy-momentum tensor. First we have considered dS spacetime with trivial topology described in flat coordinates. Unlike to the case of Minkowski spacetime, where the Poincaré invariance determines a unique vacuum state, in dS spacetime the symmetries do not determine the vacuum state completely. There are a set of vacuum states parametrized by a single complex parameter and

known as  $\alpha$  vacua. Among them only the Bunch-Davies vacuum state smoothly patches onto the Poincaré invariant Minkowski vacuum in the adiabatic limit. In free field theories (interacting only with background gravitational field), all properties of the quantum vacuum are encoded in two-point functions. For the evaluation of the Wightman function in dS spacetime with trivial topology, in section 2 we have employed the direct mode summation technique. The mode functions realizing the Bunch-Davies vacuum state are given by (11) and the Wightman function is expressed in terms of the hypergeometric function, Eq. (22). Having the Wightman function, the renormalized VEVs of the field squared and the energy-momentum tensor are found subtracting the corresponding DeWitt-Schwinger expansion truncated at the adiabatic order  $D + 1$  and taking the coincidence limit. Due to the maximal symmetry of the Bunch-Davies vacuum state these VEVs do not depend on the spacetime point. In the special case  $D = 3$  they are given by the expressions (23) and (24).

The effects of non-trivial spatial topology on properties of the Bunch-Davies vacuum state were discussed in section 3. We have considered  $(D + 1)$ -dimensional dS spacetime having the spatial topology  $R^p \times (S^1)^q$ . Both cases of the periodicity and antiperiodicity conditions along the compactified dimensions are discussed. A recurrence relation is derived which presents the vacuum energy-momentum tensor for the  $dS_{D+1}$  with topology  $R^p \times (S^1)^q$  in the form of the sum of the energy-momentum tensor for the topology  $R^{p+1} \times (S^1)^{q-1}$  and the additional part induced by the compactness of the  $(p + 1)$ th spatial dimension. The repeated application of the recurrence formula allows us to present the VEV of the energy-momentum tensor as the sum of the uncompactified dS and topological parts. Since the toroidal compactification does not change the local geometry, in this way the renormalization of the energy-momentum tensor is reduced to that for uncompactified  $dS_{D+1}$ .

At early stages of the cosmological expansion, corresponding to  $t \rightarrow -\infty$ , the vacuum energy-momentum tensor coincides with the corresponding quantity for a conformally coupled massless field and the topological part behaves like  $e^{-(D+1)t/\alpha}$ . In this limit the topological part dominates in the VEV. At late stages of the cosmological expansion,  $t \rightarrow +\infty$ , the behavior of the topological part depends on the value of  $\nu$ . For real values of this parameter the leading term in the corresponding asymptotic expansion is given by formula (41) and the vacuum stresses are isotropic. In this limit the topological part is suppressed by the factor  $e^{-(D-2\nu)t/\alpha}$ . In the same limit and for pure imaginary values of the parameter  $\nu$  the asymptotic behavior of the topological part in the VEV of the energy-momentum tensor is described by formulae (43), (45) and the topological terms oscillate with the amplitude going to the zero as  $e^{-Dt/\alpha}$  for  $t \rightarrow +\infty$ .

In section 4, we have studied the VEV of the energy-momentum tensor and the Casimir forces for a scalar field with an arbitrary curvature coupling parameter satisfying Robin boundary conditions on two parallel plates in dS spacetime. In the region between the plates, the VEV is decomposed into a boundary-free dS, a single plate-induced and an interference contributions, respectively. The vacuum energy-momentum tensor is non-diagonal, with the off-diagonal component corresponding

to the energy flux along the direction normal to the plates. Depending on the values of the coefficients in the boundary conditions and of the field mass this flux can be positive or negative. In the case of a conformally coupled massless field, the single plate contribution to the VEV of the energy-momentum tensor vanishes and the interference part is obtained from the corresponding result for the Minkowski bulk, by standard conformal transformation.

The vacuum forces acting on the plates are determined by the  $D$ -component of the stress. The normal stresses on the plates are presented as sums of single plate and interaction contributions. The contributions to the vacuum force coming from the single plate terms are the same from the left and from the right sides of the plate and thus give no contribution to the effective force. The interaction forces per unit surface are determined by formula (61) for general Robin BCs and by Eqs. (63),(64) in the special cases of Dirichlet and Neumann BCs. At small distances between the plates the vacuum forces are attractive, except for the case of Dirichlet BC on one plate and non-Dirichlet on the other, in which case the force turns out to be repulsive. At large separations and for positive values of  $\nu$ , the force acting on the plate decays monotonically as  $1/(2a/\eta)^{D-2\nu+2}$ , for non-Neumann BCs, and as  $1/(2a/\eta)^{D-2\nu}$ , in the case of Neumann BCs [see Eqs. (68)]. For imaginary values of  $\nu$  the behavior of the vacuum forces is damping oscillatory, in the leading order described by Eqs. (70). From the analysis carried out above, it follows that the curvature of the background spacetime decisively influences the behavior of the Casimir forces at distances larger than the curvature scale. As we have seen, in dS spacetime the decay of the forces at large separations between the plates is power-law. This is quite remarkable and clearly in contrast with the corresponding features of the same problem in Minkowski and AdS spacetimes.

## References

- [1] N. D. Birrell and P. C.W. Davies, *Quantum Fields in Curved Space* (Cambridge University Press, Cambridge, 1982).
- [2] A.D. Linde, *Particle Physics and Inflationary Cosmology* (Harwood Academic Publishers, Chur, Switzerland 1990).
- [3] A.G. Riess et al., *Astrophys. J.* **659**, 98 (2007); D.N. Spergel et al., *Astrophys. J. Suppl. Ser.* **170**, 377 (2007); U. Seljak, A. Slosar, and P. McDonald, *JCAP* **0610**, 014 (2006); E. Komatsu et al., arXiv:0803.0547.
- [4] S. Kachru, R. Kallosh, A. Linde, and S.P. Trivedi, *Phys. Rev. D* **68**, 046005 (2003).
- [5] E. Silverstein, arXiv:0712.1196.
- [6] N. A. Chernikov and E. A. Tagirov, *Ann. Poincare Phys. Theor. A* **9**, 109 (1968); E. A. Tagirov, *Ann. Phys.* **76**, 561 (1973); C. Schomblond and P. Spindel, *Ann.*

Inst. Henri Poincare A **25**, 67 (1976); E. Mottola, Phys. Rev. D **31**, 754 (1985); B. Allen, Phys. Rev. D **32**, 3136 (1985).

- [7] P. Candelas and D.J. Raine, Phys. Rev. D **12**, 965 (1975).
- [8] J.S. Dowker and R. Critchley, Phys. Rev. D **13**, 224 (1976).
- [9] J.S. Dowker and R. Critchley, Phys. Rev. D **13**, 3224 (1976).
- [10] T.S. Bunch and P.C.W. Davies, Proc. R. Soc. London, Ser. A **360**, 117 (1978).
- [11] A. Vilenkin and L.H. Ford, Phys. Rev. D **26**, 1231 (1982).
- [12] N. Kaloper, M. Kleban, A. Lawrence, S. Shenker, and L. Susskind, JHEP **11** (2002) 037.
- [13] P.R. Anderson, W. Eaker, S. Habib, C. Molina-París, and E. Mottola, Phys. Rev. D **62**, 124019 (2000).
- [14] G.N. Watson, *A Treatise on the Theory of Bessel Function* (Cambridge University Press, Cambridge, 1995).
- [15] I.S. Gradshteyn and I.M. Ryzhik, *Table of Integrals, Series and Products* (Academic, New York, 1980).
- [16] M. Lachièze-Rey and J.-P. Luminet, Phys. Rep. **254**, 135 (1995).
- [17] J. Levin, Phys. Rep. **365**, 251 (2002); N.J. Cornish, D.N. Spergel, G.D. Starkman, and E. Komatsu, Phys. Rev. Lett. **92**, 201302 (2004).
- [18] A. Linde, JCAP **0410**, 004 (2004).
- [19] G.D. Starkman, Class. Quantum Grav. **15**, 2529 (1998); N.J. Cornish, D.N. Spergel, and G.D. Starkman, Class. Quantum Grav. **15**, 2657 (1998).
- [20] V.M. Mostepanenko and N.N. Trunov, *The Casimir Effect and Its Applications* (Clarendon, Oxford, 1997); M. Bordag, U. Mohidden, and V.M. Mostepanenko, Phys. Rept. **353**, 1 (2001); E. Elizalde, S.D. Odintsov, A. Romeo, A.A. Bytsenko and S. Zerbini, *Zeta regularization techniques with applications* (World Scientific, Singapore, 1994).
- [21] A.A. Saharian and M.R. Setare, Phys. Lett. B **659**, 367 (2008).
- [22] S. Bellucci and A.A. Saharian, Phys. Rev. D **77**, 124010 (2008).
- [23] A.A. Saharian, Class. Quantum Grav. **25**, 165012 (2008).
- [24] E. R. Bezerra de Mello and A. A. Saharian, J. High Energy Phys. **12**, 081 (2008).

- [25] A.A. Saharian, *The Generalized Abel-Plana Formula with Applications to Bessel Functions and Casimir Effect* (Yerevan State University Publishing House, Yerevan, 2008); Preprint ICTP/2007/082; arXiv:0708.1187.
- [26] M. R. Setare and R. Mansouri, Class. Quantum Grav. **18**, 2659 (2001); M.R. Setare, Phys. Lett. B **637**, 1 (2006).
- [27] A. A. Saharian and T. A. Vardanyan, Class. Quantum Grav. **26**, 195004 (2009).
- [28] E. Elizalde, A. A. Saharian, and T. A. Vardanyan, Phys. Rev. D **81**, 124003 (2010).
- [29] K. Milton and A. A. Saharian, Phys. Rev. D **85**, 064005 (2012).
- [30] A. Romeo and A. A. Saharian, J. Phys. A: Math. Gen. **35**, 1297 (2002).
- [31] A. A. Saharian, Nucl. Phys. B **712**, 196 (2005).
- [32] A. A. Saharian, Phys. Rev. D **73**, 044012 (2006); A. A. Saharian, Phys. Rev. D **73**, 064019 (2006).
- [33] P. Breitenlohner and D. Z. Freedman, Ann. Phys. **144**, 249 (1982).

# Generation of a toroidal magnetic field in rotating neutron stars

D. M. Sedrakian

*Department of Physics, Yerevan State University  
1 Alex Manoogian Street, 0025 Yerevan, Armenia*

The electromagnetic properties of neutron stars (pulsars) are studied. It is shown that taking the presence of two angular rotation velocities of the components of neutron stars and the first corrections to the general theory of relativity into account in the equations of hydrodynamic equilibrium for the plasma and in Maxwell's equations, toroidal magnetic fields are generated.

## 1. Introduction

The possibility of field generation in neutron stars was considered in Ref. [1]. It was shown there that taking the general theory of relativity into account in the equations of hydrodynamic equilibrium for the plasma and in Maxwell's equations for the electromagnetic fields to the generation of toroidal magnetic fields. The following equation was obtained for the time derivative of the magnetic field:

$$\frac{\partial \mathbf{B}(0)}{\partial T} = \frac{mc}{e} \Omega^2 \frac{Gu(R)}{c^2 R} \sin \vartheta \cos \vartheta \boldsymbol{\tau}, \quad (1)$$

were  $R$ ,  $\vartheta$ , and  $\varphi$  are spherical coordinates,  $u(R)$  is the accumulated mass of a radius  $R$ ,  $m$  and  $e$  are the mass and charge of the proton,  $G$  and  $c$  are the gravitational constant and the speed of light,  $\Omega$  is the star's angular velocity, and  $\boldsymbol{\tau}$  is the unit vector in the  $\varphi$  direction. The equation was obtained for an initial time, when the electric current and magnetic field are zero. This result, however, was not correct, for the four-dimensional current as [1]

$$j^i = \frac{enc}{\sqrt{g_{00}}} \frac{dx^i}{dx^0}, \quad (2)$$

while the correct definition of this is

$$j^i = enu^i, \quad (3)$$

where  $u^i$  is the four-dimensional velocity. With this definition of the four-dimensional current the time derivative of the magnetic field goes to zero and no toroidal magnetic field is generated. Note that in Ref. [1] it was also assumed that in the "pre-" phase of a neutron star, all three particle species, neutrons, protons, and electrons, are normal.

However, it is well known [2] that at the temperatures  $T \leq 10^8$  of neutron star cores, neutrons and protons are more likely to be superfluid, while the electrons are normal. This means that during rotation of a neutron star its nuclear components (the neutrons and protons) will rotate with the superfluid angular velocity  $\Omega_s$ , while the normal component (and, therefore, the electrons, as well) will have an angular velocity  $\Omega_c$ . In general, the super fluid angular velocity  $\Omega_s$  and the normal angular velocity  $\Omega_c$  are not equal.

The purpose of this paper is to show that for  $\Delta\Omega = \Omega_s - \Omega_c \neq 0$ , a toroidal magnetic field can be generated and the rate of increase in the magnetic field is given by the right hand side of Eq.(1) times  $(1 - \Omega_c^2/\Omega_s^2)$ . If we assume that  $\Omega_c \ll \Omega_s$  during the lifetime of a pulsar, as occurs in several scenarios for the evolution of pulsars, then this factor may be of the order of unity [3].

## 2. The electric field of a “pre-” plasma with super fluid neutrons

The hydrodynamics equations for an individual charged component of plasma with angular velocity  $\Omega$  have the form [1]

$$\frac{\partial P}{\partial x^\alpha} - \left( \rho + \frac{P}{c^2} \right) \frac{\partial}{\partial x^\alpha} Inu^0 - \frac{1}{c} F_{\alpha i} j^i = 0, \quad (4)$$

were  $\alpha = 1, 2, 3$ ,

$$j^i = enu^i, \quad u^0 = \left( g_{00} + 2 \frac{\Omega}{c} g_{03} + \frac{\Omega^2}{c^2} g_{33} \right)^{-1/2}, \quad (5)$$

$u^i$  is the four-dimensional velocity of the plasma,  $\rho$  and  $P$  are the energy density and pressure of the plasma,  $j^i$  is the four-dimensional current, and  $F_\alpha$  is the electromagnetic field tensor. Here  $n$  is the particle number density of the plasma, while  $\rho$  and  $P$  are functions of  $n$ . Note that here, as opposed to Ref. [1], in Eq. (5) we have introduced the correct definition of the four dimensional current  $j^i$  ant the expression for  $u^0$  was obtained from the equation  $u^i u_i = 1$ .

In simple model of a neutron star its central part consists of superfluid neutrons and protons and normal electrons. The protons and electrons form an insignificant part, of the order of a few percent, of the star’s core compared to the neutrons. Thus, the bulk

of the core, the neutrons, forms a superfluid nuclear liquid. This type of core is surrounded by a solid shell made up of atomic nuclei and electrons. The dimensions of

the core of a neutron star are of the order of 10 km, and those for the shell are an order of magnitude smaller. As the neutron star rotates, the shell and the electrons in the core rotate as a normal fluid at angular velocity  $\Omega_c$ , while the bulk of the core (neutrons and protons) rotate as superfluid with angular velocity  $\Omega_s$ .

Writing Eq. (4) separately for the mixture of nuclear matter, consisting of neutrons and protons and the electrons, we obtain two equations that determine the electric field  $\mathbf{E}$  and  $\vec{\nabla}P_s(n_s)$ , where  $P_s(n_s)$  is the neutron pressure, which is equivalent of the pressure of the nuclear matter when the protons (1% of the nuclear matter) are neglected:

$$\vec{\nabla}P_s = -mc^2 n_s \vec{\nabla}Inu_s^0 \quad (6)$$

and

$$\mathbf{E} = -\frac{1}{en_e^0} \frac{\vec{\nabla}P_e}{n_e}, \quad (7)$$

where

$$u_s^0 = \left( g_{00} + 2\frac{\Omega_s}{c} g_{03} + \frac{\Omega_s^2}{c^2} g_{33} \right)^{-1/2},$$

$$u_e^0 = \left( g_{00} + 2\frac{\Omega_c}{c} g_{03} + \frac{\Omega_c^2}{c^2} g_{33} \right)^{-1/2}, \quad (8)$$

and  $P_e$  and  $n_e$  are the electron pressure and the number density. Equations (6) and (7) for  $\mathbf{E}$  and  $\vec{\nabla}P_s$  have been derived assuming that there is no initial electron current  $j^\alpha$ . Given that the neutrons form a nonrelativistic Fermi gas at the particle densities characteristic for neutron star cores ( $n \approx 10^{38} 1/cm^3$ ) and that electrons form an ultrarelativistic Fermi gas, it can be shown that

$$\frac{\vec{\nabla}P_s}{n_s} = \frac{\vec{\nabla}P_e}{n_e}. \quad (9)$$

Using Eq. (9), from Eqs. (6) and (7) we finally obtain

$$\mathbf{E} = \frac{mc^2}{e} \frac{\vec{\nabla}Inu_s^0}{n_e^0}, \quad (10)$$

where  $m$  and  $e$  are the proton mass and charge and  $c$  is the velocity of light.

### 3. Magnetic field generation effect

In a stationary gravitational field, the Maxwell equation relating the rate of change of the field,  $\partial\mathbf{B}/\partial t$ , to electric field has the form [4]

$$rot\mathbf{E} = -\frac{1}{c} \frac{\partial \mathbf{B}}{\partial t}, \quad \mathbf{B} = \frac{\mathbf{H}}{\sqrt{g_{00}}} + [\mathbf{g}\mathbf{E}]. \quad (11)$$

Here  $(\mathbf{g})_\alpha = -g_{0\alpha}/g_{00}$  and

$$(rot\mathbf{E})^\alpha = \frac{1}{2\sqrt{\gamma}} e^{\alpha\beta\gamma} \left( \frac{\partial E_\gamma}{\partial x^\beta} - \frac{\partial E_\beta}{\partial x^\gamma} \right), \quad (12)$$

where  $\gamma_{\alpha\beta} = -g_{\alpha\beta} + g_{00}g_\alpha g_\beta$  is the three-dimensional spatial metric and  $e^{\alpha\beta\gamma}$  is the unit antisymmetric tensor with  $e^{123}e_{123} = 1$ . Equation (11) shows that a magnetic field can be generated in the core of a neutron star if the curl of Eq. (10) is nonzero. In order to estimate the curl of the electric field and, therefore  $\partial\mathbf{B}/\partial t$ , the gas of nuclear particles can be treated as almost nonrelativistic and just those corrections that are linear in  $\varphi/c^2$  can be included in the components of the metric tensor [4]:

$$g_{00} = 1 + 2\varphi/c^2, \quad g_\beta^\alpha = \left(1 - \frac{2\varphi}{c^2}\right) \delta_\beta^\alpha, \quad g_{0\alpha} = 0. \quad (13)$$

Here it should be noted that in a rotating neutron star  $g_{03}$  is proportional to  $\varphi/c^2 \cdot \Omega r/c$ , where  $r$  is the distance from the axis of rotation. For these models of a neutron star the maximum value of  $\Omega r/c$  is no greater than 0.1, so we can assume that  $g_{03}$  is everywhere equal to zero. Then we can write the time component of the four dimensional velocity  $u^0$  in the form

$$u^0 = \left( g_{00} + 2\frac{\Omega}{c} g_{03} + \frac{\Omega^2}{c^2} g_{33} \right)^{-1/2} \approx 1 - \frac{\varphi}{c^2} + \frac{\Omega^2 r^2}{2c^2}.$$

Further, it is easy to see that

$$\vec{\nabla} \ln u^0 = -\frac{1}{c^2} (\vec{\nabla} \varphi - \Omega^2 \mathbf{r}). \quad (14)$$

Substituting Eq. (14) in Eq. (10), and taking Eqs. (11), (12) and (13) into account, we obtain

$$\frac{\partial \mathbf{B}}{\partial t} = \frac{m}{ec} \frac{1}{R} \frac{\partial \varphi}{\partial R} (\Omega_s^2 - \Omega_c^2) [\mathbf{r}, \mathbf{R}], \quad (15)$$

where  $\mathbf{R}$  and  $\mathbf{r}$  are the spherical and cylindrical radius vectors. Here we note again that Eq. (15) has been derived for an initial time when the electric currents  $j^\alpha = 0$  and there is no magnetic field, i.e.  $\mathbf{B} = 0$ . Expanding the vector product on the right of Eq. (15) and substituting  $d\varphi/dR = Gu(R)/R^2$  ( $u(R)$  is the accumulated mass in a sphere of radius  $R$ ), we finally obtain

$$\frac{\partial \mathbf{B}(0)}{\partial t} = \frac{mc}{e} \Omega_s^2 \left(1 - \frac{\Omega_c^2}{\Omega_s^2}\right) \frac{Gu(R)}{c^2 R} \sin \vartheta \cos \vartheta \tau. \quad (16)$$

Note that  $\partial \mathbf{B}(0)/\partial t$  is nonzero, since as the angular velocity of a neutron star (pulsar) decreases there is always a nonzero, stationary difference between the angular velocities of the superfluid and normal motions, i.e.  $\Delta\Omega = \Omega_s - \Omega_c \neq 0$ . The value of  $\Delta\Omega$  depends on the pinning of neutron vortices and, as observations of the jump in the angular velocity of the Vela pulsar show, this difference can be of the order of  $\Delta\Omega/\Omega \sim 10^{-4}$ , where  $\Delta\Omega = \Omega_s - \Omega_c$ . However, in some scenarios for the evolution of neutron stars the factor  $(1 - \Omega_c^2/\Omega_s^2)$  can be of the order of unity [3].

Therefore, from Eq. (16) it follows that a toroidal field develops in a slowing-down neutron stars and increases with time. The existence of the superfluid rotation of the nuclear component of the neutron star and taking the corrections to the Einstein theory into account mean that the electric field becomes rotational and depends on  $z$ . This, in turn, leads to the development of convection electric currents and the generation of a toroidal magnetic field [5].

## References

- [1] D. M. Sedrakian, *Astrofizika* **6**, 615 (1970).
- [2] D. M. Sedrakian and K. M. Shakhabasyan, *Usp. Fiz. Nauk* **161**, 3 (1991).
- [3] A. M. Sedrakian and D. M. Sedrakian, *Dokl. Akad. Nauk Armenii* **96**, 45 (1996).
- [4] L. D. Landau and E. M. Lifshitz, *Field Theory* (Nauka, Moscow, 1972, in Russian).
- [5] J. W. Roxburgh and P. A. Stritmatter, *Mon. Notic. Roy. Astron. Soc.* **133**, 1 (1966).

# ФИЗИЧЕСКИЕ ОСОБЕННОСТИ УФ - ГАЛАКТИК

Э.Е.Хачикян

*Бюраканская Астрофизическая Обсерватория, Бюракан, Армения*

Исследование физики Активных Галактик все еще находится в центре внимания внегалактической астрономии. Полученные наблюдательные данные по галактикам с избытком ультрафиолетового излучения в их спектре (УФ-галактики) пока не получили полного объяснения в рамках классической физики. В настоящей статье рассмотрены некоторые факты, которые, по мнению автора, не получили полного физического объяснения. Так как она представляется по случаю юбилея академика Э.В.Чубаряна, то преследует цель обратить внимание физиков, присутствующих на этом симпозиуме, на эти наблюдательные факты.

## 1. Введение

В начале прошлого века еще не было известно о существовании небесных объектов вне нашей Галактики. Лишь в конце двадцатых годов XX-го века американским астрономом Э.Хабблом были открыты новые галактики, которые им были классифицированы по их внешнему виду. Однако, по одному внешнему виду галактики невозможно судить о физических ее особенностях. В дальнейшем выяснилось, что основную роль в галактиках играет ядро или их центральная область. И первым на существенную роль ядер в эволюции галактик обратил В.Амарцумян. Часто цитируется изречение широко известного американского астрофизика А.Сандейджа: « Ни один астроном не будет сегодня отрицать, что действительно тайна окружает ядра галактик, и первым, кто осознал, какая щедрая награда содержится в этой сокровищнице, был Амбарцумян». В.А.Амбарцумян неоднократно отмечал, что наиболее важным его открытием (или идеей) является концепция об активности ядер галактик, которая была предложена им еще более чем полвека тому назад и была изложена в 1958 году в докладе на Сольвейской конференции в г. Льеже.[1]. И, действительно, ни где-либо, а в стенах Национальной Академии Наук США, это идея В.А. была оценена как революционная Коперниковского масштаба.

К активным галактикам относятся Сейфертовские галактики, Радиогалактики, галактики типа BL Lac (типа BL Ящерицы), УФ галактики (Маркаряновские и Казаряновские галактики), и Квазары. Все они в основном характеризуются наличием ярких, как разрешенных, так и запрещенных эмиссионных линий в спектре. Энергия их излучения находится в пределах  $10^{43}$ -  $10^{47}$  эрг/с. На основании наблюдательного материала, полученного на крупнейших оптических и радиотелескопах,

Амбарцумян описал следующие формы активности галактик [2]:

1. Извержение газовой материи виде джетов или облаков из области ядра со скоростью до сотен и тысячи км/с (Рис.1).

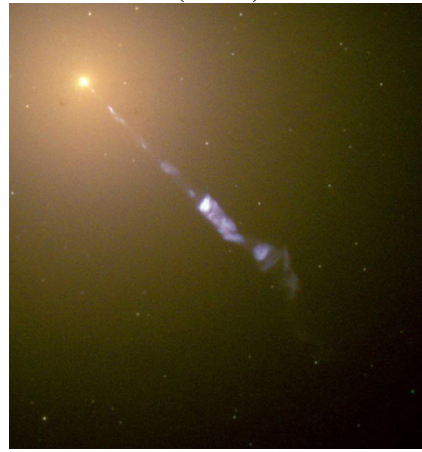


Рис.1: Virgo A (Messier 87)

2. Непрерывное истечение потока релятивистских частиц или других агентов, производящих частицы высоких энергий, в результате которого вокруг ядра может формироваться радиогало - Cygnus A (Лебедь А).( Рис.2).

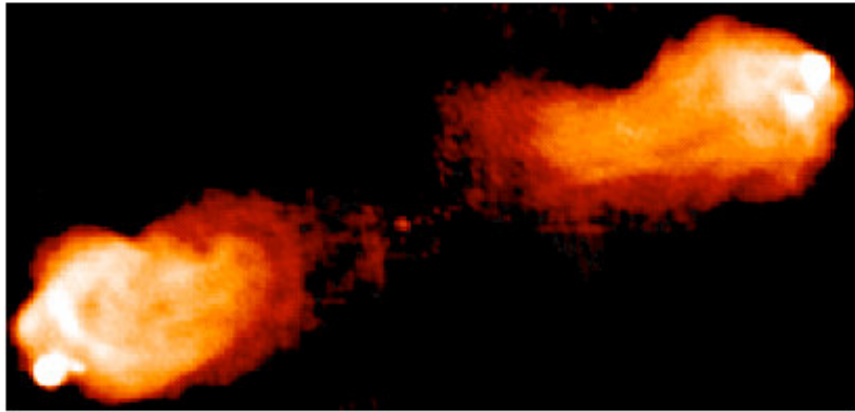


Рис2. Cygnus A (Лебедь А)

3. Эруптивные выбросы концентрированной релятивистской плазмы NGC5128 (Centaurus A) и др. (Рис.3).



Рис.3. Centaurus A

4. Эruptивные выбросы газовой материи наподобие M82.



Рис.4. M82

5. Выбросы компактных голубых конденсаций с абсолютной величиной порядка карликовых галактик (NGC3561-Ambartsumian Knot, IC1182). В этом случае возможно также деление ядра на два или более сравнимых по величине компонент, инициирующих формирование кратных галактик. (Рис5).

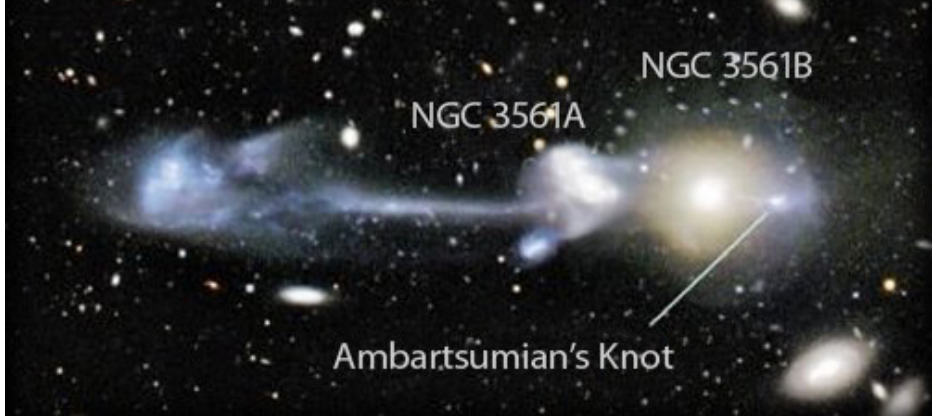


Рис.5: NGC3561-Ambartsumian’s Knot

Галактика считается активной, если в ней наблюдается хотя бы одна из форм активности. Если войти в интернет и заказать “Ambartsumians knot” то интернет выдаст вам картину которая представлена на Рис.5. Как хорошо видно на рисунке из галактики NGC3561B выброшено вправо от галактики звездообразное сгущение, которое оказалось голубого цвета.

Амбарцумян ставить задачу по выявлению новых активных галактик голубого цвета, каким обладает “Ambartsumians knot” Эту задачу Амбарцумян поручил Маркаряну и Казаряну, которые начали поиск галактик с аномально голубым цветом. Первый из них обнаружил 1500 объектов с ультрафиолетовым избытком (УФ-галактики) (Первый Бюраканский обзор (FBS) [3]), а второй - более 700 УФ-галактик, [4]. Общее число УФ-галактик составляют примерно 5% от общего числа галактик поля [3].

В настоящее время наиболее интенсивно ведутся исследования именно УФ - галактики из списков Маркаряна и Казаряна. Поэтому мы вкратце рассмотрим результаты исследования этих галактик и опишем проблемы, возникшие вследствие этих работ. Напомним, что все УФ - галактики объединены в одну группу ввиду наличия в их спектрах УФ избытка.

Хотя в настоящее время активные галактики занимают основную часть внегалактических работ, но многие исследователи и, в особенности молодые из них, не знают, что первооткрывателем активных галактик был Виктор Амбарцумян. Фактически в настоящее время почти все важнейшие идеи В.А. подтверждаются теоретически или экспериментально. Однако, одна из вышеотмеченных важнейших идей об активности галактик, в особенности природа двухъядерных галактик и галактик со сложной структурой в их центральных областях, является дискуссионной (см. пункт 5).

## 2. Основные характеристики спектров УФ-галактик

Первые же наблюдения спектров галактик из списка Маркаряна [3] и Казаряна показали[4], что эти галактики являются одними из самых активных из известных галактик. Более того, из 70 галактик первого списка Маркаряна семь оказались сейфертовскими галактиками, отличающимися широкими эмиссионными линиями в спектре, ширина которых иногда достигает 100-150 Å. А галактики № 9 и 10 показали рекордную для сейфертовских галактик высокую светимость, заполнившую пробел между нормальными гигантскими галактиками и квазарами. Галактика же под №102 в списке Казаряна оказалась самой далекой сейфертовской галактикой и самым близким квазаром(QSO) с красным смещением  $z=0.135$ . Всего же до этого времени было известно менее 10 сейфертовских галактик!

Спектры УФ-галактик по виду значительно отличаются друг от друга, как по наличию эмиссионных линий, так и по их ширине и интенсивности. В них в основном наблюдаются яркие и широкие эмиссионные линии Бальмеровской серии водорода, гелия, запрещенные линии кислорода, серы, неона, азота и других. Спектры УФ-галактик впервые были классифицированы в [5]. Подавляющее большинство УФ-галактик имеют эмиссионный спектр (85%) [6,7], среди которых сейфертовских галактик порядка 10% [8,9].

Галактики с УФ избытком не являются каким-то специальным морфологическим типом галактик: среди них имеются все Хаббловские типы галактик, галактики Цвикки и др. Их красное смещение совершенно различно от  $\sim 0.002$  до  $\sim 0.2$ . А галактика Марк132 с красным смещением  $z = 1.75$  является одним из ярчайших QSO с  $M_V \sim -28$ . Так что абсолютные звездные величины галактик с УФ избытком лежат в интервале между  $M=-13$  и  $M = -28$ . 10% УФ-галактик являются двуядерными галактиками [10-12]. Следует особо отметить тот факт, что в список галактик с УФ избытком были включены объекты, которые, как оказалось, не являются галактиками или ядрами галактик, а Сверхассоциациями вне центральных областей тех или иных определенных галактик. Впервые автором и Арпом было показано, что Марк94 **не является галактикой**, а Сверхассоциацией в спиральной галактике с перемычкой III Zw 0834 + 51[13](Рис.6). Десятки таких галактик - Сверхассоциаций были обнаружены в списках УФ - галактик[14].

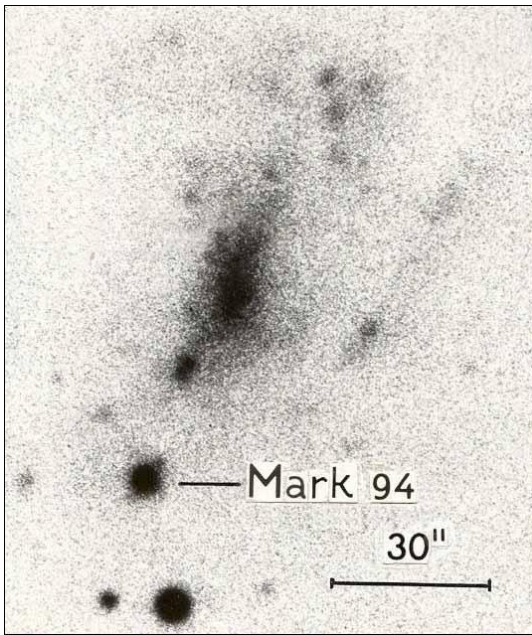


Рис.6 Фотография Марк.6, полученная на 6м. телескопе России

Переменность галактик с УФ избытком является одним из их удивительных свойств. Согласно концепции Амарцумяна, одной из форм активности галактик являются эруптивные выбросы газовой материи из их ядер, вследствие чего наблюдается изменение спектра всей галактики. Такой выброс из ядра сейфертовской галактики второго типа Sy2 Марк.6 впервые наблюдался в течении промежутка времени ,продолжительностью всего в один год [15]. В результате такого выброса у водородных эмиссионных линий появились широкие эмиссионные компоненты, смещенные в коротковолновую часть спектра. Смещение соответствовало скорости выброса порядка 3000 км/сек [15] (Рис.6а). Недавно, 24 июля 2009г спектр Маркб был наблюден на 6м телескопе САО (Рис.6б). Как видно из Рис.6б скорость выброса уменьшилось до примерно 2500 км/сек ! Обсуждение этого факта будет приведено ниже. Второй такой выброс наблюдался в 1994 году у галактики с УФ избытком Каз163 [16].

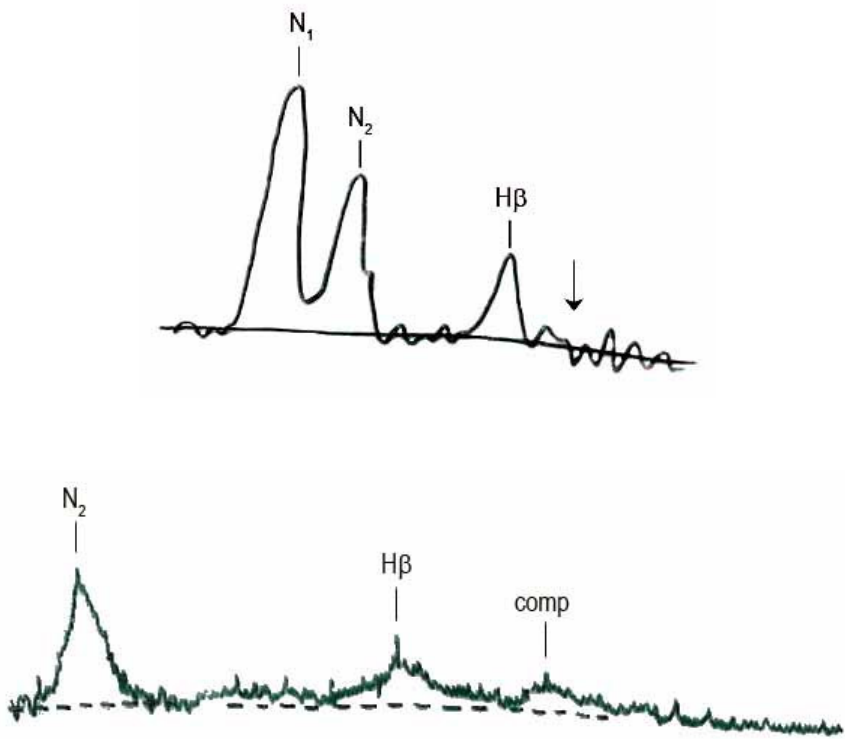
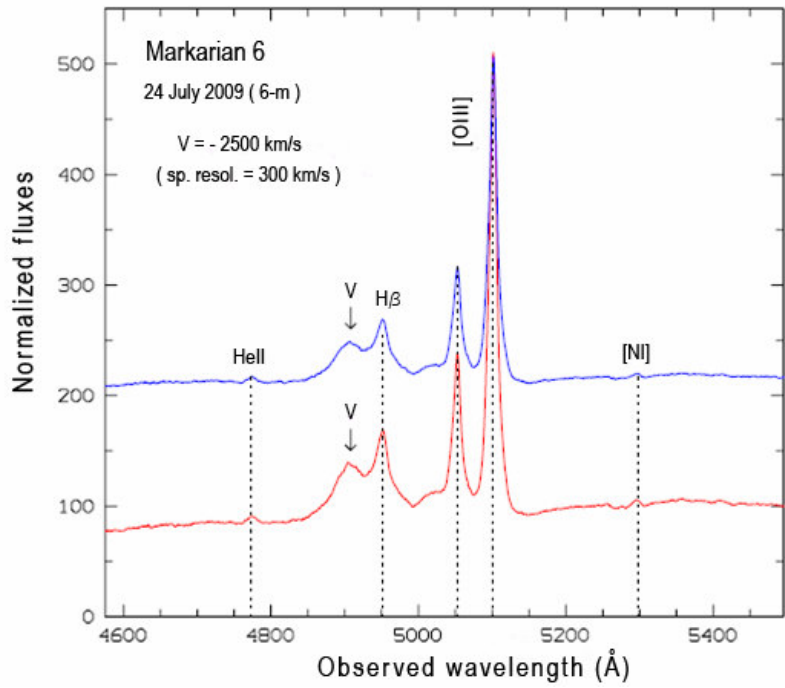


Рис 6а: Регистрация спектров Маркб в области  $H\beta$ : 5 Декабря 1967г. (верхний снимок), 27 Января 1967г. (нижний снимок).

Мы привели некоторые основные, но далеко не полные характеристики и наблюдательные данные о спектрах галактик и некоторых объектов, имеющих УФ избыток. Теперь разъясним наше понимание и оценку этих весьма интересных данных с точки зрения их физической природы.



### 3. Обсуждение

Во всех вышеупомянутых формах активности УФ-галактик основную роль играет УФ избыток в непрерывном спектре, который и объединяет их в одну группу. Любой объект при любой температуре излучает непрерывный спектр, в том числе и в области ультрафиолета, согласно закону Планка. Под выражением «избыток в ультрафиолете» предполагается, что непрерывный спектр в этой области превосходит по интенсивности таковой при излучении по закону Планка. При этом избытка в УФ области ясно не может наблюдаться, если излучение выполняется по закону Планка. Естественно возникает вопрос: **какова физическая природа источника УФ избытка**, который обнаружен у всех объектов? Что эта за субстанция? Это является основным и важнейшим вопросом в физике УФ-галактик, который, пока остается не решенным.

Некоторые из вышеупомянутых наблюдательных данных, связанных с наличием ультрафиолетового излучения, также требуют физического обоснования. Рассмотрим некоторые из них.

a). Значительное число Сверхассоциаций (СА) оказались среди активных галактик [14] (Марк59, Марк94 и др. См. Рис7). СА состоят, в основном, из звезд типа О и В, которые излучают согласно закону Планка и не имеют УФ избытка. Следовательно, кроме звезд в них имеется какой-то источник,

ответственный за УФ избыток. Так как наблюдаются изолированные СА в межгалактическом пространстве, то естественно предположить, что они являются одной из форм активности галактик.

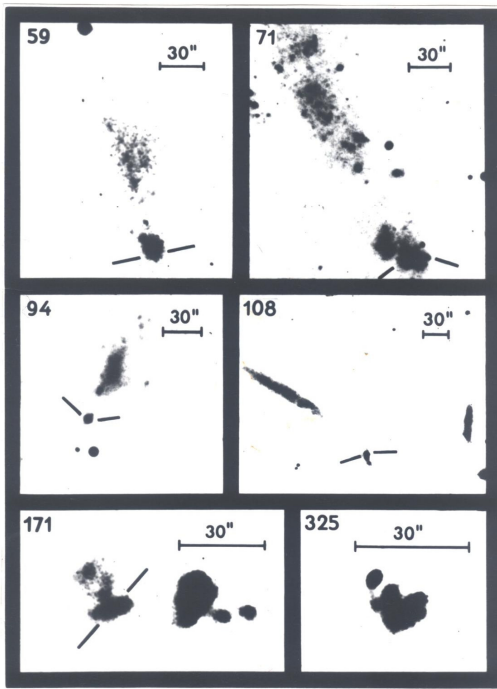
б). УФ - галактики, составляющие по количеству небольшой процент от общего числа галактик (порядка 5%), тем не менее, формируют в ряде случаев двойные и иногда более сложные системы. Отметим, например, Марк305 и Марк306, составляющие двойную систему (Рис.8)[17], Мы специально выделили эту совместную систему, потому что они сильно отличаются по своим физическим и морфологическим особенностям: Марк305 является звездообразным объектом, без каких либо эмиссионных линий в спектре, в то время как Марк306 двуядерная спиральная галактика с яркими эмиссионными линиями в спектре [18] (Рис8). Отметим, что по Маркаряну (вероятно по ошибке) приводится противоположное описание спектров этих галактик. Такими же системами являются Марк261 и Марк262, Каз.65 и 66, Каз.49 и Каз50, Каз.135 и 136 и многие другие.

в). Большой процент УФ-галактик (порядка 10%), показывают двуядерную структуру (Марк212, Марк266, Марк739,) [10-12], а некоторые галактики в центральных областях имеют многокомпонентную структуру Марк7, Марк8, Каз5 [19-21]. Механизм образования двуядерных и многокомпонентных в центральных областях галактик до конца не выяснен. Как образуются такие ядра? Каков физический механизм образования этих ядер?

В настоящее время рассматриваются две альтернативные модели по этой проблеме:

- а) физическая активность ядра-монстра, делящая на две или более части (5-ый пункт формы активности Амбарцумяна);
- б) столкновение и слияние ядер двух или более независимых галактик, вследствие их беспорядочного движения в межгалактическом пространстве. (В настоящее время мнение многих астрофизиков, ничем не подтвержденное).

Имеются многочисленные наблюдательные факты подтверждающие правильность 5-го пункта формы активности В. Амбарцумян. Приведем два примера.



ис. 7: Номера на рисунках соответствуют номерам УФ-галактик в списках Маркаряна.

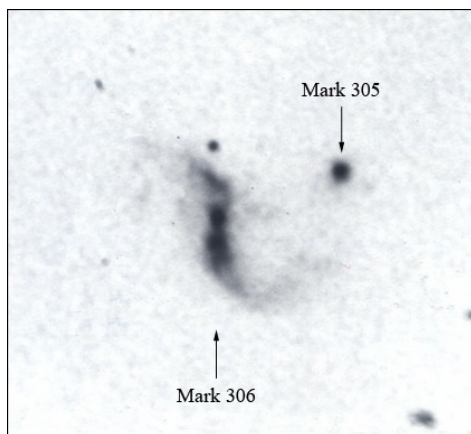


Рис. 8

В первую очередь следует представить очень интересную систему внегалактических объектов в области УФ галактик Марк261 и Марк262, составляющих, по всей вероятности, физически связанную систему в небольшом объеме порядка размеров нашей галактики ( $z=0.03$ )[22,23]. На Рис.9 приведена фотография этой области, полученная в первичном фокусе 5м. Паломарского телескопа (США).

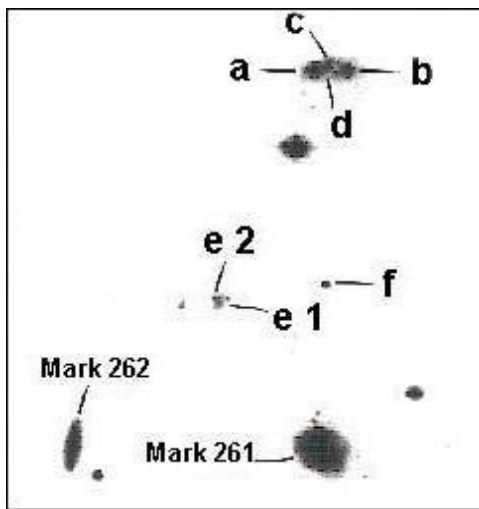


Рис. 9: Фотография получена в первичном фокусе 5м телескопа США.

Кроме Марк.261 и 262 на рисунке обозначены объекты "а", "б", "с", "д", "е" и "ф". На прямых фотографиях "а" и "б" выглядят как две слившиеся звезды примерно 18 видимой звездной величины. Спектры этих "звезд" были получены на 5м телескопе США и 6м телескопе России. Результат был неожиданный: оказалось, что это не звезды, а внегалактические объекты ( $z=0.03$ ) с яркими эмиссионными линиями. Причем спектры оказались до такой степени идентичными, что они получили название "объекты-близнецы"[22]. Но совершенно удивительным оказалось обнаружение между этими очень тесно расположенными объектами еще двух объектов ("с" и "д"), спектры которых, полученных на 6м телескопе России, оказались совершенно идентичными не только между собой, но и со спектрами "а" и "б" (Рис.10а, 10б). Выяснилось также, что объект "е" является внегалактическим, двойным ("е1","е2") , и в его спектре наблюдаются те же эмиссионные линии, что и во всех предыдущих объектах "а", "б", "с" и "д"[24] (Рис.10с).

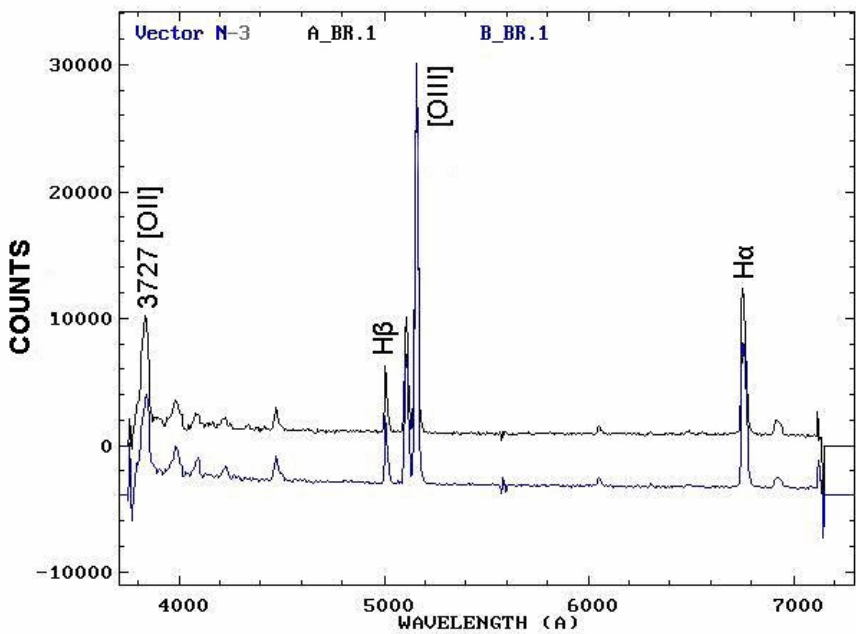


Рис. 10а: Регистрограмма спектров объектов «а» (верхний черный спектр) и «б» (нижний голубой спектр)(бм телескоп России).

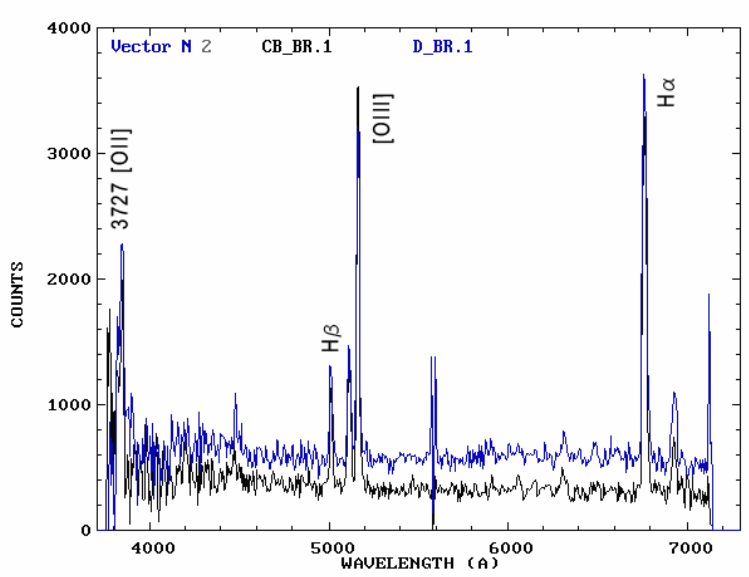


Рис. 10б: Регистрограмма спектров объектов "с" (черный нижний спектр) и "д" (голубой верхний спектр)(бм телескоп России).

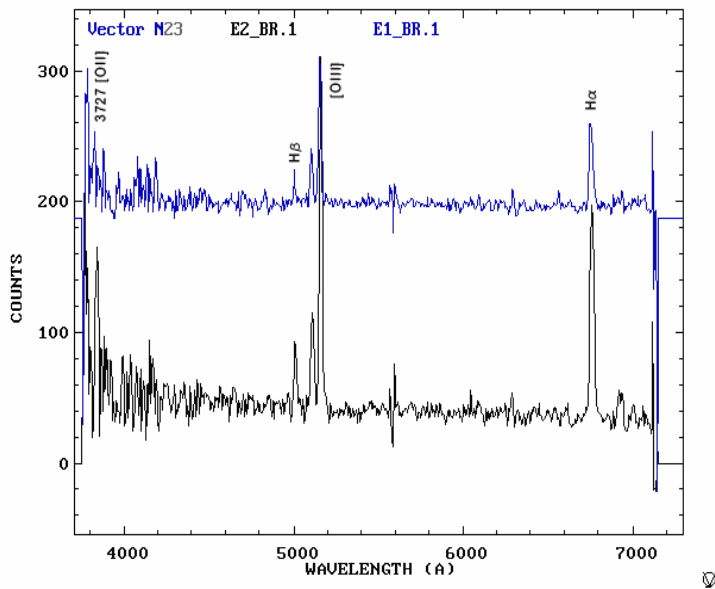


Рис. 10с: Регистрограмма спектров объектов "е1" (черный нижний спектр) и "е2" (голубой верхний спектр)(6м телескоп России).

Совершенно ясно, что вероятность образования такой системы галактик с идентичными эмиссионными спектрами при случайном движении независимых объектов ничтожно мала. Такими же системами УФ-галактик являются Марк7 и Марк8, состоящие из пяти сгущений с яркими эмиссионными линиями в спектре[19-21].

Как уже излагалось выше, одной из форм активности галактик является выбросы из ядра газовой материи в виде джетов или облаков. Большой интерес представляют галактики с джетами, причем ими могут быть и одноядерные (Марк423), и двуядерные (Марк273), и многоядерные (Марк773, Каз.5) галактики. Считаем необходимым обратить особое внимание на галактику Марк 273(Рис3)[17,25]. На левом снимке представлена фотография галактики, полученная на космическом телескопе «Хаббл». Общий размер галактики по дельта составляет примерно 70 угловых секунд. Хорошо виден джет, исходящий из южного ядра галактики и имеющий длину примерно 45 угловых секунд. Каждая угловая секунда соответствует примерно 70 пс. Удивительная картина ядра этой галактики представлена на правом рисунке. Всего примерно в 5 угловых секундах по  $\delta$  расположены все три ядра галактики: одно южное и два северных! Причем расстояние между северным ядром и двойным ядром не более 70 пс! Нет сомнения, что эта система представляет собой одну галактику со сложным ядром и джетом.

*Таким образом, ультрафиолетовый избыток является всеобщей характеристикой для всех активных галактик, независимо от их морфологии, строения центральных областей, абсолютной яркости, красного смещения, переменности и т.д.*

Физическая природа источника этого ультрафиолетового избытка остается загадкой. Для выяснения этого феномена, по нашему мнению, требуются новые как теоретические, так и наблюдательные исследования.

### Л И Т Е Р А Т У Р А

1. Ambartsumian V.A., XI Solvay Conference Report, p.241, 1958
2. Ambartsumian V.A., Transaction IAU, XIB, p.145, 1962.
3. Б.Е.Маркарян, Астрофизика, **3**, 55,1967; **5**, 443,1969; **5**,581,1969.
4. М.А.Казарян, Астрофизика, **15**, 5, 1979; **15**,193,1979; **16**, 17, 1980.
5. E.Ye.Khachikian, Astron.Journal, **73**, 891,1968.
6. Э.Е.Хачикян, Д.Видман, Астрофизика, **4**, 587, 1968.
7. Э.Е.Хачикян, Д.Видман, Астрофизика, **5**, 113, 1969.
8. E.Ye.Khachikian, D.Weedman, Bull.American Astron.Soc., March 1971.
9. Э.Е.Хачикян, Д.Видман, Астрофизика, **7**, 389, 1071.
10. А.Петросян, К.Саакян, Э.Е.Хачикян, Астрофизика, **14**, 69, 1978.
11. А.Петросян, К.Саакян, Э.Е.Хачикян, Астрофизика, **15**, 209, 1979.
12. А.Петросян, К.Саакян, Э.Е.Хачикян, Астрофизика, **15**, 373, 1979.
13. Э.Е.Хачикян, Г.Арп, Астрофизика, **10**, 173, 1974.
14. Э.Е.Хачикян, К.Саакян, Астрофизика, **11**, 207, 1975.
15. E.Ye.Khachikian, D.Weedman, Ap.J., **164**, L 109, 1971.
16. М.А.Казарян, Астрофизика, **37**,1, 1994.
17. E.Ye.Khachikian, Proceed. IAU Symp. No121, Edited by E.Khachikian, K.Fricke, J.Melnick, Byurakan, Armenia, p.65, 1987.
18. Э.Е.Хачикян, А.Петросян, М.Турато, Астрофизика, **24**, 5, 1986,
19. Э.Е.Хачикян, Астрофизика, **8**, 529, 1972.
20. А.Н.Буренков, Э.Е.Хачикян, Астрофизика, **32**. 245, 1990.
21. E.Ye.Khachikian, et al. Mon. Notice. Roy. Astron. Soc., **368**, 461, 2006.
22. Г.Арп, Э.Е.Хачикян, Дж.Айдман, Астрофизика, **10**, 7, 1974.

- 23.** Э.Е.Хачикян, Л.Саркисян, Астрофизика, **48**, 503, 2005.
- 24.** Э.Е.Хачикян, Астрофизика, **53**, 5, 2010.
- 25.** J.H.Knapen, S.,Laine, J.A.Yates, A.Robinson, A.M.Richards, R.Doyyon,,  
D.Nadeau, Ap.J.**490**, Letters 29-32, 1998.

# Tornado mechanism of astrophysical jets generation, acceleration and collimation

M. G. Abrahamyan

*Department of Physics, Yerevan State University  
1 Alex Manoogian Street, 0025 Yerevan, Armenia*

## 1. Introduction

Jet eruptions are a universal phenomenon in the universe. This phenomenon encompasses a wide range of astrophysical objects, from active galactic nuclei (AGN) to young stellar objects (YSO) within our galaxy. Supersonic outflows with less collimation are observed in massive hot stars, such as bright blue variables, as well as in low-mass stars, such as protoplanetary clouds (Gonzalez et al., 2004, Soker, 2004). These are all observed in the final evolutionary stages of these objects.

Recent extraterrestrial observations of the sun have shown that the solar corona is full of jets and flares. Although the total energy of the solar jets and flares is much less than in cosmic jets, the spectra and variability of the electromagnetic waves emitted from solar jets and flares are similar to those from cosmic flares (Shibata and Aoki, 2004)

Despite the enormous difference in their sizes and powers (AGN jets have typical sizes of  $\sim 10^6$  pc, with core velocities on the order of the speed of light, and source masses of  $\sim 10^{6-9} M_\odot$ , while the typical sizes of YSO jets are  $\sim 1$  pc, with node velocities of  $\sim 10^{-3} c$ , and masses of  $\sim M_\odot$ ). Most of the outflows are morphologically similar and apparently have a common physical origin. There is proof of the existence of an accretion disk surrounding the central sources (Königl, 1986, Dal Pino, 1995, Bridle, 1998, Reipurth & Bally, 2001).

Rotation with the velocity on the order of  $\sim 10$  km/s of many jets from YSOs has been established (Coffey et al., 2008, 2010, Chrysostomou, 2008). In some cases jets "swing" with increasing amplitude from side to side (e.g., HH83 and the jets of HH110 (Reipurth, 1989), jet of AGN object 1803+784 (Matveenko et.al, 2007), rather than appearing as chains of nodes.

The temperature of the jets from YSOs is slightly greater than  $\sim 10^4$  K, and the corresponding sound speeds are on the order of  $\sim 10$  km/s (Bacciotti & Eislöffel, 1999). The YSO jets have radii  $R_j \sim 3 \times 10^{15}$  cm, average hydrogen density  $\sim 10^{4-5}$  cm<sup>-3</sup> (Morse et al., 1992). Observations yield a somewhat uncertain value for

the ratio of the densities of the jet and surrounding medium on the order of  $\rho_j/\rho_s \sim 20$  (Perlman et al., 1999).

The origin of the jets and the mechanisms for their formation are not fully understood. Since the erupting matter is partially ionized, the strong collimation of jets is associated with magnetic fields (Bisnovatyi-Kogan, Komberg, Fridman, 1969). The magnetic field determines the direction of the jet and an axial current may stabilize the elongated shape of a jet at large distances from its source (Bisnovatyi-Kogan, 2004, 2007).

In this paper a vortical mechanism for the generation, acceleration, and collimation of astrophysical jets is proposed on the basis of exact vortical solutions of the hydrodynamic equations.

## 2. Equilibrium state of the source

Consider a rotating protostellar formation of mass  $M$  and polar radius  $R$  in an incompressible fluid model. The equilibrium state of the rotating gravitating mass is determined by Mc'Lauren spheroid (Chandrasekhar, 1969). The equilibrium of an axial cylindrical region with a lower base at depth  $H$  from the pole of the spheroid (Fig. 1) in a cylindrical coordinate system rotating with angular velocity  $\Omega$  is described by the equations

$$\frac{\partial P^0(r, z)}{\partial r} = -r(\Omega_0^2 - \Omega^2)r, \quad \frac{\partial P^0(r, z)}{\partial r} = -r\Omega_0^2 B(R - H + z), \quad (1)$$

where

$$\Omega_0^2 = 2pGrA, \quad A = \frac{2}{e^2} - \frac{2\sqrt{1-e^2}}{e^3} \arcsin e, \quad B = \frac{1-A}{A}.$$

$(R-H)$  is the distance from the center of the spheroid to the lower base of this region, which is taken as the origin for the coordinate  $z$ , and  $r$  is the radial cylindrical coordinate. Integrating Eq. (1) subject to the condition  $H \ll R$ , we find the equilibrium pressure to be<sup>1</sup>

$$P^0(r, z) \cong r\Omega_0^2 B[2RH - (1-e^2)r^2 - 2Rz - z^2] \quad (1a)$$

where we have set

$$\Omega^2 = \Omega_0^2 [1 - 2B(1-e^2)]. \quad (2)$$

---

<sup>1</sup> Here and in the following we neglect  $H^2$  compared to  $R^2$ .

These equations describe a Mc'Lauren spheroid with polar semiaxis  $R$  and eccentricity  $e$  in the meridional cross section rotating with an angular velocity  $\Omega$ .

The isobaric surfaces are obviously spheroids, while the equation for the isobar intersecting the  $z = 0$  plane in the chosen coordinate system along a circle of radius  $r_0$  at depth  $H$  from the pole of the cloud is

$$z^2 + 2Rz - (1 - e^2)(r_0^2 - r^2) = 0. \quad (3)$$

The pressure at the lower base  $z = 0$  is equal to

$$P^0(r, 0) = \rho \Omega_0^2 B (1 - e^2) (r_s^2 - r^2). \quad (3a)$$

Equation (1a) implies that the  $z = 0$  plane intersects the outer boundary of the protostar at a distance  $r_s$  from the axis of rotation (Fig. 1) given by

$$r_s^2 = \frac{2RH}{1 - e^2}. \quad (1b)$$

### 3. Development of a no stationary vortex

Let us consider the nonlinear dynamics of vortical perturbations of a protostar. At time  $t = 0$  let the selected cylindrical region be subject to a vortical perturbation with an azimuthal velocity profile of the form

$$v_j(r) = \begin{cases} \omega_{in}(t)r, & r \leq r_0, \\ \omega_e(t)r_0^2/r, & r > r_0, \end{cases} \quad (4)$$

which describes rigid-body rotation in the region  $r < r_0$  of the trunk and a differential rotation outside the trunk. The structure given by Eq. (4) is known as a Rankine vortex (Rankine, 1870, Meleshko & Konstantinov, 1993, Kundu, 1990, Pashitskii, Malnev, Naryshkin, 2007, Abrahamyan, 2008). In writing Eq. (4), we have taken into account the fact that the angular velocity of the vortex can vary with time, while the time dependence of  $\omega(t)$  can be different in different regions of the vortex.

Let us write<sup>2</sup> in the Navier-Stokes equation concerning inertial system of frame (Landau & Lifshitz, 1986)

$$P = P^0(r, z) + p(r, z, t), \quad V_\phi = \Omega r + v_\phi, \quad (5)$$

---

<sup>2</sup> Perturbations under consideration do not change the spheroid geometry. The change of gravitational potential can be caused by the mass loss. In need we can include this, considering mass of a protostar slowly decreasing. Within the framework of given approach Eqs. (6) - (9) are exact.

and including Eqs. (1) and (2), we will receive the equations for an axially symmetric flow of viscous incompressible fluid in a coordinate system rotating with angular velocity  $\Omega$  in the form

$$\frac{\partial v_r}{\partial t} + v_r \frac{\partial v_r}{\partial r} - \frac{v_j^2}{r} = -\frac{1}{r} \frac{\partial p}{\partial r} + 2\Omega v_j + n \frac{\partial}{\partial r} \left( \frac{\partial v_r}{\partial r} + \frac{v_r}{r} \right), \quad (6)$$

$$\frac{\partial v_j}{\partial t} + v_r \left( \frac{\partial v_j}{\partial r} + \frac{v_j}{r} \right) = -2\Omega v_r + n \frac{\partial}{\partial r} \left( \frac{\partial v_j}{\partial r} + \frac{v_j}{r} \right), \quad (7)$$

$$\frac{\partial v_z}{\partial t} + v_z \frac{\partial v_z}{\partial z} = -\frac{1}{r} \frac{\partial p}{\partial z} + n \frac{\partial^2 v_z}{\partial z^2}, \quad (8)$$

$$\frac{\partial v_r}{\partial r} + \frac{v_r}{r} + \frac{\partial v_z}{\partial z} = 0, \quad (9)$$

where  $p$  is the perturbation in the pressure owing to the vortical motion,  $v_r$ ,  $v_\varphi$  are the radial and rotational components of the relative velocity,  $v$  is the kinematic viscosity, and  $\rho$  is the uniform mass density of the protostar. Note that, because of the axial symmetry of the problem, in these equations we have omitted the terms containing derivatives with respect to the azimuthal coordinate  $\varphi$  and with respect to  $z$  (except for the pressure and  $v_z$ ), and we have taken  $v_z = v_z(z, t)$ .

Assuming that  $v_r = v_z = 0$  at time  $t = 0$ , from Eqs. (6) and (7) we obtain

$$\frac{\partial p}{\partial r} = r \frac{v_j^2}{r} + 2r\Omega v_j, \quad \frac{\partial v_j}{\partial t} = n \frac{\partial}{\partial r} \left( \frac{\partial v_j}{\partial r} + \frac{v_j}{r} \right). \quad (10)$$

Given Eq. (4), the solution of the first of Eqs. (10) can be written in the form

$$p = \begin{cases} p_c + r(\omega_{in}^2 + 2\Omega\omega_{in})r^2/2, & r \leq r_0, \\ rr_0^2 \left[ \frac{\omega_e^2 r_0^2}{2r^2} \left( 1 - \frac{r^2}{r_s^2} \right) + 2\Omega\omega_e \ln \frac{r_s}{r} \right], & r > r_0, \end{cases} \quad (11)$$

where it is assumed that the perturbation in the gas-kinetic pressure goes to zero at a distance  $r_s \gg r_0$  from the cylinder axis, and  $p_c$  is the pressure drop along the axis of the vortex. The requirement that the pressure perturbation be continuous at the surface of the vortex trunk yields

$$p_c = -r \frac{r_0^2}{2} [\omega_{in}^2 + 2\Omega\omega_{in} + \omega_e^2 + 4\Omega\omega_e \ln \frac{r_s}{r_0}]. \quad (12)$$

Because of the pressure drop, a longitudinal flow of matter develops through the lower base of the vortex. We write its velocity in the form

$$v_z = \begin{cases} v_{z0} + az, & r \leq r_0, \\ 0, & r > r_0, \end{cases} \quad (13)$$

where  $v_{z0}$  and  $a$  can, in general, be functions of time. The parameter  $1/a$  has the dimensions of time and characterizes the velocity gradient along the vortex trunk. In the following we shall assume  $a = \text{const}$ .

Given Eq. (13), the continuity equation (9) yields

$$v_r = -\frac{a}{2} \begin{cases} r, & r \leq r_0, \\ r_0^2/r, & r > r_0. \end{cases} \quad (14)$$

Thus, because of the pressure drop on the axis of the vortex, a *suction effect* creates, the longitudinal flow (13) develops; it creates the converging radial flow of matter (14), which, in turn, transports angular momentum and energy from outer regions into the region of the vortex trunk.

Regardless of the functional form of  $v_r$ , Eq. (7) with Eq. (4) implies that in the region of the trunk ( $r < r_0$ ) the convective and Coriolis accelerations add up, while outside the trunk ( $r > r_0$ ) they compensate one another. Given Eqs. (4) and Eq. (14) in Eq. (7), we find

$$\frac{d\omega}{dt} = \begin{cases} a(\omega + \Omega), & r \leq r_0, \\ a\Omega, & r > r_0. \end{cases} \quad (15)$$

that is, because of the transport of angular momentum by the converging radial flow (14), the angular velocity of the trunk increases with time, with different rates of change of  $\omega$  in the region of the vortex trunk ( $r < r_0$ ) and outside it ( $r > r_0$ ). Eq. (15) for the time dependence of the angular velocity of the vortex gives

$$\omega(t) = \begin{cases} (\omega_0 + \Omega)e^{at} - \Omega\varepsilon\omega_{in}, & r \leq r_0, \\ \omega_0 + a\Omega t\varepsilon\omega_e, & r > r_0, \end{cases} \quad (16)$$

where  $\omega_0$  is the angular velocity of the trunk at the time the vortex is formed.

Thus, in Eqs. (4), (11), and (12) it is necessary to assume a linear variation in the angular velocity  $\omega_e$  in the outer region of the vortex and an exponential variation  $\omega_{in}$  in the trunk; this has been done in the formulas given here.

The velocities (4), (13), and (14) drive the viscous terms in Eqs. (6) - (8) identically to zero, while the diagonal components of the viscous stress tensor are nonzero. This yields the following power for the dissipation of the kinetic energy per unit length of the vortex:

$$\frac{dE_k}{dt} \cong -4pnrr_0^2(3a^2/2 + \omega_e^2 + 2\Omega\omega_e). \quad (17)$$

Note that a rapid increase in the angular velocity only occurs in the region of the

trunk,  $r < r_0$ , where the angular velocity increases exponentially with time, while the angular velocity increases linearly in the outside region  $r > r_0$ . Thus, at the boundary  $r = r_0$  there is discontinuity in the rotational velocity which, simultaneously with the pressure drop (12) on the vortex axis, increases exponentially with time. The increase in the energy dissipation (17) proceeds much more slowly. Thus, in this vortical motion the *dissipation remains small, in spite of a rapid rise in the angular velocity of the vortex trunk.*

The tangential discontinuity in the rotational velocity at the boundary of the vortex trunk is

$$[v_j] = V = [\omega_{in}(t) - \omega_e(t)]r_0 = r_0(\omega_0 + \Omega)(e^{at} - 1) - \Omega r_0 a t, \quad (18)$$

while the discontinuity in the longitudinal velocity determined by Eq. (13) is

$$[v_z] \epsilon U = z_{z0} + az. \quad (18a)$$

#### 4. The structure of the vortex

Using Eqs. (13) and (14), Eqs. (6) and (8) can be written in the form

$$\frac{\partial p}{\partial r} = -r \begin{cases} (a^2/4 - \omega_{in}^2 - 2\Omega\omega_{in})r, & r \leq r_0, \\ \frac{r_0^4}{r^3} \left( \frac{1}{4}a^2 + \omega_e^2 \right) + 2\Omega\omega_e \frac{r_0^2}{r}, & r > r_0, \end{cases} \quad (19)$$

$$\frac{\partial p}{\partial z} = -r \begin{cases} a(v_{z0} + az) + \dot{v}_{z0}, & r \leq r_0, \\ 0, & r > r_0. \end{cases} \quad (19a)$$

Note that the first derivatives of the pressure perturbation have a discontinuity at the trunk surface. On the other hand, the pressure must be continuous at the trunk surface.

Using Eqs. (19) and (19a), for the pressure perturbation we obtain

$$p(r, z, t) = \begin{cases} p_c - (a^2/4 - \omega_{in}^2 - 2\Omega\omega_{in})r^3/2 \\ \quad - r[(\dot{v}_{z0} + av_{z0})z + a^2z^2/2] + C, & r \leq r_0, \\ -\frac{r}{2} \left[ \left( \frac{r_0^2}{r^2} - \frac{r_0^2}{r_s^2} \right) \left( \frac{1}{4}a^2 + \omega_e^2 \right) + 4\Omega\omega_e \ln \frac{r_s}{r} \right] r_0^2, & r > r_0, \end{cases} \quad (20)$$

where  $C(t)$  is determined from the requirement that the isobaric surface be continuous at the trunk boundary  $r = r_0$ . Given Eqs. (5), (1a), and (20), for the total pressure in the region  $r > r_0$  we find

$$\frac{P_e}{r} = \Omega_0^2 B [(1 - e^2)(r_s^2 - r^2) - 2Rz - z^2] - \frac{r_0^2}{2} \left[ \left( \frac{r_0^2}{r^2} - \frac{r_0^2}{r_s^2} \right) \left( \frac{1}{4} a^2 + \omega_e^2 \right) + 4\Omega \omega_e \ln \frac{r_s}{r} \right], \quad (21)$$

and in the region  $r < r_0$  of the vortex trunk,

$$\frac{P_{in}}{r} = \Omega_0^2 B (1 - e^2) (r_s^2 - r^2) - (\omega_{in}^2 + 2\Omega \omega_{in}) \frac{r_0^2 - r^2}{2} - (\omega_e^2 + 4\Omega \omega_e \ln \frac{r_s}{r_0}) \frac{r_0^2}{2} - \frac{a^2 r^2}{8} - (\Omega_0^2 B R + \dot{v}_{z0} + a v_{z0}) z - (\Omega_0^2 B + a^2) \frac{z^2}{2} + \frac{C}{r}. \quad (22)$$

The equation for the isobaric surface corresponding to a given value of  $P = P^0(r, 0)$  at the initially spheroidal surface (3) can be obtained from Eqs. (21) and (22):

$$z^2 + 2z(R + \frac{\dot{v}_{z0} + a v_{z0} - a^2 R}{\Omega_0^2 B + a^2}) - \frac{\omega_{in}^2 + 2\Omega \omega_{in} - a^2 / 4}{\Omega_0^2 B + a^2} r^2 - \frac{\Omega_0^2 B (1 - e^2)}{\Omega_0^2 B + a^2} (r_s^2 - r^2) + \frac{\omega_{in}^2 + 2\Omega \omega_{in} + \omega_e^2 + 4\Omega \omega_e \ln(r_s / r_0)}{\Omega_0^2 B + a^2} r_0^2 - \frac{2C(t)}{r(\Omega_0^2 B + a^2)} = 0, \quad (23)$$

with the unknown function  $C(t)$ , while in the outer region  $r > r_0$  this isobaric surface is described by

$$z^2 + 2Rz - (1 - e^2)(r_s^2 - r^2) + \frac{\omega_e^2 + a^2 / 4}{\Omega_0^2 B} \left( \frac{r_0^4}{r^2} - \frac{r_0^4}{r_s^2} \right) + \frac{4\Omega \omega_e}{\Omega_0^2 B} r_0^2 \ln \frac{r_s}{r} = 0. \quad (24)$$

Assuming that the size of the vortex is small compared to the protostar and requiring that the isobaric surface be continuous at the vortex trunk boundary  $r = r_0$ , we obtain the unknown function  $C(t)$  and from Eq. (23) we obtain the final form of the equation for the isobar in the region  $r < r_0$  of the vortex trunk:

$$z_{in}(r, t) = - \frac{\omega_{in}^2 + 2\Omega \omega_{in} - a^2 / 4 - \Omega_0^2 B (1 - e^2)}{2(\dot{v}_{z0} + a v_{z0} + \Omega_0^2 B R)} (r_0^2 - r^2) + \frac{1 - e^2}{2R} (r_s^2 - r_0^2) - \frac{\omega_e^2 + a^2 / 4 + 4\Omega \omega_e \ln(r_s / r_0)}{2\Omega_0^2 B R} r_0^2. \quad (25)$$

The continuation of the isobar in the outer region of the vortex is given by the solution (24):

$$z_e(r,t) = \frac{1-e^2}{2R}(r_s^2 - r^2) - \frac{\omega_e^2 + a^2/4}{2\Omega_0^2 BR} \frac{r_s^2 - r^2}{r_s^2 r^2} r_0^4 - \frac{2\Omega\omega_e}{\Omega_0^2 BR} r_0^2 \ln \frac{r_s}{r}. \quad (26)$$

In deriving Eqs. (25) and (26) we have expanded the square roots in the solutions of Eqs. (23) and (24) in series, assuming that  $\omega_{in}^2 r_0^2 \approx c_s^2 \ll \Omega_0^2 R^2$ , where  $c_s$  is the sound speed (see below).

It is evident from (23) and (24) that the problem allows the particular solution

$$\dot{v}_{z0} - a(v_{z0} - aR) = 0, \quad (27)$$

which, with the initial condition  $v_z(0) = 0$ , yields

$$v_{z0}(t) = aR(1 - e^{-at}). \quad (28)$$

Equations (25) and (26) show that the position of the intersection of the isobar with the vortex trunk surface  $r = r_0$  moves over time toward negative values of  $z$  because of the linear dependence of  $\omega_e(t)$ , i.e.

$$z_e(r_0, t) = z_{in}(r_0, t) = H - \frac{r_0^2}{2R\Omega_0^2} \left[ \frac{1}{4}a^2 + \omega_e^2(t) + 4\Omega\omega_e(t) \ln \frac{r_s}{r_0} \right]. \quad (29)$$

The isobar described by Eqs. (25) and (26) has a funnel shape which becomes deeper with time. Here the wide part of the funnel (28), which corresponds to the outer region of the vortex, develops slowly owing to the linear dependence of  $\omega_e(t)$ . In the region of the vortex trunk, on the other hand, the isobar funnel (25) develops much more rapidly, and moves into the depth of the protostar in accordance with an exponential law (Fig. 1). The bottom of the funnel lies on the axis  $r = 0$  of the vortex and its position changes with time as

$$z_{in}(0, t) = -\frac{\omega_{in}^2(t) + 2\Omega\omega_{in}(t) - a^2/4 - \Omega_0^2 B(1-e^2)}{2(\dot{v}_{z0} + av_{z0} + \Omega_0^2 BR)} r_0^2 + z(r_0, t), \quad (30)$$

where the term in parentheses in the denominator equals  $\alpha v_{z0} + \Omega_0^2 R$  - for  $v_{z0} = const$ , and  $(\alpha^2 + \Omega_0^2)R$  - for the particular solution (27).

In the initial stage of the development of the power-law instability,  $t \ll 1/2\alpha$ , for  $r_0 \ll R$  the coordinate of the bottom of the funnel varies linearly with time:

$$z(0, t) \sim -\left[ \frac{(\Omega + \omega_0)^2 R}{\dot{v}_{z0} + av_{z0} + \Omega_0^2 BR} + \frac{\Omega\omega_0 + 2\Omega^2 \ln(r_s/r_0)}{\Omega_0^2 B} \right] \frac{r_0^2}{R} at, \quad (31)$$

and at times  $t > 1/2\alpha$  the vortex deepens exponentially as

$$z(0, t) \sim -\frac{(\Omega + \omega_0)^2 e^{2at}}{\dot{v}_{z0} + av_{z0} + \Omega_0^2 BR} \frac{r_0^2}{2}. \quad (32)$$

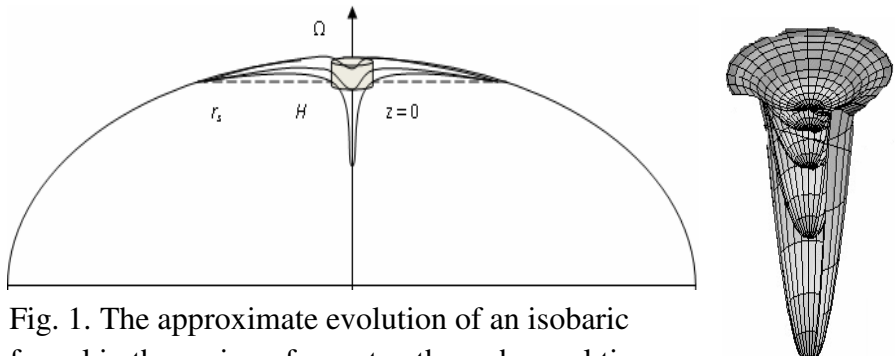


Fig. 1. The approximate evolution of an isobaric funnel in the region of a vortex through equal time steps (scale lengths are not maintained).

## 5. Instability of the tangential velocity discontinuity at the trunk boundary and the saturation of the vortex

Surfaces with a tangential velocity discontinuity are known (Landau & Lifshits, 1986) to be unstable to surface perturbations. Let us consider a two-dimensional flow of an incompressible medium with velocity discontinuities (18) and (18a) in the XZ plane (a part of the surface of the trunk with the Z axis parallel to the jet axis).

We shall study a local instability of a tangential velocity distribution; i.e., we assume that the dimensions of the segment of the surface being studied are much smaller than the corresponding dimensions of the trunk, and that the periods and reciprocal growth rates for the perturbations are much shorter than the characteristic times for growth of the angular velocity of the vortex.

In the chosen coordinate system, small perturbations of the surface of discontinuity in a coordinate system moving with the cloud are given by

$$\frac{\partial \vec{v}}{\partial t} + V \frac{\partial \vec{v}}{\partial x} + U \frac{\partial \vec{v}}{\partial z} = -\vec{C} \frac{P}{r} + 2[\vec{v} \vec{\Omega}] + n D \vec{v}, \quad \vec{C} \vec{v} = 0. \quad (33)$$

Applying the operator  $\nabla$  to both sides of the first equation, we find, using the second equation, that the perturbed pressure obeys a Laplace equation,  $\Delta P/\rho = 0$ . Thus, we write

$$P/\rho \sim e^{-k|y|} \exp\{i(k_x x + k_z z - \sigma t)\}. \quad (34)$$

where  $k$  is the wave number and  $\sigma$  is the frequency of the perturbations, and the Y axis is directed along the normal to the surface of discontinuity toward the vortex trunk.

Let  $\zeta(x, z, t)$  be the displacement, in the Y direction, of the particles in the plane of the discontinuity. Then, assuming  $v_x, v_y$  and  $\zeta \sim \exp\{i(k_x x + k_z z - \sigma t)\}$  we obtain

a dispersion relation for the perturbations of the tangential discontinuity surface:

$$\frac{(s - \vec{k}\vec{w} + ink^2)^2 - 4\Omega^2}{2\Omega k_x - k(s - \vec{k}\vec{w} + ink^2)}(s - \vec{k}\vec{w}) = \frac{(s + ink^2)^2 - 4\Omega^2}{2\Omega k_x + k(s + ink^2)}s. \quad (35)$$

We now examine the stability in two limiting cases: short and long wavelength perturbations.

*Short wavelength* - these are perturbations with a wavelength that is much shorter than the trunk radius ( $kr_0 \gg 1$ ) and are typical of perturbations that propagate along the azimuth ( $x$  - perturbations). Taking  $k_z = 0$  for simplicity, from Eq. (35) we obtain<sup>3</sup>

$$(\sigma - kV)(\sigma - kV + 2\Omega) + \sigma(\sigma - 2\Omega) + ivk^2(2\sigma - kV) = 0. \quad (36)$$

The solution of this dispersion relation is

$$\sigma_0(k) = \text{Re } \sigma = kV/2, \quad \gamma(k) = \text{Im } \sigma = [(k^2 V^2 + v^2 k^4 - 4\Omega kV)^{1/2} - vk^2]/2. \quad (37)$$

We note first that the expression under the square root in Eq. (37) becomes positive for perturbations with wave numbers

$$k > k_{cr} = 3\sqrt{\frac{2\Omega V}{n^2} \left( 1 + \sqrt{1 + \frac{V^4}{108\Omega^2 n^4}} \right)} \quad (38)$$

and the perturbations with still larger wave numbers grow. The rotation stabilizes long wavelength perturbations of the trunk boundary; thus, short wavelength perturbations which also lie in our approximation of local instability turn out to be unstable. Equation (37) for the growth rate of the perturbations implies that the maximum value is reached as  $k \rightarrow \infty$ , i.e.

$$\gamma_m = V^2/4v. \quad (39)$$

Using Eqs. (16) and (37), for the time dependence of the amplitude of the surface perturbations in the  $y = 0$  plane, in the initial stage of development of the instability over a time interval  $t \ll 1/\alpha$ , for a vortex with a power law evolution of the instability, we obtain

$$\zeta(t) \approx \zeta_0 e^{\gamma_x(t)} \sim \zeta_0 \exp\left(\frac{\omega_0^2 r_0^2 \alpha^2}{2v} t^3\right), \quad (40)$$

i.e., during the initial stage of the development of the instability the maximum growth in the amplitude with time follows  $\zeta(t) \sim \zeta_0 \exp(t^3)$  dependence.

In an inviscid fluid ( $v = 0$ ) surface perturbations with a tangential velocity discontinuity develop during the initial stage as

<sup>3</sup> Instead of  $k_x$  we shall use the notation  $k$ .

$$\zeta(t) \equiv \zeta_0 \exp(\omega_0 r_0 \alpha k t^2 / 2). \quad (41)$$

The maximum growth rate for the perturbations in a layer is known to be attained for wavelengths on the order of its thickness  $l$ , i.e., with  $k_m \sim 1/l$ . In the case of surface waves, the layer thickness is  $\ell \approx 2\zeta(t)$ , so that  $k_m \approx 1/2\zeta(t)$ . Using this in Eq. (43), we obtain

$$\ln \frac{\zeta(t)}{\zeta_0} \approx \frac{\alpha \omega_0 r_0 t^2}{2\zeta(t)}, \quad (42)$$

which implies that  $\zeta(t)$  varies with time roughly as  $t^2/\ln t$ . Thus, a turbulent transition layer of thickness  $2\zeta(t)$  develops on the surface of the vortex trunk with an effective turbulent viscosity which, in the initial stage of the development of the instability, can be estimated using the formula

$$v^*(t) \equiv \zeta^2(t) \gamma(t) \approx \frac{1}{2} \alpha v_0 |\zeta(t)| t. \quad (43)$$

The turbulent viscosity increases very rapidly with time ( $\sim t^3$ ) and can reach large values ( $v \sim v^*$ ). This leads to intense nonlinear dissipation of the growing turbulent perturbations in this layer and to a transition into a saturated state.

The turbulent perturbations saturate when the rise in the kinetic energy of the surface waves per unit time owing to instability in the tangential velocity discontinuity,  $\gamma \rho v^2/2$ , approaches, in order of magnitude, the power of the turbulent energy dissipation per unit volume,  $\rho v^3/\ell$  (Landau & Lifshits, 1986). In the estimates given above,  $v \sim d|\zeta(t)|/dt$  is the velocity of the turbulent fluctuations,  $\ell \sim |\zeta(t)|$  is their characteristic scale length, and  $\gamma \sim \pi V/|\zeta|$  is the maximum growth rate for the instabilities. This implies that the velocity of the turbulent fluctuations is essentially the same as the discontinuity in the tangential velocity, i.e.,  $v(t) \approx V(t)$ .

On the other hand, the angular acceleration in the rotation of the vortex trunk ceases when the discontinuity  $V(t)$  in the tangential velocity approaches the sound speed  $c_s$ . The characteristic time  $t_s$  for this process is given by Eq. (18) (See Eq. (53)).

Thus,  $V_m \approx c_s$  и  $\gamma_m \approx \pi c_s / \zeta_m$ , where  $\zeta_m$  is given by Eq. (42):

$$\ln \frac{\zeta_m}{\zeta_0} \equiv \frac{\alpha \omega_0 r_0 t_s^2}{2\zeta_m}. \quad (44)$$

*Long wavelength--* these are perturbations with a long wavelength exceeding the transverse dimension of the trunk, i.e.,  $kr_0 \ll 1$ . Clearly, they can arise only in longitudinal  $z$ -perturbations,

$$\zeta(z, t) = z_0 e^{\gamma_z t} \exp(ik_z z - i\sigma_0 t), \quad (45)$$

caused by the discontinuity in the longitudinal flow velocity of the material (18a). Taking  $k_x = 0$  in Eq. (35), we obtain a dispersion relation for the longitudinal perturbations of the form<sup>4</sup>

$$[(\sigma - kU + i\nu k^2)^2 - 4\Omega^2](\sigma - Uk)(\sigma + i\nu k^2) + [(\sigma + i\nu k^2)^2 - 4\Omega^2]\sigma(\sigma + i\nu k^2) = 0. \quad (35b)$$

Of course, the effect of viscosity on the long wavelength perturbations can be neglected. Then Eq. (35b) becomes much simpler:

$$(\sigma^2 - \sigma U k + U^2 k^2 / 2 - 4\Omega^2)(\sigma - U k) = 0, \quad (46)$$

and has the solutions

$$\sigma_1 = U k, \quad \sigma_{2,3} = U k / 2 \mp i\sqrt{U^2 k^2 / 4 - 4\Omega^2}. \quad (47)$$

Only the third mode, which describes oscillations with frequency  $\sigma_0 = 1/2Uk$ , yields perturbations (45) that increase in time. Here the perturbations increase only within the wavelength interval

$$2\pi r_0 \ll \lambda < \frac{\pi U}{2\Omega} \quad (1 \gg kr_0 > \frac{4\Omega r_0}{U} = \frac{4\Omega r_0}{\nu_{z0} + \alpha_z}), \quad (48)$$

with a growth rate

$$\gamma_z = \sqrt{\sigma_0^2 - 4\Omega^2}. \quad (49)$$

Given that, in the initial stage (the instability in the longitudinal perturbations sets in at a time  $t > 4\Omega/\alpha_z^2 k R_0$  of the development of the vortex in the region  $z \approx 0$ , we have  $U \approx \alpha_z^2 R_0$  (using Eq. (26)), we obtain the following for the amplitude of the particle oscillations in the long wavelength perturbations of the surface of the vortex trunk:

$$\zeta_0 e^{\gamma_z t} \sim \zeta_0 \exp(k_z \alpha_z^2 R_0 t^2 / 2). \quad (50)$$

The comparison of Eqs. (50) and (41) shows that the longitudinal long wavelength perturbations develop much more slowly than the short wavelength perturbations. Thus, saturation of the vortical motion (i.e., termination of the exponential growth in the angular velocity of the trunk and in the pressure drop on its axis) occurs when the discontinuity in the azimuthal velocity reaches the sound speed.

The time  $t_s$  for the vortex to saturate is determined from the equation

---

<sup>4</sup> Instead of  $k_z$  here we also use  $k$ .

$$e^{at_s} - \frac{\Omega at_s}{\omega_0 + \Omega} = \frac{c_s}{(\omega_0 + \Omega)r_0}. \quad (51)$$

Over this time the bottom of the isobaric funnel moves downward by a distance

$$z_s \approx \frac{(c_s + \Omega r_0 \alpha t_s)^2}{2(\dot{v}_{z0} + \alpha v_{z0} + \Omega_0^2 BR)} \quad (52)$$

and, in the case of the particular solution (28),  $v_{z0}$  increases to

$$v_{z0}(t_s) = aR \left[ 1 - \frac{(\omega_0 + \Omega)r_0}{c_s + \Omega r_0 \alpha t_s} \right]. \quad (53)$$

Equation (13) can be used to estimate the velocity of the vertical flow of matter (the jet) at the protostar's surface. If the lower base of the vortex lay at a depth  $H$  from the cloud surface at the time it was formed, then at the time the vortex saturates on emerging from the cloud, the velocity of the jet would be equal to

$$v_j \approx \begin{cases} v_{z0} + \alpha(z_s + H), & v_{z0} = \text{const}, \\ v_{z0}(t_s) + \alpha(z_s + H), & v_{z0} = \alpha R(1 - e^{-\alpha t}). \end{cases} \quad (54)$$

The mass lost by the protostar in a year is

$$dM/dt = \pi r_0^2 \rho v_j. \quad (55)$$

## 6. Generation of astrophysical jets by a vortex

The appearance of a Rankine vortex in the surface axial layer of a gravitating body, therefore, produces a longitudinal flow of matter (13) and a flow of matter which converges toward the vortex trunk (14). These flows provide for an exponential growth in the rotational velocity of the trunk and in the pressure drop on its axis. The power law increases in the angular rotation velocity and in the pressure drop cease and the vortical motion enters a state of saturation when the discontinuity in the azimuthal velocity at the surface of the trunk (as we have seen, the growth of the long wavelength perturbations proceeds much more slowly) reaches the sound speed. This takes place over a time  $t_s$  (given by Eq. (51)) following the appearance of the vortex within which the vortical motion extends to ever deeper layers of the cloud, covering a distance given by Eq. (52). On the other hand, the longitudinal velocity of the flow along the vortex trunk reaches the value given by Eq. (53) during this time, causing mass to flow out through the surface of the protostar in the form of a jet with velocity  $v_j$  (see Eq. (54)).

As an illustration of the results obtained here, let us consider a spheroidal protostar of mass  $\sim 2 M_\odot$ , polar radius 10 a.u., and eccentricity 3/4. For the mass density of the protostar we obtain  $\rho = 3 M_\odot (1-e^2)/2\pi R_0^3 \approx 10^{-11} \text{ g/cm}^3$  and, using Eq.

(2), we find its angular rotation velocity to be  $\Omega \approx 1.8 \cdot 10^{-9} \text{ s}^{-1}$  and  $\Omega_0 \approx 2 \cdot 10^{-9} \text{ s}^{-1}$ . Let a vortex (4) which appears at time  $t = 0$  in the surface polar layer of the protostar have a thickness  $H = 0.2 \text{ a.u.}$ , trunk radius  $r_0 \approx 0.5 \text{ a.u.}$ , and azimuthal velocity  $v_0 = \omega_0 r_0 \approx 0.3 \text{ km/s}$  at its surface. Taking the velocity of the radial flow (14) at the surface of the trunk to be  $v_r \approx 0.5 \text{ km/s}$ , (corresponding to  $\alpha \approx 1.3 \cdot 10^{-8} \text{ s}^{-1}$ ) and the sound speed be  $c_s \approx 10 \text{ km/s}$ , with Eq. (51) we find the saturation time for the vortex to be  $t_s \approx 2.4 \cdot 10^8 \text{ s} \approx 8 \text{ years}$ . During this time the low pressure vortical funnel spans ever deeper layers of the protostar, forming an essentially stationary cylindrical vortex of length  $\approx 1.8 \text{ a.u.}$ . The longitudinal flow velocity at the  $z = 0$  level turns out to be  $v_{z0}(t_s) \approx 19.2 \text{ km/s}$ , and at the surface of the protostar,  $v_j \approx 20 \text{ km/s}$ , while the parabolic velocity at the protostar's surface is  $\approx 12 \text{ km/s}$ . The rate of loss of mass by the protostar is then  $\approx 10^{-6} \text{ M}_\odot / \text{year}$ .

The jet velocity at the surface of the protostar can also be estimated using energy conservation arguments. In fact, equating the total work by the pressure and gravitational forces to the kinetic energy of the trunk at the surface of the protostar, i.e., taking the Bernoulli integral for the lower and upper bases of the vortex trunk, we obtain the same estimate for  $v_j$ .

We now estimate the thickness  $\zeta_m$  of the transition turbulent layer. To do this we assume that the displacement  $\zeta_0$  is on the order of the mean free path for the particles, i.e.,  $\zeta_0 \approx m_H / \pi a_H^2 \rho \approx 10^4 \text{ cm}$ , where  $m_H$  is the mass of a hydrogen atom and  $a_H$  is its Bohr radius. Then Eq. (44) gives  $\zeta_m \approx 1.5 \cdot 10^7 \text{ cm}$ . The maximum value for the coefficient of turbulent viscosity in the transition layer is then

$$\nu_m^* \equiv \frac{1}{2} \alpha v_0 \zeta_m t_s \sim 2 \cdot 10^{12} \text{ cm}^2/\text{s}. \quad (56)$$

while the ordinary kinematic viscosity of the gas is much smaller, at

$$\nu \approx v_H l / 3 \sim 3 \cdot 10^9 \text{ cm}^2/\text{s}, \quad (57)$$

where  $v_H$  is the thermal speed of the atoms and  $l$  is their mean free path. Thus, at the surface of a vortex trunk of radius  $r_0$  rotating at almost the sound speed  $v_{\varphi m} = v_0 \exp(\gamma_m t_s) \sim c_s$ , turbulence creates a layer of thickness  $\max 2\zeta_m$  with an anomalously high viscosity  $\nu_{max} \gg \nu$ .

The lifetime of the resulting vortex can be estimated by dividing the kinetic energy per unit length of the vortex in its saturated state by the energy dissipated per unit length (17):

$$t_{vortex} \approx 1.8 \times 10^7 / [\nu] \text{ year}, \quad (58)$$

where the viscosity is expressed in units of  $10^{12} \text{ cm}^2/\text{s}$ . The molecular viscosity gives an estimate in Eq. (58) of  $\sim 3 \cdot 10^9$  years, while the turbulent viscosity yields  $\sim 5 \cdot 10^6$  years for the lifetime of the vortex. Thus, these vortices are substantially dissipation-less, even when an anomalously high turbulent viscosity is assumed.

## 7. Concluding remarks

The vortical mechanism proposed in this paper for the generation of astrophysical jets is a unique way of converting gravitational energy of a source into the kinetic energy of an erupting jet. This mechanism can also provide for the acceleration and collimation of jet flows beyond the confines of a source, both in slowing-down regions and in inertial outflows.

The formation of a turbulent transition layer at the surface of a vortex trunk leads to more than the saturation of the vortex. It drives a number of hydrodynamic and physicochemical processes which merit detailed study.

As the vortex trunk emerges from the compact formation, it enters a rarefied environment and begins to expand. The following scenario for expansion of the jet can be imagined: radial distension of the jet as a whole and expansion of the surface layers into the rarefied surroundings<sup>5</sup>. Radial distension converts the jet from a dense, rapidly rotating state into a less dense, more slowly rotating state while conserving its angular momentum. At the same time, matter flows out from the jet surface: initially the layers adjacent to the boundary come into motion, and ever deeper regions away from the boundary are gradually brought into motion. A rarefaction wave develops and propagates radially into the depth of the jet, creating a "sheath" of no uniform density with a differential rotation around the jet. This leads to the recovery of equilibrium at the boundary of a uniform trunk at some radius  $R$  of the trunk. After this, the rapid expansion processes cease and a quasistationary pattern consisting of two regions is established in the jet: a *core region* that is uniform in density and rotates rigidly and a sheath region with a non-uniform density, differential rotation, and a *converging radial flow* of matter. Thus, self generation of a vortex from a bare trunk in a jet is possible (Abrahamyan, 2009). A vortex of this sort will accelerate and simultaneously collimate the core region of a jet. The result is a fast, more collimated jet inside a slow jet. "Two-velocity" CO outflows of this type have been observed in a number of molecular jet flows (so-called "molecular bullets"), such as HH211 in IC348 (Gueth & Guilloteau, 1999), L1448 (Nisini, et al., 2000, Masson et al., 1990), HH7-11 (Koo, 1990, Bachiller et al., 1998), and HH111 (Cernicharo & Reipurth, 1999, Hatchell et al., 1999).

---

<sup>5</sup> Here is significant the presence of an accreting disc component round the protostar, which can enrich angular momentum of the jet, accelerate and collimate it at the long distance from the source.

## References

- Abrahamyan M.G., 2008, *Astrofizika*, **51**, 617, [in Russian].
- Abrahamyan M.G., 2009, *Astrofizika*, **52**, 136, [in Russian].
- Bacciotti F., Eislöffel J., 1999, *Astron. Astrophys.* **342**, 717.
- Bachiller R., Martin-Pintado J., et al., 1990, *Astron. Astrophys.* **231**, 174.
- Bachiller R., Guilloteau S., et al., 1998, *Astron. Astrophys.* **339**, L49.
- Bisnovatyi-Kogan G.S., Komberg B.V., Fridman A.M., 1969, *Astron. Zh.* **46**, 465.
- Bisnovatyi-Kogan G.S., 2004, *Astrophys.* **47**, 404.
- Bisnovatyi-Kogan G.S., 2007, *Mon. Not. Roy. Astron. Soc.* **376**, 457.
- Bridle A., 1998, in: Physics of AGN Jets (<http://www.cv.nrao.edu/~abridle/bgctalk>).
- Cernicharo J. and B. Reipurth Bo, 1996, *Astrophys. J.* **460**, L57
- Chandrasekhar S., 1969, Ellipsoidal Figures of Equilibrium. Yale Univ. press, 288 p.
- Chrysostomou A., Bacciotti F., Nisini B., Ray T.P., Eislöffel P., Davis C.J., Takami M., 2008, arXiv:0802.1881.
- Coffey S.D., Bacciotti F., Chrysostomou A., Nisini B., Davis C., 2010, arXiv:1011.6619.
- Coffey S.D., Bacciotti F., Ray T.P., Eislöffel J., Woitas J., 2008, *Astron. Astrophys.*
- Dal Pino E.M.G., 1995, in: Plasma Physics and Controlled Fusion, AIP Procs. 345, 427.
- Gonzalez R., Dal Pino E.M.G., Raga A., Velazquez P., 2004, *Astrophys. J.* **600**, L59.
- Gueth F., Guilloteau S., 1999, *Astron. Astrophys.* **343**, 571.
- Hatchell J., Fuller G. A., Lada E. F., 1999, *Astron. Astrophys.* **346**, 278.
- Königl A, 1986, *Can. J. Phys.* **64**, 362.
- Koo B.C., 1990, *Astrophys. J.* **361**, 145.
- Kundu P.K., 1990, Liquid Mechanics. Academic Press Inc., p. 638.
- Landau L.D., Lifshitz E.M., 1986, Hydrodynamics [in Russian], Nauka, Moscow, 736 p.
- Matveenko L.I., Sivakon S., Ershtad S.G., Marsher A.P., 2010, *Pisma Astron. J.*, **36**, 163.
- Masson C. R., Mundi L. G., Keene J., 1990, *Astrophys. J.* **357**, L25.
- Meleshko V.V., Konstantinov M.Yu., 1993, Dynamics of Vortical Structures [in Russian], Naukova Dumka, Kiev, 282 pp.
- Morse J.A., Hartigan P., Cecil G., Raymond J.C., Heathcote S., 1992, *Astrophys. J.* **339**, 231.

- Nisini B., Benedettini M., et al., 2000, *Astron. Astrophys.* **360**, 297.  
Pashitskii E.A., Malnev E.A., Naryshkin R.A., 2007, arXiv:physics/0702229.  
Rankine W.J.M., 1870, *Phil. Mag. Ser.* **4**, 39, 211.  
Reipurth Bo & Bally J., 2001, *Ann. Rev. Astron. Astrophys.* **39**, 403.  
Reipurth Bo, 1989, *Nature* **340**, 42.  
Shibata K. and Aoki S., 2004, astro-ph/0303253.  
Soker N., 2004, *Astron. Astrophys.* **414**, 943

# ЗАВИСИМОСТЬ ФУНКЦИИ СВЕТИМОСТИ ГАЛАКТИК ОТ ИХ МОРФОЛОГИЧЕСКОГО ТИПА И ОТ ОКРУЖАЮЩЕЙ СРЕДЫ

А. П. Магтесян

*Бюраканская Астрофизическая Обсерватория, Бюракан, Армения*

## 1. Введение

Функция светимости (ФС) галактик имеет очень большое значение для исследования и понимания происхождения и эволюции галактик, для проверки космологических моделей и многих других проблем внегалактической астрономии.

Взаимодействия между галактиками играют важную роль в их эволюции. Они могут способствовать или подавлять звездообразование в галактиках. Эти взаимодействия в разных системах могут отличаться друг от друга. Например, группы галактик по сравнению со скоплениями имеют малые дисперсии лучевых скоростей, малые плотности и температуру газа, поэтому в этих окружениях эффективны такие механизмы как слияния (Toomre, Toomre 1972, White 1979), потери газа спиральными галактиками, обусловленной гравитационным взаимодействием с другими членами скопления (Spitzer, Baade 1951) или разрушения спиральных ветвей приливным обдирианием (Negroponte, White 1983). В скоплениях галактик, где дисперсия скоростей довольно высокая, эффективен механизм выметания газа из галактик лобовым давлением межгалактического газа скопления (Gunn, Gott 1972). Одиночные галактики находятся в совершенно другой ситуации. Можно предположить, что эволюция этих галактик связана с процессами, происходящими внутри их самих.

Эти механизмы могут изменить светимость галактик, и поэтому ожидается зависимость функции светимости галактик от окружающей среды.

Важно понять, как меняется ФС галактик в зависимости от их морфологического типа, а также, как влияет окружающая среда на ФС.

ФС галактик обычно представляется функцией Шехтера (Schechter 1976), которая в яркой части светимостей имеет экспоненциальную форму, а при слабых светимостях имеет степенную форму.

$$\Phi = \phi_* 10^{0.4(M_* - M)(1+\alpha)} \exp(-10^{0.4(M_* - M)}), \quad (1)$$

где  $\phi_*$  - коэффициент нормализации,  $M_*$  и  $\alpha$  определяют форму кривой. Параметр  $\alpha$  представляет логарифмический наклон в слабом конце светимостей.

Если  $\alpha$  меньше, чем -1, то ФС в слабом конце возрастающая, а при  $\alpha > -1$  она убывающая. Граничное значение  $\alpha = -1$  соответствует плоскому концу ФС.  $M_*$  показывает место изменения поведения ФС. При значениях намного меньших  $M_*$ , ФС становится экспоненциальной. ФС галактик в

скоплениях, группах и в общем поле изучены во многих работах (Oemler 1974; Schechter 1976; Felten 1977; Dressler 1978a; Sandage et al. 1985; Oegerle et al. 1986; Lluger 1986; Oegerle et al. 1987; Binggeli et al. 1988; Colless 1989; Willmer et al. 1990; Gudehus & Hegyi 1991; Garilli et al. 1991; Ferguson & Sandage 1991; Garilli et al. 1992; Loveday et al. 1992; Marzke et al. 1994; Ribeiro et al. 1994; Driver et al. 1994; Lopez-Cruz & Yee 1995; Barrientos et al. 1996; Lin et al. 1996; Andreon и др. 1997; Gaidos 1997; Jerjen & Tamman 1997; Lopez-Cruz et al. 1997; Lumsden et al. 1997; Trentham 1997; Valotto et al. 1997; Zepf et al. 1997; Andreon 1998; Bromley et al. 1998; Muriel et al. 1998; Rauzy et al. 1998; Garilli et al. 1999; Marinoni et al. 1999; Ramella et al. 1999; Zabludoff & Mulchaey 2000; Paolillo et al. 2001; de Propis et al. 2002; Goto et al. 2002; Trentham & Hodgkin 2002; Cuesta-Bolao & Serna 2003). В этих работах предметом серьезного изучения являлся вопрос об универсальности ФС.

В первых результатах было получено, что ФС галактик в скоплениях и в общем поле не отличаются друг от друга (например, Felten (1977)). В дальнейшем некоторые авторы (Loveday et al. (1992); Marzke et al. (1994); Lin et al. (1996)) для ФС галактик поля, представляя ее функцией Шехтера (1976), получили большие различия для величины  $M_*$ , но для наклона ФС в слабом конце получили подобные результаты:  $\alpha \approx -1$ .

В некоторых работах, касающихся скоплений галактик, для слабого конца ФС, также был получен плоский наклон (см. например, Garilli et al. 1999; Paolillo et al. 2001; Goto et al. 2002). Во многих других работах (Schechter 1976; Dressler 1978a; Sandage et al. 1985; Ferguson & Sandage 1991; Lluger 1986; Colless 1989; Lumsden et al. 1997; Trentham 1997; Valotto et al. 1997; Rauzy et al. 1998; Garilli et al. 1999; Paolillo et al. 2001; de Propis et al. 2002; Goto et al. 2002; Cuesta-Bolao & Serna 2003) для слабого конца ФС получены довольно большие наклоны ( $-1.5 \leq \alpha \leq -1.2$ ). Для слабого конца ФС получается довольно большой наклон ( $\alpha < -2$ ), когда рассматриваются очень слабые галактики скопления (Trentham, Hodgkin 2002). В работах Lopez-Cruz, Yee (1995) и Lopez-Cruz et al. (1997) изучены 45 скоплений Эйбла с красным смещением  $z < 0.14$  и получено, что 39 из них показывают увеличение относительного числа слабых галактик. Только 7 из них представляются ФС Шехтера с  $\alpha \approx -1$ . Оказалось, что они имеют в своем составе сD галактики и в среднем более массивны и богаты газом.

Результаты изучения ФС галактик групп разными авторами довольно сильно отличаются друг от друга. В некоторых работах, относящихся к близким группам галактик, получены согласующиеся результаты (Ferguson and Sandage 1991; Muriel et al. 1998): т. е., получена плоская ФС, похожая на ФС галактик поля. Изучение же компактных групп (Ribeiro et al. 1994; Zepf et al. 1997) также привело к плоской или слабо понижающей ФС в слабом конце светимостей. В противовес этому в работе Zabludoff and Mulchaey (2000) было показано, что в группах ФС галактик в слабом конце имеет большой логарифмический наклон. В Cuesta-Bolao, Serna (2003) показано, что как малые, так и относительно большие группы в слабом конце ФС имеют слабо понижающийся наклон подобно результату Ribeiro et al. (1994).

Известно, что существует зависимость плотность - морфологическое содержание (Dressler 1980). Согласно этой зависимости в областях высоких плотностей относительное число эллиптических и линзовидных галактик выше, чем в областях малых плотностей. Известно также, что каждый хаббловский тип галактик имеет свою характерную ФС (например, Binggeli et al. 1988). Поэтому ожидается, что суммарная ФС галактик должна быть зависима от окружения.

Представляется также важным выяснить: универсальна ли ФС для данного хаббловского типа галактик, или она зависит от окружения? В Binggeli et al. (1988), изучая ФС галактик в поле, в группах и в бедных скоплениях, было показано, что ФС галактик отдельного хаббловского типа является универсальной. Другие авторы подтвердили этот результат (например, Andreon et al. 1997; Jerjen and Tamman 1997; Andreon 1998). Они получили, что ФС галактик E, L, S не зависят от плотности окружающей среды. В противовес этому в работах (Valotto et al. 1997; Bromley et al. 1998; Marinoni et al. 1999; Ramella et al. 1999; Cuesta-Bolao, Serna 2003) получена значимая зависимость ФС галактик данного морфологического типа от плотности окружающей среды.

Такая несогласованность результатов, возможно, связана с недостаточно уверенным разделением близких и далеких фоновых галактик от галактик скопления, а для малых групп - неуверенной идентификацией их членов. Поскольку число членов групп мало, то ошибочное присоединение к данной группе одной или нескольких ложных галактик, или неприсоединение истинных членов, может значимо влиять на определение ФС.

Есть еще одна причина, которая может повлиять на достоверность результатов. Она заключается в том, что авторы часто представляют ФС функцией Шехтера во всей изучаемой области светимостей. Но изучение многих работ показывает, что эта функция довольно плохо представляет ФС как в ярком, так и в слабом конце светимостей.

Таким образом, вопрос о зависимости ФС галактик от окружающей среды, а также вопрос об универсальности ФС галактик разных морфологических типов пока остается открытым, особенно для малых групп. Этот вопрос очень важен для правильного понимания процессов происхождения и эволюции галактик.

## **2. Новый метод определения функции светимости галактик**

Классический метод определения ФС (Binggeli et al. 1987) основывается на предположении, что галактики равномерно распределены в пространстве. Чтобы вычислить ФС без любого предположения относительно пространственного распределения галактик, были предложены другие непараметрические методы (например, Lynden-Bell 1971, Choloniewski 1987) или методы, основанные на методе максимального правдоподобия (Nicoll & Segal 1983; Efstathiou et al. 1988). Для учета зависимости плотности числа галактик от расстояния, мы обобщили  $1/V_{\max}$  метод Шмидта (1968).

Галактика с абсолютной звездной величиной  $M_i$  будет видна в объеме, на границе которой она будет иметь предельную звездную величину выборки (в данном случае  $m_{\text{lim}} = 15.^m5$ ). Поскольку наша выборка ограничена расстоянием снизу и сверху, то пространственную плотность галактики с абсолютной величиной  $M_i$  мы должны оценить в объеме  $V_m^i - V_{\min}$ , когда  $M_{\max} \geq M_i \geq M_{\min}$  и в объеме  $V_{\max} - V_{\min}$ , когда  $M_i < M_{\min}$ . Где

$$V_m^i = \frac{\Omega}{3} \left( \frac{cz_m^i}{H} \right)^3$$

это тот объем, на границе которого галактика с абсолютной

звездной величиной  $M_i$  будет иметь предельную видимую звездную величину выборки  $m_{\text{lim}}$ ,  $V_{\min} = \frac{\Omega}{3} \left( \frac{cz_{\min}}{H} \right)^3$  это близкий объем, исключенный из рассмотрения, а  $V_{\max} = \frac{\Omega}{3} \left( \frac{cz_{\max}}{H} \right)^3$  есть максимальный объем,

находящиеся дальше которого галактики также не рассматриваются.  $\Omega$  - объемный угол выборки, и в нашем случае равен 4.3 ср.

Если предположить, что галактики в пространстве распределены равномерно, то следуя Schmidt (1968) и Huchra, Sargent (1973):

$$\Phi_{obs}(M_i) = \begin{cases} \frac{1}{\Delta M} \sum_{M_i \pm \Delta M / 2, j} \frac{1}{(V_m^j - V_{\min})}, & M_{\max} \geq M_i \geq M_{\min} \\ \frac{1}{\Delta M (V_{\max} - V_{\min})} \sum_{M_i \pm \Delta M / 2, j} 1, & M_i < M_{\min} \end{cases} \quad (2)$$

Поскольку галактики не распределены равномерно, и средняя пространственная плотность галактик, по крайней мере, в близкой Вселенной, зависит от расстояния (особенно в северном полушарии), то определение ФС, таким образом, приведет к повышенной оценке плотности абсолютно слабых галактик. Поэтому мы должны учитывать эту зависимость и приводить средние плотности галактик к наибольшему объему  $V_{\max}$ . Вследствие этого, уравнение (2) примет следующий вид:

$$\Phi_{obs}(M_i) = \begin{cases} \frac{1}{\Delta M} \sum_{M_i \pm \Delta M / 2, j} \frac{1}{D(r_m^j)(V_m^j - V_{\min})}, & M_{\max} \geq M_i \geq M_{\min} \\ \frac{1}{\Delta M D(r_{\max})(V_{\max} - V_{\min})} \sum_{M_i \pm \Delta M / 2, j} 1, & M_i < M_{\min} \end{cases} \quad (3)$$

где  $r_m^i = \frac{cz_m^i}{H} = \left( \frac{3V_m^i}{\Omega} \right)^{1/3}$  - расстояние соответствующее объему  $V_m^i$ .

Фактически  $D(r_m^i)$  - это плотность галактик, нормированная на объем  $V_{\max}$ :  $D(r_{\max}) = 1$ . Расчеты сделаны при  $\Delta M = 0.2$ .

Такое определение предполагает независимость ФС от пространственных координат. Мы также пренебрегаем локальными повышениями плотности в виде групп галактик, поскольку речь идет о средних плотностях галактик, в объемах намного превышающих объем групп галактик.

Среднеквадратичное отклонение  $\Phi_{obs}(M_i)$  оцениваем следующим образом:

$$\begin{aligned}\sigma(\Phi_{obs}(M_i)) &= \frac{1}{\Delta M D(r_m^i)(V_m^i - V_{\min})} \left[ n_i \left( 1 - \frac{n_i}{N} \right) \right]^{1/2}, \\ &= \frac{\Phi_{obs}(M_i)}{n_i} \left[ n_i \left( 1 - \frac{n_i}{N} \right) \right]^{1/2}\end{aligned}, \quad (4)$$

где  $n_i$  - число галактик в интервале  $M_i \pm \Delta M / 2$ ,  $N$  - общее число галактик в выборке.

В этих отношениях видимые звездные величины исправлены за галактическое поглощение (Sandage 1973, см. (3.3)) и за К - ослабление (Efstathiou et. al 1988, см. (3.4)):  $\Delta m = -A - K$ . Лучевые скорости галактик исправлены за вращение Галактики и за движение Местной системы галактик в направлении скопления в Деве (см. (2.17)-(2.19)).

$$M_i = m_i - 25 - 5 \log(cz_i / H),$$

$$M_i = m_{\lim} - 25 - 5 \log(cz_m^i / H),$$

$$M_{\min} = m_{\lim} - 25 - 5 \log(cz_{\max} / H),$$

$$M_{\max} = m_{\lim} - 25 - 5 \log(cz_{\min} / H),$$

$H = 100 km \cdot c^{-1} \cdot Mpc^{-1}$  - постоянная Хаббла,  $m$  - видимая звездная величина галактики. Как отметили выше,  $cz_{\min} = 500$  км/с,  $cz_{\max} = 20000$  км/с,  $m_{\lim} = 15.^m5$ . Поэтому  $M_{\max} = -13.^m0$ ,  $M_{\min} = -21.^m0$ .

Уравнение (3) можно также написать следующим образом:

$$\Phi_{obs}(M_i) = \begin{cases} \frac{1}{\Delta M} \frac{3}{\Omega} 10^{-0.6(m_{lim} - 25 - M_{max})} \\ \times \sum_{M_i \pm \Delta M / 2, j} \frac{(10^{-0.6(M_j - M_{max})} - 1)^{-1}}{D(10^{0.2(m_{lim} - M_j - 25)})}, M_{max} \geq M_i \geq M_{min} \\ \frac{1}{\Delta M} \frac{3}{\Omega} 10^{-0.6(m_{lim} - 25 - M_{max})} (10^{-0.6(M_{min} - M_{max})} - 1)^{-1} \\ \times \sum_{M_i \pm \Delta M / 2, j} 1, M_i < M_{min}, \end{cases} \quad (5)$$

Эти уравнения дадут истинную плотность числа галактик только в том случае, когда имеем дело с полной выборкой. Когда выборка неполная, и фактор полноты не зависит от абсолютной звездной величины, мы можем точно оценить только нормированную ФС галактик (например, Neuman, Scott 1974; Теребиж 1980).

$$\Psi(M_i) = \frac{\Phi_{obs}(M_i)}{\sum_j \Phi_{obs}(M_j)}. \quad (6)$$

Истинная плотность числа галактик с абсолютной величиной  $M_i$  будет:

$$\Phi(M_i) = P(m_{lim})^{-1} \Phi_{obs}(M_i), \quad (7)$$

а среднеквадратичное отклонение будет:

$$\sigma(\Phi(M_i)) = P(m_{lim})^{-1} \sigma(\Phi_{obs}(M_i)) \quad (8)$$

где  $P(m_{lim})$  - фактор полноты.

Для изучения полноты выборки, ограниченной звездной величиной, широко используется  $V/V_m$  метод (Schmidt 1968), где  $V$  - объем пространства, на краю которого находится галактика, а  $V_m$  - есть максимальный объем пространства, на краю которого галактика будет иметь видимую звездную величину, равную предельной звездной величине выборки. Если в Евклидовом пространстве объекты распределены равномерно, то среднее значение величины  $\langle V/V_m \rangle$  должно быть равно 0.5. При данном пространстве распределение величины  $\langle V/V_m \rangle$  строго эквивалентно распределению видимых величин (Теребиж 1980), которое при равномерном распределении объектов будет вида  $N(m) \sim 10^{0.6m}$ . Мы предполагаем, что плотность галактик зависит от расстояния, и поэтому данные методы используем для приближенной оценки полноты выборок.

### 3. Зависимость плотности галактик от расстояния

Зависимость плотности галактик от расстояния можно построить при помощи полных (по видимой и по абсолютной звездной величине) выборок. Для этого мы создали три подвыборки галактик по абсолютным величинам:

а. Выборка с  $M \leq -21''$ , которая полна по абсолютной звездной величине во всем изученном объеме. По этой выборке определена искомая зависимость при красных смещениях от 7000 км/с до 20000 км/с. При малых расстояниях эта выборка непригодна по причине малочисленности галактик.

б. Выборка с  $M \leq -20''$ . Эта выборка полна до красного смещения 12600 км/с. По этой выборке определена искомая зависимость при красных смещениях от 1700 км/с до 12600 км/с.

в. Выборка с  $M \leq -17.8''$ . По этой выборке определена искомая зависимость при красных смещениях от 500 км/с до 5000 км/с.

Эти зависимости сшиты по общим участкам и нормированы на красное смещение 20000 км/с. Полученная кривая приведена на рис. 1. Для удобства при вычислениях разные участки кривой представлены полиномами первого или второго порядка.

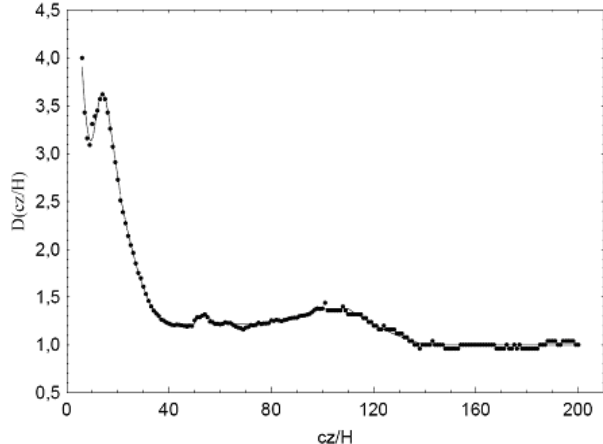


Рис. 1: Зависимость относительной плотности числа галактик от красного смещения.

#### 4. ФС галактик поля разных морфологических типов

На рис. 2 представлена нормализованная логарифмическая функция светимости (ЛФС,  $\log \Psi(M)$ ) галактик поля. Под названием “галактики поля” мы подразумеваем все галактики, расположенные в изучаемом объеме, независимо от того, входят они в группы или являются одиночными галактиками. Использован CfA2 каталог красных смещений. Выборка ограничена красным смещением  $500 \text{ km/s} \leq cz \leq 20000 \text{ km/s}$  и галактической широтой  $|b''| \geq 20^\circ$ .

На этом и на следующих рис. 3 – 6 среднеквадратичное отклонение посчитано следующим образом:

$$\sigma(\Psi(M_i)) = \frac{\Psi(M_i)}{n_i} \left[ n_i \left( 1 - \frac{n_i}{N} \right) \right]^{1/2} \quad (9)$$

Из рис. 2 видно, что ФС галактик поля можно представить функцией Шехтера с параметрами  $M_* = -19.30$  и  $\alpha = -0.90$  только в ограниченном участке светимостей:  $-21.0 \leq M \leq -17.6$ . Левее от этой области ЛФС можно представить квадратным многочленом, а правее, при слабых светимостях ЛФС можно представить линейной функцией.

На рис. 3 представлена ЛФС галактик поля с известными морфологическими типами. Видно, что она почти не отличается от ЛФС всех галактик (рис. 2).

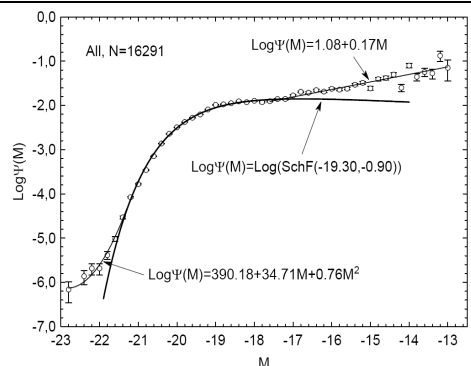


Рис. 2. ЛФС галактик поля в области  $500 \leq V \leq 20000$  км/с и  $|bII| \geq 20^\circ$ .

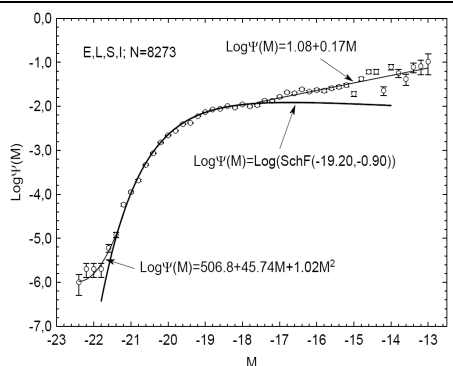


Рис. 3. ЛФС галактик поля с известными морфологическими типами в области  $500 \leq V \leq 20000$  км/с и  $|bII| \geq 20^\circ$ .

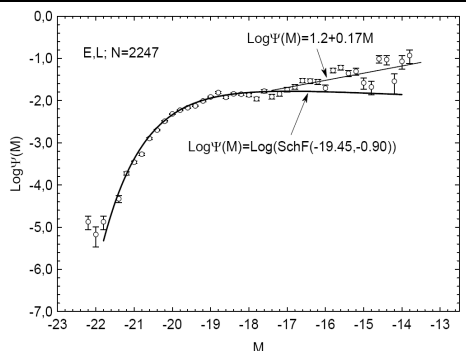


Рис. 4. ЛФС эллиптических и линзовидных галактик поля в области  $500 \leq V \leq 20000$  км/с и  $|bII| \geq 20^\circ$ .

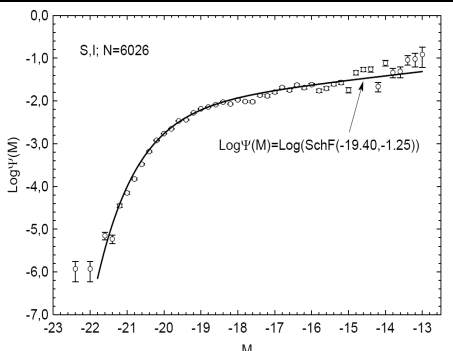


Рис. 5. ЛФС спиральных и иррегулярных галактик поля в области  $500 \leq V \leq 20000$  км/с и  $|bII| \geq 20^\circ$ .

На рис. 4 представлена ЛФС эллиптических и линзовидных галактик. Из рис. 4 видно, что для эллиптических и линзовидных галактик, как и для всех галактик, функцией Шехтера возможно представить только часть ФС. По параметру  $\alpha$  они не отличаются, а по параметру  $M_*$  отличаются мало.

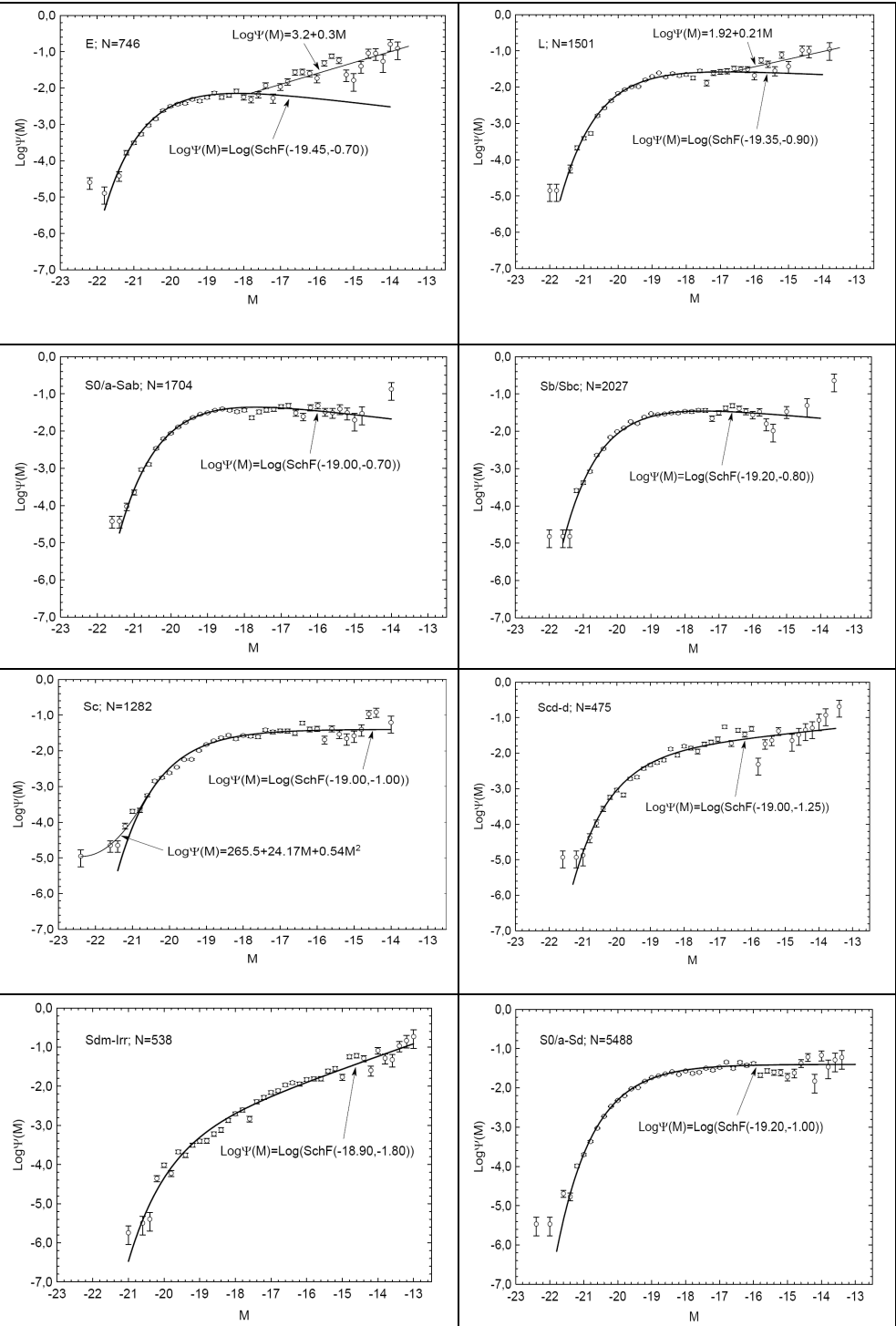


Рис. 6: ЛФС галактик поля для разных морфологических типов в области  $500 \leq V \leq 20000$  км/с и  $|bII| \geq 20^\circ$ .

На рис. 5 представлена ЛФС спиральных и иррегулярных галактик. Из рисунка видно, что ФС спиральных и иррегулярных галактик хорошо представляется функцией Шехтера с параметрами  $M_* = -19.4$  и  $\alpha = -1.25$  почти во всей изученной области светимостей:  $M \geq -21.5$ .

Значительное число галактик с известным морфологическим типом позволяют нам более подробно изучать зависимость ФС галактик от морфологии галактик. Результаты представлены на рис. 6. Из рис. 6 видно, что поведение ФС галактик типов E и L подобно поведению ФС всех галактик, т.е. не во всем диапазоне абсолютных звездных величин ФС можно представить функцией Шехтера. Данная функция для эллиптических галактик применима только в диапазоне  $-21.2 \leq M \leq -17.8$ , а для линзовидных галактик – в диапазоне  $-21.2 \leq M \leq -16.5$ .

ФС спиральных галактик можно представить функцией Шехтера в довольно широком диапазоне абсолютных звездных величин. Параметром  $M_*$  они слабо отличаются. При переходе от ранних спиралей к поздним спиралям происходит уменьшение параметра  $\alpha$  в функции Шехтера, т. е. увеличивается относительное число слабых галактик.

На последнем изображении рис. 6 приведена ЛФС спиралей без неправильных спиральных и иррегулярных галактик. Из рисунка видно, что ЛФС “чистых спиралей” в слабом конце довольно плоская и в диапазоне  $-21.5 \leq M \leq -14.0$  можно представить функцией Шехтера с параметрами  $M_* = -19.2$  и  $\alpha = -1.0$ .

## 5. Средняя плотность числа галактик разных морфологических типов

Если фактор полноты не зависит от абсолютной звездной величины, то нормированная ФС галактик не зависит от полноты выборки по видимой звездной величине (см., например, Neuman, Scott 1974, Теребиж 1980). То есть, когда выполняется это условие, то нормированную ФС галактик можно построить также по неполной выборке. Иное положение, когда оценивается средняя плотность числа галактик. Для этого надо оценить полноту изучаемых выборок.

На рис. 7 для нашей выборки представлена зависимость величин  $V/V_m$  от абсолютной звездной величины галактики. Рис. 7 не показывает какую-либо зависимость между обсуждаемыми величинами, т.е фактор полноты не зависит от абсолютной звездной величины.

Полноту CfA2 выборки можем приблизительно оценить по  $\langle V/V_m \rangle$  тесту Шмидта (Schmidt 1968), поскольку этот тест требует равномерного распределения галактик в пространстве.

В табл. 1 представлены величины  $\langle V/V_m \rangle \pm (12n)^{-1/2}$  в зависимости от видимой звездной величины, как для всех галактик, так и для галактик с известными морфологическими типами. Из таблицы видно, что выборку всех галактик можно считать полной, а выборки галактик с известными

морфологическими типами можно считать полными до видимой звездной величины  $m=14.0 - 14.5$ .

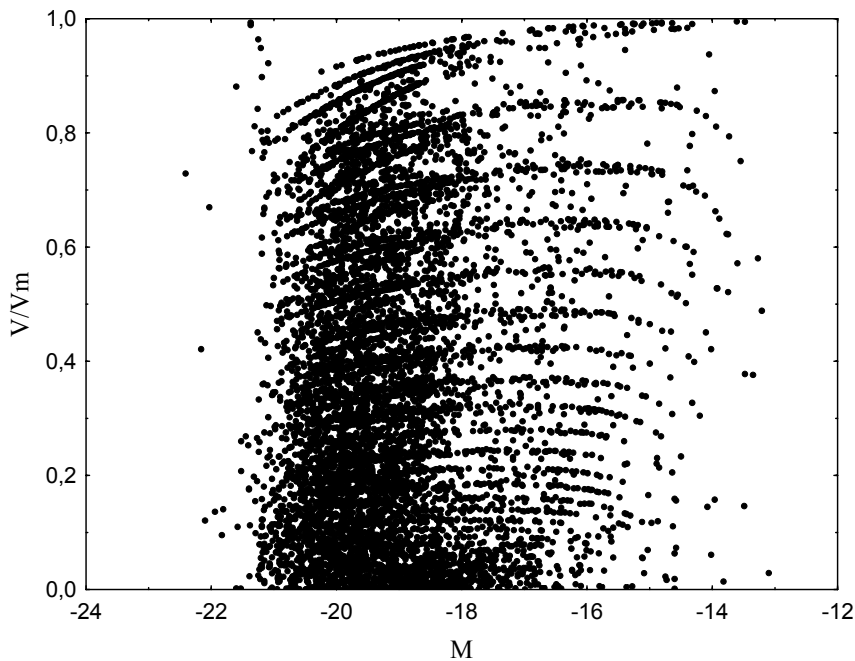


Рис. 7: Зависимость величин  $V / V_m$  от абсолютной звездной величины галактики.

На рис. 8 представлены распределения видимых звездных величин галактик разных морфологических типов. Из рисунка видно, что распределения видимых звездных величин для галактик разных морфологических типов похожи друг на друга и заметно отличаются от аналогичного распределения для всех галактик в слабом конце, начиная с  $m=14$ . Можно сказать, что нехватка морфологических типов проявляется после  $m=14-14.5$ . Причем, эти пропуски незначимо зависят от морфологического типа, и в первом приближении мы приняли, что выборки для разных морфологических типов полны до  $m=14.2$ . Также можем принять, что вся выборка безотносительно к известности морфологического типа, является полной.

Таблица 1. Величины  $\langle V / V_m \rangle$  в зависимости от видимой звездной величины для всех галактик и для галактик с известными морфологическими типами.

m	10.0	10.5	11.0	11.5	12.0	12.5
$\langle V / V_m \rangle$ все галактики	0.49± 0.077	0.54± 0.051	0.44± 0.040	0.49± 0.027	0.44± 0.021	0.45± 0.016
n	14	32	52	113	189	337
$\langle V / V_m \rangle$ Галактики с морфологичес- кими типами	0.49± 0.077	0.54± 0.051	0.44± 0.040	0.49± 0.027	0.44± 0.021	0.45± 0.016
n	14	32	52	113	188	336

Таблица 1 (продолжение)

m	13.0	13.5	14.0	14.5	15.0	15.5
$\langle V / V_m \rangle$ все галактики	0.47± 0.012	0.46± 0.009	0.46± 0.007	0.48± 0.005	0.53± 0.003	0.50± 0.002
n	611	1089	1872	3496	7773	16291
$\langle V / V_m \rangle$ Галактики с морфологичес- кими типами	0.46± 0.012	0.45± 0.009	0.45± 0.007	0.46± 0.005	0.44± 0.004	0.39± 0.003
n	597	1044	1763	3164	5338	8273

Для галактик конкретных морфологических типов фактор полноты оценили двумя способами:

а. По формуле, предложенной Теребижом (1980), которая, строго говоря, требует равномерного распределения галактик в пространстве.

$$P(m_{\text{lim}}) = 10^{-0.6(m_{\text{lim}} - m_1)} \left[ 1 + 0.6 \ln 10 \frac{N(m_{\text{lim}}) - N(m_1)}{n(m_1)} \right], \quad m_1 \leq m_{\text{lim}}, \quad (10)$$

где  $P(m_{\text{lim}})$  - фактор полноты,  $m_1$  - видимая величина, до которой выборку можно принять полной,  $N(m_1)$  - число объектов, имеющих звездные величины меньше  $m_1$ ,  $n(m_1)$  - пространственная плотность числа галактик при  $m_1$  (или число галактик в интервале  $m_1 \pm 0.5$ ),  $N(m_{\text{lim}})$  - число объектов,

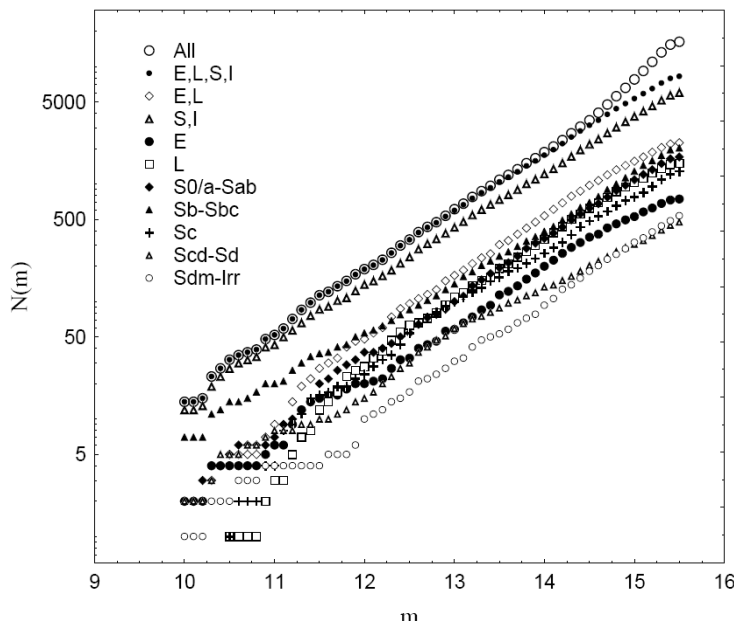


Рис. 8. Распределения видимых звездных величин галактик разных морфологических типов.

видимые величины которых меньше предельной звездной величины выборки  $m_{\lim}$ .

б. Предположим, что фактор полноты для галактик отдельных морфологических типов один и тот же. Тогда фактор полноты будет равняться отношению плотности, полученной для галактик с известными морфологическими типами, без учета этого фактора, к плотности всех галактик безотносительно к морфологическим типам. Она равняется 0.69. Ясно, что такой подход также приближенный.

Таблица 2. Факторы полноты и средние пространственные плотности числа для галактик разных морфологических типов

	T	All	E,L,S,I	E,L	S,I	S0/a-Sd	E
а способ	$P(m_{\lim})$	1	0.69	0.60	0.73	0.73	0.56
б способ	$P(m_{\lim})$	1	0.69	0.69	0.69	0.69	0.69
а способ	$\rho(Mpc^{-3})$	0.127	0.126	0.022	0.101	0.035	0.012
б способ	$\rho(Mpc^{-3})$	0.127	0.127	0.019	0.108	0.037	0.010
	n	16291	8273	2247	6026	5488	746

Таблица 2 (продолжение)

	T	L	S0/a-Sab	Sb/Sbc	Sc	Scd/Sd	Sdm/Irr
а способ	$P(m_{\text{lim}})$	0.62	0.72	0.75	0.73	0.70	0.74
б способ	$P(m_{\text{lim}})$	0.69	0.69	0.69	0.69	0.69	0.69
а способ	$\rho(Mpc^{-3})$	0.010	0.007	0.008	0.011	0.011	0.065
б способ	$\rho(Mpc^{-3})$	0.009	0.007	0.008	0.011	0.011	0.071
	n	1501	1704	2027	1282	475	538

Факторы полноты  $P(m_{\text{lim}})$  и средние пространственные плотности числа

$$\rho = P^{-1}(m_{\text{lim}}) \sum_i \Phi_{obs}(M_i), \quad (11)$$

для галактик разных морфологических типов и для обоих способов вычисления, приведены в табл. 2. Видно, что разница пространственных плотностей числа галактик разных морфологических типов, вычисленных разными способами, не отличается больше чем на 20%.

Исходя из поведения ФС эллиптических и линзовидных галактик, средние абсолютные величины галактик приведем для двух интервалов абсолютных величин,  $-23 \leq M \leq -17.8$  и  $-23 \leq M \leq -14.0$ .

Результаты приведены в табл.3, откуда видно, что при переходе от эллиптических галактик к линзовидным галактикам, к ранним спиральным галактикам, и далее, к поздним спиральным галактикам наблюдается уменьшение средней светимости ярких галактик ( $-23 \leq M \leq -17.8$ ).

Таблица 3 Средние абсолютные величины галактик разных морфологических типов

Тип	$-23 \leq M \leq -17.8$			$-23 \leq M \leq -14.0$		
	$\langle M \rangle$	$\sigma(M)$	n	$\langle M \rangle$	$\sigma(M)$	n
Все	-18.74	0.006	14646	-15.93	0.013	16269
E,L,S,I	-18.68	0.008	7154	-15.75	0.017	8257
E,L	-18.81	0.016	2027	-15.83	0.034	2245
S,I	-18.66	0.009	5127	-15.73	0.020	6012
S0/a-Sd	-18.67	0.010	4917	-16.44	0.022	5485
E	-18.92	0.030	650	-15.36	0.051	745
L	-18.78	0.019	1377	-16.35	0.042	1500
S0/a-Sab	-18.78	0.017	1586	-16.82	0.042	1704
Sb/Sbc	-18.76	0.016	1897	-17.27	0.033	2026
Sc	-18.55	0.019	1090	-16.14	0.044	1282
Scd/Sd	-18.42	0.031	344	-15.85	0.066	473
Sdm/Irr	-18.29	0.037	210	-15.03	0.043	527

## **6. Влияние окружения на функцию светимости галактик**

Для изучения ФС галактик в разных окружениях используем список групп галактик Магтесяна и Мовсесяна (2010). Для построения ФС галактик используем выше предложенный метод.

В §4 мы рассмотрели зависимость ФС галактик поля от их морфологического типа. Для оценки абсолютной величины галактик поля нами использованы собственные лучевые скорости галактик. Поскольку часть галактик поля входят в системы, то возникает вопрос, насколько изменится результат, если для оценки абсолютной величины галактик систем использовать средние лучевые скорости системы.

На рис. 9а приведена нормализованная ЛФС галактик поля, а на рис. 9б – галактик систем с числом членов от 1 до 337 для разных морфологических типов, в диапазоне лучевых скоростей  $1000 \text{ km/s} \leq V \leq 15000 \text{ km/s}$ . Эти выборки состоят из одних и тех же галактик. Разница заключается только в определении абсолютной величины галактик.

Из рис. 9а и 9б видно, что ФС галактик разных морфологических типов, всех галактик с известными морфологическими типами, всех галактик без отношения к известности морфологических типов существенно не отличаются, когда абсолютная светимость галактик оценивается индивидуальными лучевыми скоростями галактик или средними лучевыми скоростями галактик системы. Возможно, что для эллиптических и линзовидных галактик имеется некоторая несогласованность в слабом конце при  $M > -15.5$ .

На рис. 10 приведена нормализованная ЛФС галактик разных морфологических типов в разных окружениях (в системах разных кратностей). В группах абсолютные величины галактик рассчитаны по средним лучевым скоростям группы.

Из рис. 10а и 10б видно, что ФС для всех галактик, безотносительно к известности морфологических типов, и для галактик с известными морфологическими типами, не отличаются друг от друга во всех системах. Что касается зависимости ФС галактик от кратности групп, то она существенно отличается только в самых богатых группах (в скоплениях), имеющих, по крайней мере, 60 видимых членов. В этих группах ФС невозможно представить функцией Шехтера. Разные участки ЛФС можно представить линейными функциями.

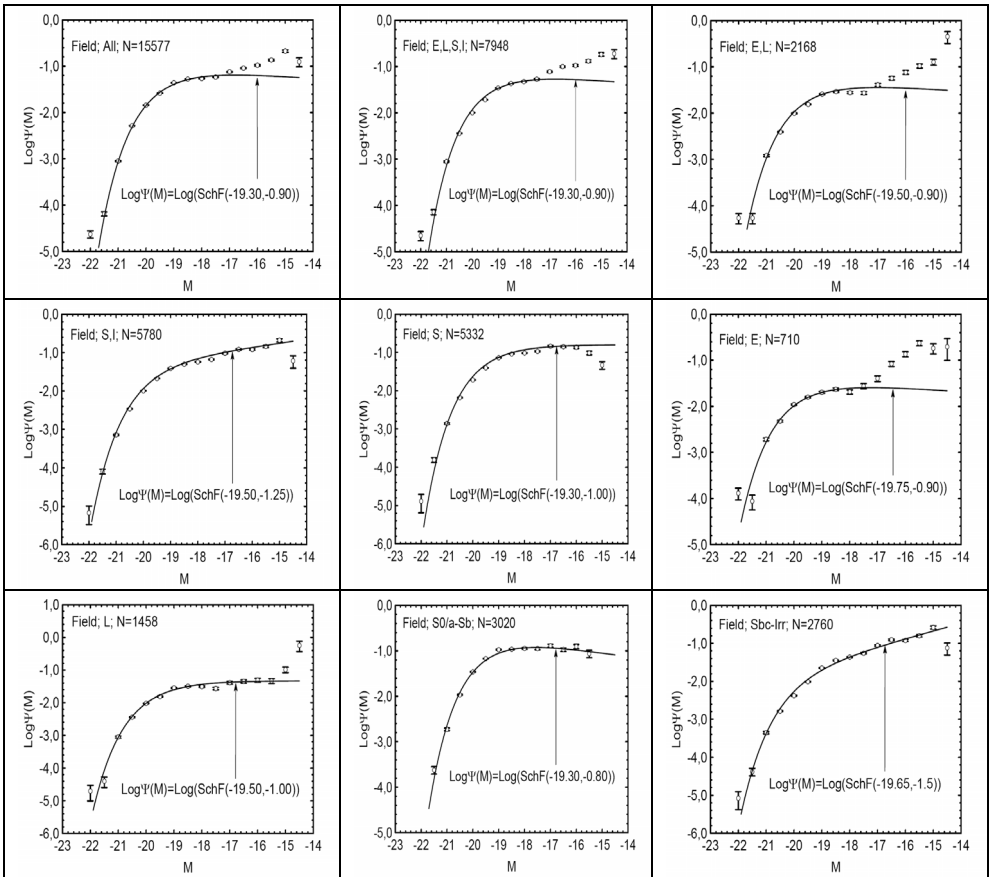


Рис. 9а. ЛФС галактик поля (каждая галактика считается индивидуальным объектом) в диапазоне лучевых скоростей  $1000 \text{ km}/c \leq V \leq 15000 \text{ km}/c$ .

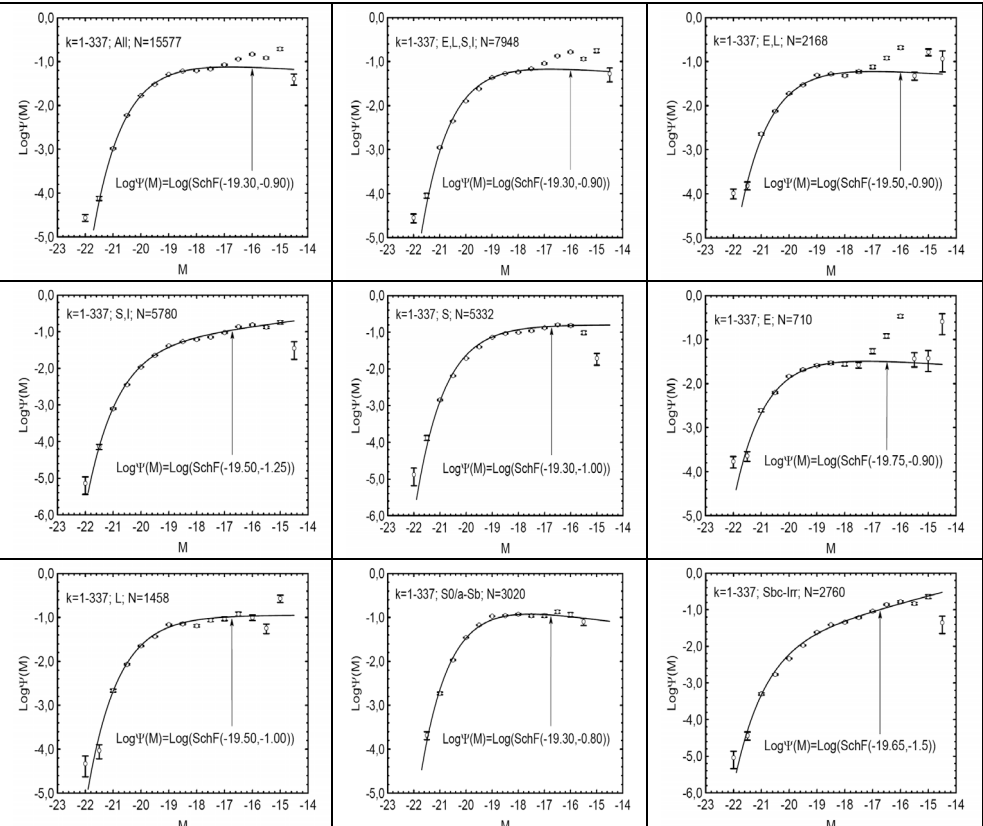


Рис. 9б. ЛФС галактик систем (одиночные галактики считаются системы с числом членов равной 1).

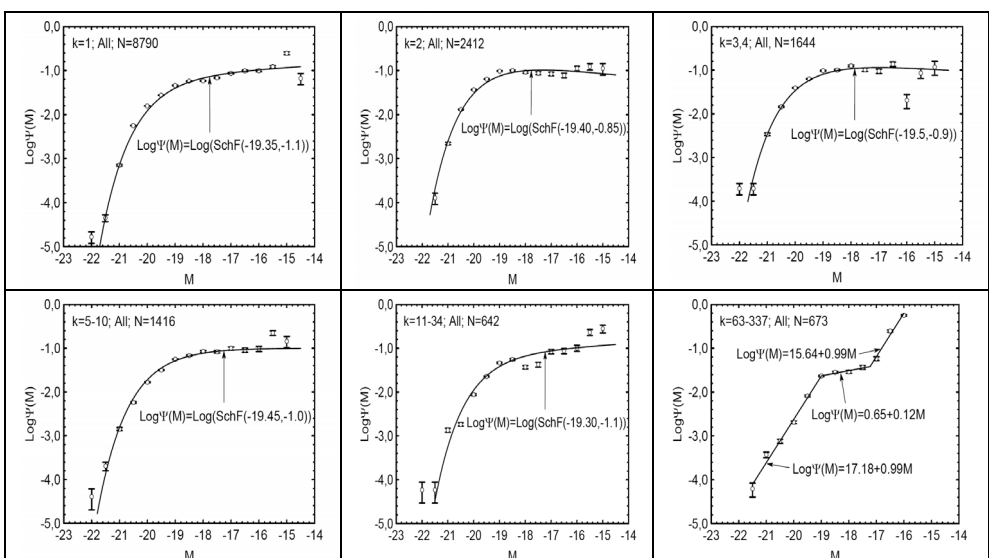


Рис. 10а. ЛФС всех галактик, безотносительно к морфологическим типам, для систем разных кратностей.

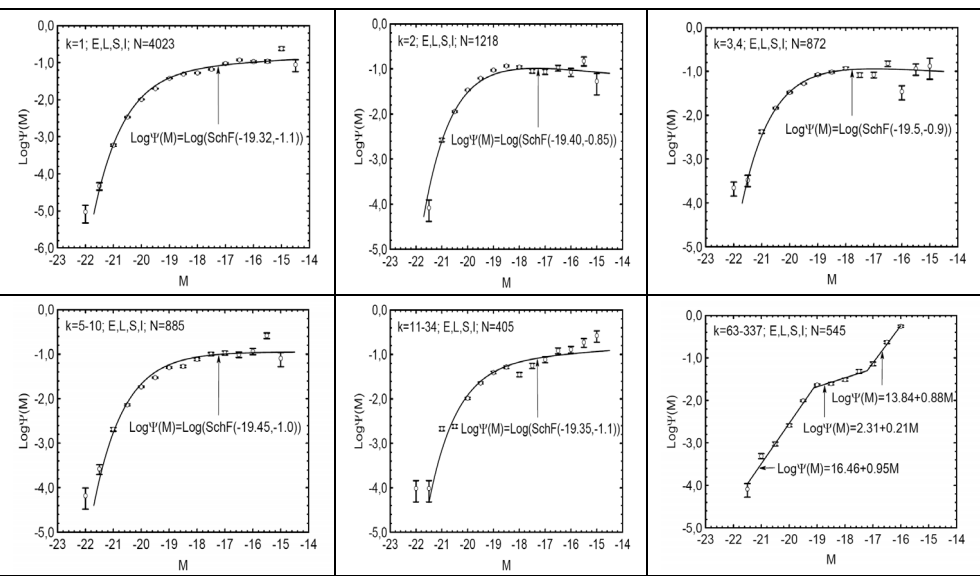


Рис. 10б. ЛФС галактик с известными морфологическими типами для систем разных кратностей.

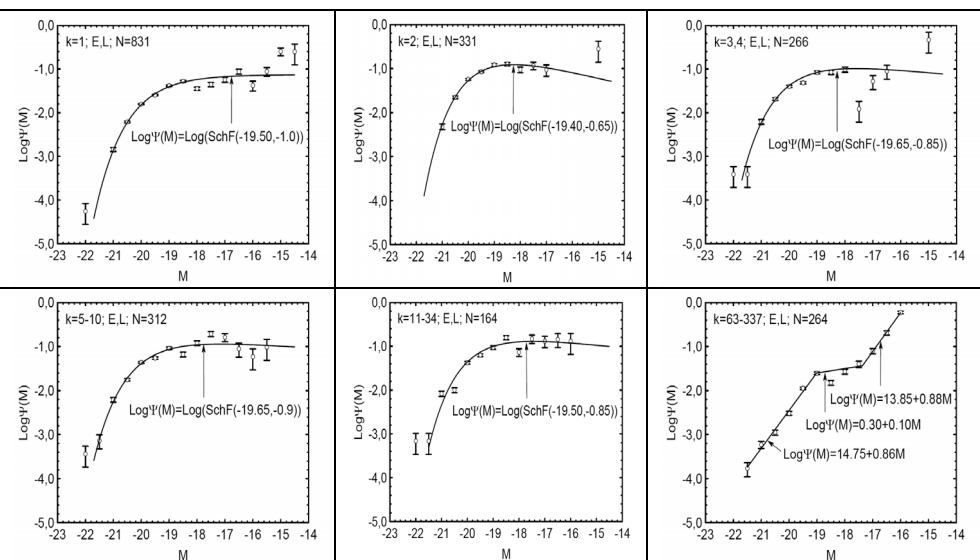


Рис. 10в. ЛФС E и L галактик для систем разных кратностей.

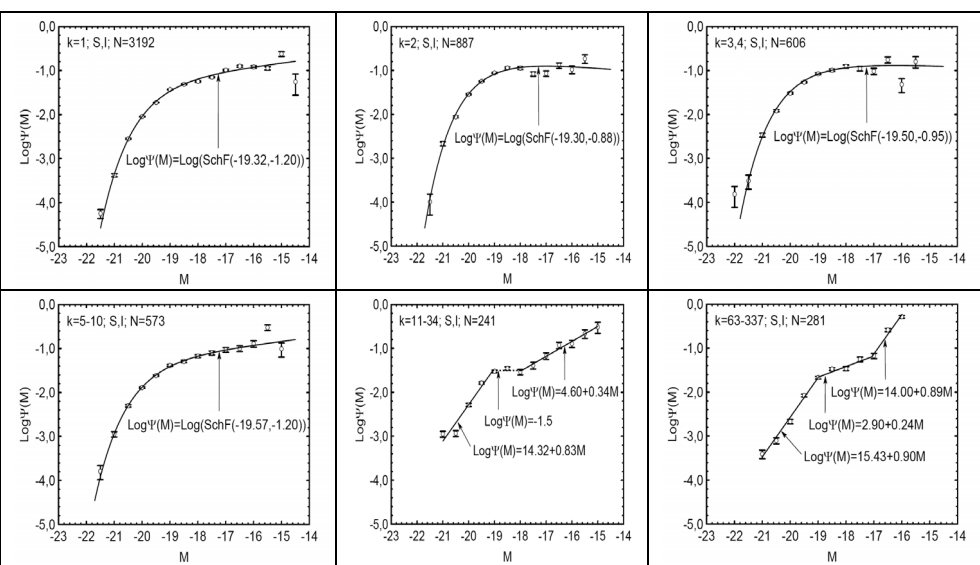


Рис. 10г: ЛФС спиральных и иррегулярных галактик для систем разных кратностей.

Наблюдается также крутой наклон в слабой части светимостей, т.е. скопления галактик отличаются большим относительным числом слабых галактик.

Сказанное относится также отдельно к галактикам разных морфологических типов (рис. 10в-10и). Возможно, что в группах имеющих два видимых члена есть нехватка слабых галактик по сравнению с остальными группами.

Таким образом, ФС всех галактик и галактик разных морфологических типов в одиночных галактиках и в малых группах ( $k < 35$ ) существенно не отличаются друг от друга. Что касается ФС скоплений галактик, то они сильно отличаются от аналогичной функции других систем. В скоплениях наблюдается большое относительное число слабых галактик.

На рис. 11 и 12 приведены функции светимости отдельно для скоплений в Деве и в Волосах Вероники. Как видно ЛФС этих скоплений можно представить линейной функцией для всех морфологических типов.

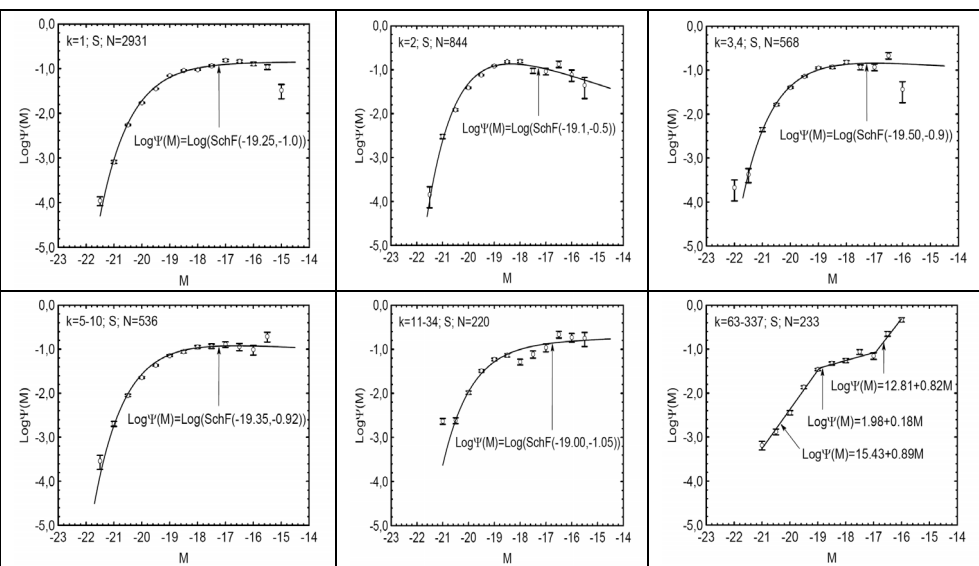


Рис. 10д: ЛФС спиральных галактик для систем разных кратностей.

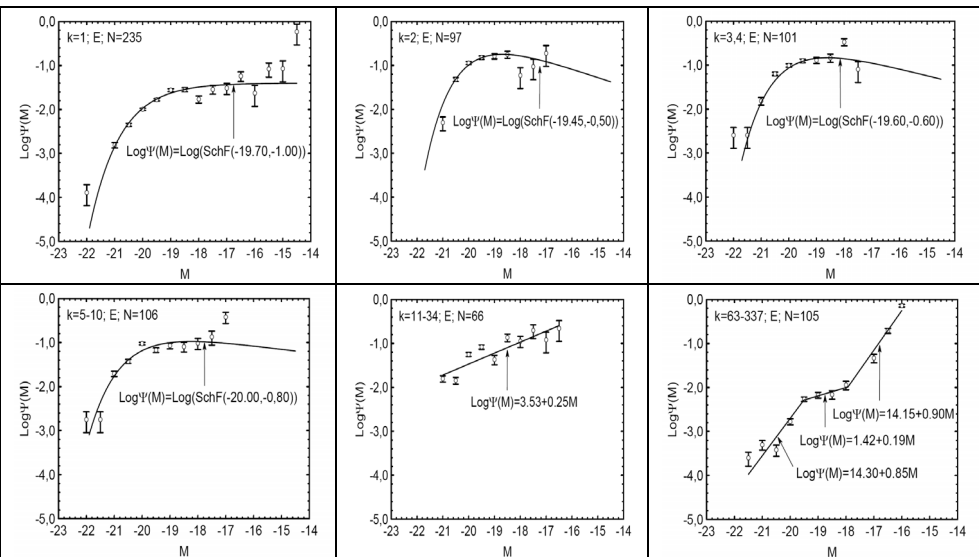


Рис. 10е: ЛФС эллиптических галактик для систем разных кратностей.

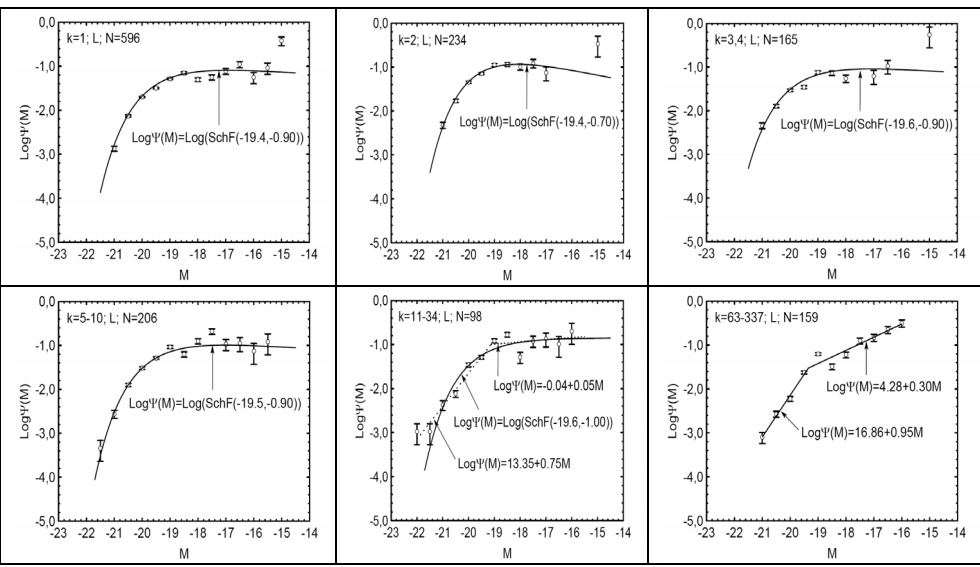


Рис. 10ж: ЛФС линзовидных галактик для систем разных кратностей.

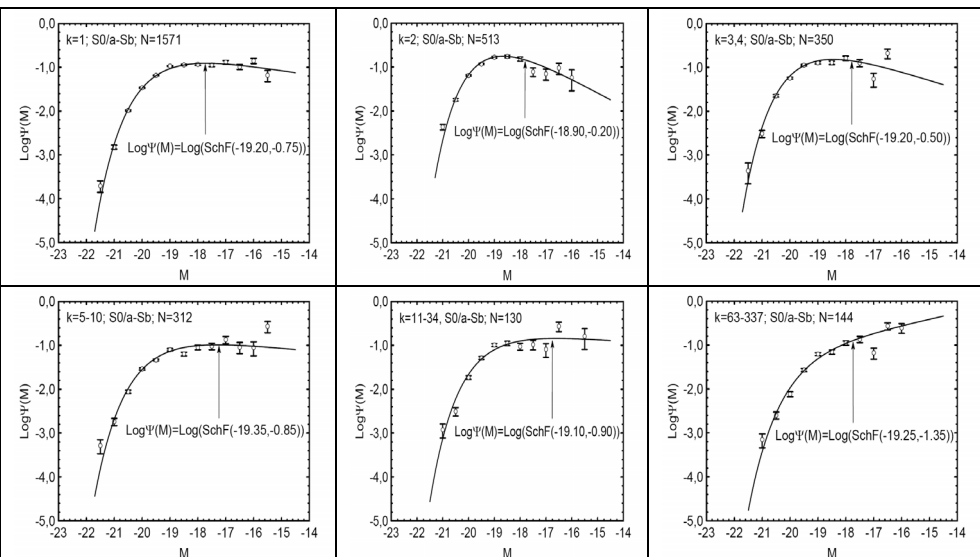


Рис. 10з: ЛФС S0/a-Sb галактик для систем разных кратностей.

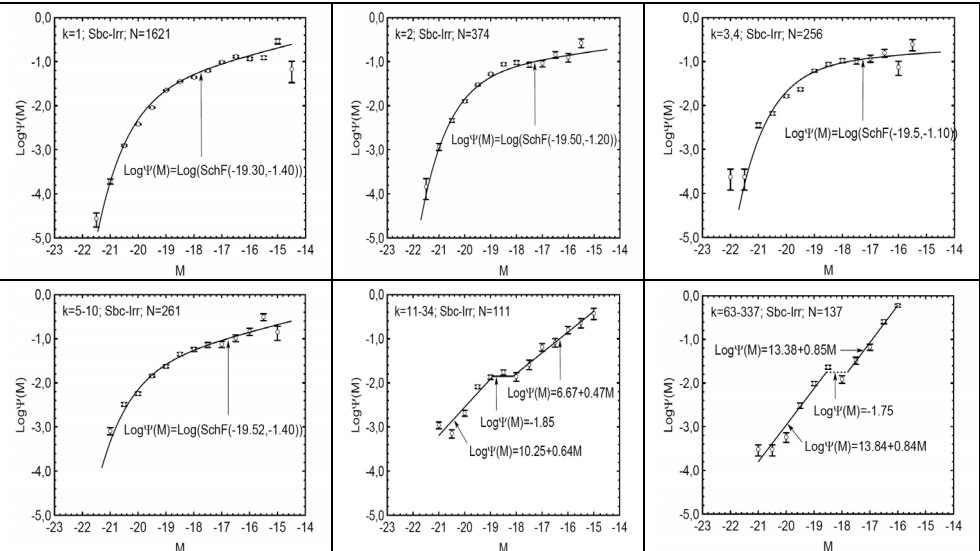


Рис. 10и: ЛФС Sbc-Irr галактик для систем разных кратностей.

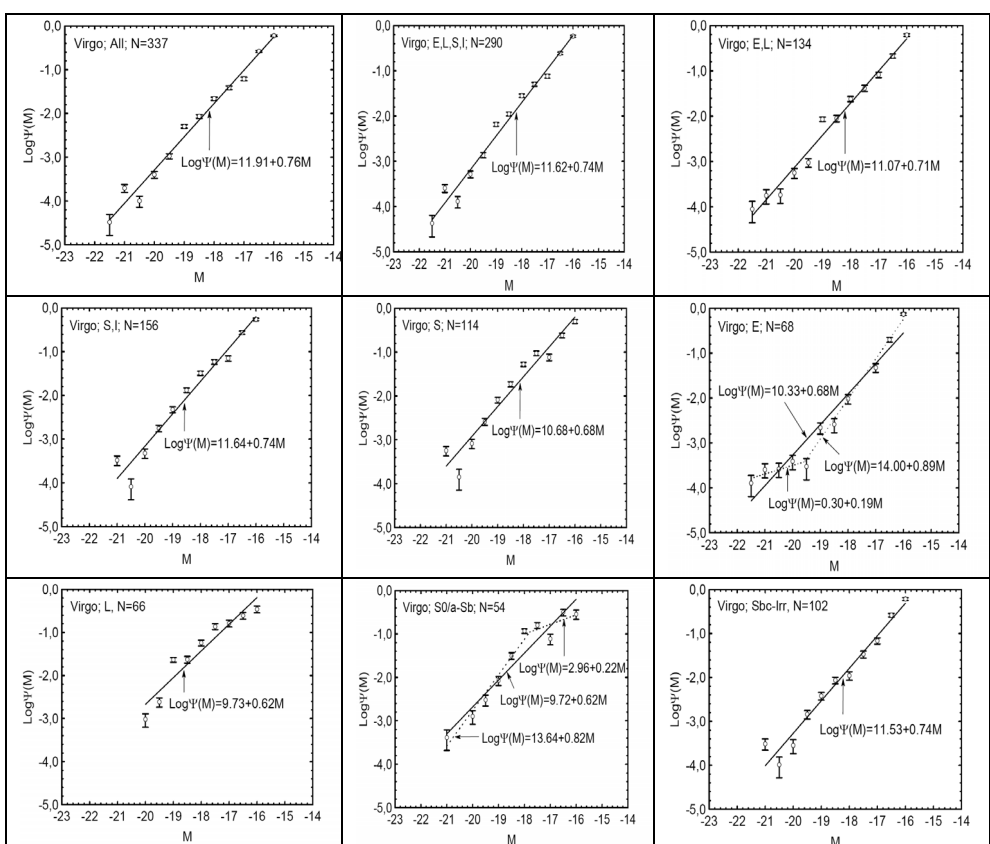


Рис. 11. ЛФС галактик разных морфологических типов скопления в Деве.

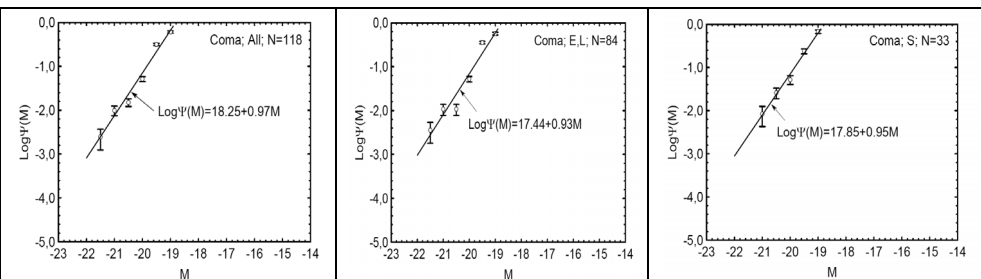


Рис. 12. ЛФС галактик разных морфологических типов скопления в Волосах Вероники.

В табл. 4 приведены средние абсолютные величины галактик в системах разных кратностей в двух интервалах абсолютных величин ( $-23 \leq M \leq -18$ ,  $-23 \leq M \leq -16$ ). В таблице, где не приводится эти величины для случая  $-23 \leq M \leq -16$ , означает, что нет данных до величины  $M = -16$ . Из таблицы видно, что средние абсолютные величины галактик в малых системах значительно не отличаются. В скоплениях же средняя абсолютная светимость галактик несколько ниже в двух изученных диапазонах абсолютных величин. Это означает, что в скоплениях галактик не работают механизмы, которые могут со временем увеличить светимость ярких галактик. Скорее происходит обратный процесс или распределение масс галактик в скоплениях (а также в малых системах) определяется начальными условиями при формировании систем.

Из табл. 4 также видно, что при переходе от эллиптических галактик к линзовидным галактикам, а далее к ранним и к поздним спиральным галактикам средняя абсолютная светимость галактик уменьшается, как в одиночных галактиках, так и в группах.

## 7. Средняя плотность числа галактик в системах разных кратностей

На рис. 12, соответственно, приведены распределения видимой звездной величины для галактик поля, для галактик групп и для одиночных галактик. Из этих рисунков видно, что во всех этих системах неполнота галактик по видимой звездной величине, с известными морфологическими типами, начинается около  $m=14^m$ . Считаем, что в изученных системах выборки всех галактик, безотносительно к известности морфологических типов, полны. Полноту выборок галактик разных морфологических типов оценим по второму методу, предложенному выше (раздел 5). То есть, фактор полноты будет равняться отношению плотности, полученной для всех галактик данной системы с известными морфологическими типами, без учета этого фактора, к плотности всех галактик безотносительно к морфологическим типам. Считаем также, что полнота выборок не зависит от морфологического типа и от абсолютной величины галактик (см. раздел 5).

$$P(m_{\text{lim}}, k)_{E,L,S,I} = \frac{\rho_{\text{obs}}(k)_{E,L,S,I}}{\rho(k)} = \frac{\sum_i \Phi_{\text{obs}}(M_i, k)_{E,L,S,I}}{\rho(k)} \quad (12)$$

Таблица 4. Средние абсолютные величины галактик в двух диапазонах абсолютных величин в группах разных кратностей.

	k	1	2	3,4	5-10	11-34	63-337	2-337	
All	M≤ -18	<b>-18.78</b> 0.008 7925	- <b>18.88</b> 0.015 2294	- <b>18.83</b> 0.019 1562	- <b>18.72</b> 0.019 1280	- <b>18.78</b> 0.026 568	<b>-18.62</b> 0.027 450	- <b>18.79</b> 0.009 6154	среднее ст. откл. n
	M≤ -16	-18.46 0.013 8679	- 17.86 0.026 2400	- 17.97 0.028 1638	- 17.56 0.031 1396	- 17.38 0.047 626	-16.48 0.031 673	- 17.26 0.015 6733	среднее ст. откл. n
E,L, S,I	M≤ -18	<b>-18.71</b> 0.011 3484	- <b>18.81</b> 0.021 1153	- <b>18.82</b> 0.026 825	- <b>18.77</b> 0.026 789	- <b>18.81</b> 0.036 354	<b>-18.64</b> 0.032 369	- <b>18.78</b> 0.012 3490	среднее ст. откл. n
	M≤ -16	-17.29 0.018 3962	- 17.86 0.035 1212	- 17.88 0.040 871	- 17.47 0.040 871	- 17.25 0.059 397	-16.51 0.035 545	- 17.14 0.019 3893	среднее ст. откл. n
E,L	M≤ -18	<b>-18.88</b> 0.025 768	- <b>18.97</b> 0.041 321	- <b>18.92</b> 0.050 260	- <b>18.90</b> 0.048 288	- <b>18.90</b> 0.058 153	<b>-18.73</b> 0.049 183	- <b>18.89</b> 0.022 1205	среднее ст. откл. n
	M≤ -16	-17.66 0.043 819	-	-	- 17.83 0.066 311	- 17.73 0.097 164	-16.47 0.050 264	- 17.06 0.034 1334	среднее ст. откл. n
S,I	M≤ -18	<b>-18.67</b> 0.012 2716	- <b>18.77</b> 0.024 832	- <b>18.78</b> 0.031 565	- <b>18.72</b> 0.031 501	- <b>18.75</b> 0.045 201	<b>-18.57</b> 0.041 186	- <b>18.74</b> 0.014 2285	среднее ст. откл. n
	M≤ -16	-17.24 0.019 3143	- 17.73 0.041 882	- 17.77 0.047 603	- 17.35 0.049 560	- 17.08 0.072 233	-16.54 0.049 281	- 17.19 0.023 2559	среднее ст. откл. n
S	M≤ -18	- <b>18.70</b> 0.013 2606	- <b>18.77</b> 0.024 806	- <b>18.81</b> 0.032 536	- <b>18.73</b> 0.032 490	- <b>18.7</b> 0.04 5 192	- <b>18.58</b> 0.044 175	- <b>18.75</b> 0.015 2199	среднее ст. откл. n
	M≤ -16	-17.46 0.021 2913	- 17.93 0.040 843	- 17.85 0.049 568	- 17.63 0.050 532	- 17.19 0.076 218	-16.72 0.062 233	- 17.43 0.025 2394	среднее ст. откл. n

Таблица 4 (продолжение)

	k	1	2	3,4	5-10	11-34	63-337	2-337	
E	M≤ -18	<b>-18.98</b> 0.049 218	<b>-19.17</b> 0.073 95	<b>-18.88</b> 0.089 100	<b>-19.20</b> 0.090 101	<b>-18.93</b> 0.105 62	<b>-18.75</b> 0.102 54	<b>-18.99</b> 0.042 412	среднее ст. откл. n
	M≤ -16	-16.70 0.102 234	- -	-	-	-	-16.23 0.054 105	-16.62 0.050 475	среднее ст. откл. n
L	M≤ -18	<b>-18.85</b> 0.030 550	<b>-18.91</b> 0.048 226	<b>-18.94</b> 0.059 160	<b>-18.80</b> 0.055 187	<b>-18.89</b> 0.068 91	<b>-18.72</b> 0.055 129	<b>-18.85</b> 0.025 793	среднее ст. откл. n
	M≤ -16	-17.65 0.050 588	- -	-	-17.75 0.078 205	-17.64 0.128 98	-16.96 0.081 159	-17.54 0.042 859	среднее ст. откл. n
S0/a-Sb	M≤ -18	<b>-18.81</b> 0.018 1473	<b>-18.88</b> 0.031 501	<b>-18.88</b> 0.040 337	<b>-18.84</b> 0.043 288	<b>-18.74</b> 0.056 119	<b>-18.57</b> 0.054 121	<b>-18.82</b> 0.019 1366	среднее ст. откл. n
	M≤ -16	-17.72 0.031 1568	-18.25 0.051 513	-18.10 0.062 350	-17.69 0.068 309	-17.69 0.096 129	-17.13 0.089 144	-17.77 0.031 1445	среднее ст. откл. n
Sbc-Irr	M≤ -18	<b>-18.56</b> 0.017 1243	<b>-18.64</b> 0.035 331	<b>-18.67</b> 0.046 228	<b>-18.60</b> 0.045 213	<b>-18.76</b> 0.074 82	<b>-18.58</b> 0.063 65	<b>-18.64</b> 0.022 919	среднее ст. откл. n
	M≤ -16	-17.06 0.024 1575	-17.42 0.059 369	-17.53 0.069 253	-17.14 0.068 251	-16.78 0.096 104	-16.37 0.055 137	-16.91 0.031 1114	среднее ст. откл. n

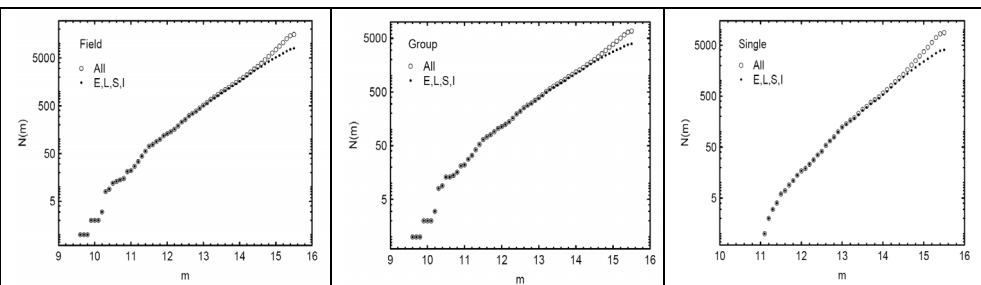


Рис. 12: Распределение видимых звездных величин галактик поля, групп и одиночных галактик в диапазоне лучевых скоростей  $1000 \text{ км} / c \leq V \leq 15000 \text{ км} / c$ .

Данные приведены в табл. 5.

Таблица 5.

Плотность числа всех галактик и наблюдаемая плотность галактик ( $\text{Мpc}^{-3}$ ) с известными морфологическими типами и фактор полноты в системах разных кратностей в диапазоне абсолютных звездных величин  $M \leq -14.5$ .

	$k$	1	2	3,4	5-10	11-34
All	$\rho(k)$	0.0369	0.00486	0.00316	0.00509	0.00352
	$n$	8790	2412	1644	1416	642
E,L,S,I	$\rho_{obs}(k)$	0.0220	0.00250	0.00187	0.00314	0.00214
	$n$	4023	1218	872	885	405
	$P(m_{lim})$	0.596	0.514	0.592	0.617	0.608

Таблица 5 (продолжение)

	$k$	63-337	2-337	1-337	field
All	$\rho(k)$	0.00665	0.0233	0.0602	0.0702
	$n$	673	6787	15577	15577
E,L,S,I	$\rho_{obs}(k)$	0.00508	0.0147	0.0367	0.0460
	$n$	545	3925	7948	7948
	$P(m_{lim})$	0.764	0.631	0.610	0.655

В табл. 6 приведена средняя плотность галактик разных морфологических типов в группах разной кратности в пределах  $M \leq -14.5$ , рассчитанной в объеме с пределами лучевых скоростей  $1000 \text{ км} / c \leq V \leq 15000 \text{ км} / c$ .

Оценим плотность галактик разных морфологических типов внутри групп. Объем произвольной группы оценим следующим образом:

$$Vol_i = \frac{4}{3} \pi R_{\max}^i \quad (13)$$

где  $R_{\max}^i$  - радиус группы (наибольшее расстояние членов группы от ее центра). Тогда суммарная плотность групп с данной кратностью будет:

$$Vol(k) = \sum_i Vol_i(k) \quad (14)$$

А плотность галактик внутри группы можно оценить следующим образом:

$$\rho_{gp}(k) = \rho(k) \frac{V_{\max} - V_{\min}}{Vol(k)} . \quad (15)$$

Таблица 6. Средняя плотность галактик ( $\rho(k)$ , Мпк<sup>-3</sup>) разных морфологических типов в группах разной кратности в диапазоне абсолютных звездных величин  $M \leq -14.5$ .

	$k$	1	2	3,4	5-10	11-34
All	$\rho(k)$	$3.69 \cdot 10^{-2}$	$4.86 \cdot 10^{-3}$	$3.16 \cdot 10^{-3}$	$5.09 \cdot 10^{-3}$	$3.52 \cdot 10^{-3}$
	$n$	8790	2412	1644	1416	642
E,L,S,I	$\rho(k)$	$3.69 \cdot 10^{-2}$	$4.86 \cdot 10^{-3}$	$3.16 \cdot 10^{-3}$	$5.09 \cdot 10^{-3}$	$3.52 \cdot 10^{-3}$
	$n$	4023	1218	872	885	405
E,L	$\rho(k)$	$6.27 \cdot 10^{-3}$	$9.23 \cdot 10^{-4}$	$8.99 \cdot 10^{-4}$	$9.21 \cdot 10^{-4}$	$4.93 \cdot 10^{-4}$
	$n$	831	331	266	312	164
S,I	$\rho(k)$	$3.05 \cdot 10^{-2}$	$3.93 \cdot 10^{-3}$	$2.26 \cdot 10^{-3}$	$4.17 \cdot 10^{-3}$	$3.03 \cdot 10^{-3}$
	$n$	3192	887	606	573	241
S	$\rho(k)$	$1.56 \cdot 10^{-2}$	$2.80 \cdot 10^{-3}$	$1.64 \cdot 10^{-3}$	$2.32 \cdot 10^{-3}$	$1.45 \cdot 10^{-3}$
	$n$	2931	844	568	536	220
E	$\rho(k)$	$2.68 \cdot 10^{-3}$	$1.61 \cdot 10^{-4}$	$1.37 \cdot 10^{-4}$	$1.88 \cdot 10^{-4}$	$1.72 \cdot 10^{-4}$
	$n$	235	97	101	106	66
L	$\rho(k)$	$3.61 \cdot 10^{-3}$	$7.62 \cdot 10^{-4}$	$7.62 \cdot 10^{-4}$	$7.33 \cdot 10^{-4}$	$3.21 \cdot 10^{-4}$
	$n$	596	234	165	206	98
S0/a-Sb	$\rho(k)$	$5.28 \cdot 10^{-3}$	$1.21 \cdot 10^{-3}$	$7.91 \cdot 10^{-4}$	$1.29 \cdot 10^{-3}$	$5.71 \cdot 10^{-4}$
	$n$	1571	513	350	312	130
Sbc-Irr	$\rho(k)$	$2.53 \cdot 10^{-2}$	$2.72 \cdot 10^{-3}$	$1.47 \cdot 10^{-3}$	$2.87 \cdot 10^{-3}$	$2.45 \cdot 10^{-3}$
	$n$	1621	374	256	261	111

Таблица 6 (продолжение)

	$k$	63-337	2-337	1-337	field
All	$\rho(k)$	$6.65 \cdot 10^{-3}$	$2.33 \cdot 10^{-2}$	$6.02 \cdot 10^{-2}$	$7.02 \cdot 10^{-2}$
	$n$	673	6787	15577	15577
E,L,S,I	$\rho(k)$	$6.65 \cdot 10^{-3}$	$2.33 \cdot 10^{-2}$	$6.02 \cdot 10^{-2}$	$7.02 \cdot 10^{-2}$
	$n$	545	3925	7948	7948
E,L	$\rho(k)$	$3.18 \cdot 10^{-3}$	$6.82 \cdot 10^{-3}$	$1.31 \cdot 10^{-2}$	$2.32 \cdot 10^{-2}$
	$n$	264	1337	2168	2168
S,I	$\rho(k)$	$3.47 \cdot 10^{-3}$	$1.65 \cdot 10^{-2}$	$4.70 \cdot 10^{-2}$	$4.70 \cdot 10^{-2}$
	$n$	281	2588	5780	5780
S	$\rho(k)$	$2.07 \cdot 10^{-3}$	$9.99 \cdot 10^{-3}$	$2.56 \cdot 10^{-2}$	$2.43 \cdot 10^{-2}$
	$n$	233	2401	5332	5332
E	$\rho(k)$	$2.16 \cdot 10^{-3}$	$3.23 \cdot 10^{-3}$	$5.91 \cdot 10^{-3}$	$7.20 \cdot 10^{-3}$
	$n$	105	475	710	710
L	$\rho(k)$	$1.02 \cdot 10^{-3}$	$3.60 \cdot 10^{-3}$	$7.21 \cdot 10^{-3}$	$1.60 \cdot 10^{-2}$
	$n$	159	862	1458	1458
S0/a-Sb	$\rho(k)$	$7.68 \cdot 10^{-4}$	$4.47 \cdot 10^{-3}$	$9.75 \cdot 10^{-3}$	$9.23 \cdot 10^{-3}$
	$n$	144	1449	3020	3020
Sbc-Irr	$\rho(k)$	$2.70 \cdot 10^{-3}$	$1.20 \cdot 10^{-2}$	$3.73 \cdot 10^{-2}$	$3.77 \cdot 10^{-2}$
	$n$	137	1139	2760	2760

Данные для групп с разным числом членов приведены в табл. 7. Как видно плотность числа галактик внутри групп с разным числом членов несколько тысяч раз больше, чем средняя плотность галактик в объеме ( $V_{\max} - V_{\min}$ ). Плотность числа галактик внутри групп с числом членов больше 3 составляет  $44 \text{ Мпк}^{-3}$ .

Коэффициенты  $(V_{\max} - V_{\min}) / Vol(k)$  можно использовать также для оценки плотности внутри групп для галактик разных морфологических типов.

Таблица 7

$k$	$Vol(k)$ Мпк <sup>3</sup>	$\frac{V_{\max} - V_{\min}}{Vol(k)}$	$\rho(k)$ Мпк <sup>-3</sup>	$\rho_{sp}(k)$ Мпк <sup>-3</sup>
3,4	600.48	8053.7	0.0032	25.77
5-10	735.14	6578.4	0.0051	33.55
11-34	728.40	6639.3	0.0035	23.24
63-337	509.87	9484.9	0.0067	63.55
3-337	2573.89	1879.9	0.0233	43.78

## 8. Зависимость ФС галактик от плотности и дисперсии скоростей галактик в группах

Исследование зависимости ФС галактик от плотности и от дисперсии лучевых скоростей галактик в группе выполнено для групп с числом членов от 5 до 34. В качестве меры для плотности будем использовать среднее парное расстояние между галактиками группы:

$$R_p = \frac{2 \sum_{j < i}^{k} \sum_{i=1}^{k-1} r_{ij}}{k(k-1)}, \quad (16)$$

где  $r_{ij} = 2(\langle V \rangle / H) \sin(d_{ij} / 2)$ , а  $d_{ij}$  - угловое расстояние между  $i$ -ым и  $j$ -ым членами группы,  $k$  - число членов в группе.

По этому параметру группы разделим на две части:  $R_p \leq 0.5 \text{ Mpc}$  и  $R_p > 0.5 \text{ Mpc}$ . По дисперсии лучевых скоростей

$$\sigma_V = \left[ \frac{1}{k-1} \sum_{i=1}^k (V_i - \langle V \rangle)^2 \right]^{1/2} \quad (17)$$

(где  $V_i$  - лучевая скорость  $i$ -ого члена данной группы,  $k$  - число членов в группе,  $\langle V \rangle$  - средняя лучевая скорость группы) также группы разделим на две части:  $\sigma_V \leq 200 \text{ km/s}$  и  $\sigma_V > 200 \text{ km/s}$ .

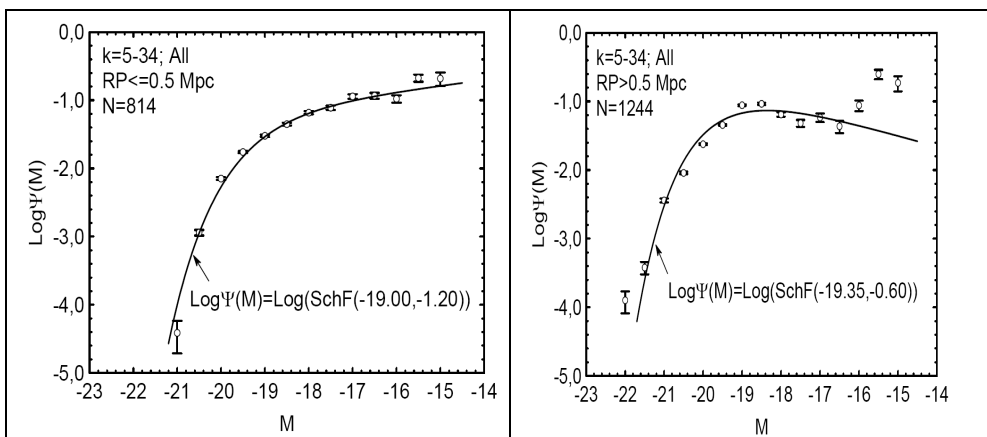


Рис. 13: ЛФС галактик групп с числом членов от 5 до 34 для двух диапазонов средних парных расстояний между галактиками.

На рис. 13 приведена ЛФС галактик для групп с средними парными расстояниями между галактиками  $R_p \leq 0.5 \text{ Mpc}$  и  $R_p > 0.5 \text{ Mpc}$ . Из рисунка видно, что в плотных группах ( $R_p \leq 0.5 \text{ Mpc}$ ) наблюдается относительно

много слабых и мало ярких галактик, чем в разреженных группах ( $R_p > 0.5 \text{Mpc}$ ). Средняя абсолютная величина галактик в диапазоне абсолютных величин  $M \leq -18$ , соответственно, равна  $\langle M \rangle = -18.58 \pm 0.024$  для групп с  $R_p \leq 0.5 \text{Mpc}$  и  $\langle M \rangle = -18.87 \pm 0.020$  для групп с  $R_p > 0.5 \text{Mpc}$ .

На рис. 14 приведена ЛФС галактик для групп с дисперсией лучевых скоростей  $\sigma_v \leq 200 \text{km/s}$  и  $\sigma_v > 200 \text{km/s}$ . Из рис. 14 видно, что в группах с меньшими дисперсиями лучевых скоростей, как и в плотных группах, наблюдается большой наклон в слабом конце ЛФС, т. е. имеется относительно много слабых галактик. Средняя абсолютная величина галактик в диапазоне абсолютных величин  $M \leq -18$ , соответственно, равна  $\langle M \rangle = -18.64 \pm 0.022$  для групп с  $\sigma_v \leq 200 \text{km/s}$  и  $\langle M \rangle = -18.86 \pm 0.022$  для групп с  $\sigma_v > 200 \text{km/s}$ .

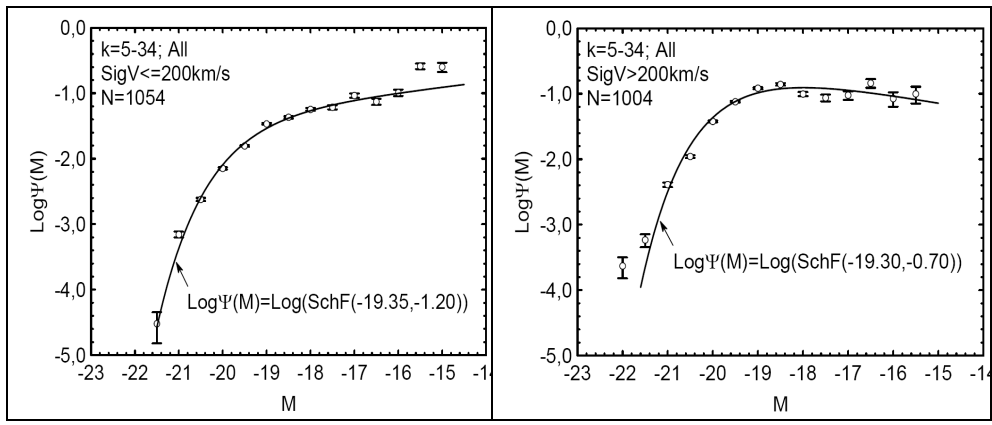


Рис. 14: ЛФС галактик групп с числом членов от 5 до 34 для двух диапазонов дисперсии лучевых скоростей галактик:  $\sigma_v \leq 200 \text{km/s}$  и  $\sigma_v > 200 \text{km/s}$ .

На рис. 15 группы галактик разделены как по средним парным расстояниям, так и по лучевым скоростям галактик. Из рис. 15 видно, что плотные группы с малыми дисперсиями лучевых скоростей ( $R_p \leq 0.5 \text{Mpc}$  и  $\sigma_v \leq 200 \text{km/s}$ ) своими ФС довольно сильно отличаются от групп имеющие малую плотность и большую дисперсию скоростей ( $R_p > 0.5 \text{Mpc}$  и  $\sigma_v > 200 \text{km/s}$ ). В группах с  $\sigma_v > 200 \text{km/s}$  и  $R_p > 0.5 \text{Mpc}$  наблюдается сильный дефицит слабых галактик, а также много ярких галактик по сравнению с группами с  $R_p \leq 0.5 \text{Mpc}$  и  $\sigma_v \leq 200 \text{km/s}$ . ФС галактик групп с  $\sigma_v > 200 \text{km/s}$  и  $R_p > 0.5 \text{Mpc}$  невозможно представить функцией Шехтера.

Таким образом, группы с малыми дисперсиями лучевых скоростей и с малыми средними парными расстояниями между членами содержат в себе относительно много слабых галактик и относительно мало ярких галактик, по сравнению с группами имеющие большие дисперсии лучевых скоростей и большие средние парные расстояния между членами.

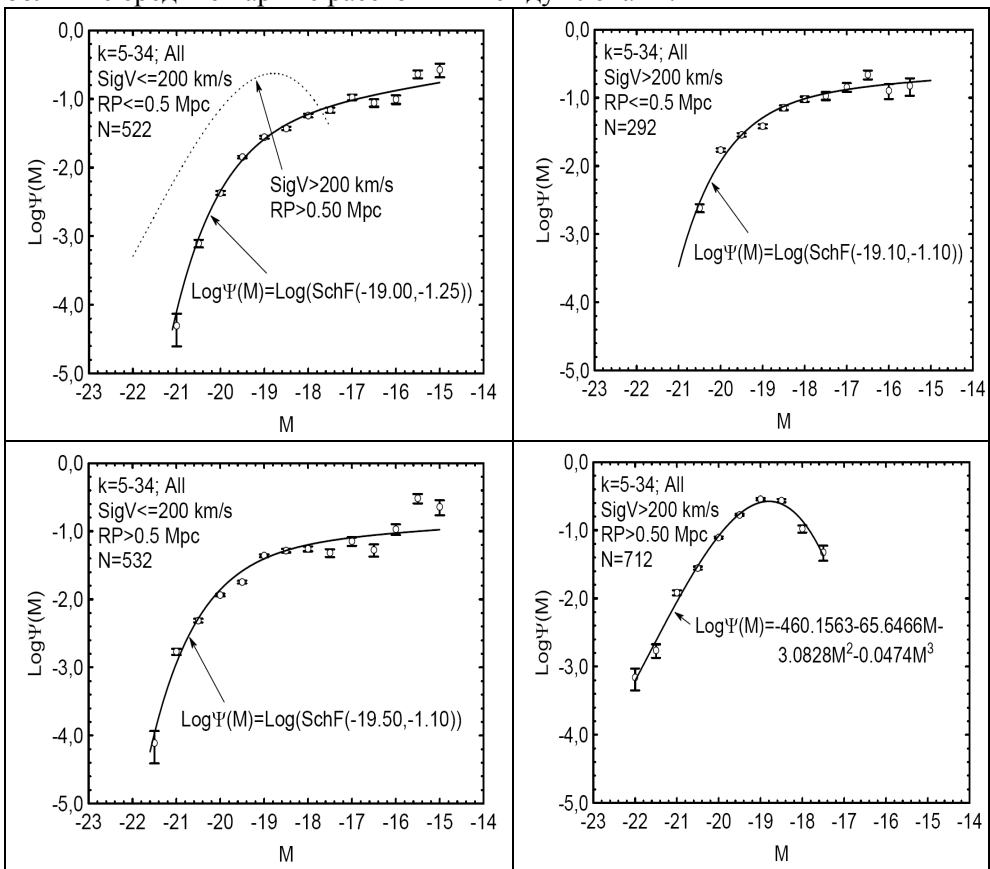


Рис. 15: ЛФС галактик в зависимости от среднего парного расстояния между галактиками и дисперсии лучевых скоростей галактик в группах с числом членов  $k=5-34$ .

Обсудим этот вопрос для галактик обоих морфологических подразделений: галактики E+L и галактики S+I. Результаты приведены на рис. 16 и 17. Эти рисунки показывают, что вышесказанное повторяется как для эллиптических и линзовидных галактик, так и для спиральных и иррегулярных галактик.

Обсудим аналогичный вопрос для групп имеющие два видимые члена. Эти группы разделим по разности лучевых скоростей и по расстоянию галактик на небесной сфере. Результат представлен на рис. 18. Как видно из рисунка получен аналогичный результат, как и для групп с числом членов от 5 до 34. Результат повторяется также для галактик разных морфологических подразделений (рис. 19).

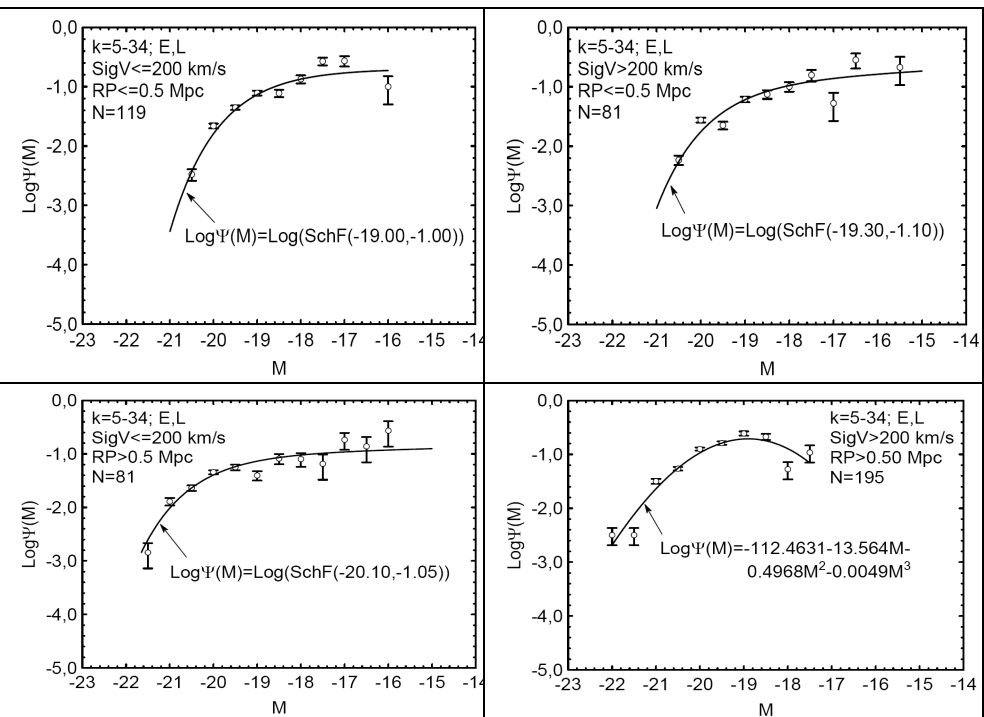


Рис. 16. То же, что и на рис. 15 для E+L галактик.

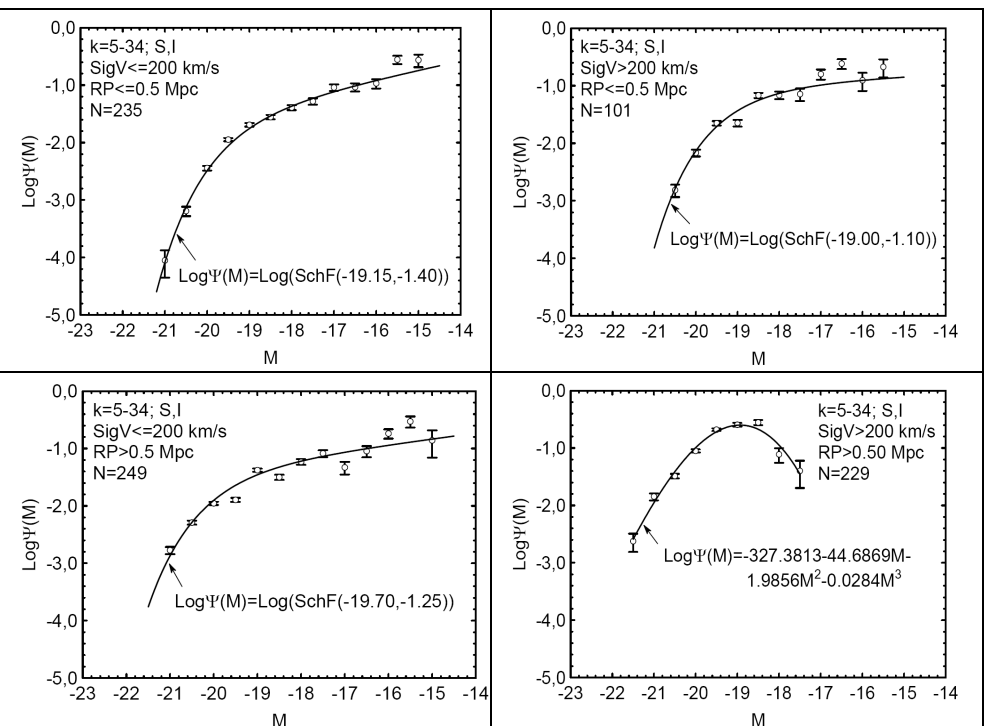


Рис. 17. То же, что и на рис. 15 для S+I галактик.

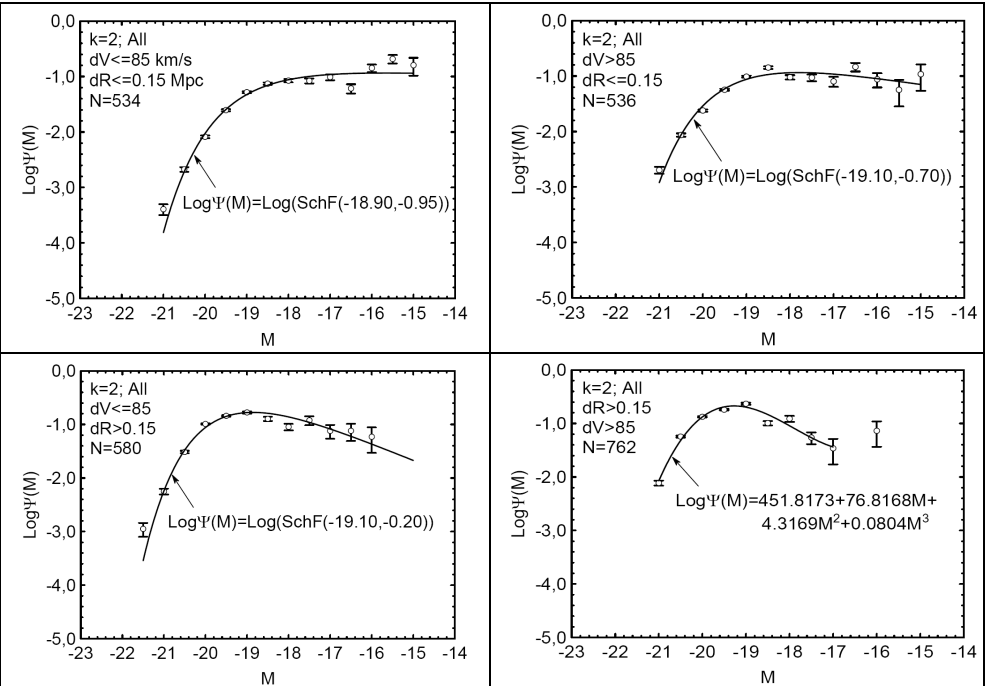


Рис. 18: ЛФС галактик в зависимости от расстояния между галактиками и разницы лучевых скоростей галактик в группах с числом членов  $k=2$ .

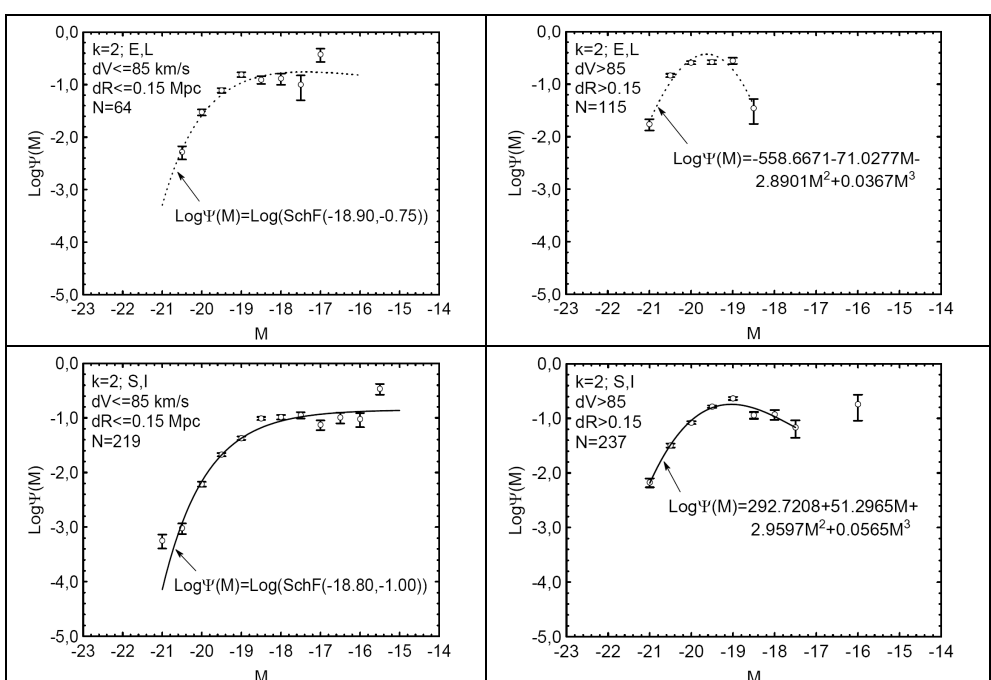


Рис. 19: ЛФС E+L и S+I галактик в зависимости от расстояния между галактиками и разницы лучевых скоростей галактик в группах с числом членов  $k=2$ .

## 9. Заключение

В данной работе предложен новый метод для определения функции светимости ( $\Phi$ С) галактик. По сути, обобщен метод Шмидта (Schmidt 1968) с учетом зависимости плотности галактик от расстояния в близкой Вселенной. Изучена  $\Phi$ С галактик поля и ее связь с морфологическими типами галактик. Получены следующие результаты:

1.  $\Phi$ С галактик поля можно представить функцией Шехтера (Schechter 1976) с параметрами  $M_* = -19.30$  и  $\alpha = -0.90$  только в ограниченном участке светимостей:  $-21.0 \leq M \leq -17.6$ . Левее от этой области Л $\Phi$ С можно представить квадратным многочленом, а правее, при слабых светимостях - линейной функцией. Л $\Phi$ С галактик поля с известными морфологическими типами почти не отличается от Л $\Phi$ С всех галактик.

2. Для эллиптических и линзовидных галактик поля, как и для всех галактик, функцией Шехтера можно представить только часть  $\Phi$ С. Причем, по параметру  $\alpha$  они не отличаются, а по параметру  $M_*$  отличаются мало.

3.  $\Phi$ С спиральных и иррегулярных галактик поля хорошо представляется функцией Шехтера с параметрами  $M_* = -19.4$  и  $\alpha = -1.25$  почти во всей изученной области светимостей:  $M \geq -21.5$ .

4. Поведение  $\Phi$ С галактик типов E и L подобно поведению  $\Phi$ С всех галактик, т.е. не во всем диапазоне абсолютных звездных величин  $\Phi$ С можно представить функцией Шехтера. Данная функция для эллиптических галактик применима только в диапазоне  $-21.2 \leq M \leq -17.8$ , а для линзовидных галактик – в диапазоне  $-21.2 \leq M \leq -16.5$ .

5.  $\Phi$ С спиральных галактик можно представить функцией Шехтера в довольно широком диапазоне абсолютных звездных величин. При переходе от ранних спиралей к поздним спиралям происходит уменьшение параметра  $\alpha$  в функции Шехтера, т. е. увеличивается относительное число слабых галактик. Параметром  $M_*$  они слабо отличаются.

6. Оценена полнота и средняя плотность выборок галактик поля разных морфологических типов. Средняя плотность числа всех галактик в диапазоне  $-23 \leq M \leq -13$  равна  $0.126 \text{ Мpc}^{-3}$ .

7. Оценены средние абсолютные звездные величины галактик поля разных морфологических типов в двух интервалах абсолютной звездной величины:  $-23 \leq M \leq -17.8$  и  $-23 \leq M \leq -14.0$ . При переходе от эллиптических галактик к линзовидным, к ранним и к поздним спиралям в яркой части абсолютных звездных величин ( $-23 \leq M \leq -17.8$ ) наблюдается уменьшение средних светимостей.

8.  $\Phi$ С всех галактик и галактик разных морфологических типов в одиночных галактиках и в малых группах ( $k < 35$ ) существенно не отличаются друг от друга. Что касается  $\Phi$ С скоплений галактик, то они сильно отличаются от аналогичной функции других систем. В скоплениях наблюдается большое относительное число слабых галактик.

9. ЛФС скоплений в Деве и в Волосах Вероники можно представить линейной функцией для всех морфологических типов.

10. Средние абсолютные величины галактик в малых системах особенно не отличаются. В скоплениях же средние абсолютные светимости галактик несколько ниже в двух изученных диапазонах абсолютной величины ( $M \leq -18$  и  $M \leq -16$ ).

11. При переходе от эллиптических галактик к линзовидным галактикам, к ранним и к поздним спиральным галактикам абсолютная светимость галактик уменьшается, как в одиночных галактиках, так и в группах (см. пункт 7).

12. Группы с малыми дисперсиями лучевых скоростей и с малыми средними парными расстояниями между членами содержат в себе относительно много слабых галактик и относительно мало ярких галактик, по сравнению с группами имеющие большие дисперсии лучевых скоростей и большие средние парные расстояния между членами. Сказанное относится как к эллиптическим и линзовидным галактикам, так и к спиральным и иррегулярным галактикам.

Поведение ФС галактик в скоплениях наводит на мысль, что возможно в этих системах в эволюции галактик важную роль может играть механизм выметания газа из галактик лобовым давлением межгалактического газа скопления, а в бедных скоплениях или в группах - приливные взаимодействия между галактиками. Но есть одна причина, которая ставит под сомнения этих механизмов. Это то, что ФС как эллиптических, так и спиральных галактик имеют подобные зависимости от окружения.

Более вероятно, что распределение масс галактик в системах определяется начальными условиями при их формировании.

## ЛИТЕРАТУРА

- Andreon, S. 1998, A&A, **336**, 98  
Andreon, S., Davoust, E., & Heim, T. 1997, A&A, **323**, 337  
Arakelian M. A., Kaloglian A. T., 1969, Astron. Let., **46**, 1215  
Barrientos, L. F., Schade, D., & Lopez-Cruz, O. 1996, ApJ, **460**, L89  
Binggeli, B., Sandage, A., & Tammann, G. A. 1988, ARA&A, **26**, 509  
Bromley, B. C., Press, W. H., Lin, H., & Kirshner, R. P. 1998, ApJ, **505**, 25  
Choloniewski J, 1987, MNRAS, **226**, 273  
Colless, M. M. 1989, MNRAS, **237**, 799  
Cuesta-Bolao M. J. & Serna A. 2003, A&A, **405**, 917  
de Propis, R., Colless, M., Driver, S., et al. 2002, preprint [astro-ph/0212562]  
Dressler, A. 1978, ApJ, **223**, 765  
Dressler, A. 1980, ApJ, **236**, 351  
Driver, S. P., Phillipps, S., Davies, J. I., Morgan, I., & Disney, M. J. 1995, MNRAS, **268**, 393  
Efstathiou, G., Ellis, R. S., & Peterson, B. A., 1988, MNRAS, **232**, 431  
Huchra J., Sargent W. L. W., 1973, ApJ, **186**, 433

- Felten, J. E. 1977, AJ, **82**, 861  
Ferguson, H. C., & Sandage, A. 1991, AJ, **101**, 765  
Gaidos, E. 1997, AJ, **113**, 117  
Garilli, B., Bottini, D., Maccagni, D., Vettolani, G., & Maccacaro, T. 1992, AJ, **104**, 1290  
Garilli, B. M., Maccagni, D., & Andreon, S. 1999, A&A, **342**, 408  
Garilli, B., Maccagni, D., & Vettolani, G. 1991, AJ, **101**, 795  
Goto, T., Okamura, S., McKay, T., et al. 2002, PASJ, **54**, 515  
Gudehus, D. H., & Hegyi, D. J. 1991, AJ, **101**, 18  
Gunn J.E., Gott J.R., Astrophys. J., 1972, **176**, 1-19.  
Jerjen, H., & Tamman, G. 1997, A&A, **321**, 713  
Lin, H., Kirshner, R. P., Shectman, S. A., Landy, S. D., Oemler, A., Tucker, D. L., & Schechter, P. L. 1996, ApJ, **464**, 60  
Lopez-Cruz, O., & Yee, H. K. C. 1995, ASP Conf. Ser. 86, Fresh Views of Elliptical Galaxies, ed. A. Buzzoni, A. Renzini, & A. Serrano (San Francisco: ASP), 279  
Lopez-Cruz, O., Yee, H. K. C., Brown, J. P., Jones, C., & Forman, W. 1997, ApJ, **475**, 97  
Loveday, J., Peterson, B. A., Efstathiou, G., & Maddox, S. J. 1992, ApJ, **390**, 338  
Lugger, P. M. 1986, ApJ, **303**, 535  
Lumsden, S. L., Collins, C. A., Nichol, R. C., Eke, V. R., & Guzzo, L. 1997, MNRAS, **290**, 119  
Lynden-Bell, D., 1971, MNRAS, **155**, 95  
Mahtessian, A. P. 1997, Astrofizika, **40**, 45  
Mahtessian, A. P., Movsessian V. H. 2010, Astrofizika, **53**, 83  
Marinoni, C., Monaco, P., Giuricin, G., & Costantini, B. 1999, ApJ, **521**, 50  
Marzke, R. O., Geller, M. J., Huchra, J. P., & Corwin, H. G. 1994, AJ, **108**, 437  
Muriel, H., Valotto C. A. & Lambas D. G. 1998, ApJ, **506**, 540  
Negroponte J., White S.D.M., MNRAS, 1983, **205**, 1009-1029  
Neyman, J., Scott, E. L. 1974, Confrontation of Cosmological Theories with Observational Data, IAUS No. 63, Ed. by Longair, 129  
Nicol, J. F., & Segal, I. E. 1983, A&A, **118**, 180  
Oegerle, W. R., Hoessel, J. G., & Ernst, R. M. 1986, AJ, **91**, 697  
Oegerle, W. R., Hoessel, J. G., & Jewison, M. S. 1987, AJ, **93**, 519  
Oemler, A., Jr. 1974, ApJ, **194**, 1  
Paolillo, M., Andreon, S., Longo, G., et al. 2001, A&A, **367**, 59  
Ramella, M., Zamorani, G., Zucca, E., et al. 1999, A&A, **342**, 1  
Rayzy, S., Adami, C., & Mazure, A. 1998, A&A, **337**, 31  
Ribeiro, A. L. B., de Carvalho, R. R., & Zepf, S. E. 1994, MNRAS, **267**, L13  
Sandage A., ApJ, 183, **711**, 1973  
Sandage, A., Binggeli, B., & Tammann, G. A. 1985, AJ, **90**, 1759  
Schechter, P. 1976, ApJ, **203**, 297  
Schmidt, M. 1968, ApJ, **151**, 393  
Spitzer L., Baade W., ApJ, 1951, **113**, 413-418.  
Terebikh V. Yu. 1980, Astrofizika, **16**, 45  
Toomre A., Toomre J., ApJ, 1972, **178**, 623-666.

- Trentham, N. 1997, MNRAS, **290**, 334  
Trentham, N., & Hodgkin, S. 2002, MNRAS, **333**, 423  
Valotto, C. A., Nicotra, M. A., Muriel, H., & Lambas, D. G. 1997, ApJ, **479**, 90  
White S.D.M., MNRAS, 1979, **189**, 831-852  
Willmer, C. N. A., Focardi, P., Chan, R., Pellegrini, P. S., & da Costa, L. N. 1991, AJ, **101**, 57  
Zabludoff, A. I., & Mulchaey, J. S. 2000, ApJ, **539**, 136  
Zepf, S. E., de Carvalho, R. R., & Ribeiro, A. L. B. 1997, ApJ, **488**, L11

# Second order operators on the algebra of densities and a groupoid of connections

H. M. Khudaverdian<sup>1\*</sup>, Th. Th. Voronov<sup>2†</sup>

<sup>1</sup>*Max-Planck-Institut für Mathematik, Vivatsgasse 7, 53111 Bonn, Germany*  
*On leave of absence of School of Mathematics, University of Manchester*  
*Oxford Road, Manchester M13 9PL, UK*

<sup>2</sup>*School of Mathematics, University of Manchester*  
*Oxford Road, Manchester M13 9PL, UK*

## Abstract

We consider the geometry of second order linear operators acting on the commutative algebra of densities on a (super)manifold introduced in our previous work. In the conventional language, operators on the algebra of densities correspond to operator pencils. This algebra has a natural invariant scalar product. We consider self-adjoint operators on the algebra of densities and analyze the corresponding “canonical operator pencils” passing through a given operator on densities of a particular weight. There are singular values for the pencil parameters. This leads to an interesting geometrical picture. In particular we obtain operators that depend on equivalence classes of connections and we study a groupoid of connections such that the orbits of this groupoid are these equivalence classes. Based on this point of view we analyze two examples: the second order canonical operator on an odd symplectic supermanifold appearing in the Batalin-Vilkovisky geometry and the Sturm-Liouville operator on the line related with classical constructions of projective geometry. We also consider a canonical second order semidensity arising on odd symplectic supermanifolds, which has some resemblance with mean curvature in Riemannian geometry.

## 1. Introduction

Second order linear operators appear in various problems in mathematical physics. A condition that an operator respects the geometrical structure of a problem under consideration usually fixes this operator almost uniquely or at least provides a great deal of information about it. For example the standard Laplacian  $\frac{\partial^2}{\partial x^2} + \frac{\partial^2}{\partial y^2} + \frac{\partial^2}{\partial z^2}$

\*E-mail: khudian@mpim-bonn.mpg.de; khudian@manchester.ac.uk

†E-mail:theodore.voronov@manchester.ac.uk

in Euclidean space  $\mathbb{E}^3$  is defined uniquely (up to a constant) by the condition that it is invariant with respect to isometries of  $\mathbb{E}^3$ . Consider an arbitrary second order operator

$$\Delta = \frac{1}{2} \left( S^{ab} \partial_a \partial_b + T^a \partial_a + R \right) \quad (1)$$

acting on functions on manifold  $M$ . It defines on  $M$  symmetric contravariant tensor  $S^{ab}$  (its principal symbol). For example for a Riemannian manifold one can take a principal symbol  $S^{ab} = g^{ab}$ , where  $g^{ab}$  is the metric tensor (with upper indices). Then one can fix the scalar  $R = 0$  in (1) by the natural condition  $\Delta 1 = 0$ . What about the first order term  $T^a \partial_a$  in the operator (1)? One can see that Riemannian structure fixes this term also. Indeed consider on  $M$  a divergence operator

$$\operatorname{div}_{\rho} \mathbf{X} = \frac{1}{\rho(x)} \frac{\partial}{\partial x^a} (\rho(x) X^a), \quad (2)$$

where  $\rho = \rho(x)|D(x)|$  is an arbitrary volume form and choose a volume form  $\rho = \rho_g = \sqrt{\det g}|D(x)|$ . On Riemannian manifold this volume form is defined uniquely (up to a constant factor) by covariance condition. Thus we come to second order operator  $\Delta_g$  such that for an arbitrary function  $f$

$$\begin{aligned} \Delta_g f &= \frac{1}{2} \operatorname{div}_{\rho_g} \operatorname{grad} f = \frac{1}{2} \frac{1}{\rho(x)} \frac{\partial}{\partial x^a} \left( \rho_g(x) g^{ab} \frac{\partial f(x)}{\partial x^b} \right) \\ &= \frac{1}{2} \left( \partial_a \left( g^{ab} \partial_b f \right) + \partial_a \log \rho_g(x) g^{ab} \partial_b f(x) \right) \\ &= \frac{1}{2} \left( g^{ab} \partial_a \partial_b f + \partial_a g^{ab} \partial_b f + \partial_a \log \sqrt{\det g} g^{ab} \partial_b f(x) \right). \end{aligned} \quad (3)$$

We see that Riemannian structure on manifold naturally defines a unique (up to a constant factor) second order operator on functions (the Laplace-Beltrami operator on Riemannian manifold  $M$ ). For this operator the terms with first derivatives contain a connection  $\nabla$  on volume forms. This connection is defined by the condition that for an arbitrary volume form  $\rho = \rho(x)|D(x)|$ ,  $\nabla_{\mathbf{X}} \rho = \partial_{\mathbf{X}} \left( \frac{\rho}{\rho_g} \right) \rho_g$ :

$$\begin{aligned} \nabla_{\mathbf{X}} \rho &= X^a (\partial_a + \gamma_a) \rho(x)|D(x)| = X^a \partial_a \left( \frac{\rho}{\rho_g} \right) \rho_g \\ &= X^a \partial_a \left( \frac{\rho(x)}{\sqrt{\det g}} \right) \sqrt{\det g} |D(x)| \\ &= X^a \left( \partial_a \rho(x) - \partial_a \log \left( \sqrt{\det g} \right) \right) |D(x)|. \end{aligned} \quad (4)$$

(Here the symbol of connection  $\gamma_a = -\partial_a(\rho_g(x)) = -\partial_a \log \sqrt{\det g}$ .)

Consider another example: Let  $S^{ab}(x)$  be an arbitrary symmetric tensor field (not necessarily non-degenerate) on manifold  $M$  equipped with affine structure with the connection on vector fields  $\nabla: \nabla_a \partial_b = \Gamma_{ab}^c \partial_c$ . The affine structure defines the second order operator  $S^{ab} \nabla_a \nabla_b = S^{ab} \partial_a \partial_b + \dots$ . Principal symbol of this operator is the

tensor field  $S^{ab}(x)$ . The affine connection induces a connection  $\nabla$  on volume forms by the relation  $\gamma_a = -\Gamma_{ab}^b$ . In the case of a Riemannian manifold the tensor  $S^{ab}$  can be fixed by Riemannian metric,  $S^{ab} = g^{ab}$ , and the Levi-Civita Theorem provides a unique symmetric affine connection which preserves the Riemannian structure. Thus we arrive again to the Beltrami-Laplace operator (3).

Often it is important to consider differential operators on densities of arbitrary weight  $\lambda$ . For example a density of weight  $\lambda = 0$  is an ordinary function, a volume form is a density of weight  $\lambda = 1$ . Wave function in Quantum Mechanics can be naturally considered as a half-density, i.e. a density of weight  $\lambda = 1/2$ .

Analysis of differential operators on densities of arbitrary weights leads to beautiful geometric constructions. ( See e.g. the works [7, 8, 16] and the book [18].) For example consider  $\text{Diff}(M)$ -modules which appear when we study operators on densities. Namely let  $\mathcal{D}_\lambda(M)$  be a space of second order linear operators acting on densities of weight  $\lambda$ . This space has a natural structure of  $\text{Diff}(M)$ -module. In the work [8] Duval and Ovsienko classified these modules for all values of  $\lambda$ . In particular they wrote down explicit expressions for  $\mathcal{D}_\lambda(M)$ -isomorphisms  $\varphi_{\lambda,\mu}$  between modules  $\mathcal{D}_\lambda(M)$  and  $\mathcal{D}_\mu(M)$  for  $\lambda, \mu \neq 0, \frac{1}{2}, 1$ . These isomorphisms have the following appearance: If an operator  $\Delta_\lambda \in \mathcal{D}_\lambda(M)$  is given in local coordinates by the expression  $\Delta_\lambda = A^{ij}(x)\partial_i\partial_j + A^i(x)\partial_i + A(x)$  then its image  $\varphi_{\lambda,\mu}(\Delta_\lambda) = \Delta_\mu \in \mathcal{D}_\mu(M)$  is given in the same local coordinates by the expression  $\Delta_\mu = B^{ij}(x)\partial_i\partial_j + B^i(x)\partial_i + B(x)$  where

$$\begin{cases} B^{ij} &= A^{ij}, \\ B^i &= \frac{2\mu-1}{2\lambda-1}A^i + \frac{2(\lambda-\mu)}{2\lambda-1}\partial_j A^{ji}, \\ B &= \frac{\mu(\mu-1)}{\lambda(\lambda-1)}A + \frac{\mu(\lambda-\mu)}{(2\lambda-1)(\lambda-1)}(\partial_j A^j - \partial_i\partial_j A^{ij}) . \end{cases} \quad (5)$$

At the exceptional cases  $\lambda, \mu = 0, 1/2, 1$ , non-isomorphic modules occur.

In work [15] it was suggested the new approach to consider the commutative algebra  $\mathcal{F}(M)$  of densities of all weights on a manifold  $M$ . This algebra possesses a canonical invariant scalar product. One can study differential operators on the algebra  $\mathcal{F}(M)$ . Due to the existence of the canonical scalar product it is possible to consider the notion of self-adjoint and antiself-adjoint differential operators on this algebra. Operators on the algebra  $\mathcal{F}(M)$  can be identified with pencils of operators acting between the spaces of densities of various weights. Self-adjoint operators of second order on  $\mathcal{F}(M)$  correspond to certain canonical pencils of operators with the same principal symbol and associated with connection on volume forms on  $M$ . This approach was suggested and developed in [15] for studying and classifying second order odd operators on odd symplectic manifolds (arising in the Batalin-Vilkovisky formalism) and on odd Poisson manifolds.

The canonical pencils of second order operators have the “universality” property: there is a unique such a pencil passing through an arbitrary second order operator acting on densities of arbitrary weight except for three singular cases. For example consider the operator  $\Delta$  of weight 0 acting on densities of weight  $\lambda$ ,  $\Delta \in \mathcal{D}_\lambda(M)$ ,  $\Delta = S^{ab}\partial_a\partial_b + \dots$ , where  $S^{ab}$  is a symmetric contravariant tensor field. Then for an arbitrary weight  $\lambda$  except for the singular cases  $\lambda = 0, \frac{1}{2}, 1$  there exists a canonical

pencil of operators which passes through the operator  $\Delta$ . These exceptional weights have deep geometrical and physical meaning. E.g. the failure to construct maps  $\varphi_\lambda, \mu$  in equation (5) for singular cases is related with existence of non-equivalent  $\text{Diff}(M)$  modules (see for detail [8]). The space  $\mathcal{D}_{1/2}(M)$  of operators on half-densities is drastically different from all other spaces  $\mathcal{D}_\lambda(M)$ , since for second order operators on half-densities there is a natural notion of a self-adjoint operator. This fact is of great importance for the Batalin-Vilkovisky geometry (see [12, 14]).

Applying the approach of the work [15] we study canonical pencils of second order operators of an arbitrary weight  $\delta$  and analyze in detail the exceptional case when these operators act on densities of weight  $\lambda = \frac{1-\delta}{2}$ . (An operator has weight  $\delta$  if it maps densities of weight  $\lambda$  into the densities of weight  $\mu = \lambda + \delta$ .) Such an operator pencil can be defined by a symmetric contravariant tensor density  $\mathbf{S} = |D(x)|^\delta S^{ab} \partial_a \otimes \partial_b$  (this field defines the principal symbol) and a connection  $\nabla$  on volume forms. Specialising the pencil to the exceptional value of weight  $\lambda = \frac{1-\delta}{2}$  we come to an operator which depends only on a equivalence class of connections. We assign to every field  $\mathbf{S}$  the certain groupoid of connections  $C_{\mathbf{S}}$ . For the exceptional weight  $\lambda = \frac{1-\delta}{2}$  the operator with the principal symbol  $\mathbf{S}$  depends on an orbit of this groupoid.

This is particularly interesting in the case of odd symplectic structures. For symplectic structures (even or odd) there is no distinguished connection. On the other hand, if a symplectic structure is odd, then the Poisson tensor is symmetric and it defines the principal symbol  $\mathbf{S}$  of an operator pencil of weight  $\delta = 0$ . It turns out that in spite of the absence of a distinguished connection, there exists a canonical class of connections on volume forms such that for them  $\gamma_a$  ( $\nabla_a = \partial_a + \gamma_a$ ) vanishes in some Darboux coordinates. Connections of this canonical class belong to an orbit of the groupoid  $C_{\mathbf{S}}$  and the corresponding operator on half-densities is the canonical operator introduced in [12]. This operator seems to be the correct clarification of the Batalin-Vilkovisky “odd Laplacian” [3]. (See for detail [14].) This approach may be used also in the case of Riemannian geometry where  $\mathbf{S}$  is defined by a Riemannian metric. However in this case there exists a distinguished connection (Levi-Civita connection). We would like to mention article [2] where an interesting attempt to compare second order operators for even Riemannian and odd symplectic structures was made.

Another important case is a canonical pencil of operators of weight  $\delta = 2$  on the line. By considering exceptional weights we come in particular to Schwarzian derivative.

The plan of the paper is as follows.

In the next section we consider second order operators on the algebra of functions. We come in this “naive” approach to preliminary relations between second order operators and connections on volume forms.

In the third section we consider first and second order operators on the algebra  $\mathcal{F}(M)$  of all densities on a manifold  $M$ . First we define an invariant canonical scalar product on the algebra  $\mathcal{F}(M)$ . This algebra can be interpreted as a subalgebra of functions on an auxiliary manifold  $\widehat{M}$ . We consider derivations (which can be

identified with vector fields on  $\widehat{M}$ ) and first order operators on the algebra  $\mathcal{F}(M)$ . The canonical scalar product on  $\mathcal{F}(M)$  leads to the canonical divergence of vector fields on  $\widehat{M}$ . We come in particular to the interpretation of Lie derivatives of densities as divergence-free vector fields on  $\widehat{M}$ .

After that we consider second order operators on the algebra  $\mathcal{F}(M)$ . We introduce our main construction: the self-adjoint second order operators on the algebra  $\mathcal{F}(M)$ , and consider the corresponding operator pencils. These considerations are due to the paper [15].

In the fourth section we consider operators of weight  $\delta$  acting on densities of exceptional weight  $\lambda = \frac{1-\delta}{2}$ . For an arbitrary contravariant symmetric tensor density  $\mathbf{S}$  of weight  $\delta$  we consider groupoid  $C_{\mathbf{S}}$ . The orbits of the groupoid  $C_{\mathbf{S}}$  are classes of connections such that operators with the principal symbol  $\mathbf{S}$  acting on densities of the exceptional weight  $\lambda = \frac{1-\delta}{2}$  depend only on these classes. This groupoid was first considered in [14, 15] for the Batalin-Vilkovisky geometry. We also give explicit description for corresponding Lie algebroids.

Then we consider various examples where these operators occur. We consider the example of operators of weight  $\delta = 0$  acting on half-densities on a Riemannian manifold and on an odd symplectic supermanifold, and the example of operators of weight  $\delta = 2$  acting on densities of weight  $\lambda = -\frac{1}{2}$  on the line. In all these examples the operators depend on classes of connections on volume forms which vanish in special coordinates (such as Darboux coordinates for symplectic case and projective coordinates for the line).

Finally we consider the example of the canonical odd invariant half-density introduced in [13]. We show that this density depends on the class of affine connections which vanish in Darboux coordinates.

By differential operators throughout this text we mean only *linear* differential operators.

For standard material from supermathematics see [5], [17] and [20].

## 2. Second order operators on functions

In what follows  $M$  is a smooth manifold or supermanifold.

Let  $L = T^a(x) \frac{\partial}{\partial x^a} + R(x)$  be a first order operator on functions on a manifold  $M$ . Under change of local coordinates  $x^a = x^a(x^{a'})$   $L$  transforms as follows:

$$L = T^a(x) \frac{\partial}{\partial x^a} + R(x) = T^a(x(x')) x_a' \frac{\partial}{\partial x^{a'}} + R(x), \quad \left( x_a' = \frac{\partial x^{a'}}{\partial x^a} \right).$$

We see that  $T^a(x) \frac{\partial}{\partial x^a}$  is a vector field and  $R(x)$  scalar field.

Now return to the second order operator (1) on a manifold  $M$ . Under a change of local coordinates  $x^a = x^a(x^{a'})$

$$\Delta = \frac{1}{2} \left( S^{ab}(x) \partial_a \partial_b + T^a(x) \partial_a + R(x) \right) = \frac{1}{2} \underbrace{x_a' S^{ab} x_b'}_{S^{a'b'}} \partial_{a'} \partial_{b'} + \dots \quad (6)$$

Top component of operator  $\Delta$ ,  $\frac{1}{2}S^{ab}\partial_a \otimes \partial_b$  defines symmetric contravariant tensor of rank 2 on  $M$  (the principal symbol of the operator  $\Delta = \frac{1}{2}(S^{ab}(x)\partial_a\partial_b + \dots)$ ).

If tensor  $S = 0$  then  $\Delta$  becomes first order operator and  $T^a\partial_a$  is a vector field. What about a geometrical meaning of the operator (6) in the case if principal symbol  $S \neq 0$ ? To answer this question we introduce a scalar product  $\langle , \rangle$  in the space of functions on  $M$  and consider the difference of two second order operators  $\Delta^+ - \Delta$ , where  $\Delta^+$  is an operator adjoint to  $\Delta$  with respect to the scalar product. A scalar product  $\langle , \rangle$  on the space of functions is defined by the following construction: an arbitrary volume form  $\rho = \rho(x)|D(x)|$  on  $M$  is chosen and

$$\langle f, g \rangle_{\rho} = \int_M f(x)g(x)\rho(x)|D(x)|. \quad (7)$$

If  $x'$  are new local coordinates  $x^a = x^a(x')$  then in new coordinates the volume form  $\rho$  has appearance  $\rho'(x')|D(x')| = \rho(x)|D(x)|$ :

$$\begin{aligned} \rho &= \rho(x)|D(x)| = \rho(x(x')) \left| \frac{D(x)}{D(x')} \right| D(x') \\ &= \rho(x(x')) \det \left( \frac{\partial x^a}{\partial x^{a'}} \right) D(x') = \rho'(x')|D(x')|, \end{aligned}$$

i.e.

$$\rho'(x') = \rho(x(x')) \det \left( \frac{\partial x^a}{\partial x^{a'}} \right).$$

In what follows we suppose that scalar product is well-defined: we suppose that  $M$  is compact orientable manifold and the oriented atlas of local coordinates is chosen (all local coordinates transformations have positive Jacobian:  $\left| \frac{\partial x}{\partial x'} \right| = \det \left( \frac{\partial x}{\partial x'} \right) > 0$ )<sup>1</sup>.

Now return to the operators  $\Delta$  and the adjoint operator  $\Delta^+$ . For operator  $\Delta$  the operator  $\Delta^+$  is defined by relation  $\langle \Delta f, g \rangle_{\rho} = \langle f, \Delta^+ g \rangle_{\rho}$ . Integrating by parts we have

$$\langle \Delta f, g \rangle_{\rho} = \int_M \underbrace{\frac{1}{2} \left( S^{ab}(x)\partial_a\partial_b f + T^a(x)\partial_a f + R(x)f \right)}_{\Delta f} g(x)\rho(x)|D(x)| =$$

$$\int_M f(x) \underbrace{\left( \frac{1}{2\rho} \partial_a \left( \partial_b (S^{ab}\rho g) \right) - \frac{1}{2\rho} \partial_a (T^a \rho g) + \frac{1}{2} R g \right)}_{\Delta^+ g} \rho(x)|D(x)| = \langle f, \Delta^+ g \rangle_{\rho}.$$

Principal symbols of operators  $\Delta$  and  $\Delta^+$  coincide. Thus the difference  $\Delta^+ - \Delta$  is a first order operator:

$$\Delta^+ - \Delta = \underbrace{\left( \partial_b S^{ab} - T^a + S^{ab} \partial_b \log \rho \right) \partial_a}_{\text{vector field}} + \text{scalar terms}. \quad (8)$$

---

<sup>1</sup>Coordinate volume form  $|D(x)|$  is usually denoted by  $dx^1 dx^2 \dots dx^n$ . We prefer our notation  $|D(x)|$  having in mind further considerations for supermanifolds.

Introducing the scalar product via chosen volume form  $\rho$  we come to the fact that for an operator  $\Delta = \frac{1}{2}(S^{ab}\partial_a\partial_b + T^a\partial_a + R)$ , and for an arbitrary volume form  $\rho = \rho(x)|D(x)|$  the expression  $(\partial_b S^{ab} - T^a + S^{ab}\partial_b \log \rho)\partial_a$  is a vector field.

*Claim : For an operator  $\Delta = \frac{1}{2}(S^{ab}\partial_a\partial_b + T^a\partial_a + R)$  the expression*

$$\gamma^a = \partial_b S^{ab} - T^a \quad (9)$$

*is an upper connection on volume forms.*

Before proving the claim we give two words about connections on the space of volume forms.

Connection  $\nabla$  on the space of volume forms defines the covariant derivative of volume forms with respect to vector fields. It obeys natural linearity properties and Leibnitz rule:

- $\nabla_{\mathbf{X}}(\rho_1 + \rho_2) = \nabla_{\mathbf{X}}(\rho_1) + \nabla_{\mathbf{X}}(\rho_2)$ ,
- for arbitrary functions  $f, g$   $\nabla_{f\mathbf{X}+g\mathbf{Y}}(\rho) = f\nabla_{\mathbf{X}}(\rho) + g\nabla_{\mathbf{Y}}(\rho)$ ,

- and the Leibnitz rule:

$$\nabla_{\mathbf{X}}(f(x)\rho) = \partial_{\mathbf{X}}f(x)(\rho) + f(x)\nabla_{\mathbf{X}}(\rho), \quad (10)$$

( $\partial_{\mathbf{X}}$  is the directional derivative of functions along vector field  $\mathbf{X}$ :  $\partial_{\mathbf{X}}f = X^a \frac{\partial f}{\partial x^a}$ ).

Denote by  $\nabla_a$  covariant derivative with respect to vector field  $\frac{\partial}{\partial x^a}$ . Due to axioms (10)

$$\nabla_a(\rho(x)|D(x)|) = (\partial_a\rho(x) + \gamma_a\rho(x))|D(x)|, \quad \text{where } \gamma_a|D(x)| = \nabla_a(|D(x)|), \quad \partial_a = \frac{\partial}{\partial x^a}. \quad .$$

Under changing of local coordinates  $x^a = x^a(x'^a)$  the symbol  $\gamma_a$  transforms in the following way:

$$\gamma_a|D(x)| = \nabla_a(|D(x)|) = x_a^{a'} \nabla_{a'} \det \frac{\partial x}{\partial x'} |D(x')| = x_a^{a'} \partial_{a'} \log \det \frac{\partial x}{\partial x'} + \gamma_{a'} |D(x)|, \quad (11)$$

i.e.

$$\gamma_a = x_a^{a'} \gamma_{a'} + \partial_{a'} \log \det \frac{\partial x}{\partial x'} = x_a^{a'} \gamma_{a'} - x_{b'}^b x_{ba}'.$$

(We use the standard formula that  $\delta \log \det M = \text{Tr}(M^{-1}\delta M)$ . We use also short notations for derivatives:  $x_a^{a'} = \frac{\partial x^{a'}(x)}{\partial x^a}$ ,  $x_{bc}^{a'} = \frac{\partial x^{a'}(x)}{\partial x^b \partial x^c}$ . The summation over repeated indices is assumed.)

Let  $S^{ab}$  be a contravariant tensor field. One can assign to this tensor field an upper connection i.e. a contravariant derivative  ${}^S\nabla$

$${}^S\nabla^a(\rho|D(x)|) = S^{ab}\partial_b + \gamma^a \rho|D(x)|. \quad (12)$$

**Remark 1** Given a contravariant tensor field  $S^{ab}(x)$  an arbitrary connection  $\nabla$  (covariant derivative) induces the upper connection (contravariant derivative)  ${}^S\nabla$ :  ${}^S\nabla^a = S^{ab}\nabla_b$ . In the case where tensor field  $S^{ab}$  is non-degenerate, the converse implication is true also. A non-degenerate contravariant tensor field  $S^{ab}(x)$  induces one-one correspondence between upper connections and usual connections. (Compare with the example 5 below where upper connection in general does not define the connection.)

Under changing of coordinates a symbol  $\gamma^a$  of upper connection (12) transforms in the following way:

$$\gamma^{a'} = x_a^{a'} \gamma^a + S^{ab} \partial_b \log \det \partial x' / \partial x \quad . \quad (13)$$

**Remark 2** From now on we refer to genuine connections (covariant derivatives) simply as connections. With some abuse of language we identify the connection  $\nabla$  with its symbol  $\boldsymbol{\gamma} = \{\gamma_a\}$ :  $\gamma_a = \nabla_a |D(x)|$ .

**Remark 3** It is worth noting that the difference of two connections is a covector field, the difference of two upper connections is a vector field. In other words the space of all connections (upper connections) is affine space associated with linear space of covector (vector) fields.

Consider two important examples of connections on volume forms.

**Example 1** An arbitrary volume form  $\rho$  defines a connection  $\boldsymbol{\gamma}^\rho$  due to the formula (4):  $\gamma_a^\rho = -\partial_a \log \rho(x)$ . This is a flat connection: its curvature vanishes:  $F_{ab} = \partial_a \gamma_b - \partial_b \gamma_a = 0$ . (Connection  $\nabla$  considered in the formula (4) is a flat connection defined by the volume form  $\rho_g$ .)

**Example 2** Let  $\nabla$  be affine connection on vector fields on manifold  $M$ . It defines connection on volume forms  $\nabla \rightarrow -\text{Tr } \nabla$  with  $\gamma_a = -\Gamma_{ab}^b$  where  $\Gamma_{bc}^a$  are Christoffel symbols of affine connection.

It is easy to see that connection and upper connection define the covariant and respectively contravariant derivative of the densities of an arbitrary weight: for  $s = s(x)|D(x)|^\lambda \in \mathcal{F}_\lambda$

$$\nabla_a s = (\partial_a s(x) + \lambda \gamma_a s(x)) |D(x)|^\lambda .$$

Respectively for upper connection

$$\nabla^a s = S^{ab} \partial_b s(x) + \lambda \gamma^a s(x) |D(x)|^\lambda . \quad (14)$$

Sometimes we will use the concept of connection of the weight  $\delta$ . This is a linear operation that transforms densities of weight  $\lambda$  to the densities of weight  $\mu = \lambda + \delta$ : for  $s = s(x)|D(x)|^\lambda \in \mathcal{F}_\lambda$

$$\nabla_a s = (\partial_a s(x) + \lambda \gamma_a s(x)) |D(x)|^{\lambda+\delta}, \quad \nabla_a |D(x)| = \gamma_a |D(x)|^{\delta+1} .$$

Respectively for upper connection

$$\nabla^a s = S^{ab} \partial_b s(x) + \lambda \gamma^a s(x) |D(x)|^{\lambda+\delta}, \quad \nabla^a |D(x)| = \gamma^a |D(x)|^{\delta+1}$$

*Proof of the claim (9):* Consider a flat connection  $\boldsymbol{\gamma}^\rho$ :  $\gamma_a^\rho = -\partial_a \log \rho$  defined by the volume form  $\rho = \rho(x)dx$  (see Example 1 above). Since the expression  $\mathbf{Y} = (\partial_b S^{ab} - T^a + S^{ab} \partial_b \log \rho) \partial_a$  in (8) is a vector field (the principal symbol of the first order operator  $\Delta^+ - \Delta$ ) and  $S^{ab} \gamma_b^\rho = -S^{ab} \partial_b \log \rho$  is an upper connection then the sum  $Y^a + S^{ab} \gamma_b^\rho$  is also upper connection:

$$S^{ab} \gamma_b^{\text{flat}} + Y^a = -S^{ab} \partial_b \log \rho + (\partial_b S^{ab} - T^a + S^{ab} \partial_b \log \rho) \partial_a = \partial_b S^{ab} - T^a .$$

Thus we have proved the claim.

Having in mind the result of the claim we can rewrite the operator  $\Delta$  on functions in a more convenient form:

$$\Delta f = \frac{1}{2} (S^{ab} \partial_a \partial_b + T^a \partial_a + R) f = \frac{1}{2} (\partial_a S^{ab} \partial_b + L^a \partial_a + R) f,$$

with  $L^a = T^a - \partial_b S^{ab}$ . We come to Proposition

**Proposition 1** For an arbitrary second order operator on functions on manifold  $M$ :

$$\Delta = \frac{1}{2} \left( S^{ab} \partial_a \partial_b + T^a \partial_a + R \right) = \frac{1}{2} \left( \partial_a \left( S^{ab} \partial_b \dots \right) + L^a \partial_a + R \right),$$

the principal symbol  $\frac{1}{2}S^{ab}$  is symmetric contravariant tensor field of rank 2, the symbol  $\gamma^a = -L^a = \partial_b S^{ba} - T^a$  defines an upper connection and the function  $R = 2\Delta 1$  is a scalar:

$$\Delta f = \frac{1}{2} \partial_a \left( \underbrace{S^{ab}}_{\text{tensor}} \partial_b f \right) - \frac{1}{2} \underbrace{\gamma^a}_{\text{connection}} \partial_a f + \underbrace{\frac{1}{2}R}_{\text{scalar}} f.$$

Second order operators on functions are fully characterised by symmetric contravariant tensors of rank 2 (principal symbol), upper connections and scalar fields. In the case if principal symbol is non-degenerate ( $\det S^{ab} \neq 0$ ) upper connection defines a usual connection on volume forms:  $\gamma_a = S^{-1}_{ab} \gamma^b$ .

### 3. Algebra of densities and second order operators on algebra of densities

#### 3.1. Algebra of densities $\mathcal{F}(M)$ . Canonical scalar product

We consider now the space of densities.

As usual we suppose that  $M$  is a compact orientable manifold with a chosen oriented atlas.

We say that  $\mathbf{s} = s(x)|D(x)|^\lambda$  is a density of weight  $\lambda$  if under changing of local coordinates it is multiplied on the  $\lambda$ -th power of the Jacobian of the coordinate transformation:

$$\mathbf{s} = s(x)|D(x)|^\sigma = s(x(x')) \left| \frac{Dx}{Dx'} \right|^\lambda |D(x')|^\lambda = s(x(x')) \left( \det \left( \frac{Dx}{Dx'} \right) \right)^\lambda |D(x')|^\lambda.$$

(Density of weight  $\lambda = 0$  is a usual function, density of weight  $\lambda = 1$  is a volume form.)

Denote by  $\mathcal{F}_\lambda = \mathcal{F}_\lambda(M)$  the space of densities of weight  $\lambda$  on the manifold  $M$ .

Denote by  $\mathcal{F} = \mathcal{F}(M)$  the space of all densities on the manifold  $M$ .

The space  $\mathcal{F}_\lambda$  of densities of the weight  $\lambda$  is a vector space. It is the module over the ring of functions on  $M$ . The space  $\mathcal{F}$  of all densities is an algebra: If  $\mathbf{s}_1 = s_1(x)|D(x)|^{\lambda_1} \in \mathcal{F}_{\lambda_1}$  and  $\mathbf{s}_2 = s_2(x)|D(x)|^{\lambda_2} \in \mathcal{F}_{\lambda_2}$  then their product is the density  $\mathbf{s}_1 \cdot \mathbf{s}_2 = s_1(x)s_2(x)Dx^{\lambda_1+\lambda_2} \in \mathcal{F}_{\lambda_1+\lambda_2}$ .

On the algebra  $\mathcal{F}(M)$  of all densities on  $M$  one can consider the canonical scalar product  $\langle , \rangle$  defined by the following formula: if  $\mathbf{s}_1 = s_1(x)|D(x)|^{\lambda_1}$  and  $\mathbf{s}_2 =$

$s_2(x)|D(x)|^{\lambda_2}$  then

$$\langle \mathbf{s}_1, \mathbf{s}_2 \rangle = \begin{cases} \int_M s_1(x)s_2(x)|D(x)|, & \text{if } \lambda_1 + \lambda_2 = 1, \\ 0 & \text{if } \lambda_1 + \lambda_2 \neq 1. \end{cases} \quad (15)$$

(Compare this scalar product with a volume form depending scalar product  $\langle \cdot, \cdot \rangle_\rho$  on algebra of functions introduced in formula (7).)

The canonical scalar product (15) was considered and intensively used in the work [15]. Briefly recall the constructions of this work.

Elements of the algebra  $\mathcal{F}(M)$  are finite combinations of densities of different weights.

It is convenient to use a formal variable  $t$  in a place of coordinate volume form  $|D(x)|$ .

An arbitrary density  $\mathcal{F} \ni \mathbf{s} = s_1(x)|D(x)|^{\lambda_1} + \cdots + s_k(x)|D(x)|^{\lambda_k}$  can be written as a function polynomial on a variable  $t$ :

$$\mathbf{s} = \mathbf{s}(x, t) = s_1(x)t^{\lambda_1} + \cdots + s_k(x)t^{\lambda_k}. \quad (16)$$

E.g. the density  $s_1(x) + s_2(x)|D(x)|^{1/2} + s_3(x)|D(x)|$  can be rewritten as  $s(x, t) = s_1(x) + \sqrt{t}s_2(x) + ts_3(x)$ . In what follows we often will use this notation.

**Remark 4** *With some abuse of language we say that a function  $f(x, t)$  is a function polynomial over  $t$  if it is a sum of finite number of monoms of arbitrary real degree over  $t$ ,  $f(x, t) = \sum_\lambda f_\lambda(x)t^\lambda$ ,  $\lambda \in \mathbb{R}$ .*

What is a global meaning of the variable  $t$ ? The relation (16) means that an arbitrary density on  $M$  can be identified with a polynomial function on the extended manifold  $\widehat{M} = \det(TM) \setminus M$  which is the frame bundle of determinant bundle of  $M$ . The natural local coordinates on  $\widehat{M}$  induced by local coordinates  $x^a$  on  $M$  are  $(x^a, t)$  where  $t$  is a coordinate which is in a place of volume form  $|D(x)|$ . Let  $x^a, x^{a'}$  be two local coordinates on  $M$ . If  $(x^a, t)$  and  $(x^{a'}, t')$  are local coordinates on  $\widehat{M}$  induced by local coordinates  $x^a$  and  $x^{a'}$  respectively then

$$x^{a'} = x^{a'}(x^a) \text{ and } t' = \det\left(\frac{\partial x'}{\partial x}\right) t. \quad (17)$$

If a function is a polynomial with respect to local variable  $t$ , then it is a polynomial with respect to local variable  $t'$  also. (As it was mentioned before we consider only oriented atlas, i.e. all changing of coordinates have positive determinant.)

It has to be emphasized that algebra  $\mathcal{F}(M)$  of all densities on  $M$  can be identified with an algebra of functions on extended manifold  $\widehat{M}$  which are polynomial on  $t$ . We do not consider arbitrary functions on  $t$ .

### 3.2. Derivations of algebra of densities (=vector fields on the extended manifold)

Consider differential operators on the algebra  $\mathcal{F}$ . (We repeat that we consider only linear operators.)

Let  $\mathbf{X}$  be a derivation of the algebra  $\mathcal{F}$ , Then for two arbitrary densities  $\mathbf{s}_1, \mathbf{s}_2$

$$\mathbf{X}(\mathbf{s}_1 \cdot \mathbf{s}_2) = (\mathbf{X}\mathbf{s}_1) \cdot \mathbf{s}_2 + \mathbf{s}_1 \cdot (\mathbf{X}\mathbf{s}_2), \quad (\text{Leibnitz rule}).$$

The derivations of the algebra  $\mathcal{F}(M)$  are vector fields on the extended manifold  $\widehat{M}$ , where coefficients are polynomials over  $t$ :

$$\mathbf{X} = X^a(x, t) \frac{\partial}{\partial x^a} + X^0(x, t) \widehat{\lambda} = \sum_{\delta} t^{\delta} \left( X_{(\delta)}^a(x) \frac{\partial}{\partial x^a} + X_{(\delta)}^0(x) \widehat{\lambda} \right). \quad (18)$$

We introduced in this formula the Euler operator

$$\widehat{\lambda} = t \frac{\partial}{\partial t}$$

which is globally defined vector field on  $\widehat{M}$  (see transformation law (17)). Euler operator  $\widehat{\lambda}$  measures a weight  $\lambda$  of density:  $\widehat{\lambda}(s(x)t^{\lambda}) = \lambda s(x)t^{\lambda}$ .

There is a natural gradation in the space of vector fields. The vector field

$$\mathbf{X} = t^{\delta} \left( X^a(x) \partial_a + X^0(x) \widehat{\lambda} \right) \quad (19)$$

is the vector field of the weight  $\delta$ . It transforms a density of weight  $\lambda$  to the density of weight  $\lambda + \delta$ .

**Remark 5** From now on considering vector fields on extended manifold  $\widehat{M}$  we suppose by default that coefficients of these vector fields are polynomial on  $t$  (see equation (18)).

Our next step is to consider adjoint operators with respect to canonical scalar product (15) on the algebra  $\mathcal{F}$ : operator  $\hat{L}^+$  is adjoint to the operator  $L$  if for arbitrary densities  $\mathbf{s}_1, \mathbf{s}_2$ ,  $\langle \hat{L}\mathbf{s}_1, \mathbf{s}_2 \rangle = \langle \mathbf{s}_1, \hat{L}^+\mathbf{s}_2 \rangle$ . One can see that

$$x^+ = x, \quad \left( \frac{\partial}{\partial x} \right)^+ = -\frac{\partial}{\partial x}, \quad \text{and} \quad \widehat{\lambda}^+ = 1 - \widehat{\lambda}.$$

Check the last relation. Let  $\mathbf{s}_1$  be a density of the weight  $\lambda_1$  and  $\mathbf{s}_2$  be a density of the weight  $\lambda_2$ . Then  $\langle \widehat{\lambda}\mathbf{s}_1, \mathbf{s}_2 \rangle = \lambda_1 \langle \mathbf{s}_1, \mathbf{s}_2 \rangle$  and  $\langle \mathbf{s}_1, \widehat{\lambda}^+\mathbf{s}_2 \rangle = \langle \mathbf{s}_1, (1 - \widehat{\lambda})\mathbf{s}_2 \rangle = (1 - \lambda_2) \langle \mathbf{s}_1, \mathbf{s}_2 \rangle$ . In the case if  $\lambda_1 + \lambda_2 = 1$  these scalar products are equal since  $\lambda_1 = 1 - \lambda_2$ . In the case if  $\lambda_1 + \lambda_2 \neq 1$  these scalar products both vanish.

**Example 3** Consider vector field on  $\widehat{M}$  ( derivation of algebra of densities):  $\mathbf{X} : \mathbf{X}\mathbf{s} = \left( X^a(x, t)\partial_a + X^0(x, t)\widehat{\lambda} \right) \mathbf{s}(x, t)$ . Then its adjoint operator is:

$$\begin{aligned} \mathbf{X}^+ : \quad \mathbf{X}^+\mathbf{s} &= \left[ \left( X^a(x, t)\partial_a + X^0(x, t)\widehat{\lambda} \right) \right]^+ \mathbf{s} \\ &= -\partial_a(X^a(x, t)\mathbf{s}) + (1 - \widehat{\lambda})(X^0(x, t)\mathbf{s}), \\ \mathbf{X}^+ &= -\partial_a X^a(x, t) - X^a(x, t)\partial_a - X^0(x, t)\widehat{\lambda} + (1 - \widehat{\lambda})X^0(x, t). \end{aligned}$$

**Definition 1** (Canonical divergence). Divergence of vector field  $\mathbf{X}$  on  $\widehat{M}$  is defined by the formula

$$\operatorname{div} \mathbf{X} = -(\mathbf{X} + \mathbf{X}^+) = \partial_a X^a + (\widehat{\lambda} - 1)X^0(x, t). \quad (20)$$

In particular for vector field  $\mathbf{X}$  of the weight  $\delta$ ,  $\mathbf{X} = t^\delta \left( X^a \partial_a + X^0 \widehat{\lambda} \right)$  (see equation(19))

$$\operatorname{div} \mathbf{X} = t^\delta (\partial_a X^a + (\delta - 1)X^0).$$

Divergence of vector field on  $\mathcal{F}$  vanishes iff this vector field is anti-self-adjoint (with respect to canonical scalar product (15)):  $\mathbf{X} = -\mathbf{X}^+ \Leftrightarrow \operatorname{div} \mathbf{X} = 0$ .

**Example 4** Divergence-less (=antiself-adjoint) vector fields of weight  $\delta = 0$  act on densities as Lie derivatives. Indeed consider vector field  $\mathbf{X} = X^a \partial_a + X^0 \widehat{\lambda}$  of the weight  $\delta = 0$ . The condition  $\operatorname{div} \mathbf{X} = \partial_a X^a - X^0 = 0$  means that  $X^0 = \partial_a X^a$ , i.e.  $\mathbf{X} = X^a \partial_a + \partial_a X^a \widehat{\lambda}$ . Hence for every  $\lambda$ ,  $\mathbf{X}|_{\mathcal{F}_\lambda} = X^a \partial_a + \lambda \partial_a X^a$ . This means that the action of divergence-free vector field  $\mathbf{X}$  of weight  $\delta = 0$  on an arbitrary density is the Lie derivative of this density: for  $\mathbf{s} \in \mathcal{F}_\lambda$

$$\mathbf{X}\mathbf{s} = (X^a \partial_a + \widehat{\lambda} \partial_a X^a)\mathbf{s} = \mathcal{L}_{\mathbf{X}}\mathbf{s} = (X^a \partial_a s(x) + \lambda \partial_a X^a s(x)) |D(x)|^\lambda. \quad (21)$$

If  $\mathbf{X}$  is divergence-free vector field on  $\widehat{M}$  of arbitrary weight then  $\operatorname{div} \mathbf{X} = 0 \Leftrightarrow \mathbf{X} = t^\delta \left( X^a \partial_a + \partial_a X^a \frac{\widehat{\lambda}}{1-\delta} \right)$ . We come to generalised Lie derivative: if  $\delta \neq 1$  then for  $\mathbf{s} \in \mathcal{F}_\lambda$

$$\mathcal{L}_{\mathbf{X}}\mathbf{s} = |D(x)|^\delta \left( X^a \partial_a + \partial_a X^a \frac{\widehat{\lambda}}{1-\delta} \right) \mathbf{s} = \left( X^a \partial_a s(x) + \frac{\lambda \partial_a X^a s}{1-\delta} \right) |D(x)|^{\lambda+\delta}. \quad (22)$$

One can consider a canonical projection  $p$  of vector fields on  $\widehat{M}$  ( derivation of algebra  $\mathcal{F}(M)$ ) on vector densities on  $M$ . It is defined by the formula  $p(\mathbf{X}) = \mathbf{X}|_{\mathcal{F}_0=C^\infty(M)}$ . In coordinates  $p$ :  $\mathbf{X} = X^a(x, t)\partial_a + X^0(x, t)\widehat{\lambda} \mapsto X^a(x, t)\partial_a$ .

We say that vector field is vertical if  $p\mathbf{X} = 0$ , i.e. if  $\mathbf{X} = X^0(x, t)\widehat{\lambda}$ . Divergence of vertical vector field  $\mathbf{X} = X^0(x, t)\widehat{\lambda}$  equals to  $\operatorname{div} \mathbf{X} = (\widehat{\lambda} - 1)X^0(x, t)$ .

**Proposition 2** Let  $\Pi$  be a projection of vector fields onto vertical vector fields such that  $\operatorname{div} \mathbf{X} = \operatorname{div}(\Pi \mathbf{X})$ , We have that

$$\Pi: \quad \mathbf{X} = t^\delta \left( X^a \partial_a + X^0 \hat{\lambda} \right) \mapsto \Pi \mathbf{X} = t^\delta \left( \frac{\partial_a X^a}{\delta - 1} + X^0 \right) \hat{\lambda}.$$

Every vector field  $\mathbf{X}$  of weight  $\delta \neq 1$  can be uniquely decomposed as the sum of a vertical vector field and divergence-free vector field, generalised Lie derivative (22)) with respect to vector field  $p\mathbf{X}$ :

$$\mathbf{X} = \Pi \mathbf{X} + (\mathbf{X} - \Pi \mathbf{X}) = \Pi \mathbf{X} + \mathcal{L}_{p\mathbf{X}}.$$

One can check the statements of this Proposition by straightforward applications of the formulae above.

What relations exist between the canonical divergence (20) of vector fields on extended manifold  $\widehat{M}$  and a divergence of vector fields on a manifold  $M$ ? Let  $\nabla$  be an arbitrary connection on volume forms. It assigns to the vector field  $\mathbf{X}$  on  $M$  a vector field  $\mathbf{X}_\gamma$  on the extended manifold  $\widehat{M}$  by the formula  $\mathbf{X}_\gamma = X^a \frac{\partial}{\partial x^a} + \hat{\lambda} \gamma_a$ , where  $\gamma = \{\gamma_a\}$  is a symbol of connection  $\nabla$  in coordinates  $x$ ,  $(\nabla_a |D(x)| = \gamma_a |D(x)|)$ . Connection  $\nabla$  defines the divergence of vector fields on  $M$  via the canonical divergence (20): for every vector field  $\mathbf{X}$  on manifold  $M$ :

$$\operatorname{div}_\gamma \mathbf{X} = \operatorname{div} \mathbf{X}_\gamma = \frac{\partial X^a}{\partial x^a} - \gamma_a X^a. \quad (23)$$

A volume form  $\rho = \rho(x) |D(x)|$  defines flat connection  $\gamma_a^\rho = -\partial_a \log \rho$  (see equation (4) and example 1). The formula (23) implies the well-known formula (see also equation (2))) for divergence of vector field on manifold equipped with a volume form

$$\operatorname{div}_\rho \mathbf{X} = \operatorname{div} \mathbf{X}_{\gamma_\rho} = \frac{\partial X^a}{\partial x^a} + X^a \partial_a \log \rho = \frac{1}{\rho} \frac{\partial}{\partial x^a} (\rho X^a). \quad (24)$$

Considering a connection corresponding to an affine connection (see Example 2) we come to  $\operatorname{div}_\nabla \mathbf{X} = \nabla_a X^a = (\partial_a X^a + X^a \Gamma_{ab}^b)$ . On Riemannian manifold  $M$  Riemannian metric defines connection on volume forms  $\gamma_a = -\partial_a \log \sqrt{\det g}$  (via Levi-Civita connection or via invariant volume form  $\rho_g$ ). We come to

$$\operatorname{div}_g \mathbf{X} = \frac{\partial X^a}{\partial x^a} + X^a \partial_a \log \sqrt{\det g} = \frac{1}{\sqrt{\det g}} \frac{\partial}{\partial x^a} \sqrt{\det g} X^a.$$

### 3.3. Second order operators on the algebra $\mathcal{F}(M)$

We will study now operators of order  $\leq 2$  on the algebra  $\mathcal{F}(M)$  of densities on manifold  $M$ .

First of all general remark about  $n$ -th order operators. 0-th order operator on the algebra  $\mathcal{F}(M)$  is just multiplication operator on non-zero density.  $L$  is  $n$ -th order operator on the algebra  $\mathcal{F}(M)$  ( $n \geq 1$ ) if for an arbitrary  $\mathbf{s} \in \mathcal{F}(M)$  the commutator  $[L, \mathbf{s}] = L \circ \mathbf{s} - \mathbf{s} \circ L$  is  $(n-1)$ -th order operator.

One can see that if  $L$  is an  $n$ -th order differential operator on  $\mathcal{F}(M)$ , then  $L + (-1)^n L^+$  is  $n$ -th order operator and  $L - (-1)^n L^+$  is an operator of the order  $\leq n-1$ . We have:

**Proposition 3** An arbitrary  $n$ -th order operator can be canonically decomposed on the sum of self adjoint and antiself-adjoint operators:

$$L = \underbrace{\frac{1}{2} (L + (-1)^n L^+)}_{n\text{-th order operator}} + \underbrace{\frac{1}{2} (L - (-1)^n L^+)}_{\text{operator of the order } \leq n-1} .$$

An operator of the even order  $n = 2k$  is a sum of self-adjoint operator of the order  $2k$  and antiself-adjoint operator of the order  $\leq 2k-1$ , and an operator of the odd order  $n = 2k+1$  is a sum of antiself-adjoint operator of the order  $2k+1$  and self-adjoint operator of the order  $\leq 2k$ .

Operators of the order 0 are evidently self-adjoint.

Let  $L = \mathbf{X} + B$  be first order antiself-adjoint operator, where  $\mathbf{X}$  is a vector field on  $\widehat{M}$  and  $B$  is a scalar term (density). We have  $L + L^+ = 0 = \mathbf{X} + \mathbf{X}^+ + 2B = 0$ . Hence  $L = \mathbf{X} + \frac{1}{2}\operatorname{div} \mathbf{X}$ .

Now study self-adjoint second order operators on  $\mathcal{F}(M)$ . Let  $\Delta$  be second order operator of the weight  $\delta$  on algebra  $\mathcal{F}(M)$  of densities. In local coordinates

$$\Delta = \frac{t^\delta}{2} \left( \underbrace{S^{ab}(x)\partial_a\partial_b + \widehat{\lambda}B^a(x)\partial_a + \widehat{\lambda}^2C(x)}_{\text{second order derivatives}} + \underbrace{D^a(x)\partial_a + \widehat{\lambda}E(x)}_{\text{first order derivatives}} + F(x) \right) . \quad (25)$$

Put normalisation condition

$$\Delta(1) = 0 \quad (26)$$

i.e. density  $\frac{F|D(x)|^\delta}{2}$  in (25) vanishes ( $F = 0$ ).

The operator  $\Delta^+$  adjoint to  $\Delta$  equals to

$$\begin{aligned} \Delta^+ &= \frac{1}{2} \left( \partial_b\partial_a \left( S^{ab}t^\delta \dots \right) - \partial_a \left( B^a\widehat{\lambda}^+t^\delta \dots \right) + \left( C(\widehat{\lambda}^+)^2t^\delta \dots \right) \right. \\ &\quad \left. - \partial_a \left( D^a t^\delta \dots \right) + \left( E\widehat{\lambda}^+t^\delta \dots \right) \right) \\ &= \frac{t^\delta}{2} \left( S^{ab}\partial_a\partial_b + 2\partial_b S^{ba}\partial_a + \partial_a\partial_b S^{ba} \right) + \frac{t^\delta}{2} \left( (\widehat{\lambda} + \delta - 1) \left( B^a\partial_a + \partial_b B^b \right) \right. \\ &\quad \left. + (\widehat{\lambda} + \delta - 1)^2 C - (\widehat{\lambda} + \delta - 1) E - D^a\partial_a - \partial_b D^b \right) . \end{aligned}$$

Comparing this operator with operator (25) we see that the condition  $\Delta^+ = \Delta$  implies that

$$\begin{aligned} \Delta &= \frac{t^\delta}{2} \left( S^{ab}(x)\partial_a\partial_b + \partial_b S^{ba}\partial_a + \left( 2\widehat{\lambda} + \delta - 1 \right) \gamma^a(x)\partial_a \right. \\ &\quad \left. + \widehat{\lambda}\partial_a\gamma^a(x) + \widehat{\lambda}(\widehat{\lambda} + \delta - 1)\theta(x) \right) . \end{aligned} \quad (27)$$

Here for convenience we denote  $\gamma^a = 2B^a$  and  $\theta = C$ . Studying how coefficients of the operator change under changing of coordinates we come to

**Theorem 1** (See [15].) Let  $\Delta$  be an arbitrary linear second order self-adjoint operator ( $\Delta^+ = \Delta$ ) on the algebra  $\mathcal{F}(M)$  of densities such that its weight equals  $\delta$  and  $\Delta(1) = 0$ . Then in local coordinates this operator has the appearance (27). The coefficients of this operator have the following geometrical meaning

- $\mathbf{S} = t^\delta S^{ab}(x) = S^{ab}(x)|D(x)|^\delta$  is symmetric contravariant tensor field-density of the weight  $\delta$ . Under changing of local coordinates  $x^{a'} = x^{a'}(x^a)$  it transforms in the following way:

$$S^{a'b'} = J^{-\delta} x_a^{a'} x_b^{b'} S^{ab},$$

- $\gamma^a$  is a symbol of upper connection-density of weight  $\delta$  (see (13) above). Under changing of local coordinates  $x^{a'} = x^{a'}(x^a)$  it transforms in the following way:

$$\gamma^{a'} = J^{-\delta} x_a^{a'} \left( \gamma^a + S^{ab} \partial_b \log J \right),$$

- and  $\theta$  transforms in the following way:

$$\theta' = J^{-\delta} \left( \theta + 2\gamma^a \partial_a \log J + \partial_a \log J S^{ab} \partial_b \log J \right)$$

Here  $J = \det \left( \frac{\partial x'}{\partial x} \right)$ , and  $x_a^{a'}$  are short notations for derivatives:  $x_a^{a'} = \partial_a x^{a'}(x) = \frac{\partial x^{a'}(x)}{\partial x^a}$ .

The object  $\theta(x)|D(x)|^\delta$  is called Brans-Dicke function <sup>2</sup>.

**Remark 6** Let  $\Delta$  be self-adjoint operator (27) and  $\boldsymbol{\gamma}' = \{\gamma'_a\}$  be an arbitrary connection on volume forms ( $\nabla|D(x)| = \gamma'_a|D(x)|$ ). Then for the upper connection-density in the equation (27) the difference  $(\gamma^a - S^{ab}\gamma'_b)|D(x)|^\delta$  is a vector density of the weight  $\delta$ . Respectively for Brans-Dicke function  $\theta$ , the difference  $\theta - \gamma'_a S^{ab} \gamma'_b$  is a density of the weight  $\delta$ . (One can easily deduce this recalling the fact that the space of genuine connections as well as the space of upper connections is an affine space: if  $\nabla$  and  $\nabla'$  are two different connections then their difference is (co)vector field:  $\nabla' - \nabla = \gamma'_a - \gamma_a = X_a$ .)

**Corollary 1** Given principal symbol  $\mathbf{S} = S^{ab}|D(x)|^\delta$  of the weight  $\delta$  and connection  $\boldsymbol{\gamma}$  on volume forms canonically define the second order self-adjoint operator (27) with upper connection  $\gamma^a = S^{ab}\gamma_b$  and Brans-Dicke function  $\theta(x) = \gamma_a S^{ab} \gamma_b$ . We denote this operator  $\Delta(\mathbf{S}, \boldsymbol{\gamma})$ .

The inverse implication is valid in the case if  $\mathbf{S} = S^{ab}|D(x)|^\delta$  is non-degenerate: Second order self-adjoint operator  $\Delta$  of weight  $\delta$  which obeys normalisation condition (26) with non-degenerate principal symbol  $\mathbf{S}$  uniquely defines connection  $\boldsymbol{\gamma}$  such that  $\Delta = \Delta(\mathbf{S}, \boldsymbol{\gamma}) + \hat{\lambda}(\hat{\lambda} + \delta - 1)F$ , where  $F$  is a density of weight  $\delta$ , and Brans-Dicke function  $\theta$  equals to  $\theta = \gamma_a \gamma^a + F = \gamma_a S^{ab} \gamma_b + F$ .

---

<sup>2</sup>Its transformation is similar to transformation of Brans-Dicke "scalar", in Kaluza-Klein reduction of 5-dimensional gravity to gravity+electromagnetism.

Consider examples.

First consider the example of operator (27) with *degenerate* principal symbol  $S^{ab}|D(x)|^\delta$ .

**Example 5** Let  $\mathbf{X} = X^a \frac{\partial}{\partial x^a}$  and  $\mathbf{Y} = Y^a \frac{\partial}{\partial x^a}$  be two vector fields on manifold  $M$ . Recall the operator of Lie derivative (see equation (21))  $\mathcal{L}_{\mathbf{X}} = X^a \partial_a + \hat{\lambda} \partial_a X^a$  and consider the operator

$$\Delta = \frac{1}{2} (\mathcal{L}_{\mathbf{X}} \mathcal{L}_{\mathbf{Y}} + \mathcal{L}_{\mathbf{Y}} \mathcal{L}_{\mathbf{X}}) = \frac{1}{2} \left( X^a \partial_a + \hat{\lambda} \partial_a X^a \right) \left( Y^a \partial_a + \hat{\lambda} \partial_a Y^a \right) + (\mathbf{X} \leftrightarrow \mathbf{Y}).$$

It is self-adjoint operator since Lie derivative is antiself-adjoint operator. Calculating this operator and comparing it with the expression (27) we come to

$$S^{ab} = X^a Y^b + Y^b X^a, \gamma^a = (\partial_b X^b) Y^a + (\partial_b Y^b) X^a, \theta = (\partial_a X^a) (\partial_b Y^b).$$

We see that in the general case (if dimension  $n$  of manifold is greater than 2) this operator has degenerate principal symbol and upper connection does not define uniquely genuine connection.

### 3.4. Canonical pencil of operators

Note that an operator  $L$  on the algebra  $\mathcal{F}(M)$  of densities defines the pencil  $\{L_\lambda\}$  of operators on spaces  $\mathcal{F}_\lambda$ :  $L_\lambda = L|_{\mathcal{F}_\lambda}$ . The self-adjoint operator  $\Delta$  on the algebra of densities (see equation (27)) defines the canonical operator pencil  $\{\Delta_\lambda\}, \lambda \in \mathbb{R}$ , where

$$\Delta_\lambda = \Delta|_{\mathcal{F}_\lambda} =$$

$$= \frac{t^\delta}{2} \left( S^{ab}(x) \partial_a \partial_b + \partial_b S^{ba} \partial_a + (2\lambda + \delta - 1) \gamma^a(x) \partial_a + \lambda \partial_a \gamma^a(x) + \lambda(\lambda + \delta - 1) \theta(x) \right) \quad (28)$$

It is canonical pencil defined by symmetric tensor density  $\mathbf{S} = S^{ab}(x)|D(x)|^\delta$ , upper connection  $\gamma^a$  and Brans-Dicke function  $\theta(x)$ . Respectively self-adjoint operator  $\Delta(\mathbf{S}, \gamma)$  on the algebra of densities defined by tensor field-density  $\mathbf{S} = S^{ab}(x)|D(x)|^\delta$  and genuine connection  $\gamma$  (see Corollary 1) defines the operator pencil  $\Delta_\lambda(\mathbf{S}, \gamma)$  with Brans-Dicke function  $\theta(x) = \gamma_a S^{ab} \gamma_b$ .

Operator  $\Delta_\lambda$  of the weight  $\delta$  maps density of weight  $\lambda$  to densities of weight  $\lambda + \delta$ . Its adjoint operator  $\Delta_\lambda^+$  maps density of weight  $1 - \delta - \lambda$  to densities of weight  $1 - \lambda$ . The condition  $\Delta = \Delta^+$  of self-adjointness of operator  $\Delta$  is equivalent to the condition

$$\Delta_\lambda^+ = \Delta_{1-\lambda-\delta}. \quad (29)$$

**Example 6** Let  $\rho = \rho(x)|D(x)|$  be a volume form on the Riemannian manifold  $M$ . We can consider an operator  $\Delta$  on functions such that  $\Delta f = \operatorname{div}_\rho \operatorname{grad} f = \frac{1}{2} \frac{1}{\rho(x)} \frac{\partial}{\partial x^a} \left( \rho(x) g^{ab} \frac{\partial f(x)}{\partial x^b} \right)$  (see equations (2) and (24) (In the case if  $\rho = \sqrt{\det g}|D(x)|$

this is just the Laplace-Beltrami operator (3).) Using this operator consider the pencil

$$\Delta_\lambda = \rho^\lambda \circ \Delta \circ \frac{1}{\rho^\lambda}: \quad \left( \text{for } \mathbf{s} \in \mathcal{F}_\lambda, \Delta_\lambda \mathbf{s} = \rho^\lambda \operatorname{div}_\rho \operatorname{grad} \left( \frac{\mathbf{s}}{\rho^\lambda} \right) \right).$$

One can see that this pencil corresponds to self-adjoint operator (see relation (29)). It coincides with the canonical pencil (28) of weight  $\delta = 0$  in the case if principal symbol is defined by Riemannian metric  $S^{ab} = g^{ab}$ , connection is a flat connection defined by the volume form (see formula (4) and Example 1):  $\gamma^a = -g^{ab}\partial_b \log \rho$ , and  $\theta = \gamma^a \gamma_a$ .

The canonical pencil (28) has many interesting properties (see for detail [15]). In particular it has the following “universality” property:

**Corollary 2** Let  $\Delta$  be an arbitrary (linear) second order operator of weight  $\delta$  acting on the space  $\mathcal{F}_\lambda$  of densities of weight  $\lambda$ ,  $\Delta: \mathcal{F}_\lambda \rightarrow \mathcal{F}_\mu$  ( $\mu = \lambda + \delta$ ). In the case if  $\lambda \neq 0, \mu \neq 1$  and  $\lambda + \mu \neq 1$  there exists a unique canonical pencil which passes through the operator  $\Delta$ .

If the operator  $\Delta$  is given by the expression  $\Delta = A^{ab}\partial_a\partial_b + A^a\partial_a + A(x)$  then the relations

$$\begin{cases} \frac{1}{2}S^{ab} &= A^{ab}, \\ \frac{1}{2}((2\lambda + \delta - 1)\gamma^a + \partial_b S^{ba}) &= A^a, \\ \frac{1}{2}(\lambda\partial_a\gamma^a + \lambda(\lambda + \delta - 1)\theta) &= A, \end{cases} \quad (\lambda \neq 0, \lambda + \mu \neq 1, \mu \neq 1).$$

uniquely define principal symbol, upper connection and Brans-Dicke field. Hence they uniquely define canonical pencil (28).

The “universality” property provides a beautiful interpretation of canonical map  $\varphi_{\lambda,\mu}$  in the relation (5). Indeed due to this Corollary we ”draw” the pencil through an arbitrary operator  $\Delta_\lambda = A^{ij}(x)\partial_i\partial_j + A^i(x)\partial_i + A(x)$  acting on densities of weight  $\lambda$ . Then the image of this operator, operator  $\Delta_\mu = \varphi_{\lambda,\mu}(\Delta_\lambda)$  is the operator of this pencil acting on densities of weight  $\mu$ .

## 4. Operators depending on a class of connections

In this section we will return to second order differential operators on manifold  $M$ . We consider second order operators acting on densities of a specially chosen given weight.

### 4.1. Operators of weight $\delta$ acting on densities of weight $\frac{1-\delta}{2}$

The Corollary 2 states that for a second order operator  $\Delta: \mathcal{F}_\lambda \rightarrow \mathcal{F}_\mu$  for all values of weights except the cases  $\lambda = 0$ ,  $\mu = 1$  or  $\lambda + \mu = 1$  there is a unique canonical

pencil (28) which passes through the operator  $\Delta$ . Consider now an exceptional case when operator  $\Delta: \mathcal{F}_\lambda \rightarrow \mathcal{F}_\mu$  is such that it has weight  $\delta$  and  $\lambda + \mu = 1$ , i.e. it acts on densities of weight  $\lambda = \frac{1-\delta}{2}$  and transforms them to densities of weight  $\mu = \frac{1+\delta}{2}$ .

Let  $\Delta_{\text{sing}}$  be such an operator which belongs to the canonical pencil (28):

$$\begin{aligned}\Delta_{\text{sing}} &= (\Delta_\lambda) \Big|_{\lambda=\frac{1-\delta}{2}} = \frac{t^\delta}{2} \left( S^{ab}(x) \partial_a \partial_b + \partial_b S^{ba} \partial_a + \lambda \partial_a \gamma^a(x) + \lambda(\lambda + \delta - 1) \theta(x) \right) \\ &= \frac{|D(x)|^\delta}{2} \left( S^{ab}(x) \partial_a \partial_b + \partial_b S^{ba} \partial_a + \frac{1-\delta}{2} \left( \partial_a \gamma^a(x) + \frac{\delta-1}{2} \theta(x) \right) \right). \quad (30)\end{aligned}$$

On the other hand let  $\Delta$  be an arbitrary second order differential operator of weight  $\delta$  which acts on densities of weight  $\frac{1-\delta}{2}$ ,  $\Delta: \mathcal{F}_{\frac{1-\delta}{2}} \rightarrow \mathcal{F}_{\frac{1+\delta}{2}}$ . Compare this operator with the operator  $\Delta_{\text{sing}}$ . The operator  $\Delta^+$  which is adjoint to the operator  $\Delta$  also acts from the space  $\mathcal{F}_{\frac{1-\delta}{2}}$  into the space  $\mathcal{F}_{\frac{1+\delta}{2}}$ , since  $\lambda + \mu = \frac{1-\delta}{2} + \frac{1+\delta}{2} = 1$  (compare with formula (29)). Hence an operator  $\Delta$  can be canonically decomposed on the sum of second order self-adjoint operator and antiself-adjoint operator of the order  $\leq 1$ . Antiself-adjoint operator is just generalised Lie derivative (22):

$$\Delta^+ - \Delta = \mathcal{L}_X \Big|_{\mathcal{F}_{\frac{1-\delta}{2}}} = |D(x)|^\delta \left( X^a \partial_a + \frac{1}{2} \partial_a X^a \right).$$

Operator  $\Delta_{\text{sing}}$  in formula (30) belongs to canonical pencil, it is self-adjoint operator:  $\Delta_{\text{sing}}^+ = \Delta_{\text{sing}}$ . Difference of two self-adjoint operators of second order with the same principal symbol is self-adjoint operator of order  $\leq 1$ . Hence it is the zeroth order operator of multiplication on the density. These considerations imply the following statement:

**Corollary 3** *Let  $\Delta$  be an arbitrary second order operator of weight  $\delta$  acting on the space of densities of weight  $\frac{1-\delta}{2}$ .*

*Let  $\mathbf{S} = S^{ab}|D(x)|^\delta$  be a principal symbol of the operator  $\Delta$ . Let  $\Delta_{\text{sing}}$  be an operator belonging to an arbitrary canonical pencil (28) with the same weight  $\delta$  and with the same principal symbol  $\mathbf{S} = S^{ab}|D(x)|^\delta$ .*

*Then the difference  $\Delta - \Delta_{\text{sing}}$  is an operator of order  $\leq 1$ . It equals to generalised Lie derivative (22) with respect to a vector field +zeroth order operator of multiplication on a density:*

$$\Delta = \Delta_{\text{sing}} + \mathcal{L}_X + F(x)|D(x)|^\delta.$$

*In the case if operator  $\Delta$  is self-adjoint,  $\Delta^+ = \Delta$ , then Lie derivative vanishes ( $\mathbf{X} = 0$ ).*

It follows from this Corollary that if the operator  $\Delta: \mathcal{F}_{\frac{1-\delta}{2}} \rightarrow \mathcal{F}_{\frac{1+\delta}{2}}$  is self-adjoint operator then it is given in local coordinates by the expression

$$\Delta = \frac{1}{2} \left( S^{ab}(x) \partial_a \partial_b + \partial_b S^{ba}(x) \partial_a + U_{\mathbf{S}}(x) \right) |D(x)|^\delta,$$

where

$$U_{\mathbf{S}}(x)|D(x)|^\delta = \frac{1-\delta}{2} \left( \partial_a \gamma^a(x) + \frac{\delta-1}{2} \theta(x) \right) |D(x)|^\delta + F(x)|D(x)|^\delta.$$

Here  $\gamma^a, \theta$  are upper connection and Brans-Dicke field defining the pencil (28), and  $F(x)|D(x)|^\delta$  is a density. In particular the self-adjoint operator  $\Delta: \mathcal{F}_{\frac{1-\delta}{2}} \rightarrow \mathcal{F}_{\frac{1+\delta}{2}}$  belongs to the canonical pencil defined by the same principal symbol  $\mathbf{S}$ , and upper connection  $\gamma^a$  but different  $\theta' = \theta - \frac{4F}{(\delta-1)^2}$ . It may belong to many other pencils with different upper connections. Self-adjoint operator  $\Delta$  acting on densities of the exceptional weight  $\lambda = \frac{1-\delta}{2}$  does not define uniquely the canonical pencil. Thus we come to

## 4.2. Groupoid of connections

We define now a groupoid  $C_{\mathbf{S}}$  of connections associated with contravariant tensor field-density  $\mathbf{S} = S^{ab}|D(x)|^\delta$  of weight  $\delta$ .

Consider a space  $\mathbf{A}$  of all connections on volume forms (covariant derivatives of volume forms) on manifold  $M$ . This is an affine space associated to the vector space of covector fields on  $M$ : difference of two connections  $\nabla$  and  $\nabla'$  is covector field (differential 1-form):

$$\nabla - \nabla' = \boldsymbol{\gamma} - \boldsymbol{\gamma}' = \mathbf{X} = X_a dx^a, \text{ where } X_a = \gamma_a - \gamma'_a.$$

Define a set of arrows as a set  $\{\boldsymbol{\gamma} \xrightarrow{\mathbf{X}} \boldsymbol{\gamma}'\}$  such that  $\boldsymbol{\gamma}, \boldsymbol{\gamma}' \in \mathbf{A}$  and  $\boldsymbol{\gamma}' = \boldsymbol{\gamma} + \mathbf{X}$ , where  $\mathbf{X}$ , difference of connections is a covector field. We come to trivial groupoid of connections:

$$-(\boldsymbol{\gamma} \xrightarrow{\mathbf{X}} \boldsymbol{\gamma}') = \boldsymbol{\gamma}' \xrightarrow{-\mathbf{X}} \boldsymbol{\gamma}, \quad (\boldsymbol{\gamma}_1 \xrightarrow{\mathbf{X}} \boldsymbol{\gamma}_2) + (\boldsymbol{\gamma}_2 \xrightarrow{\mathbf{Y}} \boldsymbol{\gamma}_3) = \boldsymbol{\gamma}_1 \xrightarrow{\mathbf{X} + \mathbf{Y}} \boldsymbol{\gamma}_3. \quad (31)$$

Pick an arbitrary contravariant symmetric tensor field-density of the weight  $\delta$ :  $\mathbf{S}(x) = S^{ab}(x)|D(x)|^\delta$ . The tensor field-density  $\mathbf{S}$  and an arbitrary connection  $\boldsymbol{\gamma}$  define the self-adjoint operator  $\Delta(\mathbf{S}, \boldsymbol{\gamma})$  on the algebra of densities. It is the operator defined in the equation (27) with principal symbol  $\mathbf{S}$ , with upper connection  $\gamma^a = S^{ab}\gamma_b$  and Brans-Dicke function  $\theta = \gamma_a\gamma^a$  (see the Corollary 1). Consider corresponding pencil of operators and the operator  $\Delta_{\text{sing}}(\mathbf{S}, \boldsymbol{\gamma})$  which belongs to this pencil and acts on densities of weight  $\frac{1-\delta}{2}$ :

$$\Delta_{\text{sing}}(\mathbf{S}, \boldsymbol{\gamma}) = \Delta(\mathbf{S}, \boldsymbol{\gamma})|_{\mathcal{F}_{\frac{1-\delta}{2}}} =$$

$$= \frac{|D(x)|^\delta}{2} \left( S^{ab}(x) \partial_a \partial_b + \partial_b S^{ba} \partial_a + \frac{1-\delta}{2} \left( \partial_a \gamma^a(x) + \frac{\delta-1}{2} \gamma_a \gamma^a(x) \right) \right). \quad (32)$$

Thus an arbitrary contravariant symmetric tensor field-density  $\mathbf{S} = S^{ab}(x)|D(x)|^\delta$  of the weight  $\delta$  and an arbitrary connection  $\boldsymbol{\gamma}$  defines self-adjoint operator  $\Delta_{\text{sing}}(\mathbf{S}, \boldsymbol{\gamma})$

by the relation (32). “Pseudoscalar” part of this operator is equal to

$$U_{\mathbf{S},\gamma}(x)|D(x)|^\delta = \left(\frac{1-\delta}{2}\right) \left(\partial_a \gamma^a(x) + \frac{\delta-1}{2} \gamma_a \gamma^a(x)\right) \frac{|D(x)|^\delta}{2}. \quad (33)$$

Let  $\gamma$  and  $\gamma'$  be two different connections. Difference of two operators  $\Delta_{\text{sing}}(\mathbf{S}, \gamma)$  and  $\Delta_{\text{sing}}(\mathbf{S}, \gamma')$  with the same principal symbol  $\mathbf{S} = S^{ab}(x)|D(x)|^\delta$  is the scalar density of the weight  $\delta$ . Calculate this density. If  $\gamma' = \gamma + \mathbf{X}$  then

$$\begin{aligned} \Delta_{\text{sing}}(\mathbf{S}, \gamma') - \Delta_{\text{sing}}(\mathbf{S}, \gamma) &= U_{\mathbf{S},\gamma'}(x)|D(x)|^\delta - U_{\mathbf{S},\gamma}(x)|D(x)|^\delta = \\ &\left(\frac{1-\delta}{4}\right) \left(\partial_a \gamma'^a(x) + \frac{\delta-1}{2} \gamma'_a \gamma'^a(x) - \partial_a \gamma^a(x) - \frac{\delta-1}{2} \gamma_a \gamma^a(x)\right) |D(x)|^\delta = \\ &\left(\frac{1-\delta}{4}\right) \left(\partial_a(S^{ab} X_b) + (\delta-1) \gamma_a(S^{ab} X_b) + \frac{\delta-1}{2} X_a S^{ab} X_b\right) |D(x)|^\delta = \\ &\frac{1-\delta}{4} \left(\text{div}_\gamma \mathbf{X} + \frac{\delta-1}{2} \mathbf{X}^2\right). \end{aligned} \quad (34)$$

Here  $\text{div}_\gamma \mathbf{X}$  is the divergence of vector density  $\mathbf{X}$  on  $M$  with respect to connection  $\gamma$  (see (23)). With some abuse of notation we denote the covector field  $X_a dx^a$  and vector density of the weight  $\delta$ ,  $X^a |D(x)|^\delta = S^{ab} X_b |D(x)|^\delta$  by the same letter  $\mathbf{X}$ .

**Definition 2** Let  $\mathbf{S} = S^{ab}(x)|D(x)|^\delta$  be contravariant symmetric tensor field-density of the weight  $\delta$ . The groupoid  $C_{\mathbf{S}}$  is a subgroupoid of arrows  $\gamma \xrightarrow{\mathbf{X}} \gamma'$  of trivial groupoid (31) such that the operators  $\Delta_{\text{sing}}(\mathbf{S}, \gamma)$  and  $\Delta_{\text{sing}}(\mathbf{S}, \gamma')$  defined by the formula (32) coincide:

$$C_{\mathbf{S}} = \{ \text{Groupoid of arrows } \gamma \xrightarrow{\mathbf{X}} \gamma' \text{ such that } \Delta_{\text{sing}}(\mathbf{S}, \gamma') = \Delta_{\text{sing}}(\mathbf{S}, \gamma) \}. \quad (35)$$

Using the formula (34) for difference of operators  $\Delta_{\text{sing}}(\mathbf{S}, \gamma')$  and  $\Delta_{\text{sing}}(\mathbf{S}, \gamma)$  rewrite the definition (35) of groupoid  $C_{\mathbf{S}}$  in the following way:

$$C_{\mathbf{S}} = \{ \text{Groupoid of arrows } \gamma \xrightarrow{\mathbf{X}} \gamma' \text{ such that } \text{div}_\gamma \mathbf{X} + \frac{\delta-1}{2} \mathbf{X}^2 = 0 \}.$$

In other words the arrow  $\gamma \xrightarrow{\mathbf{X}} \gamma'$  belongs to the groupoid  $C_{\mathbf{S}}$  if two canonical pencils  $\Delta_\lambda(\mathbf{S}, \gamma)$  and  $\Delta_\lambda(\mathbf{S}, \gamma')$  intersect at the operator  $\Delta_{\text{sing}}(\mathbf{S}, \gamma)$ .

We consider the case  $\delta \neq 1$ , The case  $\delta = 1$  is trivial <sup>3</sup>.

Denote by  $[\gamma]$  the orbit of a connection  $\gamma$  in the groupoid  $C_{\mathbf{S}}$

$$[\gamma] = \{ \gamma' : \gamma \xrightarrow{\mathbf{X}} \gamma' \in C_{\mathbf{S}} \}.$$

---

<sup>3</sup>In this case all the operators  $\Delta_{\text{sing}}(\mathbf{S}, \gamma)$  do not depend on connection  $\gamma$ . Principal symbol  $\mathbf{S} = S^{ab}|D(x)|$  defines the canonical operator  $\Delta(\mathbf{S}) : \mathcal{F}_0 \rightarrow \mathcal{F}_1$  such that in local coordinates  $\Delta(\mathbf{s})f = \partial_a S^{ab} \partial_b f / |D(x)|$ . The groupoid  $C_{\mathbf{S}}$  is the trivial groupoid of all connections.

**Proposition 4** An arbitrary contravariant symmetric tensor field  $\mathbf{S} = S^{ab}(x)|D(x)|^\delta$  of the weight  $\delta$  defines the groupoid of connections  $C_{\mathbf{S}}$  and the family of second order differential operators of the order  $\delta$  and acting on densities of the weight  $\frac{1-\delta}{2}$ :

$$\Delta([\gamma]) = \Delta_{\text{sing}}(\mathbf{S}, \gamma): \mathcal{F}_{\frac{1-\delta}{2}} \rightarrow \mathcal{F}_{\frac{1+\delta}{2}}.$$

Operators of this family have the same principal symbol and they depend on equivalence classes of connections which are orbits in the groupoid  $C_{\mathbf{S}}$ .

**Remark 7** Let  $\gamma_1, \gamma_2$  and  $\gamma_3$  be three arbitrary connections. Consider corresponding arrows  $\gamma_1 \xrightarrow{\mathbf{X}} \gamma_2$ ,  $\gamma_2 \xrightarrow{\mathbf{Y}} \gamma_3$  and  $\gamma_1 \xrightarrow{\mathbf{X}+\mathbf{Y}} \gamma_3$ . We have that  $\gamma_1 \xrightarrow{\mathbf{X}} \gamma_2 + \gamma_2 \xrightarrow{\mathbf{Y}} \gamma_3 = \gamma_1 \xrightarrow{\mathbf{X}+\mathbf{Y}} \gamma_3$ . This means that for non-linear differential equation  $\text{div}_{\gamma} \mathbf{X} + \frac{\delta-1}{2} \mathbf{X}^2 = 0$  the following property holds:

$$\begin{cases} \text{div}_{\gamma_1} \mathbf{X} + \frac{\delta-1}{2} \mathbf{X}^2 = 0 \\ \text{div}_{\gamma_2} \mathbf{Y} + \frac{\delta-1}{2} \mathbf{Y}^2 = 0 \end{cases} \Rightarrow \text{div}_{\gamma_1} (\mathbf{X} + \mathbf{Y}) + \frac{\delta-1}{2} (\mathbf{X} + \mathbf{Y})^2 = 0.$$

It follows from (34) the cocycle condition that the sum of left-hand side of first two equations is equal to the left hand-side of the third equation.

**Remark 8** Let  $\rho$  be an arbitrary volume form. Using the operator  $\Delta([\gamma]) = \Delta_{\text{sing}}(\mathbf{S}, \gamma)$  one can consider second order operator

$$\Delta: \Delta f = \rho^{-\frac{1+\delta}{2}} \Delta([\gamma]) \left( \rho^{\frac{1-\delta}{2}} f(x) \right)$$

on functions depending on volume form  $\rho$ . Calculating one comes to

$$\Delta f = \frac{1}{2} \left( S^{ab} \partial_a \partial_b + \partial_b S^{ba} \partial_a + (\delta - 1) \gamma_\rho^a \partial_a + \frac{1}{t^\delta} (U_{\mathbf{S}, \gamma} - U_{\mathbf{S}, \gamma_\rho}) \right) f$$

Here  $\gamma_\rho$ :  $\gamma_a = -\partial_a \log \rho$  is a flat connection defined by the volume form  $\rho = \rho(x)|D(x)|$ ,  $\gamma^a = S^{ab} \gamma_b$  and  $U_{\mathbf{S}, \gamma}/t^\delta$  is a "pseudoscalar" part (33) of the operator (32). The difference  $U_{\mathbf{S}, \gamma} - U_{\mathbf{S}, \gamma_\rho}$  is a density of weight  $\delta$  (see Corollary 3 and equation (34)).

We consider now examples of groupoids and corresponding operators  $\Delta_{\text{sing}}(\mathbf{S}, \gamma)$ .

### 4.3. Groupoid $C_{\mathbf{S}}$ for a Riemannian manifold

Let  $M$  be Riemannian manifold equipped with Riemannian metric  $G$ . (As always we suppose that  $M$  is orientable compact manifold with a chosen oriented atlas). Riemannian metric defines principal symbol  $\mathbf{S} = G^{-1}$ . In local coordinates  $S^{ab} = g^{ab}$  ( $G = g_{ab} dx^a dx^b$ ). It is principal symbol of operator of weight  $\delta = 0$ .

&lt;/

The operator  $\Delta([\gamma^G])$  belongs in particular to the canonical pencil associated with the Beltrami-Laplace operator (see the example 6).

On the other hand let  $\gamma$  be an arbitrary connection and let  $\rho$  be an arbitrary volume form on the Riemannian manifold  $M$ . One can assign to volume form  $\rho$  the flat connection  $\gamma^\rho: \gamma_a^\rho = -\partial_a \log \rho$ . Consider operator  $\frac{1}{\sqrt{\rho}}\Delta([\gamma])\sqrt{\rho}$  on functions (see Remark 8.) We come to scalar operator on functions

$$\Delta f = \frac{1}{2} \left( \partial_a \left( g^{ab} \partial_b f \right) - \gamma^{\rho a} \partial_a + R \right)$$

where scalar function  $R$  equals to

$$R = U_{G,\gamma} - U_{G,\gamma^\rho} = \frac{1}{2} \text{div} \mathbf{X} - \frac{1}{4} \mathbf{X}^2.$$

Here vector field  $\mathbf{X}$  is defined by the difference of the connections:  $\mathbf{X} = \gamma - \gamma^\rho$ .

It is interesting to compare formulae of this subsection with constructions in the paper [2] for a case of Riemannian structure.

Our next example is a groupoid on odd symplectic supermanifold. Before discussing it sketch shortly what happens if we consider supermanifolds instead manifolds.

#### 4.4. Supermanifold case

Let  $M$  be  $n|m$ -dimensional supermanifold. Denote local coordinates of supermanifold by  $z^A = (x^a, \theta^\alpha)$  ( $a = 1, \dots, n; \alpha = 1, \dots, m$ ). Here  $x^a$  are even coordinates and  $\theta^\alpha$  odd coordinates:  $z^A z^B = (-1)^{p(A)p(B)} z^B z^A$ , where  $p(z^A)$ , or shortly  $p(A)$  is a parity of coordinate  $z^A$ ; ( $p(x^a) = 0, p(\theta^\alpha) = 1$ ).

We would like to study second order linear differential operators  $\Delta = S^{AB} \partial_A \partial_B + \dots$ . Principal symbol of this operator is supersymmetric contravariant tensor field  $\mathbf{S} = S^{AB}$ . This field may be even or odd:

$$S^{AB} = (-1)^{p(A)p(B)} S^{BA}, \quad p(S^{AB}) = p(\mathbf{S}) + p(A) + p(B).$$

The analysis of second order operators can be performed in supercase in a way similar to usual case. We have just to worry about sign rules. E.g. the formula (28) for canonical pencil of operators has to be rewritten in the following way

$$\begin{aligned} \Delta_\lambda &= \frac{t^\delta}{2} \left( S^{AB}(x) \partial_B \partial_A + (-1)^{p(A)p(\mathbf{S}+1)} \partial_B S^{BA} \partial_A \right) + \\ &+ \frac{t^\delta}{2} \left( (2\lambda + \delta - 1) \gamma^A(x) \partial_A + (-1)^{p(A)p(\mathbf{S}+1)} \lambda \partial_A \gamma^A(x) + \lambda (\lambda + \delta - 1) \theta(x) \right). \end{aligned} \quad (36)$$

Here  $\Delta$  is even (odd) operator if principal symbol  $\mathbf{S}$  is even (odd) tensor field (see for detail [15]).

In the case if  $\mathbf{S}$  is an even tensor field and it is non-degenerate then it defines Riemannian structure on (super)manifold  $M$ . We come to groupoid  $C_{\mathbf{S}}$  in a same

way as in a case of usual Riemannian manifold considered in the previous subsection. (We just must worry about signs arising in calculations.) In particular for even Riemannian supermanifold there exists distinguished Levi-Civita connection which canonically induces the unique connection on volume forms. This connection is a flat connection of the canonical volume form:

$$\rho_g = \sqrt{\text{Ber } g_{AB}} |D(z)|, \gamma_A = -\partial_A \log \rho(z) = -(-1)^B \Gamma_{BA}^B. \quad (37)$$

Here  $g_{AB}$  is a covariant tensor defining Riemannian structure, ( $S^{AB} = g^{AB}$ ) and  $\Gamma_{BC}^A$  are Christoffel symbols of Levi-Civita connection of this Riemannian structure.  $\text{Ber } g_{AB}$  is Berezinian (superdeterminant) of the matrix  $g_{AB}$ . It is super analog of determinant. The matrix  $g_{AB}$  is  $n|m \times n|m$  even matrix and its Berezinian is given by the formula

$$\text{Ber } g_{AB} = \text{Ber} \begin{pmatrix} g_{ab} & g_{a\beta} \\ g_{\alpha b} & g_{\alpha\beta} \end{pmatrix} = \det \left( \frac{g_{ab} - g_{a\gamma} g^{\gamma\delta} g_{\delta b}}{\det g_{\alpha\beta}} \right). \quad (38)$$

(Here as usual  $g^{\gamma\delta}$  stands for the matrix inverse to the matrix  $g_{\gamma\delta}$ .)

The situation is essentially different in the case if  $\mathbf{S} = S^{AB}$  is an odd supersymmetric contravariant tensor field and respectively  $\Delta = S^{AB} \partial_A \partial_B + \dots$  is an odd operator. In this case one comes naturally to the odd Poisson structure on supermanifold  $M$  if tensor  $\mathbf{S}$  obeys additional conditions.

Namely, consider cotangent bundle  $T^*M$  to supermanifold  $M$  with local coordinates  $(z^A, p_B)$  where  $p_A$  are coordinates in fibres dual to coordinates  $z^A$  ( $p_A \sim \frac{\partial}{\partial z^A}$ ). Supersymmetric contravariant tensor field  $\mathbf{S} = S^{AB}$  defines quadratic master-Hamiltonian, odd function  $H_{\mathbf{S}} = \frac{1}{2} S^{AB} p_A p_B$  on cotangent bundle  $T^*M$ . This quadratic master-Hamiltonian defines the odd bracket on the functions on  $M$  as a derived bracket:

$$\{f, g\} = ((f, H_{\mathbf{S}}), g), \quad p(\{f, g\}) = p(f) + p(g) + 1. \quad (39)$$

Here  $(, )$  is canonical Poisson bracket on the cotangent bundle  $T^*M$ . The odd derived bracket is anti-commutative with respect to shifted parity and it obeys Leibnitz rule:

$$\{f, g\} = -(-1)^{(p(f)+1)(p(g)+1)} \{g, f\}, \quad \{f, gh\} = \{f, g\}h + (-1)^{p(g)p(h)} \{f, h\}g.$$

This odd derived bracket becomes *an odd Poisson bracket* in the case if it obeys Jacobi identity

$$\begin{aligned} & (-1)^{p((f)+1)p((h)+1)} \{\{f, g\}, h\} + (-1)^{p((g)+1)p((f)+1)} \{\{g, h\}, f\} \\ & + (-1)^{p((h)+1)p((g)+1)} \{\{h, f\}, g\} = 0. \end{aligned} \quad (40)$$

It is a beautiful fact that *the condition that derived bracket (39) obeys Jacobi identity can be formulated as a quadratic condition  $(H, H) = 0$  for the master-Hamiltonian*:

$$(H_{\mathbf{S}}, H_{\mathbf{S}}) = 0 \Leftrightarrow \text{Jacobi identity for the derived bracket } \{, \} \text{ holds.} \quad (41)$$

(See for detail [14]). In the case if  $\mathbf{S}$  is an even field (Riemannian geometry) master-Hamiltonian  $H$  is even function and Jacobi identity is trivial (see for detail [14] and [15].)

From now on suppose that tensor field  $\mathbf{S}$  is odd and it defines an odd Poisson bracket on the supermanifold  $M$ , i.e. the relation (41) holds. This odd Poisson bracket corresponds to an odd symplectic structure in the case if the bracket is non-degenerate, i.e. the odd tensor field  $\mathbf{S}$  is non-degenerate tensor field. The condition of non-degeneracy means that there exists inverse covariant tensor field  $S_{BC}$ :  $S^{AB}S_{BC} = \delta_C^B$ . Since the matrix  $S^{AB}$  is an odd matrix ( $p(\mathbf{S}^{AB}) = p(A) + p(B) + 1$ ) this implies that matrix  $S^{AB}$  has equal number of even and odd dimensions. We come to conclusion that for an odd symplectic supermanifold even and odd dimensions have to coincide. It is necessarily  $n|n$ -dimensional.

The basic example of an odd symplectic supermanifold is the following: for an arbitrary usual manifold  $M$  consider its cotangent bundle  $T^*M$  and change parity of the fibres in this bundle. We come to an odd symplectic supermanifold  $\Pi T^*M$ . To arbitrary local coordinates  $x^a$  on  $M$  one can associate local coordinates  $(x^a, \theta_a)$  in  $\Pi T^*M$ , where odd coordinates  $\theta_a$  transform as  $\partial_a$ :

$$x^{a'} = x^{a'}(x^a), \quad \theta_{a'} = \frac{\partial x^a}{\partial x^{a'}} \theta_a. \quad (42)$$

In these local coordinates the non-degenerate odd Poisson bracket is well-defined by the relations

$$\{x^a, \theta_b\} = \delta_b^a, \quad \{x^a, x^b\} = 0, \quad \{\theta_a, \theta_b\} = 0. \quad (43)$$

(These relations are invariant with respect to coordinate transformations (42).)

**Remark 9** An arbitrary odd symplectic supermanifold  $E$  is symplectomorphic to cotangent bundle of a usual manifold  $M$ . One may take  $M$  as even Lagrangian surface in  $M$ . (See for detail [12].) One can consider instead supermanifold  $E$  the cotangent bundle  $\Pi T^*M$  for usual manifold  $M$ . The difference between cotangent bundle to  $M$  with changed parity of fibres and supermanifold  $\Pi T^*M$  is that in the supermanifold  $\Pi T^*M$  one may consider arbitrary parity preserving coordinate transformations of local coordinates  $x$  and  $\theta$  which may destroy vector bundle structure, not only the transformations (42) which preserve the structure of vector bundle.

#### 4.5. Groupoid $C_S$ for an odd symplectic supermanifold

Let  $E$  be  $(n|n)$ -dimensional odd symplectic supermanifold, where an odd symplectic structure and respectively odd non-degenerate Poisson structure are defined by contravariant supersymmetric non-degenerate odd tensor field  $\mathbf{S} = S^{AB}$  such that Jacobi identities (40) hold. We study second order odd operators  $\Delta = \frac{1}{2}S^{AB} + \dots$  of weight  $\delta = 0^4$ .

---

<sup>4</sup>The following construction of groupoid is obviously valid in the general Poisson case, but in this subsection we are mainly interested in the odd symplectic case

Let  $\gamma$  be an arbitrary connection on volume forms. The differential operator  $\Delta = \Delta_{\text{sing}}(\mathbf{S}, \gamma)$  of weight  $\delta = 0$  with principal symbol  $\mathbf{S}$  defined by equation (32) transforms half-densities to half-densities. Due to the formulae (32), (33) and (36) this operator equals to

$$\begin{aligned} \Delta_{\text{sing}}(\mathbf{S}, \gamma) : \quad & \mathcal{F}_{\frac{1}{2}} \rightarrow \mathcal{F}_{\frac{1}{2}}, \\ \Delta_{\text{sing}}(\mathbf{S}, \gamma) &= \frac{1}{2} \left( S^{AB} \partial_B \partial_A + \partial_B g^{BA} \partial_a + \frac{1}{2} \partial_A \gamma^A - \frac{1}{4} \gamma_A \gamma^A \right). \end{aligned} \quad (44)$$

We come to the groupoid

$$C_{\mathbf{S}} = \left\{ \text{Groupoid of arrows } \gamma \xrightarrow{\mathbf{X}} \gamma' \text{ such that } \operatorname{div}_{\gamma} \mathbf{X} - \frac{1}{2} \mathbf{X}^2 = 0 \right\}$$

and to the operator on half-densities depending on the class of connections

$$\Delta([\gamma]) = \frac{1}{2} (S^{AB} \partial_B \partial_A + \partial_B g^{BA} \partial_a + U_{\mathbf{S}}([\gamma])), \text{ where } U_{\mathbf{S}}([\gamma]) = \frac{1}{2} \partial_A \gamma^A - \frac{1}{4} \gamma_A \gamma^A. \quad (45)$$

It is here where a similarity with Riemannian case finishes. On Riemannian manifold one can consider canonical volume form and distinguished Levi-Civita connection which induces canonical flat connection  $\gamma$  (see equation (37)). On an odd symplectic supermanifold there is no canonical volume form <sup>5</sup> and there is no distinguished connection on vector fields. On the other hand it turns out that in this case one can construct the class of distinguished connections which belong to an orbit of groupoid  $C_{\mathbf{S}}$ . Namely study the equation

$$\operatorname{div}_{\gamma} \mathbf{X} - \frac{1}{2} \mathbf{X}^2 = 0, \quad (46)$$

which defines the groupoid  $C_{\mathbf{S}}$ . According to equations (34), (44) and (45) we see that for operators  $\Delta([\gamma])$  acting on half-densities we have that

$$\Delta([\gamma']) - \Delta([\gamma]) = \Delta_{\text{sing}}(\mathbf{S}, \gamma') - \Delta_{\text{sing}}(\mathbf{S}, \gamma) = \frac{1}{4} \left( \operatorname{div}_{\gamma} \mathbf{X} - \frac{1}{2} \mathbf{X}^2 \right). \quad (47)$$

We call the equation (46) *Batalin-Vilkovisky equation*. Study this equation.

It is convenient to work in *Darboux coordinates*. Local coordinates  $z^A = (x^a, \theta_b)$  on supermanifold  $E$  are called Darboux coordinates if non-degenerate odd Poisson bracket has the appearance (43) in these coordinates.

We say that connection  $\gamma$  is Darboux flat if it vanishes in some Darboux coordinates.

**Lemma 1** *Let  $\gamma, \gamma'$  be two connections such that both connection  $\gamma$  and  $\gamma'$  are Darboux flat. Then the arrow  $\gamma \xrightarrow{\mathbf{X}} \gamma'$  belongs to the groupoid  $C_{\mathbf{S}}$ . i.e. the Batalin-Vilkovisky equation  $\operatorname{div}_{\gamma} \mathbf{X} - \frac{1}{2} \mathbf{X}^2 = 0$  holds for covector field  $\mathbf{X} = \gamma' - \gamma$ .*

---

<sup>5</sup>Naive generalisation of formulae (37) and (38) does not work since in particular  $S^{AB}$  is not an even matrix

We will prove this lemma later.

**Remark 10** In fact lemma implies that a class of locally defined Darboux flat connections defines globally the pseudoscalar function  $U_S$  in (44). Let  $\{z_{(\alpha)}^A\}$  be an arbitrary atlas of Darboux coordinates on  $E$ . We say that the collection of local connections  $\{\gamma_{(\alpha)}\}$  is adjusted to Darboux atlas  $\{z_{(\alpha)}^A\}$  if every local connection  $\gamma_{(\alpha)}$  (defined in the chart  $z_{(\alpha)}^A$ ) vanishes in these local Darboux coordinates  $z_{(\alpha)}^A$ . Let  $\{\gamma_{(\alpha)}\}$  and  $\{\gamma'_{(\alpha')}\}$  be two families of local connections adjusted to Darboux atlases  $\{z_{(\alpha)}^A\}$  and  $\{z_{(\alpha')}^{A'}\}$  respectively. Then due to Lemma all arrows  $\gamma_{(\alpha)} \xrightarrow{x} \gamma_{(\alpha')}$ ,  $\gamma'_{(\alpha)} \xrightarrow{x} \gamma'_{(\alpha')}$  and  $\gamma_{(\alpha)} \xrightarrow{x} \gamma'_{(\alpha')}$  belong to local groupoid  $C_S$  (if charts  $(z_{(\alpha)}^A)$ ,  $(z_{(\alpha')}^{A'})$ ,  $(z_{(\alpha)}^{A'})$  and  $(z_{(\alpha')}^{A'})$  intersect). This means that in spite of the fact that the family  $\{\gamma_\alpha\}$  does not define the global connection, still equations (46) hold locally and operator  $\Delta = \Delta(S, \gamma_\alpha)$  globally exists. (These considerations for locally defined groupoid can be performed for arbitrary case. One can consider the family of locally defined connections  $\{\gamma_a\}$  such that they define global operator (32).) On the other hand in a case of an odd symplectic supermanifold there exists a global Darboux flat connection, i.e. the connection  $\gamma$  such in a vicinity of an arbitrary point this connection vanishes in some Darboux coordinates. Show it.

Without loss of generality suppose that  $E = \Pi T^*M$  (see Remark (9).) Let  $\sigma$  be an arbitrary volume form on  $M$  (we suppose that  $M$  is orientable). Choose an atlas  $\{x_{(\alpha)}^a\}$  of local coordinates on  $M$  such that  $\sigma$  is the coordinate volume form, i.e.  $\sigma = dx_{(\alpha)}^1 \wedge \dots dx_{(\alpha)}^n$ . Then consider associated atlas  $\{x_{(\alpha)}^a, \theta_a(\alpha)\}$  in supermanifold  $\Pi T^*M$  which is an atlas of Darboux coordinates. For this atlas as well as for the atlas  $\{x_{(\alpha)}^a\}$  Jacobians of coordinate transformations are equal to 1. Thus we constructed atlas of special Darboux coordinates in which all the Jacobians of coordinate transformations are equal to 1. The coordinate volume form  $\rho = D(x, \theta)$  is globally defined. The flat connection defined by this volume form vanishes. We defined globally Darboux flat connection.

We come to Proposition

**Proposition 5** In an odd symplectic supermanifold there exists a canonical orbit of connections. It is the class  $[\gamma]$  in the groupoid  $C_S$ , where  $\gamma$  is an arbitrary Darboux flat connection. We will call this canonical class of connections “the class of Darboux flat connections”.

For any connection belonging to the canonical orbit of connections, the pseudoscalar function  $U_S$  in (45) vanishes in arbitrary Darboux coordinates<sup>6</sup>. The operator  $\Delta = \Delta[\gamma]$  on half-densities corresponding to this class of connections has the following appearance in arbitrary Darboux coordinates  $z^A = (x^a, \theta_b)$ :

$$\Delta = \frac{\partial^2}{\partial x^a \partial \theta_a}. \quad (48)$$

(This canonical operator on half-densities was introduced in [12].)

Now prove Lemma 1.

For an arbitrary volume form  $\rho$  consider an operator

$$\Delta_\rho f = \frac{1}{2} \operatorname{div}_\rho \operatorname{grad} f. \quad (49)$$

---

<sup>6</sup>This function vanishes not only for globally defined Darboux flat connection but for a family of connections adjusted to an arbitrary Darboux atlas (see Remark 10)

Here  $\text{grad } f$  is Hamiltonian vector field  $\{f, z^A\} \frac{\partial}{\partial z^A}$  corresponding to the function  $f$ . (Compare with (2).) This is the famous Batalin-Vilkovisky odd Laplacian on functions. In the case if  $z^A = (x^a, \theta_a)$  are Darboux coordinates and a volume form  $\rho$  is the coordinate volume form, i.e.  $\rho = D(x, \theta)$ , then odd Laplacian in these Darboux coordinates has the appearance

$$\Delta = \frac{\partial^2}{\partial x^a \partial \theta_a}. \quad (50)$$

(This is the initial form of the Batalin-Vilkovisky operator in [3]. (Geometrical meaning of BV operator, and how formulae (49) and (50) are related with canonical operator (48) on semidensities see in [10, 19, 12].)

The equation (46) characterising the groupoid (the Batalin-Vilkovisky equation) is related with the Batalin-Vilkovisky operator by the following identity:

$$-e^{\frac{F}{2}} \Delta_{\rho} e^{-\frac{F}{2}} = \frac{1}{4} \text{div}_{\gamma} \mathbf{X} - \frac{1}{8} \mathbf{X}^2, \quad (51)$$

where connection  $\gamma$  is a flat connection induced by volume form ( $\gamma_a = -\partial_a \log \rho$ ) and vector field  $\mathbf{X}$  is Hamiltonian vector field of the function  $F$ .

We use this identity to prove the lemma. Let connection  $\gamma$  vanishes in Darboux coordinates  $z^A = (x^a, \theta_a)$  and connection  $\gamma'$  vanishes in Darboux coordinates  $z^{A'} = (x'^a, \theta'_a)$ . Then (compare with equation (11)) connection  $\gamma'$  has in Darboux coordinates  $z^A = (x^a, \theta_a)$  the following appearance

$$\gamma'_A = \frac{\partial z^{A'}(z^A)}{\partial z^A} (\gamma_{A'} + \partial_{A'} \log J),$$

where  $J$  is Jacobian of Darboux coordinates transformation  $J = \text{Ber } J = \text{Ber} \frac{\partial(x, \theta)}{\partial(x', \theta')}$  (see also the formula (38))

Hence for the arrow  $\gamma \xrightarrow{\mathbf{X}} \gamma'$  the covector field  $\mathbf{X}$  equals to

$$X_A = -\frac{\partial}{\partial z^a} \log \text{Ber} \frac{\partial(x', \theta')}{\partial(x, \theta)}.$$

Apply identity (51) where  $\gamma_a = 0$ ,  $\rho = D(x, \theta)$  is coordinate volume form and  $F = -\log \text{Ber} \frac{\partial(x', \theta')}{\partial(x, \theta)}$ . Using (49) and (50) we arrive at

$$\frac{1}{4} \text{div}_{\gamma} \mathbf{X} - \frac{1}{8} \mathbf{X}^2 = -e^{\frac{F}{2}} \Delta_{\rho} e^{-\frac{F}{2}} = - \left( \sqrt{\text{Ber} \frac{\partial(x, \theta)}{\partial(x', \theta')}} \right) \frac{\partial^2}{\partial x^a \partial \theta_a} \left( \sqrt{\text{Ber} \frac{\partial(x', \theta')}{\partial(x, \theta)}} \right) = 0.$$

The last identity is the famous Batalin-Vilkovisky identity [4] which stands in the core of the geometry of Batalin-Vilkovisky operator.

Lemma is proved.

**Remark 11** The canonical operator (48) assigns to every even non-zero half density  $s$  and to every volume form  $\rho$  the functions  $\sigma_s$  and  $\sigma_\rho$ :

$$\sigma(s) = \frac{\Delta s}{s}, \quad \sigma(\rho) = \frac{\Delta \sqrt{\rho}}{\rho}$$

(see [12]). In the articles [1, 2] Batalin and Bering considered geometrical properties of the canonical operator (48) on semidensities. In these considerations they used the formula for expressing the canonical operator (48) in arbitrary coordinates. This formula was suggested by Bering in [6]. Clarifying geometrical meaning of this formula and analysing the geometrical meaning of the scalar function  $\sigma(\rho)$  they come to beautiful result: if  $\nabla$  is an arbitrary torsion-free affine connection in an odd symplectic supermanifold which is compatible with volume form  $\rho$ , then the scalar curvature of this connection equals (up to a coefficient) to the function  $\sigma_\rho$ .

**Remark 12** In work [14] we have considered in particular the following “Batalin–Vilkovisky groupoid” of volume forms on an odd Poisson manifold: the arrows  $\rho \xrightarrow{J} \rho'$ , where  $J = \frac{\rho'}{\rho}$ , are defined by the Batalin–Vilkovisky equation  $\Delta_\rho \sqrt{J} = 0$ . The operator  $\Delta_\rho$  is defined by equation (49). Assign to each arrow  $\rho \xrightarrow{J} \rho'$  the arrow  $\gamma \xrightarrow{X} \gamma'$  of the groupoid  $C_S$  such that the connections  $\gamma, \gamma'$  are defined by volume forms  $\rho, \rho'$  respectively ( $\gamma_a = -\partial_a \log \rho$  and  $\gamma'_a = -\partial_a \log \rho'$ ). Then it follows from equation (51) that the groupoid of volume forms is a subgroupoid of the groupoid  $C_S$ .

Both the Batalin–Vilkovisky groupoid and the groupoid of connections  $C_S$  considered here can be regarded as Lie groupoids over infinite-dimensional manifolds, which are the space  $\text{Vol}^\times(M)$  of the non-degenerate volume forms and the space  $\text{Conx}(M)$  of the connections on densities on a manifold  $M$  respectively. The corresponding Lie algebroids can be described as follows.

For the Batalin–Vilkovisky groupoid, the Lie algebroid is the vector bundle over the (infinite-dimensional) manifold  $\text{Vol}^\times(M)$  whose the fiber over the point  $\rho$  is the vector space of all solutions of the equation  $\Delta F = 0$  where  $F \in C^\infty(M)$ . The anchor is tautological: it sends a function  $F$  to the infinitesimal shift  $\rho \mapsto \rho + \varepsilon \rho F$ . A section of this bundle is a functional  $F[\rho]$  of a volume form with values in functions on  $M$  such that for each  $\rho$ , the above equation is satisfied. The Lie bracket is the restriction of the canonical commutator of vector fields on  $\text{Vol}^\times(M)$  and can be expressed by an explicit formula

$$[F, G][\rho; x] = \int_M Dy \rho(y) \left( F[\rho; y] \frac{\delta G[\rho; x]}{\delta \rho(y)} - G[\rho; y] \frac{\delta F[\rho; x]}{\delta \rho(y)} \right).$$

Here we write  $F[\rho; x]$  for the value of  $F[\rho] \in C^\infty(M)$  at  $x \in M$ .

For the groupoid of connections (with a fixed tensor density  $S^{ab}$  of weight  $\delta$ ), the Lie algebroid is the vector bundle over  $\text{Conx}(M)$  whose fiber over  $\gamma \in \text{Conx}(M)$  is the vector space of all solutions of the equation  $\text{div}_\gamma X = 0$ . A section is a functional of a connection taking values in these vector spaces. The anchor is tautological: it

sends a covector field  $X_a$  to the infinitesimal shift of the connection  $\gamma_a \mapsto \gamma_a + \varepsilon X_a$ . The Lie bracket can be expressed by the formula

$$[X, Y]_a[\gamma; x] = \int_M Dy \left( X_b[\gamma; y] \frac{\delta Y_a[\gamma; x]}{\delta \gamma_b(y)} - Y_b[\gamma; y] \frac{\delta X_a[\gamma; x]}{\delta \gamma_b(y)} \right).$$

(For supermanifolds the formulas for the brackets contain extra signs.) Note that since the groupoids in question are subgroupoids of the trivial (pair) groupoids, these Lie algebroids are subalgebroids of the respective tangent bundles.

#### 4.6. Groupoid $C_S$ for the line

We return here to simplest possible manifold—real line. The symmetric tensor field  $\mathbf{S}$  of rank 2 and of weight  $\delta$  on real line  $\mathbb{R}$  is a density of the weight  $\delta - 2$ :  $\mathbf{S} = S\partial_x^2|D(x)|^\delta \sim S|D(x)|^{\delta-2}$ . Consider on  $\mathbb{R}$  the canonical vector density  $|D(x)|\partial_x$  which is invariant with respect to change of coordinates. Its square defines canonical tensor density  $\mathbf{S}_{\mathbb{R}} = |D(x)|^2(\partial_x)^2$  of weight  $\delta = 2$ .

We see that on the line there is a canonical pencil of second order operators of the weight  $\delta = 2$ :  $|D(x)|^2(\partial_x^2 + \dots)$  with canonical principal symbol  $\mathbf{S}_{\mathbb{R}} = |D(x)|^2(\partial_x)^2$ . The operator (32) belonging to this pencil acts on densities of weight  $\frac{1-\delta}{2} = -\frac{1}{2}$  and transforms them into densities of weight  $\frac{1+\delta}{2} = \frac{3}{2}$ . According to (32) It has the following appearance:

$$\Delta(\gamma): \quad \Psi(x)|Dx|^{-\frac{1}{2}} \mapsto \Phi(x)|D(x)|^{\frac{3}{2}} = \frac{1}{2} \left( \frac{\partial^2 \Psi(x)}{\partial x^2} + U(x)\Psi(x) \right) |Dx|^{\frac{3}{2}},$$

where according to the equation (33)

$$U_{\gamma}(x) = -\frac{1}{4} \left( \gamma_x + \frac{1}{2}\gamma^2 \right) |D(x)|^2. \quad (52)$$

This is Sturm-Liouville operator recognisable by specialists in projective geometry and integrable systems<sup>7</sup> (see e.g. [9] or the book [18]).

We see that in this case the difference of operators is

$$\begin{aligned} \Delta(\gamma') - \Delta(\gamma) &= -\frac{1}{4} \left( \gamma'_x + \frac{1}{4} (\gamma')^2 \right) |D(x)|^2 + \frac{1}{4} \left( \gamma_x + \frac{1}{2} (\gamma)^2 \right) |D(x)|^2 = \\ &\quad -\frac{1}{4} \left( \operatorname{div} \mathbf{X} + \frac{1}{2} \mathbf{X}^2 \right). \end{aligned}$$

Here  $\mathbf{X} = (\gamma' - \gamma)|D(x)|^2\partial_x$  is vector density of the weight  $\delta = 2$ . (compare with formulae(34) and (47)).

---

<sup>7</sup>The operator  $\Delta$  corresponds to a curve  $t \mapsto [u_1(t) : u_2(t)]$ ,  $\mathbb{R} \rightarrow \mathbb{R}P^1$  in projective line defined by the solutions of equation  $\Delta u = 0$ .

Using formulae (35) we come to the following canonical groupoid  $C_{\mathbb{R}}$  on the line:

$$C_{\mathbb{R}} = \{\text{Groupoid of arrows } \gamma \xrightarrow{\mathbf{X}} \gamma' \text{ such that } \Delta(\gamma') = \Delta(\gamma), \text{ i.e. } U_{\gamma'} = U_{\gamma}\} = \\ = \{\text{Groupoid of arrows } \gamma \xrightarrow{\mathbf{X}} \gamma' \text{ such that } \operatorname{div}_{\gamma} \mathbf{X} + \frac{1}{2} \mathbf{X}^2 = 0\},$$

where  $\Delta(\gamma)$  is the Sturm-Liouville operator (52). It depends on the orbit of connection  $\gamma$ , the class  $[\gamma]$ .

Analyse the equation  $\operatorname{div} \mathbf{X} + \frac{1}{2} \mathbf{X}^2 = 0$  defining the canonical groupoid  $C_{\mathbb{R}}$  and compare it with the cocycle related with the operator.

If covector field equals to  $\gamma' - \gamma = a(x)dx$ , then the vector density equals to  $S_{\mathbb{R}}(a(x)dx) = a(x)|D(x)|^2 \partial_x$ . Hence  $\mathbf{X}^2 = a^2(x)|D(x)|^2$  and  $\operatorname{div} \mathbf{X} = (a_x + \gamma a)|D(x)|^2$ . We come to the equation:

$$\operatorname{div} \mathbf{X} + \frac{1}{2} \mathbf{X}^2 = \left( a_x + \gamma a + \frac{1}{2} a^2 \right) |D(x)|^2 = 0.$$

Solve this differential equation. Choose coordinate such that  $\gamma$  vanishes in this coordinate. Then

$$\mathbf{X} = \frac{2dx}{C+x}, \quad \text{where } C \text{ is a constant.} \quad (53)$$

On the other hand analyze the action of diffeomorphisms on the connection  $\gamma$  and the Sturm-Liouville operator (52). Let  $f = f(x)$  be a diffeomorphism of  $\mathbb{R}$ . (We consider compactified  $\mathbb{R} \sim S^1$  and diffeomorphisms preserving orientation.) The new connection  $\gamma^{(f)}$  equals to  $y_x (\gamma|_{y(x)} + (\log x_y)_x) dx$  and the covector field  $\gamma^{(f)} - \gamma$  equals to

$$\mathbf{X}^{(f)} = \gamma^{(f)} - \gamma = \gamma(y(x))dy + (\log x_y)_y dy - \gamma(x)dx.$$

We come to cocycle on group of diffeomorphisms:

$$c_{\gamma}(f) = \Delta^f(\gamma) - \Delta(\gamma) = \Delta(\gamma^{(f)}) - \Delta(\gamma) = \frac{1}{4} (U_{\gamma^{(f)}} - U_{\gamma}) = \\ -\frac{1}{4} \left( \operatorname{div} \mathbf{X}^{(f)} + \frac{1}{2} (\mathbf{X}^{(f)})^2 \right). \quad (54)$$

In coordinate such that  $\gamma = 0$ ,  $\mathbf{X}^{(f)} = (\log x_y)_y dy$ . Combining with a solution (53) we come to equation  $(\log x_y)_x = \frac{2}{C+x}$ . Solving this equation we see that

$$\operatorname{div} \mathbf{X}^{(f)} + \frac{1}{2} (\mathbf{X}^{(f)})^2 = 0 \Leftrightarrow y = \frac{ax+b}{cx+d} \text{ is a projective transformation.}$$

The cocycle (54) is coboundary in the space of second order operators and it is a non-trivial cocycle in the space of densities of the weight 2. This cocycle vanishes

on projective transformations. This is well-known cocycle related with Schwarzian derivative (see the book [18] and citations there):

$$\begin{aligned} c_{\gamma}(f) &= \Delta^f(\gamma) - \Delta(\gamma) = \Delta(\gamma^f) - \Delta(\gamma) \\ &= \frac{1}{2} (U_{\gamma^f} - U_{\gamma}) = -\frac{1}{4} \left( \operatorname{div} \mathbf{X}^{(f)} + \frac{1}{2} \left( \mathbf{X}^{(f)} \right)^2 \right) \\ &= -\frac{1}{4} (U_{\gamma}(y)|D(y)|^2 + \mathcal{S}(x(y))|D(y)|^2 - U_{\gamma}(x)|D(x)|^2), \end{aligned}$$

where

$$\mathcal{S}(x(y)) = \frac{x_{yyy}}{x_y} - \frac{3}{2} \left( \frac{x_{yy}}{x_y} \right)^2.$$

is *Schwarzian* of the transformation  $x = x(y)$ . If  $\gamma = 0$  in coordinate  $x$  then  $c(f) = \mathcal{S}(x(y))|D(y)|^2$ .

#### 4.7. Invariant densities on 1|1-codimension submanifolds in an odd symplectic supermanifold and mean curvature

In the previous examples we considered second order operators which depend on a class of connections on volume forms. In particular we considered for odd symplectic supermanifold the canonical class of Darboux flat connections (see the Proposition 5) and with use of this class redefined the canonical operator (48).

Now we consider an example of geometrical constructions which depend on second order derivatives and on a class of *Darboux flat affine connections*.

Let  $E$  be an odd symplectic supermanifold equipped with volume form  $\rho$ . Let  $C$  be a non-degenerate submanifold of codimension (1|1) in  $E$  (induced Poisson structure on  $C$  is non-degenerate). We call such a submanifold "hypersurface".

For an arbitrary affine connection  $\nabla$  and arbitrary vector field  $\Psi$  consider the following object:

$$A(\nabla, \Psi) = \operatorname{Tr}(\Pi(\nabla\Psi)) - \operatorname{div}_{\rho}\Psi, \quad (55)$$

where  $\Pi$  is the projector on (1|1)-dimensional planes which are symplectoorthogonal to hypersurface  $C$  at points of this hypersurface. (We define these objects in a vicinity of  $C$ .)

Let vector field  $\Psi$  be symplectoorthogonal to the hypersurface  $C$  at points of  $C$ . Then one can see that at points of  $C$

$$A(\nabla, f\Psi) = fA(\nabla, \Psi) \quad (56)$$

for an arbitrary function  $f$ . Thus  $A(\nabla, \Psi)$  is well-defined on  $C$  in the case if  $\Psi$  is a vector field defined only at  $C$  and  $\Psi$  is symplectoorthogonal to  $C$ . This object is interesting since it is related with canonical vector valued half-density and canonical scalar half-density on the manifold  $C$  (see for detail [11].)

Namely let  $\Psi$  be a vector field on hypersurface  $C$  symplectoorthogonal to  $C$ . From now on we suppose that it also obeys to following additional conditions

- it is an odd vector field  $p(\Psi = \Psi^A \partial_A) = p(\Psi^A) + p(A) = 1$ ,
- it is non-degenerate, i.e. at least one of components is not-nilpotent,
- $\omega(\Psi, \Psi) = 0$ , where  $\omega$  is the symplectic form in  $E$ , defining its symplectic structure.

One can see that these conditions uniquely define vector field  $\Psi$  at every point of  $C$  up to a multiplier function. Consider now a following volume form  $\rho_\Psi$  on  $C$ : Let  $\mathbf{H}$  be an even vector field on hypersurface  $C$  such that it is symplectoorthogonal to  $C$  and  $\omega(\mathbf{H}, \Psi) = 1$ . Define an half-density  $\rho_\Psi$  by the condition that for an arbitrary basis  $\{\mathbf{e}_1, \dots, \mathbf{e}_{n-1}; \mathbf{f}_1, \dots, \mathbf{f}_{n-1}\}$  of surface  $C$

$$\rho_\Psi(\mathbf{e}_1, \dots, \mathbf{e}_{n-1}; \mathbf{f}_1, \dots, \mathbf{f}_{n-1}) = \rho(\mathbf{e}_1, \dots, \mathbf{e}_{n-1}, \mathbf{H}; \mathbf{f}_1, \dots, \mathbf{f}_{n-1}, \Psi).$$

(Here  $\mathbf{e}_1, \dots, \mathbf{e}_{n-1}$  are even basis vectors and  $\mathbf{f}_1, \dots, \mathbf{f}_{n-1}$  are odd basis vectors.) Using formula (38) for Berezinian and relation (56) one can see that for an arbitrary function  $f$ ,

$$\rho_{f\Psi} = \frac{\rho_\Psi}{f^2}.$$

We come to conclusion that vector valued half-density  $\Psi\sqrt{\rho_\Psi}$  is well-defined odd half-density on hypersurface  $C$ . Applying equation (55) we come to well-defined half-density on hypersurface  $C$ :  $\mathbf{s}_C(\nabla) = A(\nabla, \Psi)\sqrt{\rho_\Psi}$ . This half-density depends only on affine connection  $\nabla$ .

We say that affine supersymmetric connection  $\nabla$  on  $E$  with Christoffel symbols  $\Gamma_{AB}^C$  is Darboux flat affine if there exist Darboux coordinates  $z^A = (x^a, \theta_b)$  such that in these Darboux coordinates the Chrsitoffel symbols of the connection vanish:  $\nabla_A \partial_B = 0$ . (Darboux flat affine connection on  $E$  induces Darboux flat connection  $\gamma$ :  $\gamma_A = (-1)^B \Gamma_{AB}^B$  on volume forms.)

**Proposition 6** *The half-density  $\mathbf{s}_C(\nabla)$  does not depend on a connection in the class of Darboux flat connections:  $\mathbf{s}_C(\nabla) = \mathbf{s}_C(\nabla')$  for two arbitrary Darboux flat affine onnections  $\nabla$  and  $\nabla'$ .*

This statement in not explicit way in fact was used in the work [11] where the half-density was constructed in Darboux coordinates.

The Proposition implies the existence of canonical half-density on hyperLsurfaces in odd symplectic supermanifold. This semidensity was first calculated straightforwardly in [13].

On one hand the invariant semindensity in odd symplectic supermanifold is an analogue of Poincare-Cartan integral invariants. On the other hand the constructions above are related with mean curvature of hypersurfaces (surfaces of codimension 1) in the even Riemannian case: if  $C$  is surface of codimension  $(1|0)$  in Riemannian manifold  $M$  then one can consider the canonical Levi-Civita connection and canonical volume form. Applying constructions above we come to mean curvature.

In the odd symplectic case there is no preferred affine connection compatible with the symplectic structure(see for detail [11]).

**Acknowledgment** We are grateful to O.Little for useful discussions which were helpful for understanding the relation of formula (55) with invariant half-density. Khudaverdian is very happy to acknowledge the wonderful environment of the MPI which facilitates the working on this paper.

## References

- [1] I. A. Batalin, K. Bering, J. Math. Phys. **49**, 033515 (2008).
- [2] I. A. Batalin, K. Bering, J. Math. Phys. **50**, 073504 (2009).
- [3] I. A. Batalin, G. A. Vilkovisky, Phys. Lett. B **102**, 27 (1981).
- [4] I. A. Batalin, G. A. Vilkovisky, Nucl.Phys. B **234**, 106 (1984).
- [5] F. A. Berezin, *Introduction in superanalysis*. Expanded translation from the Russian: Introduction to analysis with anticommuting variables. A. A. Kirillov (Editor), Moscow State University, Moscow (1983). Translation edited by D. A. Leites, D. Reidel, Dordrecht (1987).
- [6] K. Bering, J. Math. Phys. **47**, 123513 (2006).
- [7] P. Cohen, Y. Manin, D. Zagier. *Automorphic pseudodifferential operators. Algebraic aspects of Integrable systems.*, A. S. Fokas and I. M. Gelfand (Editors). Boston, Burkhauser, (1997), pp.17-47.
- [8] C. Duval, V. Yu. Ovisenko, Advances in Mathematics **132**, 316 (1997).
- [9] N. J. Hitchin, G. B. Segal and R. S. Ward *Integrable systems*. The Clarendon Press, Oxford Univ. Press, New-York (1999).
- [10] O. M. (H. M.) Khudaverdian, J. Math. Phys. **32**, 1934 (1991).
- [11] O. M. (H. M.) Khudaverdian, Comm. Math. Phys. **198**, 591 (1998).
- [12] H. M. Khudaverdian, Comm. Math. Phys. **247**, 353 (2004).
- [13] O. M. (H. M.) Khudaverdian, R. L. Mkrtchian, Lett. Math. Phys. **18**, 229 (1989).
- [14] H. M. Khudaverdian, T. Voronov, Lett. Math. Phys. **62**, 127 (2002).
- [15] H. M. Khudaverdian, T. Voronov, In Amer. Math. Soc. Transl.(2), Vol.212, 179 (2004).

- [16] P. Lecomte *Classification projective des espaces d'operateurs differentiels agissant sur les densities.* C. R. Acad. Sci. Paris.–Ser.1 Math. (1999), **328**. 4, pp.287–290.
- [17] D. A. Leites, The theory of Supermanifolds. Karelskij Filial AN SSSR (in Russian) (1983). Seminar on Supermanifolds, D. Leites (Editor). Reports of Stockholm University, 1986 V1990. V. 1 V35. ca 2000 pp.
- [18] V. Ovsienko, S. Tabachnikov *Projective Differential Geometry Old and New From Schwarzian Derivative to the Cohomology of Diffeomorphism Groups.* Cambridge University Press (2005).
- [19] A. S. Schwarz, Comm. Math. Phys. **155**, 249 (1993).
- [20] T. Voronov *Geometric integration theory on supermanifolds.* Sov. Sci. Rev. C, Math. **9**, 1 (1992).

# Quantum superpositional beam-splitter for a two-bunch atom interferometer

Lilit A. Hovhannisyan, Gevorg Muradyan, Atom Zh. Muradyan  
*Department of Physics, Yerevan State University*  
*1 Alex Manoogian Street, 0025 Yerevan, Armenia*

## Abstract

The problem of Kapitza - Dirac diffraction is solved in Raman-Nath approximation without imitations on resonance detuning. A formula for the scattering amplitude in a definite integral form is obtained. It shows that in case of initial superposition state of discrete Gaussian form the scattering spectrum has a new regularity, more usable for the atomic optics.

## 1. Introduction

Interaction of atoms with electromagnetic field has a double nature: it changes the population of energy levels and a momentum exchange takes place between the field and the atom, as a result of which the speed of atoms changes [1]. The mean power, which has an effect on the atom, has a resonance nature and changes the sign when crossing the resonance [2].

The problem of motion of scattering atoms in the field of counterpropagating waves, attracts a constant attention in atomic optics and atomic interferometry [3,4]. The mechanism of atom scattering in this case is the re-emission of photons of one wave into the other counterpropagating wave, when due to each reemitted photon the atom acquires recoil momentum  $2\hbar k$ , where  $k$  -is the wave vector [5,6]. As an unknown for each process of scattering, stand the scattering probability amplitudes  $a_n$ , corresponding to the number  $n$  of the re-emitted photons for  $t$  interaction time [7]. Analytical results for the scattering amplitudes, outside of Bragg regime, is possible to obtain only for short times of interaction, when the operator of kinetic energy of the atom can be neglected. This is mathematically equivalent to the Raman-Nath approximation. By this approximation the scattering amplitude with an accuracy of a phase factor are given by the  $n$ -order Bessel function

$$a_m(t) = J_m(\Omega_{Rabi} t), \quad (1)$$

where the argument is a product of the Rabi frequency of the optical transition between the energy levels of the atom during interaction with the counterpropagating waves field [8].

The characteristic form of the temporal development of the diffraction of atomic wave according to the formula (1) for high Rabi frequencies is shown in Fig.1. The development is described by two characteristics: first, the momentum spectrum is symmetrical and monotonic and second, the maximum scattering

amplitudes always remain grouped on the boundaries of distribution. For later discussion is important that formula (1) nevertheless is related to the case of zero or large resonance detuning  $\Delta = \omega - \omega_0$ , where  $\omega$  is the field frequency and  $\omega_0$  is the atomic transition frequency. In the presented paper the expression for scattering amplitude, derived without limitations for  $\Delta$ , will have a form of a definite integral, which in the limit of small and large  $\Delta$  passes into a Bessel function. Thus it can be viewed as the generalized form of a Bessel function.

Detailed comparison with formula (1) shows, that differences have quantitative nature only if the atom before interaction has a definite momentum. But if the moving atom is in the superposition state of many momentum states the evolution of atom acquires a qualitatively new content compared to the case of zero or asymptotically large detunings. In particular a periodic oscillillation of atomic beam direction from the initial one is possible too.

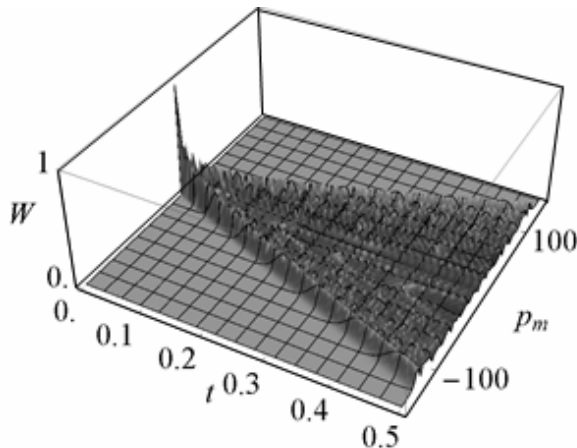


Figure 1: Temporal evolution of the atomic diffraction probability in the field of two counterpropagating optical waves, in case of the high intensitiestransitions.

## 2. Scattering amplitudes

The two-level atom interacts with the field of counterpropaating waves. The electric field is

$$E(z,t) = E_1(t)e^{i(kz-\omega t)} + E_2(t)e^{-i(kz-\omega t)} + c.c, \quad (2)$$

where  $k = \omega/c$ ,  $z$  is the atomic center of mass coordinate and for amplitudes  $E_1(t)$  и  $E_2(t)$  is taken a simple law of instantaneous turn-on. Limiting with dipole approximation, for the interacting atom Hamiltonian we will have

$$\hat{H} = -\frac{\hbar^2}{2M} \frac{\partial^2}{\partial z^2} + \hat{H}_0 - \hat{d} E(z, t), \quad (3)$$

where  $\hat{H}_0$  is the Hamiltonian of free and immovable atom,  $M$  is atomic mass, and  $d$  – operator of dipole moment. The atomic wavefunction can be written in the following form:

$$\psi(z, \mathbf{r}, t) = a(z, t) \psi_1(\mathbf{r}) e^{-i \frac{\epsilon_1 t}{\hbar}} + b(z, t) \psi_2(\mathbf{r}) e^{-i \frac{\epsilon_2 t}{\hbar} - i \Delta t}, \quad (4)$$

where  $a(z, t)$  and  $b(z, t)$  are the sought probability amplitudes of the atom being in ground and excited states, respectively,  $\epsilon_1$ ,  $\epsilon_2$  and  $\psi_1(\mathbf{r}), \psi_2(\mathbf{r})$  are eigenvalues and eigenfunctions of the free atoms Hamiltonian,  $\mathbf{r}$  – the radius-vector of optical electron relative to the center of mass.

The Raman – Nath approximation assumes that the atomic displacement during interaction is considerably smaller than the light wavelength. Hence it proves to be possible to neglect the kinetic energy operator, after which equation for the probability amplitudes substantially simplifies and takes the following form:

$$i\hbar \frac{\partial}{\partial t} a(z, t) = -d \left( E_1^* e^{-i k z} + E_2^* e^{i k z} \right) b(z, t), \quad (5)$$

$$\left( i\hbar \frac{\partial}{\partial t} - \hbar \Delta \right) b(z, t) = -d^* \left( E_1 e^{i k z} + E_2 e^{-i k z} \right) a(z, t). \quad (6)$$

Since the right side coefficient of equation (5) does not depend on time, the equation for the amplitude of the ground state  $a(z, t)$  can be obtained from it by simply acting from the left side with operator  $i\hbar \frac{\partial}{\partial t} - \hbar \Delta$ , and using equation (6).

This will bring to

$$\left( \frac{\partial}{\partial t} + i\Delta \right) \frac{\partial}{\partial t} a(z, t) = -\frac{|d|^2}{\hbar^2} \left( E_1^2 + E_2^2 + 2 E_1 E_2 \cos(2kz) \right) a(z, t). \quad (7)$$

The solution of this equation we can present in the form of Fourier- transformation in terms of dimensionless space coordinate  $2kz$ :

$$a(z, t) = \sum_{n=-\infty}^{\infty} a_n(t) e^{i n 2kz}, \quad (8)$$

where the unknown amplitude  $a_n(t)$  will be sought in the form of a definite integral

$$a_n(t) = \frac{1}{\pi} \int_0^\pi e^{i \lambda(\varphi) t} \cos(n\varphi) d\varphi \quad (9)$$

with unknown function  $\lambda(\varphi)$ . Substitution of (8) and (9) into (7) gives two possible expressions for  $\lambda(\varphi)$ :

$$\lambda(\varphi) = -i \frac{\Delta}{2} \pm i \frac{|\Delta|}{2} \sqrt{1 + \xi(\varphi)}, \quad (10)$$

where  $\xi(\varphi) \equiv \xi_1 + \xi_2 + 2\sqrt{\xi_1 \xi_2} \cos(\varphi)$  and  $\xi_{1,2} = 4d^2 E_{1,2}^2 / \hbar^2 \Delta^2$ .

The general solution, as usually, is presented as a superposition of two linearly independent solutions

$$a_n(t) = C_1 \int_0^\pi \exp(i\lambda_1(\varphi)t) \cos(n\varphi) d\varphi + C_2 \int_0^\pi \exp(i\lambda_2(\varphi)t) \cos(n\varphi) d\varphi. \quad (11)$$

The coefficients  $C_1$  and  $C_2$  are determined from initial conditions. If, for example, before interaction the atom resided on the ground state and was in rest, then

$$C_1 = \frac{1}{2} + \frac{\text{sign}[\Delta]}{4\sqrt{1+\xi}} \left( F\left(\frac{4\sqrt{\xi_1\xi_2}}{1+\xi}\right) \right)^{-1}, \quad C_2 = \frac{1}{2} - \frac{\text{sign}[\Delta]}{4\sqrt{1+\xi}} \left( F\left(\frac{4\sqrt{\xi_1\xi_2}}{1+\xi}\right) \right)^{-1}, \quad (12)$$

where  $F(x)$  is the elliptic integral of the first kind. The obtained solution (11) with coefficients (12) and integrands (10) is the generalization of known formula (1) in the case of arbitrary resonance detuning.

### 3. Numerical calculations

As shows the more detailed analysis of the situation, the biggest differences from the Bessel regularities are obtained, when the initial state of the atom is a superpositional one. For example, when at the beginning it has the following discrete Gaussian distribution [9]:

$$a(z, t=0) = \sum_{n=-\infty}^{\infty} s_n e^{in2kz}, \quad (13)$$

$$s_n = \frac{1}{\sqrt{\pi}} e^{i\alpha n} \frac{1}{\sqrt[4]{\sigma}} e^{-i\alpha v - \frac{(n-v)^2}{2\sigma}}, \quad (14)$$

where  $s$  is the distribution FWHM and  $\alpha$  is the initial phase of each scattering component  $n = 0, \pm 1, \pm 2, \dots$ . Then for the scattering amplitudes instead of (11) we will have the following, more general expression

$$\begin{aligned} a_n(t) &= \frac{1}{\sqrt{\pi}} e^{i\alpha n} \frac{1}{\sqrt[4]{\sigma}} \\ &\left( C_1 \int_0^\pi \exp\left(-i\frac{\Delta t}{2} + i\frac{|\Delta|t}{2}\sqrt{1+\xi(\varphi)}\right) \sum_{v=-\infty}^{\infty} \exp\left(-i\alpha v - \frac{(n-v)^2}{2\sigma}\right) \cos(v\varphi) d\varphi + (15) \right. \\ &\left. + C_2 \int_0^\pi \exp\left(-i\frac{\Delta t}{2} - i\frac{|\Delta|t}{2}\sqrt{1+\xi(\varphi)}\right) \sum_{v=-\infty}^{\infty} \exp\left(-i\alpha v - \frac{(n-v)^2}{2\sigma}\right) \cos(v\varphi) d\varphi \right), \end{aligned}$$

with the same coefficients  $C_1, C_2$  that appear in (12).

For illustrating the new regularities, we will limit the discussion to the cases  $\alpha=0$  and  $\alpha=\pi/2$ . In the case  $\alpha=0$ , for example was obtained<sup>9</sup> that if we proceed from the Bessel approximation for the scattering amplitudes, then initial Gaussian distribution in the course of interaction monotonically increases its width and only. Calculations according to the formula (15) give a qualitatively different result: the distributions are split into two identical peaks, which preserving the form, symmetrically move away from the distribution center. Fig.2 illustrates this

picture at  $t = 18 \times 10^6$  (here and afterwards  $t$  is given in  $\Delta^{-1}$  units).

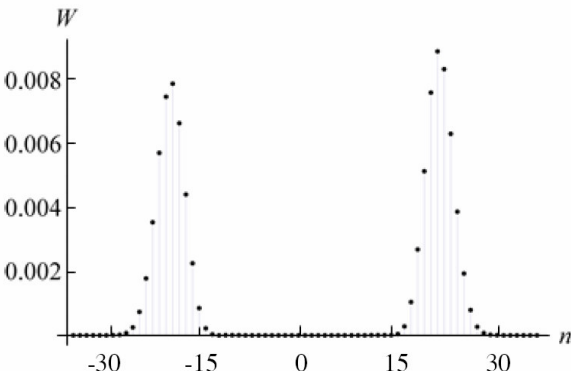


Figure 2: Picture of the momentum distribution for a moving atom scattering in the field of counterpropagating waves at  $t = 59 \times 10^7$ . Initial distribution had a Gaussian form (14) with the phase parameter  $\alpha = 0$ , with half-width  $\sigma = 10$ .

Qualitative differences are present also for  $\alpha = \pi/2$ . Within the framework of the Bessel approximation the initial Gaussian distribution is monotonically moving to one side with a weak change of the form. Formula (15) gives a new, oscillatory behavior: in the beginning the Gaussian peak, as in Bessel approximation case, is moving in one direction, but soon in symmetrically opposite direction gradually appears a new peak, the growth of which is accompanied by the decrease of the first one, before it totally disappears as in Fig.3. Subsequently the reverse process occurs, and two peaks, oscillating in reversed phase, monotonically are moving away from the distribution center (Fig.4(a) and Fig.4(b)). It is evident that the atomic wave packet evolution preserves the Gaussian form.

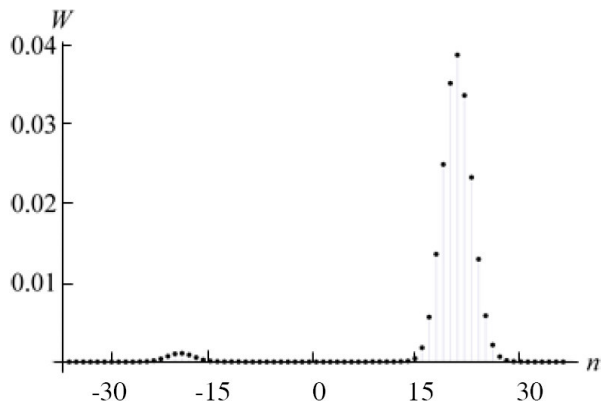


Figure 3: Appearance of a new peak in the momentum distribution of atom, when scattering in the field of intense counterpropagating waves for  $\alpha = \pi/2$ ,  $\sigma = 10$ ,  $t = 6 \times 10^7$ .

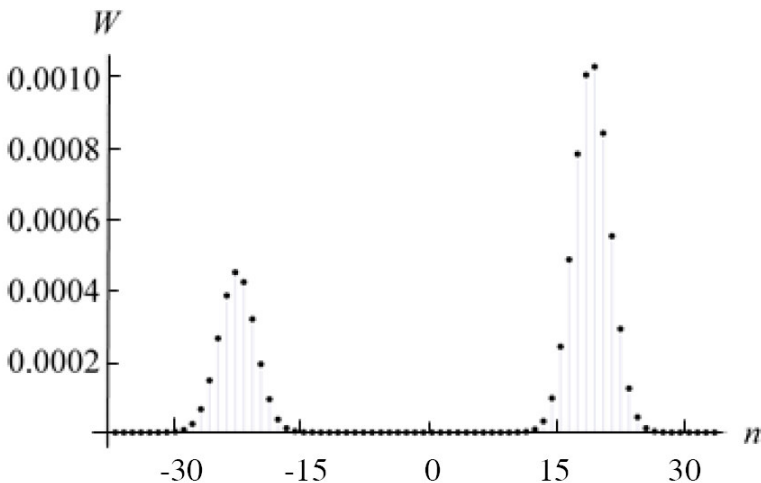


Figure 4a: Appearance of a new peak in the momentum distribution of atom, when scattering in the field of intense counterpropagating waves for  $\alpha=\pi/2$ ,  $\sigma=10$ ,  $t=6.07\times 10^7$ .

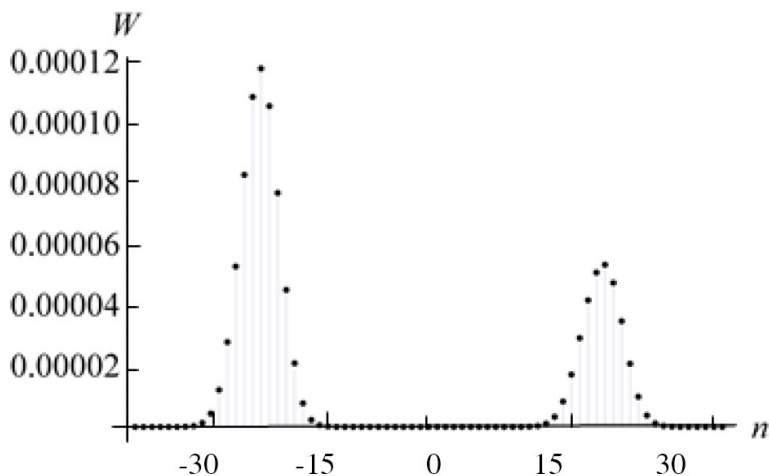


Figure 4b: Appearance of a new peak in the momentum distribution of atom, when scattering in the field of intense counterpropagating waves  $\alpha=\pi/2$ ,  $\sigma=10$ ,  $t=6.12\times 10^7$ .

Not less interesting, especially for applied optics, appears the case  $\alpha=\pi$ . In this case it proves to be possible to obtain a table-shaped form of momentum distribution, which is the base form for high resolution spectroscopy [10]. Such a distribution is shown in Fig.5.

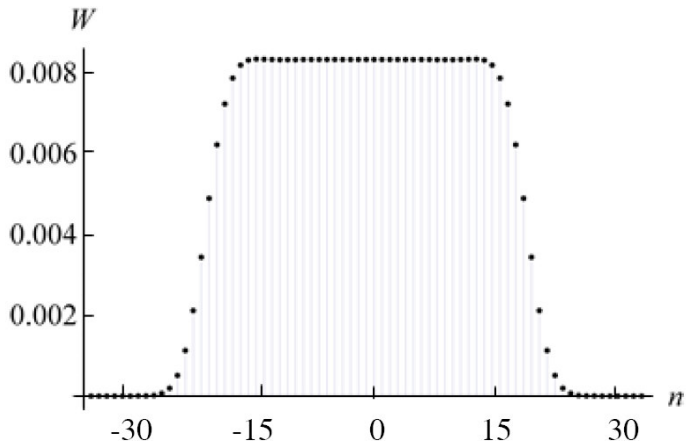


Figure 5: Form “of the table” of the momentum distribution for a moving atom in the Raman - Nath approximation.  $\alpha = \pi$ ,  $\sigma = 10$ ,  $t = 17.8 \times 10^6$ .

#### 4. Conclusion

The problem of resonance Kapitza-Dirac scattering of atom in the laser field of counterpropagating waves is solved in Raman-Nath approximation without the limitations put on the resonance detuning. The obtained formulas somewhat generalize the known Bessel functions expression for the scattering amplitudes. More valuable is the fact that the refinement of formula allows to obtain table-like momentum distribution forms, desirable in applied atomic optics and interferometry.

#### References

- [1] S. Stenholm, *Basics of laser spectroscopy* (Mir, Moscow, 1987); V.G. Minogin, V.S. Letokhov, *Pressure of laser radiation on the atoms* (Nauka, Moscow, 1986); A.P. Kazantsev, G.I. Surdutovich, V.P. Yakovlev, *Mechanical action of light on atoms* (Nauka, Moscow, 1991).
- [2] G.A. Askaryan, JETP **42**, 1567 (1962).
- [3] E. Arimodo, H. Lew, T. Oka, Phys. Rev. Lett. **43**, 753 (1979); W.D. Phillips, J.V. Prodan, H.J. Metcalf, J. Opt. Soc. Am. B **2**, 1751 (1985).
- [4] H.J. Metcalf, P. van der Straten, *Laser cooling and trapping* (Springer, New York, 1999); Ch.J. Foot, *Atomic Physics* (Oxford University Press, New York, 2005); Y. Castin, arXiv:cond-mat/0105058 (2001).
- [5] J.K. Pachos, P.L. Knight, Phys. Rev. Lett. **91**, 107902 (2003); I. Bloch, Nature Physics **1**, 23 (2005); J.K. Chin, D.F. Miller, Y. Liu, C. Stan, W. Setiawan, C. Sanner, K. Xu, W. Ketterle, Phys. Rev. Lett., Nature **443**, 961 (2006); S.P. Papp, J.M. Pino, R.J. Wild, S. Ronen, C.E. Wieman, D.E. Jin, E.A. Cornell, Phys. Rev. Lett. **101**, 135301 (2008).

- [6] P. Berman, *Atom Interferometry* (Acad. Press, New York, 1997); A.D. Cronin, J. Schmiedmayer, D.E. Pritchard, arXiv:0712.3703 (2007); J.M. Hogen, D.M.S. Johnson, M.A. Kasevich, arXiv:0806:3261 (2008).
- [7] A.Zh. Muradyan, Proceedings of AN ARM. SSR, Physics **10**, 361 (1975).
- [8] V.M. Arutyunyan, A.Zh. Muradyan, Reports to AN ARM. SSR **60**, 275 (1975); R.J. Cook, A.F. Bernhardt, Phys. Rev. A **18**, 2533 (1978); P.J. Martin, P.L. Gould, B.J. Oldaker, A.H. Miklich, D.E. Pritchard, Phys.Rev.A **36**, 2495 (1987).
- [9] A.M. Ishkhanyan, Phys.Rev.A **61**, 063611 (2000).
- [10] J. Ye, S.T. Cundiff, *Femtosecond Optical Frequency Comb Technology* (Springer, New York, 2005).

# АДИАБАТИЧЕСКОЕ ОПИСАНИЕ КОЛЬЦЕОБРАЗНЫХ НАНОСТРУКТУР

Э.М. Казарян<sup>1</sup>, А.А. Саркисян<sup>1,2</sup>

<sup>1</sup>*Российско-Армянский (Славянский) университет  
0051 О.Эмина 123, Ереван, Армения*

<sup>2</sup>*Ереванский государственный университет,  
0025 А. Манукяна 1, Ереван, Армения*

В кратком обзоре представлена процедура адиабатического описания электронных состояний в квантовых системах с нетривиальной геометрией. На примере полупроводниковых наноструктур с кольцеобразной геометрией показано, что при малых значениях толщины квантового кольца характерные частоты радиального квантования настолько велики, по сравнению с частотами углового квантования, что систему можно рассматривать как совокупность быстрой и медленной подсистем. Последнее обстоятельство позволяет применить модель плоского ротора для описания электронных состояний в квантовом кольце. Если к тому же квантовое кольцо помещено в аксиальное магнитное поле, то возникают условия для проверки эффекта Ааронова-Бома для связанных состояний. Обсуждается также случай узкозонного квантового кольца из InSb с кейновским законом дисперсии электрона. Показано, что благодаря наличию непараболичности закона дисперсии носителей заряда меняется характер зависимости энергии электрона от величины потока магнитного поля пронизывающего квантовое кольцо.

## 1. Введение

Приближенные методы решения квантомеханических задач всегда являлись важной составной частью теоретического аппарата исследователей, изучающих особенности микромира, начиная с описания поведения нуклонов в ядрах и заканчивая сугубо прикладными проблемами микро- и наноэлектроники [1, 2]. На основе таких методов, как стационарная и нестационарная теория возмущений, вариационное приближение, адиабатическое приближение, метод канонических преобразований, метод осцилляторного представления и т.д., удается получить приближенные аналитические выражения, которые зачастую, несмотря на сравнительную простоту окончательных соотношений, хорошо согласуются с результатами численного моделирования и эксперимента [3–6]. Ясно, что наличие аналитических выражений для различных физических параметров, характеризующих квантовые системы, значительно упрощает процедуру анализа полученных результатов и их сравнение с данными эксперимента. Поэтому, наряду с мощным аппаратом численного решения различных уравнений квантовой механики, приближенные аналитические методы активно применяются для качественного анализа математических моделей [7, 8].

Классическим примером применения приближенного метода

стационарной теории возмущений, для описания квантовой системы, является проблема атома водорода в слабом электрическом поле (эффект Штарка) (см., напр. [1]). В рамках этой задачи была продемонстрирована сравнительная простота и эффективность аппарата теории возмущений, а также обоснована специфика штарковского расщепления уровней атома водорода, связанная со случайным вырождением невозмущенного спектра.

Вариационное приближение является эффективным инструментом описания квантовых систем, например, в тех случаях, когда поля являются промежуточными, или же невозможно осуществить разделение переменных в уравнении Шредингера (см. напр., [9–11]). Типичным примером такой ситуации является проблема связанных состояний частицы, находящейся в центрально-симметричном поле, когда на систему наложено внешнее магнитное поле [4, 9]. В этом случае угловая часть в уравнении Шредингера не отделяется, и поэтому, даже простейшая одночастичная проблема решается на основе численного моделирования [12] или же соответствующего подбора пробных вариационных волновых функций [13, 14].

С другой стороны, наряду с вышеперечисленными методами довольно эффективным механизмом описания квантовых систем является адиабатическое приближение. В предлагаемом кратком обзоре представлена схема адиабатического описания одночастичных состояний в квантовых системах со специфической геометрией. На примере кольцеобразных квантовых точек (КТ) выявляются особенности одноэлектронного спектра в случае малых толщин изучаемых структур. При этом предполагается, что выбранная геометрия рассматриваемых КТ позволяет эффективно пользоваться так называемым приближением “геометрической адиабатики”.

## 2. Адиабатическое приближение в стационарных задачах

Суть адиабатического подхода состоит в возможности представления рассматриваемой системы в виде совокупности двух подсистем: “медленной” и “быстрой”, когда описание поведения “медленной” подсистемы осуществляется путем усреднения по движению “быстрой” [7]. При этом, область применимости адиабатического подхода может определяться различными физическими факторами, например:

- существенное различие эффективных масс, характеризующих “быструю” и “медленную” подсистемы (приближение Борна–Опенгеймера);
- наличие существенной разницы в значениях поперечной и продольной эффективных масс частицы в кристалле (экзитон в анизотропном кристалле);
- наличие существенной диэлектрической анизотропии в исследуемом кристалле (экзитон в анизотропном кристалле);

- наличие сильных внешних полей (атом водорода в экстремально сильном магнитном поле).

В твердотельных задачах адиабатический метод широко применяется при описании свойств кристаллической решетки. Здесь в качестве “быстрой” подсистемы рассматриваются электроны, в усредненном эффективном поле которых движутся в окрестности узлов кристаллической решетки массивные ионы [15].

Интересная ситуация возникает в анизотропных кристаллах, когда имеется место существенная разница в значениях продольной и поперечной эффективных масс [16]. Например, если продольная эффективная масса намного больше поперечной, то медленное продольное движение усредняется по поперечному движению “быстрой” подсистемы.

Из задач астрофизики хорошо известно, что в таких системах, как квазары, водородоподобные атомы под воздействием экстремально сильных магнитных полей (порядка  $10^{12}$  Гс) принимают игольчатую форму. Последнее является следствием сильной локализации электрона вокруг ядра в перпендикулярной к полю плоскости. В такой системе можно предполагать, что в перпендикулярной к полю плоскости электрон совершает движение без влияния кулонова поля ядра. В направлении же поля совершается одномерное движение в усредненном по поперечному движению эффективном кулоновском поле [1].

### **3. Математический аппарат адиабатического приближения стационарных задач**

Одним из важных критериев применимости адиабатического описания поведения стационарной квантовой системы является не только возможность ее разбиения на подходящие “быструю” и “медленную” взаимодействующие между собой подсистемы, которые, соответственно, характеризуются большими и малыми частотами колебаний, но и возможность представления ее гамильтониана  $\hat{H}(x_1, x_2)$  в виде суммы гамильтониана быстрой подсистемы  $\hat{H}_1(x_1)$ , гамильтониана медленной подсистемы  $\hat{H}_2(x_2)$  и оператора взаимодействия подсистем  $\hat{V}(x_1, x_2)$ :

$$\hat{H}(x_1, x_2) = \hat{H}_1(x_1) + \hat{H}_2(x_2) + \hat{V}(x_1, x_2). \quad (1)$$

Уравнение Шредингера для волновой функции  $\Psi(x_1, x_2)$  такой квантовой системы с гамильтонианом  $\hat{H}(x_1, x_2)$  и энергией  $E$  имеет вид [7]:

$$(\hat{H}(x_1, x_2) - E)\Psi(x_1, x_2) = 0. \quad (2)$$

С учетом того, что характерные частоты 1-й подсистемы намного больше характерных частот 2-й, проблему вычисления энергетических уровней

совокупной системы приближенно можно свести к решению уравнений Шредингера для отдельных ее подсистем. Действительно, если зафиксировать координату “медленной” подсистемы  $x_2$ , то, обозначив через  $\Phi_{n_1}(x_1; x_2)$  и  $E_{n_1}(x_2)$  собственные функции и собственные значения оператора

$$\hat{H}_f(x_1; x_2) = \hat{H}_1(x_1) + \hat{V}(x_1, x_2), \quad (3)$$

придем к уравнению, определяющему  $\Phi_{n_1}(x_1; x_2)$  и  $E_{n_1}(x_2)$ :

$$[\hat{H}_1(x_1) + \hat{V}(x_1, x_2)]\Phi_{n_1}(x_1; x_2) = E_{n_1}(x_2)\Phi_{n_1}(x_1; x_2), \quad (4)$$

с дополнительными условиями ортогональности и нормировки собственных функций  $\Phi_{n_1}(x_1, x_2) \in F_{x_2}$ :  $L_2(\Omega(x_1))$  в виде внутреннего скалярного произведения

$$(\Phi_{n'_1}, \Phi_{n_1}) = \int \Phi_{n'_1}^*(x_1; x_2)\Phi_{n_1}(x_1; x_2)dx_1 = \delta_{n'_1, n_1}. \quad (5)$$

Далее, представим полную волновую функцию системы  $\Psi(x_1, x_2)$  в приближенном виде

$$\Psi(x_1, x_2) \approx \Phi_{n_1}(x_1; x_2)\chi_{n_1, n_2}(x_2). \quad (6)$$

С учетом (6) уравнение

$$\begin{aligned} & (\hat{H}_1(x_1) + \hat{V}(x_1, x_2) + \hat{H}_2(x_2))\Phi_{n_1}(x_1; x_2)\chi_{n_1, n_2}(x_2) = \\ & = E_{n_1, n_2}\Phi_{n_1}(x_1; x_2)\chi_{n_1, n_2}(x_2) \end{aligned} \quad (7)$$

после умножения обоих частей на  $\Phi_{n_1}^*(x_1; x_2)$  и интегрирования по координате  $x_1$ , приводится к так называемому грубому адиабатическому приближению

$$(\hat{H}_2(x_2) + E_{n_1}(x_2))\chi_{n_1, n_2}(x_2) = E_{n_1, n_2}\chi_{n_1, n_2}(x_2). \quad (8)$$

При этом, пренебрегают действием оператора  $\hat{H}_2(x_2)$  на переменную  $x_2$ , входящую в  $\Psi_{n_1}(x_1, x_2)$ , иначе говоря, предполагают, что имеет место приближенное равенство:

$$\hat{H}_2(x_2)\Phi_{n_1}(x_1, x_2)\chi_{n_1, n_2}(x_2) \approx \Phi_{n_1}(x_1, x_2)\hat{H}_2(x_2)\chi_{n_1, n_2}(x_2). \quad (9)$$

Из уравнения (9) следует, что собственные значения  $E_{n_1}(x_2)$ , так называемые термы или потенциальные кривые, играют роль эффективной потенциальной энергии для “медленной” подсистемы. Таким образом, задача сводится к решению соответствующих уравнений Шредингера для двух подсистем, связь между которыми устанавливается посредством энергии “быстрой” подсистемы, параметрически зависящей от координаты  $x_2$  “медленной” подсистемы. Решение уравнения (8), использующее разложение

терма  $E_{n_1}(x_2)$  в ряд Тейлора в окрестности точки устойчивого равновесия до квадратичных членов, соответствует приближению Борна-Опенгеймера [17].

Следует отметить, что адиабатическое приближение может оказаться исключительно эффективным инструментом для теоретического описания полупроводниковых КТ, обладающих нетривиальной геометрией. При этом, сама nanoструктура может диктовать условия применимости этого подхода в зависимости от соотношений различных геометрических масштабов локализации носителей заряда в конкретно изучаемых образцах. Таким образом, в КТ реализация условий адиабатического описания может быть обусловленной сугубо геометрическими особенностями изучаемых систем. Иными словами, в таких случаях можно говорить о реализации условий применимости “геометрической адиабатики”. Блестящей иллюстрацией применения “геометрической адиабатики” является задача приведенная в задачнике [8], в которой необходимо определить уровни энергии электрона в двумерной непроницаемой эллипсоидальной яме полуоси которой сильно отличаются друг от друга. С математической точки зрения эта задача сводится к решению уравнения Шредингера с потенциальным членом имеющим вид:

$$V(x, y) = \begin{cases} 0, & \frac{x^2}{a^2} + \frac{y^2}{b^2} \leq 1 \\ \infty, & \frac{x^2}{a^2} + \frac{y^2}{b^2} > 1 \end{cases}, \quad (10)$$

где  $a$  и  $b$  соответственно малая и большая полуоси эллипса. При наличии условия

$$b \gg a, \quad (11)$$

становится ясно, что “быстрым” является движение вдоль оси  $oX$ , а “медленным” – вдоль оси  $oY$ . Применяя схему представленную выше заметим, что движение вдоль  $oX$ , при фиксированном значении координаты  $y$ , имеет место в бесконечно глубокой яме шириной

$$a(y) = 2a\sqrt{1 - y^2/b^2}. \quad (12)$$

Таким образом, для волновой функции и энергетического спектра “быстрой” подсистемы можем записать:

$$\Phi_{n_1}(x, y) = \sqrt{\frac{2}{a(y)}} \sin \frac{\pi(n_1 + 1)(x + a(y)/2)}{a(y)}, \quad (13)$$

$$E_{n_1}(y) = \frac{\pi^2 \hbar^2 (n_1 + 1)^2}{2\mu a^2(y)}, \quad (14)$$

где  $\mu$  – масса электрона.

Учитывая соотношение (8) заключаем, что движение электрона вдоль оси  $oY$  определяется потенциалом

$$V(y) = \begin{cases} E_{n_1}(y) = \frac{\pi^2 \hbar^2 (n_1 + 1)^2}{8\mu a^2 (1 - y^2/b^2)}, & |y| < b, \\ \infty, & |y| > b. \end{cases} \quad (15)$$

Одномерное уравнение Шредингера с потенциалом (15) точно не решается. С другой стороны можно заметить, что для сравнительно низких уровней областю локализации электрона является центральная часть двумерной эллиптической квантовой ямы. Иначе говоря, имеет место условие  $|y| << b$ , благодаря которому потенциал (15) можно разложить в ряд Тейлора

$$V(y) \approx \frac{\pi^2 \hbar^2 (n_1 + 1)^2}{8\mu a^2} + \frac{\pi^2 \hbar^2 (n_1 + 1)^2}{8\mu a^2 b^2} y^2. \quad (16)$$

Для “медленной” подсистемы получается уравнение гармонического осциллятора с частотой

$$\omega_{n_1} = \frac{\pi \hbar (n_1 + 1)}{2\mu a b}. \quad (17)$$

Таким образом, для энергетического спектра и волновых функций системы окончательно можем записать

$$E_{n_1 n_2} = \frac{\pi^2 \hbar^2 (n_1 + 1)^2}{8\mu a^2} + \frac{\pi^2 \hbar^2 (n_1 + 1)^2}{8\mu a b} (n_2 + 1/2), \quad n_{1,2} = 0, 1, 2, \dots$$

$$\psi_{n_1, n_2}(x, y) = \left[ \frac{\exp[-y^2/(2y_0^2)]}{(\sqrt{\pi} y_0 2^{n_2} n_2!)^{1/2}} H_{n_2}\left(\frac{y}{y_0}\right) \right]$$

$$\times \left[ \sqrt{\frac{2}{a(y)}} \sin \frac{\pi(n_1 + 1)(x + a(y)/2)}{a(y)} \right], \quad (18)$$

где  $y_0 = \sqrt{\frac{2ab}{\pi(n_1 + 1)}}$ .

#### 4. Кольцеобразные квантовые точки

В последние годы удалось реализовать и теоретически исследовать слоистые и кольцеобразные КТ сферической и цилиндрической геометрий [18-24]. Исключительная важность изучения таких систем, в первую очередь, связана с возможностью экспериментальной проверки эффекта Ааронова-Бома для связанных состояний. Как известно, этот эффект, не имеющий классического аналога, по сути, свидетельствует об огромной роли векторного и магнитного потенциалов в квантовых системах. В рамках классической электродинамики  $\vec{A}$  и  $\varphi$  играют формальную роль и определяются с точностью до некоторого калибровочного преобразования.

Действительно, так как

$$\vec{E} = -\vec{\nabla}\varphi + \frac{1}{c} \frac{\partial \vec{A}}{\partial t} \quad (19)$$

и

$$\vec{H} = \text{rot } \vec{A} \quad (20)$$

то легко заметить, что, например, если вместо  $\vec{A}$  взять  $\vec{A}' = \vec{A} + \vec{\nabla}f$  (где  $f$  – некоторая скалярная функция), и с учетом равенства

$$\text{rot}(\vec{\nabla}f) = 0 \quad (21)$$

получаем

$$\text{rot } \vec{A} = \text{rot } \vec{A}' = \vec{H}. \quad (22)$$

С другой стороны, реально измеряемые физические величины в классической физике являются  $\vec{E}$  и  $\vec{H}$ , вследствие чего переход от  $\vec{A}$  к  $\vec{A}'$  никоим образом не повлияет на физическую картину классической системы. В случае квантового описания системы вместо обычного оператора импульса  $\vec{p}$  вводится оператор обобщенного импульса  $\vec{P}$ , определяемый соотношением

$$\vec{P} = \vec{p} - \frac{e}{c} \vec{A}, \quad (23)$$

где  $e$  – заряд частицы,  $c$  – скорость света. При этом оператор Гамильтона рассматриваемой системы приобретает следующий вид:

$$\hat{H} = \frac{1}{2\mu} \left( \vec{p} - \frac{e}{c} \vec{A} \right)^2 + U(\vec{r}). \quad (24)$$

Как следует из (24), векторный потенциал  $\vec{A}$  в явном виде фигурирует в выражении для  $\hat{H}$ . Следовательно, наличие электромагнитного потенциала отразится на виде волновой функции электрона, и при выборе определенной геометрии квантовой системы это обстоятельство может привести к наблюдаемому интерференционному эффекту. Впервые на это обстоятельство обратили внимание в 1949 году британские физики Эренберг и Сидай, которые подчеркнули принципиально важную роль электромагнитных потенциалов в квантовой физике. В дальнейшем Ааронов и Бом провели детальный анализ влияния этих потенциалов на поведение квантовых систем. В результате этого они пришли к выводу, что поведение квантовой частицы, непосредственно не находящейся в поле  $\vec{H}$ , но движущейся в области, где  $\vec{A} \neq 0$ , тем не менее, при определенных условиях претерпевает изменение, что может отразиться на ее энергетическом спектре. Таким образом, был продемонстрирован нелокальный характер взаимодействия заряженных квантовых частиц с электромагнитным полем. Наиболее наглядным образом это утверждение можно продемонстрировать на примере плоского ротора, находящегося в магнитном поле. Однако, прежде чем перейти к этой задаче, выведем ряд полезных соотношений.

Рассмотрим следующий интеграл от  $\vec{A}(\vec{r})$  по замкнутому контуру  $\Gamma$ :

$$\int_{\Gamma} \vec{A} d\vec{l} = I. \quad (25)$$

Согласно теореме Стокса,

$$\int_{\Gamma} \vec{A} d\vec{l} = \int_S \text{rot } \vec{A} d\vec{S} = \int_S \vec{H} d\vec{S} = \Phi, \quad (26)$$

где  $\Phi$  – поток магнитного поля сквозь площадь  $S$ . Если рассмотреть движение частицы по окружности радиуса  $R$  в магнитном поле  $\vec{H}$ , то, выбирая в качестве контура  $\Gamma$  именно эту окружность для потока  $\Phi$ , можем записать

$$\Phi = \pi R^2 H. \quad (27)$$

В том случае, когда поле сконцентрировано внутри площади контура  $\Gamma$  и при этом на самом контуре имеет место условие

$$\text{rot } \vec{A} = 0, \quad \vec{A} \neq 0, \quad (28)$$

можно утверждать, что заряженная частица не находится в магнитном поле. Однако, как будет показано ниже, наличие на контуре  $\Gamma$  ненулевого значения  $\vec{A}$  приводит к возникновению эффекта смещения уровней энергии плоско вращающейся частицы (плоского ротора) по сравнению со случаем отсутствия поля.

В 2000 году было сообщено об экспериментальной реализации полупроводниковых кольцеобразныхnanoструктур [18]. На основе метода самоорганизации удалось вырастить полупроводниковые квантовые кольца из *InGaAs*. При этом для одно- и двухэлектронных состояний исследовались основной, а также возбужденные уровни при наличии однородного магнитного поля, направленного перпендикулярно плоскости квантового кольца и меняющегося в пределах от 0 до 12Т. Обратимся теперь к теоретическому описанию поведения электрона в квантовом кольце при наличии однородного магнитного поля, направленного вдоль оси кольца OZ. Рассматривая кольцо малой толщины, будем предполагать, что по сравнению с осцилляциями вдоль радиуса кольца, вращение по окружности происходит значительно медленнее. Иначе говоря, радиальное квантование намного сильнее вращательного, вследствие чего в первом приближении можно считать, что электрон находится на основном радиальном уровне. С другой стороны, считая, что электрон локализован на середине кольца и вводя радиус

$$R = \frac{R_1 + R_2}{2}, \quad (29)$$

где  $R_{1(2)}$  – внутренний (внешний) радиус, задачу будем решать в рамках модели плоского ротора в магнитном поле. Выбирая вектор–потенциал в виде

$$\vec{A} = [\vec{H}\vec{r}]/2, \quad (30)$$

для гамильтониана системы можем записать

$$\hat{H} = -\frac{\hbar^2}{2I} \frac{d^2}{d\phi^2} + \frac{ieH}{2mc} \frac{d}{d\phi} + \frac{e^2 H^2}{8\mu^2 c^2} I, \quad (31)$$

где  $I = \mu R^2$  – момент инерции плоского ротора. Благодаря тому, что оператор проекции момента импульса

$$\hat{l}_z = -i\hbar \frac{\partial}{\partial z}, \quad (32)$$

коммутирует с гамильтонианом (31), а также учитывая цилиндрическую симметрию системы для угловой волновой функции, можем сразу записать:

$$\phi_m(\varphi) = \frac{1}{\sqrt{2\pi}} e^{im\varphi} (m = 0; \pm 1; \pm 2; \dots). \quad (33)$$

Подставляя (33) в (31) для вращательных уровней энергии, получим:

$$E_m = \frac{\hbar^2}{2I} \left( m - \frac{\Phi}{\Phi_0} \right)^2, \quad (34)$$

где  $\Phi = \pi R^2 H$  – введенный выше (см. формулу (54)) магнитный поток, пронизывающий рассматриваемое кольцо, величина  $\Phi_0 = \frac{2\pi\hbar c}{e}$ , входящая в выражение (34), называется квантом магнитного потока и определяет поток магнитного поля сквозь окружность, описываемую электроном в однородном магнитном поле. Согласно соотношению (34), с увеличением значения магнитного поля основной уровень системы сначала соответствует значению магнитного квантового числа  $m = 0$ , далее с ростом  $\vec{H}$  наимизшему уровню соответствует значение  $m = -1$ , после –  $m = -2$  и т.д. Таким образом, возникают так называемые ааронов-бомовские осцилляции основного состояния, представленные на рис.1. Отметим, что уровни, соответствующие отрицательным значениям магнитного квантового числа, сначала опускаются, а потом начинают подниматься, в то время как уровни с положительными  $m$  сразу начинают подниматься.

Как видим, кольцеобразные системы являются очень удобными системами, где непосредственно можно создать условия для проверки эффекта Ааронова-Бома в случае связанных состояний. Действительно, если рассмотреть ситуацию, когда окружность, прочерчиваемая электроном, охватывает поток магнитного поля, однако на самой окружности значение этого поля равно нулю, то уровни энергии такой системы будут определяться в точности формулой (34), так как эта она определяется не локальным значением магнитного поля в своей точке нахождения, а величиной потока магнитного поля пронизывающего квантовое кольцо. Ясно, что если отношение  $\frac{\Phi}{\Phi_0}$  будет целочисленным, то пронизывающий кольцо поток

никоим образом не перестроит спектр ротора, который соответствует

случаю отсутствия поля. Однако при иных значениях этого отношения энергетический спектр претерпевает изменения. Сказанное становится более наглядным, если учесть, что в процессе включения магнитного поля возникает вихревое электрическое поле, изменяющее энергию электрона.

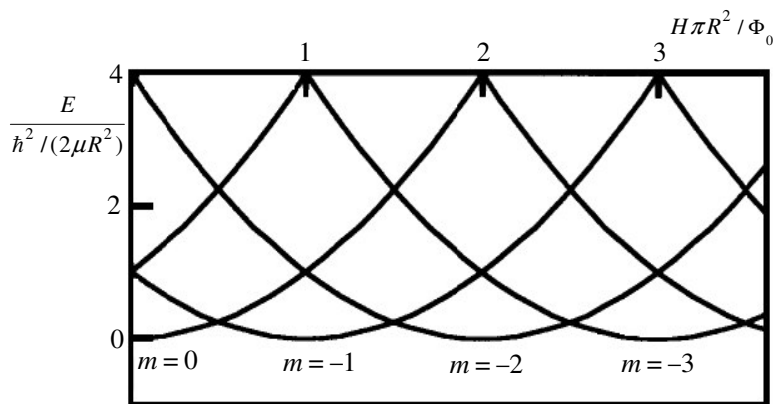


Рис. 1. Ааронов-бомовские осцилляции основного состояния.

Интересная ситуация возникает при описании поведения электрона в цилиндрических нанослоях с узкой запрещенной зоной. Обсудим этот случай на примере нанослоя из *InSb*, для которого зависимость энергии электрона от его импульса является непараболическим и определяется законом Кейна, по виду совпадающим с релятивистским

$$E = \sqrt{p^2 s^2 + \mu^2 s^4} - \mu s^2, \quad (35)$$

где  $s \sim 10^8$  см/с – так называемый кейновский параметр непараболичности. Естественно, ни о каком настоящем релятивизме речь не идет. Данный закон отражает тот факт, что в узкозонных полупроводниках, а для *InSb*  $E_g = 0.18$  эВ, электрон, находясь в зоне проводимости, чувствует влияние также валентной зоны.

В квантовой механике показано, что частицы для которых имеет место дисперсия типа (35), описываются в рамках уравнения Клейна-Гордона, которое в случае стационарных полей после ряда преобразований сводится к уравнению шредингеровского типа [8]. Если теперь рассматривать тонкий цилиндрический нанослой из *InSb*, то в приближении непроницаемых прямоугольных стенок поведение электрона в плоскости слоя снова можно описать с помощью модели плоского ротора радиуса  $R$ . Однако в этом случае нужно учесть, что дисперсия электрона будет отличаться от стандартной квадратичной и, в свою очередь, будет определяться согласно (35). Считая, что в направлении оси нанослоя электрон находится в прямоугольной, бесконечно глубокой яме ширины  $L$

для волновых функций углового движения, а также движения вдоль оси слоя,  $OZ$  можем записать [23]:

$$\phi_m(\varphi) = \frac{1}{\sqrt{2\pi}} e^{im\varphi}, \quad (36)$$

а также

$$\chi_n(z) = \sqrt{\frac{2}{L}} \begin{cases} \sin\left(\frac{\pi n}{L} z\right), & n = 2k \\ \cos\left(\frac{\pi n}{L} z\right), & n = 2k+1 \end{cases} \quad (k = 1, 2, 3, \dots), \quad (37)$$

где  $n$  – квантовое число, характеризующее состояния вдоль оси  $OZ$ . Воспользовавшись выражениями (36) и (37), можно на основе детальных расчетов вычислить энергию электрона в рассматриваемой системе [23]:

$$E_{m,n} = \sqrt{2\mu s^2 \left\{ \frac{\hbar^2}{2I} \left( m - \frac{\Phi}{\Phi_0} \right)^2 + \frac{\pi^2 \hbar^2 n^2}{2\mu L^2} \right\} + \mu^2 s^4}, \quad (38)$$

где второй член в подкоренном выражении определяет энергию, приходящуюся на направление  $OZ$ . Как видим, учет непараболичности закона дисперсии приводит к тому, что соотношение  $\left( m - \frac{\Phi}{\Phi_0} \right)^2$  в выражении для энергии электрона находится под корнем, в то время как в случае стандартной дисперсии реализуется прямая пропорциональность.

## 5. Заключение

Таким образом, использование адиабатического приближения может существенным образом облегчить описание физических свойств КТ с нетривиальной геометрией, позволяя получить аналитические выражения для энергетического спектра и волновых функций электрона как при отсутствии, так и при наличии внешних полей. Ясно, что наличие аналитических выражений для энергии и волновых функций носителей заряда позволяет провести расчеты конкретных физических характеристик изучаемых систем: коэффициентов межзонного и внутризонного поглощения, релаксационного времени и т.д. Последнее, в свою очередь, позволяет провести более детальный анализ физических характеристик изучаемых структур, что, в конечном счете, очень важно при конструировании (проектировании) полупроводниковых приборов нового поколения, в которых эти системы играют роль элементной базы.

## Литература

1. Л.Д. Ландау, Е.М. Лифшиц, *Квантовая механика, Нерелятивистская теория*, М.: Наука, 1989.
2. G. Bastard, *Wave mechanics applied to semiconductor heterostructures*, Halsted, New York, 1988.
3. Г. Вете, Э. Солпитер, *Квантовая механика атомов с одним и двумя электронами*. М.: Физматгиз, 1960.
4. P.A. Braun, Discrete semiclassical methods in the theory of Rydberg atoms in external fields. *Rev. Mod. Phys.* **65**, 115 (1993).
5. М. Динейхан, Г.В. Ефимов, Квантовая механика связанных состояний в осциллятором представлении. *ЭЧАЯ* **26**, 651 (1995).
6. R.G. Nazmitdinov. Hidden symmetries of two-electron quantum dots in a magnetic field. *Phys. Rev. B* **67**, 041305 (2003).
7. А.Б. Мигдал, В.П. Крайнов, *Приближенные методы квантовой механики*. М.: Наука, 1966.
8. В.М. Галицкий, Б.М. Карнаков, В.И. Коган, *Задачи по квантовой механике*. М.: Наука, 1981.
9. A. Corella-Madueno et al., Hydrogenic impurities in spherical quantum dots in a magnetic field. *J. Appl. Phys.* **90**, 2333 (2001).
10. A.Kh. Manaselyan, A.A. Kirakosyan. Effect of the dielectric-constant mismatch and magnetic field on the binding energy of hydrogenic impurities in a spherical quantum dot. *Physica E* **22**, 825 (2004).
11. K.G. Dvoyan, E.M. Kazaryan. Impurity states in a weakly prolate (oblate) ellipsoidal microcrystal placed in a magnetic field. *Phys. Status Sol. B* **288**, 695 (2001).
12. M.S. Kaschiev, S.I. Vinitsky, F.R. Vukajlovic, Hydrogen atom H and H<sup>2+</sup> in strong magnetic fields. *Phys. Rev. A* **22**, 557 (1980).
13. L.B. Zhao, P.C. Stancil, Hydrogen photoionazation cross sections for strong-field magnetic white dwarfs. *Phys. Rev. A* **74**, 055401 (2006).
14. C.V. Clark, K.T. Lu, A.F. Starace, *Effects of magnetic and electric fields on highly excited atoms. Progress on atomic spectroscopy Part C*. Ed. H.G. Beyer. New-York: Plenum. 1984. Р. 247-320.
15. А.И. Ансельм. *Введение в теорию полупроводников*. М.: Наука. 1978.
16. Ф. Бассани, Дж. Пастори Парравичини, *Электронные состояния и оптические переходы в твердых телах*. М.: Наука. 1982.
17. M. Born, R. Oppenheimer, Zur quantentheorie der moleküle. *Annalen der Physic.* **84**, 457 (1927).
18. A. Lorke et al. Spectroscopy of nanoscopic semiconductor rings. *Phys. Rev. Lett.* **22**, 860 (2000).
19. T. Chakraborty, P.Pietilainen, Electron-electron interaction and the persistent current in a quantum ring, *Phys. Rev. B* **50**, 8460 (1994).
20. V.A. Harutyunyan, K.S. Aramyan, H.Sh. Petrosyan, G.H. Demirjian, Optical transitions in spherical quantized layer under the presence of radial electrical field, *Physica E* **24**, 173 (2004).

21. V.A. Harutyunyan, E. M. Kazaryan, A. A. Kostanyan, H. A. Sarkisyan, Interband transitions in cylindrical layer quantum dot: influence of magnetic and electric fields, *Physica E* **36**, 114 (2007).
22. E.M. Kazaryan, A.A. Kostanyan, H.A. Sarkisyan, Interband transitions in a spherical quantum layer in the presence of an electric field: spherical rotator model, *Journal of Contemporary Physics* **42**, 145 (2007).
23. M. Zuhair, A.Kh. Manaselyan, H.A. Sarkisyan, Magneto- and electroabsorption in narrow-gap InSb cylindrical layer quantum dot, *Physica E* **41**, 1583 (2009).
24. A.K. Atayan, E.M. Kazaryan, A.V. Meliksetyan, H.A. Sarkisyan, Interband magnetoabsorption in cylindrical quantum layer with Smorodinsky-Winternitz confinement potential, *Journal of Computational and Theoretical Nanoscience* **7**, N6 (2010).

# Pulsed "three-photon" light

T. V. Gevorgyan<sup>1</sup>, G. Yu. Kryuchkyan<sup>1,2</sup>

<sup>1</sup>*Institute for Physical Research, National Academy of Sciences  
Ashtarak-2, 0203, Armenia*

<sup>2</sup>*Department of Physics, Yerevan State University  
1 Alex Manoogian Street, 0025 Yerevan, Armenia*

## Abstract

Generating multi-photon entangled states is a primary task for applications of quantum information processing. We investigate production of photon-triplet in a regime of light amplification in second-order nonlinear media under action of a pulsed laser beam. For this goal the process of cascaded three-photon splitting in an optical cavity driven by a sequence of laser pulses with Gaussian time-dependent envelopes is investigated. Considering production of photon-triplet for short-time regime and in the cascaded three-wave collinear configuration we shortly analyze preparation of polarization-non-product states looking further applications of these results in the cascaded optical parametric oscillator. It is also demonstrated the nonclassical characteristics of the photon-triplet in phase-space on the base of the Wigner function. Calculating the normalized third-order correlation functions below-and at the generation threshold of cascaded optical parametric oscillator, we demonstrate that in the pulsed regime, depending on the duration of pulses and the time-interval separations between them, the degree of three-photon-number correlation essentially exceed the analogous one for the case of continuous pumping.

## 1. Introduction

Multiphoton entangled states have attracted a great interest in probing the foundations of quantum theory and constitute a powerful quantum resource with promising potential for various applications in quantum information technologies. Recently, experimental efforts in the direct production of multiphoton joint states, particularly, three- or four-photon states have paved a new stage for the study of multipartite entanglement [1]. Indeed, the simultaneous generation of three photons is at the origin of intrinsic three-particle quantum properties such as Greenberger-Horne-Zeilinger (GHZ) -class and W-class quantum entanglement [2] - [5]. Up to now, several physical systems have been proposed for the generation of photon triplet including third-order nonlinear medium [6] and cascaded spontaneous parametric down-conversion (PDC) [7, 8]. Experimentally, three-photon down-conversion was

studied in third-order nonlinear media [9] - [11] and also by using cascaded second-order nonlinear parametric processes [12]. Direct generation of photon triplets using cascaded photon-pairs has been demonstrated in periodically poled lithium niobate crystals [1]. The distinction of three-photon GHZ and W states entangled in time and space has been also reported [13, 14]. It was also shown that intracavity three-photon down-conversion can be effectively realized in cascaded optical parametric oscillator (OPO) [15]. This scheme that involves cascading second-order nonlinearities is based on the parametric processes of splitting and summing in which the frequencies between the pump and two subharmonics frequencies are in the ratio of 3 : 2 : 1. Experimental realization of cascaded OPO by using the dual-grid method of quasi-phase matching (QPM) has been done in Ref. [16]. Most recently, joint quantum states of three-photons with arbitrary spectral characteristics have been studied on the base of optical superlattices [17] for the cascaded configuration proposed in [15]. Two cascaded configurations have been considered in [17] that lead to production of spontaneous photon triplet in cascaded PDC and generation of high intensity mode due to cascaded three-photon splitting in optical cavity.

In this paper we continue the investigation of cascaded three-photon splitting in an optical cavity following the paper [17]. Our goal is twofold. In one part of the present paper we extend our previous results regarding three-photon splitting in optical cavity for an experimentally available scheme that is a cascaded parametric oscillator pumped by a sequence of Gaussian laser pulses (see, Sects. II and III). The other part of the paper is devoted to studies of quantum properties of "three-photon" mode. We discuss preparation of non-product states that are superposition of three-photon polarization states, however, without any consideration of cavity effects (see, Sec. IV). We also calculate the Wigner function of the subharmonic, i.e. "three-photon mode" showing the negativity in phase-space (see, Sec. V). Our analysis includes calculation of third-order correlation function of photon numbers for various operational regimes of pulsed OPO (see, Sec. VI). It is known, that it is possible to control the behavior of quantum dissipative system by a train of pulses. In this paper, we use this approach for suppression of dissipation and cavity induced feedback in cascaded OPO that leads to increasing the level of three-photon-number correlation.

## 2. Periodically pulsed cascaded OPO: Generation threshold

In this section we briefly describe the cascaded optical parametric oscillator (OPO) with a triply resonant optical ring cavity driven by a sequence of laser pulses. The semiclassical and quantum theories of this device for the monochromatic pump field were developed in Refs. [15, 17] and here we only add some important details regarding cascaded OPO under laser pulses with Gaussian time-dependent envelopes. This cascaded configuration involves the fundamental mode driven by an external pump field at the central frequency  $\omega_0$  with an amplitude  $E_L$  and two subharmonic modes at the frequencies  $\omega_1 = \frac{\omega_0}{3}$  and  $\omega_2 = \frac{2\omega_0}{3}$ . Due to intracavity parametric type-

I three-wave interactions pump field is converted to the subharmonics throughout two cascaded processes:  $\omega_0 \rightarrow \omega_1 + \omega_2$  and  $\omega_2 \rightarrow \omega_1 + \omega_1$ . Subharmonic modes have the same plane polarizations and are all propagating in the same direction. The pump field consists from the sequence of Gaussian laser pulses with the amplitude

$$E(t, z) = E_L f(t) e^{-i(\omega_0 t - k_L z)}, \quad (1)$$

$$f(t) = \sum_{n=0}^{\infty} e^{-(t-t_0-n\tau)^2/T^2}, \quad (2)$$

where  $T$  is the duration of pulses that are separated by time intervals  $\tau$ . The cascaded OPO is dissipative, because the modes suffer from losses due to partially transmission of light through the mirrors of the cavity. We consider below the case of high cavity losses for the pump mode ( $\gamma_0 \gg \gamma, \gamma_1 = \gamma_2 = \gamma$ ), when the pump mode is eliminated adiabatically in non-depletion approximation. In this case, the effective interaction Hamiltonian in the rotating wave approximation reads as

$$H_{int} = i\hbar\chi_1 E_0 f(t) (a_1^+ a_2^+ - a_1 a_2) + i\hbar\chi_2 (a_1^{+2} a_2 - a_1^2 a_2^+), \quad (3)$$

where  $E_0 = E_L/\gamma_0$ ,  $a_i$  ( $i=1,2$ ) are the operators of the modes at the frequencies  $\omega_1 = \frac{\omega_0}{3}$  and  $\omega_2 = \frac{2\omega_0}{3}$  and the coupling constants between the modes are expressed through the Fourier spectra of the second-order susceptibilities of nonlinear crystals of the length  $L$

$$\chi_1 = \int_0^L dz \chi^{(2)}(z) e^{i\Delta k_1(z)z}, \quad (4)$$

$$\chi_2 = \int_0^L dz \chi^{(2)}(z) e^{i\Delta k_2(z)z}. \quad (5)$$

We assume collinear, one-dimensional on  $z$  quasi-phase-matching with the phase mismatch vectors

$$\Delta k_1(z) = k_L(\omega_0, z) - k_1(\omega_1, z) - k_2(\omega_2, z), \quad (6)$$

$$\Delta k_2(z) = k_2(\omega_2, z) - 2k_1(\omega_1, z) \quad (7)$$

analyzed in the details [17].

In this regime, the stochastic equations of motion for the complex c-number variables  $\alpha_{1,2}$  and  $\beta_{1,2}$  corresponding to the operators  $a_{1,2}$  and  $a_{1,2}^+$ , have the following form

$$\frac{d\alpha_1}{dt} = -\gamma_1 \alpha_1 + E_0 f(t) \chi_1 \beta_2 + 2\chi_2 \alpha_2 \beta_1 + W_{\alpha_1}(t), \quad (8)$$

$$\frac{d\beta_1}{dt} = -\gamma_1 \beta_1 + E_0 f(t) \chi_1 \alpha_2 + 2\chi_2 \beta_2 \alpha_1 + W_{\beta_1}(t). \quad (9)$$

The equations for  $\alpha_2, \beta_2$  are obtained from (8), (9) by exchanging the subscripts (1)  $\rightleftharpoons$  (2). Our derivation is based on the Ito stochastic calculus, and the nonzero stochastic correlators are:

$$\langle W_{\alpha_1}(t)W_{\alpha_2}(t') \rangle = \chi_1 \frac{E_L f(t)}{\gamma_0} \delta(t - t'), \quad (10)$$

$$\langle W_{\alpha_1}(t)W_{\alpha_1}(t') \rangle = 2\chi_2 \alpha_2 \delta(t - t'), \quad (11)$$

$$\langle W_{\beta_1}(t)W_{\beta_1}(t') \rangle = 2\chi_2 \beta_2 \delta(t - t'), \quad (12)$$

$$\langle W_{\alpha_2}(t)W_{\alpha_2}(t') \rangle = 2\chi_2 \alpha_1 \delta(t - t'). \quad (13)$$

The Eqs. (8), (9) and the correlation functions modifies the analogous ones derived for OPO with monochromatic pumping [15] on the case of non-stationary pump field.

In accordance with the cited paper, for the monochromatic driven cascaded OPO, zero-amplitude solutions  $\alpha_1 = \alpha_2 = 0$  of Eqs. (8), (9) with  $f(t) = 1$  are stable, if  $E_L < E_{th} = \frac{\gamma_0}{\chi_1} \sqrt{\gamma_1 \gamma_2}$ , while steady-state photon numbers  $n_1$  and  $n_2$  displays histeresis-cycle behavior in a small domain  $\frac{2\sqrt{2}}{3} < E_L/E_{th} < 1$ . Thus, remarkable feature of OPO under monochromatic pump is comparatively low generation threshold in comparison with the scheme of direct intracavity three-photon down-conversion, where the pump power threshold is determined by third-order susceptibility [9].

Below, we derive the threshold value for OPO driven by trains of Gaussian pulses. The analysis of stochastic equations shows that similar to the standard OPO with monochromatic pump field amplitude, the periodically pulsed OPO also exhibits threshold behavior, which is easily described through the period averaged pump field amplitude  $\overline{f(t)} = \frac{1}{\tau} \int_0^\tau f(t) dt$ . We demonstrate this statement analyzing the stability of zero-amplitude solutions of  $\alpha_1 = \alpha_2 = 0$  of Eqs. (8), (9) for both modes below threshold and for  $\gamma_1 = \gamma_2 = \gamma$ . To check the stability we turn to the linearized on the small deviations  $\delta\alpha_i, \delta\beta_i$  the equations in the semicalssical approach without noise terms. These equations can be rewritten in the following form:

$$\frac{d}{dt} \delta X_\pm = (-\gamma \pm \frac{E_L}{\gamma_0} \chi_1 f(t)) \delta X_\pm, \quad (14)$$

$$\frac{d}{dt} \delta Y_\pm = (-\gamma \pm \frac{E_L}{\gamma_0} \chi_1 f(t)) \delta Y_\pm, \quad (15)$$

through the quadrature field variables defined as  $\delta\alpha_\pm = \delta\alpha_1 \pm \delta\alpha_2$  and  $\delta X_\pm = \frac{1}{2}(\delta\alpha_\pm + \delta\alpha_\pm^*), \delta Y_\pm = \frac{1}{2i}(\delta\alpha_\pm - \delta\alpha_\pm^*)$ . In these variables the time evolution has the simple form

$$\delta X_\pm(t) = \Lambda_\pm(t, t_0) \delta X_\pm(t_0), \quad (16)$$

$$\delta Y_{\pm}(t) = \Lambda_{\mp}(t, t_0) \delta Y_{\pm}(t_0), \quad (17)$$

$$\Lambda_{\pm}(t, t_0) = \exp(\pm \frac{E_L \chi_1}{\gamma_0} \int_0^t f(t') dt' - \gamma(t - t_0)). \quad (18)$$

Analyzing semiclassical equations and operational regimes we choose the switching time in infinity, i.e.  $t_0 \rightarrow -\infty$ , and add in (2) terms with negative  $n$ . In this case, the function  $f(t)$  is periodic on time  $f(t + \tau) = f(t)$  and the analysis is simplified. Since the function  $f(t)$  is periodic on time, we can obtain the general formula  $\int_{t_0}^t f(t) dt = \overline{f(t)}(t - t_0) + F(t) - F(t_0)$ , where  $F(t)$  is a periodic function,  $F(t + \tau) = F(t)$ . Therefore, we see from (16), (17), (18) that the solution  $\alpha_i = 0$  below-threshold is stable if  $E_L < \frac{\gamma_0 \tau}{\chi_1} \overline{f(t)}$ . It is easy to check also that due to noted periodicity of the amplitude the following formula takes place (see, for example [18])

$$\int_0^\tau dt \sum_{n=-\infty}^{\infty} e^{-(t-n\tau)^2/T^2} = \int_{-\infty}^{\infty} dt e^{-t^2/T^2}. \quad (19)$$

This formula allows us to calculate the averaged value of the amplitude  $f(t)$ . On the whole, we arrive to the result that for the case of Gaussian pulses above threshold regime is realized if

$$E_L \geq \overline{E_{th}} = \frac{\tau}{T\sqrt{\pi}} E_{th} = \frac{\tau}{T\sqrt{\pi}} \frac{\gamma_0 \gamma}{\chi_1}. \quad (20)$$

The important peculiarity of the system proposed is that the threshold value  $\overline{E_{th}}$  depends on the coupling constant  $\chi_1$  which is related to the second-order susceptibility as well as depends on the characteristics of laser pulses.

### 3. Numerical simulation of dissipation and decoherence

The cascaded OPO is dissipative, because the modes suffer from losses due to partial transmission of light through the mirrors of the cavity and due to quantum fluctuations. We analyse dissipative and decoherence effects on the base of master equation for the density operator of the cavity modes in the Limbland form

$$\frac{\partial \rho}{\partial t} = \frac{1}{i\hbar} [H_{int}, \rho] + \sum_{i=1,2} \gamma_i (2a_i \rho a_i^+ - a_i^+ a_i \rho - \rho a_i^+ a_i). \quad (21)$$

We calculate the quantities of interest (the photon number distributions, Wigner functions, etc.) mainly for the subharmonic mode (1) by using the reduced density operator  $\rho_1(t)$  which is constructed from the density operator  $\rho(t)$  of both modes by tracing over the mode (2),  $\rho_1(t) = Tr_2(\rho)$ . We analyze the master equation numerically using quantum state diffusion method (QSD) [19]. According to this method, the reduced density operator is calculated as the ensemble mean

$$\rho(t) = M(|\psi_\xi(t)\rangle\langle\psi_\xi(t)|) = \lim_{N \rightarrow \infty} \frac{1}{N} \sum_{\xi}^N |\psi_\xi(t)\rangle\langle\psi_\xi(t)| \quad (22)$$

over the stochastic pure states  $|\psi_\xi(t)\rangle$  describing evolution along a quantum trajectory. The stochastic equation for the state  $|\psi_\xi(t)\rangle$  involves Hamiltonian described by Eq. (3) and the Linblad operators described by noise terms in the master equation (21). We calculate the density operator using an expansion of the state vector  $|\psi_\xi\rangle$  in a truncated basis of Fock's number states of modes of the subharmonics (1) and (2)

$$|\psi_\xi(t)\rangle = \sum_n a_{n_1, n_2}^\xi(t) |n_1\rangle_1 |n_2\rangle_2. \quad (23)$$

Details of analogous calculations for an anharmonic oscillator in time-modulated field can be found in [20]). The numerical simulations are performed in the truncated Fock basis of the subharmonic modes that are limited by 500 photons. This approximation is valid for the case of strong nonlinear couplings  $\chi_1$  and  $\chi_2$  with respect to the dissipation parameters.

#### 4. Production of polarization, non-product states of photon triplet in collinear configuration

Three-photon correlations allow the creation of tripartite entangled states such as the GHZ state. For cascaded SPDC in noncollinear configuration spatially-polarization GHZ states has been considered in [17]. Below we apply the results obtained for preparation of three-photon polarization states in collinear configuration of interacting waves. Recently, a simple but highly efficient source of polarization-entangled photon pairs at nondegenerate wavelengths and in collinear configuration has been demonstrated [21]. We consider the production of polarization-entangled photon triplet. It is possible for the case when cascaded processes involve polarized photons.

Thus, we modify the above results considering three-wave interaction with the indexes of polarization states. Looking further applications of above results for intracavity three-photon down-conversion in collinear configuration of cascading processes we concentrate on consideration of non-product states that are entangled only on polarization degree of freedom but not on spatial variables. Thus, including into consideration the polarization states of the photons we assume that the type-II process  $\omega_0 \rightarrow \omega_1 + \omega_2$  create the pair of photons with a vertical  $V$ ,  $(a_1(V), (a_2(V))$  and horizontal  $H$ ,  $(a_1(H), (a_2(H))$  polarizations in collinear configuration. If the pump field is oriented at  $45^\circ$  to the horizontal and vertical axes two processes  $\omega_0 \rightarrow \omega_1(V) + \omega_2(H)$  and  $\omega_0 \rightarrow \omega_1(H) + \omega_2(V)$  take place in the first crystal. The next process is considered as the type-I parametric process. In type-I conversion, photon pairs are created with the same polarization state, but orthogonal to the input mode. Therefore, the second, type-I crystal is arranged in the manner that the following process:  $\omega_2(H) \rightarrow \omega_1(V) + \omega_1(V)$  and  $\omega_2(V) \rightarrow \omega_1(H) + \omega_1(H)$  should be realized.

For simplicity, we restrict our attention considering frequency-uncorrelated three-photon states and assume that the process under photons with ( $V$ ) and ( $H$ ) polar-

izations are described by the equal coupling constants. Thus, we assume that photon pairs in three-wave processes :  $\omega_0 \rightarrow \omega_1 + \omega_2$ ,  $\omega_2 \rightarrow \omega'_1 + \omega''_1$  have correlations on the polarization, but not on the spectral lines. In analogy with Eq.(3), we model the sum of the corresponding parametric interactions by the following effective Hamiltonian

$$H = H_1 + H_2, \quad (24)$$

$$H_1 = i\hbar\chi E_0 f(t)(a_1^+(V)a_2^+(H) + a_1^+(H)a_2^+(V)) + h.c., \quad (25)$$

$$H_2 = i\hbar k[(a_2(V)(a_1^+(H))^2 + a_2(H)(a_1^+(V))^2)] + h.c.. \quad (26)$$

Here,  $a_1(V)$  and  $a_2(V)$  are the annihilation operators of modes (1) and (2) at vertical polarizations, while the operators  $a_1(H), a_2(H)$  corresponds to the horizontal polarized photons of the frequencies  $\omega_1$  and  $\omega_2$ , respectively.

We focus on analysing the generation of non-product states for one-passing configuration of cascaded parametric spontaneous processes without consideration of cavity dynamics and feedback effects. This approach is valid for short interaction time intervals much shorter than the characteristics relaxation time. In this case time-evolution of the vector state of the system is described by the second-order term of the perturbation theory. Choosing the initial state as a vacuum state  $|\psi_{in}\rangle = |0\rangle_{a_1(H)}|0\rangle_{a_2(H)}|0\rangle_{a_1(V)}|0\rangle_{a_2(V)}$  for all modes we derive the final state during time evaluation in the following form

$$|\psi(t)\rangle = \left(-\frac{i}{\hbar}\right)^2 t^2 H_2 H_1 |\psi\rangle_{in} = \\ \bar{\chi} \bar{k} E_0 (|V\rangle|V\rangle|V\rangle + |H\rangle|H\rangle|H\rangle)|0\rangle_{a_2(H)}|0\rangle_{a_2(V)}, \quad (27)$$

where  $\bar{\chi} = \chi t$  and  $\bar{k} = kt$  are the coupling constants and the states  $|V\rangle = a_1^+(V)|0\rangle_{a_1(V)}$ ,  $|H\rangle = a_1^+(H)|0\rangle_{a_1(H)}$  present the vertical and horizontal polarization states of photons at the frequency  $\omega_1 = \frac{\omega_0}{3}$ . Thus, we demonstrate that in this collinear, one-dimensional cascaded scheme triple photons can constitutes the polarization entangled (non-product) states of light. It should be noted that under cavity feedback effects the non-product quantum state cannot be described by this simple expression and we should include the higher-order terms of the perturbation expansion into consideration.

## 5. Photon triplet in phase-space: Wigner functions and photon number distributions in the pulsed regime

Quantum interference signature of three-photon states in phase-space has been demonstrated for the direct three-photon down-conversion in third-order nonlinear medium [6, 9] as well as in the cascaded scheme [17] for the case of monochromatic pumping. We demonstrate now this effect for the pulsed regime of cascaded OPO. We illustrate these effects numerically on the base of the master equation, however,

in the regimes when the dissipation in the cavity is unessential and the dynamic of modes is almost unitary. For the cavity configuration presented, the validity of such approximation is guaranteed by consideration of short interaction time for which the duration of pulses are much shorter than the characteristics relaxation time,  $1/(\chi_1 E_0)$ ,  $1/\chi_2 \ll t \ll 1/\gamma_{1,2}$ , provided that the nonlinear coupling constants exceed the dumping rates for the modes.

Below, we present the results on the photon-number distributions and Wigner functions for three-photon mode. The photon number distribution for  $\omega_1 = \frac{\omega_0}{3}$  mode is calculated as the diagonal element  $P_1(n) = \langle n | \rho | n \rangle$  of photonic Fock states while calculations of the Wigner function for the this mode are performed by using its standard formula in a Fock space:

$$W_1(\rho, \theta) = \sum_{m,n} \rho_{1,mn} W_{mn}(\rho, \theta) \quad (28)$$

Here,  $\rho, \theta$  are the polar coordinates in the complex phase space which is determined by the position and the momentum of quadratures  $x = (a + a^+)/\sqrt{2}, y = (a - a^+)/\sqrt{2i}$ , respectively, while the coefficients  $W_{mn}(\rho, \theta)$  are the Fourier transforms of the matrix elements of the Wigner characteristic function.

Three-photon structure of the mode is shown on photon-number distributions in Figs. 1 (a, d). As we see, for short time-intervals, the most probable values of photon numbers are separated by three photons. In Figs. 1 (b, e) we present results on the Wigner functions that clearly exhibit phase-space quantum interfringes. These results describe the case of cascaded OPO under two consecutive pulses with the duration  $T\gamma = 1 * 10^{-3}$  separated by the interval  $\tau\gamma = 6 * 10^{-3}$ . Fig. 1(b) shows the Wigner function evolved for a time interval  $t = t_0 + 6.2 * 10^{-3}\gamma^{-1}$  that corresponds to maximal photon number  $n_{max}$  of the first pulse; Fig. 1(e) shows the Wigner function at  $t = t_0 + 6.2 * 10^{-2}\gamma^{-1}$  corresponding to  $n_{max}$  of the second pulse. The Wigner function shows three phase components with an interference pattern in the regions between them. We show the regions of quantum interference in the contour plots (see, Figs. 1 (c, f)) depicting negative regions of the interference terms in black. Note that threefold symmetry of the Wigner function and interference pattern has been demonstrated for the direct three-photon down-conversion in  $\chi^{(3)}$  media [6, 9]. However, we note that the results presented here for the pulsed cascaded configuration are also different in details from the analogous calculation of the Wigner function for the case of monochromatic pump field [17].

## 6. Photon-number correlation in the pulsed regime

The experimental verification of time-dependent correlation between photons in triplet has been demonstrated for one-passing configuration of cascaded SPDC [1]. Considering production of photon triplet in a cavity, it seems that the correlation

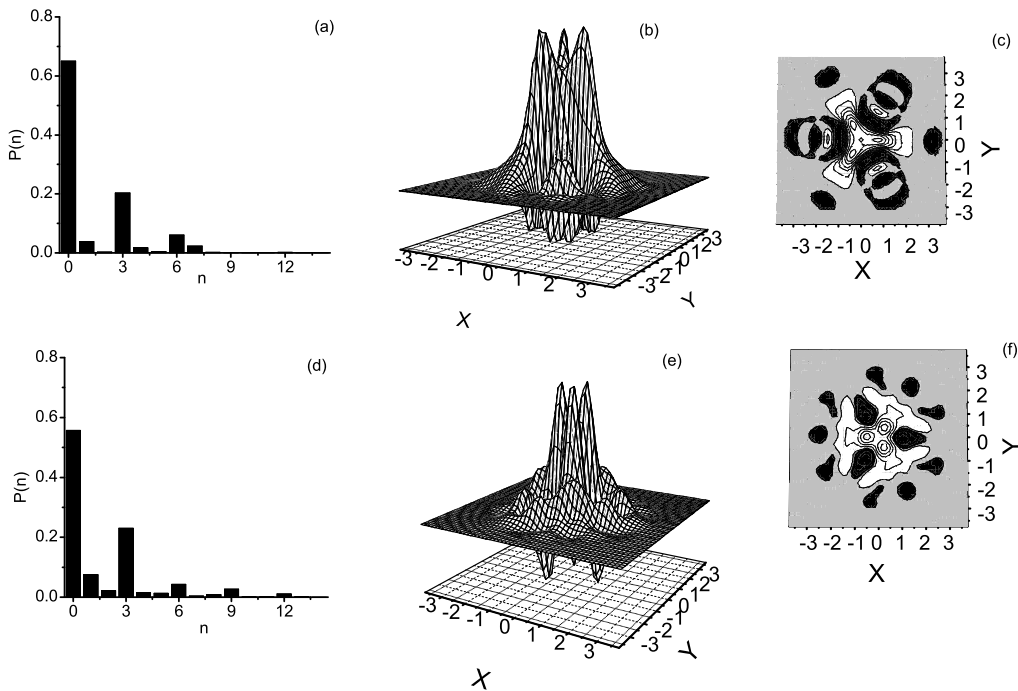


Figure 1: The photon number distributions (a, d), the Wigner functions (b, e) and its contour plots (c, f) for  $\omega_1$ -mode and for different time intervals:  $t = t_0 + 6.2 \times 10^{-3} \gamma^{-1}$  (a, b, c);  $t = t_0 + 6.2 \times 10^{-2} \gamma^{-1}$  (d, e, f). The other parameters are:  $\chi_1/\gamma_1 = 200$ ,  $\chi_2/\gamma_1 = 100$ ,  $\gamma_2 = \gamma_1 = \gamma$ ,  $T\gamma = 1 \times 10^{-3}$ ,  $\tau\gamma = 6 \times 10^{-3}$ .

between photons can be evidently displayed for short interaction time intervals much shorter than the relaxation time. Nevertheless, the three-photon number correlation exceeding the coherent level, (that means the normalized third-order correlation function  $g^{(3)} > 1$ ), has been demonstrated for cascaded OPO driven by monochromatic pumping, in over transient regime for modes generated below the threshold [17]. This effect decreases if the system moves to the range of the generation threshold. At the threshold, the typical value for the normalized third-order correlation function for zero delay-time,  $g^{(3)} = 1.2$ , has been obtained.

In this Section, we demonstrate the new regimes of strong three-photon correlation for the pulsed cascaded OPO. We concentrate on numerical simulation of both the mean photon number of subharmonics as well as the third-order correlation function. Let us now discuss photon-number correlation in the time domain, considering output twin light beams from the pulsed cascaded OPO on the base of normalized third-order photon-numbers correlation function  $g^{(3)}$  for the mode (1)

$$g^{(3)}(t) = \text{Tr}(a_1^+ a_1^3 \rho_1(t)) / n^3(t). \quad (29)$$

Here,  $n(t) = \text{Tr}(a_1^+ a_1 \rho_1(t))$  is the mean photon number. Considering three-photon number correlation for the intensive cavity mode in the presence of dissipation and cavity induced feedback, we control quantum dynamics of dissipative systems by a train of pulses. Here, we use this approach for controlling quantum statistics of mode, particularly for increasing the level of three-photon-number correlation. We analyze the cases in which  $T\gamma \leq 1$  and  $\tau\gamma \geq 1$ , for over transient time-intervals,  $t \gg \gamma^{-1}$ , considering the operational regimes below-and at the generation threshold. Typical results for the mean photon numbers and the correlation function  $g^{(3)}$  for two different parameters of the Gaussian pulses :  $T = \gamma^{-1}, \tau = 10\gamma^{-1}$  and  $T = \gamma^{-1}, \tau = 5\gamma^{-1}$  are presented in Figs. (2) and (4). As we see from these figures, the time-dependence of these quantities repeat the periodicity of the pump laser over transient time intervals. We also conclude that the maxima of the three-photon correlation are realized for the definite time intervals for which the mean photon number of mode (1) is in the ranges between its maxima and minima. As shown our calculations, such strong photon correlations take place in nonstationary regime of cascaded OPO when duration of pulses is close to a characteristic dissipation time. In Figs. (2) we analyze the mean photon number (Fig. 2(a)) and the correlation function (Fig. 2(b)) in the operational regimes of OPO at the generation threshold. In the regime below the generation threshold, at  $E/\overline{E}_{th} = 0.5$  the correlation function display two-peak structure (see, curve (2)). The lower peak corresponds to the time intervals for which the mean photon number is between its minimal and maximal values. More correctly, for the period trains of intervals  $t = t_0 + m11.6\gamma^{-1}$ , ( $m = 1, 2, \dots$ ), the mean photon number  $n = 50$  and the correlation function  $g^{(3)} = 8.9$ . The other peaks correspond to the minimal values of the mean photon number. At the threshold (see, curves (1)) the effect of photon correlation is decreased, although the level of correlation exceeds the coherent level,  $g^{(3)} > 1$ , particularly, we get  $g^{(3)} = 3.4$  for the mean photon number  $n=251$ . Thus, we found a remarkable result that the degree of three-photon number correlation for the pulsed regime of OPO surpass the analogous result for

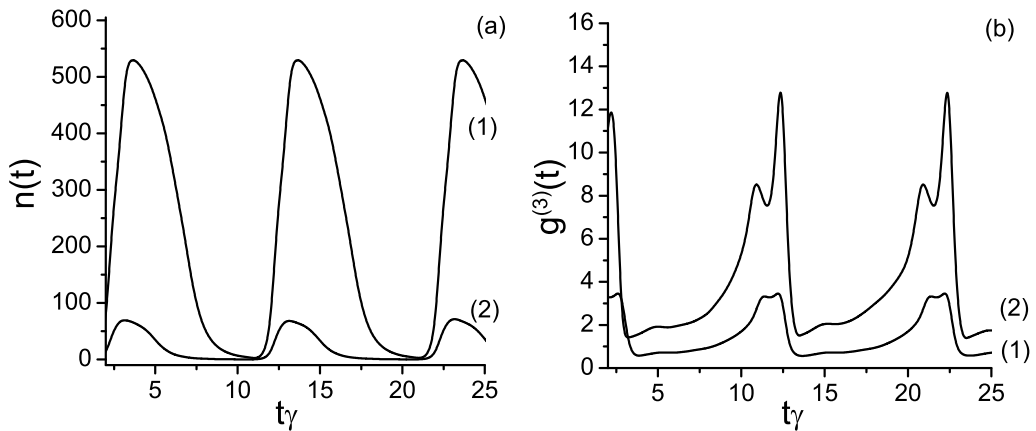


Figure 2: The mean photon number (a) and the third-order correlation function (b) versus  $t\gamma$  at the threshold  $E_L/\overline{E_{th}} = 1$ , curves (1) and below the threshold  $E_L/\overline{E_{th}} = 0.5$ , curves (2). The parameters are:  $\chi_1/\gamma = 0.2$ ,  $\chi_2/\gamma = 0.1$ ,  $\gamma_2 = \gamma_1 = \gamma$ ,  $\tau\gamma = 10$ ,  $T\gamma = 1$ .

OPO with continuous pumping for the same mean photon numbers. Indeed, this conclusion is illustrated in Figs. (2) and (3), where the comparison of the results on pulsed regime with the calculations based on the Hamiltonian (3) with  $f = 1$  is done. Note, that the ideal limit of continuous pumping is realized if  $T \rightarrow 0$ ,  $\tau \rightarrow \infty$  for the case of infinity numbers of pulses. We present on the Figs. (3) the results for OPO with continuous pumping at the threshold  $E_L = E_{th}$ , in which the mean photon number  $n = 52$  in the steady state regime (curve (2), Fig. 2(a)) approximately equals to the maximal value of the photon number in the pulsed regime. However, as we see, the level of the maximal correlation,  $g^{(3)} = 9$  in this case exceeds the analogous one for the case of continuous pumping,  $g^{(3)} = 1.2$ .

It is natural to explain such improvement of three-photon correlation by control the behavior of a quantum system by an external time-dependent force. The presence of these effects in the cascaded OPO, particularly, can been seen from the noise-correlation functions. Indeed, the equation (10) describes a multiplicative noise-term, where the level of noise is determined by the amplitude of pulsed driving field  $E_L f(t)$  leading to the control of dissipation. In this spirit, we emphasize that the idea of controlling the dynamics of a quantum system in the presence of dissipation and decoherence by an external periodic driving was exploited by many authors (see, for example, [22] and the references therein). In one of the standard techniques control of the optical quantum system is achieved through the application of suitable tailored, synchronized laser pulses [23]. In this way, it is interesting to analyze

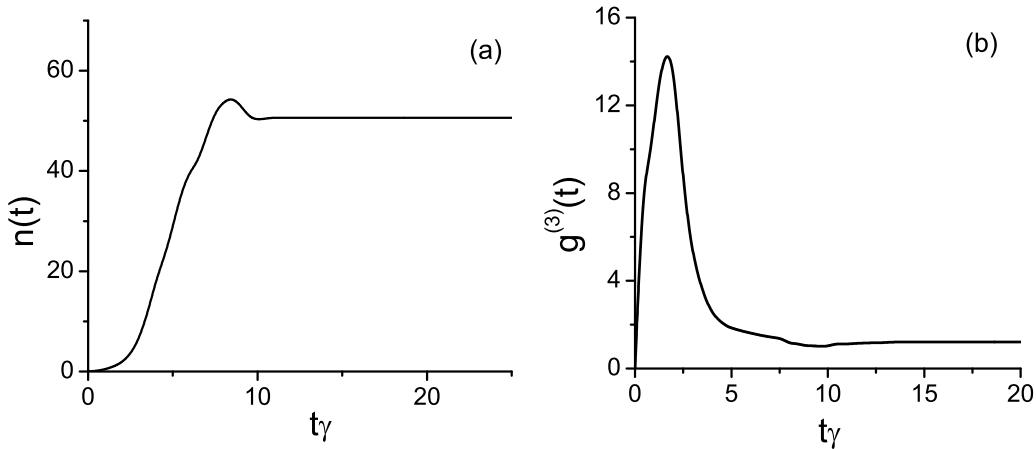


Figure 3: Mean photon number (a) and the correlation function (b) for continuously pumped OPO at the threshold  $E_L/E_{th} = 1$ . The parameters are:  $\chi_1/\gamma = 0.2$ ,  $\chi_2/\gamma = 0.1$ ,  $\gamma_2 = \gamma_1 = \gamma$ .

the three-photon correlation function in dependence of the time-separation between pulses, i.e. for the other parameters of driving pulses in additional to the parameters considered in Figs. 2. The results are presented in Figs. 4 in the regime below the threshold where strong three-photon correlations are realized. As we see, in this case the correlation function reach to  $g^{(3)} = 75$  for  $n = 1.1$  (curves (1)) for time-intervals between pulses,  $\tau = 10\gamma^{-1}$ . Decreasing of the time-separation between pulses leads to decreasing of the correlation function (see, curves (2), where  $\tau = 5\gamma^{-1}$ ).

## 7. Conclusion

In conclusion, we have studied quantum properties of photon triplet cardinally different from those of twin photons. Because photon-triplet originates from a single laser photon, the quantum correlations take place between all three photons allowing the creation of entangled, non-product states. The production of photon-triplets in the presence of stimulation radiative processes, cavity feed-back effects and dissipation have been investigated. We have demonstrated the possibility to create polarization, non-product states of photon-triplet for one-passing, collinear configuration of cascaded parametric spontaneous processes. We have also illustrated three-photon structure of sub-harmonic mode on the base of both the photon-number distribution and the Wigner function. We have demonstrated the operational regimes depending on the durations of pulses and the intervals between them that guarantees strong

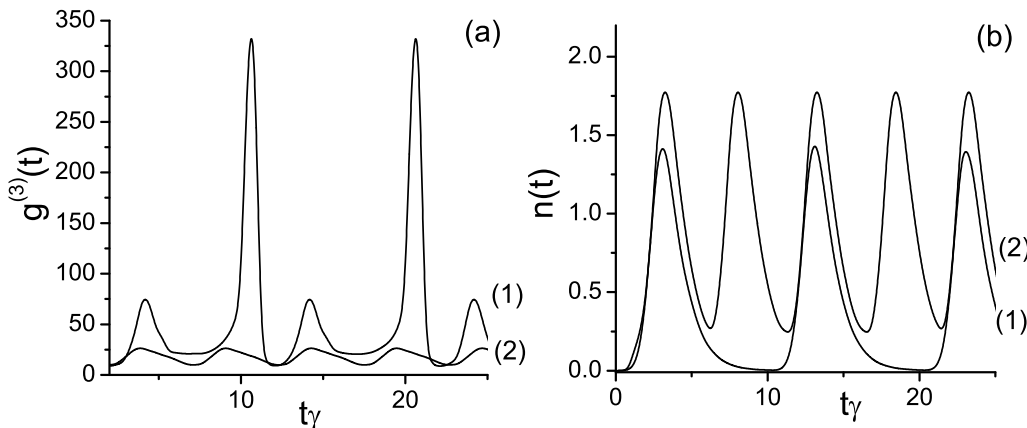


Figure 4: The correlation functions (a) and the mean photon numbers (b) at  $E_L/\overline{E_{th}} = 0.2$  for time-separation between pulses:  $\tau\gamma = 10$ , curves (1);  $\tau\gamma = 5$ , curves (2). The parameters are:  $\chi_1/\gamma = 0.2$ ,  $\chi_2/\gamma = 0.1$ ,  $\gamma_2 = \gamma_1 = \gamma$ ,  $T\gamma = 1$ .

three-photon-number correlations . This effect of strong correlation takes place for the definite time intervals corresponding to generation of high intensity "three-photon mode" in over transient regime and for wide ranges of the system parameters. We hope that these results could be of interest in areas of quantum communications and photonic quantum computing.

## References

- [1] H. Hubel *et al*, Nature Photonics Lett. **466**, 09175 (2010).
- [2] D.M. Greenberger, M.A. Horne, and A. Zeilinger, in Bell's Theorem, Quantum Theory, and Conceptions of the Universe, M. Kafatos, ed. (Kluwer, 1989).
- [3] D. Bouwmeester *et al*, Phys. Rev. Lett. **82**, 1345 (1999); J.-W. Pan *et al*, Nature (London) **403**, 515 (2000).
- [4] M. Eibl, N. Kiesel, M. Bourennane, C. Kurtsiefer, and H. Weinfurter, Phys. Rev. Lett. **92**, 077901 (1998).
- [5] W.Dür, G. Vidal, and J. I. Cirac, Phys. Rev. A **62**, 062314 (2000).
- [6] K.Banaszek and P.Knight, Phys. Rev. A **55**, 2368 (1997).

- [7] D.M. Greenberger, M.A. Horne, A. Shimony, and A. Zellinger, Am. J. Phys. **58**, 1131 (1990).
- [8] T.E. Keller, M.H. Rubin, Y. Shih, and L.A. Wu, Phys. Rev. A **57**, 2076 (1998).
- [9] T. Felbinger, S. Schiller, and J. Mlynek, Phys. Rev. Lett. **80**, 492 (1998).
- [10] J. Douady, and B. Boulanger, Opt. Lett. **29**, 2794 (2004).
- [11] K. Bencheikh, F. Gravier, J. Douady, J.A. Levenson, and B. Boulanger, C.R. Phys. **8**, 206 (2007).
- [12] H.C. Guo, Y.Q. Qin, and S.H. Tang, Appl. Phys. Lett. **87**, 161101 (2005).
- [13] J.M. Wen and M. H. Rubin, Phys. Rev. A **79**, 025802 (2009).
- [14] J. Wen, E. Oh, and Sh. Du, J. Opt. Soc. Am. B **27**, (6), A11 (2010).
- [15] G.Yu. Kryuchkyan, N.T. Muradyan, Phys. Lett. A **286**, 113 (2001); G.Yu. Kryuchkyan, L.A. Manukyan and N.T. Muradyan, Opt. Comm. **190**, 245 (2001).
- [16] J.J. Zondy, A. Tallet, E. Ressayre, and M. LeBerre, Phys. Rev. A **63**, 023814 (2001).
- [17] D.A. Antonosyan, T.V. Gevorgyan, and G.Yu. Kryuchkyan, Phys. Rev. A **83**, 043807 (2011).
- [18] N.H. Adamyan, H.H. Adamyan, and G.Yu. Kryuchkyan, Phys. Rev. A **77**, 023820 (2008).
- [19] N. Gisin and I.C. Percival, J. Phys. A **25**, 5677 (1992); I.C. Percival, Quantum State Diffusion (Cambridge University Press, Cambridge, 2002).
- [20] H.H. Adamyan, S.B. Manvelyan and G.Yu. Kryuchkyan, Phys. Rev. A **63** 022102 (2001); S.B. Manvelyan and G.Yu. Kryuchkyan, Phys. Rev. Lett. **88** 094101 (2002); T. V. Gevorgyan, A.R. Shahinyan, G.Yu. Kryuchkyan, Phys. Rev. A **79** 094101 (2009).
- [21] P. Trojek and H. Weinfurter, Appl. Phys. Lett. **92**, 211103 (2008).
- [22] L. Viola, E. Knill, and S. Lloyd, Phys. Rev. Lett. **82** 2414 (1999); L. Viola and E. Knill, Phys. Rev. Lett. **90**, 037901 (2003).
- [23] G.J. Milburn *et al* Rev. Mod. Phys. **79**, 135 (2007).

# Magnetic properties, classical and quantum phase transitions in anti-ferromagnetic models

N.S. Ananikian

*A.I. Alikhanyan National Science Laboratory  
2 Alikhanyan Brothers Street, 0036 Yerevan, Armenia*

## Abstract

The magnetization plateaus, bifurcation points and chaos are playing the greatest role in the classical and quantum phase transitions. We obtained three-cycle windows of antiferromagnetic Potts and magnetization plateaus of anti-ferromagnetic Ising model with multisite interactions. Using Gibbs-Bogolubov inequality the quantum entanglement (concurrence) of antiferromagnetic spin-1/2 Ising-Heisenberg model on the triangulated kagome and two dimensional kagome (fluid  $^3\text{He}$ ) lattices are investigated.

## 1. Introduction

Entanglement is considered to play a key role for the understanding of strongly correlated quantum systems, quantum phase transitions and collective quantum phenomena in particular many-body spin and fermionic lattice models [1]. One can introduce the fundamental connection between quantum transitions in  $d$  dimensions and certain well studied finite temperature phase transitions in classical statistical mechanics in  $d+1$  dimension [2]. The magnetization plateaus have played a great role in understanding of a large family of nontrivial quantum phenomena of spin systems [3]. The experimental [4] and theoretical [5] studies suggest that three-site exchanges are dominant in solid  $^3\text{He}$  atoms, which have 1/2 spin [6]. One can obtain magnetization plateaus with multiple-spin exchange using the dynamical and transfer matrix methods [7]. In this paper I would pay attention to the researching of classical phase transitions, magnetisation plateaus, stable cycles of Potts antiferromagnetic model and quantum entanglement of spin-1/2 Ising-Heisenberg model on the triangulated kagome lattice, solid and fluid  $^3\text{He}$  models with multi spin-exchanges.

## 2. Bifurcation points and chaos

The Potts and Ising models played an important role in the theories of phase transitions and critical phenomena [8]. The aim of this section is to analyze the cyclic period-3 window for rational mappings describing the antiferromagnetic  $Q$ -state Potts model on the Bethe lattice ( $Q < 2$ ) and the antiferromagnetic Ising model with three-site interaction on the Husimi cactus (tree). This window is represented

by the laminar phase with an incorporated chaotic behavior. The transition from the chaotic regime to the period-3 regime occurring through tangent bifurcation (type-I intermittency) [9], as well as subsequence doubling of the period through the type-II intermittency (doubling bifurcation), is considered.

In the presence of external magnetic field, the  $Q$ -site Potts model on the Bethe lattice is specified by the Hamiltonian

$$\mathcal{H} = -J \sum_{(i,j)} \delta(\sigma_i, \sigma_j) - H \sum_i \delta(\sigma_i, Q), \quad (1)$$

where  $\sigma_i = 1, 2, \dots, Q$ ; and  $\delta(x, y)$  is the Kronecker delta; the first and second sums are taken over all of the edges and sites of the lattice, respectively; and  $J < 0$  corresponds to antiferromagnetic pairing. The partition function and magnetization at the central site can be represented as

$$\mathcal{Z} = \sum_{\{\sigma\}} e^{-\frac{\mathcal{H}}{k_B T}}, \quad M = \langle \delta(\sigma_0, Q) \rangle = \mathcal{Z}^{-1} \sum_{\{\sigma\}} \delta(\sigma_0, Q) e^{-\frac{\mathcal{H}}{k_B T}}, \quad (2)$$

where  $k_B$  is the Boltzmann constant (below, we set  $k_B = 1$ ). Cutting the Bethe lattice at the central site into  $\gamma$  identical branches ( $\gamma$  is the coordination number), we represent the partition function in the form

$$\mathcal{Z} = \sum_{\{\sigma_0\}} \exp\left\{\frac{H}{T} \cdot \delta(\sigma_0, Q)\right\} [g_n(\sigma_0)]^\gamma, \quad (3)$$

where  $\sigma_0$  is the central spin and  $g_n(\sigma_0)$  is the contribution of each of the identical branches. Following a known procedure described in [10], we obtain

$$x_n = f_1(x_{n-1}), \quad f_1(x) = \frac{e^{\frac{H}{T}} + (e^{\frac{J}{T}} + Q - 2)x^{\gamma-1}}{e^{\frac{H+J}{T}} + (Q - 1)x^{\gamma-1}},$$

where  $x_n = g_n(\sigma \neq Q)/g_n(\sigma = Q)$ . Using these equations, one can express magnetization via  $x$ .

We study the transition from the chaotic regime to the cyclic period-3 regime through tangent bifurcation. Certain values of the temperature  $T$  and magnetic field  $H$  specify a curve separating the chaotic and period-3 regimes (the mapping in the latter regime has three stable stationary points). In this curve, tangent bifurcation occurs under the condition

$$\begin{cases} f_i^{(3)}(x) = x \\ (f_i^{(3)}(x))' = 1, (i = 1, 2). \end{cases} \quad (4)$$

where  $f^{(3)}(x) = f\{f[f(x)]\}$ . Subsequent bifurcations, responsible for the appearance of a stable cycle with a period of  $3 \times 2^n (n = 2, 3, \dots)$ , correspond to the doubling of the period.

When an  $H = \text{const}$  line intersects only the upper curve (corresponding to Eq. (4) with  $i = 1$ ), the boundaries of the cyclic window are strictly distinguished (tangent

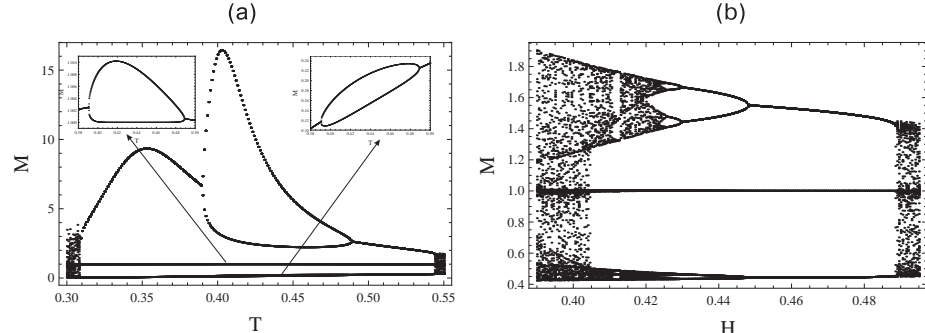


Figure 1: Magnetization in the cyclic period-3 window for the Potts model at  $Q = 1.1$ ,  $J = 1$ , and  $\gamma = 3$  (a) versus the temperature for  $H = 1.24$  (inset shows the details of the modulated period-six phase) and (b) versus the magnetic field for  $T = 1$ .

bifurcation occurs at both edges). This window is represented only by the 3M0 phase (a stable period-3 cycle) (see Fig. 1a). The phase transition between the 3M0 and 3M1 phases, accompanied by a change in symmetry, occurs at the bifurcation points. With a further decrease in the field, new bubbles corresponding to modulated phases with larger periods will appear on bifurcation diagrams. Finally, the chaotic regime, which is localized inside the cyclic period-3 window, will be reached. At the same time, when the magnetization is considered as a function of the temperature  $T$  at a fixed value  $H < 0.1$  or as a function of the magnetic field  $H$  at any fixed temperature, tangent bifurcation occurs only at one edge of the cyclic window [11]. A crisis [12, 13], i.e., the collision of the chaotic attractor with the independent unstable stationary point with a period of 3, occurs at the other edge (see Fig. 1b). In this case, modulated phases with a period of  $3 \times 2^n$  are not localized inside the window (similarity with logistic mapping).

### 3. Magnetization plateaus and frustrated systems

In this section the dynamical (recursive) approach was used to study magnetic properties of a kagome chain. The magnetization plateaus were found at low temperatures and moreover, the kagome chain was separated into four sublattices with different magnetizations. Two of these exhibited plateaus, whereas the others did not. The stability of the system is described by Lyapunov exponents [15] by means of which the exponential rate is measured, at which the adjacent orbits converge or diverge [14, 15]. It is interesting to check whether the maximum Lyapunov exponent has plateaus that coincide with the magnetization one. According to [7] the multiple spin exchanges Hamiltonian can be written as

$$H_{ex} = J_2 \sum_{Pairs} P_2 - J_3 \sum_{Triangles} (P_3 + P_3^{-1}) + J_6 \sum_{Hexagons} (P_6 + P_6^{-1}), \quad (5)$$

where  $P_2$  is the pair transposition operator,  $P_3$  ( $P_6$ ) is the operator making a cyclic rearrangement in the triangle (hexagon). The explicit expression of pair transposi-

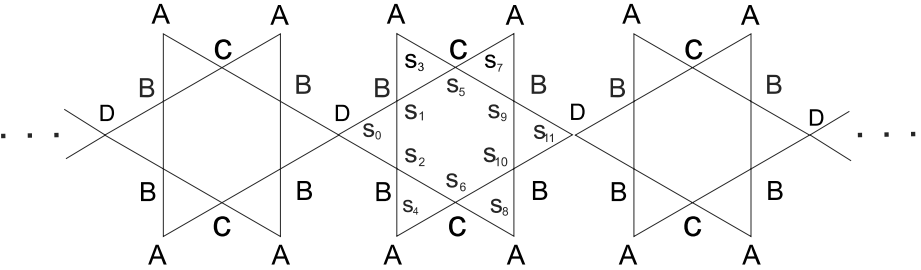


Figure 2: Sublattices on the kagome chain.

tion operator  $P_{ij}$  was been given by Dirac

$$P_2 \equiv P_{ij} = \frac{1}{2} (1 + \boldsymbol{\sigma}_i \boldsymbol{\sigma}_j), \quad (6)$$

where  $\boldsymbol{\sigma}_i$  is the Pauli matrix, acting on the spin at the  $i$ -th site. The expressions for  $P_3, P_4, \dots$  can be calculated using (6). By using these expressions one can rewrite the Heisenberg Hamiltonian in terms of Pauli matrices. By taking into account that in a strong external magnetic field directed along the z-axis the contribution from x and y spin component will be negligible and the only relevant contribution will come from the z component (which can effectively take values  $s_z = \pm 1$ ), we may consider an Ising model instead of Heisenberg one. By using expressions for  $P_3$ , and  $P_6$  and by substituting the Pauli matrix with  $s_z$  we get the Ising approximation of the Heisenberg Hamiltonian:

$$H = \frac{J_2}{2} \sum_{Pairs} s_i s_j - \frac{J_3}{2} \sum_{Triangles} (s_i s_j + s_j s_k + s_k s_i) + \frac{J_6}{2} \sum_{Hexagons} H^{(6)} - h \sum_i s_i, \quad (7)$$

where  $H^{(6)}$  represents the six particle exchange term in each hexagon:

$$H^{(6)} = \frac{1}{8} \left( \sum_{\mu < \nu} s_\mu s_\nu + \sum_{\mu < \nu < \lambda < \rho} s_\mu s_\nu s_\lambda s_\rho + s_1 s_2 s_5 s_6 s_9 s_{10} \right) \quad (8)$$

where the first sum goes over all pairs in the hexagon, and the second one goes over all quartets in the hexagon.

To obtain recursion relations for the partition function one can separate the kagome ladder into two identical parts (branches) and firstly perform a summation over all spin configurations on each branch, and secondly sum over the central spin variable (see Fig. 2). The summation on each branch yields the same result and such a term only depends on the value of central spin:

$$Z = \sum_{s_0} e^{\frac{h}{T} s_0} g_n^2(s_0) = e^{\frac{h}{T}} g_n^2(+) + e^{-\frac{h}{T}} g_n^2(-), \quad (9)$$

where  $g_n(s_0)$  denotes the contribution of each branch. The expression for  $g_n(s_0)$  can be written ( $s_1 \dots s_{11}$ , see Fig. 2) in the form:

$$g_n(s_0) = \sum_{s_1, s_3 \dots s_{11}} e^{k(s_0, \dots, s_{11})} g_{n-1}(s_{11}), \quad (10)$$

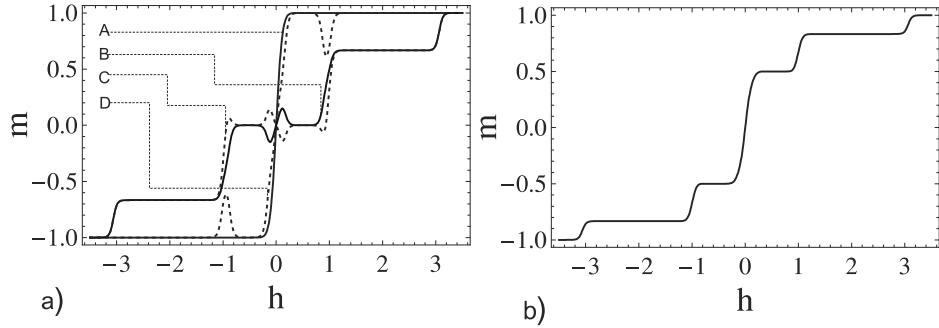


Figure 3: Magnetization curves for  $J_2 = 2mK, J_3 = 1.5mK, J_6 = 2mK, T = 0.04mK$  for a) sublattice  $A, B, C, D$  b) Average magnetization of all sublattices.

where and  $n$  is the number of generations and the expression for  $k(s_0, \dots s_{11})$  has the following form:

$$\begin{aligned} k(s_0, \dots s_{11}) &= -\frac{J_2}{2T} \sum_{18 \text{ pairs}} s_i s_j + \frac{J_3}{2T} \sum_{6 \text{ triangles}} (s_i s_j + s_j s_k + s_k s_i) - \\ &- \frac{J_6}{2T} \cdot H^{(6)} + \frac{h}{T} \sum_{i=1}^{11} s_i. \end{aligned} \quad (11)$$

The recursion relation is obtained by introducing a new variable  $x_n = g_n(+) / g_n(-)$ :

$$x_n = \frac{K(+,+)x_{n-1} + K(+,-)}{K(-,+)x_{n-1} + K(-,-)}. \quad (12)$$

where

$$K(s_1, s_{12}) = \sum_{s_2, s_3, \dots, s_{11}} e^{k(s_0, \dots, s_{11})}. \quad (13)$$

By using this equations one can write for the magnetization of the central vertex

$$m = \frac{e^{\frac{h}{T}} g_n^2(+) - e^{-\frac{h}{T}} g_n^2(-)}{e^{\frac{h}{T}} g_n^2(+) + e^{-\frac{h}{T}} g_n^2(-)} = \frac{e^{\frac{2h}{T}} x_n^2 - 1}{e^{\frac{2h}{T}} x_n^2 + 1}. \quad (14)$$

At the same way one can obtain the magnetizations of the non-central vertexes. Because of the symmetry of the Hamiltonian, the values of magnetization for some spins are equal: we have in general (See Fig. 2),

$$\begin{aligned} m(s_3) &= m(s_4) = m(s_7) = m(s_8) && - A \\ m(s_1) &= m(s_2) = m(s_9) = m(s_{10}) && - B \\ && m(s_5) = m(s_6) && - C \\ m(s_0) &= m(s_{11}) && - D \end{aligned} \quad (15)$$

In Figure 3a magnetization curves are plotted for different sites. As it can be seen from the figures, the magnetization functions have plateaus only for the sublattices B and C. In magnetisation curves there are regions with unusual nonmonotonous

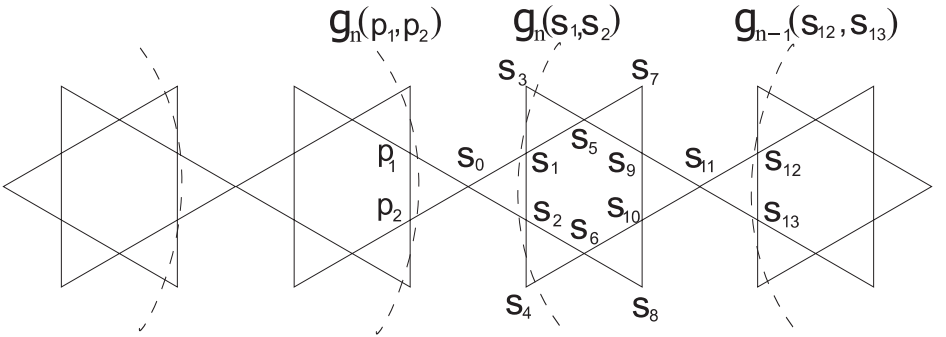


Figure 4: The kagome chain.

magnetisation behaviour. In Figure 3b plotted the average magnetization of all sublattices and the figure show that the curve is smooth and monotonous as it should be.

It is interesting to calculate the Lyapunov exponent near plateaus but one cannot use recurrent function (12) because it is related to  $s_1$  site. To obtain the recursion relation for the partition function that is related to  $s_2$  site one can separate the kagome chain into two identical parts as shown in Figure 4:

$$Z = \sum_{s_1, s_2, p_1, p_2} N_{p_1, p_2}^{s_1, s_2} \cdot g_n(s_1, s_2) \cdot g_n(p_1, p_2), \quad (16)$$

where

$$N_{p_1, p_2}^{s_1, s_2} = \sum_{s_0} e^{\left\{ \frac{h}{T}(s_1 + s_2 + s_0 + p_1 + p_2) + \frac{J_3 - J_2}{2T} (H^{(2,3)}(s_0, s_1, s_2) + H^{(2,3)}(s_0, p_1, p_2)) - \frac{J_6}{2T} H^{(6)} \right\}} \quad (17)$$

and the contribution of each branch is denoted by  $g_n(s_1, s_2)$ . The recursion relations for  $g_n$  can be obtained by performing eleven ( $s_3 \dots s_{13}$ , see Fig. 4) summations in the kagome chain:

$$g_n(s_1, s_2) = \sum_{s_{12}, s_{13}} K_{s_{12}, s_{13}}^{s_1, s_2} \cdot g_{n-1}(s_{12}, s_{13}), \quad (18)$$

where  $K_{s_{12}, s_{13}}^{s_1, s_2}$  is as follows

$$K_{s_{12}, s_{13}}^{s_1, s_2} = \sum_{s_3 \dots s_{11}} e^{\frac{J_3 - J_2}{2T} \sum_{6 \text{ Triangle}} H^{(2,3)} - \frac{J_6}{2T} H^{(6)} + \frac{h}{T} \sum_{i=3}^{13} s_i}. \quad (19)$$

Since  $K_{s_{12}, s_{13}}^{s_1, s_2} = K_{s_{12}, s_{13}}^{s_2, s_1}$ ,  $K_{s_{12}, s_{13}}^{s_1, s_2} = K_{s_{13}, s_{12}}^{s_1, s_2}$  one can show that  $g_n(+, -) = g_n(-, +)$  and, hance, the recurrence relations are two-dimensional. By introducing  $x_n = g_n(+, +)/g_n(-, -)$  and  $y_n = g_n(+, -)/g_n(-, -)$  the recursion relations may be written in the following form:

$$\begin{aligned} x_n = \Phi(x_{n-1}, y_{n-1}), \quad \Phi(x, y) &= \frac{K_{+,+}^{+,+} x + 2K_{+,-}^{+,+} y + K_{-,-}^{+,+}}{K_{+,-}^{-,-} x + 2K_{+,-}^{-,-} y + K_{-,-}^{-,-}}, \\ y_n = \Psi(x_{n-1}, y_{n-1}), \quad \Psi(x, y) &= \frac{K_{+,+}^{+,-} x + 2K_{+,-}^{+,-} y + K_{-,-}^{+,-}}{K_{+,-}^{-,+} x + 2K_{+,-}^{-,+} y + K_{-,-}^{-,+}}. \end{aligned} \quad (20)$$

The magnetization can be expressed in terms of  $x_n, y_n$  with due regard for (16) and (17)

Relations (20) permit the calculation of Lyapunov exponents near the plateaus. At first we shall give definition of Lyapunov exponent for an one-dimensional case. For display  $x_{n+1} = f(x_n)$  Lyapunov exponent characterizes exponential divergence of two next points after  $n$  iterations [14, 15]. By definition in the two-dimensional space Lyapunov exponent defined as

$$\lambda_{1,2} = \lim_{N \rightarrow \infty} \frac{1}{N} \ln (\text{eigenvalues}\{\mathbf{\Lambda}(x_1, y_1) \cdot \mathbf{\Lambda}(x_2, y_2) \cdots \mathbf{\Lambda}(x_N, y_N)\}), \quad (21)$$

where  $\mathbf{\Lambda}(x_i, y_i)$  is Jacobian matrix evaluated at the  $(x_i, y_i)$  point

$$\mathbf{\Lambda}(x_i, y_i) = \left( \begin{array}{cc} \frac{\partial \Phi}{\partial x} & \frac{\partial \Phi}{\partial y} \\ \frac{\partial \Psi}{\partial x} & \frac{\partial \Psi}{\partial y} \end{array} \right) \Big|_{x_i, y_i}. \quad (22)$$

One of the basic features of chaos is the sensitive dependence on initial conditions and the Lyapunov exponents provide quantitative measures of response sensitivity of a dynamical system to small changes in initial conditions. For a chaotic orbit at least one Lyapunov exponents is positive, implying exponential divergence of nearby orbits, while in the case of regular orbits all Lyapunov exponents are zero. Therefore, the presence of positive Lyapunov exponent is a signature of chaotic behavior. Usually the computation of only the maximal Lyapunov exponent is sufficient for determining the nature of an orbit, because it guarantees that the orbit is chaotic. The results of calculation are shown in Fig. 5 with the corresponding magnetization function: it is seen in the figures that the maximum Lyapunov exponent also exhibits plateaus. Moreover, for the maximum Lyapunov exponent the location of magnetization plateaus coincide with those of magnetization curves.

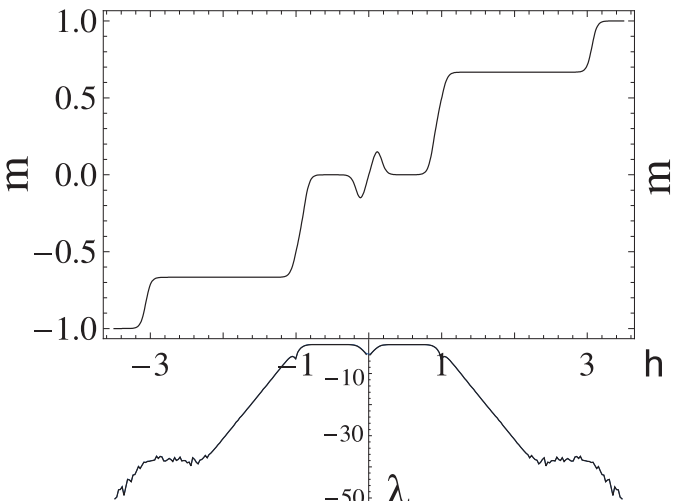


Figure 5: Coincidence of magnetization plateaus and the maximum of Lyapunov exponent.

## 4. Thermal entanglement on a triangulated Kagome lattice

The efforts aimed at better understanding of the aforementioned phenomena stimulated an intensive search of two-dimensional geometrically frustrated topologies. From this perspective, the most interesting geometrically frustrated topologies are the magnetic materials in form of two-dimensional isostructural polymeric coordination compounds  $\text{Cu}_9\text{X}_2(\text{cpa})_6 \cdot n\text{H}_2\text{O}$  ( $\text{X} = \text{F}, \text{Cl}, \text{Br}$  and  $\text{cpa} = \text{carboxypentonic acid}$ ) [16].

We consider the spin- $\frac{1}{2}$  Ising-Heisenberg model on triangulated kagome lattice (TKL) (Fig. 6) consisting of two types of sites ( $a$  and  $b$ ). Since the exchange coupling between  $\text{Cu}^{2+}$  ions are almost isotropic, the application of the  $XXX$  Heisenberg model is more appropriate. There is a strong Heisenberg  $J_{aa}$  exchange coupling between trimeric sites of  $a$  type and weaker Ising-type one ( $J_{ab}$ ) between trimeric  $a$  and monomeric  $b$  ones. Thus, the kagome lattice of the Ising spins (monomers) contains inside of each triangle unit a smaller triangle of the Heisenberg spins (trimer). The Hamiltonian can be written as follows:

$$\mathcal{H} = J_{aa} \sum_{(i,j)} \mathbf{S}_i^a \mathbf{S}_j^a - J_{ab} \sum_{(k,l)} (\mathbf{S}^z)_k^a \cdot (\mathbf{S}^z)_l^b - H \sum_{i=1}^{2N} 3[(\mathbf{S}^z)_j^a + \frac{1}{2}(\mathbf{S}^z)_j^b], \quad (23)$$

where  $\mathbf{S}^a = \{S_x^a, S_y^a, S_z^a\}$  is the Heisenberg spin- $\frac{1}{2}$  operator,  $S^b$  is the Ising spin.  $J_{aa} > 0$  corresponds to antiferromagnetic Heisenberg coupling and  $J_{ab} > 0$  to ferromagnetic Ising-Heisenberg one. The first two summations run over  $a - a$  and  $a - b$  nearest neighbors respectively and the last sum incorporates the effect of uniform magnetic field (we have assumed that the total number of sites is  $3N$ ).

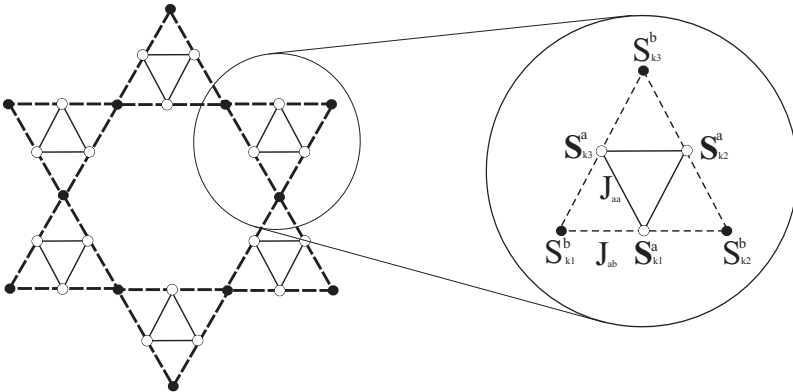


Figure 6: A cross-section of TKL structure. Solid lines represent the intra-trimer Heisenberg interactions  $J_{aa}$ , while the broken ones label monomer-trimer Ising interactions  $J_{ab}$ . The circle marks  $k$ -th cluster (Heisenberg trimer).  $\mathbf{S}_k^a$  presents the Heisenberg and  $S_k^b$  the Ising spins.

Using Gibbs-Bogoliubov inequality [17]

$$F \leq F_0 + \langle \mathcal{H} - \mathcal{H}_0 \rangle_0, \quad (24)$$

where  $\mathcal{H}$  is the real Hamiltonian which describes the system and  $\mathcal{H}_0$  is the trial one.  $F$  and  $F_0$  are free energies corresponding to  $\mathcal{H}$  and  $\mathcal{H}_0$  respectively and  $\langle \dots \rangle_0$  denotes the thermal average over the ensemble defined by  $\mathcal{H}_0$ . Following [18] we introduce the trial Hamiltonian in the following form:

$$\mathcal{H}_0 = \sum_{k \in trimers} \mathcal{H}_{c_0}, \quad (25)$$

$$\mathcal{H}_{c_0} = \lambda_{aa} (\mathbf{S}_{k_1}^a \mathbf{S}_{k_2}^a + \mathbf{S}_{k_2}^a \mathbf{S}_{k_3}^a + \mathbf{S}_{k_1}^a \mathbf{S}_{k_3}^a) - \sum_{i=1}^3 \left[ \gamma_a (S^z)_{k_i}^a + \frac{\gamma_b}{2} (S^z)_{k_i}^b \right]. \quad (26)$$

Using the fact that in terms of (26)  $\mathbf{S}^a$  and  $\mathbf{S}^b$  are statistically independent, one obtains  $\langle \mathbf{S}^a \cdot \mathbf{S}^b \rangle_0 = \langle \mathbf{S}^a \rangle_0 \cdot \langle \mathbf{S}^b \rangle_0$ . Besides, taking into account that  $\langle (S^z)^a \rangle_0 = m_a$  (single  $a$ -site magnetization),  $\langle (S^z)^b \rangle_0 = m_b$  (single  $b$ -site magnetization), we obtain the following expression:

$$f \leq f_0 + (J_{aa} - \lambda_{aa}) \langle \mathbf{S}_{k_1}^a \mathbf{S}_{k_2}^a + \mathbf{S}_{k_2}^a \mathbf{S}_{k_3}^a + \mathbf{S}_{k_1}^a \mathbf{S}_{k_3}^a \rangle_0 - 6J_{ab}m_a m_b - 3Hm_a - \frac{3Hm_b}{2} + 3\gamma_a m_a + \frac{3\gamma_b m_b}{2}. \quad (27)$$

Minimizing the RHS of (27) in order to  $\gamma_a$ ,  $\gamma_b$  and  $\lambda_{aa}$  and using the fact, that  $\frac{\partial f_0}{\partial \gamma_a} = -3m_a$ ,  $\frac{\partial f_0}{\partial \gamma_b} = -3/2m_b$ ,  $\frac{\partial f_0}{\partial \lambda_{aa}} = \langle \mathbf{S}_{k_1}^a \mathbf{S}_{k_2}^a + \mathbf{S}_{k_2}^a \mathbf{S}_{k_3}^a + \mathbf{S}_{k_1}^a \mathbf{S}_{k_3}^a \rangle_0$ , we obtain the following values for the variational parameters:  $\lambda_{aa} = J_{aa}$ ,  $\gamma_a = 2J_{ab}m_b + H$ ,  $\gamma_b = 4J_{ab}m_a + H$ . Parameters  $\gamma_a$  and  $\gamma_b$ , which have a meaning of a magnetic field, are interconnected, which is the consequence of its' apparent self-consistency.

As for defined above  $a$ - and  $b$ -single site magnetizations we obtain:

$$m_a = -\frac{1}{3} \frac{\partial f_0}{\partial \gamma_a} = \frac{1}{6} \frac{3 \sinh\left(\frac{3\gamma_a}{2T}\right) + 2e^{\frac{3\lambda_{aa}}{2T}} \sinh\left(\frac{\gamma_a}{2T}\right) + \sinh\left(\frac{\gamma_a}{2T}\right)}{\cosh\left(\frac{3\gamma_a}{2T}\right) + 2e^{\frac{3\lambda_{aa}}{2T}} \cosh\left(\frac{\gamma_a}{2T}\right) + \cosh\left(\frac{\gamma_a}{2T}\right)}, \quad (28)$$

$$m_b = -\frac{\partial f_0}{\partial \gamma_b} = \frac{1}{2} \tanh\left(\frac{\gamma_b}{2T}\right). \quad (29)$$

We study *concurrence*  $C(\rho)$ , to quantify pairwise entanglement [19], defined as

$$C(\rho) = \max\{\lambda_1 - \lambda_2 - \lambda_3 - \lambda_4, 0\}, \quad (30)$$

where  $\lambda_i$  are the square roots of the eigenvalues of the corresponding operator for the density matrix

$$\tilde{\rho} = \rho_{12} (\sigma_1^y \otimes \sigma_2^y) \rho_{12}^* (\sigma_1^y \otimes \sigma_2^y) \quad (31)$$

in descending order. Since we consider pairwise entanglement, we use reduced density matrix  $\rho_{12} = \text{Tr}_3 \rho$ . We can calculate the concurrence for each of them on cluster level individually in effective magnetic field. In our case the density matrix has the following form

$$\rho = \frac{1}{Z_{0a}} \sum_{k=1}^8 \exp(-E_k/T) |\psi_k\rangle \langle \psi_k|, \quad (32)$$

$E_k$ ,  $|\psi_k\rangle$  and  $Z_{0a}$  are taken from equations (7), (8) and (9) respectively. The construction process of matrix (31) does not depend whether  $\gamma_a$  is effective or real

magnetic field, although the presence of effective field  $\gamma_a$  plays crucial role for the self-consistent solution. Here we skip the specific details and provide the result of final calculations of the matrix  $\rho_{12}$ , taking into account that the Hamiltonian  $\mathcal{H}_{c_0}$  is translationary invariant with a symmetry  $[S_z, \mathcal{H}_{c_0}] = 0$  ( $S_z = \sum_{k=1}^3 (S_z)_{k_i}^a$ ). Hence

$$\rho_{12} = \begin{pmatrix} u & 0 & 0 & 0 \\ 0 & w & y & 0 \\ 0 & y^* & w & 0 \\ 0 & 0 & 0 & v \end{pmatrix}, \quad (33)$$

where  $u, v, w$  and  $y$  are some functions of  $\gamma_a, \lambda_{aa}$  and  $T$ . The concurrence  $C(\rho)$  of such a density matrix has the following form:

$$C(\rho) = \frac{2}{Z} \max(|y| - \sqrt{uv}, 0). \quad (34)$$

Finally, we consider transcendental equations (28) and (29) by taking into account the values of variational parameters:  $\lambda_{aa} = J_{aa}$ ,  $\gamma_a = 2J_{ab}m_b + H$ ,  $\gamma_b = 4J_{ab}m_a + H$ , and, therefore, one can use these parameters to calculate  $C(\rho)$ . First, we study the behavior of  $C(\rho)$  at  $H = 0$ . The temperature dependence of  $C(\rho)$  is shown in figure 7a.

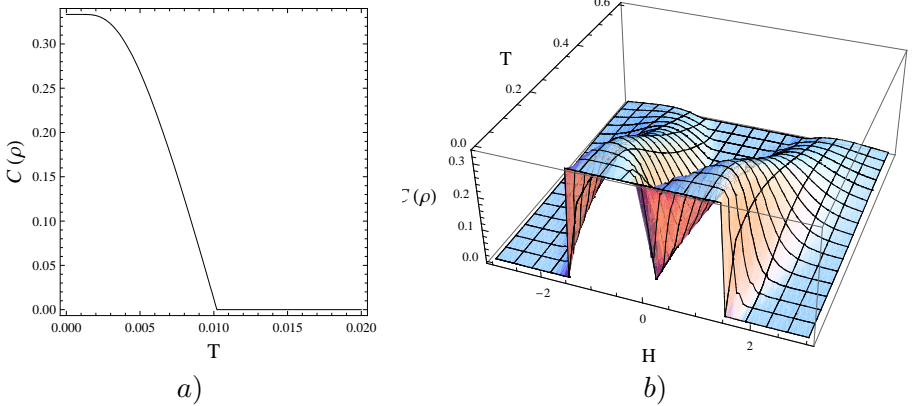


Figure 7: a) Concurrence  $C(\rho)$  versus temperature field for  $J_{aa} = 1$ ,  $\alpha = 0.025$  and  $H = 0$ , b) Concurrence  $C(\rho)$  versus temperature  $T$  and external magnetic field  $H$  for  $J_{aa} = 1$ ,  $\alpha = 0.025$ .

Another important observation is that threshold temperature at which entanglement  $C(\rho)$  disappear is identical to the critical temperature  $T_c$  of second order phase transition between ordered and disordered phases. This implies that the concurrence vanishes precisely at  $T_c$ , the same temperature of specific heat discontinuity. This is the consequence of the fact that at  $T_c$  the system undergoes order-disorder phase transition and the second term in  $\gamma_a$  vanishes, too ( $m_b = 0$ , when  $H = 0$  and  $T \geq T_c$ ). This factor implies the strong relationship between magnetic and entanglement properties of the system. In figure 7b we present the three dimensional plot of the concurrence as a function of the temperature and external magnetic field.

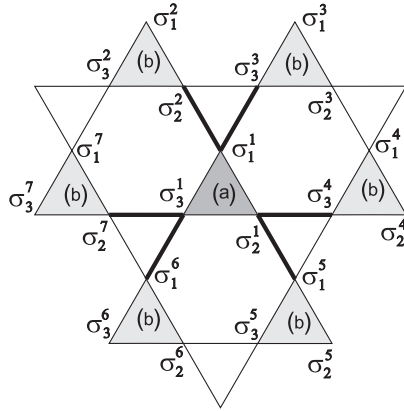


Figure 8: Kagome lattice.

## 5. Magnetic properties and concurrence for ${}^3\text{He}$

In the present section mean-field like approach, based on the Gibbs-Bogoliubov inequality (24), was used to study entanglement and magnetic properties of a two dimensional kagome lattice. The key result of the section is concentrated on the comparison of specific (peaks and plateaus) features in magnetization, susceptibility and thermal entanglement properties in the above mentioned model using variational mean-field like Gibbs-Bogoliubov inequality.

According [6] the third layer of  ${}^3\text{He}$  system is kagome lattice (see Fig 8) and Hamiltonian for kagome lattice can be written in the following form:

$$H = \sum_{\text{Triangles}} \left[ \frac{J_2 - J_3}{2} (\boldsymbol{\sigma}_i \boldsymbol{\sigma}_j + \boldsymbol{\sigma}_j \boldsymbol{\sigma}_k + \boldsymbol{\sigma}_k \boldsymbol{\sigma}_i) - \frac{h}{2} (\sigma_i^z + \sigma_j^z + \sigma_k^z) \right]. \quad (35)$$

We introduce the trial Hamiltonian  $H_0$  as a set of noninteracting clusters (triangles) on two sublattices in different external self-consistent fields:

$$H_0 = \sum_{\Delta_i} H_0^{(i)}, \quad (36)$$

where

$$H_0^{(i)} = \lambda \times (\boldsymbol{\sigma}_1^i \boldsymbol{\sigma}_2^i + \boldsymbol{\sigma}_2^i \boldsymbol{\sigma}_3^i + \boldsymbol{\sigma}_3^i \boldsymbol{\sigma}_1^i) - \gamma_v \times [(\sigma_1^i)^z + (\sigma_2^i)^z + (\sigma_3^i)^z],$$

where  $\lambda$  and  $\gamma_v$  variational parameters, and the index of summation  $\Delta_i$  labels different non-interacting rectangles (see Fig. 8 ) and

$$\begin{aligned} \gamma_v &= \gamma_a && \text{for sublattice (a),} \\ \gamma_v &= \gamma_b && \text{for sublattice (b).} \end{aligned}$$

It should be emphasized that in trial Hamiltonian spins  $\boldsymbol{\sigma}_k^i$  of the  $\Delta_i$ -th triangle do not interact with the spins  $\boldsymbol{\sigma}_k^j$  of the  $\Delta_j$  triangle if  $i \neq j$ , therefore these spins are

statistically independent. The real Hamiltonian  $H$  (35) can be represented in the following form

$$H = \sum_{\Delta_i} H^{(i)}, \quad (37)$$

where  $H^{(i)}$  is the contribution of spins on the single triangle in real Hamiltonian  $H$  and index of summation  $\Delta_i$  runs over the different triangles (see Fig. 8, grey triangles). Terms of real Hamiltonian  $\sigma_1^i \sigma_2^i + \sigma_2^i \sigma_3^i + \sigma_3^i \sigma_1^i$  must be included in  $H^{(i)}$ , but terms like  $\sigma_a^i \sigma_b^j$  (see Fig. 8 tick lines) should be included both in  $H^{(i)}$  and  $H^{(j)}$ . Consequently,  $H^{(i)}$  has the following form:

$$H^{(i)} = \frac{J_2 - J_3}{2} \left( \alpha^{(i)} + \sum_{a=2,3} \frac{\sigma_1^i \sigma_a^j}{2} + \sum_{a=1,3} \frac{\sigma_2^i \sigma_a^k}{2} + \sum_{a=1,2} \frac{\sigma_3^i \sigma_a^l}{2} \right) - h \sum_{a=1}^3 (\sigma_a^i)^z, \quad (38)$$

where

$$\alpha^{(i)} = \sigma_1^i \sigma_2^i + \sigma_2^i \sigma_3^i + \sigma_3^i \sigma_1^i. \quad (39)$$

One can rewrite Gibbs-Bogoliubov inequality for each sublattice as follows:

$$\begin{aligned} f_v &\leq (f_0)_v + \left( \frac{J_2 - J_3}{2} - \lambda \right) \langle \alpha \rangle_0 + \frac{J_2 - J_3}{4} 6(2m_a 2m_b) - (h - \gamma_v) 6m_v. \\ \gamma_a &= h - (J_2 - J_3)m_b, \quad \gamma_b = h - (J_2 - J_3)m_a. \end{aligned} \quad (40)$$

Minimizing the right hand side of (40) in order to  $\gamma_a, \gamma_b$  and  $\lambda$  and using the fact, that  $\frac{\partial f_0}{\partial \lambda} = \langle \alpha \rangle_0$  and  $\frac{\partial f_0}{\partial \gamma_v} = -6m_v$  we obtain the following values for the variational parameters:

$$\lambda = \frac{J_2 - J_3}{2}; \quad \gamma_a = h - (J_2 - J_3)m_b; \quad \gamma_b = h - (J_2 - J_3)m_a. \quad (41)$$

According to (41) the Hamiltonian of sublattice (*a*) depends on  $m_b$  through  $\gamma_a$  and vice versa. For defined above magnetization we obtain the following expression:

$$m_a = \frac{1}{6} \cdot \frac{3 \sinh \left( \frac{3\gamma_a}{T} \right) + \sinh \left( \frac{\gamma_a}{T} \right) + 2e^{\left( \frac{6\lambda}{T} \right)} \sinh \left( \frac{\gamma_a}{T} \right)}{\cosh \left( \frac{3\gamma_a}{T} \right) + \cosh \left( \frac{\gamma_a}{T} \right) + 2e^{\left( \frac{6\lambda}{T} \right)} \cosh \left( \frac{\gamma_a}{T} \right)}, \text{ and } \gamma_a = h - (J_2 - J_3)m_b. \quad (42)$$

The dependance of magnetization  $m_a$  from external magnetic field  $h$  can be found by solving the this recursive equation for each value of magnetic field  $h$ . At relatively high temperatures the recursive equation has one stable solution and therefore magnetization curves of sublattices (*a*) and (*b*) coincide (see Fig. 9(a)). With decreasing temperature the solution of recursive equation ceases to be stable and, therefore, the magnetization of different sublattices are no longer equal. The partially saturated phase emerges in form of the magnetization plateaus (see Fig. 9(b) for  $T = 0.01 \text{ mK}$ ,  $J_2 = 3 \text{ mK}$ ,  $J_3 = 2.5 \text{ mK}$ ), which can be associated with a staggered magnetization or short range antiferromagnetism (AF) in frustrated kagome geometry. Indeed, the appearance of plateaus in magnetization curve at  $m = \pm 1/6$  can be explained as stability of trimeric states in available  $(\uparrow\downarrow\downarrow, \uparrow\uparrow\downarrow, \downarrow\downarrow\uparrow)$  and  $(\uparrow\downarrow\downarrow, \downarrow\uparrow\downarrow, \uparrow\downarrow\downarrow)$  configurations.

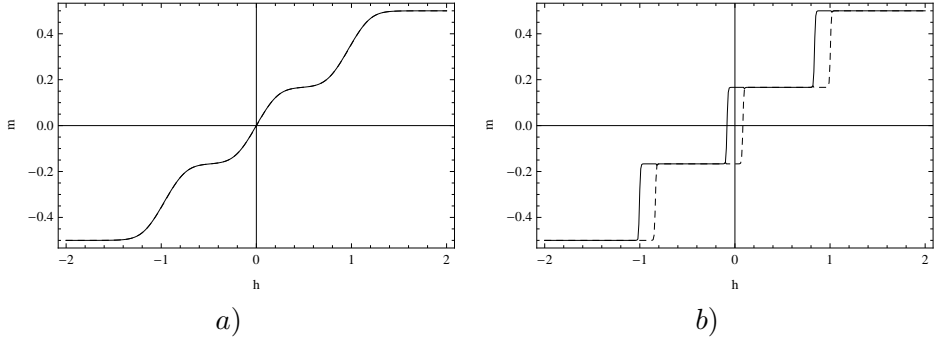


Figure 9: Magnetization  $m_a$  versus external magnetic field  $h$  for  $J_2 = 3 \text{ mK}$ ,  $J_3 = 2.5 \text{ mK}$ . at a)  $T=0.15 \text{ mK}$  b)  $T=0.01 \text{ mK}$ .

It is curious to discuss some similarities of statistical and quantum characteristics of our system. We consider magnetization as a statistical characteristic. In figure 10(a) plotted the magnetization as a function of the coupling constant  $J_2$  (for fixed value of  $J_3 = 2.5 \text{ mK}$ ) and the external field  $h$ , at a relatively high temperature  $T = 0.2 \text{ mK}$ . As a quantum characteristic we consider entanglement (concurrence  $C(\rho)$ ). In figure 10(b) the concurrence as a function of the  $J_2$  ( $J_3 = 2.5 \text{ mK}$ ) is shown for the same value of temperature. Our calculations show that the magnetic characteristics is similar to that of bipartite entanglement. Indeed, comparison of figures 10(a) and 10(b) shows that regions corresponding to the magnetization plateaus, coincide with the plateaus on concurrence plot.

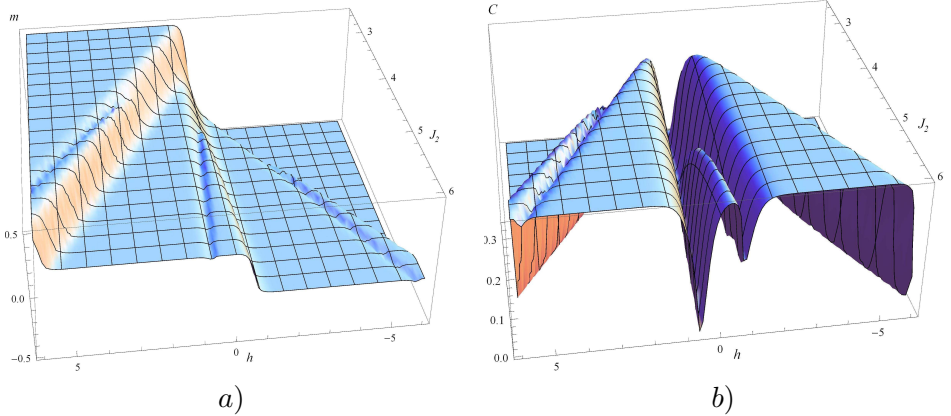


Figure 10: Dependence for (a) magnetization  $m$  and (b) concurrence  $C(\rho)$  versus the magnetic field  $h$  and the coupling constant  $J_2$  at  $J_3 = 2.5 \text{ mK}$  and  $T = 0.2 \text{ mK}$ .

## 6. Conclusions

A cyclic period-3 window has been studied in the antiferromagnetic Potts model on the Bethe lattice. We have analyzed the mechanism of the transition from the chaotic regime to the cyclic period-3 window through tangent bifurcation followed by the doubling cascade  $3 \times 2^n (n = 2, 3, \dots)$ . In the present paper the theory of dynamical systems has been used to study magnetization on the kagome chain. Exact recursion relations have been derived for the partition function. The magnetization curves for different temperatures and exchange parameters were obtained and the kagome chain was observed to split into four sublattices with different magnetizations. A multidimensional mapping was deduced to study the maximum Lyapunov exponent near the plateaus and it was shown that the location of plateaus on the maximal Lyapunov exponent and for magnetization was the same. We found strong correlations between magnetic properties and quantum entanglement in spin- $\frac{1}{2}$  Ising-Heisenberg model on triangulated kagome lattice, which has been proposed to understand a frustrated magnetism of the series of  $\text{Cu}_9\text{X}_2(\text{cpa})_6 \cdot n\text{H}_2\text{O}$  polymeric coordination compounds. We also find strong correlations between magnetic properties and quantum entanglement in the Heisenberg model with two-, and three-site exchange interactions in strong magnetic field on the kagome lattice, which correspond to the third layer of fluid  $^3\text{He}$  absorbed on the surface of graphite. We adopted variational mean-field-like treatment (based on the Gibbs-Bogoliubov inequality) of separate clusters in effective magnetic fields and studied magnetic properties and concurrence as a measure of pairwise thermal entanglement. We have found, that in the antiferromagnetic region behavior of the concurrence coincides with the magnetization one. The comparison of magnetization and concurrence shows that regions corresponding to the magnetization plateaus, coincide with the plateaus on concurrence plot.

## References

- [1] L. Amico, R. Fazio, A. Osterloh, V. Vedral, Rev. Mod. Phys. **80**, 517 (2008); R. Horodecki, P. Horodecki, M. Horodecki, K. Horodecki, Rev. Mod. Phys. **81**, 865 (2009); O. Gühne and G. Tóth, Phys. Rep. **474**, 1 (2009).
- [2] M. Suzuki, Prog. Theor. Phys. **46**, 1337 (1971); M. Suzuki, Prog. Theor. Phys. **56**, 1454 (1976); M. Suzuki, Phys. Rev. B **31**, 2957 (1985); M. Suzuki, Commun. Math. Phys. **51**, 183 (1976); **57**, 193 (1977); N.S. Ananikian, S.S. Poghosyan, Statphys 23 (2007, Genova, Italy), Programme and Abstract, p. 71.
- [3] K. Kubo and T. Momoi, Z. Phys. B: Condens. Matter **103**, 485 (1997); K. Hida, J. Phys. Soc. Jpn. **63**, 2359 (1994); K. Okamoto T. Tonegawa, T. Nakao, and M. Kaburagi, J. Phys. Soc. Jpn. **65**, 3317 (1996); K. Totsuka, Phys. Rev. B **57**, 3454 (1998); T. Sakai and M. Takahashi, ibid. **57**, R3201 (1998); F. Mila, Eur. Phys. J. B **6**, 201 (1998).
- [4] M. Siqueira, J. Nyeki, B. Cowan, and J. Saunders, Phys. Rev. Lett. **76**, 1884 (1996); K. Ishida, M. Morishita, K. Yawata, and H. Fukuyama, Phys. Rev.

Lett. **79**, 3451 (1997); M. Roger, C. Baüerle, Yu.M. Bunkov, A.-S. Chen, and H. Godfrin, Phys. Rev. Lett. **80**, 1308 (1998).

- [5] J. Delrieu, M. Roger, and J.H. Hetherington, J. Low Temp. Phys. **40**, 71 (1980); M. Roger, Phys. Rev. B **30**, 6432 (1984); B. Bernu, D. Ceperley, and C. Lhuillier, J. Low Temp. Phys. **89**, 589 (1992).
- [6] M. Roger, J. H. Hetherington, J. M. Delrieu, Magnetism in solid  $^3\text{He}$ , Rev. Mod. Phys. **55**, 1 (1983).
- [7] A. Arakelyan, V. R. Ohanyan, L. N. Ananikyan N. S. Ananikian and M. Roger, Phys. Rev. B **67** 024424 (2003); V. V. Hovhannisyan, L. N. Ananikyan, and N. S. Ananikian, Int. J. of Mod. Phys. B **21**, 3567 (2007); V. V. Hovhannisyan and N. S. Ananikian, Phys. Lett. A **372**, 3363(2008).
- [8] R. J. Baxter, Exactly Solved Models in Statistical Mechanics (Academic Press, New York, 1982; Mir, Moscow, 1985); F. Y. Wu, Rev. Mod. Phys. **54**, 235 (1982); N. S. Ananikyan and A. Z. Akheyyan, Sov. Phys. JETP **80**, 105 (1995).
- [9] P. Manneville and Y. Pomeau, Phys. Lett. A **75**, 1 (1979); Physica D 1, 219 (1980); A. E. Hramov, A. A. Koronovskii, and M. K. Kurovskayaet, Phys. Rev. E **76**, 2 (2007).
- [10] L. N. Ananikyan, Int. J. Mod. Phys. B **21**, 755 (2007).
- [11] L. N. Ananikyan, N. S. Ananikian, and L. A. Chakhmakhchyan, Fractals **18**, 371 (2010).
- [12] C. Grebogi, E. Ott, and J. A. Yorke, Physica D **7**, 181 (1983).
- [13] S. Zambrano, I. P. Marino, and M. A. F. Sanjun, New J. Phys. **11**, 023025 (2009).
- [14] V. I. Oseledec, A multiplicative ergodic theorem,Trans. Moskow Math. Soc. **19**, 197 (1968); J. P. Eckmann and D. Ruelle, Ergodic theory of chaos and strange attractors, Rev. Mod. Phys. **57**, 617 (1985); İ. Birol and A. Hacinliyan, Approximately conserved quantity in the He'non-Heiles problem, Phys. Rev. E **52**, 4750 (1995).
- [15] G. Casati, B. V. Chirikov, Quantum chaos: between order and disorder (Cambridge University Press, 1995).
- [16] R. E. Norman, N. J. Rose and R. E. Stenkamp, J. Chem. Soc.: Dalton Trans. 2905 (1987); M. Gonzalez, F. Cervantes-Lee and L. W. Haar, Mol. Cryst. Liq. Cryst. **233**, 317 (1993); S. Maruti and L. W. ter Haar, J. Appl. Phys. **75**, 5949 (1994); S. Ateca, S. Maruti, and L. W. ter Haar, J. Magn. Magn. Mater. **147**, 398 (1995).
- [17] N.N. Bogoliubov J. Phys. (USSR) **11**, 23 (1947); R. P. Feynman , Phys. Rev. **97**, 660 (1955).

[18] J. Strečka, J. Magn. Magn. Mater. **316**, e346 (2007).

[19] S. Hill and W. K. Wootters, Phys. Rev. Lett. **78**, 5022 (1997); W. K. Wootters, Phys. Rev. Lett. **80**, 2245 (1998).

# Work extraction from microcanonical bath

Armen E. Allahverdyan <sup>1,2</sup> and Karen V. Hovhannisyan <sup>1</sup>

<sup>1</sup>Yerevan Physics Institute,  
Alikhanian Brothers Street 2, 0036 Yerevan, Armenia

<sup>2</sup>Laboratoire de Physique Statistique et Systèmes Complexes, ISMANS,  
44 ave. Bartholdi, 72000 Le Mans, France

## Abstract

We determine the maximal work extractable via a cyclic Hamiltonian process from a positive-temperature ( $T > 0$ ) microcanonical state of a  $N \gg 1$  spin bath. The work is much smaller than the total energy of the bath, but can be still much larger than the energy of a single bath spin, e.g. it can scale as  $\mathcal{O}(\sqrt{N \ln N})$ . Qualitatively same results are obtained for those cases, where the canonical state is unstable (e.g., due to a negative specific heat) and the microcanonical state is the only description of equilibrium. For a system coupled to a microcanonical bath the concept of free energy does *not generally* apply, since such a system—starting from the canonical equilibrium density matrix  $\rho_T$  at the bath temperature  $T$ —can enhance the work extracted from the microcanonical bath without changing its state  $\rho_T$ . This is impossible for any system coupled to a canonical thermal bath due to the relation between the maximal work and free energy. But the concept of free energy still applies for a sufficiently large  $T$ . Here we find a compact expression for the *microcanonical free-energy* and show that in contrast to the canonical case it contains a *linear entropy* instead of the von Neumann entropy.

## 1. Introduction

How much work can be extracted from a state of a physical system via cyclic processes? This question governs our understanding of energy conversion and storage, and hence is central for thermodynamics [1]–[8]. The basic answer, known as the Thomson’s formulation of the second law, is that an equilibrium state cannot yield work. This formulation is an axiom in thermodynamics, but its first-principle derivations were given in literature for a *canonical* (Gibbsian) equilibrium state [2]. The main consequence of the Thomson’s formulation is that only non-equilibrium states can be sources of work. The maximal work extractable from such states via a cyclic process was studied both for macroscopic [1] and finite systems [4, 5, 6].

One instance of the maximal work is especially well-known, because it provides the physical meaning of free energy [1]. Consider a quantum system with Hamil-

Assuming no system-bath coupling both initially and finally, the maximal work extracted by the fields reads [1, 9]

$$W_{\max} = F[\rho] - F[\rho_{\text{eq}}], \quad F[\rho] = \text{tr}(\rho H) + T \text{tr}(\rho \ln \rho), \quad (1)$$

where  $F[\rho]$  is the free energy and  $\rho_{\text{eq}} = e^{-H/T}/\text{tr}[e^{-H/T}]$  is the canonical equilibrium state of the system, which is its final state after work-extraction [1]. The maximal work is determined by the deviation of  $\rho$  from its canonical equilibrium value  $\rho_{\text{eq}}$  as quantified by the free energy (1).

One notes however that *all* above results refer to a specific notion of equilibrium, viz. the canonical state. Another concept of equilibrium is given by the microcanonical state, which describes an isolated system equilibrated due to its internal mechanism [10], or an open system coupled weakly to its environment (so weak that no energy is exchanged) [8, 11]. This is a more fundamental notion of equilibrium: *(i)* under certain conditions the canonical state can be derived from it for a weakly coupled subsystem [1]. *(ii)* In contrast to the canonical state, whose preparation refers to an external thermal bath, the microcanonical state can be applied to a closed few-body system provided that it satisfies certain chaoticity features [12, 13]. *(iii)* Since *local* stability conditions of the canonical state are more demanding—a fact closely related to the no work-extraction feature[1]—there are situations, where the equilibrium can be described by the microcanonical state only, since the canonical state for them is unstable [14]. For such systems, frequently realized via long-range interactions, the entropy is a non-concave function of energy, and hence the notorious *macroscopic* equivalence between canonical and microcanonical state is broken [14]. Even if this macroscopic equivalence holds, it is by no means obvious that in the argument around (1) one can substitute the canonical state of the thermal bath by the microcanonical state [with the same temperature], because *in general* the work (1) is not a macroscopic quantity, i.e. it does not scale with the number of bath particles. This is however widely done in literature, e.g., when introducing the free energy as in (1) one basically never specifies the equilibrium state of the bath; see, e.g. [1, 7].

We revisit the maximal work-extraction problem for a thermal bath in a quantum microcanonical state. It was noted already some work can be extracted via a cyclic Hamiltonian process from a *few-particle* microcanonical system [3]. Recent papers studied to which extent the extraction of work from one-particle classical microcanonical system can be carried out by physically realistic Hamiltonians [15, 16]. Our purposes here are different:

- We focus on finding the maximal amount of work extractable from a *macroscopic* microcanonical state of  $N \gg 1$  particle thermal bath.
- We also determine the work extracted via a system coupled to a microcanonical thermal bath, and check whether the reasoning (1) generalizes *at least* qualitatively, i.e. whether the concept of free energy applies to the microcanonical situation.

The subject of work extraction via a system coupled to a thermal bath is an active research topic. Refs. [16, 17, 18, 19, 20] discuss various set-ups for this problem: quantum, classical, with or without state-dependent feedback *etc*. Recall that (1) is at the core of relations between statistical thermodynamics and information theory [7]. The term  $\text{tr}([\rho - \rho_{\text{eq}}]H)$  in the right-hand-side of (1) is the energy extracted from the system, while the remaining (entropic) part comes from the bath. If  $\text{tr}([\rho - \rho_{\text{eq}}]H)$  is negligible (e.g., because  $H$  contains only few almost degenerate energy levels), the work is extracted from the bath due to the difference between the initial entropy and its canonical equilibrium value. This relation between the entropy and work is the essential part of information driven engines (e.g., Szilard's engine) [7]. In contrast, various forms of fuel operate due to the initial non-equilibrium energy, i.e. the term  $\text{tr}([\rho - \rho_{\text{eq}}]H)$  in (1).

## 2. Microcanonical thermal bath

The microcanonical state is characterized by two parameters: energy  $E$  and width  $\sigma$  [1]. The corresponding density matrix is diagonal in the energy representation, all energies within the interval  $[E, E - \sigma]$  have equal probabilities, all other energies have probability zero. For a  $N \gg 1$ -particle system the number  $d(E, \sigma)$  of energy levels within the interval  $[E, E - \sigma]$  defines the microcanonical entropy [1]:

$$S(E) = \ln d(E, \sigma) = \mathcal{O}(N), \quad (2)$$

where the choice of  $\sigma$  should not influence the leading  $\mathcal{O}(N)$  behavior of  $S(E)$ . Eq. (2) is the von Neumann entropy for the microcanonical density matrix (6); see also [21]. For clarity we want to work with a specific model of a macroscopic microcanonical system (bath). This is the basic model of the field:  $N \gg 1$  uncoupled two-level spins; each spin has energies 0 and  $\delta > 0$  [8]. Some of our results extend to more general bath models, as seen below.

The bath Hamiltonian reads (diag[...] means diagonal matrix in the energy representation)

$$H = \text{diag}[0, \delta, 2\delta \dots, \delta N], \quad (3)$$

where each element  $\delta k$  is repeated  $d_k$  times,

$$d_k \equiv \frac{N!}{k!(N-k)!}. \quad (4)$$

Hence every energy shell  $\delta k$  is  $d_k$ -degenerate. Denote

$$\mathbf{e}_k = (1, \dots, 1), \quad \mathbf{0}_k = (0, \dots, 0), \quad D_k \equiv \sum_{m=0}^k d_m, \quad (5)$$

where  $\mathbf{e}_k$  ( $\mathbf{0}_k$ ) is the vector of  $k$  1's (0's).

For the present model of bath the microcanonical state is easy to define: all energies  $\delta M$  have equal probability  $\frac{1}{d_M}$ ; all other energies have zero probability.

Thus we put  $\sigma \rightarrow 0$ , the *minimal* thermodynamically consistent width for this model. Note that the degeneracy of the energy levels is convenient, since it allows to set  $\sigma \rightarrow 0$ . It is however not essential: an effective degeneracy will be anyhow regained for a small but finite  $\sigma > 0$ , since the energy levels of a macroscopic system are located very densely [1]. The bath initial state reads in representation (3)

$$\Omega_i = \frac{1}{d_M} \text{diag}[\mathbf{0}_{D_{M-1}}, \mathbf{e}_{d_M}, \mathbf{0}_{D_N - D_M}]. \quad (6)$$

For  $N \gg 1$  this microcanonical state does have desired features expected from thermodynamics, e.g. macroscopic equivalence with the canonical state, equilibration of a small subsystem, third law [8]. The density matrix of a single bath spin is Gibbsian  $\propto \text{diag}[1, e^{-\delta/T}]$  with [8]

$$e^{-\delta/T} = m/(1-m), \quad m = M/N. \quad (7)$$

The same  $T$  is recovered as microcanonical temperature [1]

$$1/T = \partial S(E)/\partial E, \quad E = \delta M, \quad S(E) = \ln d_M, \quad (8)$$

where  $S(E)$  is the microcanonical entropy (2). This equivalence can be shown via formula (17) that is proven below.

Note that although the spins are uncoupled, the microcanonical state does not reduce to the tensor product of the separate spin states (otherwise it would amount to the canonical state). It contains inter-spin correlations. Ultimately, this is the reason why, as seen below, a microcanonical bath can yield work in a cyclic process.

We restrict ourselves with  $M/N \leq 1/2$ , i.e. *positive* temperatures. The case with  $M/N > 1/2$  is definitely less interesting, because now each spin of the bath is in a state with a negative temperature. Such states are trivially active, i.e. they yield work in a cyclic process.

### 3. Work extraction

At some initial time  $t = 0$  the bath Hamiltonian  $H(t)$  becomes time-dependent due to interaction with sources of work. Consider a cyclic process

$$H(0) = H(\tau) = H, \quad (9)$$

where  $\tau$  is the final time. The work extracted in this thermally isolated cyclic Hamiltonian process is

$$W = \text{tr}(H[\Omega_i - \Omega_f]) = \delta M - \text{tr}(H\Omega_f), \quad \Omega_f = U\Omega_i U^\dagger, \quad (10)$$

where  $\Omega_f$  is the final state of the bath, and  $U = \mathcal{T}e^{-(i/\hbar) \int_0^\tau ds H(s)}$ ;  $\mathcal{T}$  means chronologicalization. Conversely, for a given unitary  $U$  one can construct a class of Hamiltonians that generate  $U$  and satisfies (9) [5].

Condition (9) is necessary for the system to be an autonomous carrier of energy

that should deliver work to another system (e.g., to a work-source) via an interaction which switches on and off at well-defined times. Hence this is a cyclic Hamiltonian process.

We now maximize the work  $W$ —or minimize the final energy  $\text{tr}(H\Omega_f)$ —over all cyclic Hamiltonians, i.e. over unitary operators  $U$ . Note from (10) that

$$\text{tr}(H\Omega_f) = \sum_{a,b=1}^{2^N} E_a C_{ab} \langle b|\Omega_i|b\rangle, \quad C_{ab} \equiv |\langle b|U|a\rangle|^2, \quad (11)$$

$$C_{ab} \geq 0, \quad \sum_{a=1}^{2^N} C_{ab} = \sum_{b=1}^{2^N} C_{ab} = 1, \quad (12)$$

where  $\{E_a\}_{a=1}^{2^N}$  and  $\{|a\rangle\}_{a=1}^{2^N}$  are, respectively, the eigenvalues and eigenvectors of  $H$  [see (3)], and the elements  $\{\langle b|\Omega_i|b\rangle\}_{b=1}^{2^N}$  are defined in (6). Three conditions in (12) mean that the matrix  $C_{ab}$  is double-stochastic [22]. Conversely, every such matrix can be represented as  $C_{ab} \equiv |\langle b|U|a\rangle|^2$  for some unitary  $U$  [22]. Every double-stochastic matrix equals to a convex sum of permutation matrices  $\Pi^{[\alpha]}$  (Birkhoff's theorem [22]):  $C = \sum_{\alpha} \lambda_{\alpha} \Pi^{[\alpha]}$ ,  $\sum_{\alpha} \lambda_{\alpha} = 1$ ,  $\lambda_{\alpha} \geq 0$ , where each matrix  $\Pi^{[\alpha]}$  acting on a column-vector  $x$  amounts to permuting (in a certain way) the elements of  $x$ . Eq. (11) shows that  $\text{tr}(H\Omega_f)$  is a linear function of the matrix  $C = \{C_{ab}\}$ . Hence its minimum over the unitary operators  $U$ , that is its minimum over double-stochastic matrices  $C_{ab}$ , is reached for  $C_{ab}$  equal to some permutation matrix  $\tilde{\Pi}$ . It is clear from (11) that  $\tilde{\Pi}$ , when acting on the vector  $\langle b|\Omega_i|b\rangle$  permutes its elements such that all its non-zero [equal to each other] elements concentrate at lowest energies  $\{E_a\}_{a=1}^{2^N}$  [5]. For the final state we have  $\langle a|\Omega_f|a\rangle = \sum_b \tilde{\Pi}_{ab} \langle b|\Omega_i|b\rangle$ . Hence the lowest-energy final state compatible with  $\Omega_i$  reads

$$\Omega_f = \frac{1}{d_M} \text{diag}[\mathbf{e}_{d_M}, \mathbf{0}_{D_N - d_M}]. \quad (13)$$

Once  $\tilde{\Pi}$  is found we can employ the standard procedure of constructing the corresponding unitary operator  $U$  and the cyclic Hamiltonian [5]. Note that  $\tilde{\Pi}$  does depend on the energy of the initial state  $\Omega_i$ :  $\tilde{\Pi}$  applied on a microcanonical state with a different energy will not lead to the maximal work-extraction. This does not differ from (say) the ordinary Carnot cycle, whose implementation also demands knowing the initial state of the working body.

The maximal work  $W_{\max}$  reads from (13, 10):  $W_{\max} = \delta M - \frac{\delta}{d_M} [\sum_{k=0}^{M-\ell} k d_k + (M - \ell + 1)(d_M - \sum_{k=0}^{M-\ell} d_k)]$ . After summation by parts,

$$W_{\max} = \delta \left[ \ell - 1 + \frac{1}{d_M} \sum_{k=0}^{M-\ell} D_k \right], \quad (14)$$

where  $D_k$  is defined in (5), and where integer  $\ell = \ell(M)$  is found from

$$\sum_{k=0}^{M-\ell+1} d_k > d_M \geq \sum_{k=0}^{M-\ell} d_k. \quad (15)$$

Eq. (14, 15) hold for any microcanonical state (3, 6); the specific form (4) is not necessary.

We shall now calculate  $W_{\max}$  for two limits:  $T \rightarrow \infty$  and a finite  $N$ , and then  $N \rightarrow \infty$  and a finite  $T$ .

#### 4. Doubly maximized work

We set the number of spins  $N$  to a large, but a finite number, and maximize  $W_{\max}(T)$  over all positive temperatures of the  $N$ -spin bath. The maximum is reached for  $T = \infty$  (or  $M = N/2$  as (7) shows) and provides an upper bound for the work extractable from the positive temperature bath. We now calculate  $W_{\max}(\infty)$ . Consider the sum  $\sum_{k=0}^{\frac{N}{2}-\ell} d_k = \sum_{m=\ell}^{\frac{N}{2}} d_{\frac{N}{2}-m}$  in (15). The dominant summation region is  $m \sim \ell$ . We shall see below that  $\ell \ll N$ . Hence for (4) we use the Gaussian approximation  $d_{\frac{N}{2}-m} = 2^{\frac{N}{2}} e^{-\frac{m^2}{N/2}}$  [23], change the sum to integral, and find  $\ell$  from  $1 = \int_{\ell}^{\infty} dx e^{-\frac{x^2}{(N/2)}}$ :  $\ell = \sqrt{\frac{N}{4} \ln \left[ \frac{N}{4 \ln(N/4)} \right] + \frac{N}{4} \mathcal{O} \left[ \frac{\ln \ln(N/4)}{\ln(N/4)} \right]}$ . The second term under square root is negligible if  $\ln N$  is large. Eq. (14) then implies (for  $N \gg 1$ ):

$$W_{\max} = \delta \int_{\ell}^{\infty} dx x e^{-\frac{x^2}{(N/2)}} = \delta \ell \approx \frac{\delta}{2} \sqrt{N \ln N}. \quad (16)$$

This is a reachable upper bound for the work extractable from the  $N$ -spin microcanonical bath.

#### 5. Finite temperatures and thermodynamic limit

We employ (4) and assume the standard thermodynamic limit:  $m = M/N < 1/2$  (and hence  $T > 0$ ) in (7) is a fixed finite number for  $M, N \rightarrow \infty$ . We note from (4) and (7) that for any fixed finite numbers  $m, \ell$  and  $N \rightarrow \infty$ ,

$$\frac{d_{Nm-\ell}}{d_{Nm}} = e^{-\ell \delta/T} [1 + \mathcal{O}(\frac{1}{N})]. \quad (17)$$

Since the sums in (14, 15) are dominated by their largest terms, using (17) (with  $m < 1$  and integer  $\ell$ ) amounts to calculating these sums via geometrical progression, e.g.,  $\frac{1}{d_M} \sum_{k=0}^{M-\ell+1} d_k = \sum_{k=\ell-1}^{\infty} e^{-\delta k/T}$ . We get for  $\ell$  and  $W_{\max}$

$$W_{\max}(T) = \delta \left[ \ell - 1 + v^{\ell} (1-v)^{-2} \right], \quad (18)$$

$$v \equiv e^{-\delta/T}, \quad \ell = \left\lceil \frac{\ln(1-v)}{\ln v} \right\rceil, \quad (19)$$

where  $\lceil x \rceil$  is the ceiling (upper) integer part of  $x$ , e.g.,  $\lceil 0.99 \rceil = 1$ ,  $\lceil -0.99 \rceil = 0$ . According to (19),  $\ell$  grows to infinity with  $T$ :  $\ell = 1$  for  $e^{-\delta/T} \leq \frac{1}{2}$ ,  $\ell = 2$  for  $\frac{2}{1+\sqrt{5}} \geq e^{-\delta/T} \geq \frac{1}{2}$ ,  $\ell = 3$  for  $0.68232 \geq e^{-\delta/T} \geq \frac{2}{1+\sqrt{5}}$  etc.

$W_{\max}(T)$  is a continuous function of  $T$ , but  $\frac{dW_{\max}}{dT}$  has jumps at the temperatures, where  $\ell$  changes, and one energy shell in the final density matrix (13) is completely filled; see (15) and Fig. 1. Hence

$$W_{\max}(T) = \mathcal{O}(\delta) \quad \text{for } N \gg 1 \quad \text{and } T = \mathcal{O}(\delta). \quad (20)$$

The situation is symmetric with respect to different spins of the bath. Hence after the work-extraction the initial energy of each bath spin changes negligibly  $= \mathcal{O}(\frac{1}{N})$ . The final state of each spin is diagonal in the energy representation and thus after work-extraction it has a well-defined temperature that differs from the initial temperature by  $\mathcal{O}(\frac{1}{N})$ . Recall that the Gibbsian state as such cannot yield work in a cyclic process (9) [2]. Hence the work is extracted due to inter-spin correlations present initially in the microcanonical state.

Eq. (18) shows that  $W_{\max}(T)$  increases faster than  $T$ :

$$W_{\max}(T) = T \left[ \ln \left( \frac{T}{\delta} \right) + 1 \right] \quad \text{for } T \gg \delta, \quad (21)$$

where we used  $\left\lceil \frac{\ln(1-v)}{\ln v} \right\rceil \approx \frac{\ln(1-v)}{\ln v}$ . Eq. (21) is practically good already for  $T > 1.5\delta$ . Now  $W_{\max}$  can be much larger than the energy of a single bath spin. In the limit  $T \gg \delta$  this energy is equal to  $\delta/2$ ; see (7).

## 6. Microcanonical states not equivalent to the canonical one

Eq. (20) does not depend on the concrete form (4) of  $d_k$ . What is needed for (20) is that the sum  $\sum_{k=0}^M d_k$  is dominated by its last term  $d_M$ . Then (15) implies  $\ell = \mathcal{O}(1)$ , and (14) leads to (20). Hence (20) generalizes the Thomson's formulation of the second law to the microcanonical situation. In particular, (20) holds for those  $d_k$ , where the macroscopic equivalence between microcanonical and canonical states is violated. As an example consider (3, 6) with  $d_M = e^{N(M/N)^2}$ . This spectrum satisfies all above conditions and leads to (20). Now the entropy  $\ln d_M$  is a *convex function* of energy  $\delta M$ . Hence the specific heat  $C = [\frac{dT}{d(\delta M)}]^{-1}$  calculated from (8) is *negative*, and the macroscopic equivalence between canonical and microcanonical states is clearly violated, because  $C > 0$  is an automatic consequence of the canonical state [1]. Such convex-entropy spectra are realized in macroscopic long-range interacting systems [14].

Another example of convex entropy and canonical-microcanonical non-equivalence where still (20) holds, is the *first-order microcanonical* phase transition [1, 14], where in the vicinity of some critical energy  $E_c$ ,  $\frac{dS(E)}{dE}$  has a jump:  $\frac{dS(E)}{dE}|_{E \rightarrow E_c+} = \frac{1}{T_h}$ ,  $\frac{dS(E)}{dE}|_{E \rightarrow E_c-} = \frac{1}{T_l}$ . This describes coexistence of two phases with different temperatures. Since a more stable phase should have a larger entropy, we get  $T_h < T_l$  [1]. The above non-equivalence is seen here, because at a canonical first-order phase transition different phases have the same temperature [1]. Even though two phases at different temperatures do co-exist, the extracted work has the same order of magnitude (20) as for a homogeneous-temperature microcanonical state.

## 7. System coupled to the bath

An important instance of the maximal work problem is the amount of work extractable from a thermal bath in the presence of a smaller system coupled to it; see (1). How much work can be extracted from a combined state of a two level system with energies 0 and  $\epsilon > 0$  and the microcanonical thermal bath? Answering this question will allow us to understand to which extent the concept of the free energy applies to the microcanonical situation. Before starting the analysis we should like to stress again that so far the statistical physics literature does not distinguish between canonical and microcanonical situations when introducing and applying the free energy concept; see e.g. [1].

Let the initial density matrix of the two-level system be  $\rho_i$ ; its eigenvalues are  $\pi_0 > \pi_1$ . The spectrum of the overall initial state  $R_i \equiv \rho_i \otimes \Omega_i$  reads [see (6, 5)]

$$\text{Spec}[R_i] = \frac{1}{d_M} [\pi_0 \mathbf{e}_{d_M}, \pi_1 \mathbf{e}_{d_M}, \mathbf{0}_{2D_N - 2d_M}], \quad \pi_0 > \pi_1. \quad (22)$$

Both initially and finally the two-level system and bath do not interact. Hence the overall Hamiltonian  $\mathcal{H}$  reads

$$\mathcal{H} = \mathcal{H}(\tau) = H_S \otimes 1 + 1 \otimes H \quad (23)$$

$$= \text{diag}[0, \delta, 2\delta \dots, \delta N, \epsilon, \epsilon + \delta, \dots, \epsilon + \delta N], \quad (24)$$

where  $H$  is given by (3), and  $H_S$  is the two-level Hamiltonian with energies 0 and  $\epsilon$ . We recall that each symbol  $k\delta$  (or  $\epsilon + k\delta$ ) in (24) is repeated  $d_k$  times. Once we consider unitary work-extraction processes, the final state of the overall system will have the same eigenvalues (22). Recalling our discussion between (11) and (13) it should be clear that the minimal final energy for the overall system is achieved for the unitary operator that forces  $R_f$  to have the same eigenvectors as  $\mathcal{H}$  and permutes the eigenvalues (22) such that the largest eigenvalue is matched with the smallest energy, next to the largest eigenvalue with the next to the smallest energy and so on. Note that  $\text{Spec}[R_i]$  is already ordered in a non-increasing way. It remains to order (24) in a non-decreasing way and write the lowest final average energy as scalar product of two vectors

$$\begin{aligned} \text{tr}(\mathcal{H}R_f) &= \text{Spec}[R_i] \cdot [0, \delta, \dots, \alpha\delta, \epsilon, \\ &(\alpha+1)\delta, \epsilon+\delta, \dots, \delta N, \epsilon+\delta(N-\alpha), \dots, \epsilon+\delta N], \end{aligned} \quad (25)$$

where  $\alpha = \lfloor \frac{\epsilon}{\delta} \rfloor$ , and  $\lfloor x \rfloor$  is the floor (lower) integer part of  $x$ , e.g.,  $\lfloor 0.99 \rfloor = 0$ ,  $\lfloor -0.99 \rfloor = -1$ .

Consider the work extracted from the overall system that is maximized over all unitary dynamic operators. Since the system and bath do not interact both initially and finally, this work separates into two parts coming, respectively, from the system and bath [see (10, 14)]:

$$\text{tr}(\mathcal{H}[R_i - R_f]) = W_{\max} + W_{\text{sur}} + \text{tr}(H_S[\rho_i - \rho_f]), \quad (26)$$

where  $\text{tr}(H_S[\rho_i - \rho_f])$  is the energy change of the two-level system.  $W_{\max} + W_{\text{sur}}$  is the work coming from the bath. Here  $W_{\max}$  is given by (14) (the maximal work extracted from the bath alone) and we defined the surplus work  $W_{\text{sur}}$  (work extracted from the bath, but due to the system).

Obviously,  $W_{\text{sur}} + \text{tr}(H_S[\rho_i - \rho_f]) \geq 0$ , since  $\text{tr}(\mathcal{H}[R_i - R_f])$  results from optimizing over a larger set of parameters than  $W_{\max}$ . Note that  $\text{tr}(H_S[\rho_i - \rho_f])$  appears also in the right-hand-side of (1), and there is some analogy between  $W_{\text{sur}}$  and the entropy difference  $T(\text{tr}[-\rho_{\text{eq}} \ln \rho_{\text{eq}} + \rho \ln \rho])$  in (1), which is the work extracted from the canonical bath. There the work  $W_{\max}$  extracted from the canonical equilibrium bath alone (without the system) is zero.

Scalar product (25) is calculated straightforwardly; for clarity we focus on the thermodynamic limit regime (17):

$$W_{\max} + W_{\text{sur}} = \delta[\pi_1 F_2 + (\pi_0 - \pi_1)F_1], \quad (27)$$

$$\text{tr}(H_S \rho_f) = \epsilon[\pi_1 P_2 + (\pi_0 - \pi_1)P_1], \quad (28)$$

where  $W_{\max}$  is given by (18) and we defined for  $k = 1, 2$ :

$$F_k \equiv k(\ell_{1k} - 1) + v^{\ell_{1k}} \frac{1+v^\alpha}{1-v} \left[ \frac{1}{1-v} + \frac{\alpha v^\alpha}{1+v^\alpha} \right] + \alpha \text{sign}(\ell_{1k} - \ell_{2k}) \left[ k - \frac{v^{\ell_{2k}}(1+v^{1+\alpha})}{1-v} \right], \quad (29)$$

$$P_k \equiv \frac{v^{\ell_{1k}+\alpha}}{1-v} + \text{sign}(\ell_{1k} - \ell_{2k}) \left[ k - \frac{v^{\ell_{2k}}(1+v^{1+\alpha})}{1-v} \right], \\ \ell_{1k} \equiv \left\lceil \frac{\ln \left( \frac{k(1-v)}{1+v^\alpha} \right)}{\ln v} \right\rceil, \quad \ell_{2k} \equiv \left\lceil \frac{\ln \left( \frac{k(1-v)}{1+v^{1+\alpha}} \right)}{\ln v} \right\rceil. \quad (30)$$

Recall that  $\text{sign}(0) = 0$ ,  $\alpha = \lfloor \frac{\epsilon}{\delta} \rfloor$ , and that  $\lfloor x \rfloor$  and  $\lceil x \rceil$  are defined after (25) and (18), respectively.

The final state  $\rho_f$  of the two-level system is diagonal in its energy representation. The eigenvalues of  $\rho_f$  are read-off from (28). The excited state of  $\rho_f$  is less populated than the ground-state; otherwise it can still provide work via a cyclic process. In this specific sense the two-level system *partially* equilibrates; recall that  $\rho_i$  is arbitrary.

Fig. 1 displays  $W_{\max}(T)$  and  $W_{\text{sur}}(T)$  for a representative range of parameters. It is seen that for  $\alpha = 0$ ,  $W_{\text{sur}} \geq 0$  and both  $W_{\max}$  and  $W_{\text{sur}}$  monotonically increase with  $T$ . For  $\alpha > 0$  the positivity of  $W_{\text{sur}}$  is recovered only for a sufficiently high  $T$  provided that  $\pi_0 \neq \pi_1$ ; see Fig. 1. For  $\pi_0 = \pi_1$ , we always get  $W_{\text{sur}} < 0$ .

Consider now  $\epsilon < \delta$  [i.e.  $\alpha = 0$  in (25)] and assume  $v \equiv e^{-\delta/T} \leq 1/3$  for simplicity. Eqs. (27–30) produce

$$W_{\text{sur}} = v\delta(2\pi_0 - 1)(1-v)^{-2}, \quad (31)$$

$$\text{tr}(H_S \rho_f) = \epsilon[v\pi_0 + (1-3v)\pi_1](1-v)^{-1}. \quad (32)$$

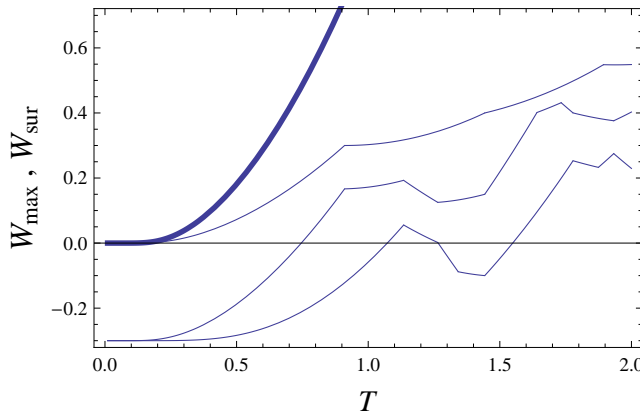


Figure 1: Thick curve:  $W_{\max}$  given by (14) as a function of temperature  $T$  for  $\delta = 1$ . Normal curves show  $W_{\text{sur}}$  given by (27) as a function of  $T$  for  $\delta = 1$ ,  $\pi_1 = 0.3$  and (from top to bottom):  $\alpha = \lfloor \frac{\epsilon}{\delta} \rfloor = 0, 1, 2$ .

Eq. (31) shows that, in addition to  $W_{\text{sur}} + \text{tr}(H_S[\rho_i - \rho_f]) \geq 0$ , the work extracted from the bath is enhanced,  $W_{\text{sur}} > 0$ , for any state of the two-level system besides the completely mixed one, where  $\pi_0 = \pi_1 = \frac{1}{2}$ .

The energy difference  $\text{tr}(H_S[\rho_i - \rho_f])$  can be positive or negative. Hence parameters can be tuned such that it is zero, e.g., from (32) and for  $\epsilon = T \ln 2 < T \ln 3 < \delta$  we get that initially canonical *equilibrium* two-level system,  $\pi_0 = 1 - \pi_1 = (1 + e^{-\epsilon/T})^{-1} = \frac{2}{3}$ , enhances the work extracted from the bath *without* changing its marginal state:  $\text{tr}(H_S \rho_f) = 0$ . Hence for enhancing the work extracted from the microcanonical bath one needs that the system is ordered: its state should not be completely mixed, while the maximal enhancing is achieved for a pure state. But the state of the system need not change.

A non-equilibrium system coupled to canonical equilibrium bath can enhance the work extracted from the bath *only* at the cost of changing (towards equilibrium) its initially non-equilibrium state; see (1). The free energy measures this change. For the microcanonical bath, the work can be enhanced already by an equilibrium two-state system without changing its marginal state. We conclude that the concept of the free energy does not *generally* apply to a system coupled to a microcanonical bath.

But this concept applies in the high-temperature limit. For  $T \gg \delta, \epsilon$  we get from (27–30) and from (21):

$$W_{\text{sur}} = (1 - 2\pi_1)T \ln 2, \quad (33)$$

$$\text{tr}(H_S \rho_f) = \epsilon/2. \quad (34)$$

Eq. (34) means that the final state of the two-level system is completely mixed, which for the present high-temperature case coincides with the canonical equilibrium state. Eq. (33) predicts work-enhancement only if initially the two-level system was out

of equilibrium [recall that  $\frac{1}{2} \geq \pi_1$ ]. Hence for  $T \gg \delta, \epsilon$  we recover the logics of the canonical-bath situation, but not its letter, because for a canonical bath  $W_{\text{sur}}$  reduces to the difference between two von Neumann entropies that are logarithmic functions of the initial eigenvalues  $\pi_0$  and  $\pi_1$ ; cf. our remark after (26).

We shall show elsewhere that for a  $\mu$ -level system in a state (density matrix)  $\rho$  with eigenvalues ordered as  $\pi_0 \geq \pi_1 \geq \dots \geq \pi_{\mu-1}$ , we can define the *linear entropy* as

$$\mathcal{L}[\rho] = \sum_{k=1}^{\mu-1} \pi_k [(k+1) \ln(k+1) - k \ln k]. \quad (35)$$

Generalizing (33), the surplus work  $W_{\text{sur}}$  extracted from a high-temperature microcanonical bath in contact with this system is then  $W_{\text{sur}} = T(\ln \mu - \mathcal{L}[\rho]) = T(\mathcal{L}[\frac{1}{\mu}] - \mathcal{L}[\rho])$ , where  $\frac{1}{\mu}$  is the maximally mixed state of the  $\mu$ -level system. For the canonical situation this expression involves the von Neumann entropy  $-\text{tr}[\rho \ln \rho]$  instead of  $\mathcal{L}[\rho]$ . Note that  $\ln \mu \geq \mathcal{L}[\rho] \geq 0$ : the upper (lower) limit is reached for the maximally mixed (pure)  $\rho$ .

Hence for a system in initial state  $\rho$  and Hamiltonian  $H_S$  coupled to the *high-temperature* microcanonical bath one can define the *microcanonical* free energy  $\mathcal{F}[\rho] = \text{tr}(H_S \rho) - T\mathcal{L}[\rho]$ , whose difference  $\mathcal{F}[\rho] - \mathcal{F}[\rho_{\text{eq}}]$  (after adding to  $W_{\text{max}}$  extracted from the bath alone) defines the maximal work extracted from the system+bath.

## 8. Summary

We reformulated the Thomson's formulation of the second law for a  $N \gg 1$  particle *equilibrium* bath in a microcanonical state: if the bath temperature  $T$  is finite, the maximal work extractable from the bath via a cyclic Hamiltonian process is  $\gtrsim \delta$ , where  $\delta$  is the energy of a single bath particle. The maximal work tends to  $\delta \sqrt{N \ln N}$  if  $N$  is large but fixed and  $T \rightarrow \infty$ . The reformulation applies equally well to both ordinary microcanonical states, which are macroscopically equivalent to canonical states, and convex-entropy microcanonical states for which no canonical state can be defined, e.g., because of a negative specific heat [14]. The existence of such states demonstrates that a viewpoint on a microcanonical state as emerging from measuring the energy of the canonical state is not generally valid. Thermodynamics of such systems can have peculiarities [24], but we saw that they satisfy the same generalized Thomson's formulation much in the same way as ordinary microcanonical states. The work extraction is possible, since the microcanonic state of the bath is not Gibbsian, though each its constituent can be in a Gibbsian state.

It is widely known that only a non-equilibrium system can lead—at expense of changing its state towards equilibration—to work extraction from a canonical bath [1]. This work is given by the free energy difference (1). In contrast, a canonical equilibrium system (having the same temperature as the bath) can enhance the work extracted from the microcanonical bath without changing its marginal state. Hence

the concept of free energy, in the sense of the maximal work, does not generally apply to the microcanonical situation. The application of the concept is recovered for  $T \gg \delta$ , but the canonical expression of the free energy is not restored, instead it should be formulated via the linear entropy (35).

## Acknowledgements

We thank our colleagues Guenter Mahler, Dominik Janzing and Roger Balian for discussions that motivated this work. We were supported by Volkswagenstiftung.

## References

- [1] L.D. Landau and E.M. Lifshitz, *Statistical Physics, I*, (Pergamon Press Oxford, 1978).
- [2] A. Lenard, J. Stat. Phys. **19**, 575 (1978).  
I.M. Bassett, Phys. Rev. A **18**, 2356 (1978).
- [3] A. E. Allahverdyan and Th. M. Nieuwenhuizen, Physica A **305**, 542 (2002).
- [4] G.N. Hatsopoulos and E.P. Gyftopoulos, Found. Phys. **6**, 127 (1976).
- [5] A.E. Allahverdyan, R. Balian and Th.M. Nieuwenhuizen, Europhys. Lett. **67**, 565 (2004).
- [6] D. Janzing, J. Stat. Phys. **112**, 3, 531 (2006).
- [7] K. Maruyama, F. Nori and V. Vedral, Rev. Mod. Phys. **81**, 1 (2009).
- [8] J. Gemmer, M. Michel and G. Mahler, *Quantum Thermodynamics* (Springer, NY, 2004).
- [9] The maximization of work is carried out over all cyclic and time-dependent (in the sense of (9)) Hamiltonians acting on the system+bath [1]; for more details see, e.g., Appendix E of [26]. One can show that the work (1) can be achieved for a Hamiltonian, where external fields act only on the system and on its coupling to the bath [25, 26]. This set-up is local (advantage), but it has to be slow (drawback).
- [10] A. Polkovnikov *et al.*, arXiv:1007.5331.
- [11] L. van Hove in *Fundamental Problems in Statistical Mechanics*, edited by E.D.G. Cohen (North Holland, Amsterdam, 1962), p. 157; N.G. van Kampen, *ibid.*, p. 173. M. Bander, arXiv:cond-mat/9609218.

- [12] V. L. Berdichevsky, *Thermodynamics of Chaos and Order* (Addison Wesley Longman, Essex, England, 1997).
- [13] F. Borgonovi and F. M. Izrailev, Phys. Rev. E **62**, 6475 (2000).
- [14] A. Campa *et al.*, Phys. Rep. **480**, 57 (2009).
- [15] R. Marathe and J.M.R. Parrondo, Phys. Rev. Lett. **104**, 245704 (2010).
- [16] S. Vaikuntanathan and C. Jarzynski, arXiv:1105.1744
- [17] A.E. Allahverdyan and D.B. Saakian, EPL, **81**, 30003 (2008).
- [18] D. Abreu and U. Seifert, EPL, **94**, 10001 (2011).
- [19] Th.M. Nieuwenhuizen and A.E. Allahverdyan, Phys. Rev. E, **66**, 036102, (2002).
- [20] T. Sagawa and M. Ueda, Phys. Rev. Lett. **100**, 080403 (2008).
- [21] Eq. (2) is one of two standard definitions of the microcanonical entropy [1]. Another definition is  $\ln \text{tr}[\rho P_{E,E_0}]$ , where  $E_0$  is the lowest energy and  $P_{E,E_0}$  is the projector on the subspace  $[E, E_0]$ . For macroscopic systems both definitions typically agree with each other within the order  $\mathcal{O}(N)$ , where  $N \gg 1$  is the number of particles. For finite systems the second definition is preferable [12, 17].
- [22] A.W. Marshall and I. Olkin, *Inequalities: Theory of Majorization* (Academic Press, New York, 1979).
- [23] It is derived from (4) via the Stirling's formula  $N! \simeq (N/e)^N$  and expanding over  $m$ .
- [24] A. Ramirez-Hernandez *et al.*, Phys. Rev. E **78**, 061133 (2008). D.H.E.Gross and J.F.Kenney, J. Chem. Phys. **122**, 224111 (2005). J. Oppenheim, Phys. Rev. E **68**, 016108 (2003).
- [25] R. Alicki *et al.*, Open Syst. Inf. Dyn. **11**, 205 (2004).
- [26] A.E. Allahverdyan, R. S. Johal and G. Mahler, Phys. Rev. E **77**, 041118 (2008).

# M theory on $AdS_4 \times S^7$ and $AdS_4 \times S^7/\mathbb{Z}_k$

Marine Samsonyan

*Yerevan Physics Institute*

*Alikhanian Brothers Street 2, 0036 Yerevan, Armenia*

## Abstract

We revisit Kaluza-Klein compactification of 11-d supergravity on  $S^7$  and go to  $S^7/\mathbb{Z}_k$  using group theory techniques. We show that there is no Higgs mechanism responsible for the supersymmetry breaking. We analyze Kaluza-Klein towers and compute their partition functions.

## 1. Some generalities on Superstring Theory

A theory of fundamental one-dimensional objects, strings, arose in the late 1960s in an attempt to understand the strong nuclear force [1]. String theory contains open and closed strings. Open strings can end on a  $(p+1)$  dimensional hypersurface called D $p$ -brane. In this theory specific particles correspond to specific oscillation modes (or quantum states) of the string. One of the most important features of string theory is that it contains general relativity. The graviton is in the spectrum of closed string. Bosonic string theories are inconsistent. The consistency of the theory requires supersymmetry. There are five superstring theories- Type IIA, Type IIB, Type I, Heterotic  $SO(32)$  and Heterotic  $E_8 \times E_8$ . They predict the spacetime dimension in which they live to be ten. This means that the six dimensions must be compactified on an internal manifold with the size of Planck length. String theories are related via dualities. T-duality implies that in many cases two different geometries for the extra dimensions are physically equivalent. It relates the two Type II and the two Heterotic theories. Therefore the Type IIA and Type IIB theories (also the two Heterotic theories) should be regarded as a single theory. The S-duality relates the string coupling constant to its inverse. This duality connects the Type I theory to the  $SO(32)$  Heterotic string theory and the Type IIB theory to itself. Thus knowing the behaviour of these theories at small coupling limit, we learn how they behave at strong coupling limit. This means that we know how Type I, Type IIB and Heterotic  $SO(32)$  theories behave at strong coupling limit. At this limit in the Type IIA and Heterotic  $E_8 \times E_8$  theories arises an eleventh dimension of size  $g\ell$  ( $\ell$  is the string length,  $g$  is the coupling constant). This dimension is a circle in the Type IIA case and a line interval in the Heterotic theory. When it is large a new type of quantum theory in eleven dimensions arises. This is called M-theory. The low energy limit of this theory is 11-dimensional supergravity.



coupling constant becomes infinite one reaches the conformally invariant fixed-point theory describing a stack of coincident M2-branes in 11 dimensions. This theory has  $SO(8)$  R-symmetry which corresponds to the rotations in the eight dimensions transverse to the M2-branes in 11 dimensions. The isometry group of  $AdS_4 \times S^7$  metric is  $SO(3, 2) \times SO(8) \approx Sp(4) \times Spin(8)$ .  $SO(3, 2)$  is the symmetry of  $AdS_4$  and in the dual theory it corresponds to the conformal symmetry group. The isometry group  $SO(8)$  of  $S^7$  corresponds to the R-symmetry of the dual gauge theory. There are 32 conserved supercharges (maximal supersymmetry). In the dual gauge theory 16 of these supersymmetries are realized linearly and the other 16 are conformal supersymmetries. The isometry superalgebra becomes  $OSp(8|4)$  once these supersymmetries are included. The 32 fermionic generators transform as  $(\mathbf{8}, \mathbf{4})$  under  $Spin(8) \times Sp(4)$ .

**The ABJM model:** Aharony, Bergman, Jafferis and Maldacena have conjectured that 11-d supergravity on  $AdS_4 \times S^7/\mathbb{Z}_k$ , corresponding to the near horizon geometry of  $N$  M2-branes at a  $\mathbb{C}^4/\mathbb{Z}_k$  singularity, be dual to  $\mathcal{N} = 6$  Chern-Simons (CS) theory in  $d = 3$  with gauge group  $U(N)_k \times U(N)_{-k}$  and opposite CS couplings  $k_1 = k = -k_2$  [5]. The metric reads

$$ds_{11}^2 = \frac{1}{4}L^2 ds_{AdS}^2 + L^2 ds_{S^7}^2 \quad (1)$$

for later use, note that  $L_{AdS} = L/2$  with  $L$  the radius of  $S^7$  and henceforth the metrics of the subspaces are for unit curvature radii.

The Type IIA solution which corresponds to the ABJM model reads

$$ds_{IIA}^2 = 4\frac{\rho^2}{L^2}dx \cdot dx + 4\frac{L^2}{4\rho^2}d\rho^2 + L^2 ds_{\mathbb{CP}^3}^2 = \frac{1}{4}L^2 ds_{AdS}^2 + L^2 ds_{\mathbb{CP}^3}^2 \quad (2)$$

where  $L = \left(\frac{32\pi^2 N}{k}\right)^{1/4}$  is the curvature radius in string units. The string coupling, related to the VEV of the dilaton, is given by  $g_s = L/k = \left(\frac{32\pi^2 N}{k^5}\right)^{1/4}$ . Thus the perturbative Type IIA description should be valid for  $L \gg 1$  and  $g_s \ll 1$  i.e. for  $N^{1/5} \ll k \ll N$ .  $\lambda = N/k$  is the 't Hooft coupling of the boundary CS theory.

When one goes from Type IIA on  $AdS_4 \times \mathbb{CP}^3$  to M-theory on  $AdS_4 \times S^7$  an uplift to 11 dimensions occur, the  $\mathbb{CP}^3$  becomes the base of a Hopf fibration  $S^7 = \mathbb{CP}^3 \times S^1$  whose metric reads

$$ds_{S^7}^2 = ds_{\mathbb{CP}^3}^2 + (d\tau + \mathcal{A})^2 \quad (3)$$

with  $d\mathcal{A} = 2\mathcal{J}_{\mathbb{CP}^3}$ , the Kähler form on  $\mathbb{CP}^3$  normalized so that  $dV(\mathbb{CP}^3) = \mathcal{J} \wedge \mathcal{J} \wedge \mathcal{J}/6$  and  $V(\mathbb{CP}^3) = \pi^3/6$ . There are R-R fluxes

$$g_s F_2 = 2L\mathcal{J} \quad , \quad g_s F_4 = 6L^3 dV(AdS_4) \quad , \quad g_s F_6 = 6L^5 dV(\mathbb{CP}^3). \quad (4)$$

In the ABJM model  $B_2 = 0$ . When there are also fractional M2-branes one has the ABJ model. In that case the boundary theory is  $\mathcal{N} = 6$  CS theory with

$U(N)_k \times U(N+k-l)_{-k}$  gauge group [6]. In this model  $B_2 = \mathcal{J}l/k$ , with  $l = 1, \dots, k-1$ .

The 11-d supergravity approximation should be valid in the double-scaling limit  $k \rightarrow \infty$ ,  $N \rightarrow \infty$  with  $\lambda = N/k$  fixed and large. The CFT description should instead be valid when  $\lambda \ll 1$ , i.e.  $k \gg N$ . As  $\lambda \rightarrow 0$  higher spin symmetry enhancement takes place [3], [4].

$\mathcal{N} = 6$  d = 3 boundary CS theory: Three dimensional  $\mathcal{N} = 6$  CS theories are constructed from CS theories with  $\mathcal{N} = 3$  supersymmetry. These  $\mathcal{N} = 3$  theories come from the  $\mathcal{N} = 4$  case in three dimensions which in turn are obtained from  $\mathcal{N} = 2$  in  $d = 3$ .  $d = 3$  theories with  $\mathcal{N} = 2$  supersymmetry are the dimensional reductions of  $\mathcal{N} = 1$  theories in four dimensions. The chain connecting these theories is the following:

$$\mathcal{N} = 6_{(d=3)} \leftarrow \mathcal{N} = 3_{(d=3)} \leftarrow \mathcal{N} = 4_{(d=3)} \leftarrow \mathcal{N} = 2_{(d=3)} \leftarrow \mathcal{N} = 1_{(d=4)} \quad (5)$$

The field contents of the theories are the following:

$$\begin{aligned} d = 4, \mathcal{N} = 1 \quad V_{\mathcal{N}=1} &= (A_\mu, \chi, D) \in \text{Adj} \quad Q_i = (\phi_i, \psi_i) \in R_i \\ d = 3, \mathcal{N} = 2 \quad V_{\mathcal{N}=2} &= (A_m, \chi, D, \sigma) \in \text{Adj} \quad Q_i = (\phi_i, \psi_i) \in R_i \\ d = 3, \mathcal{N} = 4 \quad V_{\mathcal{N}=4} &= V_{\mathcal{N}=2} + \Phi \in \text{Adj} \quad Q_i \in R_i, \tilde{Q}_i \in \bar{R}_i \end{aligned} \quad (6)$$

The vector multiplet of  $\mathcal{N} = 4$  theory consists of an  $\mathcal{N} = 2$  vector multiplet plus one chiral multiplet in the adjoint representation  $\Phi = \Phi_a t^a$  and there are hypermultiplets  $Q$  and  $\tilde{Q}$  in the real (reducible) representations. Adding to the  $\mathcal{N} = 4$  superpotential  $W = \tilde{Q}\Phi Q$  the CS term, giving a mass  $m = g_{YM}^2 \frac{k}{4\pi}$  to the vectors, and a CS superpotential  $W = -\frac{k}{8\pi} \text{Tr} \Phi^2$  breaks  $\mathcal{N} = 4$  to  $\mathcal{N} = 3$ . Integrating out  $\Phi$  yields the superpotential

$$W = \frac{4\pi}{k} (\tilde{Q} t^a Q)(\tilde{Q} t^a Q). \quad (7)$$

The resulting  $\mathcal{N} = 3$  theory has  $SO(3) \approx SU(2)$  R-symmetry group.

The case of  $\mathcal{N} = 6$  is special. It comes from the  $\mathcal{N} = 3$  theory when one takes the gauge group to be  $G = U(N)_k \times U(N)_{-k}$  and 2 hypermultiplets in the bifundamental representation  $H_i = Q_i + \tilde{Q}_i$ ,  $i = 1, 2$ . The chiral superfields  $Q_i = (A_1, A_2)$  are in the bifundamental representation  $(\mathbf{N}, \mathbf{N}^*)$  and  $\tilde{Q}_i = (B_1, B_2)$  are in the anti- bifundamental representation  $(\mathbf{N}^*, \mathbf{N})$ . In this case the superpotential (7) becomes:

$$W = \frac{2\pi}{k} \text{tr}(A_i B_i A_j B_j - B_i A_i B_j A_j) = \frac{4\pi}{k} \text{tr}(A_1 B_1 A_2 B_2 - A_1 B_2 A_2 B_1). \quad (8)$$

This can be written in a more compact way:

$$W = \frac{2\pi}{k} \epsilon^{ab} \epsilon^{\dot{a}\dot{b}} \text{tr}(A_a B_{\dot{a}} A_b B_{\dot{b}}). \quad (9)$$

The  $\mathcal{N} = 3$  CS theory has a  $SU(2) \times U(1)$  flavour symmetry. This  $SU(2)$  rotates  $A$ 's and  $B$ 's together. (9) has a symmetry under  $SU(2) \times SU(2) \times U(1)_B$  which acts on  $A$ 's and  $B$ 's separately. This symmetry does not commute with R-symmetry  $SO(3) \approx SU(2)$  under which  $A$  and  $B$  form doublets. Hence the  $\mathcal{N} = 3$  CS theory in this specific case has a larger  $SU(4) \approx SO(6)$  symmetry. This is the R-symmetry group of  $\mathcal{N} = 6$ .

Compactification on  $S^7$ : For the later use let us briefly review the mass spectrum of the Freund-Rubin solution of  $d = 11$  supergravity on  $S^7$  [8–10]. The gravitino field as well as all the fermions are set to zero, the  $AdS_4$  Riemann tensor and the three-form field strength are given by:

$$R_{\mu\nu\rho\sigma} = -4(g_{\mu\rho}(x)g_{\nu\sigma}(x) - g_{\mu\sigma}(x)g_{\nu\rho}(x)) \quad (10)$$

$$F_{\mu\nu\rho\sigma} = 3\sqrt{2}\sqrt{-\det g_{\mu\nu}(x)}\varepsilon_{\mu\nu\rho\sigma} \quad (11)$$

where  $\varepsilon_{0123} = -1$ . The metric and the three form field with mixed indices vanish:

$$g_{\mu\alpha} = F_{\mu\nu\rho\alpha} = F_{\mu\nu\alpha\beta} = F_{\mu\alpha\beta\gamma} = 0 \quad (12)$$

and also

$$F_{\alpha\beta\gamma\delta}(y) = 0 \quad (13)$$

$$R_{\alpha\beta} = -6g_{\alpha\beta}(y) \quad (14)$$

$\mu, \nu, \rho = 0, \dots, 3$  are  $d = 4$  indices,  $\alpha, \beta, \gamma = 1, \dots, 7$  are internal indices.

Then one considers fluctuations around the Freund-Rubin solution. The linearized field equations are obtained by replacing the background fields in the  $d = 11$  field equations by background fields plus arbitrary fluctuations. An elegant and quite general method to determine the complete mass spectrum on any coset manifold relies on generalized harmonic expansion. In our case, one expands the fluctuations in a complete set of spherical harmonics of  $S^7 = SO(8)/SO(7)$ . The coefficient functions of the spherical harmonics correspond to the physical fields in  $d = 4$ . In order to diagonalize the linearized equations it turns out to be convenient to parameterize the fluctuations as follows:

$$g_{\mu\nu}(x, y) = g_{\mu\nu}(x) + h_{\mu\nu}(x, y) \quad (15)$$

$$h_{\mu\nu}(x, y) = h'_{\mu\nu}(x, y) - \frac{1}{2}g_{\mu\nu}(x)h_\alpha^\alpha(x, y) \quad (16)$$

$$g_{\alpha\beta}(x, y) = g_{\alpha\beta}(x) + h_{\alpha\beta}(x, y) \quad (17)$$

$$g_{\mu\alpha}(x, y) = h_{\mu\alpha}(x, y) \quad (18)$$

$$A_{\mu\nu\rho}(x, y) = A_{\mu\nu\rho}(x) + a_{\mu\nu\rho}(x, y) \quad (19)$$

In particular the Weyl rescaled spacetime metric appears in (16) so as to put the  $d = 4$  Einstein action in the canonical form. The spherical harmonic expansions of

Spin	Field	$SO(7)$	$SO(8)$	$4(ML)^2$	$\Delta$	$\ell$
$2^+$	$h'_{(\mu\nu)}$	$N_1$	$(\ell, 0, 0, 0)$	$\ell(\ell + 6)$	$\Delta = \frac{\ell}{2} + 3$	$\ell \geq 0$
$1_1^-$	$h_{\mu\alpha}$	$N_7$	$(\ell, 1, 0, 0)$	$\ell(\ell + 2)$	$\Delta = \frac{\ell}{2} + 2$	$\ell \geq 0$
$1_2^-$	$A_{\mu\nu\alpha}$	$N_7$	$(\ell - 2, 1, 0, 0)$	$(\ell + 6)(\ell + 4)$	$\Delta = \frac{\ell}{2} + 4$	$\ell \geq 2$
$1^+$	$A_{\mu\alpha\beta}$	$N_{21}$	$(\ell - 1, 0, 1, 1)$	$(\ell + 2)(\ell + 4)$	$\Delta = \frac{\ell}{2} + 3$	$\ell \geq 1$
$0_1^+$	$A_{\mu\nu\rho}$	$N_1$	$(\ell + 2, 0, 0, 0)^*$	$(\ell + 2)(\ell - 4)$	$\Delta = \frac{\ell}{2} + 1$	$\ell \geq 0$
$0_2^+$	$h_{\alpha\alpha}, h'_{\lambda\lambda}$	$N_1$	$(\ell - 2, 0, 0, 0)$	$(\ell + 10)(\ell + 4)$	$\Delta = \frac{\ell}{2} + 5$	$\ell \geq 2$
$0_3^+$	$h_{(\alpha\beta)}$	$N_{27}$	$(\ell - 2, 2, 0, 0)$	$\ell(\ell + 6)$	$\Delta = \frac{\ell}{2} + 3$	$\ell \geq 2$
$0_1^-$	$A_{\alpha\beta\gamma}$	$N_{35}$	$(\ell, 0, 2, 0)$	$(\ell - 2)(\ell + 4)$	$\Delta = \frac{\ell}{2} + 2$	$\ell \geq 0$
$0_2^-$	$A_{\alpha\beta\gamma}$	$N_{35}$	$(\ell - 2, 0, 0, 2)$	$(\ell + 8)(\ell + 2)$	$\Delta = \frac{\ell}{2} + 4$	$\ell \geq 2$

Table 1: Bosonic KK towers after compactification on  $S^7$

the fluctuations of the metric and of the antisymmetric tensor fields are given by:

$$\begin{aligned}
h'_{(\mu\nu)}(x, y) &= \sum H_{\mu\nu}^{N_1}(x) Y^{N_1}(y) \\
h_{\mu\alpha}(x, y) &= \sum B_\mu^{N_7}(x) Y_\alpha^{N_7}(y) + B_\mu^{N_1}(x) D_\alpha Y^{N_1}(y) \\
h_{(\alpha\beta)}(x, y) &= \sum \phi^{N_{27}}(x) Y_{(\alpha\beta)}^{N_{27}}(y) + \phi^{N_7}(x) D_{(\alpha} Y_{\beta)}^{N_7}(y) + \phi^{N_1}(x) D_{(\alpha} D_{\beta)} Y^{N_1}(y) \\
h_\alpha^\alpha(x, y) &= \sum \pi^{N_1}(x) Y^{N_1}(y) \\
A_{\mu\nu\rho}(x, y) &= \sum a_{\mu\nu\rho}^{N_1}(x) Y^{N_1}(y) \\
A_{\mu\nu\alpha}(x, y) &= \sum a_{\mu\nu}^{N_7}(x) Y_\alpha^{N_7}(y) + a_{\mu\nu}^{N_1}(x) D_\alpha Y^{N_1}(y) \\
A_{\mu\alpha\beta}(x, y) &= \sum a_\mu^{N_{21}}(x) Y_{\alpha\beta}^{N_{21}}(y) + a_\mu^{N_7}(x) D_{[\alpha} Y_{\beta]}^{N_7} \\
A_{\alpha\beta\gamma}(x, y) &= \sum a^{N_{35}}(x) Y_{\alpha\beta\gamma}^{N_{35}}(y) + a^{N_{21}}(x) D_{[\alpha} Y_{\beta\gamma]}^{N_{21}}(y)
\end{aligned} \tag{20}$$

All superscripts  $N_r$  ( $r = 1, 7, 21, 27, 35$ ) have infinite range, since they should provide a basis for arbitrary fields on the 7-sphere. The index  $r$  specifies the  $SO(7)$  representation of the corresponding spherical harmonic. For example,  $Y_{\alpha\beta\gamma}^{N_{35}}$  is in the third rank totally antisymmetric representation of  $SO(7)$  with dimension 35, while  $Y_{(\alpha\beta)}^{N_{27}}$  is in the symmetric traceless 27-dimensional representation. Derivatives of  $Y$ 's appear in the expansions since any tensor can be decomposed into its transverse and longitudinal parts. Then one has to fix all local symmetries and substitute the resulting expansions into the  $d = 11$  field equations. The coefficients of each independent spherical harmonic will yield the  $d = 4$  field equations. After diagonalizing the bosonic field equations one obtains the mass spectrum summarized in Table 1. The resulting bosonic spectrum includes the massless graviton, **28** massless vectors of  $SO(8)$ , corresponding to a combination of  $B_\mu$  (in  $h_{\mu\alpha}$ ) and  $C_\mu$  (in  $A_{\mu\nu\alpha}$ ), **35**<sub>s</sub> scalars ( $\Delta = 1$ ) and **35**<sub>s</sub> ( $\Delta = 2$ ) pseudoscalars with  $(ML_{AdS})^2 = -2$ . In the supergravity literature [8–10] masses of scalars are often shifted by  $-R/6$  so that  $(ML_{AdS})^2 \rightarrow (ML_{AdS})^2 = (ML_{AdS})^2 + 2$ . The 70 (pseudo)scalars in the  $\mathcal{N} = 8$  su-

Spin	$SO(8)$	$4(ML)^2$	$\Delta$	$\ell$
$(\frac{3}{2})_1$	$(\ell, 0, 0, 1)$	$(\ell + 2)^2$	$\Delta = \frac{\ell}{2} + \frac{5}{2}$	$\ell \geq 0$
$(\frac{3}{2})_2$	$(\ell - 1, 0, 1, 0)$	$(\ell + 4)^2$	$\Delta = \frac{\ell}{2} + \frac{7}{2}$	$\ell \geq 1$
$(\frac{1}{2})_1$	$(\ell + 1, 0, 1, 0)^*$	$\ell^2$	$\Delta = \frac{\ell}{2} + \frac{3}{2}$	$\ell \geq 0$
$(\frac{1}{2})_2$	$(\ell - 1, 1, 1, 0)$	$(\ell + 2)^2$	$\Delta = \frac{\ell}{2} + \frac{5}{2}$	$\ell \geq 1$
$(\frac{1}{2})_3$	$(\ell - 2, 1, 0, 1)$	$(\ell + 4)^2$	$\Delta = \frac{\ell}{2} + \frac{7}{2}$	$\ell \geq 2$
$(\frac{1}{2})_4$	$(\ell - 2, 0, 0, 1)$	$(\ell + 6)^2$	$\Delta = \frac{\ell}{2} + \frac{9}{2}$	$\ell \geq 2$

Table 2: Fermionic KK towers after compactification on  $S^7$

pergravity multiplet are massless in the sense that  $(\tilde{M}L_{AdS})^2 = 0$ . Moreover, there are three families of scalars and two families of pseudoscalar excitations. Three of them ( $0_2^+$ ,  $0_3^+$  and  $0_2^-$ ) contain only states with positive mass square and correspond to irrelevant operators in the dual CFT. The remaining families  $0_1^+$  and  $0_1^-$  contain states with positive, zero and negative mass squared corresponding to irrelevant, marginal and relevant operators, respectively.

A similar analysis can be performed for fermionic fluctuations. In Table 2 we summarize the fermionic mass spectrum.

The KK spectrum does not include the states with \* for  $\ell = -1$ , since they do not propagate in the bulk but live on the conformal boundary of  $AdS_4$ . They correspond to the singleton representation of  $Osp(8|4)$  that consists of  $8_v$  bosons  $X^i$  with  $\Delta = \frac{1}{2}$ ,  $(ML)^2 = -\frac{5}{4}$  and  $8_c$  fermions  $\psi^a$  with  $\Delta = 1$ ,  $ML = \frac{1}{2}$ , both at the unitary bound.

### 3. From $S^7$ to $S^7/\mathbb{Z}_k$ and $\mathbb{CP}^3 \times S^1$

$S^7$  is a  $U(1)$  bundle over  $\mathbb{CP}^3$ . The  $\mathbb{CP}^3$  solution of the  $d = 10$  theory can be obtained from the  $S^7$  solution of the  $d = 11$  theory by Hopf fibration, *i.e.* keeping only  $U(1)$  invariant states [7]. The compactification on  $\mathbb{CP}^3$  of the  $d = 10$  theory yields a four dimensional theory with  $\mathcal{N} = 6$  supersymmetry and with gauge group  $SO(6) \times SO(2)$ . In order to decompose KK harmonics on  $S^7 = SO(8)/SO(7)$  into KK harmonics on  $\mathbb{CP}^3 = U(4)/U(3) \times U(1)$ , we constructed an arbitrary representations of  $SO(8)$  in the space of polynomials of 12 variables. The latter are the coordinates of the subgroup  $Z_+^{SO(8)}$  generated by the raising operators of  $SO(8)$ . Then we developed a technique which allows to identify which of the above polynomials correspond to highest weight states of representations of  $U(4) \subset SO(8)$ . In this case the number of variables reduces to 6 and in this case the polynomials will depend on these six variables. The method we used is quite standard in representation theory of Lie groups (see *e.g.* Chapter 16 of [11]). The details can be found in the original paper [3] or in the [4]. We just give the *indicator* system one has to

solve for the highest weight states:

$$\begin{aligned} (a_{23}\partial_{a_{13}} + a_{24}\partial_{a_{14}})^{\ell_1+1} f(a) &= 0 \\ (a_{13}\partial_{a_{12}} + a_{34}\partial_{a_{24}})^{\ell_2+1} f(a) &= 0 \\ (a_{14}\partial_{a_{13}} + a_{24}\partial_{a_{23}})^{\ell_3+1} f(a) &= 0 \\ (\partial_{a_{34}})^{\ell_4+1} f(a) &= 0. \end{aligned} \quad (21)$$

Solving these equations one can fully decompose KK harmonics on  $S^7$  into KK harmonics of  $\mathbb{CP}^3 \times S^1$  which is our next task.

In the following we will give only a couple of examples how KK towers of  $S^7$  decompose into KK towers of  $S^7/\mathbb{Z}_k$ . For the decomposition of all towers see [3], [4]. For scalar spherical harmonics with Dynkin labels  $(\ell, 0, 0, 0)$  one finds as independent polynomials  $\{a_{14}^m \mid m = 0, \dots, \ell\}$ . Thus the following decomposition holds:

$$(\ell, 0, 0, 0) \rightarrow \bigoplus [0, \ell - m, m]_{\ell-2m} \quad (22)$$

where the subscript is the  $SO(2)$  charge  $Q$  of the appropriate representation.

For vector spherical harmonics with  $SO(8)$  Dynkin labels  $(\ell - 2, 1, 0, 0)$  one gets  $\{a_{12}a_{14}^m, a_{24}a_{14}^m, (a_{13}a_{24} - a_{14}a_{23})a_{14}^m, a_{14}^m \mid m = 0, \dots, \ell\}$  as independent polynomials. The  $SO(8)$  representation decomposes into  $SO(6)$  representations as:

$$\begin{aligned} (\ell, 1, 0, 0) \rightarrow & \quad \bigoplus [0, \ell - m, m]_{\ell-2m} \oplus [0, \ell - m + 1, m + 1]_{\ell-2m} \\ & \quad \bigoplus [1, \ell - m, m]_{\ell-2m-2} \oplus [1, \ell - m, m]_{\ell-2m+2} \end{aligned} \quad (23)$$

The zero charge spectrum *i.e.* the states which constitute the KK spectrum of Type IIA supergravity on  $\mathbb{CP}^3$  can be easily identified in the decompositions.

The  $\mathbb{Z}_k$  orbifold projection on  $S^7$  gives  $S^7/\mathbb{Z}_k \approx \mathbb{CP}^3 \times S^1$ . In this way the supersymmetry breaks. It appears not to be spontaneous supersymmetry breaking. Massless scalars, corresponding to marginal operators with  $\Delta = 3$  on the boundary, only appear in higher KK multiplets, *i.e.* in the **840<sub>vc</sub>** = (2, 0, 2, 0) and **1386** = (6, 0, 0, 0). None of these can play the role of Stückelberg field for the 12 coset vectors in the **6**<sub>+2</sub> + **6**<sub>-2</sub> of  $SO(8)/SO(6) \times SO(2)$ .

Indeed, using the group theory techniques described in Section 3 the decomposition of **840<sub>vc</sub>** = (2, 0, 2, 0) under  $SO(8) \rightarrow SO(6) \times SO(2)$  reads

$$\begin{aligned} \mathbf{840}_{\mathbf{vc}}(2, 0, 2, 0) \rightarrow & \quad \mathbf{84}_{+4}[0, 2, 2] + \mathbf{70}_{+2}[0, 3, 1] + \mathbf{70}_{+2}[0, 1, 3] + \mathbf{64}_{+2}[1, 1, 1] \\ & + \mathbf{84}_0[0, 2, 2] + \mathbf{45}_0[1, 2, 0] + \mathbf{45}_0[1, 0, 2] \\ & + \mathbf{35}_0[0, 4, 0] + \mathbf{35}_0[0, 0, 4] + \mathbf{20}'_0[2, 0, 0] \\ & + \mathbf{84}_{-4}[0, 2, 2] + \mathbf{70}_{-2}[0, 3, 1] + \mathbf{70}_{-2}[0, 1, 3] + \mathbf{64}_{-2}[1, 1, 1] \end{aligned} \quad (24)$$

This means that the massless scalars in the **840<sub>vc</sub>**(2, 0, 2, 0) cannot account for the needed Stückelberg fields in the **6**<sub>+2</sub> + **6**<sub>-2</sub>. One can recognize massless scalars neutral under  $SO(2)$  that survive in  $k \rightarrow \infty$  limit and transform non-trivially under  $SO(6)$ .

The

The same applies to the other massless scalars in the **1386**(6,0,0,0). The decomposition reads

$$\begin{aligned} \mathbf{1386}(6,0,0,0) \rightarrow & \quad \mathbf{84}_{+6}[0,6,0] + \mathbf{189}_{+4}[0,5,1] + \mathbf{270}_{+2}[0,4,2] \\ & + \mathbf{300}_0[0,3,3] \\ & + \mathbf{84}_{-6}[0,0,6] + \mathbf{189}_{-4}[0,1,5] + \mathbf{270}_{-2}[0,2,4] \end{aligned} \quad (25)$$

It

is

obvious

that

there

are

no

**6****+2****-2**

. In

this

case,

neutral

fields

appear

in

the

**300**

representation

of

*SO*(6).

Thus,

we

see

that

there

is

no

Higgs

mechanism

for

the

breaking

of

*SO*(8)

to

*SO*(6)

×

*SO*(2).

One

observes

that

in

the

large

*k*

limit

only

*SO*(2)

singlets

survive.

Only

states

with

 $\ell$ 

even

on

 $S^7$ 

give

rise

to

neutral

states.

This

means

that

the

parent

theory

could

be

either

a

compactification

on

 $S^7$ 

or

on

 $\mathbb{RP}^7 = S^7/\mathbb{Z}_2$ .

Indeed

both

lead

to

*SO*(8)

gauged

supergravity

with

the

massless

multiplet

{ $\{g_{\mu\nu}, 8\psi_\mu, 28A_\mu, 56\lambda, 35^+ + 35^- \varphi\}$ }.

## 4. KK towers

Let

us

now

focus

on

the

KK

excitations.

One

can

write

the

single-particle

partition

function

on

 $S^7$ ,

decompose

it

into

super-characters

and

identify

the

*SO*(2)

charge

sectors,

relevant

for

the

subsequent

 $\mathbb{Z}_k$ 

projection

*i.e.*

compactification

on

 $\mathbb{CP}^3$ .

Introducing

a

chemical

potential

for

the

charge

 $Q$ 

(

 $t^Q$ )

, the

super-character

of

an

ultra-short

1/2

BPS

representation

of

*Osp*(8|4)

reads:

$$\begin{aligned} \mathcal{X}_\ell^{1/2BPS}(q,t) = & \frac{t^{-2-\ell} q^{2+\ell}}{6(1-t^2)^5(1+q)^3} \left[ \ell^3 (-1+t^2)^2 (-1+q)^3 \right. \\ & \times \left( t^{6+2\ell} (t^2-q)^2 - (-1+t^2 q)^2 \right) - 6\ell^2 (-1+t^2) (-1+q)^2 \\ & \times \left( t^{6+2\ell} (t^2-q)^2 (-3+2t^2+q) + (2+t^2(-3+q)) (-1+t^2 q)^2 \right) \\ & + 6t^{6+2\ell} (t^2-q)^2 (-35+q(35+(-9+q)q)+2t^4(-5+q^2) \\ & + t^2(35+q(-13+(-7+q)q))) - (2(-5+q^2) \\ & + t^4(-35+q(35+(-9+q)q))+t^2(35+q(-13+(-7+q)q))) \\ & \times 6(-1+t^2 q)^2 - \ell(-1+q) \left( t^{6+2\ell} (t^2-q)^2 (-107+(70-11q)q \right. \\ & \left. + t^4(-47+(-2+q)q)-2t^2(-71+q(22+q))) + (-1+t^2 q)^2 \right. \\ & \left. \times (47-(-2+q)q+2t^2(-71+q(22+q))+t^4(107+q(-70+11q))) \right]. \end{aligned} \quad (26)$$

For

 $\ell=0$ ,

corresponding

to

the

gauged

supergravity

multiplet,

there

is

further

shortening

(null

descendants)

due

to

the

presence

of

conserved

'currents'

*i.e.*

stress-

tensor,

*SO*(8)

vector

currents

and

**8**<sub>s</sub>

supercurrents.

Taking

this

into

account

one

finds the following super-character

$$\begin{aligned} \mathcal{X}_{\ell=0}^{1/2BPS}(q) = \frac{1}{(1-q^2)^3} & [(10t^2 + 15 + 10t^{-2})q^2 - \\ & 2(15t^2 + 10 + 6 + 10 + 15t^{-2})q^3 + \\ & (10t^2 + 15 + 10t^{-2} + 3(6t^2 + 15 + 1 + 6t^{-2}))q^4 - \\ & 4(t^2 + 6 + t^{-2})q^5 - (6t^2 + 15 + 1 - 5 + 6t^{-2})q^6 + \\ & 2(t^2 + 6 + t^{-2})q^7 - 3q^8]. \end{aligned} \quad (27)$$

The denominator takes into account derivatives (descendants). Quite remarkably this formula coincides with the previous one when  $\ell = 0$ .

After some algebra, putting  $t = 1$  (*i.e.* not keeping the track of  $SO(2)$  charge), one finds

$$\mathcal{X}_{\ell=0}^{1/2BPS}(q) = \frac{q^2(3q^3 - 7q^2 - 7q + 35)}{(1+q)^3}. \quad (28)$$

A factor  $(1-q)^2$  cancels between numerator and denominator meaning that not only the number of bosons equals to the number of fermions and the sum with  $\Delta^1$  vanishes but also the sum with  $\Delta^2$  should vanish. This should be related to the absence of quantum corrections to the negative vacuum energy, *i.e.* cosmological constant in the bulk.

The  $1/2$  BPS partition function is given by

$$\mathcal{Z}_{1/2BPS}^{\mathcal{N}=8} = \sum_{\ell} \mathcal{X}_{\ell}^{1/2BPS} = \frac{35q^2}{(1-q^2)^2}. \quad (29)$$

The simplicity of the result is due to miraculous cancellations between bosonic and fermionic operators with the same scaling dimensions in different KK multiplets *i.e.* with different  $\ell$ 's.

In order to perform the  $\mathbb{Z}_k$  projection it is useful to decompose into  $SO(2)$  charge sectors according to

$$\mathcal{Z}_{1/2BPS}^{\mathcal{N}=8 \rightarrow \mathcal{N}=6}(q, t) = \frac{q^2[(1+q^6)P_2(t) - (q+q^5)P_3(t) + (q^2+q^4)P_4(t) - q^3P_5(t)]}{(1-qt)^4(1-qt^{-1})^4(1+q)^2}, \quad (30)$$

where

$$\begin{aligned} P_2(t) &= 10t^{+2} + 15 + 10t^{-2} \\ P_3(t) &= 20t^{+3} + 10t^{+2} + 64t^{+1} + 22 + 64t^{-1} + 10t^{-2} + 20t^{-3} \\ P_4(t) &= 15t^{+4} + 8t^{+3} + 104t^{+2} + 48t^{+1} + 175 + 48t^{-1} + 104t^{-2} + 8t^{-3} + 15t^{-4} \\ P_5(t) &= 4t^{+5} + 2t^{+4} + 64t^{+3} + 40t^{+2} + 196t^{+1} + 88 + \\ &+ 196t^{-1} + 40t^{-2} + 64t^{-3} + 2t^{-4} + 4t^{-5}. \end{aligned} \quad (31)$$

Depending on the choice of  $k$  one can recognize the surviving  $1/2$  BPS states as those with  $Q = kn$ . In formulae one has to replace  $t$  with  $\omega^r$  and sum over  $r = 0, \dots, k-1$ .

## 5. Conclusions

We have re-analyzed the KK spectrum of 11 dimensional supergravity on  $AdS_4 \times S^7$  which is the low energy limit of M-theory on  $AdS_4 \times S^7$ . A compactification on  $AdS_4 \times S^7/\mathbb{Z}_k$  with  $k \rightarrow \infty$  corresponds to the low energy limit of Type IIA theory on  $AdS_4 \times \mathbb{CP}^3$ . We presented group theoretical method showing how the R-symmetry group of the theory on  $AdS_4 \times \mathbb{CP}^3$  is embedded into the R-symmetry group of the theory on  $AdS_4 \times S^7$ . This gives a very nice way to decompose the KK towers of  $S^7$  into those of  $S^7/\mathbb{Z}_k$ . Going from M-theory on  $AdS_4 \times S^7$  to Type IIA theory on  $AdS_4 \times \mathbb{CP}^3$  the supersymmetry breaks. We show that this breaking is not spontaneous. Massless scalars, corresponding to marginal operators with  $\Delta = 3$  on the boundary, only appear in higher KK multiplets, *i.e.* in the **840<sub>vc</sub>** = (2, 0, 2, 0) and **1386** = (6, 0, 0, 0). We have shown that none of these can play the role of Stückelberg field for the 12 coset vectors in the **6<sub>+2</sub> + 6<sub>-2</sub>** of  $SO(8)/SO(6) \times SO(2)$ . In the last section we discussed KK excitations in details computing different super-characters and partition functions.

## References

- [1] M.B. Green, J.H. Schwarz and E. Witten, *Superstring Theory* (Cambridge University Press, Cambridge, 1988); J. Polchinski, *String Theory* (Cambridge University Press, Cambridge, 1998); K. Becker, M. Becker, J.H. Schwarz *String Theory and M-Theory* (Cambridge University Press, Cambridge, 2007); E. Kiritsis *String Theory in a Nutshell* (Princeton University Press, Princeton, 2007).
- [2] J. M. Maldacena, Adv. Theor. Math. Phys. **2** (1998) 231 [Int. J. Theor. Phys. **38** (1999) 1113] [arXiv:hep-th/9711200].
- [3] M. Bianchi, R. Poghossian and M. Samsonyan, JHEP **1010**, 021 (2010) [arXiv:1005.5307].
- [4] M. Samsonyan, arXiv:1102.1357.
- [5] O. Aharony, O. Bergman, D. L. Jafferis and J. Maldacena, JHEP **0810**, 091 (2008) [arXiv:0806.1218].
- [6] O. Aharony, O. Bergman and D. L. Jafferis, JHEP **0811**, 043 (2008) [arXiv:0807.4924].
- [7] B. E. W. Nilsson and C. N. Pope, Class. Quant. Grav. **1**, 499 (1984).
- [8] L. Castellani, R. D'Auria, P. Fre, K. Pilch and P. van Nieuwenhuizen, Class. Quant. Grav. **1**, 339 (1984).
- [9] P. Van Nieuwenhuizen, In \*Les Houches 1983, Proceedings, Relativity, Groups and Topology, II\*, 823-932

[10] E. Sezgin, Phys. Lett. B **138**, 57 (1984).

[11] D. P. Zhelobenko “Compact Lie groups and their representations”. Translations of mathematical monographs, V. 40, AMS (1973).

# Casimir-Polder forces in the geometry of cosmic string

A. S. Kotanjyan, A. A. Saharian, V. M. Bardeghyan

*Department of Physics, Yerevan State University*

*1 Alex Manoogian Street, 0025 Yerevan, Armenia*

## Abstract

Combined effects on the Casimir-Polder potential due to a cosmic string and coaxial metallic cylindrical shell are investigated. For the both regions inside and outside the shell, the potential is decomposed into pure string and shell-induced parts. In a special case of an isotropic polarizability tensor, the Casimir-Polder force in the interior region is attractive with respect to the shell. In the exterior region the force is attractive near the shell and repulsive at large distances from the shell.

## 1. Introduction

The Casimir-Polder (CP) forces have attracted a great deal of attention because of their important role in many areas of science, including material sciences, physical chemistry, nanotechnology, and atom optics (for reviews see Refs. [1, 2]). In this paper we present the results of the investigation of the CP forces due to the non-trivial topology induced by a straight cosmic string and boundaries. Cosmic strings are among the most interesting classes of topological defects which could arise as a result of symmetry breaking phase transitions during the evolution of the early universe [3]. They are candidates for the generation of a variety of interesting physical effects, including gravitational lensing, anisotropies in the cosmic microwave background radiation, the generation of gravitational waves, high-energy cosmic rays, and gamma ray bursts.

The nontrivial topology of the cosmic string spacetime results in the distortion of the zero-point vacuum fluctuations of quantized fields and induces non-zero vacuum expectation values for physical observables. Combined effects of topology and boundaries on the quantum vacuum in the geometry of a cosmic string have been investigated for scalar [4], vector [5, 6] and fermionic fields [7, 8], with boundary conditions on cylindrical surfaces. The vacuum energy for massless scalar fields subject to Dirichlet, Neumann and hybrid boundary conditions in the setting of the conical piston has been analyzed in Ref. [9]. The vacuum polarization effects in a cosmic string spacetime induced by a scalar field obeying Dirichlet or Neumann boundary conditions on a flat boundary orthogonal to the string are considered in Ref. [10]. Here we consider the effects of cosmic string and coaxial metallic cylindrical shell on

the CP force. The CP interaction potential of a microparticle with an ideal metal cylindrical shell in background of Minkowski spacetime has been investigated in a number of papers (see references in Ref. [11]). Recently, the exact potential for a microparticle outside a cylindrical shell has been found in Ref. [11] using the Hamiltonian approach. The CP potential for both regions inside and outside an ideal metal cylindrical shell is investigated in Ref. [12] using the Green function method.

The paper is based on Refs. [13, 14, 15] and is organized as follows. In the next section the CP potential is investigated for a polarizable microparticle in a boundary-free cosmic string geometry. The part in the CP potential induced by a metallic cylindrical shell is studied in Sec. 3 for both interior and exterior regions. The main results are summarized in Sec. 4.

## 2. Casimir-Polder potential in boundary-free cosmic string geometry

For an infinitely long straight cosmic string the line element has the form

$$ds^2 = dt^2 - dr^2 - r^2 d\phi^2 - dz^2, \quad (1)$$

where  $0 \leq r < \infty$ ,  $-\infty < z < +\infty$ ,  $0 \leq \phi \leq \phi_0$  and the spatial points  $(r, \phi, z)$  and  $(r, \phi + \phi_0, z)$  are to be identified. For an infinite straight cosmic string the line element (1) has been derived in Ref. [16] in the weak-field approximation. In this approximation the planar angle deficit is small and it is related to the mass  $\mu_0$  per unit length of the string by  $2\pi - \phi_0 = 8\pi G\mu_0$ , with  $G$  being the gravitational constant. The validity of the line element (1) has been extended beyond linear perturbation theory by several authors [17] (see also Ref. [3]). In this case the planar angle deficit need not to be small. An interesting limiting case with  $\phi_0 \ll 2\pi$  has been discussed in Ref. [3].

First we consider the CP potential for a microparticle with the polarizability tensor  $\alpha_{jl}(\omega)$  in the boundary-free cosmic string geometry. For a microparticle at a point  $\mathbf{r}$ , the potential is given by the expression [2]

$$U_0(\mathbf{r}) = \frac{1}{2\pi} \int_0^\infty d\xi \alpha_{jl}(i\xi) G_{jl}^{(s)}(\mathbf{r}, \mathbf{r}; i\xi), \quad (2)$$

where summation is understood over the indices  $j, l = 1, 2, 3$ ,

$$G_{jl}^{(s)}(\mathbf{r}, \mathbf{r}'; \omega) = \int_{-\infty}^{+\infty} d\tau \left[ G_{jl}^{(0)}(x, x') - G_{jl}^{(M)}(x, x') \right] e^{i\omega\tau}, \quad (3)$$

and  $x = (t, \mathbf{r})$ ,  $x' = (t', \mathbf{r}')$ ,  $\tau = t - t'$ . In (3),  $G_{jl}^{(0)}(x, x')$  is the retarded Green tensor for the electromagnetic field in the geometry of the cosmic string and  $G_{jl}^{(M)}(x, x')$  is the corresponding tensor in the Minkowski spacetime. Outside the string core the spacetime is flat and the renormalization is reduced to the subtraction of the Minkowskian part.

In the problem under consideration the off-diagonal components,  $G_{jl}^{(s)}(\mathbf{r}, \mathbf{r}; i\xi)$ ,  $j \neq l$ , vanish and for the diagonal components we have the expression:

$$G_{ll}^{(s)}(\mathbf{r}, \mathbf{r}; i\xi) = 2\xi^3 \left[ \sum_{k=1}^{[q/2]} f_l(2\xi rs_k, s_k) - \frac{q}{\pi} \sin(q\pi) \int_0^\infty dy \frac{f_l(2\xi r \cosh y, \cosh y)}{\cosh(2qy) - \cos(q\pi)} \right], \quad (4)$$

where  $q = 2\pi/\phi_0$ ,  $[q/2]$  stands for the integer part of  $q/2$  and

$$s_k = \sin(\pi k/q). \quad (5)$$

In (6), the function  $f_l(u, v)$  is defined as

$$f_l(u, v) = e^{-u} \sum_{p=1}^3 b_{lp}(v) u^{p-4}, \quad b_{lp}(v) = b_{lp}^{(0)} + b_{lp}^{(1)} v^2, \quad (6)$$

with the coefficients matrices

$$b_{lp}^{(0)} = \begin{pmatrix} 1 & 1 & 1 \\ -2 & -2 & 0 \\ 1 & 1 & 1 \end{pmatrix}, \quad b_{lp}^{(1)} = \begin{pmatrix} 1 & 1 & -1 \\ 1 & 1 & -1 \\ 0 & 0 & 0 \end{pmatrix}. \quad (7)$$

The CP potential is evaluated by using the formula (2). By taking into account (4) and introducing the notation

$$h_{lp}(y) = \int_0^\infty dx x^{p-1} e^{-x} \alpha_{ll}(ix/y), \quad (8)$$

the potential is expressed as

$$\begin{aligned} U_0(r) &= \frac{r^{-4}}{16\pi} \sum_{l,p=1}^3 \left[ \sum_{k=1}^{[q/2]} \frac{b_{lp}(s_k)}{s_k^4} h_{lp}(2rs_k) - \frac{q}{\pi} \sin(q\pi) \right. \\ &\quad \times \left. \int_0^\infty dy \frac{h_{lp}(2r \cosh y)}{\cosh(2qy) - \cos(q\pi)} \frac{b_{lp}(\cosh y)}{\cosh^4 y} \right]. \end{aligned} \quad (9)$$

The corresponding force is perpendicular to the string and is directed along the radial direction. Expression (9) is simplified for integer values of the parameter  $q$ :

$$U_0(r) = \frac{r^{-4}}{32\pi} \sum_{k=1}^{q-1} \sum_{l,p=1}^3 \frac{b_{lp}(s_k)}{s_k^4} h_{lp}(2rs_k). \quad (10)$$

In (24),  $\alpha_{ll}(i\xi)$  are the (physical) components of the polarizability tensor in the cylindrical coordinates  $x^l = (r, \phi, z)$ . These components depend on the orientation of the polarizability tensor principal axes. As a consequence, the CP potential depends on the distance of the microparticle from the string and on the angles determining the orientation of the principal axes. Let us introduce Cartesian coordinates  $x^l =$

$(x', y', z')$  with the  $z'$ -axis along the string and with the particle location at  $(r, 0, 0)$  and let  $\beta_{ln}$  be the cosine of the angle between  $x'^l$  and the  $n$ -th principal axis of the polarizability tensor. One has  $\sum_{n=1}^3 \beta_{ln}^2 = 1$ . Now we can write  $\alpha_{ll}(\omega) = \sum_{n=1}^3 \beta_{ln}^2 \alpha_n(\omega)$ , where  $\alpha_n(\omega)$  are the principal values of the polarizability tensor. The coefficients  $\beta_{ln}$  can be expressed in terms of the Euler angles determining the orientation of the principal axes with respect to the coordinate system  $x'^l$ . In the isotropic case  $\alpha_n(\omega) \equiv \alpha(\omega)$  and we have  $\alpha_{ll}(\omega) = \alpha(\omega)$ .

At large distances from the string to the leading order one finds

$$U_0(r) \approx \frac{(q^2 - 1)(q^2 + 11)}{360\pi r^4} [\alpha_{11}(0) - \alpha_{22}(0) + \alpha_{33}(0)]. \quad (11)$$

with  $\alpha_{ll}(0)$  being the static polarizability of a particle. The force corresponding to (11) can be either attractive or repulsive.

For an isotropic polarizability tensor,  $\alpha_{jl}(\omega) = \delta_{jl}\alpha(\omega)$ , we can explicitly sum over  $l$  and the expression for the CP potential is obtained from (9) by making the replacement

$$\sum_{l=1}^3 b_{lp}(v) h_{lp}(2rv) \rightarrow b_p(v) h_p(2rv), \quad (12)$$

where we have defined  $h_p(y) = \int_0^\infty dx x^{p-1} e^{-x} \alpha(ix/y)$  and

$$b_1(v) = b_2(v) = 2v^2, \quad b_3(v) = 2 - 2v^2. \quad (13)$$

For the further transformation of the general expression (9) for the CP potential we need to specify the functional form of the polarizability tensor. For the corresponding principal values we use the anisotropic oscillator model with

$$\alpha_n(i\xi) = \sum_j \frac{g_j^{(n)}}{\omega_j^{(n)2} + \xi^2}, \quad (14)$$

and with  $\omega_j^{(n)}$  and  $g_j^{(n)}$  being the oscillator frequencies and strengths, respectively. This model for the dynamic polarizability works well over a wide range of separations. Now for the function (8) one gets

$$h_{lp}(y) = y^2 \sum_{n=1}^3 \sum_j g_j^{(n)} \beta_{ln}^2 B_p(y\omega_j^{(n)}). \quad (15)$$

with

$$B_p(z) = \int_0^\infty dx \frac{x^{p-1} e^{-x}}{x^2 + z^2}. \quad (16)$$

The integral in (16) is expressed in terms of the functions  $\text{Si}(x)$  and  $\text{Ci}(x)$ . As a

result, for the CP potential in the oscillator model we find the following expression

$$U_0(r) = \frac{1}{4\pi r^2} \sum_{l,n,p=1}^3 \sum_j g_j^{(n)} \beta_{ln}^2 \left[ \sum_{k=1}^{[q/2]} \frac{b_{lp}(s_k)}{s_k^2} B_p(2r\omega_j^{(n)} s_k) - \frac{q}{\pi} \sin(q\pi) \int_0^\infty dy \frac{B_p(2r\omega_j^{(n)} \cosh y)}{\cosh(2qy) - \cos(q\pi)} \frac{b_{lp}(\cosh y)}{\cosh^2 y} \right]. \quad (17)$$

The corresponding formula for the isotropic case is obtained from (17) by the replacement

$$\sum_{l,n=1}^3 \beta_{ln}^2 b_{lp}(v) B_p(2rv\omega_j^{(n)}) \rightarrow b_p(v) B_p(2rv\omega_j). \quad (18)$$

The corresponding force is repulsive.

At small distances from the string,  $r \ll 1/\omega_j^{(n)}$ , the dominant contribution in (17) comes from the term with  $p = 1$  in the leading order and to the leading order we get

$$U_0(r) \approx \frac{1}{16r^3} \sum_{l,n=1}^3 \sum_j \eta_j^{(n)} \beta_{ln}^2 [b_{l1}^{(0)} g_3(q) + b_{l1}^{(1)} g_1(q)], \quad (19)$$

where  $\eta_j^{(n)} = g_j^{(n)} / \omega_j^{(n)}$  and

$$b_{l1}^{(0)} = (1, -2, 1), \quad b_{l1}^{(1)} = (1, 1, 0). \quad (20)$$

In (19) we have defined the function

$$g_n(q) = \sum_{k=1}^{[q/2]} s_k^{-n} - \frac{q}{\pi} \sin(q\pi) \int_0^\infty dy \frac{\cosh^{-n}(y)}{\cosh(2qy) - \cos(q\pi)}. \quad (21)$$

With dependence of the orientation of the polarizability tensor principal axes and on the values of  $\eta_j^{(m)}$ , the corresponding force can be either repulsive or attractive. In the isotropic case the asymptotic expression at large distance takes the form

$$U_0(r) \approx \frac{g_1(q)}{8r^3} \sum_j \frac{g_j}{\omega_j}, \quad (22)$$

and the corresponding force is repulsive.

The dependence of the CP potential on the orientation of the polarizability tensor principal axes with respect to the string will also lead to the moment of force acting on the particle. As a consequence, the influence of the cosmic string on the system of particles with anisotropic polarizability results in the macroscopic polarization.

### 3. Casimir-Polder potential for a metallic cylinder in cosmic string spacetime

In this section we consider the CP potential for a microparticle inside and outside a metallic cylindrical shell with radius  $a$ . The CP potential is presented in the decomposed form (details will be presented in Ref. [15])

$$U(r) = U_0(r) + U_b(r), \quad (23)$$

where the term

$$\begin{aligned} U_b(r) &= -\frac{2q}{\pi^2} \sum_{m=0}^{\infty}' \sum_{\lambda=0,1} \sum_{l=1}^3 \int_0^\infty d\xi \alpha_{ll}(i\xi) (-\xi^2)^\lambda \int_\xi^\infty d\gamma \gamma \\ &\times \frac{(\gamma^2 - \xi^2)^{1-\lambda}}{\sqrt{\gamma^2 - \xi^2}} \frac{K_{qm}^{(\lambda)}(a\gamma)}{I_{qm}^{(\lambda)}(a\gamma)} |i_l^{(\lambda)}(\gamma r, \gamma/\sqrt{\gamma^2 - \xi^2})|^2, \end{aligned} \quad (24)$$

is induced by the presence of the cylindrical shell. In (24),  $I_\nu(x)$ ,  $K_\nu(x)$  are the modified Bessel functions and the functions  $i_l^{(\lambda)}(x, y)$  are defined as

$$\begin{aligned} i_1^{(0)}(x, y) &= I'_{q|m|}(x), i_2^{(0)}(x, y) = i \frac{qm}{x} I_{q|m|}(x), i_3^{(0)}(x, y) = iy I_{q|m|}(x), \\ i_1^{(1)}(x, y) &= \frac{qm}{x} I_{q|m|}(x), i_2^{(1)}(x, y) = -i I'_{q|m|}(x), i_3^{(1)}(x, y) = 0, \end{aligned} \quad (25)$$

and the prime on the summations sign means that the term  $m = 0$  should be taken with the coefficient  $1/2$ . In the absence of the string we have  $q = 1$  and the formula (24) is reduced to the expression for the CP potential for a cylindrical shell in Minkowski spacetime derived in Ref. [12].

For the isotropic polarizability tensor the general expression (24) for the boundary-induced part in the CP potential takes the form

$$\begin{aligned} U_b(r) &= -\frac{2q}{\pi^2} \sum_{m=0}^{\infty}' \int_0^\infty d\xi \alpha(i\xi) \int_\xi^\infty \frac{\gamma d\gamma}{\sqrt{\gamma^2 - \xi^2}} \\ &\times \left\{ \frac{K_{qm}(a\gamma)}{I_{qm}(a\gamma)} \left[ (\gamma^2 - \xi^2) F_{qm}(\gamma r) + \gamma^2 I_{qm}^2(\gamma r) \right] - \xi^2 \frac{K'_{qm}(a\gamma)}{I'_{qm}(a\gamma)} F_{qm}(\gamma r) \right\}. \end{aligned} \quad (26)$$

with the notation  $F_{qm}(x) = I_{qm}^2(x) + (qm/x)^2 I_{qm}^2(x)$ . The boundary-induced part of the potential diverges on the cylindrical shell. The leading term in the corresponding asymptotic expansion over the distance from the boundary coincides with the CP potential for a metallic plate in Minkowski spacetime.

For the anisotropic oscillator model, Eq. (14), the expression for the potential takes the form

$$\begin{aligned} U_b(r) &= -\frac{q}{\pi} \sum_{m=0}^{\infty}' \sum_{n=1}^3 \sum_j g_j^{(n)} \sum_{\lambda=0,1} \int_0^\infty d\gamma \gamma \frac{K_{qm}^{(\lambda)}(a\gamma)}{I_{qm}^{(\lambda)}(a\gamma)} \\ &\times [\sqrt{1 + \gamma^2/\omega_j^{(n)2}} - 1] f_{\lambda, qm}(\gamma r, \sqrt{1 + \gamma^2/\omega_j^{(n)2}}), \end{aligned} \quad (27)$$

where we have introduced the notations

$$\begin{aligned} f_{0,qm}(x, y) &= \beta_{1n}^2 I_{qm}^{\prime 2}(x) + \beta_{2n}^2 \left(\frac{qm}{x}\right)^2 I_{qm}^2(x) + \left(1 + \frac{1}{y}\right) \beta_{3n}^2 I_{qm}^2(x), \\ f_{1,qm}(x, y) &= -\frac{1}{y} \left[ \beta_{1n}^2 \left(\frac{qm}{x}\right)^2 I_{qm}^2(x) + \beta_{2n}^2 I_{qm}^{\prime 2}(x) \right]. \end{aligned} \quad (28)$$

In the isotropic case we have

$$\begin{aligned} U_b(r) &= \frac{q}{\pi} \sum_{m=0}^{\infty}' \sum_j \frac{g_j}{\omega_j^2} \int_0^{\infty} d\gamma \gamma^3 \left\{ \frac{K'_{qm}(a\gamma)}{I'_{qm}(a\gamma)} \frac{F_{qm}(\gamma r)}{s_j(\gamma)[s_j(\gamma) + 1]} \right. \\ &\quad \left. - \frac{K_{qm}(a\gamma)}{I_{qm}(a\gamma)} \left[ \frac{F_{qm}(\gamma r)}{s_j(\gamma) + 1} + \frac{I_{qm}^2(\gamma r)}{s_j(\gamma)} \right] \right\}, \end{aligned} \quad (29)$$

with the notation

$$s_j(\gamma) = \sqrt{1 + \gamma^2/\omega_j^2}. \quad (30)$$

For the boundary-induced part in the CP force we have  $\mathbf{F}_b = F_{b,r} \mathbf{n}_r$ , where  $\mathbf{n}_r$  is the unit vector along the radial coordinate  $r$  and  $F_{b,r} = -\partial_r U_b(r)$ . In the isotropic case one has  $F_{b,r} > 0$  and the boundary-induced part in the CP force inside the cylindrical shell is directed toward the shell. The pure string part of the force has the same direction and the total force in the isotropic case is repulsive with respect to the string and attractive with respect to the shell.

Similar to the interior case, the CP potential for the exterior region is presented in the decomposed form (23). The formulas for the boundary-induced part are obtained from expressions (24), (26) and (29) by the interchange  $I_{qm} \rightleftarrows K_{qm}$ . At large distances from the shell, to the leading order we find

$$U_b(r) \approx -\frac{q\alpha_{11}(0)}{6\pi r^4 \ln(r/a)}. \quad (31)$$

At large distances the CP potential is dominated by the pure string part and the corresponding force in the isotropic case is repulsive.

In figure 1 we display the total CP potential  $U(r)$  (full curve) for both interior and exterior regions as a function of  $r/a$  for  $q = 2$  and  $a/\lambda_0 = 1$ , with  $\lambda_0 = 2\pi/\omega_0$ . The dot-dashed and dashed curves correspond to the pure string ( $U_0(r)$ ) and boundary-induced ( $U_b(r)$ ) parts in the potential, respectively. In the numerical evaluation the single oscillator model is used with isotropic polarizability and with the parameters  $g_j = g_0$  and  $\omega_j = \omega_0$ . The potential is dominated by boundary-induced part near the cylindrical shell and by the pure string part for points near the string and at large distances from the cylindrical shell.

## 4. Conclusion

We have presented the results of the investigation of the CP potential for a microparticle with anisotropic polarizability tensor in the geometry of a straight

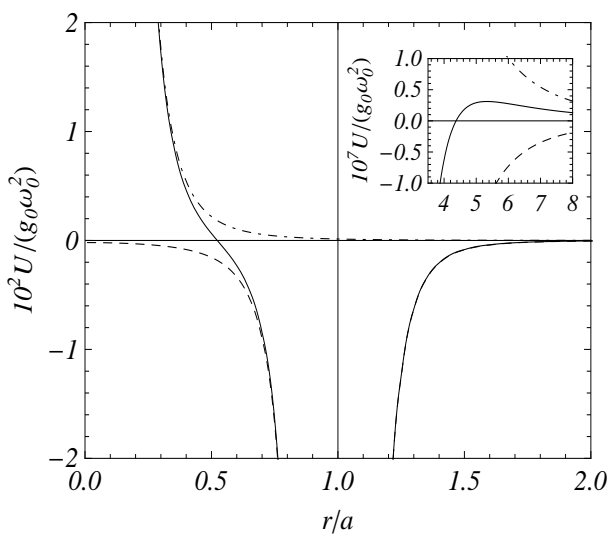


Figure 1: CP potential as a function of  $r/a$  for  $a/\lambda_0 = 1$  and  $q = 2$ .

cosmic string with coaxial metallic cylindrical shell. For the both exterior and interior regions of the shell the potential is decomposed into the boundary-free and shell-induced part. The former dominates for points near the string and at large distances from the shell, whereas the shell-induced part is dominant near the shell. The potential depends on the distance of the microparticle from the string and on the angles determining the orientation of the principal axes. In the anisotropic case, with dependence of orientation, the corresponding forces can be either attractive or repulsive. As a model for a polarizability tensor we have taken anisotropic oscillator model which works well over a wide range of separations. Within this model, for an isotropic polarizability tensor the boundary-free part of the CP force is repulsive with respect to the cosmic string for all distances and the shell-induced part is attractive with respect to the shell. At large distances from the shell (retarded regime), the dominant contribution to the CP potential comes from low frequencies and it scales as  $1/r^4$ . At large distances from the shell, the shell-induced part behaves as  $1/[r^4 \ln(r/a)]$ . At distances from the string smaller than the relevant transition wavelengths the potential behaves as  $1/r^3$  power law. In the case of anisotropic polarizability, the dependence of the CP potential on the orientation of the polarizability tensor principal axes will also lead to the moment of force acting on the particle.

## References

- [1] V.A. Parsegian, *Van der Waals forces: A Handbook for Biologists, Chemists, Engineers, and Physicists* (Cambridge University Press, Cambridge, 2005).

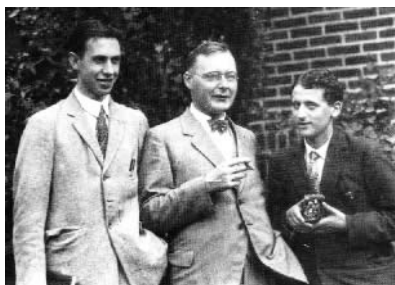
- [2] S.Y. Buhmann, D.-G. Welsch, Prog. Quantum Electron. **31**, 51 (2007).
- [3] A. Vilenkin and E.P.S. Shellard, *Cosmic Strings and Other Topological Defects* (Cambridge University Press, Cambridge, England, 1994).
- [4] E.R. Bezerra de Mello, V.B. Bezerra, A.A. Saharian and A.S. Tarloyan, Phys. Rev. D **74**, 025017 (2006).
- [5] I. Brevik and T. Toverud, Class. Quantum Grav. **12**, 1229 (1995).
- [6] E.R. Bezerra de Mello, V.B. Bezerra and A.A. Saharian, Phys. Lett. B **645**, 245 (2007).
- [7] E.R. Bezerra de Mello, V.B. Bezerra, A.A. Saharian and A.S. Tarloyan, Phys. Rev. D **78**, 105007 (2008).
- [8] E.R. Bezerra de Mello, V.B. Bezerra, A.A. Saharian and V.M. Bardeghyan, Phys. Rev. D **82**, 085033 (2010); S. Bellucci, E.R. Bezerra de Mello and A.A. Saharian, Phys. Rev. D **83**, 085017 (2011).
- [9] G. Fucci and K. Kirsten, JHEP **03**, 016 (2011); G. Fucci and K. Kirsten, J. Phys. A **44**, 295403 (2011).
- [10] E.R. Bezerra de Mello and A.A. Saharian, Class. Quantum Grav. **28**, 145008 (2011).
- [11] C. Eberlein and R. Zietal, Phys. Rev. A **80**, 012504 (2009).
- [12] V.B. Bezerra, E.R. Bezerra de Mello, G.L. Klimchitskaya, V.M. Mostepanenko and A.A. Saharian, Eur. Phys. J. C **71**, 1614 (2011).
- [13] V.M. Bardeghyan and A.A. Saharian, J. Contemp. Phys. **45**, 1 (2010).
- [14] A.A. Saharian and A.S. Kotanjyan, Eur. Phys. J. C **71**, 1765 (2011).
- [15] A.A. Saharian and A.S. Kotanjyan, arXiv:1201.0135.
- [16] A. Vilenkin, Phys. Rev. D **23**, 852 (1981).
- [17] J. R. Gott III, Astrophys. J. **288**, 422 (1985); W. Hiscock, Phys. Rev. D **31**, 3288 (1985); B. Linet, Gen. Relativ. Gravit. **17**, 1109 (1985); D. Garfinkle, Phys. Rev. D **32**, 1323 (1985).

# В ответ на любимую историю Э. Чубаряна о несостоявшейся статье С. Гаудсмита и Дж. Уленбека о спине

В. М. Мыхитарян<sup>1</sup>

Институт физических исследований НАН Армении, Аштарак

А история, которую любил рассказывать уважаемый юбиляр, следующая:



Джордж Уленбек (слева) и  
Сэмюэл Гаудсмит (справа)

В октябре 1925 года Сэмюэл Гаудсмит (Samuel Goudsmit) и Джордж Уленбек (George Uhlenbeck), молодые сотрудники Паула Эренфеста (Paul Ehrenfest), ввели в физику концепцию спина. Они предложили рассматривать электрон как «вращающийся волчок», обладающий собственным механическим моментом, равным  $\hbar/2$ , и собственным магнитным моментом, равным магнетону Бора. Они сообщили о своей гипотезе Эренфесту, которому она понравилась. Он предложил своим ученикам написать небольшую заметку для

журнала *Die Naturwissenschaften* и показать ее Хендрику Лоренцу.

Лоренц произвел ряд вычислений электромагнитных свойств вращающегося электрона и продемонстрировал нелепость выводов, к которым приводит эта гипотеза. Согласно расчетам, основанным на классических подходах, скорость на поверхности электрона должна превышать скорость света. Уленбек и Гаудсмит посчитали за лучшее не публиковать свою статью, однако было поздно: Эренфест уже отоспал ее в печать<sup>2</sup>.

По этому поводу Эренфест заметил: «Вы оба достаточно молоды, чтобы позволить себе сделать одну глупость!».

Мы повторим «глупость» молодых, но сделаем расчет в рамках релятивистских подходов. Предположим, что вращению электрона можно сопоставить твердое вращение заряженной сферы с угловой скоростью  $\Omega$ , у которого удаленная относительно оси вращения точка поверхности движется со скоростью света.

Одна из особенностей группы представления (преобразования) Пуанкаре в том, что представляемое пространство не только меняет метрические свойства, но и может оказаться ограниченным в размерах. Преобразования указывают не только на изменении метрики, но и на то, что при вращении пространство (где описывается физический объект) само ограничено размерами. Т.е. в общем случае они осуществляют отображение бесконечного, неограниченного в размерах импульсного пространства в ограниченную в размерах пространственную область. Таким образом, всякое вращение описывается представлением импульсного пространства в координатном пространстве как ограниченную область.

<sup>1</sup> Email: [vm@ipr.sci.am](mailto:vm@ipr.sci.am)

<sup>2</sup> Uhlenbeck G. E., Goudsmit S.— *Naturwissenschaften*, 1925, Hf. 47, S. 953.

Это особенно наглядно на примере собственного вращения физического объекта или вращающейся системы отсчета с угловой скоростью  $\Omega$  вокруг оси  $z$ . В этом случае скорость в точке  $\rho$  можно представить как  $[\Omega \times \rho]$  и обобщенный импульс  $d\mathbf{P}$  элемента объема  $dv$  в точке  $\rho$  с энергией покоя  $d\varepsilon$  и импульсом  $d\mathbf{p}$  представится в виде

$$d\mathbf{P} = \left( \frac{d\varepsilon + \frac{1}{c} [\Omega \times \rho] \cdot d\mathbf{p}}{\sqrt{1 - [\Omega \times \rho]^2/c^2}}, \quad d\mathbf{p}_{0\perp} + \frac{d\mathbf{p}_{0\parallel} + \frac{d\varepsilon}{c} [\Omega \times \rho]}{\sqrt{1 - [\Omega \times \rho]^2/c^2}} \right),$$

где  $\varepsilon_0$  и  $\mathbf{p}_0$ , соответственно, энергия и импульс без вращения. Как видим, импульсное пространство отображено в ограниченной области координатного пространства размером  $\rho_c = c/\Omega$  на плоскости  $(x, y)$ . Соответственно, при вращении пространство описания частицы ограничено преобразованием в область  $\rho \leq \rho_c = c/\Omega$ . Т.е. вращение представляется как отображение в ограниченное пространство – ограниченное преобразованием пространство и есть вращающаяся частица, физический объект, описываемая система.

По сути, вращение это переход в другую систему отсчета, где пространство описания частицы уже имеет другие размеры отображения и соответствующую метрику. При этом частица всегда одна и та же, но отображено (упаковано) в пространстве иных размеров.

Рассмотрим сначала вопрос об энергии собственного вращения частицы. Если частица не вращается и имеет бесконечные размеры (например, электрон), то в состоянии вращения она (или вращающаяся часть) будет упакована в конечных размерах. Т.е. при вращении область вовлечения равна  $\rho_c = c/\Omega$  и количество вовлеченной массы равно  $m_0$ . Конкретно, рассмотрим твердое вращение частицы с энергией покоя  $\varepsilon_0 = m_0 c$ , которая при вращении упакована в сферу радиусом  $\rho_c = c/\Omega$ . Энергия  $d\varepsilon$  в элементе объема  $dv$  в точке  $\rho$  выражается в виде

$$d\varepsilon = c \frac{dm}{\sqrt{1 - \frac{\Omega^2}{c^2} \rho^2 \sin^2 \theta}} = \frac{3}{2} \varepsilon_0 \frac{\rho^2 \sin \theta d\theta d\rho}{\rho_c^3 \sqrt{1 - \frac{\Omega^2}{c^2} \rho^2 \sin^2 \theta}}.$$

Сделав замену переменной и интегрируя, имеем

$$\begin{aligned} \varepsilon &= \frac{3}{2} \varepsilon_0 \int_0^{\rho_c} \int_0^\pi \frac{\rho^2 \sin \theta d\theta d\rho}{\rho_c^3 \sqrt{1 - \Omega^2 \rho^2 \sin^2 \theta / c^2}} \\ &= \frac{3}{2} \varepsilon_0 \int_0^1 \int_0^\pi \frac{x^2 \sin \theta d\theta dx}{\rho_c^3 \sqrt{1 - x^2 \sin^2 \theta}} = \frac{3}{2} \varepsilon_0 = \frac{3}{2} m_0 c^2 = mc^2. \end{aligned}$$

Результат весьма неожиданный, так как энергия собственного вращения релятивистской частицы оказалось не зависящим от угловой скорости вращения, а относительно покоя отличается постоянным коэффициентом 3/2. Если рассматривать частицу с более сложным распределением плотности массы, все равно бы имели аналогичный результат с какой-то средней плотностью и

с другим постоянным коэффициентом. Это обусловлено характером выражения интеграла энергии, где после замены переменной интегрирования исчезает зависимость от угловой скорости и получается постоянное число.

Таким образом, релятивистская энергия собственного вращения пространственной частицы отличается от энергии покоя на постоянное число, вне зависимости от скорости вращения. Это фундаментальное свойство можно выразить следующим образом – энергия собственного вращения частицы имеет только два дискретных значения и описывает всего лишь качество состояния – вращается или не вращается, обладает спином или нет.

Из постоянства и дискретности энергии собственного вращения следует весьма существенный вывод – непрерывный переход во вращательное состояние не возможен, так как вращательная энергия может иметь относительно покоя только определенную, не зависящую от состояния собственного вращения, энергию. Это свойство можно сформулировать и как инвариантность энергии собственного вращения – в любой (и вращательной) системе отсчета энергия собственного вращения постоянна.

Конечно, размеры области представления и скорость вращения частицы соответственно меняются. Но при преобразованиях группы Пуанкаре размеры и скорость вращения частицы преобразуются таким образом, что энергия собственного вращения остается постоянным. Когда скорость вращения увеличивается, то, соответственно, размеры частицы и момент инерции уменьшаются, поэтому и энергия собственного вращения остается неизменной. Возможность релятивистской частицы при постоянной энергии иметь различные скорости вращения является фундаментальным для понимания независимости энергии частицы от состояния собственного вращения – спина.

Для момента импульса собственного вращения частицы имеем

$$s = \varepsilon_0 \frac{3}{4\pi c \rho_c^3} \int_0^{\rho_c} \frac{[\mathbf{p} \times [\Omega \times \mathbf{p}]]}{\sqrt{1 - [\Omega \times \mathbf{p}]^2/c^2}} d\mathbf{p}^3.$$

Так как направление момента  $s$  совпадает с направлением вращения  $\Omega$ , то умножая выражение для  $s$  на единичный вектор  $\Omega/\Omega$ , получим

$$s = \varepsilon_0 \frac{3}{4\pi c \Omega \rho_c^3} \int_0^{\rho_c} \frac{[\Omega \times \mathbf{p}]^2}{\sqrt{1 - [\Omega \times \mathbf{p}]^2/c^2}} d\mathbf{p}^3 =$$

$$\frac{\varepsilon c}{\Omega} \int_0^1 dx \int_0^\pi \frac{x^2 \sin^3 \theta}{\sqrt{1 - x^2 \sin^2 \theta}} d\theta = \frac{\varepsilon c}{2\Omega} = \frac{E}{2\Omega}.$$

Если представить энергию  $E$  в виде энергии ротатора  $\hbar\Omega$ , то получим

$$s = \frac{E}{2\Omega} = \frac{\hbar}{2}; \quad \rho_c = \frac{c}{\Omega} = \frac{\hbar}{\varepsilon} = \frac{\hbar}{mc} = \lambda_m;$$

где  $\lambda_m$  – длина волны де Броイラ для частицы с массой  $m$ .

Как видим, все как то неожиданно, но уже не так глупо, как казалось в 1925 г.